Towards a Global Estimate for Generalized Parton Distributions

Dissertation

zur Erlangung des Doktorgrades
der Naturwissenschaften (Dr. rer. nat.)
der Fakultät für Physik
der Universität Regensburg

vorgelegt von

Tobias Lautenschlager

aus Neumarkt

Juni 2014

Promotionsgesuch eingereicht am 24.06.2014

Prüfungsausschuss:

Prof. Dr. S. Ganichev
Prof. Dr. A. Schäfer
Prof. Dr. V. M. Braun
Prof. Dr. I. Morgenstern

Termin Promotionskolloquium: 29. April 2015

Contents

1 Introduction

The theory of the strong interaction quantum chromodynamics (QCD) is an asymptotically free theory. In the limit of small separations, the coupling constant tends to zero and we utilize perturbation theory in the small coupling. However, the description of hard exclusive processes involves hadrons consisting of confined quarks. For their respective momentum, the coupling is large and perturbation theory is not applicable. The solution to this problem are factorization theorems.

The idea of all factorization theorems is to introduce an artificial factorization scale. A given observable like a cross section involving a hard scale $\mathcal{Q}^2$ is expressed as a convolution of two functions that take into account the hard (small-distance) and soft (large-distance) effects, respectively. The hard function can be treated within perturbation theory describing the evolution of the system at small distances. On the other hand, all information about the transition of asymptotically free quarks and gluons into hadrons is contained in the soft function. It only involves partons with momenta below the factorization scale. As a consequence, the dependence on the hard scale is only contained in the hard part. Furthermore, the soft nonperturbative functions are universal entering various processes. They are expressed as hadronic matrix elements of well defined quark-gluon operators sandwiched between hadronic states.

In this thesis, we discuss three hard processes. In deeply inelastic scattering (DIS), a lepton interacts with the nucleon via a virtual photon, with the nucleon fragmenting into a number of hadrons. The corresponding nonperturbative functions are the well known parton distribution functions (PDFs). Furthermore, we investigate deeply virtual Compton scattering (DVCS) [MRG+94, Rad96b, Ji97a]. In the process (Fig. 1.1(a)), the lepton interacts with the nucleon via a virtual photon under the emission of a photon. This process involves generalized parton distributions (GPDs). And finally, we investigate deeply virtual meson production (DVMP) [CFS97]. A lepton is scattered off a nucleon target via the exchange of a virtual photon (Fig. 1.1(b)). It interacts with the target in such a way, that a nucleon and a meson are produced. Depending on the particular meson, the nucleon in the in and outgoing state may be different. As a crucial difference to the two previous processes, the latter one involves two nonperturbative functions. In addition to the GPDs, the transition from asymptotically free partons into a meson is described by a distribution amplitude (DA). The basic object for the factorization theorem of DVCS is the virtual Compton scattering amplitude, which is defined as the off-forward matrix element of the time-ordered product of

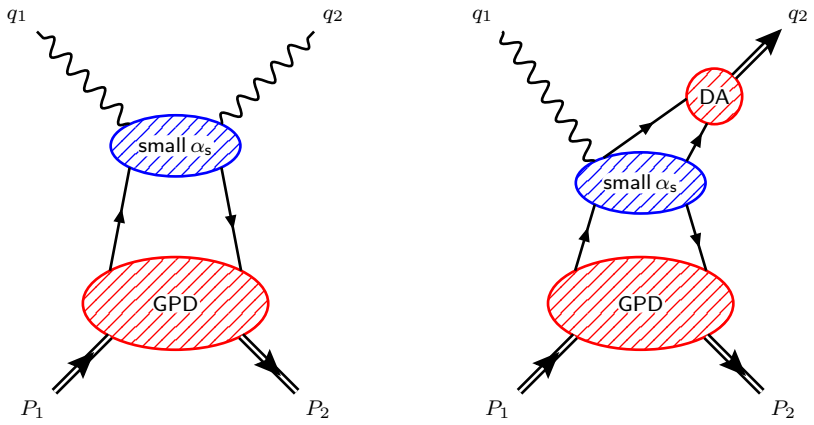

(a) DVCS (b) DVMP

Figure 1.1.: Factorization for DVCS and DVMP involving generalized parton distributions and distribution amplitudes.

two quark electromagnetic currents

$$T^{\mu\nu} = i \int \mathrm{d}^4 z \; e^{iq.z} \left\langle \mathrm{P}_2 | T\{ j^\mu(\tfrac{z}{2}) \, j^\nu(-\tfrac{z}{2}) \} \, | \mathrm{P}_1 \right\rangle ,$$

where

$$j_\mu(z) = \sum_q Q_q \bar{\psi}_q(z) \gamma_\mu \psi_q(z) , \quad q \in \{u, d, s, c\} , \quad Q_u = Q_c = 2/3 , \; Q_d = Q_s = 1/3 .$$

The amplitude factorizes in a hard scattering amplitude and generalized parton distributions in the limit where at least one of the invariants q_1^2, q_2^2 is large and the Mandelstam variable $s = (P_1 + q_1)^2$ is large as well, whereas the respective ratios q_1^2/s, q_2^2/s are fixed [CF99, JO98a]. This particular limit is called the generalized Bjorken limit. In this limit, the dominant contribution originates in the region $0 \leq z^2 \leq \mathrm{const}/(-q_1^2)$ [Mut98]. As a consequence, a particular useful coordinate system are light-cone coordinates. We introduce two independent vectors n^μ and $\tilde{n}^\mu$ with $n^2 = \tilde{n}^2 = 0$. A arbitrary four-vector a^μ can be decomposed into the two components into the direction of the two light-like vectors and a component perpendicular to both:

$$a^\mu = a^+ \tilde{n}^\mu + a^- n^\mu + a_\perp^\mu , \qquad \text{with} \quad a^+ = a.n , \; a^- = a.\tilde{n} .$$

In a reference frame, where the proton is at rest and the virtual photon moves along the opposite z-axis, its four-momentum becomes

$$q_1^\mu = \left(\frac{\mathcal{Q}^2}{2 M x_\mathrm{B}}, 0, 0, \frac{\mathcal{Q}^2}{2 M x_\mathrm{B}} \sqrt{1 + \frac{4 M^2 x_\mathrm{B}}{\mathcal{Q}^2}} \right) ,$$

with the momentum transfer $\mathcal{Q}^2 = -q_2^2$, the Bjorken variable $x_\mathrm{B} = \mathcal{Q}^2/(2P_1.q_1)$ and the nucleon mass $P_1^2 = M^2$. For sufficiently large values of $\mathcal{Q}^2$, the light-cone components are

$$q_1^- \approx \frac{\mathcal{Q}^2}{M x_\mathrm{B}}\,, \qquad q_1^+ \approx M x_\mathrm{B}\,.$$

The integrand in the virtual Compton amplitude is a oscillating function and only provides a result if the distances of the electromagnetic currents are

$$z^- \approx \frac{1}{M x_\mathrm{B}}\,, \qquad z^+ \approx \frac{M x_\mathrm{B}}{\mathcal{Q}^2}\,.$$

Thus, assuming that the transverse separations $z_\perp$ are small, the dependence on the z^+ coordinate component can be neglected and the only relevant component is z^-. The latter is called Ioffe time [GIP66, Iof69] and corresponds to the longitudinal distance probed in the process.
The systematic analysis of the virtual Compton amplitude is achieved via the operator product expansion (OPE) near the light-cone. The product of two electromagnetic currents takes the form

$$j_\perp(z) j_\perp(0) \sim \sum_{i,j} C_j^{(i)}\big(z^2\big)\,(-iz^-)^j\, n^{\mu_1}\ldots n^{\mu_j}\,\mathcal{O}^{(i)}_{\mu_1\ldots\mu_j}\,,$$

where the index (i) denotes the different type of local composite operators and we anticipated the Lorentz structure of the unpolarized dominant contribution. In a free field theory the singularity structure follows by analyzing the canonical dimensions of the operators in the OPE. The canonical dimension of the electromagnetic current is denoted by l^can and the one of the local composite operator depends in general on j is denoted by l_j^can. Therefore, the coefficient function $C_j^{(i)}(z^2)$ has the structure

$$C_j^{(i)}(z^2) \sim \left(\frac{1}{z^2}\right)^{l^\mathrm{can}+j/2-l_j^\mathrm{can}/2}\,.$$

Hence, the strength of the singularity is completely determined by the so called twist [GT71]

$$\tau = l_j^\mathrm{can} - j\,.$$

An example for such an local composite operator appearing in the LO analysis of DVCS is the bilocal quark operator

$$\mathcal{O}_\alpha^{qq}(-z^-, z^-) = \bar\psi(-z^-)\gamma_\alpha\psi(z^-)\,.$$

The definition of twist is only valid for local operators and consequently, the operator above does not transform in an irreducible representation of the Lorentz group. A Taylor expansion in terms of local operators leads to

$$\mathcal{O}_\alpha^{qq}(-z, z) = \sum_{j=0}^{\infty}\frac{1}{j!}(-iz^-)^j n^{\mu_1}\ldots n^{\mu_j}\mathcal{O}^{qq}_{\alpha\mu_1\ldots\mu_j}\,,$$

with

$$\mathcal{O}^{qq}_{\alpha\mu_1\ldots\mu_j} = \bar{\psi}\gamma_\alpha i\overset{\leftrightarrow}{D}_{\mu_1}\ldots i\overset{\leftrightarrow}{D}_{\mu_j}\psi\,,$$

where the covariant left-right derivative is defined by $\overset{\leftrightarrow}{D}_\mu = \vec{D}_\mu - \overset{\leftarrow}{D}_\mu$. This nonlocal operator does not transform in an irreducible representation of the Lorentz group and thus has no definite twist. The indices $\mu_1\ldots\mu_j$ are symmetric and transform in the irreducible representation $(j/2, j/2)$ of the Lorentz group. Therefore, including a free Lorentz index α in the representation $(1/2, 1/2)$ leads to the following irreducible representation

$$\boxed{\mu_1|\mu_2|\cdots|\mu_j} \otimes \boxed{\alpha} = \boxed{\mu_1|\mu_2|\cdots|\mu_j|\alpha} \oplus \begin{array}{|c|}\hline \mu_1|\mu_2|\cdots|\mu_j \\ \hline \alpha \\ \hline \end{array}\,.$$

The first one denotes the fully symmetric combination of the indices. It corresponds to the operator

$$\mathcal{R}^{2,qq}_{\alpha\mu_1\ldots\mu_j} = \underset{\alpha\mu_1\ldots\mu_j}{\mathbf{S}}\,\bar{\psi}\gamma_\alpha i\overset{\leftrightarrow}{D}_{\mu_1}\ldots i\overset{\leftrightarrow}{D}_{\mu_j}\psi\,,$$

where $\mathbf{S}$ is the operator of symmetrization and trace subtraction. The operator above transforms in the irreducible representation $((j+1)/2, (j+1)/2)$ with dimension $j+2$. As a consequence, its twist is two. This is the leading contribution.
In an interaction theory, the counting of the canonical dimension is no longer valid, since the canonical dimensions have to be modified by the anomalous dimensions. The full singularity structure is obtained by the renormalization group equation [Col84]. The three nonperturbative functions mentioned before are matrix elements of the local composite operators.
A meson distribution amplitude describes a vacuum-to-hadron (Fig. 1.2(a)) or hadron-to-

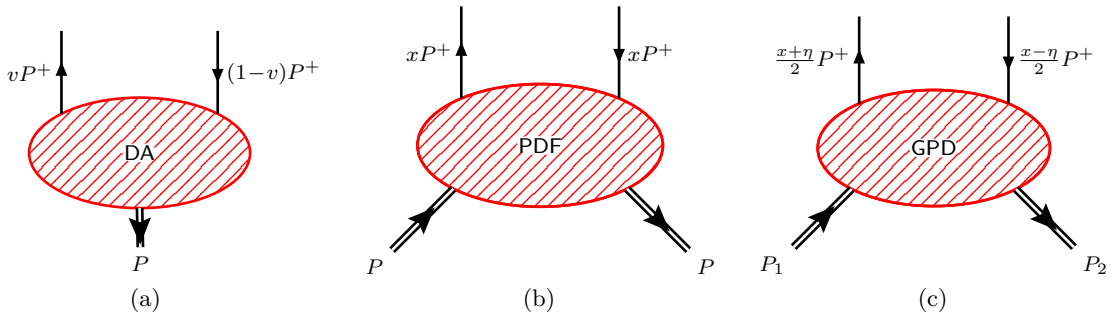

Figure 1.2.: The three nonperturbative functions utilized in this thesis: the distribution amplitude, the parton distribution function and the generalized parton distribution.

vacuum matrix element of non-local light-cone operators, where a quark-antiquark pair with the longitudinal momentum fractions v and $1-v$ is absorbed or emitted, respectively. The momentum fraction v is in the interval $[0, 1]$.
The PDF describes the emission and absorption of a quark and antiquark with the longitudinal momentum fraction x of the longitudinal nucleon momentum P^+. The momentum fraction x is in the interval $[-1, 1]$, whereas it is positive for quarks and negative for antiquarks.

The GPD (Fig. 1.2(c)) depends on the variable x, which is the Fourier conjugate to the Ioffe time. In addition, it also depends on the t-channel momentum transfer $\Delta^2 = (P_1 + P_2)^2$ and the skewness

$$\eta = -\frac{\Delta^+}{P^+} .$$

The longitudinal components of the incoming and outgoing parton momenta k_1^+ and k_2^+ are therefore

$$k_1^+ = \frac{x+\eta}{P^+} , \qquad k_2^+ = \frac{x-\eta}{P^+} .$$

The variable x in terms of the parton momenta reads

$$x = \frac{k_1^+ + k_2^+}{P^+} ,$$

which has the support in the region $x \in [-1, 1]$. It can be split in three different regions. In the region $x \in [\eta, 1]$, the parton momenta k_1^+ and k_2^+ are positive and can be interpreted as the emission and absorption of a quark. In the central region $x \in [-\eta, \eta]$, $k_1 \geq 0$ and $k_2 \leq 0$. Thus, this region corresponds to the emission of a quark-antiquark pair. In the third region we have the opposite situation as in the first one, which can be viewed as the emission and reabsorption of a antiquark.
In Ch. 2 we introduce the definition of the leading twist-2 GPDs and its properties, which are employed throughout this thesis. For an extensive review on GPDs see [Die03, BR05].
In the next chapter 3, we study the three processes involving GPDs. Since in the forward case, they are equal to PDFs, we present a full analysis of DIS and the unpolarized structure functions at LO of perturbation theory. This also serves as a show case, where the methods are introduced first in a simpler scenario.
This is followed by the derivation of the deeply virtual Compton scattering cross section. We introduce the Compton form factors (CFFs) as the basic non-separable objects involving GPDs. This allows a clear separation of the perturbative hard scattering amplitude and the perturbative evaluation procedure at amplitude level. We study its properties and perturbative evolution in detail.
For deeply virtual meson production we derive the cross section at LO of perturbation theory, which in contrast to the hand bag approach for DVCS also involves gluon GPDs making the analysis more intricate. As in the previous case, we identify the basic non-separable objects involving the GPDs and DAs, which are called transition form factors (TFFs). This is followed by an extensive study of its properties including the perturbative evolution. In addition, we present the hard scattering amplitudes in the momentum fraction representation at NLO of perturbation theory in a systematic way. We define basic building blocks and calculate their imaginary parts. Moreover, we identify the most singular parts. The given representation is much more suited for latter purposes than the original form in [ISK04] allowing the derivation of the conformal moments also for the non-separate building blocks.
In Ch. 4 we reanalyze the three processes utilizing conformal symmetry. As the main result, we derive the Mellin-Barnes representations of CFFs and TFFs, which is a convenient

representation for their numerical evaluation from the respective GPDs. The Mellin-Barnes representation demands the analytic continuation of the conformal moments of the hard scattering amplitudes. The solution was already known for the hard scattering amplitudes of DVCS. However, due to the non-separate building blocks it was only solved recently for DVMP in [MLPKS14]. We benefit from the systematic representation of the NLO hard scattering amplitude in the previous chapter and derive a method which allows the numerical and analytical evaluation of conformal moments of the hard scattering amplitude, ensuring the correct analytic continuation to complex conformal moments.
In the field of high energy physics, it is common to utilize the least squares estimate to analyze GPDs and PDFs, since it is easy to implement and most standard software packages provide its methods. However, this so called orthodox statistics (OS) relies on several assumptions. In Ch. 5 we give a detailed and exhaustive introduction to probability theory as extended logic (PTEL). This answers all the questions related to the parameter estimation in this thesis. We derive the product and sum rule of probability theory, which are the essential equations to solve all estimation problems from the basic desiderata of G. Pòlya [Pól45, Pól54]. This is followed by the introduction of hypothesis tests and the extension to probability distribution functions. We introduce several generic probability distributions. Afterward, we derive the relevant formulae for the estimation of parameters from data. Furthermore, we study the propagation of uncertainties and investigate the consequences of employing a Gaussian distribution for the experimental data. In the appendix, we derive the methods of orthodox statistics and their assumptions from PTEL. This brings the reader in a position to choose the most efficient method for a given problem. However, OS is not applicable to the given parameter estimation problem of this thesis.
The parametrization of GPDs is discussed in Ch. 6. We parametrize the conformal Mellin moments providing a fast numerical evaluation. First, we introduce the parametrization utilized in [KMPK08, KM10] for the analysis of data for DIS and DVCS. Second, we discuss a full parametrization to prepare a complete study of the available parametrizations.
In the last chapter 7, we present our results for a global GPD analysis based on PTEL [LMS13] utilizing the result of all previous chapters. We repeat the estimate in [KMPK08, KM10] to show advantages of probability theory in contrast to the usual least square estimate.

2

Generalized parton distributions

In this chapter, we introduce the leading twist-2 generalized parton distributions and their basic properties. We present the forward limit which is equal to the common parton distribution functions. Furthermore, we study the symmetry properties of the GPDs. For a review see [Die03, BR05].

2.1. Operators

We briefly discussed the twist decomposition of the relevant operators in the introduction. Let us introduce the leading twist-2 quark and gluon operators.
The vector and axial-vector leading twist-2 bilocal quark operators read

$$\begin{aligned}\mathcal{O}^{qq}(z_1^-, z_2^-) &= \bar{\psi}(z_1^-)\gamma^+ \quad \psi(z_2^-)\,,\\ \tilde{\mathcal{O}}^{qq}(z_1^-, z_2^-) &= \bar{\psi}(z_1^-)\gamma^+\gamma^5\psi(z_2^-)\,,\end{aligned} \tag{2.1}$$

where we suppressed the Wilson line since we work in the light-cone gauge $A^+=0$. The total symmetry is ensured by the contraction of the bilocal operator in the introduction with the light-like vector n^α.
The two leading twist vector and axial-vector gluon operators are

$$\begin{aligned}\mathcal{O}^{gg}(z_1^-, z_2^-) &= F_a^{+\mu}(z_1^-)\; g_{\mu\nu}F_b^{\nu+}(z_2^-)\,,\\ \tilde{\mathcal{O}}^{gg}(z_1^-, z_2^-) &= F_a^{+\mu}(z_1^-) i\epsilon^\perp_{\mu\nu}F_a^{\nu+}(z_2^-)\,,\end{aligned} \tag{2.2}$$

respectively. Note, that we suppressed the Wilson line as well.

2.2. Matrix elements

In this thesis, we will only deal with spin-$\frac{1}{2}$ hadrons. It is convenient to express the expectation values of local operators in terms of the spinor bilinears

$$\begin{aligned} b &= \bar{U}(P_2) \quad U(P_1)\,, & \tilde{b} &= \bar{U}(P_2) \quad \gamma^5 U(P_1)\,,\\ h^\mu &= \bar{U}(P_2)\,\gamma^\mu \quad U(P_1)\,, & \tilde{h}^\mu &= \bar{U}(P_2)\,\gamma^\mu \quad \gamma^5 U(P_1)\,,\\ t^{\mu\nu} &= \bar{U}(P_2)\, i\sigma^{\mu\nu} U(P_1)\,, & \tilde{t}^{\mu\nu} &= \bar{U}(P_2)\, i\sigma^{\mu\nu}\gamma^5 U(P_1)\,. \end{aligned} \tag{2.3}$$

However, the spinor bilinears above are not independent. An independent basis is given by

$$h^\mu\,, \qquad e^\mu = \frac{t^{\nu\mu}\Delta_\nu}{M_{H_1}+M_{H_2}}\,, \qquad \tilde{h}^\mu\,, \qquad \tilde{e}^\mu = -\frac{\Delta^\mu \tilde{b}}{M_{H_1}+M_{H_2}}\,. \tag{2.4}$$

For the vector and axial-vector operators (2.1) there are two independent Dirac structures. The corresponding operators the decomposition of the matrix elements is [Ji97a]

$$\begin{aligned}
\langle \mathrm{P}_2|\mathcal{O}^{qq}(-z^-,z^-)\,|\mathrm{P}_1\rangle &= \int_{-1}^{1}\mathrm{d}x\; e^{-ixP.z}\big[h^+H^q\big(x,\eta,\Delta^2\big)+e^+E^q\big(x,\eta,\Delta^2\big)\,\big]\,,\\
\langle \mathrm{P}_2|\tilde{\mathcal{O}}^{qq}(-z^-,z^-)\,|\mathrm{P}_1\rangle &= \int_{-1}^{1}\mathrm{d}x\; e^{-ixP.z}\big[\tilde{h}^+\tilde{H}^q\big(x,\eta,\Delta^2\big)+\tilde{e}^+\tilde{E}^q\big(x,\eta,\Delta^2\big)\,\big]\,.
\end{aligned} \tag{2.5}$$

The matrix element of the twist-2 gluon operators (2.2) is defined as

$$\begin{aligned}
\langle \mathrm{P}_2|\mathcal{O}^{gg}(-z^-,z^-)\,|P_1\rangle &= \frac{1}{4}P^+\int_{-1}^{1}\mathrm{d}x\; e^{-ixP.z}\big[h^+H^{\mathrm{G}}\big(x,\eta,\Delta^2\big)+e^+E^{\mathrm{G}}\big(x,\eta,\Delta^2\big)\,\big]\,,\\
\langle \mathrm{P}_2|\tilde{\mathcal{O}}^{gg}(-z^-,z^-)\,|\mathrm{P}_1\rangle &= \frac{1}{4}P^+\int_{-1}^{1}\mathrm{d}x\; e^{-ixP.z}\big[\tilde{h}^+\tilde{H}^{\mathrm{G}}\big(x,\eta,\Delta^2\big)+\tilde{e}^+\tilde{E}^{\mathrm{G}}\big(x,\eta,\Delta^2\big)\,\big]\,.
\end{aligned} \tag{2.6}$$

We also introduce the target-independent, boost invariant form of GPDs. In the parity even sector, the definition is

$$\begin{aligned}
\langle \mathrm{P}_2|\mathcal{O}^{qq}(-z^-,z^-)\,|\mathrm{P}_1\rangle &= P^+\int_{-1}^{1}\mathrm{d}x\; e^{-ixP.z}\,F^q\big(x,\eta,\Delta^2\big)\,,\\
\langle \mathrm{P}_2|\mathcal{O}^{gg}(-z^-,z^-)\,|\mathrm{P}_1\rangle &= \frac{1}{4}(P^+)^2\int_{-1}^{1}\mathrm{d}x\; e^{-ixP.z}\,F^{\mathrm{G}}\big(x,\eta,\Delta^2\big)\,,
\end{aligned} \tag{2.7}$$

with $A=(q,\mathrm{G})$. The functions F^A are defined as

$$F^A\big(x,\eta,\Delta^2\big) = \frac{h^+}{P^+}H^A\big(x,\eta,\Delta^2\big)+\frac{e^+}{P^+}E^A\big(x,\eta,\Delta^2\big)\,. \tag{2.8}$$

In the parity odd sector, the corresponding definitions are

$$\begin{aligned}
\langle \mathrm{P}_2|\tilde{\mathcal{O}}^{qq}(-z^-,z^-)\,|\mathrm{P}_1\rangle &= P^+\int_{-1}^{1}\mathrm{d}x\; e^{-ixP.z}\,F^q\big(x,\eta,\Delta^2\big)\,,\\
\langle \mathrm{P}_2|\tilde{\mathcal{O}}^{gg}(-z^-,z^-)\,|\mathrm{P}_1\rangle &= \frac{1}{4}(P^+)^2\int_{-1}^{1}\mathrm{d}x\; e^{-ixP.z}\,F^{\mathrm{G}}\big(x,\eta,\Delta^2\big)\,.
\end{aligned} \tag{2.9}$$

The respective GPDs read

$$F^A\big(x,\eta,\Delta^2\big) = \frac{\tilde{h}^+}{P^+}\tilde{H}^A\big(x,\eta,\Delta^2\big)+\frac{\tilde{e}^+}{P^+}\tilde{E}^A\big(x,\eta,\Delta^2\big)\,. \tag{2.10}$$

Moreover, it is possible to write the quark and gluon GPD as Fourier transformation of the corresponding matrix elements:

$$\begin{aligned}
F^q\big(x,\eta,\Delta^2\big) &= \int\frac{\mathrm{d}z^-}{2\pi}e^{ixP.z}\langle P_2|\mathcal{O}^{qq}(-z,z)|P_1\rangle\,,\\
F^g\big(x,\eta,\Delta^2\big) &= \frac{4}{P^+}\int\frac{\mathrm{d}z^-}{2\pi}e^{ixP.z}\langle P_2|\mathcal{O}^{gg}(-z,z)|P_1\rangle\,.
\end{aligned} \tag{2.11}$$

Analogous equation follow for the parity odd sector.
The time-reversal and hermicity imply that the GPDs are real and that

$$F^A\big(x,\eta,\Delta^2\big) = F^A\left(x,-\eta,\Delta^2\right), \qquad F\in\{H,\tilde{H},E,\tilde{E}\}, \qquad A\in\{q,\mathrm{G}\}. \tag{2.12}$$

2.3. Definite charge parity

The quark GPDs defined in (2.5) do not posses a definite symmetry under the transformation $x\to -x$. GPDs with a definite symmetry can be defined by utilizing the decomposition

$$F(x) = \frac{1}{2}\left[F(x)+F(x)+F(-x)-F(-x)\right] = \frac{1}{2}\left[F(x)-F(-x)\right]+\frac{1}{2}\left[F(x)+F(-x)\right], \tag{2.13}$$

where we suppressed the dependence in the skewness and the t-channel momentum transfer. Therefore, we introduce the two GPD combinations

$$\begin{aligned} F^{q(\pm)}\big(x,\eta,\Delta^2\big) &\equiv F^q\big(x,\eta,\Delta^2\big) \mp F^q\big(-x,\eta,\Delta^2\big), \qquad F\in\{H,E\},\\ F^{q(\pm)}\big(x,\eta,\Delta^2\big) &\equiv F^q\big(x,\eta,\Delta^2\big) \pm F^q\big(-x,\eta,\Delta^2\big), \qquad F\in\{\widetilde{H},\widetilde{E}\}, \end{aligned} \tag{2.14}$$

where $F^{q(+)}$ and $F^{q(-)}$ refer to even and odd charge parity, respectively. A general notation using a signature factor is

$$F^{q(C)}\big(x,\eta,\Delta^2\big) \equiv F^q\big(x,\eta,\Delta^2\big) - \sigma F^q\big(-x,\eta,\Delta^2\big). \tag{2.15}$$

Summarizing the properties of the quark GPDs with definite charge parity and the gluon GPDs leads to

$$\begin{aligned} H^{q(C)},\, E^{q(C)} &: C=\pm 1,\ \sigma=\pm 1,\\ \widetilde{H}^{q(C)},\, \widetilde{E}^{q(C)} &: C=\pm 1,\ \sigma=\mp 1. \end{aligned} \tag{2.16}$$

As a consequence, we have the following symmetries with respect to the transformation $x\to -x$

$$F^{q(\pm)}\big(-x,\eta,\Delta^2\big) = \mp F^{q(+)}\big(x,\eta,\Delta^2\big), \qquad F\in\{H,E\}, \tag{2.17}$$

$$F^{q(\pm)}\big(-x,\eta,\Delta^2\big) = \pm F^{q(+)}\big(x,\eta,\Delta^2\big), \qquad F\in\{\widetilde{H},\widetilde{E}\}. \tag{2.18}$$

Utilizing the signature we obtain

$$F^{q(C)}\big(-x,\eta,\Delta^2\big) = -\sigma F^{q(C)}\big(x,\eta,\Delta^2\big). \tag{2.19}$$

2.4. Forward limit

For spin-$\frac{1}{2}$ hadrons, we have in addition to the unpolarized quark $q(x)$ and antiquark $\bar{q}(x)$ distributions the polarized quark $\Delta q(x)$ and antiquark $\Delta\bar{q}(x)$ distributions. For $\eta = 0$, the

GPDs are equal to PDFs. In this limit, where only the GPDs H and $\widetilde{H}$ survive, we have equality to the parton densities mentioned above. For the vector and axial-vector case:

$$\begin{aligned} H^q\big(x,\eta{=}0,\Delta^2{=}0\big) &= \quad f^q(x) = \quad q(x)\theta(x) - \quad \bar{q}(-x)\theta(-x)\,, \\ \widetilde{H}^q\big(x,\eta{=}0,\Delta^2{=}0\big) &= \Delta f^q(x) = \Delta q(x)\theta(x) + \Delta\bar{q}(-x)\theta(-x)\,. \end{aligned} \tag{2.20}$$

The gluon GPD in the forward case is equal to

$$\begin{aligned} H^{\mathrm{G}}\big(x,\eta{=}0,\Delta^2{=}0\big) &= f^{\mathrm{G}}(x) \quad = xg(x)\theta(x) - xg(-x)\theta(-x)\,, \\ \widetilde{H}^{\mathrm{G}}\big(x,\eta{=}0,\Delta^2{=}0\big) &= \Delta f^{\mathrm{G}}(x) = x\Delta g(x)\theta(x) + x\Delta g(-x)\theta(-x)\,. \end{aligned} \tag{2.21}$$

Furthermore, the forward matrix elements of the vector and axial-vector quark GPD are defined as

$$\begin{aligned} \big\langle \mathrm{P}|\mathcal{O}^{qq}(-z^-,z^-)\,|\mathrm{P}\big\rangle &= h^+\int_{-1}^{1}\mathrm{d}x\, e^{-ix2P.z}\; f^q(x)\,, \qquad h^+ = 2P^+\,, \\ \big\langle \mathrm{P}|\tilde{\mathcal{O}}^{qq}(-z^-,z^-)\,|\mathrm{P}\big\rangle &= \tilde{h}^+\int_{-1}^{1}\mathrm{d}x\; e^{-ix2P.z}\Delta f^q(x)\,. \end{aligned} \tag{2.22}$$

For the gluonic operators the forward matrix elements read

$$\begin{aligned} \big\langle \mathrm{P}|\mathcal{O}^{gg}(-z^-,z^-)\,|\mathrm{P}\big\rangle &= \frac{1}{2}P^+h^+\int_{-1}^{1}\mathrm{d}x\; e^{-ix2P.z}\; f^{\mathrm{G}}(x)\,, \\ \big\langle \mathrm{P}|\tilde{\mathcal{O}}^{gg}(-z^-,z^-)\,|P\big\rangle &= \frac{1}{2}P^+\tilde{h}^+\int_{-1}^{1}\mathrm{d}x\; e^{-ix2P.z}\Delta f^{\mathrm{G}}(x)\,. \end{aligned} \tag{2.23}$$

As for GPDs (2.53), the two gluon PDFs have definite symmetry under the transformation $x\to -x$, namely

$$f^{\mathrm{G}}(-x) = f^{\mathrm{G}}(x) \qquad \Delta f^{\mathrm{G}}(-x) = -\Delta f^{\mathrm{G}}(x)\,. \tag{2.24}$$

For quark PDFs, such a symmetry is absent:

$$\begin{aligned} f^q(-x) &= \quad q(-x)\theta(-x) - \quad \bar{q}(x)\theta(x)\,, \\ \Delta f^q(-x) &= \Delta q(-x)\theta(-x) + \Delta\bar{q}(x)\theta(x)\,. \end{aligned} \tag{2.25}$$

We can introduce PDFs with such a symmetry analogously to GPDs with definite charge parity (2.14)

$$\begin{aligned} f^{q(\pm)}(x) &= f^q(x) \mp f^q(-x) & f^{q(\pm)}(-x) &= \mp f^{q(\pm)}(x)\,, \\ \Delta f^{q(\pm)}(x) &= \Delta f^q(x) \pm \Delta f^q(-x) & \Delta f^{q(\pm)}(-x) &= \pm f^{q(\pm)}(x)\,. \end{aligned} \tag{2.26}$$

It is customary to decompose the quark PDFs into valence and sea contributions, we write

$$f^q(x) = f^q_{\mathrm{val}}(x) + f^q_{\mathrm{sea}}(x)\,, \qquad \Delta f^q(x) = \Delta f^q_{\mathrm{val}}(x) + \Delta f^q_{\mathrm{sea}}(x)\,, \tag{2.27}$$

where the respective valence and sea contribution is defined as

$$f^q_{\text{val}}(x) = [q(x) - \bar{q}(x)]\,\theta(x)\,, \qquad \Delta f^q_{\text{val}}(x) = [\Delta q(x) - \Delta\bar{q}(x)]\,\theta(x)\,,$$
$$f^q_{\text{sea}}(x) = \bar{q}(x)\theta(x) - \bar{q}(-x)\theta(-x)\,, \qquad \Delta f^q_{\text{sea}}(x) = \Delta\bar{q}(x)\theta(x) + \Delta\bar{q}(-x)\theta(-x)\,. \tag{2.28}$$

The decomposition for PDFs with definite charge parity reads

$$f^{q(+)}(x) = f^q_{\text{val}}(x) + 2f^q_{\text{sea}}(x)\,, \qquad \Delta f^{q(+)}(x) = \Delta f^q_{\text{val}}(x) + 2\Delta f^q_{\text{sea}}(x)\,, \tag{2.29}$$
$$f^{q(-)}(x) = f^q_{\text{val}}(x)\,, \qquad \Delta f^{q(-)}(x) = \Delta f^q_{\text{val}}(x)\,. \tag{2.30}$$

This decomposition in terms of partonic degrees of freedom is very useful for the phenomenological description. Note, these decompositions equivalently hold for GPDs.

2.5. Distribution amplitudes

In case the incoming or outgoing momentum is set to zero, the GPD reduces to the meson distribution amplitude. It parametrizes a vacuum-to-hadron or hadron-vacuum matrix element of a non-local light-cone operator

$$\big\langle \mathrm{P}|\bar{\psi}(z_1^-)\gamma^+\psi(z_2^-)|0\big\rangle = -iP^+ f_{\mathrm{M}} \int_0^1 \mathrm{d}v\, e^{iP.(vz_1^- + \bar{v}x_2^-)}\, \varphi(v)\,. \tag{2.31}$$

The distribution amplitudes enter as nonperturbative functions numerous exclusive processes via factorization with GPDs. Therefore, they are treated like the GPD as a unknown quantity. As a consequence, a understanding of the DA is crucial for the estimation of the GPDs in such processes. Let us list the DAs of longitudinally polarized vector mesons as they are the main objective in the present thesis

$$P^+ f_{\rho^+} \int_0^1 \mathrm{d}v\, e^{iP.(vz_1^- + \bar{v}x_2^-)}\, \varphi_{\rho^+}(v) = \big\langle \rho^+_{\mathrm{L}}(P)|\bar{u}(z_1^-)\gamma^+ d(z_2^-)|0\big\rangle\,. \tag{2.32}$$

$$P^+ f_{\rho^0} \int_0^1 \mathrm{d}v\, e^{iP.(vz_1^- + \bar{v}x_2^-)}\, \varphi_{\rho^0}(v) = \big\langle \rho^0_{\mathrm{L}}(P)|\tfrac{1}{\sqrt{2}}\big[\bar{u}(z_1^-)\gamma^+ u(z_2^-) - \bar{d}(z_1^-)\gamma^+ d(z_2^-)\big]|0\big\rangle\,. \tag{2.33}$$

$$P^+ f_{\omega^0} \int_0^1 \mathrm{d}v\, e^{iP.(vz_1^- + \bar{v}x_2^-)}\, \varphi_{\omega^0}(v) = \big\langle \omega^0_{\mathrm{L}}(P)|\tfrac{1}{\sqrt{2}}\big[\bar{u}(z_1^-)\gamma^+ u(z_2^-) + \bar{d}(z_1^-)\gamma^+ d(z_2^-)\big]|0\big\rangle\,. \tag{2.34}$$

$$P^+ f_{\phi} \int_0^1 \mathrm{d}v\, e^{iP.(vz_1^- + \bar{v}x_2^-)}\, \varphi_{\phi}(v) = \big\langle \phi_{\mathrm{L}}(P)|\bar{s}(z_1^-)\gamma^+ s(z_2^-)|0\big\rangle\,. \tag{2.35}$$

2.6. Polynomiality

In this section, we introduce the generic properties of the GPDs like the polynomiality in the skewness parameter η. For this purpose, we perform a Taylor expansion of the non-local

light-cone operators resulting in a tower of local operators

$$\mathcal{O}^{qq}(-z^-,z^-) = \sum_{j=0}^{\infty} \frac{1}{j!}(-iz^-)^j n^{\mu_0} n^{\mu_1} \dots n^{\mu_j} \mathcal{R}^{2,qq}_{\mu_0\mu_1\dots\mu_j}\,, \tag{2.36}$$

$$\mathcal{O}^{gg}(-z^-,z^-) = \sum_{j=0}^{\infty} \frac{1}{j!}(-iz^-)^j n^{\mu_0} n^{\mu_1} \dots n^{\mu_{j+1}} \mathcal{R}^{2,gg}_{\mu_0\mu_1\dots\mu_{j+1}}\,, \tag{2.37}$$

in terms of the twist-2 local operators

$$\mathcal{R}^{2,qq}_{\mu_0\mu_1\dots\mu_j} = \underset{\mu_0\mu_1\dots\mu_j}{\mathbf{S}} \bar{\psi}\gamma_{\mu_0} i\overset{\leftrightarrow}{D}_{\mu_1} \dots i\overset{\leftrightarrow}{D}_{\mu_j}\psi\,, \tag{2.38}$$

$$\mathcal{R}^{2,gg}_{\mu_0\mu_1\dots\mu_j} = \underset{\mu_0\mu_1\dots\mu_j}{\mathbf{S}} F_{\mu_0\nu} i\overset{\leftrightarrow}{D}_{\mu_1} \dots i\overset{\leftrightarrow}{D}_{\mu_{j-1}} F^{\nu}{}_{\mu_j}\,, \tag{2.39}$$

where $\mathbf{S}$ is the operator of symmetrization and trace subtraction, that projects out the leading twist contribution. The covariant left-right derivative is defined as

$$\overset{\leftrightarrow}{D}_\mu = \vec{D}_\mu - \overset{\leftarrow}{D}_\mu\,. \tag{2.40}$$

Let us in the following consider the parametrization of the matrix elements.

2.6.1. Parton distribution functions

For instructive purposes, we start by discussing the Mellin moments of PDFs. Sandwiching the vector operator in (2.1) between two equal proton states as in the definition of the quark PDF (2.22) leads to

$$\langle \mathrm{P}|\mathcal{O}^{qq}(-z^-,z^-)|\mathrm{P}\rangle = \sum_{j=0}^{\infty} \frac{(-iz^-)^j}{j!} n^{\mu_0} n^{\mu_1} \dots n^{\mu_j} \langle \mathrm{P}|\mathcal{R}^{2,qq}_{\mu_0\mu_1\dots\mu_j}|\mathrm{P}\rangle\,. \tag{2.41}$$

For example in case of $j = 0$, we obtain

$$\langle \mathrm{P}|\mathcal{O}^{qq}(-z,z)|\mathrm{P}\rangle = n^{\mu_0}\langle \mathrm{P}|\mathcal{R}_{\mu_0}|\mathrm{P}\rangle\,. \tag{2.42}$$

The parametrization of the matrix element of the completely symmetrized and traceless operators (2.36) yields

$$\langle \mathrm{P}|\mathcal{R}^{2,qq}_{\mu_0\mu_1\dots\mu_j}|\mathrm{P}\rangle = \underset{\mu_0\mu_1\dots\mu_j}{\mathbf{S}} 2P_{\mu_0} 2P_{\mu_1} \dots 2P_{\mu_j} f_j^q\,. \tag{2.43}$$

in terms of the moments f_j^q, since the only available momentum is the nucleon momentum P. Let us recall the definition of the quark PDF (2.22):

$$\langle \mathrm{P}|\mathcal{O}^{qq}(-z^-,z^-)|\mathrm{P}\rangle = 2P_+ \int_{-1}^{1} \mathrm{d}x\; e^{-ix2P.z} f^q(x)\,.$$

Expanding both sides with respect to z^-, we obtain:

$$f_j^q = \int_{-1}^{1} \mathrm{d}x\, x^j f^q(x), \tag{2.44}$$

where the coefficients f_j^q are denoted as Mellin moments, with $j = 0, 1, 2, 3, \ldots$. For gluons, expressing the matrix element of the corresponding operator in (2.2) by the matrix element of (2.36) leads to

$$\langle \mathrm{P}|\mathcal{O}^{gg}(-z^-, z^-)|\mathrm{P}\rangle = \sum_{j=0}^{\infty} \frac{(-iz^-)^j}{j!} n^{\mu_0} n^{\mu_1} \ldots n^{\mu_{j+1}} \langle \mathrm{P}|\mathcal{R}^{2,gg}_{\mu_0\mu_1\ldots\mu_{j+1}}|\mathrm{P}\rangle\,. \tag{2.45}$$

The parametrization involves the reduced matrix elements f^{G}. We have

$$\langle \mathrm{P}|\mathcal{R}^{2,gg}_{\mu_0\mu_1\ldots\mu_j}|\mathrm{P}\rangle = \frac{1}{2} \underset{\mu_0\mu_1\ldots\mu_j}{\mathbf{S}} 2P_{\mu_0} 2P_{\mu_1} \ldots 2P_{\mu_j} f_j^{\mathrm{G}}\,. \tag{2.46}$$

As in the previous case, we recall the definition of the gluon PDF (2.23)

$$\langle \mathrm{P}|\mathcal{O}^{gg}(-z^-, z^-)|\mathrm{P}\rangle = \left(P^+\right)^2 \int_{-1}^{1} \mathrm{d}x\, e^{-ix2P.z} f^{\mathrm{G}}(x)\,.$$

Taylor expanding both sides with respect to z^- leads to

$$f_j^{\mathrm{G}} = \int_{-1}^{1} \mathrm{d}x\, x^{j-1} f^{\mathrm{G}}(x)\,, \tag{2.47}$$

with $j = 2, 4, 6, \ldots$ [1], due to the symmetry of the gluon PDF.

2.6.2. Generalized parton distributions

The nucleon matrix elements of twist-2 quark operators sandwiched between two different nucleon states are parametrized in terms of form factors in the following way

$$\begin{aligned}\langle \mathrm{P}_2|\mathcal{R}^{2,qq}_{\mu_0\mu_1\ldots\mu_j}|\mathrm{P}_1\rangle = &\underset{\mu_0\mu_1\ldots\mu_j}{\mathbf{S}} h_{\mu_0} \left[P_{\mu_1}\ldots P_{\mu_j} H^q_{j,0}\left(\Delta^2\right) + \cdots + \Delta_{\mu_1}\ldots\Delta_{\mu_j} H^q_{j,j}\left(\Delta^2\right)\right] \\ &+ \underset{\mu_0\mu_1\ldots\mu_j}{\mathbf{S}} e_{\mu_0} \left[P_{\mu_1}\ldots P_{\mu_j} E^q_{j,0}\left(\Delta^2\right) + \cdots + \Delta_{\mu_1}\ldots\Delta_{\mu_j} E^q_{j,j}\left(\Delta^2\right)\right] \\ &+ \underset{\mu_0\mu_1\ldots\mu_j}{\mathbf{S}} \frac{b}{2m_{\mathrm{N}}} \Delta_{\mu_0}\ldots\Delta_{\mu_j} D^q_j\left(\Delta^2\right)\,,\end{aligned} \tag{2.48}$$

where in contrast to the previous case also the difference of the two nucleon momenta appears. The reduced matrix elements H^q, E^q and D^q can be expressed by moments of the parity-even quark GPDs. Utilizing the relation $\Delta_+ = \eta P_+$ leads to [MRG+94, Ji97b, Rad97]

$$\begin{aligned}H^q_j(\eta, \Delta^2) &= \sum_{k=0}^{j} \eta^k H^q_{j,k}\left(\Delta^2\right) + \eta^{j+1} D^q_j\left(\Delta^2\right) = \int_{-1}^{1} \mathrm{d}x\, x^j H^q\left(x, \eta, \Delta^2\right)\,, \\ E^q_j(\eta, \Delta^2) &= \sum_{k=0}^{j} \eta^k E^q_{j,k}\left(\Delta^2\right) - \eta^{j+1} D^q_j\left(\Delta^2\right) = \int_{-1}^{1} \mathrm{d}x\, x^j E^q\left(x, \eta, \Delta^2\right)\,.\end{aligned} \tag{2.49}$$

[1] In the literature, it is also common to define the Mellin moments as $j \geq 1$.

For gluon GPDs, the parametrization involves the form factors H^{G}, E^{G}, D^{G}:

$$\begin{aligned}\left\langle \mathrm{P}_2|\mathcal{R}^{2,gg}_{\mu_0\mu_1\cdots\mu_j}|\mathrm{P}_1\right\rangle = &\frac{1}{2}\underset{\mu_0\mu_1\ldots\mu_j}{\mathbf{S}} h_{\mu_0}\left[P_{\mu_1}\ldots P_{\mu_{j-1}}H^{\mathrm{G}}_{j,0}\left(\Delta^2\right)+\ldots+\Delta_{\mu_1}\ldots\Delta_{\mu_{j-1}}H^{\mathrm{G}}_{j,j-1}\left(\Delta^2\right)\right]P_{\mu_j}\\ &+\frac{1}{2}\underset{\mu_0\mu_1\ldots\mu_j}{\mathbf{S}} e_{\mu_0}\left[P_{\mu_1}\ldots P_{\mu_{j-1}}E^{\mathrm{G}}_{j,0}\left(\Delta^2\right)+\ldots+\Delta_{\mu_1}\ldots\Delta_{\mu_{j-1}}E^{\mathrm{G}}_{j,j-1}\left(\Delta^2\right)\right]P_{\mu_j}\\ &+\frac{1}{2}\underset{\mu_0\mu_1\ldots\mu_j}{\mathbf{S}}\frac{b}{2m_{\mathrm{N}}}\Delta_{\mu_0}\ldots\Delta_{\mu_j}D^{\mathrm{G}}_j\left(\Delta^2\right)\,. \end{aligned} \tag{2.50}$$

Whereas the relations to the Mellin moments of the gluon GPDs are given by

$$\begin{aligned}H^g_j\left(\eta,\Delta^2\right) &= \sum_{k=0}^{j-1}\eta^k H^g_{j,k}\left(\Delta^2\right)+\eta^{j+1}D^g_j\left(\Delta^2\right) = \int_{-1}^{1}\mathrm{d}x\; x^{j-1}H^g\left(x,\eta,\Delta^2\right)\,,\\ E^g_j\left(\eta,\Delta^2\right) &= \sum_{k=0}^{j-1}\eta^k E^g_{j,k}\left(\Delta^2\right)-\eta^{j+1}D^g_j\left(\Delta^2\right) = \int_{-1}^{1}\mathrm{d}x\; x^{j-1}E^g\left(x,\eta,\Delta^2\right)\,. \end{aligned} \tag{2.51}$$

The quark GPD does not possess a definite symmetry under the transformation $x\to -x$. On the other hand, the gluon GPDs do. Due to the fact, that gluons are their own antiparticles, we have the following symmetries:

$$\begin{aligned}F^{\mathrm{G}}\left(-x,\eta,\Delta^2\right) &= \;\;F^{\mathrm{G}}\left(x,\eta,\Delta^2\right)\,, \qquad F\in\{H,E\}\,,\\ F^{\mathrm{G}}\left(-x,\eta,\Delta^2\right) &= -F^{\mathrm{G}}\left(x,\eta,\Delta^2\right)\,, \qquad F\in\{\widetilde{H},\widetilde{E}\}\,. \end{aligned} \tag{2.52}$$

Utilizing the signature σ, the relations above can be written as:

$$F^{\mathrm{G}}\left(-x,\eta,\Delta^2\right) = \sigma F^{\mathrm{G}}\left(x,\eta,\Delta^2\right) \qquad \forall F\in\{H,E\}:\sigma=+1 \qquad \forall F\in\{\widetilde{H},\widetilde{E}\}:\sigma=-1\,. \tag{2.53}$$

2.7. GPD decomposition

In order to separate quark degrees and gluonic ones in the cleanest manner we change from a quark/gluon basis to group theoretical irreducible SU(N_{f}) multiplets, which consist of the flavor non-singlet (NS) multiplets (F^3, F^8, …, $F^{N_{\mathrm{f}}^2-1}$) and the flavor singlet (S) one (F^0). Utilizing this decomposition, we solve the quark-gluon mixing appearing in the perturbatively predicted evolution. The group theoretical decomposition of quark GPDs for $N_{\mathrm{f}}=4$[2] reads

$$\begin{aligned}F^0 &= F^u+F^d+F^s+F^c\,,\\ F^3 &= F^u-F^d\,,\\ F^8 &= F^u+F^d-2F^s\,,\\ F^{15} &= F^u+F^d+F^s-3F^c\,. \end{aligned} \tag{2.54}$$

[2]The derivation of the case $N_{\mathrm{f}}=3$ is straight forward and is presented in [MLPKS14].

Consequently, expressing GPDs in the quark/gluon basis by the SU(N_f) multiplets leads to

$$\begin{aligned} F^u &= \tfrac{1}{4}F^0 + \tfrac{1}{2}F^3 + \tfrac{1}{6}F^8 + \tfrac{1}{12}F^{15}\,, \\ F^d &= \tfrac{1}{4}F^0 - \tfrac{1}{2}F^3 + \tfrac{1}{6}F^8 + \tfrac{1}{12}F^{15}\,, \\ F^s &= \tfrac{1}{4}F^0 - \tfrac{1}{3}F^8 + \tfrac{1}{12}F^{15}\,, \\ F^c &= \tfrac{1}{4}F^0 - \tfrac{1}{4}F^{15}\,. \end{aligned} \tag{2.55}$$

This decomposition holds for the parity even as well as for the parity odd sector (Sec. 2.3). However, since a gluon has charge parity even the decomposition is not necessary in the parity odd sector, since no mixing occurs. In the analysis of hard exclusive processes we will deal with a definite flavor combination of GPDs. A arbitrary sum of GPDs in the quark/gluon basis can be rewritten as

$$\begin{aligned} F &= \hat{c}^u F^u + \hat{c}^d F^d + \hat{c}^s F^s + \hat{c}^c F^c \\ &= \hat{c}^0 F^0 + \hat{c}^3 F^3 + \hat{c}^8 F^8 + \hat{c}^{15} F^{15}\,, \end{aligned} \tag{2.56}$$

where $\hat{c}$ are the corresponding coefficients. The coefficients of the SU(N_f) multiplets read

$$\begin{aligned} \hat{c}^0 &= \tfrac{1}{4}\left(\hat{c}^u + \hat{c}^d + \hat{c}^s + \hat{c}^c\right)\,, \\ \hat{c}^3 &= \tfrac{1}{2}\left(\hat{c}^u - \hat{c}^d\right)\,, \\ \hat{c}^8 &= \tfrac{1}{6}\left(\hat{c}^u + \hat{c}^d - 2\hat{c}^s\right)\,, \\ \hat{c}^{15} &= \tfrac{1}{12}\left(\hat{c}^u + \hat{c}^d + \hat{c}^s - 3\hat{c}^c\right)\,. \end{aligned} \tag{2.57}$$

Since only the singlet part F^0 mixes with the gluon contribution under evolution, all remaining contributions are summed in the non-singlet contribution:

$$\begin{aligned} \hat{c}^3 F^3 + \hat{c}^8 F^8 + \hat{c}^{15} F^{15} = {} & \tfrac{1}{4}\Big(3\hat{c}^u - \hat{c}^d - \hat{c}^s - \hat{c}^c\Big) F^u + \tfrac{1}{4}\Big(-\hat{c}^u + 3\hat{c}^d - \hat{c}^s - \hat{c}^c\Big) F^d \\ & + \tfrac{1}{4}\Big(-\hat{c}^u - \hat{c}^d + 3\hat{c}^s - \hat{c}^c\Big) F^s + \tfrac{1}{4}\Big(-\hat{c}^u - \hat{c}^d - \hat{c}^s + 3\hat{c}^c\Big) F^c\,. \end{aligned} \tag{2.58}$$

3
Phenomenology

3.1. Deeply inelastic scattering

Deeply inelastic scattering is phenomenologically one of the most important hard processes. A lepton interacts with the nucleon via a virtual photon, with the nucleon fragmenting into a number of hadrons X. In this work, we focus on the scattering of an electron on a proton target. Schematically, the reaction is

$$e^-(k_1) + N(P) \to e^-(k_2) + X(R)\,, \tag{3.1}$$

and it is depicted in figure 3.1.

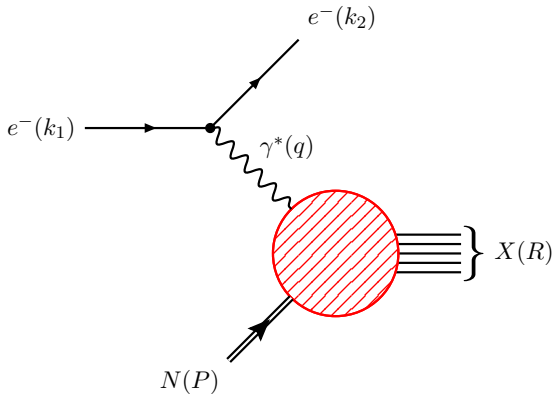

Figure 3.1.: Deeply inelastic scattering. An electron with momentum k_1 is scattered off a nucleon with momentum P. The interaction takes place via a virtual photon with momentum q. In the final state, only the momentum k_2 of the scattered electron is observed.

In this section, we derive the DIS cross section in terms of the structure functions F_1 and F_2 utilizing the parton model and a rigorous field theoretical treatment.

3.1.1. Kinematics

The incoming and outgoing electrons have four-momenta k_1 and k_2, respectively. Furthermore, the nucleon momenta is denoted by P and the combined momentum of all hadrons in

the final state is R. In order to work out the kinematics, we choose the laboratory frame, where the nucleon target is at rest and the leptons only move in the x-z-plane. The coordinate system is rotated in such a way, that the momentum of the virtual photon $q=k_1-k_2$ points along the negative z-axes, see Fig. 3.2. Consequently, the four-momenta of all relevant

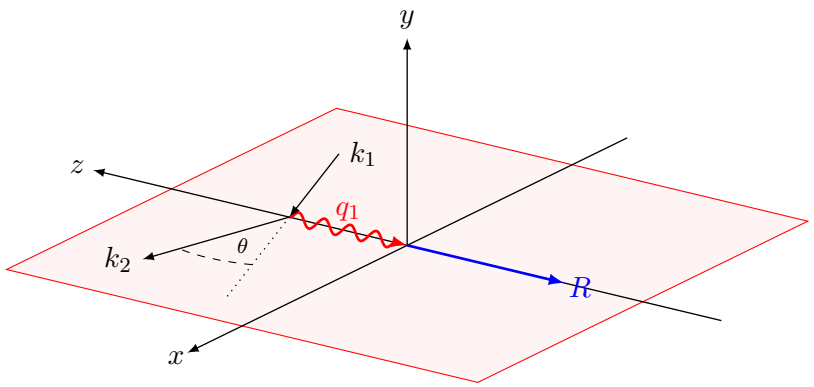

Figure 3.2.: Deeply inelastic scattering in the laboratory frame. The leptons move only in the x-z-plane. The coordinate system is rotated in such a way, that the momentum of the virtual photon $q=k_1-k_2$ points along the negative z-axes.

particles in this frame are given by

$$\begin{aligned} P^\mu &= (M,0,0,0)\,, & k_1^\mu &= (\omega_1, k_1^x, 0, k_1^z)\,, \\ q^\mu &= (\nu,0,0,-q^z)\,, & k_2^\mu &= (\omega_2, k_2^x, 0, k_2^z)\,. \end{aligned} \tag{3.2}$$

In the process, we have two particles in the final state. All recoiling hadrons remain unobserved. However, their total momentum R is known due to momentum conservation. Therefore, an experiment only measures the four momentum components of the scattered electron. Since its mass is small compared to momentum transfer q, it is neglected providing the condition $k_2^2=0$. The freedom in the choice of the reference frame eliminates another degree of freedom. Hence, only two components of the electron momentum remain unknown. A convenient choice is the energy of the final electron ω_2 and its scattering angle with respect to the incident beam.
For the theoretical description, we use Lorentz scalars instead. A common choice is the square of the space like momentum transfer and the Bjorken scaling variable

$$\mathcal{Q}^2 = -q^2\,, \qquad x_\mathrm{B} = \frac{\mathcal{Q}^2}{2P.q}\,. \tag{3.3}$$

In addition, common choices are the relative energy loss y or the invariant mass of the hadronic system:

$$y = \frac{P.q}{P.k_1}\,, \qquad W^2 = (P^2+q^2) = M^2 + 2P.q - \mathcal{Q}^2\,. \tag{3.4}$$

Note, for elastic scattering, we would have $W^2=M^2$. In terms of the independent components of electron momentum (ω_2,θ) and the known momentum components, cf. (3.2), the four

Lorentz scalars are given by

$$\mathcal{Q}^2 = 4\omega_1\omega_2 \sin^2(\theta/2)\,, \qquad y = \frac{\omega_1 - \omega_2}{\omega_1}\,,$$
$$x_{\mathrm{B}} = \frac{4\omega_1\omega_2 \sin^2(\theta/2)}{2M(\omega_1 - \omega_2)}\,, \qquad W^2 = M^2 + 2M(\omega_1 - \omega_2) - \mathcal{Q}^2\,, \tag{3.5}$$

where we neglected the electron mass compared to its energy. From the equation above, we see, that the Bjorken variable lies in the interval $x_{\mathrm{B}} \in [0,1]$. For elastic scattering we have $x_{\mathrm{B}} = 1$. The Mandelstam variables are given by

$$\hat{s} = (P + k_1)^2\,, \qquad \hat{t} = (k_1 - k_2)^2\,, \qquad \hat{u} = (P - k_2)^2\,. \tag{3.6}$$

The cross section is obtained as the sum over all possible final hadronic states, involving n particles and integrated over each of their respective phase space Π_n. Thus, the cross section for deeply inelastic scattering reads

$$\mathrm{d}\sigma^{ep\to eX} = \frac{1}{4M\omega_1} \frac{\mathrm{d}^3k_2}{(2\pi)^2 2\omega_2} \sum_X \int \mathrm{d}\Pi_n \, |\mathcal{M}(ep \to eX)|^2 \; (2\pi)^4 \delta^{(4)}(k_1 + P - k_2 - R)\,. \tag{3.7}$$

The invariant matrix element is given by the interacting part of the S-matrix (iT-matrix). Since the electromagnetic coupling is much smaller than the momentum transfer, we restrict our analysis to single photon exchange. The iT-matrix is proportional to the second order in the electromagnetic current:

$$\langle \mathrm{k_2 R}|iT|\mathrm{k_1 P}\rangle = * = (-ie)^2 \int \mathrm{d}^4y \int \mathrm{d}^4z \, \langle \mathrm{k_2 R}|\bar{\psi}(y) \not{A}(y) \psi(y) \cdot Q_q \bar{\psi}_q(z) \not{A}(z) \psi_q(z)|\mathrm{k_1 P}\rangle\,, \tag{3.8}$$

where we have omitted the sum over all possible quark flavors q, but always imply its presence. The quark charges are

$$Q_u = Q_c = \frac{2}{3}\,, \qquad Q_d = Q_s = -\frac{1}{3}\,. \tag{3.9}$$

Separating the leptonic interaction in the iT-matrix leads to

$$* = \bar{u}(k_2)\gamma^\mu u(k_1) \int \mathrm{d}^4y \, \mathrm{d}^4z \int \frac{\mathrm{d}^4q}{(2\pi)^4} \, e^{-iq(y-z)} e^{-i(k_1-k_2)y} \frac{ie^2}{l^2 + i\epsilon} \langle \mathrm{R}|Q_a \bar{\psi}_a(z) \gamma_\mu \psi_a(z)|\mathrm{P}\rangle\,,$$
$$* = \bar{u}(k_2)\gamma^\mu u(k_1) \int \mathrm{d}^4z \int \frac{\mathrm{d}^4q}{(2\pi)^4} \, e^{iqz} \frac{ie^2}{q^2 + i\epsilon} \langle \mathrm{R}|j_\mu(z)|\mathrm{P}\rangle \cdot (2\pi)^4 \delta^{(4)}(k_1 + q - k_2)\,, \tag{3.10}$$

where we introduced the electromagnetic current

$$j_\mu(z) = \sum_q Q_q \bar{\psi}_q(z) \gamma_\mu \psi_q(z)\,. \tag{3.11}$$

The immanent δ-function stems from a shift of the electromagnetic current to the origin leading to a factor of $e^{-i(P-R)z}$. Hence, we get rid of the integration with respect to the photon momentum q. Thus,

$$\langle \mathrm{k_2 R}|iT|\mathrm{k_1 P}\rangle = \frac{ie^2}{q^2 + i\epsilon} \bar{u}(k_2)\gamma^\mu u(k_1) \int \mathrm{d}^4z \, e^{iqz} \langle \mathrm{R}|j_\mu(z)|\mathrm{P}\rangle (2\pi)^4 \delta^{(4)}(k_1 + P - k_2 - R)\,. \tag{3.12}$$

To further simplify the expression, we introduce the leptonic current

$$L^\mu = \frac{-i}{q^2 + i\epsilon} \bar{u}(k_2)\gamma^\mu u(k_1)\,, \tag{3.13}$$

and the Fourier transform of the electromagnetic current

$$j_\mu(q) = \int \mathrm{d}^4 z\, e^{iq.z}\; j_\mu(z)\,. \tag{3.14}$$

With these abbreviations, we read off the invariant matrix element as

$$i\mathcal{M}(ep \to eX) = -4\pi\alpha_{\mathrm{em}} L^\mu \big\langle R|j_\mu(q)|P\big\rangle\,, \quad \text{with} \quad \alpha_{\mathrm{em}} = \frac{e^2}{4\pi}\,. \tag{3.15}$$

It enters the cross section (3.7) as absolute value squared:

$$|\mathcal{M}(ep \to eX)|^2 = (4\pi)^2 \alpha_{\mathrm{em}}^2 L^\mu \left(L^\nu\right)^\dagger \big\langle P|j_\nu^\dagger(q)|R\big\rangle\big\langle R|j_\mu(q)|P\big\rangle\,. \tag{3.16}$$

Conveniently, we unite the hadronic part of the cross section in the hadronic tensor

$$W_{\mu\nu}(P,q) = \frac{1}{2\pi}\sum_X \int \mathrm{d}\Pi_n \big\langle P|j_\nu^\dagger(q)|R\big\rangle\big\langle R|j_\mu(q)|P\big\rangle \cdot (2\pi)^4 \delta^{(4)}(k_1 + P - k_2 - R)\,. \tag{3.17}$$

Note, the factor of $\frac{1}{2\pi}$ is conventional and differs in the literature. Taking advantage of the unitarity of the S-matrix, the hadronic tensor is given as the imaginary part of the forward Compton tensor

$$T_{\mu\nu}(P,q) = i\int \mathrm{d}^4 z\, e^{iq.z} \big\langle \mathrm{P}|T\{j_\mu(z) j_\nu(0)\}|\mathrm{P}\big\rangle\,. \tag{3.18}$$

The relation is also known as the optical theorem (cf. Fig. 3.3), namely

$$\sum_X \int \mathrm{d}\Pi_X \big\langle P|j_\mu^\dagger(q)|R\big\rangle\big\langle R|j_\nu(q)|P\big\rangle = 2\Im\mathrm{m}\; i\int \mathrm{d}^4 z\, e^{iq.z} \big\langle \mathrm{P}|T\{j_\mu(z) j_\nu(0)\}|\mathrm{P}\big\rangle\,. \tag{3.19}$$

Hence, the relation between the hadronic tensor and the forward Compton tensor is

$$W_{\mu\nu}(P,q) = \frac{1}{\pi}\,\Im\mathrm{m}\, T_{\mu\nu}(P,q)\,, \tag{3.20}$$

Employing the hadronic tensor and the leptonic current, the cross section for deeply inelastic scattering (3.7) becomes

$$\mathrm{d}\sigma^{ep\to eX} = \frac{2\pi}{4M\omega_1} \cdot \frac{\mathrm{d}^3 k_2}{(2\pi)^2 2\omega_2} \cdot (4\pi)^2 \alpha_{\mathrm{em}}^2 L_\mu L_\nu^\dagger W^{\mu\nu}\,. \tag{3.21}$$

At this point, the leptonic part is completely separated and we shift our attention to the hadronic tensor.

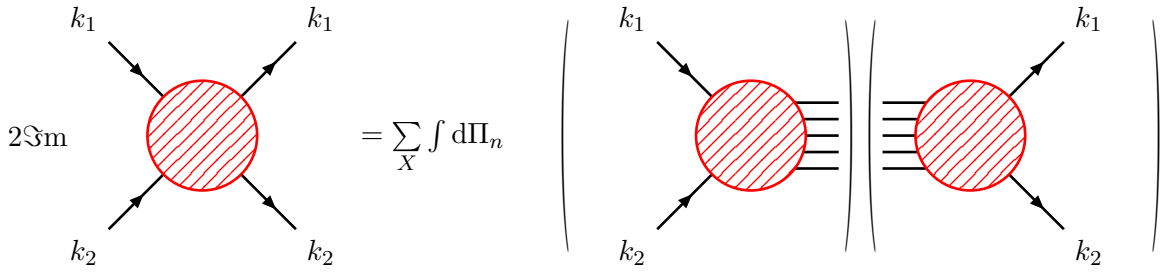

Figure 3.3.: Optical Theorem: The sum over all possible hadrons in the final state integrated over their phase space is equal to the imaginary part of the forward Compton amplitude.

It decomposes into several structure functions, which depend on the two Lorentz invariant quantities[1]. For a unpolarized spin 1/2 target, its structure is

$$\begin{aligned} W_{\mu\nu}(P,q) = {} & P_\mu P_\nu \, A\big(P.q, q^2\big) + (P_\mu q_\nu + P_\nu q_\mu) \; B\big(P.q, q^2\big) \\ & + q_\mu q_\nu \, C\big(P.q, q^2\big) + g_{\mu\nu} \, D\left(P.q, q^2\right) . \end{aligned} \tag{3.22}$$

The hadronic tensor is gauge invariant. Therefore, the corresponding Ward identity requires

$$q^\mu \, W_{\mu\nu} = W_{\mu\nu} \, q^\nu = 0 \, . \tag{3.23}$$

Imposing the conditions leads to

$$\begin{aligned} q^\mu W^{\mu\nu} &= P.q \, P^\nu A + \big(P.q \, q^\nu + P^\nu q^2\big) \, B + q^2 \, q^\nu C + q^\nu D \\ &= \big(P.q \, A + q^2 \, B\big) \, P^\nu + \big(P.q \, B + q^2 \, C + D\big) \, q^\nu \, , \end{aligned} \tag{3.24}$$

where we omitted the arguments of the structure function. Hence, we can eliminate the functions B and C. The complete decomposition for the unpolarized case is

$$W^{\mu\nu} = \left(P^\mu - \frac{P.q}{q^2} q^\nu\right) \left(P^\nu - \frac{P.q}{q^2} q^\mu\right) A\big(P.q, q^2\big) + \left(g_{\mu\nu} - \frac{q^\mu q^\nu}{q^2}\right) D\big(P.q, q^2\big) \, . \tag{3.25}$$

Conventionally, the nomenclature in the literature is

$$A\big(P.q, q^2\big) = W_2\big(P.q, q^2\big) \, , \qquad D\big(P.q, q^2\big) = -W_1\big(P.q, q^2\big) \, . \tag{3.26}$$

Using this notation, the decomposition of the hadronic tensor reads

$$W^{\mu\nu}(P,q) = \left(-g_{\mu\nu} + \frac{q^\mu q^\nu}{q^2}\right) W_1\big(P.q, q^2\big) + \left(P^\mu - q^\nu \frac{P.q}{q^2}\right) \left(P^\nu - q^\mu \frac{P.q}{q^2}\right) W_2\big(P.q, q^2\big) \, . \tag{3.27}$$

[1] We choose $P.q$ instead of x_B

To complete the consideration of the kinematics, we combine the Lorentz structure of the hadronic tensor with the leptonic currents in (3.21).
Summing over the electron polarizations, the products are

$$\frac{1}{2}\sum_s L^\mu \left(L^\nu\right)^\dagger = \frac{1}{2\mathcal{Q}^4}\mathrm{tr}(\not{k}_2\gamma^\mu \not{k}_1\gamma^\nu) = \frac{2}{\mathcal{Q}^4}(k_1^\mu k_2^\nu + k_1^\nu k_2^\mu - g^{\mu\nu}k_1.k_2)\,. \tag{3.28}$$

The contraction of the equation above with the hadronic tensor is

$$\frac{1}{2}\sum_s L^\mu (L^\nu)^\dagger W_{\mu\nu}(P,q) = \frac{2}{\mathcal{Q}^4}\left[2k_1.k_2\ W_1 + 2P.k_1 P.k_2\ W_2\right]\,. \tag{3.29}$$

For the cross section, we still have to express all products of particle momenta by the energy and the scattering angle of the outgoing electron.
In terms of the particle momenta defined in (3.2), the vector products in the equation above read

$$\begin{aligned} 2k_1.k_2 &= 2\omega_1\omega_2(1-\cos\theta) = 4\omega_1\omega_2\sin^2(\theta/2)\,,\\ 2P.k_1 P.k_2 &= 2M^2\omega_1\omega_2\,. \end{aligned} \tag{3.30}$$

Expressing the phase space in terms of the same variables, we get

$$\frac{\mathrm{d}^3k_2}{(2\pi)^3 2\omega_2} = \frac{|\vec{k}_2|^2\mathrm{d}|\vec{k}_2|\mathrm{d}(\cos\theta)2\pi}{(2\pi)^3 2\omega_2} = \frac{\omega_2\mathrm{d}\omega_2\mathrm{d}(\cos\theta)}{2(2\pi)^2}\,. \tag{3.31}$$

Thus, the unpolarized cross section becomes

$$\frac{\mathrm{d}\sigma^{ep\to eX}}{\mathrm{d}\omega_2\mathrm{d}(\cos\theta)} = \frac{8\pi\alpha_{\mathrm{em}}^2}{\mathcal{Q}^4}\omega_2^2\left[\frac{\sin^2(\theta/2)}{M}\ W_1 + \frac{M}{2}\ W_2\right]\,. \tag{3.32}$$

It is preferable to express the cross section in terms of two of the Lorentz scalars x_{B}, $\mathcal{Q}^2$ (3.3), y and W^2 (3.4). We introduce the two choices

$$x_{\mathrm{B}} \wedge \left(y \vee \mathcal{Q}^2\right)\,. \tag{3.33}$$

For the first choice (x_{B}, y), we express the relative energy loss in terms of the Mandelstam variable $\hat{s}$, namely

$$\hat{s} = (P+k_1)^2 = M^2 + 2P.k_1 = M^2 + 2M\omega_1 \approx 2M\omega_1 = 2P.k_1\,, \tag{3.34}$$

$$y = \frac{P.q}{P.k_1} = \frac{\mathcal{Q}^2}{2x_{\mathrm{B}}P.k_1} \approx \frac{\mathcal{Q}^2}{\hat{s}x_{\mathrm{B}}}\,, \qquad \bar{y} = 1-y\,. \tag{3.35}$$

From (3.5), we obtain the determinant of the Jakobian matrix of the variable transformation

$$\left|\frac{\partial(x_{\mathrm{B}},y)}{\partial(\omega_2,\cos\theta)}\right| = \frac{2\omega_2}{y2M\omega_1}\,. \tag{3.36}$$

After the transformation, the cross sections in terms of the Lorentz scalars reads

$$\frac{\mathrm{d}\sigma^{ep\to eX}}{\mathrm{d}x_{\mathrm{B}}\mathrm{d}y} = \frac{2\pi\alpha_{\mathrm{em}}^2}{\mathcal{Q}^4}\frac{\hat{s}}{2}\left[2x_{\mathrm{B}}y^2\ W_1 + sy\bar{y}\ W_2\right]\,. \tag{3.37}$$

As stated before, instead of the variable y one also uses the momentum transfer $\mathcal{Q}^2 = x_\mathrm{B} y \hat{s}$. The cross section turns into

$$\frac{\mathrm{d}\sigma^{ep\to eX}}{\mathrm{d}x_\mathrm{B}\mathrm{d}\mathcal{Q}^2} = \frac{2\pi\alpha_\mathrm{em}^2}{\mathcal{Q}^4}\frac{1}{2x_\mathrm{B}}\left[2x_\mathrm{B}y^2\, W_1 + \hat{s}y\bar{y}\, W_2\right] . \tag{3.38}$$

As shown in [Bjo69], we can replace the structure functions W_1 and W_2 by dimensionless structure functions

$$W_1\big(P.q, \mathcal{Q}^2\big) = F_1\big(P.q, \mathcal{Q}^2\big) , \qquad P.q\, W_2\big(P.q, \mathcal{Q}^2\big) = F_2\big(x_\mathrm{B}, \mathcal{Q}^2\big) , \tag{3.39}$$

where we also write $P.q = M\nu = y\hat{s}/2$. The purpose of this replacement becomes obvious in the next section. Thus, the final form of the DIS cross section is

$$\frac{\mathrm{d}\sigma^{ep\to eX}}{\mathrm{d}x_\mathrm{B}\mathrm{d}y} = \frac{2\pi\alpha_\mathrm{em}^2}{\mathcal{Q}^4}\frac{\hat{s}}{2}\left[2x_\mathrm{B}y^2\, F_1\big(x_\mathrm{B}, \mathcal{Q}^2\big) + 2\bar{y}\, F_2\big(x_\mathrm{B}, \mathcal{Q}^2\big)\right] . \tag{3.40}$$

3.1.2. Parton model

The basic hypothesis of the parton model [Fey69] is, that at a large energy and momentum transfer by the virtual photon to the nucleon, the interaction of the virtual photon and the nucleon can be described by an incoherent sum of interactions between the electron and the partons. The interpretation of the scattering process simplifies drastically in the infinite momentum frame, in which the nucleon moves along the z-axes with a large (infinite) momentum.
Due to the Lorentz contraction in the z-direction, the nucleon is deformed to a disk. Consequently, the momenta p of the partons can be written as the momentum fraction x of the total nucleon momentum and a component transverse to the z-axes:

$$p = xP + p_\perp . \tag{3.41}$$

For now, we will neglect the transverse momentum $p_\perp$.
Since the time scale of the interaction is of the order $(\mathcal{Q}^2)^{-1/2}$, at a sufficiently high momentum transfer, this time scale is much less than the typical time scale of the electromagnetic interaction among the partons. Therefore, the virtual photon only interacts with one of the partons. However, the partons always interact through strong interactions. This is neglected by the naive parton model. The field theoretical treatment is outlined in Sec. 3.1.3.
Final-state interactions cause the quarks to reform into the nucleon. These interactions occur at time scales, which are too long to interfere with the hard photon scattering.
The probability for a parton to have the momentum fraction x, $0 \leq x \leq 1$, is given by the function $q(x)$. These functions are called parton distribution functions (PDFs) and they are in fact probability distribution functions (pdfs) in the sense of chapter 5. Under the assumption of elastic electron-quark scattering and the neglect of the small parton mass in comparison to the momentum transfer $\mathcal{Q}^2$, we have

$$0 \approx (p+q)^2 \approx 2xP.q - \mathcal{Q}^2 . \tag{3.42}$$

Thus, the longitudinal momentum fraction is equal to the Bjorken scaling variable (3.3)

$$x = \frac{\mathcal{Q}^2}{2P.q} = x_{\mathrm{B}}\,. \tag{3.43}$$

Consequently, in the infinite momentum frame, the parton has the momentum fraction $x = x_{\mathrm{B}}$ in order to absorb the virtual photon.
With the picture above, the forward Compton scattering tensor (3.18) is given by

$$T^{\mu\nu} = i \int \mathrm{d}^4 z\, e^{iq.z} \sum_q \int_0^1 \frac{\mathrm{d}x}{x}\, q(x) \left\langle \mathrm{p}|T\{j_\mu(z) j_\nu(0)\}|\mathrm{p}\right\rangle \Big|_{p=xP}, \quad \text{with } q = \{u, d, \dots\}\,. \tag{3.44}$$

Note, the factor $1/x$ takes into account the different flux factors of electron-nucleon and electron-parton scattering. Furthermore, the square of the electron-parton center of mass energy is given as the electron-proton one as

$$\tilde{s} = (p + k_1)^2 = 2p.k_1 = 2xP.k_1 = x\hat{s}\,. \tag{3.45}$$

The evaluation of the amplitude for parton electron scattering in LO of perturbation theory is a straight forward task. We display the corresponding Feynman diagrams in figure 3.4. Using the quark propagator in coordinate space (A.2) the time ordered product of the two

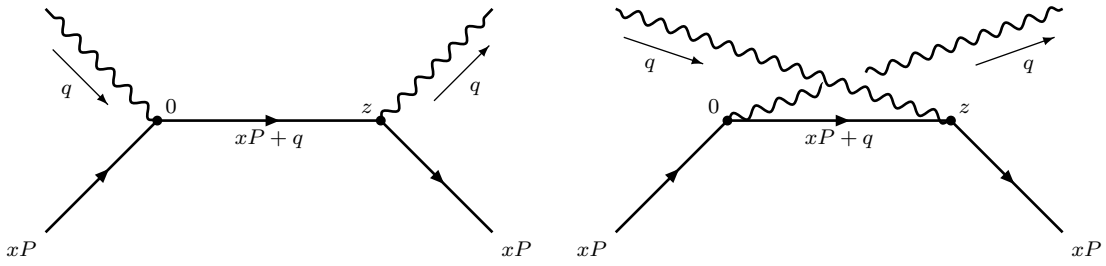

Figure 3.4.: Feynman diagrams for elastic photon-parton scattering at LO.

electromagnetic currents yields

$$iT\{j_\mu(\tfrac{z}{2})\, j_\nu(-\tfrac{z}{2})\} = i \sum_q Q_q^2 \left\{\bar{\psi}_q(\tfrac{z}{2})\, \gamma_\mu \not{p}(z) \gamma_\nu \psi_q(-\tfrac{z}{2}) + \bar{\psi}_q(-\tfrac{z}{2})\, \gamma_\nu \not{p}(-z) \gamma_\mu \psi_q(\tfrac{z}{2})\right\}. \tag{3.46}$$

Note, we shifted the arguments of the electromagnetic currents by $-z/2$. Making use of the Chisholm identity

$$\gamma_\mu\gamma_\alpha\gamma_\nu = (g_{\mu\alpha}g_{\nu\beta} - g_{\mu\nu}g_{\alpha\beta} + g_{\mu\beta}g_{\nu\alpha} + i\epsilon_{\mu\alpha\nu\beta}\gamma_5)\,\gamma^\beta = (s_{\mu\alpha\nu\beta} + i\epsilon_{\mu\alpha\nu\beta}\gamma_5)\,\gamma^\beta\,, \tag{3.47}$$

and neglecting the structure proportional to the totally antisymmetric tensor which only contributes in case of a polarized nucleon target, we get

$$iT\{j_\mu(\tfrac{z}{2})\, j_\nu(-\tfrac{z}{2})\} = \sum_q Q_q^2 \frac{1}{2\pi^2} \frac{s_{\mu\alpha\nu\beta} z^\alpha}{(z^2 - i\epsilon)^2} \left\{-\bar{\psi}_q(\tfrac{z}{2})\, \gamma_\beta \psi_q(-\tfrac{z}{2}) + \bar{\psi}_q(-\tfrac{z}{2})\, \gamma_\beta \psi_q(\tfrac{z}{2})\right\}. \tag{3.48}$$

Plugging the expression into the forward Compton tensor leads to

$$T^{\mu\nu} = -\int \mathrm{d}^4 z\, e^{iqz} \sum_q Q_q^2 \int_0^1 \frac{\mathrm{d}x}{x}\, q(x)\, \frac{1}{2\pi^2} \frac{s_{\mu\alpha\nu\beta} z^\alpha}{(z^2 - i\epsilon)^2} \left[e^{ipz} \bar{u}(p) \gamma_\beta u(p) - \{p \leftrightarrow -p\} \right] \Big|_{p=xP} . \tag{3.49}$$

Now we can perform the integration with respect to the coordinate z, namely

$$T^{\mu\nu} = \sum_q Q_q^2 \int_0^1 \frac{\mathrm{d}x}{x}\, q(x)\, s_{\mu\alpha\nu\beta} \left[\frac{2(p+q)^\alpha p^\beta}{-(p+q)^2 - i\epsilon} + \{p \leftrightarrow -p\} \right] \Big|_{p=xP} . \tag{3.50}$$

Reformulating the denominator, while neglecting the parton masses we obtain

$$-(p \pm q)^2 - i\epsilon = \mp 2xP.q + \mathcal{Q}^2 - i\epsilon = 2P.q\, x_\mathrm{B} \mp x - i\epsilon\,. \tag{3.51}$$

Therefore, the forward Compton amplitude in the LO approximation reads

$$T^{\mu\nu} = \frac{1}{P.q} \sum_q Q_q^2 \int_0^1 \mathrm{d}x\, q(x)\, s_{\mu\alpha\nu\beta} P^\beta \left[\frac{(q + xP)^\alpha}{x_\mathrm{B} - x - i\epsilon} + \frac{(q - xP)^\alpha}{x_\mathrm{B} + x - i\epsilon} \right] . \tag{3.52}$$

As mentioned before, the hadronic tensor of DIS is given as the imaginary part of the forward Compton scattering amplitude. Since the parton distribution function $q(x)$ is real valued, the only source for an imaginary part is the hard scattering amplitude. Hence,

$$\Im\mathrm{m} \frac{1}{x_\mathrm{B} \pm x - i\epsilon} = \pi \delta(x \pm x_\mathrm{B})\,. \tag{3.53}$$

Note, that the second diagram has no contribution in the physical region of DIS, since the momentum fraction x and also the Bjorken variable x_B are positive. Therefore, the result is resolving the Lorentz structure

$$\begin{aligned} W^{\mu\nu} &= \frac{1}{\pi} \Im\mathrm{m}\, T^{\mu\nu} = \frac{1}{P.q} \sum_q Q_q^2 q(x_\mathrm{B})\, s_{\mu\alpha\nu\beta} P^\beta\, (q + x_\mathrm{B} P)^\alpha \\ &= \left[\frac{2x_\mathrm{B}}{P.q} \left(P^\mu + \frac{q^\mu}{2x_\mathrm{B}} \right) \left(P^\nu + \frac{q^\nu}{2x_\mathrm{B}} \right) + \left(-g_{\mu\nu} + \frac{q^\mu q^\nu}{q^2} \right) \right] \sum_q\, Q_q^2 q(x_\mathrm{B})\,. \end{aligned} \tag{3.54}$$

From the comparison of the equation above with the general structure of the hadronic tensor (3.27) with the dimensional structure functions F_1 and F_2 (cf. Eq. 3.39) we obtain

$$F_1\big(x_\mathrm{B}, \mathcal{Q}^2\big) = \sum_q Q_q^2\, q(x_\mathrm{B}) \qquad F_2\big(x_\mathrm{B}, \mathcal{Q}^2\big) = 2x_\mathrm{B} \sum_q\, Q_q^2\, q(x_\mathrm{B})\,. \tag{3.55}$$

This result is the Callan-Gross relation [CG69]

$$F_2(x_\mathrm{B}) = 2x_\mathrm{B} F_1(x_\mathrm{B})\,, \tag{3.56}$$

which predicted, that partons are indeed spin 1/2 particles.
The parton model provides an intuitive picture of DIS and Bjorken scaling. However, this can not be a replacement of a rigorous treatment within a field theory.

3.1.3. Field theoretical treatment

The analysis in this section will look very similar to the parton model. However, in contrast to the parton model, we are able to calculate corrections to the given picture. To do so, we calculate the forward Compton scattering amplitude (3.18) in the leading order approximation in the strong coupling using the matrix elements defined in chapter 2. Shifting the coordinates leads to

$$T^{\mu\nu} = i \int \mathrm{d}^4 z \; e^{iq.z} \left\langle \mathrm{P} | T\{ j^\mu(\tfrac{z}{2}) \, j^\nu(-\tfrac{z}{2}) \} \, | \mathrm{P} \right\rangle .$$

At leading order, we have the same Feynman diagrams as before in figure 3.4. Thus, the time ordered product of the two electromagnetic currents is the same as in (3.48). We recall

$$iT\{ j_\mu(\tfrac{z}{2}) \, j_\nu(-\tfrac{z}{2}) \} = \sum_q Q_q^2 \frac{1}{2\pi^2} \frac{s_{\mu\alpha\nu\beta} z^\alpha}{(z^2 - i\epsilon)^2} \left\{ -\bar{\psi}_q(\tfrac{z}{2}) \, \gamma^\beta \psi_q(-\tfrac{z}{2}) + \bar{\psi}_q(-\tfrac{z}{2}) \, \gamma^\beta \psi_q(\tfrac{z}{2}) \right\} .$$

The corresponding unpolarized twist-2 quark PDFs (2.22) are defined as

$$\left\langle \mathrm{P} | \bar{\psi}_a(-z) \gamma^\beta \psi_a(z) | \mathrm{P} \right\rangle = \int_{-1}^{1} \mathrm{d}x \, e^{-ix2P.z} \; h^\beta \, f^q(x) . \tag{3.57}$$

We remind ourselves, that in order to pick up the leading twist contribution, a contraction of the open Lorentz index with the light-like vector n is required. Consequently, we obtain for the amplitude

$$T_{\mu\nu} = \sum_q Q_q^2 \int \mathrm{d}^4 z \, e^{iq.z} \, \frac{s_{\mu\alpha\nu\beta} z^\alpha}{2\pi^2 \, (z^2 - i\epsilon)^2} \int_{-1}^{1} \mathrm{d}x \, \left(e^{-ixP.z} - e^{ixP.z} \right) h^\beta f^q(x) . \tag{3.58}$$

The integration with respect to z is

$$\int \mathrm{d}^4 z \; e^{i(q \pm xP.z)} \, \frac{z^\alpha}{2\pi^2 \, (z^2 - i\epsilon)^2} = \frac{q^\alpha \pm xP.z}{(q \pm xP.z)^2 + i\epsilon} . \tag{3.59}$$

The denominator simplifies to

$$(q \pm xP)^2 = 2P.q \left(\frac{q^2}{2P.q} \pm x + \frac{x^2 P^2}{2P.q} \right) = 2P.q \left(-x_\mathrm{B} \pm x + \frac{x^2 P^2}{2P.q} \right) , \tag{3.60}$$

where the parton masses are neglected in comparison to the momentum transfer. Therefore, the forward Compton tensor reads

$$T_{\mu\nu} = \frac{1}{2P.q} \int_{-1}^{1} \mathrm{d}x \; s_{\mu\alpha\nu\beta} h^\beta \left(\frac{q^\alpha + xP^\alpha}{x_\mathrm{B} - x - i\epsilon} - \frac{q^\alpha - xP^\alpha}{x_\mathrm{B} + x - i\epsilon} \right) \sum_q Q_q^2 \, f^q(x) . \tag{3.61}$$

For the hadronic tensor $W_{\mu\nu}$, we only need to pick up the imaginary part

$$\Im\mathrm{m} \frac{1}{x_\mathrm{B} \pm x - i\epsilon} = \pi \delta(x_\mathrm{B} \pm x) . \tag{3.62}$$

Note that, in this case, the second Feynman diagram does contribute, since the definition of $f^q(x)$ contains quarks and anti-quarks, whereas $q(x)$ was defined only for quarks. Thus, we obtain

$$W^{\mu\nu} = \frac{1}{\pi} T^{\mu\nu} = \frac{1}{2P.q}\, s_{\mu\alpha\nu\beta} h^\beta \left(q^\alpha + x_\mathrm{B} P^\alpha\right) \sum_q Q_q^2 \left[f^q(x_\mathrm{B}) - f^q(-x_\mathrm{B})\right] . \tag{3.63}$$

Since the nucleon spinors are normalized by $\bar{U}(P)\gamma^\beta U(P) = 2P^\beta$, the Lorentz structure collapses to

$$s_{\mu\alpha\nu\beta}(q + x_\mathrm{B} P)^\alpha P^\beta = 2x_\mathrm{B} \left(P_\mu + \frac{q_\mu}{2x_\mathrm{B}}\right)\left(P_\nu + \frac{q_\nu}{2x_\mathrm{B}}\right) + P.q \left(-g_{\mu\nu} + \frac{q_\mu q_\nu}{q^2}\right) . \tag{3.64}$$

Therefore, the final result for the hadronic tensor is

$$W^{\mu\nu} = \left[\frac{2x_\mathrm{B}}{P.q}\left(P_\mu + \frac{q_\mu}{2x_\mathrm{B}}\right)\left(P_\nu + \frac{q_\nu}{2x_\mathrm{B}}\right) + \left(-g_{\mu\nu} + \frac{q_\mu q_\nu}{q^2}\right)\right] \sum_q Q_q^2 \left[f^q(x_\mathrm{B}) - f^q(-x_\mathrm{B})\right] . \tag{3.65}$$

We have shown in the previous section, the parton distribution function for anti-quarks is given by

$$f^q(-x) = -\bar{q}(x) , \tag{3.66}$$

where q denotes the specific quark flavor. Consequently, the structure function $F_1(x_\mathrm{B}, \mathcal{Q}^2)$ in LO of perturbation theory reads

$$F_1(x_\mathrm{B}) = \sum_q Q_q^2 \left[f^q(x_\mathrm{B}) - f^q(-x_\mathrm{B})\right] = \sum_q Q_q^2 \left[q(x_\mathrm{B}) + \bar{q}(x_\mathrm{B})\right] . \tag{3.67}$$

The result above agrees with the one from the parton model at LO, whereas we also included the anti-quark distributions. Furthermore, we are able to calculate corrections leading to a violation of the Bjorken scaling.

3.2. Deeply virtual Compton scattering

Deeply virtual Compton scattering is the cleanest hard exclusive process providing access to generalized parton distributions. In the process, the lepton interacts with the nucleon via a virtual photon under the emission of a photon. In this work, we focus on the scattering of an electron on a proton target. Schematically, the reaction is

$$e^-(k_1) + N(P_1) = e^-(k_2) + N(P_2) + \gamma(q_2) . \tag{3.68}$$

The reaction is depicted in figure 3.5(a). Due to the unresolvable structure of the photon, the GPD is the only nonperturbative distribution in the process. However, the process of virtual Compton scattering is entangled with the Bethe-Heitler bremsstrahlungs process (Fig. 3.5(b),3.5(c)), where the interaction with the virtual photon is described by electromagnetic form factors of the nucleon. We will not consider the extraction of the DVCS amplitude

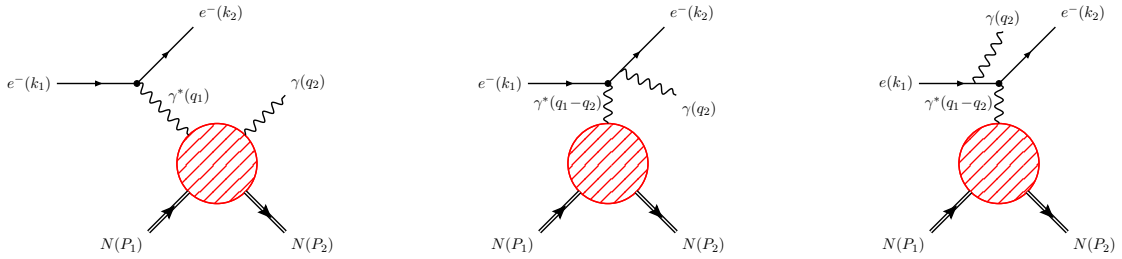

(a) DVCS (b) BH (c) BH

Figure 3.5.: DVCS and Bethe Heitler process.

in this work.
The factorization of the DVCS amplitude was shown in [CF99, JO98a] at twist-2 level. In leading order of $1/\mathcal{Q}$, the amplitude factorized in a hard scattering part and twist-2 generalized parton distributions, which describes the transition from the nucleon target to the nucleon in the final state.
Beyond leading power, twist-3 GPDs were introduced in [APT00, PPSS00, RW00, BM00]. Kinematical power-corrections for DVCS are studied in [BM11, BM12, BMP12a, BMP12b]. The hard scattering amplitudes are known up to NLO of perturbation theory from diagrammatical evaluation in momentum fraction representation [MPS+98, JO98b, JO98a]. Utilizing conformal symmetry, they can be related to the perturbative corrections for DIS [ZvN92, ZvN94, vNV00, VMV04, MVV04], see Sec. 4.3. Therefore, they are known also at NNLO. Note, that the conformal symmetry is broken in the $\overline{\text{MS}}$ scheme.
In this section, we give an introduction to deeply virtual Compton scattering. We investigate the kinematics of the process and explicitly calculate the unpolarized cross section in LO approximation of perturbation theory using twist-2 GPDs to obtain the general Lorentz structure. We also include the transverse degrees of freedom to ensure the gauge invariance of the Compton tensor. In the end, we present the approximation of the cross section for small values of x_B.

3.2.1. Variables of the Compton amplitude

Before analyzing the DVCS process, we first introduce a set of variables to describe the Compton amplitude (Fig. 3.6). The appendant Mandelstam variables are

$$s = (P_1 + q_1)^2 \,, \qquad t = (P_2 - P_1)^2 \,, \qquad u = (P_2 - q_1)^2 \,. \tag{3.69}$$

It is convenient to use symmetric combinations of the particle momenta to describe the photon-nucleon system. Energy-momentum conservation restricts the number of independent four-momenta to three. We choose[2]

$$q = \frac{1}{2}(q_1 + q_2) \,, \qquad P = P_1 + P_2 \qquad \Delta = P_2 - P_1 = q_1 - q_2 \,. \tag{3.70}$$

[2]There are several definitions in the literature and same care is necessary to convert the expressions, e.g., in [BR05] $\Delta = P_1 - P_2$. The notation in this work is consistent with [KMPK08, MLPKS14].

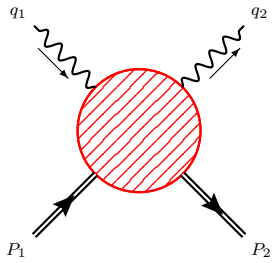

$$q = \frac{1}{2}(q_1 + q_2) \qquad P = P_1 + P_2 \qquad \Delta = P_2 - P_1 = q_1 - q_2$$

$$Q^2 = -q^2 \qquad \xi = \frac{Q^2}{P.q} \qquad \eta = -\frac{\Delta.q}{P.q}$$

$$\mathcal{Q}^2 = -q_1^2 \qquad x_{\mathrm{B}} = \frac{\mathcal{Q}^2}{2P_1.q_1}$$

Figure 3.6.: Compton amplitude and the corresponding variables.

Inverting the definitions leads to

$$P_1 = \frac{P - \Delta}{2}, \qquad P_2 = \frac{P + \Delta}{2}, \qquad q_1 = q + \frac{\Delta}{2}, \qquad q_2 = q - \frac{\Delta}{2}. \tag{3.71}$$

These three invariants can be traded for Lorentz scalars: The averaged photon virtuality and two scaling variables

$$Q^2 = -q^2\,, \qquad \xi = \frac{Q^2}{P.q}\,, \qquad \eta = -\frac{\Delta.q}{P.q}\,. \tag{3.72}$$

The first scaling variable ξ is called the generalized Bjorken variable, whereas the latter variable is the skewness η. For the forward Compton amplitude, the skewness is zero and the generalized Bjorken variable coincides with the Bjorken variable. In addition, there are three further Lorentz scalars to describe the process. Our choice is

$$\Delta^2 = t\,, \qquad M^2 = P^2 + \frac{1}{4}\Delta^2\,, \qquad P.\Delta = 0\,, \tag{3.73}$$

where the last scalar vanishes if the mass of the in and out going nucleons is equal. Although these variables are suited for a theoretical description of DVCS, on the experimental side, the masses of the incoming and outgoing photons, and the Bjorken variable (3.3) are conveniently accessible. In terms of the particle momenta, they are defined as

$$\mathcal{Q}^2 = -q_1^2\,, \qquad q_2^2 = 0\,, \qquad x_{\mathrm{B}} = \frac{\mathcal{Q}^2}{2P_1.q_1}\,. \tag{3.74}$$

Section B.2 in the appendix gives the transformations between the theoretical variables in (3.70) and the ones used by the experimental analysis in (3.74) using (3.73) for general q_2^2 and $P.\Delta$, namely

$$Q^2 = \frac{1}{2}\left(\mathcal{Q}^2 - q_2^2 + \frac{\Delta^2}{2}\right), \quad \xi = \frac{\mathcal{Q}^2 - q_2^2 + \frac{\Delta^2}{2}}{\frac{2-x_{\mathrm{B}}}{x_{\mathrm{B}}}\mathcal{Q}^2 - q_2^2 + \Delta^2}, \quad \eta = \frac{\mathcal{Q}^2 + q_2^2}{\frac{2-x_{\mathrm{B}}}{x_{\mathrm{B}}}\mathcal{Q}^2 - q_2^2 + \Delta^2}. \tag{3.75}$$

The inverse transformations are

$$\mathcal{Q}^2 = \left(1+\frac{\eta}{\xi}\right)Q^2 - \frac{\Delta^2}{4}, \quad q_2^2 = -\left(1-\frac{\eta}{\xi}\right)Q^2 + \frac{\Delta^2}{4}, \quad x_{\mathrm{B}} = \frac{(\xi+\eta)\,Q^2 - \xi\Delta^2/4}{(1+\eta)\,Q^2 - \xi\Delta^2/2}. \tag{3.76}$$

The perturbative approach to the Compton amplitude is only justified in the generalized Bjorken limit, in which the Mandelstam variable s and at least one of the photon virtualities have to be infinite, whereas both scaling variables ξ and η are kept finite. This work, we consider the two limiting cases:
The forward Compton amplitude for deeply inelastic scattering (Sec. 3.1) is obtained by

$$\Delta = 0\,, \qquad \eta = 0\,, \qquad \xi = x_{\mathrm{B}}\,, \tag{3.77}$$

and the Bjorken kinematics are given by the condition

$$s \sim -q_1^2 = -q_2^2 \to \infty\,. \tag{3.78}$$

The DVCS and DVMP amplitude are characterized by

$$q_2^2 = 0\,, \qquad \eta \simeq \xi\,, \tag{3.79}$$

such that

$$s \sim -q_1^2 \to \infty\,, \qquad -\Delta^2 \ll s\,. \tag{3.80}$$

Some consequences of the generalized Bjorken kinematics and the variables of the Compton amplitude are

$$\mathcal{Q}^2 \simeq 2Q^2\,, \qquad \xi \simeq \frac{x_{\mathrm{B}}}{2 - x_{\mathrm{B}}}\,, \qquad s \simeq 2P.q\,, \tag{3.81}$$

which we will use extensively throughout this chapter. The limits on the momentum transfer in the t-channel are given by

$$\Delta^2_{\mathrm{min,max}} = -\frac{\mathcal{Q}^2}{4x_{\mathrm{B}}(1 - x_{\mathrm{B}}) + \epsilon^2}\left[2(1 - x_{\mathrm{B}}) + \epsilon^2 \mp 2(1 - xB)\sqrt{1 + \epsilon^2}\right]\,. \tag{3.82}$$

3.2.2. Kinematics

As mentioned in the introduction we concentrate our attention on the DVCS cross section, see figure 3.5(a). In contrast to the forward Compton amplitude, the incoming and outgoing nucleon have different momenta P_1 and P_2, respectively. We denote the momentum of the detected real photon by q_2, whereas the virtual photon for the interaction between the electron and the nucleon has the space like momentum q_1. Analog to DIS, the incoming and outgoing electron have momenta k_1 and k_2, respectively.
Schematically, the reaction is

$$e^-(k_1) + N(P_1) = e^-(k_2) + N(P_2) + \gamma(q_2)\,. \tag{3.83}$$

In contrast to deeply inelastic scattering, the nucleon stays intact during the scattering process and it is exclusive. We describe the reaction in the laboratory frame as displayed in figure 3.7. The nucleon target is at rest and the leptons only move in the x-z-plane (leptonic plane) in such a way, that the momentum of the virtual photon moves in the negative z directions.

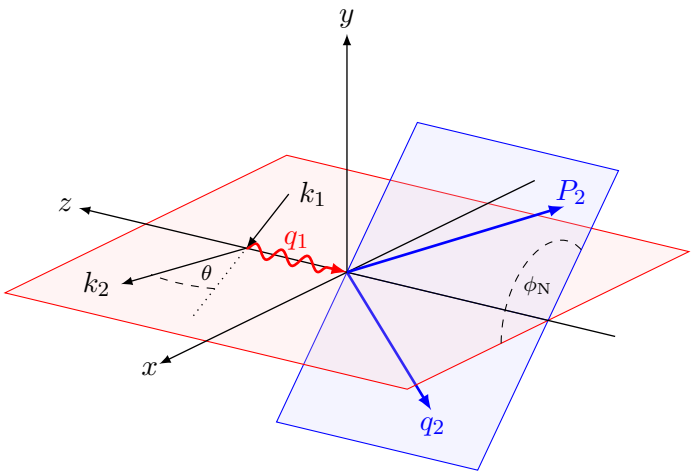

Figure 3.7.: DVCS in the target rest frame. The leptonic and hadronic plane are colored in red and blue, respectively.

The momenta of the scattered proton and the outgoing photon span the hadronic plane. Therefore, the components of the particle momenta can be written as

$$\begin{aligned} P_1^\mu &= (M, \vec{0})\,, & P_2^\mu &= (E_2, \vec{P}_2)\,, \\ k_1^\mu &= (\omega_1, \vec{k}_1)\,, & k_2^\mu &= (\omega_2, \vec{k}_2)\,, \\ q_1^\mu &= (\nu_1, 0, 0, -q_1^z)\,, & q_2^\mu &= (\nu_2, \vec{q}_2)\,. \end{aligned} \tag{3.84}$$

The cross section for the electroproduction of a real photon is given by

$$\mathrm{d}\sigma^{eN\to e\gamma N} = \frac{1}{4M\omega_1}\,|\mathcal{M}(eN\to e\gamma N)|^2\,\mathrm{d}\Pi_3\,, \tag{3.85}$$

where $\mathrm{d}\Pi_3$ is the three-body Lorentz invariant phase space (LIPS) defined as

$$\mathrm{d}\Pi_3 = (2\pi)^4\delta^{(4)}(k_1+P_1-k_2-q_2-P_2)\,\frac{\mathrm{d}^3k_2}{2(2\pi)^3\omega_2}\,\frac{\mathrm{d}^3q_2}{2(2\pi)^3\nu_2}\,\frac{\mathrm{d}^3P_2}{2(2\pi)^3E_2}\,. \tag{3.86}$$

The invariant matrix element $\mathcal{M}$ is obtained from the expression for the S-matrix. In order to obtain a photon in the final state, we have to include the third order in the electromagnetic coupling. The interacting part (iT-matrix) reads

$$\begin{aligned} \langle \mathrm{k_2 q_2 P_2}|iT|\mathrm{k_1 P_1}\rangle = (-ie)^3 \sum\nolimits_{q,h} \int \mathrm{d}^4y \int \mathrm{d}^4z \int \mathrm{d}^4w \\ \times \langle \mathrm{k_2 q_2 P_2}|\bar\psi(y)\not{A}(y)\psi(y)\cdot Q_q\bar\psi_q(z)\not{A}(z)\psi_q(z)\cdot Q_h\bar\psi_h(w)\not{A}(w)\psi_h(w)|\mathrm{k_1 P_1}\rangle\,. \end{aligned} \tag{3.87}$$

Contracting the photon vector field of the electrons, with one of the remaining ones and separating off the leptonic contribution results into

$$\langle \mathrm{k_2 q_2 P_2}|iT|\mathrm{k_1 P_1}\rangle = e^3 L^\mu \epsilon^{\nu *}(q_2) \int \mathrm{d}^4z \int \mathrm{d}^4w\, e^{-iq_1 z + iq_2 w}\,\langle \mathrm{P_2}|j_\mu(z) j_\nu(w)|\mathrm{P_1}\rangle\,, \tag{3.88}$$

where we utilize the electromagnetic current (3.11) and the leptonic current[3] L^μ (3.13). ϵ^ν is the polarization vector of the outgoing photon.
With the electromagnetic interaction separated, we introduce the Compton tensor for the description of the hadronic dynamics,

$$T_{\mu\nu}(q,P,\Delta) = i\int \mathrm{d}^4z\,\mathrm{d}^4w\; e^{-iq_1z+iq_2w}\left\langle \mathrm{P}_2|j_\mu(z)j_\nu(w)|\mathrm{P}_1\right\rangle . \tag{3.89}$$

For $P_1 = P_2$ it coincides with the forward Compton tensor (3.18). Introducing the symmetric variables

$$W = \frac{z+w}{2}\,, \qquad Z = z-w\,, \tag{3.90}$$

the Compton tensor transforms into

$$T_{\mu\nu}(q,P,\Delta) = i\int \mathrm{d}^4W\,\mathrm{d}^4Z\, e^{-i(q_1-q_2)W+i(q_1+q_2)\frac{Z}{2}}\left\langle P_2|T\left\{j_\mu\left(W+\tfrac{Z}{2}\right)j_\nu\left(W-\tfrac{Z}{2}\right)\right\}|P_1\right\rangle . \tag{3.91}$$

Shifting the variables by

$$\langle P_2\,|j_\mu(W)|\,P_1\rangle = \left\langle P_2\,|j_\mu(0)|\,P_1\right\rangle e^{-i(P_1-P_2)W}\,, \tag{3.92}$$

we eliminate one of the integrations, which results in the explicit momentum conservation of the photon-nucleon system

$$\int \mathrm{d}^4W\, e^{-i(q_1-q_2)W}\; e^{-i(P_1-P_2)W} = (2\pi)^4\,\delta^{(4)}(P_1+q_1-P_2-q_2)\;. \tag{3.93}$$

Therefore,

$$T_{\mu\nu}(P,q,\Delta) = (2\pi)^4\,\delta^{(4)}(P_1+q_1-P_2-q_2)\cdot i\int \mathrm{d}^4z\; e^{iq.z}\left\langle \mathrm{P}_2|T\left\{j_\mu(\tfrac{z}{2})\,j_\nu(-\tfrac{z}{2})\right\}|\mathrm{P}_1\right\rangle . \tag{3.94}$$

To shorten the notation, we define the reduced Compton tensor[4] as

$$\mathcal{T}_{\mu\nu}(P,q,\Delta) = i\int \mathrm{d}^4z\; e^{iq.z}\;\left\langle \mathrm{P}_2\right|T\left\{j_\mu(\tfrac{z}{2})\,j_\nu(-\tfrac{z}{2})\right\}\left|\mathrm{P}_1\right\rangle\;. \tag{3.95}$$

From the matrix element of the iT-matrix (3.88) and the definition of the Compton tensor (3.94), we read off the invariant matrix element, namely

$$i\mathcal{M}(eN\to e\gamma N) = e^3 L_\mu \epsilon^*_\nu(q_2) T^{\mu\nu}\,. \tag{3.96}$$

Its absolute value squared enters the unpolarized cross section. Summing over the polarizations of the outgoing photon ($\sum \epsilon^*_\mu\epsilon_\nu \to -g_{\mu\nu}$) gives

$$|\mathcal{M}|^2 = e^3 L_\mu L^\alpha_\dagger T^{\mu\beta} T_{\alpha\beta} = (4\pi)^3\alpha^3_{\mathrm{em}}\,|\mathcal{T}_{\mathrm{DVCS}}|^2\;, \tag{3.97}$$

[3] For DVCS we have to make the substitution $q \to q_1$.
[4] In the literature, sometimes the argument of the electromagnetic currents is shifted by $z/2$, giving rise to the exponent $\exp(-i\Delta.z/2)$.

where we used the squared DVCS scattering amplitude

$$|\mathcal{T}_{\mathrm{DVCS}}|^2 = L_\mu L^\alpha_\dagger T^{\mu\beta} T_{\alpha\beta} \,. \tag{3.98}$$

Thus, the unpolarized cross section for the electro production of a photon reads

$$\mathrm{d}\sigma^{eN\to e\gamma N} = \frac{1}{4M\omega_1}(4\pi)^3\alpha_{\mathrm{em}}^3 \left|\mathcal{T}^2_{\mathrm{DVCS}}\right| \mathrm{d}\Pi_3 \,. \tag{3.99}$$

The last step is expressing the cross section in terms of a set of independent variables. In general, there are three outgoing particles, of which one momentum can be obtained by total four-momentum conservation. Therefore, it is required to measure eight vector components. However, the electron, nucleon and photon mass ($k_2^2 = 0$, $P_2^2 = M$ and $q_2^2 = 0$) are known beforehand, reducing the number of degrees of freedom by three. Likewise, the freedom in the choice of the reference frame eliminates another variable. Hence, there are only four independent variables left. We choose the energy and the scattering angle of the incident electron and the energy and the azimuthal angle of the recoiling nucleon[5]

$$\omega_2,\ \theta,\ E_2,\ \phi_{\mathrm{N}} \,, \tag{3.100}$$

respectively. As derived in appendix B.1, the Lorentz invariant phase space in terms of the previous quantities can be cast into the form

$$\mathrm{d}\Pi_3 = \frac{1}{8(2\pi)^4}\frac{\omega_2}{|\vec{q}_1|} \cdot \mathrm{d}\omega_2\ \mathrm{d}(\cos\theta) \cdot \mathrm{d}E_2\ \mathrm{d}\phi_{\mathrm{N}} \,. \tag{3.101}$$

Since the four-momentum components are not Lorentz invariant, one conventionally uses the variables

$$x_{\mathrm{B}} \wedge \left(y \vee \mathcal{Q}^2\right) \wedge \Delta^2 \wedge \phi_{\mathrm{N}} \,. \tag{3.102}$$

They are given in terms of the variables in (3.100) by (cf. Sec. B.1 and Eq. 3.5)

$$x_{\mathrm{B}} = \frac{4\omega_1\omega_2\sin^2(\theta/2)}{2M(\omega_1-\omega_2)} \,, \qquad y = \frac{\omega_1-\omega_2}{\omega_1} \,, \qquad \Delta^2 = M^2 - 2ME_2 \,. \tag{3.103}$$

In terms of the Lorentz invariant variables, the Lorentz invariant phase space is (cf. B.1)

$$\mathrm{d}\Pi_3 = \frac{1}{16(2\pi)^4}\frac{\mathrm{d}x_{\mathrm{B}}\mathrm{d}y\mathrm{d}\Delta^2\mathrm{d}\phi_{\mathrm{N}}}{\sqrt{1+\epsilon^2}} \,, \qquad \text{with } \epsilon = \frac{2x_{\mathrm{B}}M}{\mathcal{Q}} \,. \tag{3.104}$$

Thus, the cross section of the electroproduction of a photon becomes

$$\frac{\mathrm{d}\sigma^{eN\to e\gamma N}}{\mathrm{d}x_{\mathrm{B}}\mathrm{d}y\mathrm{d}\Delta^2\mathrm{d}\phi_{\mathrm{N}}} = \frac{\alpha_{\mathrm{em}}^3 x_{\mathrm{B}} y}{8\pi\mathcal{Q}^2\sqrt{1+\epsilon^2}} \left|\mathcal{T}_{\mathrm{DVCS}}\right|^2 \,. \tag{3.105}$$

[5] At the experiments at the HERA collider, the real photon is detected, whereas the recoiled nucleon remains unobserved.

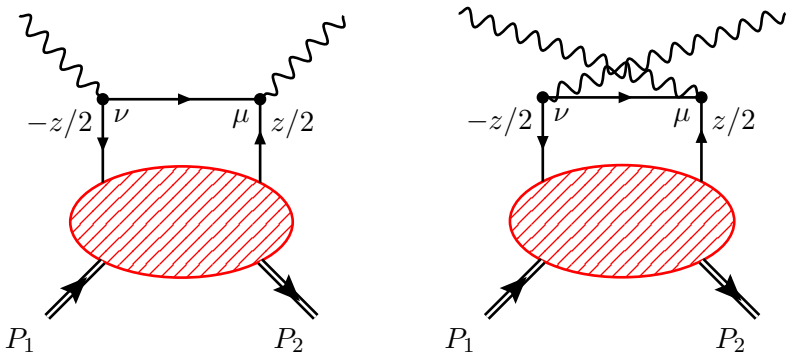

(a) s-channel (b) u-channel

Figure 3.8.: Deeply virtual Compton scattering in LO of perturbation theory. The dashed blob symbolizes the quark GPD.

3.2.3. Dynamics

As in DIS, we use a factorization theorem [CF99, JO98a] to separate two kinematical regions: The hard scattering amplitude calculable in perturbation theory and the soft short distance contribution, which is parametrized by GPDs. Here, we derive the Compton tensor in the leading twist-2 approximation in LO of perturbation theory. Let us recall the reduced Compton tensor (3.95), namely

$$\mathcal{T}_{\mu\nu} = i \int \mathrm{d}^4 z \; e^{iq.z} \left\langle \mathrm{P}_2 | T\{ j_\mu(\tfrac{z}{2}) \, j_\nu(-\tfrac{z}{2}) \} \, | \mathrm{P}_1 \right\rangle$$

To calculate the result in the handbag approximation (Born level) shown in figure 3.8 we employ the massless quark propagator in coordinate space (A.2). From equation (3.48), the time ordered product for the two contributions reads

$$iT\{ j_\mu(\tfrac{z}{2}) \, j_\nu(-\tfrac{z}{2}) \} = i \sum_q Q_q^2 \left\{ \bar{\psi}_q(\tfrac{z}{2}) \, \gamma_\mu \not{n}(z) \gamma_\nu \psi_q(-\tfrac{z}{2}) + \bar{\psi}_q(-\tfrac{z}{2}) \, \gamma_\nu \not{n}(-z) \gamma_\mu \psi_q(\tfrac{z}{2}) \right\} .$$

Current conservation is not fulfilled for the parity even and odd terms separately. By parametrization of the matrix elements with GPDs, the contributions proportional to the vector GPDs H and E will not be gauge invariant without the axial GPDs $\tilde{H}$ and $\tilde{E}$, although, they are dynamically independent. The situation is resolved by the inclusion of operators with total derivatives, which have twist-3, but are kinematically related to twist-2 operators [APT00, PPSS00, RW00, BM00]. Neglecting such contributions, we fall back on the conventional leading twist contribution [MRG+94, Ji97b, Rad96b, BR00, BGR99].
In a full twist-3 analysis we also have to include quark-gluon-quark operators. Since our aim is to derive the gauge invariant Compton tensor in the twist-2 approximation, we neglect such contributions and only take into account operators with total derivatives. In contrast to the derivation of the forward Compton tensor (Sec. 3.1.3), we use the quark propagator in momentum space (A.1) and also include its transverse components. For the time ordered

product, we derive

$$iT\{j_\mu(\tfrac{z}{2})\, j_\nu(-\tfrac{z}{2})\} = iQ_q^2 \left\{\bar\psi_q(\tfrac{z}{2})\,\gamma_\mu \not{S}(q_1)\gamma_\nu\psi_q(-\tfrac{z}{2}) - \bar\psi_q(-\tfrac{z}{2})\,\gamma_\nu \not{S}(q_1)\gamma_\mu\psi_q(\tfrac{z}{2})\right\}, \tag{3.106}$$

where we used the quark propagator[6] in momentum space (A.1)

$$\not{S}(q_1) = \int \frac{\mathrm{d}^4k_1}{(2\pi)^4}\, e^{-i(k_1+q_1).z}\, \frac{i(\not{k}_1 + \not{q}_1)}{(k_1+q_1)^2 + i\epsilon}\,. \tag{3.107}$$

Making use of the identity (3.47)

$$\gamma_\mu\gamma_\alpha\gamma_\nu = (s_{\mu\alpha\nu\beta} + i\epsilon_{\mu\alpha\nu\beta}\gamma_5)\,\gamma^\beta\,, \qquad \gamma_\nu\gamma_\alpha\gamma_\mu = (s_{\mu\alpha\nu\beta} - i\epsilon_{\mu\alpha\nu\beta}\gamma_5)\,\gamma^\beta\,,$$

we cast Eq. 3.106 into the form

$$\begin{aligned} iT\{j_\mu(\tfrac{z}{2})\, j_\nu(\text{-}\tfrac{z}{2})\} &= Q_q^2 \int \frac{\mathrm{d}^4k_1}{(2\pi)^4}\, e^{-i(k_1+q_1).z}\, \frac{(k_1+q_1)^\alpha}{(k_1+q_1)^2 - i\epsilon} \\ &\times \left\{ s_{\mu\alpha\nu\beta}\left[\text{-}\bar\psi_q(\tfrac{z}{2})\gamma^\beta\psi_q(\text{-}\tfrac{z}{2}) + \{z\leftrightarrow\text{-}z\}\right] - i\epsilon_{\mu\alpha\nu\beta}\gamma_5\left[\bar\psi_q(\tfrac{z}{2})\gamma^\beta\psi_q(\text{-}\tfrac{z}{2}) + \{z\leftrightarrow\text{-}z\}\right]\right\}. \end{aligned}$$

As argued before, the dominant contribution is proportional to the plus component of the parton momentum. Thus, its Sudakov decomposition yields

$$k_1^\mu = k_1^+\tilde n^\mu + k_\perp^\mu\,, \qquad k_1^+ = x+\eta\,, \qquad k_1^- \simeq 0\,. \tag{3.108}$$

Therefore, the denominator can be written as

$$(k_1+q_1)^2 = P.q\,(x-\xi)\,, \tag{3.109}$$

where we used $\mathcal{Q}^2 = 2Q^2$ (3.81) and the fact that the momentum of the virtual photon has no transverse component in the laboratory frame. The numerator on the other hand emerges as

$$k_1^\alpha + q_1^\alpha = (x-\xi)\,\tilde n^\alpha + {k_1}_\perp^\alpha + \frac{P.q}{2} n^\alpha\,. \tag{3.110}$$

Inserting the time ordered product of two electromagnetic currents (3.106) into the reduced Compton tensor (3.95), we find

$$\begin{aligned} \mathcal{T}^{\mu\nu} &= Q_q^2 \int \mathrm{d}^4z \int \frac{\mathrm{d}^4k_1}{(2\pi)^4}\, e^{i(q-k_1-q_1).z}\, \frac{(k_1+q_1)^\alpha}{(k_1+q_1)^2 + i\epsilon} \\ &\times \left\{ s_{\mu\alpha\nu\beta}\left[\langle\text{-}\bar\psi_q(\tfrac{z}{2})\gamma^\beta\psi_q(\text{-}\tfrac{z}{2})\,\rangle + \{z\leftrightarrow\text{-}z\}\right] - i\epsilon_{\mu\alpha\nu\beta}\gamma_5\left[\langle\bar\psi_q(\tfrac{z}{2})\gamma^\beta\psi_q(\text{-}\tfrac{z}{2})\,\rangle + \{z\leftrightarrow\text{-}z\}\right]\right\}. \end{aligned} \tag{3.111}$$

Note, that we omitted the nucleon states in the matrix elements for brevity in the previous expression. With the denominator (3.109) and numerator (3.110), the previous equation can be written as

$$\mathcal{T}^{\mu\nu} = \frac{Q_q^2}{P.q}\int_{-1}^{1}\mathrm{d}x \int \frac{\mathrm{d}^4z}{2\pi}\int\frac{\mathrm{d}k_1^-}{2\pi}\frac{\mathrm{d}^2k_1^\perp}{(2\pi)^2}\, e^{i(q-k_1-q_1).z}\, \frac{\frac{P.q}{2}n^\alpha + (x-\xi)\,\tilde n^\alpha + k_{1\perp}^\alpha}{x-\xi+i\epsilon} \times \{\ldots\}\,, \tag{3.112}$$

[6] In order to agree with the literature, we use the same letter as for the electron momentum. The distinction is clear form the context.

where the ellipsis corresponds to the term in brackets in (3.111). We also interchanged the integration with respect to the plus component of the parton momentum k_1^+ with the one over the momentum fraction x, see Eq. 3.108. Expressing the exponents in terms of the light-cone coordinates we obtain

$$(q-k_1-q_1).z = -\left(\tfrac{\Delta^+}{2}+k_1^+\right)z^- - \left(\tfrac{\Delta^-}{2}+k_1^-\right)z^+ - k_1^\perp.z^\perp\,. \tag{3.113}$$

At this point, we first perform the integration with respect to the minus component of the quark momentum. We obtain the δ-function $\delta(z^+)$ as seen from the previous equation. With it, we evaluate the z^+ integration. Thus,

$$\mathcal{T}^{\mu\nu} = \frac{Q_q^2}{P.q}\int_{-1}^{1}\mathrm{d}x\int\frac{\mathrm{d}z^-\mathrm{d}^2z_\perp}{2\pi}\int\frac{\mathrm{d}^2k_1^\perp}{(2\pi)^2}\,e^{-i(xz^-+k_1^\perp.z^\perp)}\,\frac{\frac{P.q}{2}n^\alpha+(x-\xi)\,\tilde{n}^\alpha+k_{1\perp}^\alpha}{x-\xi+i\epsilon}\times\{\ldots\}\,. \tag{3.114}$$

We get rid of the transverse parton momentum in the numerator utilizing a derivative with respect to the transverse component of the light-like distance z, namely

$$\frac{\partial}{\partial z_\perp^\alpha}e^{-ik_1^\perp.z^\perp} = \partial_\perp^\alpha e^{-ik_1^\perp.z^\perp} = -ik_{1\perp}^\alpha e^{-ik_1^\perp.z^\perp}\,. \tag{3.115}$$

By partial integration, we shift the derivative from acting on the exponential to acting on the operators in (3.111). The occurring operators are the following

$$\begin{aligned}
\mathcal{O}^\beta(-z^-,z^-) &= \bar\psi(-z)\gamma^\beta\psi(z)\,, & \tilde{\mathcal{O}}^\beta(-z^-,z^-) &= \bar\psi(-z)\gamma^\beta\gamma^5\psi(z)\,,\\
\mathcal{K}^\beta(-z^-,z^-) &= \bar\psi(-z)i\overset{\leftrightarrow}{\partial}{}_\perp^\beta\gamma^+\psi(z)\,, & \tilde{\mathcal{K}}^\beta(-z^-,z^-) &= \bar\psi(-z)\overset{\leftrightarrow}{\partial}{}_\perp^\beta\gamma^+\gamma^5\psi(z)\,.
\end{aligned} \tag{3.116}$$

Note, in order to obtain the twist-2 contribution, we have to perform Sudakov decomposition. The operators in the first row are the familiar twist-2 vector and axial-vector operators introduced in Sec. 2.1. Their matrix elements are parametrized as

$$\int\frac{\mathrm{d}z^-}{2\pi}e^{ixP^+z^-}\langle \mathrm{P}_2|\bar\psi(\text{-}z)\gamma^\beta(\gamma^5)\psi(z)|\mathrm{P}_1\rangle = F^\beta_{V(A)}\big(x,\eta,\Delta^2\big)\,. \tag{3.117}$$

This is the boost invariant form of the definition (2.7, 2.9). We have

$$\begin{aligned}
F_V^\beta\big(x,\eta,\Delta^2\big) &= \frac{h^\beta}{P^+}H\big(x,\eta,\Delta^2\big)+\frac{e^\beta}{P^+}E\big(x,\eta,\Delta^2\big)\,,\\
F_A^\beta\big(x,\eta,\Delta^2\big) &= \frac{\tilde h^\beta}{P^+}\tilde H\big(x,\eta,\Delta^2\big)+\frac{\tilde e^\beta}{P^+}\tilde E\big(x,\eta,\Delta^2\big)\,.
\end{aligned}$$

This definition is not exactly the form present in (3.111). We have to apply the transformations $z\to z/2$ and $x\to -x$

$$\begin{aligned}
\int\frac{\mathrm{d}z^-}{2\pi}e^{-ixz^-}\langle \mathrm{P}_2|\bar\psi\left(-\tfrac{z}{2}\right)\gamma^\beta(\gamma^5)\psi\left(\tfrac{z}{2}\right)|\mathrm{P}_1\rangle &= 2F^\beta_{V(A)}(-x)\,,\\
\int\frac{\mathrm{d}z^-}{2\pi}e^{-ixz^-}\langle \mathrm{P}_2|\bar\psi\left(\tfrac{z}{2}\right)\gamma^\beta(\gamma^5)\psi\left(-\tfrac{z}{2}\right)|\mathrm{P}_1\rangle &= 2F^\beta_{V(A)}(\quad x)\,.
\end{aligned} \tag{3.118}$$

Since the only relevant argument of the GPD is the momentum fraction x, we hide all others. In addition, the operators $\mathcal{K}$ and $\tilde{\mathcal{K}}$ are introduced. The matrix element of the vector operator is parametrized by

$$\int \frac{\mathrm{d}z^-}{2\pi} e^{ixP^+z^-} \langle \mathrm{P}_2|\bar{\psi}(-z) i\overset{\leftrightarrow}{\partial}{}^{\beta}_{\perp} \gamma^+(\gamma^5)\psi(z)|\mathrm{P}_1\rangle = K^{\beta}_{V(A)}(x)\,. \tag{3.119}$$

With the adjustments for our situation, we receive

$$\int \frac{\mathrm{d}z^-}{2\pi} e^{-ixz^-} \langle \mathrm{P}_2|\bar{\psi}\left(-\tfrac{z}{2}\right) i\overset{\leftrightarrow}{\partial}{}^{\beta}_{\perp} \gamma^+(\gamma^5)\psi\left(\tfrac{z}{2}\right)|\mathrm{P}_1\rangle = \quad K^{\beta}_{V(A)}(-x)\,, \tag{3.120}$$

$$\int \frac{\mathrm{d}z^-}{2\pi} e^{-ixz^-} \langle \mathrm{P}_2|\bar{\psi}\left(\tfrac{z}{2}\right) i\overset{\leftrightarrow}{\partial}{}^{\beta}_{\perp} \gamma^+(\gamma^5)\psi\left(-\tfrac{z}{2}\right)|\mathrm{P}_1\rangle = -K^{\beta}_{V(A)}(\quad x)\,. \tag{3.121}$$

Applying the parametrizations above to the reduced Compton tensor (3.114) and integrating out the two transverse variables $z^\perp$ and $k_1^\perp$, we get

$$\begin{aligned}\mathcal{T}^{\mu\nu} = \frac{Q_q^2}{P.q}\int_{-1}^{1}\mathrm{d}x \qquad\qquad\qquad\qquad\qquad\qquad\qquad\qquad\qquad\qquad\qquad\qquad (3.122)\\ \times\Bigg\{\frac{\frac{P.q}{2}n^\alpha+(x-\xi)\,\tilde{n}^\alpha}{x-\xi+i\epsilon}\Big[2s_{\mu\alpha\nu\beta}\Big(-F_V^\beta(x)+F_V^\beta(-x)\Big)+2i\epsilon_{\mu\alpha\nu\beta}\Big(-F_A^\beta(x)-F_A^\beta(-x)\Big)\Big]\\ +\frac{1}{x-\xi+i\epsilon}\Big[s_{\mu\alpha\nu\beta}\,\tilde{n}^\alpha\Big(-K_V^\beta(x)-K_V^\beta(-x)\Big)-i\epsilon_{\mu\alpha\nu\beta}\tilde{n}^\alpha\Big(-K_A^\beta(x)+K_A^\beta(-x)\Big)\Big]\Bigg\}.\end{aligned}$$

In the next step, we introduce the common notation for the LO hard scattering amplitudes $C_0^{(\pm)}(x,\xi)$. Schematically, we have

$$\begin{aligned}\int \mathrm{d}x\frac{1}{x-\xi+i\epsilon}\left[-F(x)\pm F(-x)\right] &= \left(\frac{1}{\xi-x-i\epsilon}\mp\frac{1}{\xi+x-i\epsilon}\right)F(x) = \quad C_0^{(\mp)}(x,\xi)F(x)\,,\\ \int \mathrm{d}x\frac{x}{x-\xi+i\epsilon}\left[-F(x)\pm F(-x)\right] &= \left(\frac{x}{\xi-x-i\epsilon}\pm\frac{x}{\xi+x-i\epsilon}\right)F(x) = x\,C_0^{(\pm)}(x,\xi)F(x)\,.\end{aligned} \tag{3.123}$$

Note, in (3.122) the combination of the GPD F_V is odd under the transformation $x\to -x$. Thus, the term proportional to $x-\xi$ does not contribute for the vector GPDs. However, it contributes to the even axial-vector GPD F_A combination. Rearranging (3.122) leads to

$$\begin{aligned}\mathcal{T}_{\mu\nu} = \frac{Q_q^2}{P.q}\int_{-1}^{1}\mathrm{d}x\, C_0^{(-)}(x,\xi)\left[P.q\, s_{\mu\alpha\nu\beta}\, n^\alpha F_V^\beta(x) + i\epsilon_{\mu\alpha\nu\beta}\,\tilde{n}^\alpha\left(2xF_A^\beta(x) - K_A^\beta(x)\right)\right]\\ +\frac{Q_q^2}{P.q}\int_{-1}^{1}\mathrm{d}x\, C_0^{(+)}(x,\xi)\left[2i\epsilon_{\mu\alpha\nu\beta}\, q^\alpha F_A^\beta(x) + s_{\mu\alpha\nu\beta}\,\tilde{n}^\alpha K_V^\beta(x)\right]\,.\end{aligned} \tag{3.124}$$

To shorten the notation, we have omitted the unimportant arguments of the GPDs. We use now QCD equation of motions to express the GPDs K by twist-2 GPDs and ones with higher twist contributions [BM00], namely

$$\frac{\partial}{\partial z^-}\mathcal{O}^\beta - i\epsilon_\perp^{\beta\rho}\partial^+\tilde{\mathcal{O}}_\rho + i\mathcal{K}^\beta + i\epsilon_\perp^{\beta\rho}\partial_\rho^\perp\tilde{\mathcal{O}}_+ = 0\,, \tag{3.125}$$

$$\partial^+\mathcal{O}_\alpha - i\epsilon_{\alpha\beta}^\perp\frac{\partial}{\partial z^-}\tilde{\mathcal{O}}^\beta + \epsilon_{\alpha\beta}^\perp\tilde{\mathcal{K}}^\beta - \partial_\alpha^\perp\mathcal{O}_+ = 0\,, \tag{3.126}$$

where we omitted operators with an additional gluon field. For brevity, the argument $(-z^-, z^-)$ of all operators is suppressed. In terms of the corresponding matrix elements neglecting twist-3 contributions the identities yield

$$i\epsilon_\perp^{\beta\rho}\Delta_\rho^\perp F_A^+(x) - K_V^\beta(x) = 0\,, \tag{3.127}$$

$$-\Delta_\alpha^\perp F_V^+(x) + 2xi\epsilon_{\alpha\beta}^\perp F_A^\beta(x) + 2\eta F_V^\beta(x) - i\epsilon_{\alpha\beta}^\perp K_A^\beta(x) = 0\,. \tag{3.128}$$

Therefore, we are able to replace the GPDs K_V and K_A in (3.124) by

$$K_V^\beta(x) = i\epsilon_\perp^{\beta\rho}\Delta_\rho^\perp\, F_A^+(x)\,, \quad i\epsilon_{\alpha\beta}^\perp\, K_A^\beta(x) = -\Delta_\alpha^\perp\, F_V^+(x) + 2xi\epsilon_{\alpha\beta}^\perp\, F_A^\beta(x) + 2\eta\, F_V^\beta(x)\,, \tag{3.129}$$

respectively. The two accompanying Lorentz structures are

$$s_{\mu\alpha\nu\beta}\,\tilde{n}^\alpha \cdot i\epsilon_\perp^{\beta\rho}\Delta_\rho^\perp F_A^+(x) = \frac{i}{2}\left(\epsilon_\perp^{\mu\sigma}\Delta_\sigma^\perp P^\nu(x) + \epsilon_\perp^{\nu\sigma}\Delta_\sigma^\perp P^\mu\right) F_A^+(x) \tag{3.130}$$

and

$$i\epsilon_{\mu-\nu\beta}\, K_A^\beta(x) \approx \tilde{n}^\nu\left[-\Delta_\mu^\perp\, F_V^+(x) - \eta\,\tilde{n}^\mu\, F_V^+(x)\right] + \tilde{n}^\nu xi\epsilon_{\mu\beta}^\perp\, F_A^\beta(x)\,, \tag{3.131}$$

which arises from the Sudakov decomposition of the totally antisymmetric tensor (B.30). The two remaining Lorentz structures of the genuine twist-2 GPDs are

$$\begin{aligned} &s_{\mu\alpha\nu\beta}\, n^\alpha\tilde{n}^\beta = -g_{\mu\nu} + \tilde{n}^\mu n^\nu + \tilde{n}^\nu n^\mu = -g_{\mu\nu} + \tilde{n}^\mu\,(q^\nu + \xi\tilde{n}^\nu) + \tilde{n}^\nu\,(q^\mu + \xi\tilde{n}^\mu) = -g_{\mu\nu}^\perp\,, \\ &i\epsilon_{\mu-\nu\beta}\left[2xF_A^\beta(x) - K_A^\beta(x)\right] = \frac{1}{2}\left(-\tilde{n}^\mu\Delta_\nu^\perp + \tilde{n}^\nu\Delta_\mu^\perp\right) F_V^+(x)\,. \end{aligned} \tag{3.132}$$

Assembling everything together, we get for the reduced Compton tensor

$$\mathcal{T}_{\mu\nu} = t_{\mu\nu}^{(-)}\, Q_q^2 \int_{-1}^{1} \mathrm{d}x\, C_0^{(-)}(x,\xi)\, F_V^q\big(x,\eta,\Delta^2\big) + t_{\mu\nu}^{(+)}\, Q_q^2 \int_{-1}^{1} \mathrm{d}x\, C_0^{(+)}(x,\xi)\, F_A^q\big(x,\eta,\Delta^2\big)\,. \tag{3.133}$$

The two Lorentz structures for the vector and axial-vector part are

$$t_{\mu\nu}^{(-)} = -g_{\mu\nu} + \tilde{n}^\mu\left(q^\nu + \xi\tilde{n}^\nu - \tfrac{1}{2}\Delta_\perp^\nu\right) + \tilde{n}^\nu\left(q^\mu + \xi\tilde{n}^\mu + \tfrac{1}{2}\Delta_\perp^\mu\right)\,, \tag{3.134}$$

$$t_{\mu\nu}^{(+)} = \frac{i}{P.q}\left[\epsilon_{\mu\nu\alpha\beta}\, q^\alpha P^\beta + \tfrac{1}{2}\epsilon_\perp^{\alpha\beta}\Delta_\beta^\perp\left(\tilde{n}_\mu g_{\alpha\nu} + \tilde{n}_\nu g_{\alpha\mu}\right)\right]\,. \tag{3.135}$$

Note, that the occurring GPDs are of twist-2. The Compton tensor in the twist-2 approximation is explicitly gauge invariant. We conclude this section with the derivation of the forward limit.

In DIS only the vector part of the Compton amplitude contributes in the unpolarized case. The corresponding Lorentz structure neglecting contributions proportional to $\Delta_\perp$ can be written as

$$t_{\mu\nu}^{(-)} = -g_{\mu\nu}^\perp = \left(-g^{\mu\nu} + \frac{q^\mu q^\nu}{q^2}\right) + \frac{\xi}{P.q}\left(P^\mu + \frac{q^\mu}{\xi}\right)\left(P^\nu + \frac{q^\nu}{\xi}\right)\,. \tag{3.136}$$

To obtain the forward case, we have to choose the momenta $P_1 = P_2 = P$ and $q_1 = q_2 = q$. Thus, the replacement rules are

$$P \to 2P\,, \qquad q \to q\,, \qquad \xi \to x_{\mathrm{B}}\,. \tag{3.137}$$

Making use of these rules, the Lorentz structure in the forward limit becomes

$$t^{(-)}_{\mu\nu} \to \left(-g^{\mu\nu} + \frac{q^\mu q^\nu}{q^2}\right) + \frac{2x_{\mathrm{B}}}{P.q}\left(P^\mu + \frac{q^\mu}{2x_{\mathrm{B}}}\right)\left(P^\nu + \frac{q^\nu}{2x_{\mathrm{B}}}\right)\,. \tag{3.138}$$

It coincides with the result in (3.65). The forward case of the GPD F^q_V is given by

$$F^q_V(x,0,0) = \frac{h^+}{P^+} H^q(x,0,0) = f^q(x)\,. \tag{3.139}$$

Taking the imaginary part, we obtain the hadronic tensor

$$W_{\mu\nu} = t^{(-)}_{\mu\nu}\frac{1}{\pi}\,\Im\mathrm{m}\int_{-1}^{1}\mathrm{d}x\, C_0^{(-)}(x,x_{\mathrm{B}})\sum_q Q_q^2\, f^q(x)\,. \tag{3.140}$$

At this point, we can precede in two ways. Since the PDF is real valued, we can take the imaginary part of the hard scattering amplitude as done in Sec. 3.1.3. Second, we first evaluate the convolution and take the imaginary part afterward. Since the imaginary part is only contained in the outer region $x \in [-x_{\mathrm{B}}, x_{\mathrm{B}}]$, we adjust the integration and obtain

$$W_{\mu\nu} = t^{(-)}_{\mu\nu}\frac{1}{\pi}\,\Im\mathrm{m}\int_{x_{\mathrm{B}}}^{1}\mathrm{d}x\, C_0^{(-)}(x,x_{\mathrm{B}})\sum_q Q_q^2\,[q(x)+\bar{q}(x)]\,. \tag{3.141}$$

The latter approach has the advantage that its notation is very close to the notation of Compton form factors which we introduce in the next section.

3.2.4. Compton form factors

In analogy to the structure functions in DIS, we split off the Lorentz structure and introduce the quark Compton form factors (CFFs) consisting of the hard scattering amplitude and the GPD

$$\mathcal{F}^q\big(\xi,\Delta^2,\mathcal{Q}^2\big) \overset{\mathrm{LO}}{=} \int_{-1}^{1}\frac{\mathrm{d}x}{2\xi}\left[\frac{2(\xi-i\epsilon)}{\xi-x-i\epsilon} - \frac{2(\xi-i\epsilon)}{\xi+x-i\epsilon}\right]F^q\big(x,\eta,\Delta^2\big)\,, \qquad \mathcal{F}\in\{\mathcal{H},\mathcal{E}\}\,, \tag{3.142a}$$

$$\mathcal{F}^q\big(\xi,\Delta^2,\mathcal{Q}^2\big) \overset{\mathrm{LO}}{=} \int_{-1}^{1}\frac{\mathrm{d}x}{2\xi}\left[\frac{2(\xi-i\epsilon)}{\xi-x-i\epsilon} + \frac{2(\xi-i\epsilon)}{\xi+x-i\epsilon}\right]F^q\big(x,\eta,\Delta^2\big)\,, \qquad \mathcal{F}\in\{\widetilde{\mathcal{H}},\widetilde{\mathcal{E}}\}\,. \tag{3.142b}$$

For practical reasons, which become clear later, we pulled out a factor of 2ξ and decorated the generalized Bjorken variable ξ with an imaginary part $-i\epsilon$ to obtain the imaginary part according to Feynman's causality prescription. The Compton form factors, which enter the reduced Compton tensor (3.133) can be represented by the sum

$$\mathcal{F} = \sum_q Q_q^2\,\mathcal{F}^q \qquad \text{with } q\in\{u,d,s,c,\dots\}, \quad \mathcal{F}\in\{\mathcal{H},\mathcal{E},\widetilde{\mathcal{H}},\widetilde{\mathcal{E}}\}\,. \tag{3.143}$$

Since the convolution of the hard scattering amplitude and the GPD can not be resolved, the CFFs are the basic objects in a GPD analysis. In the rest of the section, we study its symmetry properties and perturbative expansion. We also give a convenient representation for the evolution.

3.2.4.1. Definite intrinsic parity

As visible in (3.142), the symmetry under the transformation $x \to -x$ is contained in the hard scattering part. Using GPDs with definite charge parity (2.14)

$$F^q(x,\eta,\Delta^2) = \frac{1}{2}\left[F^{q(+)}(x,\eta,\Delta^2) + F^{q(-)}(x,\eta,\Delta^2)\right] ,$$

and definite symmetry properties

$$F^{q(\pm)}(-x,\eta,\Delta^2) = \mp F^{q(\pm)}(x,\eta,\Delta^2) ,$$

we shift this symmetry to the GPDs.[7] The LO Compton form factor is then

$$\mathcal{F}^{q(+)}(\xi,\Delta^2,\mathcal{Q}^2) \overset{\text{LO}}{=} \int_{-1}^{1} \frac{\mathrm{d}x}{2\xi}\, {}^{\mathrm{q}}\hat{T}^{(0)}\left(\frac{\xi+x-i\epsilon}{2(\xi-i\epsilon)}\right) F^{q(+)}(x,\eta,\Delta^2) , \quad \mathcal{F} \in \{\mathcal{H},\mathcal{E},\widetilde{\mathcal{H}},\widetilde{\mathcal{E}}\} , \tag{3.144}$$

where the hard scattering amplitude is given by

$${}^{\mathrm{q}}T^{(0)}\left(\frac{\xi+x-i\epsilon}{2(\xi-i\epsilon)}\right) = \frac{2(\xi-i\epsilon)}{\xi-x-i\epsilon} . \tag{3.145}$$

The index q is used to stress the hard scattering amplitude involving a quark GPD, albeit it is equivalent for all quark flavors.

3.2.4.2. Perturbative expansion

In section 3.2.3, we derived the hard scattering amplitudes in leading order. Starting at NLO, also the gluon GPD contributes to DVCS. Concurrently, renormalization and factorization logarithms arise. Approximating the hard scattering amplitude up to NLO, we write

$$T\left(\tfrac{\xi+x}{2\xi}\middle|\, \alpha_{\mathrm{s}}(\mu_{\mathrm{R}}), \tfrac{\mathcal{Q}^2}{\mu_{\mathrm{F}}^2}\right) = T^{(0)}\left(\tfrac{\xi+x}{2\xi}\right) + \frac{\alpha_{\mathrm{s}}^2(\mu_{\mathrm{R}})}{2\pi}\, T^{(1)}\left(\tfrac{\xi+x}{2\xi}\middle|\, \tfrac{\mathcal{Q}^2}{\mu_{\mathrm{F}}^2}\right) , \tag{3.146}$$

where μ_{R} and μ_{F} are the renormalization and factorization scale, respectively. The requirement, that the hard scattering amplitude is independent of the renormalization scale manifests itself in the renormalization group equation

$$\left[\mu_{\mathrm{R}}\frac{\partial}{\partial\mu_{\mathrm{R}}} + \beta(\alpha_{\mathrm{s}})\frac{\partial}{\partial\alpha_{\mathrm{s}}}\right] T\left(\tfrac{\xi+x}{2\xi}\middle|\, \alpha_{\mathrm{s}}(\mu_{\mathrm{R}}), \tfrac{\mathcal{Q}^2}{\mu_{\mathrm{F}}^2}\right) = 0 . \tag{3.147}$$

[7] This reverts the definitions introduced in Eq. 3.123.

The running of the strong coupling is controlled by the equation

$$\mu \frac{\mathrm{d}}{\mathrm{d}\mu} \alpha_\mathrm{s}(\mu) = \beta_0 \frac{\alpha_\mathrm{s}^2(\mu)}{2\pi} + O(\alpha_\mathrm{s}^3) \quad \text{with} \quad \beta_0 = -\left(-\frac{2N_\mathrm{f}}{3} + 11\right) . \tag{3.148}$$

Therefore, the CFF in arbitrary order of perturbation theory can be written as

$$\mathcal{F}_\gamma^A(\xi, \Delta^2, \mathcal{Q}^2) = {}^A T\left(\tfrac{\xi+x-i\epsilon}{2(\xi-i\epsilon)}, \xi \,\middle|\, \alpha_\mathrm{s}(\mu_\mathrm{R}), \tfrac{\mathcal{Q}^2}{\mu_\mathrm{F}^2}\right) \overset{x}{\otimes} F^A(x, \eta, \Delta^2, \mu_\mathrm{F}^2) , \tag{3.149}$$

where the index A runs now also over the gluon contribution G, $A \in \{u^{(+)}, d^{(+)}, s^{(+)}, c^{(+)}, \ldots, \mathrm{G}\}$. The explicit dependence of the hard scattering amplitude on the generalized Bjorken variable ξ is important for the latter. For convenience, we define

$${}^\mathrm{G} T\left(\tfrac{\xi+x-i\epsilon}{2(\xi-i\epsilon)}, \xi \,\middle|\, \alpha_\mathrm{s}(\mu_\mathrm{R}), \tfrac{\mathcal{Q}^2}{\mu_\mathrm{F}^2}\right) \equiv \frac{1}{\xi} {}^\mathrm{G} T\left(\tfrac{\xi+x-i\epsilon}{2(\xi-i\epsilon)} \,\middle|\, \alpha_\mathrm{s}(\mu_\mathrm{R}), \tfrac{\mathcal{Q}^2}{\mu_\mathrm{F}^2}\right) . \tag{3.150}$$

Whereas in the quark channel, the explicit dependence on ξ can be neglected. For the integration over the momentum fraction x we use the abbreviation

$$f(x) \overset{x}{\otimes} g(x) \equiv \int_{-1}^{1} \frac{\mathrm{d}x}{2\xi} f(x)\, g(x) . \tag{3.151}$$

Adding the gluon contribution to the sum over quark CFF in (3.143), we write

$$\mathcal{F}_\gamma = \sum_A Q_A^2 \, \mathcal{F}^A , \tag{3.152}$$

where

$$Q_\mathrm{G}^2 = \frac{1}{N_\mathrm{f}} \sum_q Q_q^2 . \tag{3.153}$$

This basis of CFFs is denoted as the quark/gluon basis.

3.2.4.3. Evolution basis

Up to this point, we have represented the CFFs in the quark/gluon basis (3.143). For general notation, we use

$$\mathcal{F}_\gamma = \sum_A \hat{c}_\gamma^A \, \mathcal{F}_\gamma^A , \qquad A \in \{u^{(+)}, d^{(+)}, s^{(+)}, c^{(+)}, \ldots, \mathrm{G}\} , \qquad \mathcal{F} \in \{\mathcal{H}, \mathcal{E}, \widetilde{\mathcal{H}}, \widetilde{\mathcal{E}}\} , \tag{3.154}$$

where the index γ indicates the DVCS process. The coefficients $\hat{c}$ are obtained by comparison with (3.152)

$$\hat{c}_\gamma^{q(+)} = Q_q^2 , \qquad \hat{c}_\gamma^\mathrm{G} = Q_\mathrm{G}^2 . \tag{3.155}$$

As we will see in section D.1, the singlet and gluon GPD mix under evolution. In order to resolve the situation, we represent the quark GPDs by irreducible SU(N_f) multiplets (see Sec. 2.7). In the evolution basis the sum over CFFs is

$$\mathcal{F}_\gamma = \sum_A \hat{c}_\gamma^A \, \mathcal{F}_\gamma^A \,, \qquad A \in \{0^{(+)}, 3^{(+)}, 8^{(+)}, 15^{(+)}, \mathrm{G}\} \,. \tag{3.156}$$

The flavor singlet Compton form factor $\mathcal{F}^{0^{(+)}}$ mixes with the gluon one. On the other hand, the multiplets $3^{(+)}$, $8^{(+)}$ and $15^{(+)}$ evolve according to the non-singlet evolution operator (D.15). Following Sec. 2.7, the coefficients in the evolution basis are given by

$$\begin{aligned}
\hat{c}_\gamma^{0^{(+)}} &= \frac{1}{4}\left(\hat{c}_\gamma^u + \hat{c}_\gamma^d + \hat{c}_\gamma^s + \hat{c}_\gamma^c\right) = \frac{5}{18} \,, & \hat{c}_\gamma^{3^{(+)}} &= \frac{1}{2}\left(\hat{c}_\gamma^u - \hat{c}_\gamma^d\right) = \frac{1}{6} \,, \\
\hat{c}_\gamma^{8^{(+)}} &= \frac{1}{6}\left(\hat{c}_\gamma^u + \hat{c}_\gamma^d - 2\hat{c}_\gamma^s\right) = \frac{1}{18} \,, & \hat{c}_\gamma^{15^{(+)}} &= \frac{1}{12}\left(\hat{c}_\gamma^u + \hat{c}_\gamma^d + \hat{c}_\gamma^s - 3\hat{c}_\gamma^c\right) = -\frac{1}{18} \,.
\end{aligned} \tag{3.157}$$

To simplify the notation and the numerical treatment, the non-singlet contributions are merged into the non-singlet Compton form factor

$$\mathcal{F}^{\mathrm{NS}^{(+)}} = \hat{c}_\gamma^{3^{(+)}} \mathcal{F}^{3^{(+)}} + \hat{c}_\gamma^{8^{(+)}} \mathcal{F}^{8^{(+)}} + \hat{c}_\gamma^{15^{(+)}} \mathcal{F}^{15^{(+)}} = \frac{1}{6}\left(\mathcal{F}^{u^{(+)}} - \mathcal{F}^{d^{(+)}} - \mathcal{F}^{s^{(+)}} + \mathcal{F}^{c^{(+)}}\right) . \tag{3.158}$$

For the quark singlet contribution, it is common to use the notation

$$\mathcal{F}_\gamma^\Sigma = \hat{c}_\gamma^{0^{(+)}} \mathcal{F}_\gamma^{0^{(+)}} \,. \tag{3.159}$$

Summarized with the gluon contribution, we obtain the singlet contribution

$$\mathcal{F}_\gamma^\mathrm{S} = \mathcal{F}_\gamma^\Sigma + \hat{c}_\gamma^\mathrm{G} \mathcal{F}_\gamma^\mathrm{G} = \hat{c}_\gamma^{0^{(+)}} \mathcal{F}_\gamma^{0^{(+)}} + \hat{c}_\gamma^\mathrm{G} \mathcal{F}^\mathrm{G} \,. \tag{3.160}$$

To solve the mixing problem, we take advantage of the equality of the quark singlet and gluon coefficient (3.153) and define the singlet coefficient as

$$\hat{c}_\gamma^\mathrm{S} = \hat{c}_\gamma^{0^{(+)}} = \hat{c}_\gamma^\mathrm{G} \,. \tag{3.161}$$

This enables us, to write down the singlet CFF in a matrix notation. We combine the singlet GPD and the gluon GPD in a vector

$$\boldsymbol{F}(x,\eta,\Delta^2) = \begin{pmatrix} F^{0^{(+)}} \\ F^\mathrm{G} \end{pmatrix}(x,\eta,\Delta^2) \,. \tag{3.162}$$

Accordingly, the hard scattering amplitudes for the quark and gluon CFF are written as a row vector

$$\boldsymbol{T}\left(\tfrac{\xi+x}{2\xi},\xi\right) = \left({}^\mathrm{q}T\left(\tfrac{\xi+x}{2\xi}\right) \quad \tfrac{1}{\xi}\,{}^\mathrm{G}T\left(\tfrac{\xi+x}{2\xi}\right)\right), \tag{3.163}$$

where the extra factor of $1/\xi$ originates from the specific characteristics of the gluon GPD definition (2.6). Thus, the singlet Compton form factor in matrix notation reads

$$\mathcal{F}_\gamma^\mathrm{S}(\xi,\Delta^2,\mathcal{Q}^2) = \boldsymbol{T}\left(\tfrac{\xi+x-i\epsilon}{2(\xi-i\epsilon)},\xi\right) \overset{x}{\otimes} \boldsymbol{F}(x,\eta,\Delta^2) \,. \tag{3.164}$$

Employing the singlet CFF, the initial sum (3.154) reads

$$\mathcal{F}_\gamma = \hat{c}_\gamma^\mathrm{S} \mathcal{F}_\gamma^\mathrm{S} + \mathcal{F}_\gamma^\mathrm{NS} \,. \tag{3.165}$$

3.2.5. Cross section

Before expressing the cross section in terms of CFFs, let us recapitulate the analysis up to this point. In section 3.2.2 we derived the cross section for the electroproduction of a photon in dependence of the Compton amplitude (3.105). We parametrized the amplitude using twist-2 GPDs at LO of perturbation theory (3.133). To simplify the expressions, we introduced several Compton form factors, which are the basic irreducible building blocks involving GPDs, see Sec. 3.2.4. Then, we studied their symmetry properties and introduced their perturbative expansion . Now we combine the results of all previous sections, to write down the cross section in terms of twist-2 Compton form factors. Recall the DVCS scattering amplitude (3.98)

$$|\mathcal{T}_{\text{DVCS}}|^2 = L^\mu L^\dagger_\alpha T_{\mu\beta} T^{\beta\alpha}\,,$$

where the reduced Compton tensor is given in (3.133). Evaluating the products of its Lorentz structures (3.134) one get the three different results

$$t^{(-)}_{\mu\beta}\, t^{\beta\alpha}_{(-)} \approx g^{\perp\alpha}_\mu\,, \qquad t^{(+)}_{\mu\beta} \left(t^{\beta\alpha}_{(+)}\right)^* \approx g^{\perp\alpha}_\mu\,, \qquad t^{(+)}_{\mu\beta} \left(t^{\beta\alpha}_{(-)}\right)^* \approx i\epsilon^{\perp\alpha}_\mu\,. \tag{3.166}$$

Contracting the terms above with the leptonic tensor in the unpolarized case leads to

$$g^{\mu\alpha}_\perp\, L_\mu L^\dagger_\alpha = \frac{2(2-2y+y^2)}{y^2\mathcal{Q}^2}\,, \qquad i\epsilon^{\mu\alpha}_\perp\, L_\mu L^\dagger_\alpha = 0\,, \tag{3.167}$$

Thus, the part from the transverse polarization of the totally antisymmetric tensor vanishes for unpolarized electrons and products of vector and axial-vector CFFs are absent. To evaluate the products of nucleon spinor bilinear forms, we need to evaluate

$$\sum_{S_2} \bar{U}(P_1,S_1)\Gamma_1 U(P_2,S_2)\bar{U}(P_2,S_2)\Gamma_2 U(P_1,S_1)\,, \tag{3.168}$$

where the Lorentz structures $\Gamma_{1,2}$ can be read of from the possible GPD bilinear forms. Recall from (2.3)

$$\begin{aligned} h^+ &= \bar{U}(P_2)\gamma^+ U(P_1)\,, & e^+ &= \bar{U}(P_2)\frac{i\sigma^{+\Delta}}{2M}U(P_1)\,,\\ \tilde{h}^+ &= \bar{U}(P_2)\gamma^+\gamma^5 U(P_1)\,, & \tilde{e}^+ &= \bar{U}(P_2)\frac{-\Delta^+\gamma^5}{2M}U(P_1)\,. \end{aligned}$$

The bilinear e^+ can be decomposed with the help of the Gordon identity

$$\bar{U}(P_2,S_2)\gamma^\mu U(P_1,S_1) = \bar{U}(P_2,S_2)\left[\frac{P^\mu}{2M} + \frac{i\sigma^{\mu\nu}\Delta_\nu}{2M}\right]U(P_1,S_1)\,. \tag{3.169}$$

Thus, the occurring Lorentz structures[8] are

$$\frac{\gamma^+}{P^+}\,, \qquad \frac{P^+}{2MP^+}\,, \qquad \left(\to \frac{i\sigma^{+\Delta}}{2MP^+}\right), \qquad \frac{\gamma^+\gamma_5}{P^+}\,, \qquad \frac{\Delta^+\gamma^5}{2MP^+}\,. \tag{3.170}$$

Γ_1 \ Γ_2	γ^+	$\frac{P^+}{2M}$	$\frac{i\sigma^{+\Delta}}{2M}$	$\gamma^+\gamma_5$	$\frac{\Delta^+\gamma^5}{2M}$
γ^+	$1-\xi^2$	1	$-\xi^2$		
$\frac{P^+}{2M}$	1	$1-\frac{\Delta^2}{4M^2}$			
$\frac{i\sigma^{+\Delta}}{2M}$	$-\xi^2$		$-\xi^2-\frac{\Delta^2}{4M^2}$		
$\gamma^+\gamma_5$				$1-\xi^2$	$-\xi^2$
$-\frac{\Delta^+\gamma^5}{2M}$				$-\xi^2$	$-\xi^2\frac{\Delta^2}{4M^2}$

Table 3.1.: Evaluation of the product of nucleon spinor bilinear forms. We omitted the term P^+ in the nominator of the gamma structures Γ_1 and Γ_2 for a clear presentation.

The result for the summation over the spin of the recoiled nucleon is given in table 3.1. Therefore, the squared vector and axial-vector Compton form factors read

$$\begin{aligned}\left(\frac{h^+}{P^+}\mathcal{H}+\frac{e^+}{P^+}\mathcal{E}\right)^2 &= \left(1-\xi^2\right)\mathcal{H}\mathcal{H}^*-\xi^2\left(\mathcal{H}\mathcal{E}^*+\mathcal{E}\mathcal{H}^*\right)-\left(\xi^2+\frac{\Delta^2}{4M^2}\right)\mathcal{E}\mathcal{E}^*\,,\\ \left(\frac{\tilde{h}^+}{P^+}\widetilde{\mathcal{H}}+\frac{\tilde{e}^+}{P^+}\widetilde{\mathcal{E}}\right)^2 &= \left(1-\xi^2\right)\widetilde{\mathcal{H}}\widetilde{\mathcal{H}}^*-\xi^2\left(\widetilde{\mathcal{H}}\widetilde{\mathcal{E}}^*+\widetilde{\mathcal{E}}\widetilde{\mathcal{H}}^*\right)-\xi^2\frac{\Delta^2}{4M^2}\widetilde{\mathcal{E}}\widetilde{\mathcal{E}}^*\,.\end{aligned} \tag{3.171}$$

Combining the result from the Lorentz structures (3.167) and the one of the Dirac bilinears (3.171) the DVCS scattering amplitudes casts into the form

$$\begin{aligned}|\mathcal{T}_{\rm DVCS}|^2 =&\frac{2(2-2y+y^2)}{y^2\mathcal{Q}^2(2-x_{\rm B})^2}\Bigg[4(1-x_{\rm B})\left(\mathcal{H}\mathcal{H}^*+\widetilde{\mathcal{H}}\widetilde{\mathcal{H}}^*\right)-x_{\rm B}^2\left(\mathcal{H}\mathcal{E}^*+\mathcal{E}\mathcal{H}^*+\widetilde{\mathcal{H}}\widetilde{\mathcal{E}}^*+\widetilde{\mathcal{E}}\widetilde{\mathcal{H}}^*\right)\\ &-\left(x_{\rm B}^2+(2-x_{\rm B})^2\frac{\Delta^2}{4M^2}\right)\mathcal{E}\mathcal{E}^*-x_{\rm B}^2\frac{\Delta^2}{4M^2}\widetilde{\mathcal{E}}\widetilde{\mathcal{E}}^*\Bigg]\,.\end{aligned} \tag{3.172}$$

Since the scaling variable ξ is not directly measurable in an experiments, we expressed it in terms of the Bjorken scaling variable $x_{\rm B}$ using (3.81). For the polarized result and higher twist contributions see [BMK02, BR05]. Let us recall the cross section formula (3.105):

$$\frac{{\rm d}\sigma^{eN\to e\gamma N}}{{\rm d}x_{\rm B}{\rm d}y{\rm d}\Delta^2{\rm d}\phi_{\rm N}}=\frac{\alpha_{\rm em}^3 x_{\rm B}y}{8\pi\mathcal{Q}^2\sqrt{1+\epsilon^2}}\left|\mathcal{T}_{\rm DVCS}\right|^2\,.$$

Since we are only interested in the leading twist-2 contribution, we integrate out the azimuthal angle $\phi_{\rm N}$ of the recoiled nucleon. In addition, the H1 and ZEUS collaboration published the photo-production cross section. Thus, we first express the relative energy loss of the electron by the squared of momentum transfer $\mathcal{Q}^2$ utilizing the relation (3.81)

$$y=\frac{\mathcal{Q}^2}{x_{\rm B}s}\quad\frac{1}{{\rm d}y}=x_{\rm B}s\frac{1}{{\rm d}\mathcal{Q}^2}\,. \tag{3.173}$$

[8] The factor P^+ stems form the boost invariant form of GPDs (2.7, 2.9).

The resulting cross section is

$$\frac{\mathrm{d}\sigma^{eN\to e\gamma N}}{\mathrm{d}x_{\mathrm{B}}\mathrm{d}\mathcal{Q}^2\mathrm{d}\Delta^2} = \frac{\alpha_{\mathrm{em}}^3 x_{\mathrm{B}} y^2}{4\mathcal{Q}^4\sqrt{1+\epsilon^2}} \left|\mathcal{T}_{\mathrm{DVCS}}\right|^2 .$$

To completely remove the electron contribution we have to remove the phase space of the outgoing electron, the term stemming from the leptonic currents, the electromagnetic coupling and the flux factor. Instead, we add the term from the virtual photon and the photon flux factor according to Hand's convention [Han63]. Taking everything together, we obtain the factor

$$\frac{g_\perp^{\mu\alpha}\epsilon_\mu\epsilon_\alpha^*}{P_1.q_1}\left(e^2\frac{g_\perp^{\mu\alpha}L_\mu L_\alpha^\dagger}{P_1.k_1}\cdot\frac{\mathrm{d}^3k_2}{(2\pi)^3 2\omega_2}\right)^{-1} = \frac{1}{\alpha_{\mathrm{em}}}\cdot\frac{2\pi}{2-2y+y^2}\frac{x_{\mathrm{B}}}{\mathrm{d}x_{\mathrm{B}}}\frac{\mathcal{Q}^2}{\mathrm{d}\mathcal{Q}^2}, \tag{3.174}$$

where the individual terms are

$$g_\perp^{\mu\alpha}\epsilon_\mu\epsilon_\alpha^* = 1\,, \qquad g_\perp^{\mu\alpha}\,L_\mu L_\alpha^\dagger = \frac{2(2-2y+y^2)}{y^2\mathcal{Q}^2}\,, \tag{3.175}$$

and

$$\frac{\mathrm{d}^3k_2}{2\omega_2} = \frac{\pi y}{2x_{\mathrm{B}}}\mathrm{d}x_{\mathrm{B}}\mathrm{d}\mathcal{Q}^2\,, \qquad P_1.q_1 = \frac{\mathcal{Q}^2}{2x_{\mathrm{B}}}\,, \qquad P_1.k_1 = \frac{\mathcal{Q}^2}{2yx_{\mathrm{B}}}\,. \tag{3.176}$$

Therefore, the cross section for the photo-production of a real photon together with the DVCS scattering amplitude (3.172) reads

$$\frac{\mathrm{d}\sigma^{\gamma^*N\to\gamma N}}{\mathrm{d}\Delta^2} = \frac{\pi\alpha_{\mathrm{em}}^2}{\mathcal{Q}^4\sqrt{1+\epsilon^2}}\frac{x_{\mathrm{B}}^2}{(2-x_{\mathrm{B}})^2}\left[\ldots\right]. \tag{3.177}$$

where the ellipsis denotes the term in the square brackets in (3.172).
Finally, the experiments considered in this work measure the cross section in the small-x_{B} kinematics. Expanding the cross section in x_{B} around the vicinity of zero gives

$$\frac{\mathrm{d}\sigma^{\gamma^*N\to\gamma N}}{\mathrm{d}\Delta^2} = \frac{\pi\alpha_{\mathrm{em}}^2 x_{\mathrm{B}}^2}{\mathcal{Q}^4}\left[|\mathcal{H}|^2 + |\widetilde{\mathcal{H}}|^2 - \frac{\Delta^2}{4M^2}|\mathcal{E}|^2\right]. \tag{3.178}$$

To present the result in the same form as the H1 and ZEUS collaboration, we employ the invariant mass $W=(P_1+q_1)^2$ instead of the Bjorken variable x_{B}. The transformation is

$$W^2 = M^2 + q_1^2 + 2P_1.q_1 = M^2 - \mathcal{Q}^2 + \frac{\mathcal{Q}^2}{x_{\mathrm{B}}} \quad \to x_{\mathrm{B}} = \frac{\mathcal{Q}^2}{W^2+\mathcal{Q}^2-M^2}\,. \tag{3.179}$$

Thus,

$$\frac{\mathrm{d}\sigma^{\gamma^*N\to\gamma N}}{\mathrm{d}\Delta^2} = \frac{\pi\alpha_{\mathrm{em}}^2}{(W^2+\mathcal{Q}^2)^2}\left[|\mathcal{H}|^2 + |\widetilde{\mathcal{H}}|^2 - \frac{\Delta^2}{4M^2}|\mathcal{E}|^2\right]. \tag{3.180}$$

This is the final formula, which we employ in the data analysis in Ch. 7.
In this section, we calculated the lepton- and photon-production cross section of a real photon at LO accuracy of perturbation theory involving Compton form factors of leading twist-2. We took into account transverse degree of freedom of the exchanged parton and obtained the gauge invariant expression of the Compton amplitude.

3.3. Deeply virtual meson production

Deeply virtual meson production belongs to the class of hard exclusive processes that provides access to generalized parton distributions. The process is in various ways similar to DVCS. A lepton is scattered of a nucleon target via the exchange of a virtual photon. It interacts with the target in such a way, that a nucleon and a meson are produced. Depending on the the particular meson, the nucleon in the in and outgoing state may be different. In this work, we focus on the scattering of an electron on a proton target. Schematically, the reaction is

$$e^-(k_1) + P(P_1) = e^-(k_2) + N(P_2) + M(q_2)\,, \tag{3.181}$$

where the N is a outgoing nucleon. The reaction is depicted in figure 3.9.

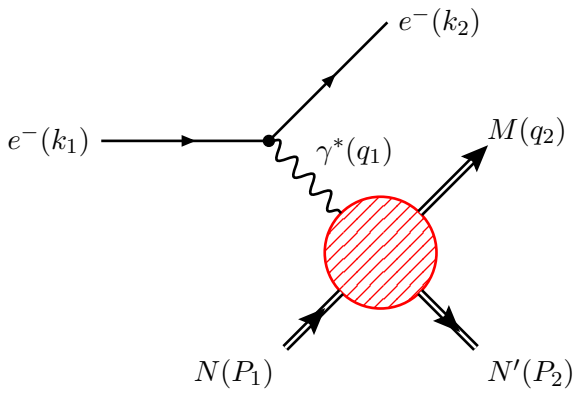

Figure 3.9.: Deeply virtual meson production.

The factorization of the DVMP amplitude was shown in [CFS97] for light (pseudoscalar) and longitudinal vector mesons. In leading order of $1/\mathcal{Q}$, the DVMP amplitude factorized in a hard scattering part and two nonperturbative distributions. The transition from the nucleon target to the nucleon in the final state is described by twist-2 GPDs, whereas a twist-2 distribution amplitude specifies the formation of the particular meson. Beyond leading order, the factorization may be broken by final state interaction. Thus, the suitability of DVMP for a GPDs analysis of higher twist remains unclear.
At LO accuracy of perturbation theory, numerous channels have been studied [FKS96,Rad96a, FKS98, MPW98, MPW99, MPR99, FPSV00, FPPS99]. The phenomenological description can be extended to the level of NLO perturbation theory [BM01, ISK04]. The hard scattering amplitudes at NLO accuracy in momentum fraction representation are already known. Either from analytic continuation [BM01, DK07] of the diagrammatical result [MNP99] for the pion form factor or the diagrammatical evaluation in [ISK04]. However, the present form is not advantageous for a global GPD analysis.
In the present section, we introduce the properties and flavor content of various pseudoscalar and vector mesons. We focus our considerations on the vector mesons ρ^0, ω and ϕ. Throughout this section, the expressions for these three mesons are complete, whereas for other mesons they can be obtained easily following our considerations. We investigate the kinematics of the DVMP cross section for the single photon exchange in the laboratory frame analog to

DVCS. This is followed by a detailed analysis of the dynamics in LO accuracy of perturbation theory. We introduce TFFs given as the convolution of the hard scattering amplitude, the two nonperturbative distributions as the basic irreducible object containing GPDs. We study their properties and perturbative expansion as well. In the last part of the section, we present the results for the hard scattering amplitudes at the level of NLO perturbation theory following [MLPKS14].

3.3.1. Preliminaries

In the quark model, the general Fock state expansion for mesons can be written as

$$\big|M\big\rangle = c_M^{ij}\,\big|q_i\bar{q}_j\big\rangle\ , \tag{3.182}$$

where c_M^{ij} are Clebsch-Gordon coefficients which we denote here as Fock coefficients. Due to the prove of factorization we restrict our analysis on vector mesons (V) and pseudoscalar mesons (PS). For a longitudinally polarized vector meson, we introduce the symbol V_L. Let us first list the mesons of interest in this work. We consider the neutral vector mesons (V^0)

$$|\rho^0\rangle = \frac{1}{\sqrt{2}}\left(|u\bar{u}\rangle - |d\bar{d}\rangle\right)\ , \qquad |\omega\rangle = \frac{1}{\sqrt{2}}\left(|u\bar{u}\rangle + |d\bar{d}\rangle\right)\ , \qquad |\phi\rangle = |s\bar{s}\rangle\,. \tag{3.183}$$

The corresponding Fock coefficients are

$$c_{\rho^0} = \frac{1}{\sqrt{2}}\begin{pmatrix}1 & 0\\ 0 & 1\end{pmatrix}, \quad c_\omega = \frac{1}{\sqrt{2}}\begin{pmatrix}1 & 0\\ 0 & -1\end{pmatrix}, \quad c_\phi = \frac{1}{\sqrt{2}}\begin{pmatrix}0 & 0 & 0\\ 0 & 0 & 0\\ 0 & 0 & 1\end{pmatrix}. \tag{3.184}$$

We also consider ρ^+ as an example for a charged vector meson ($V^\pm$), which possesses a non-diagonal flavor content

$$|\rho^+\rangle = |u\bar{d}\rangle\,, \qquad c_{\rho^+} = \begin{pmatrix}0 & 1\\ 0 & 0\end{pmatrix}. \tag{3.185}$$

This process will introduce GPDs with flavor changing transitions. These GPDs can be reduced to conventional flavor diagonal GPDs relying on SU(3) flavor symmetry. In the case above, the proton target changes into a neutron.
On the other hand, we consider the following neutral (PS^0) and charged ($PS^\pm$) pseudoscalar mesons

$$\begin{aligned} |\pi^0\rangle &= \frac{1}{\sqrt{2}}\left(|u\bar{u}\rangle - |d\bar{d}\rangle\right), & |\eta^{(0)}\rangle &= \frac{1}{\sqrt{3}}\left(|u\bar{u}\rangle + |d\bar{d}\rangle + |s\bar{s}\rangle\right),\\ |\pi^+\rangle &= |u\bar{d}\rangle, & |\eta^{(8)}\rangle &= \frac{1}{\sqrt{6}}\left(|u\bar{u}\rangle + |d\bar{d}\rangle - 2|s\bar{s}\rangle\right). \end{aligned} \tag{3.186}$$

Their respective Fock coefficients are

$$c_{\pi^0} = \frac{1}{\sqrt{2}}\begin{pmatrix}1 & 0\\ 0 & 1\end{pmatrix}, \quad c_{\eta^{(0)}} = \frac{1}{\sqrt{3}}\begin{pmatrix}1 & 0 & 0\\ 0 & 1 & 0\\ 0 & 0 & 1\end{pmatrix}, \quad c_{\eta^{(8)}} = \frac{1}{\sqrt{6}}\begin{pmatrix}1 & 0 & 0\\ 0 & 1 & 0\\ 0 & 0 & -2\end{pmatrix}, \quad c_{\pi^+} = \begin{pmatrix}0 & 1\\ 0 & 0\end{pmatrix}. \tag{3.187}$$

Due to the meson-pole contribution in the GPD $\tilde{E}$ the SU(3) flavor symmetry is strongly violated and we can only reduce the GPD $\tilde{H}$ to flavor diagonal GPDs. Note, we do not discuss the η/η' mixing problem and rather provide only the expressions for the pure octet and singlet states. Furthermore, the singlet state $\eta^{(0)}$ possesses a two gluon component, which is beyond the scope of our considerations. One may also include the neutral and charged kaon production, where the targeted proton transforms into a hyperon. Table 3.2 gives overview of the mesons and their respective properties. Various of these DVMP channels have been

meson	J^{PC}	quark content	process	SU(3)	TFFs
ρ^0	1^{--}	$\frac{1}{\sqrt{2}}\left(\lvert u\bar{u}\rangle - \lvert d\bar{d}\rangle\right)$	$\rho^0_{\mathrm{L}} p$		$\mathcal{H}^{q(+)}, \mathcal{E}^{q(+)}, \mathcal{H}^{\mathrm{G}}, \mathcal{E}^{\mathrm{G}}$
ω	1^{--}	$\frac{1}{\sqrt{2}}\left(\lvert u\bar{u}\rangle + \lvert d\bar{d}\rangle\right)$	$\omega_{\mathrm{L}} p$		$\mathcal{H}^{q(+)}, \mathcal{E}^{q(+)}, \mathcal{H}^{\mathrm{G}}, \mathcal{E}^{\mathrm{G}}$
ϕ	1^{--}	$\lvert s\bar{s}\rangle$	$\phi_{\mathrm{L}} p$		$\mathcal{H}^{q(+)}, \mathcal{E}^{q(+)}, \mathcal{H}^{\mathrm{G}}, \mathcal{E}^{\mathrm{G}}$
ρ^+	1^{-}	$\lvert u\bar{d}\rangle$	$\rho^+_{\mathrm{L}} n$	$F^u - F^d$	$\mathcal{H}^{q(\pm)}, \mathcal{E}^{q(\pm)}$
π^0	0^{-+}	$\frac{1}{\sqrt{2}}\left(\lvert u\bar{u}\rangle - \lvert d\bar{d}\rangle\right)$	$\rho^0 p$		$\widetilde{\mathcal{H}}^{q(-)}, \widetilde{\mathcal{E}}^{q(-)}$
$\eta^{(0)}$	0^{-+}	$\frac{1}{\sqrt{3}}\left(\lvert u\bar{u}\rangle + \lvert d\bar{d}\rangle + \lvert s\bar{s}\rangle\right)$	$\eta^{(0)} p$		$\widetilde{\mathcal{H}}^{q(-)}, \widetilde{\mathcal{E}}^{q(-)}$
$\eta^{(8)}$	0^{-+}	$\frac{1}{\sqrt{6}}\left(\lvert u\bar{u}\rangle + \lvert d\bar{d}\rangle - 2\lvert s\bar{s}\rangle\right)$	$\eta^{(8)} p$		$\widetilde{\mathcal{H}}^{q(-)}, \widetilde{\mathcal{E}}^{q(-)}$
π^+	0^{-}	$\lvert u\bar{d}\rangle$	$\pi^+ n$	$H^u - H^d$	$\widetilde{\mathcal{H}}^{q(\pm)}, \widetilde{\mathcal{E}}^{q(\pm)}$

Table 3.2.: Properties of specific mesons. The process denotes the result of the photoproduction $\gamma^* p \to \ldots$.

considered, see [BR05] for LO factorization formulae.
To obtain further insights, we introduce discrete t-channel quantum numbers. Consider the t-channel reaction, where a photon scattered on a $q\bar{q}$ or gg described by GPDs and forms a meson:

$$\gamma^* q\bar{q}(gg) \to M^0. \tag{3.188}$$

From charge parity conservation, we realize that the $q\bar{q}$ state has to satisfy

$$C = C_\gamma \, C_{M^0} = -C_{M^0}, \tag{3.189}$$

where the charge parity of the photon is $C_\gamma = -1$. The charge parity of the particular meson can be read off from the nomenclature for the total angular momentum, parity and charge parity J^{PC}, see Tab. 3.2. Since the charge parity of the gluon state is $C_{gg} = 1$, only neutral vector mesons (1^{--}) contain the contribution involving a gluon GPD. On the same lines, we realize, that there are no gg Fock states in neutral vector mesons. The CP quantum number of the $q\bar{q}$ state is given by

$$CP = C_\gamma P_\gamma \cdot C_{M^0} P_{M^0} = C_{M^0} P_{M^0}\,, \tag{3.190}$$

since the photon has parity is $P_\gamma = -1$. Therefore, the production of neutral vector mesons is described by GPDs with even charge parity $H^{q(+)}, E^{q(+)}, H^{\mathrm{G}}, E^{\mathrm{G}}$, whereas the production of neutral pseudoscalar mesons is described by the odd intrinsic parity GPDs $H^{q(-)}, E^{q(-)}$.

3.3.2. Kinematics

The cross section for exclusive electroproduction of a mesons from a nucleon target is given by

$$\mathrm{d}\sigma^{eN\to eN'M} = \frac{1}{4M\omega_1}\mathrm{d}\Pi_3\,|\mathcal{M}(eN\to eN'M)|^2\cdot 2\pi\,\delta^{(4)}(P_1+q_1-P_2-q_2)\;, \tag{3.191}$$

with the flux factor $4M\omega_1$ as in DVCS, see Sec. 3.2.2. The corresponding particle four-momenta are equivalent to DVCS and we display them in figure 3.9. For the derivation of the invariant matrix elements $\mathcal{M}$ we write down the iT-matrix

$$\begin{aligned}\left\langle \mathrm{k_2 q_2 P_2}|iT|\mathrm{k_1 P_1}\right\rangle = (-ie)^2\int \mathrm{d}^4y\int \mathrm{d}^4z\\ \times\left\langle \mathrm{k_2 q_2 P_2}|\,\bar\psi(y)\not{A}(y)\psi(y)\cdot Q_q\bar\psi_q(z)\not{A}(z)\psi_q(z)\,|\mathrm{k_1 P_1}\right\rangle,\end{aligned} \tag{3.192}$$

where the sum over the quark flavors q is suppressed for brevity. In contrast to DVCS, due to the missing real photon in the final state the leading contribution of the lepton-hadron interaction is proportional second-order of the electromagnetic coupling constant e. Hence the numerically larger cross section in comparison to DVCS. We restrict our considerations to the single photon exchange, since the electromagnetic coupling constant is much smaller than the strong one. By contracting the two photon fields (A.5), the iT-matrix splits up in the leptonic and hadronic part, namely

$$\left\langle \mathrm{k_2 q_2 P_2}|iT|\mathrm{k_1 P_1}\right\rangle = \frac{ie^2}{q_1^2+i\epsilon}\bar u(k_2)\gamma^\mu u(k_1)\int \mathrm{d}^4z\; e^{-iq_1z}\left\langle \mathrm{P_2}|j_\mu(z)|\mathrm{P_1}\right\rangle. \tag{3.193}$$

Therefore, using the leptonic current[9] (3.13), the invariant matrix element becomes

$$i\mathcal{M}(eN\to eN'M) = e^2L_\mu A^\mu\,, \tag{3.194}$$

where we employed the transition amplitude

$$A_\mu = \int\mathrm{d}^4z\; e^{-iq_1z}\left\langle \mathrm{q_2P_2}|j_\mu(z)|\mathrm{P_1}\right\rangle = i(2\pi)^4\delta^{(4)}(P_1+q_1-P_2-q_2)\,\mathcal{A}_\mu\,. \tag{3.195}$$

Analog to DVCS, we introduced the reduced transition amplitude $\mathcal{A}_\mu$ by separation of the δ-function of the four-momentum conservation. Utilizing the same set of variables as in DVCS and the three-body phase space (B.14) the cross section for the electroproduction of a meson reads

$$\mathrm{d}\sigma^{eN\to eN'M} = \frac{\alpha_{\mathrm{em}}^2 x_{\mathrm{B}}y}{32\pi^2\mathcal{Q}^2\sqrt{1+\epsilon^2}}\,|L_\mu\mathcal{A}^\mu|^2\,\mathrm{d}x_{\mathrm{B}}\mathrm{d}y\mathrm{d}\Delta^2\mathrm{d}\phi_{\mathrm{N}}\,. \tag{3.196}$$

[9] For DVMP we have to make the substitution $q\to q_1$.

3.3.3. Dynamics

3.3.3.1. Flavor non-singlet channel

The reduced transition amplitude for the electroproduction of mesons as stated in equation (3.195) reads

$$A_\mu = \int \mathrm{d}^4 z \, e^{-iq_1 z} \langle \mathrm{q_2 P_2} | j_\mu(z) | \mathrm{P_1} \rangle = i(2\pi)^4 \delta^{(4)}(P_1 + q_1 - P_2 - q_2) \, \mathcal{A}_\mu \, .$$

The leading contribution is of order $\mathcal{O}(\alpha_\mathrm{s})$. Thus,

$$\begin{aligned} A_\mu =& (-ig)^2 \int \mathrm{d}^4 z \int \mathrm{d}^4 y \int \mathrm{d}^4 w \, e^{-iq_1 z} \\ & \times \langle \mathrm{q_2 P_2} | Q_q \bar{\psi}_q^a(z) \gamma_\mu \psi_q^a(z) \cdot t^A_{bc} \, \bar{\psi}_g^b(y) \not{A}^A(y) \psi_g^c(y) \cdot t^B_{de} \, \bar{\psi}_h^d(w) \not{A}^B(w) \psi_h^e(w) | \mathrm{P_1} \rangle \, . \end{aligned} \tag{3.197}$$

The matrices t^A are the Gell-Mann matrices λ^A divided by two. The lower indices on the spinor fields denote the quark flavor. The remaining indices are the matrix indices of the Gell-Mann matrices (SU(3) color gauge group). For brevity, we do not display the sums over the flavor indices q, g and h, but always imply their presence. As depicted in figure 3.10 at LO there is a one gluon exchange. Contracting both gluon fields (A.3) leads to

$$\begin{aligned} A_\mu =& \, ig^2 \, Q_q \, t^A_{bc} t^A_{de} \int \mathrm{d}^4 z \int \mathrm{d}^4 y \int \mathrm{d}^4 w \int \frac{\mathrm{d}^4 l}{(2\pi)^4} \, e^{-iq_1 z} e^{-il(y-w)} \frac{1}{l^2 + i\epsilon} \\ & \times \langle \mathrm{q_2 P_2} | \bar{\psi}_q^a(z) \gamma_\mu \psi_q^a(z) \cdot \bar{\psi}_g^b(y) \gamma_\alpha \psi_g^c(y) \cdot \bar{\psi}_h^d(w) \gamma^\alpha \psi_h^e(w) | \mathrm{P_1} \rangle \, , \end{aligned} \tag{3.198}$$

where l denotes the four-momentum of the exchanged gluon. For the parametrization of the cross section by means of GPDs and DAs, we have to contract two quark fields in such a way, that the resulting diagram is connected. Thereby, we only consider contractions between fields at the z and y, hence the amplitude is symmetric under the exchange of y and w. We obtain the following two structures $\boxed{1}$ and $\boxed{2}$

$$\begin{aligned} A_\mu =& -g^2 \, Q_q \, t^A_{bc} t^A_{de} \int \mathrm{d}^4 z \int \mathrm{d}^4 y \int \mathrm{d}^4 w \int \frac{\mathrm{d}^4 l}{(2\pi)^4} \int \frac{\mathrm{d}^4 k}{(2\pi)^4} \, e^{-iq_1 z} e^{-il(y-w)} \frac{1}{l^2 + i\epsilon} \frac{1}{k^2 + i\epsilon} \\ \boxed{1} & \times e^{-ik(z-y)} \, \langle \mathrm{q_2 P_2} | \bar{\psi}_q^b(z) \gamma_\mu \not{k} \gamma_\alpha \psi_q^c(y) \cdot \bar{\psi}_h^d(w) \gamma^\alpha \psi_h^e(w) | \mathrm{P_1} \rangle \\ \boxed{1} & \times e^{-ik(y-z)} \, \langle \mathrm{q_2 P_2} | \bar{\psi}_q^b(y) \gamma_\alpha \not{k} \gamma_\mu \psi_q^c(z) \cdot \bar{\psi}_h^d(w) \gamma^\alpha \psi_h^e(w) | \mathrm{P_1} \rangle \, . \end{aligned} \tag{3.199}$$

To parametrize the quark fields with GPDs and a DA, we apply a Fierz transformation [Fie37] of the two matrix elements in the previous equation. The two structures above transform into

$$\begin{aligned} \boxed{1} & \; -\frac{1}{16} \mathrm{Tr}\left(\gamma^\alpha \gamma_\sigma \gamma_\mu \not{k} \gamma_\alpha \gamma_\rho\right) \; \bar{\psi}_h^d(w) \gamma^\rho (\gamma^5) \psi_q^c(y) \cdot \bar{\psi}_q^b(z) \gamma^\sigma (\gamma^5) \psi_h^e(w) \, , \\ \boxed{2} & \; -\frac{1}{16} \mathrm{Tr}\left(\gamma^\alpha \gamma_\sigma \gamma_\alpha \not{k} \gamma_\mu \gamma_\rho\right) \; \bar{\psi}_h^d(w) \gamma^\rho (\gamma^5) \psi_q^c(z) \cdot \bar{\psi}_q^b(y) \gamma^\sigma (\gamma^5) \psi_h^e(w) \, . \end{aligned} \tag{3.200}$$

We also included the additional γ^5-matrix Lorentz structure for pseudoscalar mesons in brackets. In structure $\boxed{1}$, the momentum flow in the quark propagator is always from the y-vertex

to the z-vertex and vice versa for the second structure. Inserting the Fierz transformation (3.200) into (3.199), we can identify both of the quark operators with the GPD or DA, respectively. Table 3.3 shows the possibilities with the corresponding Feynman diagrams. This identification results in four different Feynman diagrams (see Fig. 3.10).

structure	$\bar{\psi}_h^d(w)\gamma^\rho(\gamma^5)\psi_q^c(y)$	$\bar{\psi}_q^b(z)\gamma^\sigma(\gamma^5)\psi_h^e(w)$	diagram
1	GPD	DA	A
1	DA	GPD	B
structure	$\bar{\psi}_h^d(w)\gamma^\rho(\gamma^5)\psi_q^c(z)$	$\bar{\psi}_q^b(y)\gamma^\sigma(\gamma^5)\psi_h^e(w)$	diagram
2	GPD	DA	C
2	DA	GPD	D

Table 3.3.: All possible identifications with GPDs and a DA in (3.200).

To continue, we recall the definition of the twist-2 DA (2.33)

$$\langle \mathrm{q}_2|\bar{\psi}_q^a(y)\gamma^+(\gamma^5)\psi_h^b(z)|0\rangle = c_M^{hq}\frac{\delta^{ab}}{N_\mathrm{c}}\, q_2^+ f_\mathrm{M}\int_0^1 \mathrm{d}v\; e^{iq_2(vy+\bar{v}z)}\varphi\,(v)\;, \tag{3.201}$$

where we included the Fock coefficients c_M to specify the flavor content of the particular meson M. Parametrizing the matrix elements by a DA according to table 3.3, we realize, that the diagrams $\boxed{A,C}$ and $\boxed{B,D}$ possess the same flavor structures

$$\sum_{q,h} Q_q\, c_{hq}^M \left\langle \mathrm{P}_2|\bar{\psi}_h\gamma^+\psi_q|\mathrm{P}_1\right\rangle, \qquad \sum_{q,h} Q_q\, c_{qh}^M \left\langle \mathrm{P}_2|\bar{\psi}_q\gamma^+\psi_h|\mathrm{P}_1\right\rangle, \tag{3.202}$$

respectively. Interchanging the nomenclature in the latter term, we obtain the form

$$\sum_{q,h} Q_h\, c_{hq}^M \left\langle \mathrm{P}_2|\bar{\psi}_h\gamma^+\psi_q|\mathrm{P}_1\right\rangle. \tag{3.203}$$

Thus, the four diagrams only differ in the quark charge and we continue parametrizing the remaining matrix element by GPDs. We work here with the general prescription and show the result for specific mesons in the end. To parametrize the GPD, let us repeat the definition of the twist-2 quark GPDs (2.5)

$$\left\langle \mathrm{P}_2|\mathcal{O}^{qq}(-z,z)|\mathrm{P}_1\right\rangle = \int_{-1}^1 \mathrm{d}x\; e^{-ixP.z}\left[h^+H^q\big(x,\eta,\Delta^2\big)+e^+E^q\big(x,\eta,\Delta^2\big)\right].$$

For the given problem, we have to shift the variables and incorporate the flavor content of the meson. Thus,

$$\left\langle \mathrm{P}_2|\bar{\psi}_h^a(y)\gamma^+\psi_q^b(z)|\mathrm{P}_1\right\rangle = \frac{\delta^{ab}}{N_\mathrm{c}}\int_{-1}^1 \mathrm{d}x\, e^{i\left(\frac{\Delta+xP}{2}\right).y} e^{i\left(\frac{\Delta-xP}{2}\right).z}\Big[h^+H^{hq}+e^+E^{hq}\Big]\big(x,\eta,\Delta^2\big)\,. \tag{3.204}$$

As already mentioned depending on the particular meson, this GPDs might induce a flavor transition. The quark operators in the transition amplitude as presented in (3.199) do not

have definite twist, yet. Therefore, we leave the Lorentz indices open and keep in mind, that we have to make Sudakov decomposition to project onto the leading twist-2 contribution. After inserting the parametrizations, the exponent of all four Feynman diagrams are

$$\begin{aligned}
&\boxed{\text{A}} \quad (-q_1 - k + vq_2)\,.z + (-l + k + K_-)\,.y + (l + K_+ + \bar{v}q_2)\,.w\,,\\
&\boxed{\text{B}} \quad (-q_1 - k + K_+)\,.z + (-l + k + \bar{v}q_2)\,.y + (l + K_- + vq_2)\,.w\,,\\
&\boxed{\text{C}} \quad (-q_1 + k + K_-)\,.z + (-l - k + vq_2)\,.y + (l + K_+ + \bar{v}q_2)\,.w\,,\\
&\boxed{\text{D}} \quad (-q_1 + k + \bar{v}q_2)\,.z + (-l - k + K_+)\,.y + (l + K_- + vq_2)\,.w\,,
\end{aligned} \tag{3.205}$$

where we introduced the abbreviation

$$K_\pm = \frac{\Delta \pm xP}{2}\,. \tag{3.206}$$

Integration with respect to the coordinates z, y and w leads to three δ-functions, determining the momenta of the propagators. Two of them fix the quark and gluon momenta to the expressions shown in figure 3.10. The third one provides the conservation of the total momenta in the transition amplitude (3.195). In the next step, we approximate the denominators from

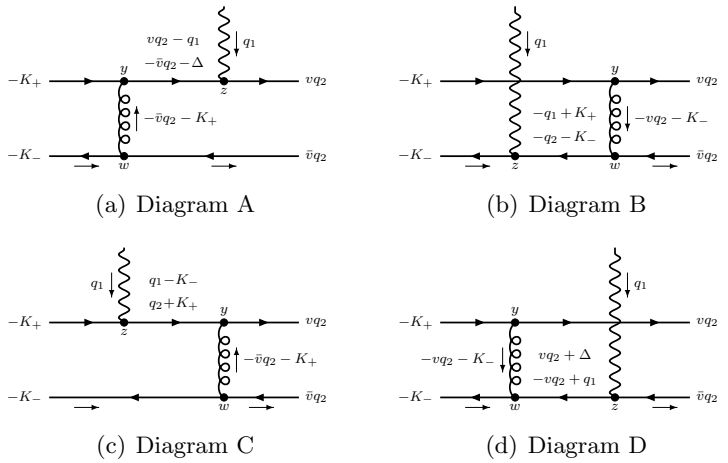

(a) Diagram A (b) Diagram B

(c) Diagram C (d) Diagram D

Figure 3.10.: LO Feynman diagrams for the flavor non-singlet channel.

the quark and gluon propagators in (3.199) analog to DVCS, see Sec. 3.3.3. Moreover, we neglect contributions proportional to $\Delta^2/P.q$ and $M^2/P.q$. As in DVCS, in the generalized Bjorken limit, we have $\eta \simeq \xi$, $q_2^2 = 0$ and $M_1 = M_2 = M$. Consequently, $P.\Delta = 0$. Hence, the denominators of all four diagrams are

$$\begin{aligned}
&\boxed{\text{A}} \quad (vq_2 - q_1)^2 \quad (\bar{v}q_2 + K_+)^2 \quad = 2\,(P.q)^2\ \bar{v}^2 \quad (\xi - x - i\epsilon)\,,\\
&\boxed{\text{C}} \quad (q_2 + K_+)^2 \quad (\bar{v}q_2 + K_+)^2 \quad = \quad (P.q)^2\ \bar{v} \quad (x - \xi + i\epsilon)^2\,,\\
&\boxed{\text{B}} \quad (-q_2 - K_-)^2\,(-vq_2 - K_-)^2 = \quad (P.q)^2\ v \quad (\xi + x - i\epsilon)^2\,,\\
&\boxed{\text{D}} \quad (vq_2 + \Delta)^2 \quad (-vq_2 - K_-)^2 = 2\,(P.q)^2\ v^2\xi\,(\xi + x - i\epsilon)\,.
\end{aligned} \tag{3.207}$$

As mentioned before, we still have to apply Sudakov decomposition (B.26) to γ^ρ and γ^σ in (3.200). Expressing the decomposition with the vectors P and q, the Sudakov decomposition keeping only the twist-2 contribution is

$$\gamma^\alpha = \frac{\gamma^+}{2} P^\mu + \dots \,. \tag{3.208}$$

Making use of the Sudakov decomposition above, the traces in (3.200) are evaluated to

$$\begin{aligned}
&\boxed{\text{A}} \quad \frac{1}{16}\mathrm{Tr}\left[\gamma^\alpha \not{q}_2 \gamma_\mu \left(v\not{q}_2 - \not{q}_1\right)\gamma_\alpha \not{P}\right] \approx \bar{v} P.q \left(q^\mu + \frac{\xi}{2}P^\mu\right) , \\
&\boxed{\text{C}} \quad \frac{1}{16}\mathrm{Tr}\left[\gamma^\alpha \not{q}_2 \gamma_\alpha \left(\not{q}_2 + \not{K}_+\right)\gamma_\mu \not{P}\right] \approx \frac{1}{2}\left(\xi - x\right) P.q \; P^\mu , \\
&\boxed{\text{B}} \quad \frac{1}{16}\mathrm{Tr}\left[\gamma^\alpha \not{P} \gamma_\mu \left(\not{q}_2 - \not{K}_-\right)\gamma_\alpha \not{q}_2\right] \approx -\frac{1}{2}\left(\xi + x\right) P.q \; P^\mu , \\
&\boxed{\text{D}} \quad \frac{1}{16}\mathrm{Tr}\left[\gamma^\alpha \not{P} \gamma_\alpha \left(\not{q}_2 + \not{K}_+\right)\gamma_\mu \not{q}_2\right] \approx -v P.q \left(q^\mu + \frac{\xi}{2}P^\mu\right) .
\end{aligned} \tag{3.209}$$

In order to obtain the last equation, we used $\Delta^\alpha = -\eta P^\alpha$, which is valid within our approximations. Combining the results for the traces and the denominators, we obtain

$$\begin{aligned}
&\boxed{\text{A}} \quad \frac{q^\mu + \frac{\xi}{2}P^\mu}{\mathcal{Q}^2}\frac{1}{\bar{v}\left(\xi - x - i\epsilon\right)} , \qquad
&&\boxed{\text{C}} \quad \frac{\xi P^\mu}{\mathcal{Q}^2}\frac{1}{\bar{v}\left(\xi - x - i\epsilon\right)} , \\
&\boxed{\text{D}} \quad -\frac{q^\mu + \frac{\xi}{2}P^\mu}{\mathcal{Q}^2}\frac{1}{v\left(\xi + x - i\epsilon\right)} , \qquad
&&\boxed{\text{B}} \quad -\frac{\xi P^\mu}{\mathcal{Q}^2}\frac{1}{v\left(\xi + x - i\epsilon\right)} .
\end{aligned} \tag{3.210}$$

The only thing left is the color structure, namely

$$\frac{\mathrm{Tr}\left(t^A t^A\right)}{N_\mathrm{c}^2} = \frac{N_\mathrm{c}^2 - 1}{2N_\mathrm{c}^2} = \frac{C_\mathrm{F}}{N_\mathrm{c}} , \tag{3.211}$$

for all diagrams. Finally, taking everything together, the result for the reduced transition amplitude in the non-singlet channel reads

$${}^{\mathrm{q}}\mathcal{A}_\mu^M \overset{\mathrm{LO}}{=} \frac{2\pi}{\mathcal{Q}^2}\, c_M^{hq}\, \frac{f_M C_\mathrm{F}}{N_\mathrm{c}}\, j_\mu \int_{-1}^{1}\frac{\mathrm{d}x}{2\xi}\int_0^1 \mathrm{d}v\; \varphi(v)\, \alpha_\mathrm{s}\, {}^{\mathrm{q}}\hat{T}^{(0)}(\xi, x, v)\left[\frac{h^+}{2}H^{hq} + \frac{e^+}{2}E^{hq}\right]\left(x, \eta, \Delta^2\right) , \tag{3.212}$$

where we used the abbreviation

$$j_\mu = 2q_\mu + 3\xi P_\mu \,. \tag{3.213}$$

and introduced the familiar factor of 2ξ. The hard scattering amplitude ${}^{\mathrm{q}}\hat{T}(\xi, x, v)$ is given by

$${}^{\mathrm{q}}\hat{T}^{(0)}\left(\tfrac{\xi + x - i\epsilon}{2(\xi - i\epsilon)}, v\right) = \left[\frac{Q_q\, 2(\xi - i\epsilon)}{\bar{v}\left(\xi - x - i\epsilon\right)} - \frac{Q_h\, 2(\xi - i\epsilon)}{v\left(\xi + x - i\epsilon\right)}\right] , \tag{3.214}$$

where we restored the correct $i\epsilon$ prescription according to Feynman's causality principle. In order to bring the result in the familiar form known from DVCS, we take out the quark charges. Thus,

$$
\begin{aligned}
{}^{\mathrm{q}}\hat{T}^{(0)}\left(\tfrac{\xi+x-i\epsilon}{2(\xi-i\epsilon)}, v\right) = \frac{Q_q+Q_h}{2}\left[\frac{2(\xi-i\epsilon)}{\bar{v}\,(\xi-x-i\epsilon)} - \frac{2(\xi-i\epsilon)}{v\,(\xi+x-i\epsilon)}\right] \\
+ \frac{Q_q-Q_h}{2}\left[\frac{2(\xi-i\epsilon)}{\bar{v}\,(\xi-x-i\epsilon)} + \frac{2(\xi-i\epsilon)}{v\,(\xi+x-i\epsilon)}\right] .
\end{aligned} \tag{3.215}
$$

The two terms have definite symmetry with respect to $x \to -x$. For later symmetry considerations, we introduce the amplitude ${}^{\mathrm{q}}T(\cdots)$ without that symmetry. It is defined as

$$
{}^{\mathrm{q}}T^{(0)}\left(\tfrac{\xi+x-i\epsilon}{2(\xi-i\epsilon)}, v\right) = \frac{2(\xi-i\epsilon)}{\bar{v}\,(\xi-x-i\epsilon)} . \tag{3.216}
$$

The notation simplifies drastically, by introducing the variable

$$
u = \frac{\xi+x}{2\xi} , \qquad \bar{u} = \frac{\xi-x}{2\xi} . \tag{3.217}
$$

The transformation $x \to -x$ is equivalent to $u \to \bar{u}$. Restricting the the momentum fraction x to the central region of the GPD $[-\eta, \eta]$ the variable u is positive $0 < u < 1$ and the kinematic reduce to the one of the pion form factor. Thus, the Feynman diagrams are equivalent. For DVMP, we also include the imaginary part which is present in the outer region of the GPD. To complete the picture, for the pion form factor, we identify

$$
K_+^\mu = \bar{u}\Delta^\mu , \qquad K_-^\mu = u\Delta^\mu , \tag{3.218}
$$

where Δ corresponds in this case to momentum of the pion.
In the following, we utilize the variable u, to simplify the considerations of the general flavor structure. The GPDs F^{hq} are flavor diagonal for neutral mesons and flavor off-diagonal for charged ones. In the off-diagonal case, we can utilize SU(3) flavor symmetry ignoring symmetry breaking effects to write

$$
F^{hq} = \lambda^{hq} F^q , \qquad F \in \{H, E, \tilde{H}, \tilde{E}\} . \tag{3.219}
$$

For neutral mesons, the matrix λ is the Kronecker delta $\lambda_{hq} = \delta_{hq}$, whereas for charged mesons its components are determined by the SU(3) flavor decomposition, see table 3.2 for the mesons of interest in this work. Therefore, the flavor structure of the transition amplitude (3.212) utilizing the variable u and omitting all unimportant factors becomes

$$
\sum_{q,h} c_M^{hq}\, \varphi(v) \left\{ \frac{Q_q+Q_h}{2}\left[\frac{1}{\bar{u}\bar{v}} - \frac{1}{uv}\right] + \frac{Q_q-Q_h}{2}\left[\frac{1}{\bar{u}\bar{v}} + \frac{1}{uv}\right] \right\} \lambda^{hq} F^q(u) . \tag{3.220}
$$

Since the second term does not contribute for neutral mesons, the structure of the transition amplitude is very similar to the structure of the Compton amplitude. If SU(3) flavor symmetry breaking effects are ignored, the meson distribution amplitudes for both vector and pseudoscalar mesons are symmetric under the transformation $v \to \bar{v}$. As a consequence, at

LO the symmetry of the DA can be used to take out its momentum fraction and express the transition amplitude by Compton form factors of even charge parity and a prefactor depending on the meson DA. For DVMP, we are going to take a similar approach and introduce the convolution of the GPD, DA and the hard scattering amplitude as the irreducible object containing GPDs. We call this convolution analog to DVCS a transition form factor. However, there is a subtlety due to the complicated flavor structure in DVMP. In DVCS, we could easily dispense of the quark charges (cf. Eq. 3.133) and express the Compton amplitude as the sum over Compton form factors of a definite flavor (3.143). At first, these CFFs involved the symmetric hard scattering amplitude (3.142). However, in (3.220) both terms contribute for charged mesons and we are not able to take of the quark charges so easily. To avoid a new notation, we do not attempt to define a TFF using the symmetric hard scattering amplitudes, we rather first transfer the symmetry with respect to $u \to \bar{u}$ to the GPD introducing GPDs with definite charge parity (2.15) and define the TFF only with definite intrinsic parity as done for CFFs in Sec. 3.2.4.1. After the transfer, (3.220) reads

$$\sum_{q,h} c_M^{hq}\, \varphi(v)\, \lambda^{hq}\, \frac{1}{\bar{u}\bar{v}} \left\{ \frac{Q_q + Q_h}{2} F^{q(+)}(u) + \frac{Q_q - Q_h}{2} F^{q(-)}(u) \right\} , \tag{3.221}$$

This is the desired form. We are able to define the transition form factor involving quark GPDs with definite charge parity, the asymmetric hard scattering amplitude (3.216) and a distribution amplitude, namely

$$\mathcal{F}_M^{q(\pm)}(\xi, \Delta^2, \mathcal{Q}^2) = \frac{f_M C_\mathrm{F}}{\mathcal{Q} N_\mathrm{c}} \int_{-1}^{1} \frac{\mathrm{d}x}{2\xi} \int_0^1 \mathrm{d}v\, \varphi_M(v)\, {}^{\mathrm{q}}T^{(0)}\left(\tfrac{\xi + x - i\epsilon}{2(\xi - i\epsilon)}, v\right) F^{q(\pm)}(x, \eta, \Delta^2) . \tag{3.222}$$

Analog to DVCS, we write the contribution of the TFFs to the transition amplitude (3.212) as the sum over TFFs with definite flavor

$$\mathcal{F}_M = \sum_{q,h} c_M^{hq}\, \lambda^{hq} \left\{ \frac{Q_q + Q_h}{2}\, \mathcal{F}^{q(+)} + \frac{Q_q - Q_h}{2}\, \mathcal{F}^{q(-)} \right\} . \tag{3.223}$$

Let us illustrate the flavor structure by two examples. For a neutral meson like ρ^0, the matrix c_M only has diagonal entries and the matrix λ_{hq} for a possible SU(3) flavor decomposition is the Kronecker delta δ_{hq}. Hence, the second term in the equation above vanishes and we obtain

$$\mathcal{F}_{\rho^0} = \sum_q c_{\rho^0}^{qq}\, Q_q\, \mathcal{F}^{q(+)} = \frac{Q_u}{\sqrt{2}}\, \mathcal{F}^{u(+)} - \frac{Q_d}{\sqrt{2}}\, \mathcal{F}^{d(+)} . \tag{3.224}$$

Note, in case of neutral vector mesons, we also have a gluon contribution. The situation gets more complicated in case of charged mesons. The flavor decomposition for ρ^+ becomes

$$\begin{aligned} \mathcal{F}_{\rho^+} &= \sum_{q,h} c_M^{hq} \left\{ \frac{Q_q + Q_h}{2}\, \left(\mathcal{F}^{q(+)} - \mathcal{F}^{q(+)}\right) + \frac{Q_q - Q_h}{2}\, \left(\mathcal{F}^{q(-)} - \mathcal{F}^{d(-)}\right) \right\} \\ &= \frac{Q_u + Q_d}{2}\, \left(\mathcal{F}^{u(+)} - \mathcal{F}^{d(+)}\right) + \frac{Q_u - Q_d}{2}\, \left(\mathcal{F}^{q(-)} - \mathcal{F}^{d(-)}\right) . \end{aligned} \tag{3.225}$$

In both cases, the structure is equivalent to the one in DVCS and we can treat both processes in the same manner. The flavor structure for other mesons can by easily obtained from table 3.2. Before introducing the properties of the TFF, we first derive the hard scattering amplitude involving a gluon GPD.

3.3.3.2. Gluon-quark channel

Now we evaluate the transition amplitude (3.195) with a gluon GPD. Following the structure of the previous section, we calculate the Feynman diagrams shown in figure 3.11. The

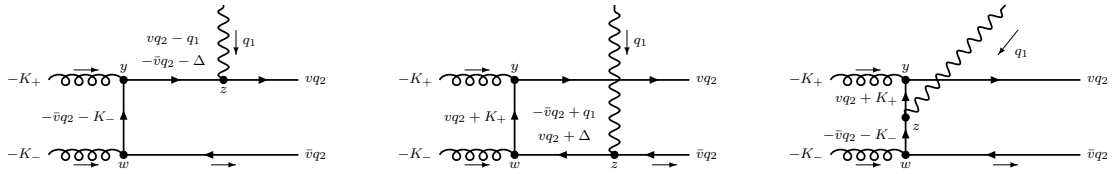

(a) Diagram E (b) Diagram F (c) Diagram G

Figure 3.11.: Feynman diagrams for the gluon-quark channel.

definition of the gluon GPD written in a Gauge invariant way (2.6) is

$$\langle \mathrm{P}_2|F^{+\mu}(-z)g_{\mu\nu}F^{\nu+}(z)|\mathrm{P}_1\rangle = \frac{1}{4}P^+\int_{-1}^{1}\mathrm{d}x\; e^{-ixP.z}\left[h^+H^g + e^+E^g\right](x,\eta,\Delta^2)\;.$$

Unfortunately, we only have the vector field A available. In light-cone gauge, we are able to rewrite [Rad96a, Hoo97]:

$$n_\mu A^\mu(z;q) = 0, \qquad F^{+\mu}(z) = \partial^+ A^\mu(z), \qquad A^\mu(z) = \int_0^\infty \mathrm{d}a\; F^{+\mu}(z+an). \tag{3.226}$$

Thus, the matrix element of two vector fields can be written as

$$\langle \mathrm{P}_2|A^\alpha(y)g_{\alpha\beta}A^\beta(z)|\mathrm{P}_1\rangle = -\int_0^\infty \mathrm{d}a\mathrm{d}b\,\langle \mathrm{P}_2|F^{+\alpha}(y+an)g_{\alpha\beta}F^{\beta+}(z+bq)|\mathrm{P}_1\rangle\,. \tag{3.227}$$

Using the definition of the gluon GPD on the right-hand side and performing out the integration over the auxiliary variables a and b we obtain

$$\langle \mathrm{P}_2|A^A_\alpha(y)g_{\alpha\beta}A^B_\beta(z)|\mathrm{P}_1\rangle = \frac{\delta^{AB}}{N_\mathrm{c}^2-1}\frac{P^+}{4}\int_{-1}^{1}\mathrm{d}x\; e^{i\left(\frac{\Delta+xP}{2}\right)y}e^{i\left(\frac{\Delta-xP}{2}\right)z}\frac{\left[h^+H^g+e^+E^g\right](x,\eta,\Delta^2)}{(\xi-x)(\xi+x)}, \tag{3.228}$$

where we used the integral

$$\int_0^\infty \mathrm{d}a\,\mathrm{d}b\, e^{i\left(\frac{\Delta+xP}{2}\right).na}e^{i\left(\frac{\Delta-xP}{2}\right).nb} = \frac{i}{K_+.n}\frac{i}{K_-.n} = -\frac{1}{(\xi-x)}\frac{1}{(\xi+x)}\,, \tag{3.229}$$

and $K_\pm.q = K_\pm.q_2$. In the same manner as in the previous section, we obtain the exponents of the three Feynman diagrams, which provide us the total momentum conservation. After that, the combination of the numerator and denominator provides us with the general expression. Introducing two quark propagators in the transition amplitude (3.195), the three combinations possess the exponents

$$\begin{aligned}
&\boxed{\text{E}} \quad (-q_1 - l + vq_2)z + (l - k + K_+)y + (k + \bar{v}q_2 + K_-)w\,,\\
&\boxed{\text{F}} \quad (-q_1 + l + \bar{v}q_2)z + (-k + vq_2 + K_+)y + (-l + k + K_-)w\,,\\
&\boxed{\text{G}} \quad (-q_1 - l + k)z + (l + \bar{v}q_2 + K_+)y + (-k + vq_2 + K_-)w\,.
\end{aligned} \tag{3.230}$$

As before, the integrals over the coordinates fix the momenta of the quark propagators and ensure momentum conservation. In the next step, we evaluate the corresponding traces

$$\begin{aligned}
&\boxed{\text{E}} \quad \bar{\psi}(z)\gamma_\mu \not{l}\gamma_\alpha \not{k}\gamma_\beta\psi(w) \to \frac{1}{4}\mathrm{Tr}\left(\gamma_\mu \not{l}\gamma_\alpha \not{k}\gamma_\beta \not{q}_2\right) \approx g_{\alpha\beta}\,\frac{1}{2}\bar{v}(\xi + x)\,(2q_\mu + \xi P_\mu)\,P.q\,,\\
&\boxed{\text{F}} \quad \bar{\psi}(y)\gamma_\alpha \not{k}\gamma_\beta \not{l}\gamma_\mu\psi(z) \to \frac{1}{4}\mathrm{Tr}\left(\gamma_\alpha \not{k}\gamma_\beta \not{l}\gamma_\mu \not{q}_2\right) \approx g_{\alpha\beta}\,\frac{1}{2}v(\xi - x)\,(2q_\mu + \xi P_\mu)\,P.q\,,\\
&\boxed{\text{G}} \quad \bar{\psi}(y)\gamma_\alpha \not{k}\gamma_\mu \not{l}\gamma_\beta\psi(w) \to \frac{1}{4}\mathrm{Tr}\left(\gamma_\alpha \not{k}\gamma_\mu \not{l}\gamma_\beta \not{q}_2\right) \approx g_{\alpha\beta}\,\frac{1}{2}(\xi - x)(\xi + x)P_\mu P.q\,,
\end{aligned} \tag{3.231}$$

where we neglect contributions proportional to $\Delta^2/P.q$ and $M^2/P.q$. The denominators simplify to

$$\begin{aligned}
&\boxed{\text{E}} \quad (vq_2 - q_1)^2 \quad \cdot(-\bar{v}q_2)^2 \quad\;\; = 2\bar{v}^2\,\xi(\xi + x)(P.q)^2\,,\\
&\boxed{\text{F}} \quad (-\bar{v}q_2 + q_1)^2 \;\cdot(vq_2 + K_+)^2 = 2v^2\,\xi(\xi - x)(P.q)^2\,,\\
&\boxed{\text{G}} \quad (-\bar{v}q_2 - K_-)^2\cdot(vq_2 + K_+)^2 = v\bar{v}\,(\xi - x)(\xi + x)(P.q)^2\,.
\end{aligned} \tag{3.232}$$

Combining the numerators (3.231) and denominators (3.232) we obtain

$$\frac{2q_\mu + \xi P_\mu}{4\bar{v}\xi P.q} + \frac{2q_\mu + \xi P_\mu}{4v\xi P.q} + \frac{2\xi P_\mu}{4v\bar{v}\xi P.q} = \frac{2q_\mu + 3\xi P_\mu}{2v\bar{v}\mathcal{Q}^2}. \tag{3.233}$$

The color structure of all three diagrams is

$$\frac{\mathrm{Tr}\left(t^A t^A\right)}{N_\mathrm{c}(N_\mathrm{c}^2 - 1)} = \frac{1}{2N_\mathrm{c}}\,. \tag{3.234}$$

The reduced transition amplitude involving a gluon GPD reads

$${}^{\mathrm{G}}\mathcal{A}_\mu^M \overset{\mathrm{LO}}{=} \frac{2\pi}{\mathcal{Q}^2}Q_q\,c_M^{qq}\,\frac{f_\mathrm{M}}{N_\mathrm{c}}\,j_\mu \int_0^1 \mathrm{d}v \int_{-1}^1 \frac{\mathrm{d}x}{2\xi}\,\varphi(v)\,\alpha_\mathrm{s}\,{}^{\mathrm{G}}\hat{T}^{(0)}(\xi, x, v)\left[\frac{h^+}{2}H^{\mathrm{G}} + \frac{e^+}{2}E^{\mathrm{G}}\right](x, \eta, \Delta^2)\,. \tag{3.235}$$

Thus, the hard scattering amplitude is given by

$${}^{\mathrm{G}}\hat{T}^{(0)}\,(\xi, x, v) = \frac{\xi - i\epsilon}{v\bar{v}(\xi - x - i\epsilon)(\xi + x - i\epsilon)}\,. \tag{3.236}$$

As in the non-singlet channel, it has definite symmetry under the exchange $x \to -x$. The full symmetry is revealed by the decomposition

$$ {}^{\mathrm{G}}\hat{T}^{(0)}(\xi,x,v) = \frac{1}{4\xi}\left[\frac{2(\xi-i\epsilon)}{\bar{v}(\xi-x-i\epsilon)} + \frac{2(\xi-i\epsilon)}{v(\xi-x-i\epsilon)} + \frac{2(\xi-i\epsilon)}{\bar{v}(\xi+x-i\epsilon)} + \frac{2(\xi-i\epsilon)}{v(\xi+x-i\epsilon)}\right] . \tag{3.237} $$

The hard scattering amplitude is symmetric as it is the gluon GPD (2.53). For later purposes, we define the hard scattering amplitude without symmetry properties:

$$ {}^{\mathrm{G}}T^{(0)}\left(\tfrac{\xi+x-i\epsilon}{2(\xi-i\epsilon)}, v\right) = \frac{2(\xi-i\epsilon)}{\bar{v}(\xi-x-i\epsilon)} . \tag{3.238} $$

Analog to the flavor non-singlet channel in the previous section, we do not attempt to define a TFF using the symmetric hard scattering amplitude ${}^{\mathrm{G}}T(\cdots)$, but exploit the symmetry with respect to $x \to -x$ or equivalent $u \to \bar{u}$ first. Utilizing the variable u, we schematically obtain

$$ \varphi(v)\,\frac{1}{4\xi}\frac{1}{u\bar{u}v\bar{v}}\,F^{\mathrm{G}}(u) = \varphi(v)\,\frac{1}{4\xi}\left(\frac{1}{\bar{u}\bar{v}} + \frac{1}{\bar{u}v} + \frac{1}{u\bar{v}} + \frac{1}{uv}\right)F^{\mathrm{G}}(u) \to \varphi(v)\,\frac{1}{\xi}\frac{1}{\bar{u}\bar{v}}\,F^{\mathrm{G}}(u) . \tag{3.239} $$

Analog to the quark transition form factor, we define the gluon one as

$$ \mathcal{F}_M^{\mathrm{G}}(\xi,\Delta^2,\mathcal{Q}^2) = \frac{f_M C_{\mathrm{F}}}{\mathcal{Q}N_{\mathrm{c}}}\int_{-1}^{1}\frac{\mathrm{d}x}{2\xi}\int_0^1 \mathrm{d}v\;\varphi_M(v)\,\frac{1}{\xi C_{\mathrm{F}}}\,{}^{\mathrm{G}}T^{(0)}\left(\tfrac{\xi+x-i\epsilon}{2(\xi-i\epsilon)}, v\right)F^{\mathrm{G}}(x,\eta,\Delta^2) . \tag{3.240} $$

The factor $1/\xi$ stems from the peculiarity of the definition of the gluon GPD, whereas the factor $1/C_{\mathrm{F}}$ compensates for the different prefactor in the quark and gluon case (cf. Eq. 3.222).

3.3.4. Transition form factors

Due to the intricate flavor structure of the transition amplitude of DVMP we already defined the quark and gluon TFF with definite intrinsic parity in the previous two sections. We obtained the results (3.222, 3.240)

$$ \begin{aligned} \mathcal{F}_M^{q(\pm)}(\xi,\Delta^2,\mathcal{Q}^2) &= \frac{f_M C_{\mathrm{F}}}{\mathcal{Q}N_{\mathrm{c}}}\int_{-1}^{1}\frac{\mathrm{d}x}{2\xi}\int_0^1 \mathrm{d}v\;\varphi_M(v)\qquad {}^{\mathrm{q}}T^{(0)}\left(\tfrac{\xi+x-i\epsilon}{2(\xi-i\epsilon)}, v\right)F^{q(\pm)}(x,\eta,\Delta^2) , \\ \mathcal{F}_M^{\mathrm{G}}(\xi,\Delta^2,\mathcal{Q}^2) &= \frac{f_M C_{\mathrm{F}}}{\mathcal{Q}N_{\mathrm{c}}}\int_{-1}^{1}\frac{\mathrm{d}x}{2\xi}\int_0^1 \mathrm{d}v\;\varphi_M(v)\,\frac{1}{\xi C_{\mathrm{F}}}\,{}^{\mathrm{G}}T^{(0)}\left(\tfrac{\xi+x-i\epsilon}{2(\xi-i\epsilon)}, v\right)F^{\mathrm{G}}(x,\eta,\Delta^2) . \end{aligned} $$

The TFFs that enter the transition amplitude can be represented by the sum

$$ \mathcal{F}_M = \sum_{q,h} c_M^{hq}\left\{\frac{Q_q+Q_h}{2}\,\lambda_{hq}\,\mathcal{F}^{q(+)} + \frac{Q_q-Q_h}{2}\,\lambda_{hq}\,\mathcal{F}^{q(-)} + Q_q\,\delta_{qh}\,\mathcal{F}^{\mathrm{G}}\right\} . \tag{3.241} $$

Note, that the gluon contribution is only present for neutral vector mesons. The matrices c_M are presented in (3.184). For the three vector mesons of particular interest in this work, we

obtain

$$\begin{aligned}\mathcal{F}_{\rho^0} &= \frac{Q_u}{\sqrt{2}}\,\mathcal{F}_{\rho^0}^{u} - \frac{Q_d}{\sqrt{2}}\,\mathcal{F}_{\rho^0}^{d} + \frac{Q_u - Q_d}{\sqrt{2}}\,\mathcal{F}_{\rho^0}^{\mathrm{G}}\,,\\ \mathcal{F}_{\omega} &= \frac{Q_u}{\sqrt{2}}\,\mathcal{F}_{\omega}^{u} + \frac{Q_d}{\sqrt{2}}\,\mathcal{F}_{\omega}^{d} + \frac{Q_u + Q_d}{\sqrt{2}}\,\mathcal{F}_{\omega}^{\mathrm{G}}\,,\\ \mathcal{F}_{\phi} &= Q_s\;\mathcal{F}_{\phi}^{s} \qquad\qquad + \qquad Q_s\;\mathcal{F}_{\phi}^{\mathrm{G}}\,.\end{aligned} \tag{3.242}$$

In the rest of the section, we present the perturbative expansion of TFFs and introduce the evolution basis as in DVCS.

3.3.4.1. Perturbative expansion

The introduction of the perturbative expansion is analog to the considerations for the Compton form factor in section 3.2.4.2. The approximation of the hard scattering amplitude up to NLO is

$$T\left(u,v\middle|\alpha_{\mathrm{s}}(\mu_{\mathrm{R}}),\tfrac{\mathcal{Q}^2}{\mu_{\mathrm{F}}^2},\tfrac{\mathcal{Q}^2}{\mu_{\varphi}^2},\tfrac{\mathcal{Q}^2}{\mu_{\mathrm{R}}^2}\right) = \alpha_{\mathrm{s}}(\mu_{\mathrm{R}})\,T^{(0)}(u,v) + \frac{\alpha_{\mathrm{s}}^2(\mu_{\mathrm{R}})}{2\pi}T^{(1)}\left(u,v\middle|\tfrac{\mathcal{Q}^2}{\mu_{\mathrm{F}}^2},\tfrac{\mathcal{Q}^2}{\mu_{\varphi}^2},\tfrac{\mathcal{Q}^2}{\mu_{\mathrm{R}}^2}\right)\,. \tag{3.243}$$

In contrast to DVCS, it also depends on the factorization scale of the distribution amplitude μ_φ and its momentum fraction v. Whereas it fulfills the renormalization group equation (3.147) as well. As a peculiarity, from NLO on there is a pure singlet contribution [ISK04]. At arbitrary order of perturbation theory, the transition form factor is given by

$$\mathcal{F}^{q(\pm)}\left(\xi,\Delta^2,\mathcal{Q}^2\right) = \frac{fC_{\mathrm{F}}}{\mathcal{Q}N_{\mathrm{c}}}\,\varphi(v)\overset{v}{\otimes}{}^{\mathrm{q}}T\left(\tfrac{\xi+x-i\epsilon}{2(\xi-i\epsilon)},v,\xi\middle|\alpha_{\mathrm{s}}(\mu_{\mathrm{R}}),\tfrac{\mathcal{Q}^2}{\mu_{\mathrm{F}}^2},\tfrac{\mathcal{Q}^2}{\mu_{\varphi}^2},\tfrac{\mathcal{Q}^2}{\mu_{\mathrm{R}}^2}\right)\overset{x}{\otimes}F^{q(\pm)}\left(x,\eta,\Delta^2\right)\,, \tag{3.244}$$

where we use the short hand notations of the integrations

$$f(x)\overset{x}{\otimes}g(x) \equiv \int_{-1}^{1}\frac{\mathrm{d}x}{2\xi}\,f(x)\,g(x)\,,\qquad f(v)\overset{v}{\otimes}g(v) \equiv \int_{0}^{1}\mathrm{d}v\,f(v)\,g(v)\,. \tag{3.245}$$

Including the pure singlet contribution, the transition form factor is

$$\mathcal{F}_{\rho^0} = \frac{Q_u}{\sqrt{2}}\,\mathcal{F}_{\rho^0}^{u(+)} - \frac{Q_d}{\sqrt{2}}\,\mathcal{F}_{\rho^0}^{d(+)} + \frac{Q_u - Q_d}{\sqrt{2}}\left(\mathcal{F}_{\rho^0}^{\mathrm{G}} + \mathcal{F}_{\rho^0}^{\mathrm{pS}}\right)\,, \tag{3.246a}$$

$$\mathcal{F}_{\omega} = \frac{Q_u}{\sqrt{2}}\,\mathcal{F}_{\omega}^{u(+)} + \frac{Q_d}{\sqrt{2}}\,\mathcal{F}_{\omega}^{d(+)} + \frac{Q_u + Q_d}{\sqrt{2}}\left(\mathcal{F}_{\omega}^{\mathrm{G}} + \mathcal{F}_{\omega}^{\mathrm{pS}}\right)\,, \tag{3.246b}$$

$$\mathcal{F}_{\phi} = Q_s\;\mathcal{F}_{\phi}^{s(+)} \qquad\qquad + Q_s\qquad \left(\mathcal{F}_{\phi}^{\mathrm{G}} + \mathcal{F}_{\phi}^{\mathrm{pS}}\right)\,. \tag{3.246c}$$

3.3.4.2. Evolution basis

To solve the mixing problem, we introduce the evolution basis for transition form factors. In the quark/gluon basis, we have the general notation

$$\mathcal{F}_M = \sum_A \hat{c}_M^A \mathcal{F}_M^A\,, \qquad A \in \{u^{(\pm)}, d^{(\pm)}, \dots, \mathrm{pS}, \mathrm{G}\}\,, \qquad \mathcal{F} \in \{\mathcal{H}, \mathcal{E}, \widetilde{\mathcal{H}}, \widetilde{\mathcal{E}}\}\,. \tag{3.247}$$

Comparing with equation (3.246) we have the coefficients

$$\hat{c}_{\rho^0}^{u(+)} = \frac{Q_u}{\sqrt{2}}, \quad \hat{c}_{\rho^0}^{d(+)} = -\frac{Q_d}{\sqrt{2}}, \quad \hat{c}_{\rho^0}^{\mathrm{G}} = \hat{c}_{\rho^0}^{\mathrm{pS}} = \frac{Q_u - Q_d}{\sqrt{2}C_{\mathrm{F}}}\,, \tag{3.248a}$$

$$\hat{c}_{\omega}^{u(+)} = \frac{Q_u}{\sqrt{2}}, \quad \hat{c}_{\omega}^{d(+)} = \frac{Q_d}{\sqrt{2}}, \quad \hat{c}_{\omega}^{\mathrm{G}} = \hat{c}_{\omega}^{\mathrm{pS}} = \frac{Q_u + Q_d}{\sqrt{2}C_{\mathrm{F}}}\,, \tag{3.248b}$$

$$\hat{c}_{\phi}^{s(+)} = Q_s, \qquad \hat{c}_{\phi}^{\mathrm{G}} = \hat{c}_{\phi}^{\mathrm{pS}} = Q_s\,. \tag{3.248c}$$

Following Sec. 2.7 we introduce the summation with respect to irreducible $\mathrm{SU}(N_\mathrm{f})$ multiplets:

$$\mathcal{F}_M = \sum_A \hat{c}_M^A\ \mathcal{F}_M^A\,, \qquad A \in \{0^{(\pm)}, 3^{(\pm)}, 8^{(\pm)}, 15^{(\pm)}, \mathrm{pS}, \mathrm{G}\}\,. \tag{3.249}$$

The coefficients are given in table 3.4. To simplify the notation, the non-singlet contributions

c_M^A	$0^{(+)}$	$3^{(+)}$	$8^{(+)}$	$15^{(+)}$
ρ^0	$\frac{Q_u-Q_d}{4\sqrt{2}}$	$\frac{Q_u+Q_d}{2\sqrt{2}}$	$\frac{Q_u-Q_d}{6\sqrt{2}}$	$\frac{Q_u-Q_d}{12\sqrt{2}}$
ω	$\frac{Q_u+Q_d}{4\sqrt{2}}$	$\frac{Q_u-Q_d}{2\sqrt{2}}$	$\frac{Q_u+Q_d}{6\sqrt{2}}$	$\frac{Q_u+Q_d}{12\sqrt{2}}$
ϕ	$\frac{Q_s}{4\sqrt{2}}$	0	$-\frac{Q_s}{3}$	$\frac{Q_s}{12}$

c_M^A	$0^{(+)}$	$3^{(+)}$	$8^{(+)}$	$15^{(+)}$
ρ^0	$\frac{1}{4\sqrt{2}}$	$\frac{1}{6\sqrt{2}}$	$\frac{1}{6\sqrt{2}}$	$\frac{1}{12\sqrt{2}}$
ω	$\frac{1}{12\sqrt{2}}$	$\frac{1}{2\sqrt{2}}$	$\frac{1}{18\sqrt{2}}$	$\frac{1}{36\sqrt{2}}$
ϕ	$-\frac{1}{12}$	0	$\frac{1}{9}$	$-\frac{1}{36}$

Table 3.4.: $\mathrm{SU}(N_\mathrm{f}{=}4)$ factors for the longitudinal vector mesons ρ^0, ω and ϕ. The quark charges for the numerical evaluation in the right table are given in (3.9).

merge in the non-singlet transition form factor

$$\mathcal{F}_M^{\mathrm{NS}} = \hat{c}_M^3 \mathcal{F}_M^3 + \hat{c}_M^8 \mathcal{F}_M^8 + \hat{c}_M^{15} \mathcal{F}_M^{15}\,, \tag{3.250}$$

whose flavor composition is in general different for all mesons. Expressing the non-singlet TFFs in terms of quark ones, we have

$$\mathcal{F}_{\rho^0}^{\mathrm{NS}(+)} = \frac{3Q_u+Q_d}{4\sqrt{2}}\mathcal{F}_{\rho^0}^{u(+)} + \frac{-Q_u-3Q_d}{4\sqrt{2}}\mathcal{F}_{\rho^0}^{d(+)} + \frac{-Q_u+Q_d}{4\sqrt{2}}\mathcal{F}_{\rho^0}^{s(+)} + \frac{-Q_u+Q_d}{4\sqrt{2}}\mathcal{F}_{\rho^0}^{c(+)}\,, \tag{3.251a}$$

$$\mathcal{F}_{\omega}^{\mathrm{NS}(+)} = \frac{3Q_u-Q_d}{4\sqrt{2}}\mathcal{F}_{\omega}^{u(+)} + \frac{-Q_u+3Q_d}{4\sqrt{2}}\mathcal{F}_{\omega}^{d(+)} + \frac{-Q_u-Q_d}{4\sqrt{2}}\mathcal{F}_{\omega}^{s(+)} + \frac{-Q_u-Q_d}{4\sqrt{2}}\mathcal{F}_{\omega}^{c(+)}\,, \tag{3.251b}$$

$$\mathcal{F}_{\phi}^{\mathrm{NS}(+)} = -\frac{Q_s}{4}\mathcal{F}_{\phi}^{u(+)} - \frac{Q_s}{4}\mathcal{F}_{\phi}^{d(+)} + \frac{3Q_s}{4}\mathcal{F}_{\phi}^{s(+)} - \frac{Q_s}{4}\mathcal{F}_{\phi}^{c(+)}\,. \tag{3.251c}$$

Inserting the quark charges leads to the numerical values

$$\mathcal{F}^{\mathrm{NS}}_{\rho^0} = \frac{1}{12\sqrt{2}}\left(5\mathcal{F}^{u(+)}_{\rho^0} + \mathcal{F}^{d(+)}_{\rho^0} - 3\mathcal{F}^{s(+)}_{\rho^0} - 3\mathcal{F}^{c(+)}_{\rho^0}\right), \tag{3.252a}$$

$$\mathcal{F}^{\mathrm{NS}}_{\omega} = \frac{1}{12\sqrt{2}}\left(7\mathcal{F}^{u(+)}_{\omega} - 5\mathcal{F}^{d(+)}_{\omega} - 3\mathcal{F}^{s(+)}_{\omega} - 3\mathcal{F}^{c(+)}_{\omega}\right), \tag{3.252b}$$

$$\mathcal{F}^{\mathrm{NS}}_{\phi} = \frac{1}{12}\left(\mathcal{F}^{u(+)}_{\phi} + \mathcal{F}^{d(+)}_{\phi} - 3\mathcal{F}^{s(+)}_{\phi} + \mathcal{F}^{c(+)}_{\phi}\right). \tag{3.252c}$$

For the quark singlet contribution we also include the pure singlet contribution:

$$\mathcal{F}^{\Sigma} = \hat{c}^0_{\gamma}\,\mathcal{F}^0 + \hat{c}^{\mathrm{pS}}_{M}\,\mathcal{F}^{\mathrm{pS}}_{M}. \tag{3.253}$$

Together with the gluon contribution, we receive the singlet contribution

$$\mathcal{F}^{\mathrm{S}}_{M} = \mathcal{F}^{\Sigma}_{M} + \hat{c}^{\mathrm{G}}_{M}\,\mathcal{F}^{\mathrm{G}} = \hat{c}^0_{M}\,\mathcal{F}^0 + \hat{c}^{\mathrm{pS}}_{M}\,\mathcal{F}^{\mathrm{pS}}_{M} + \hat{c}^{\mathrm{G}}_{\gamma}\,\mathcal{F}^{\mathrm{G}}. \tag{3.254}$$

The advantage is, that we can now introduce a very convenient representation for the singlet TFF in matrix notation by using the relation

$$\hat{c}^0_{M} = \frac{1}{N_{\mathrm{f}}}\hat{c}^{\mathrm{pS}}_{M}, \qquad \hat{c}^{\mathrm{G}}_{M} = \frac{1}{C_{\mathrm{F}}}\hat{c}^{\mathrm{pS}}_{M}, \tag{3.255}$$

which allows to pull out the coefficient $\hat{c}^{\mathrm{pS}}_{M}$ and the remains are added to the hard scattering amplitudes. Combining the singlet and gluon GPD, we employ the definition (3.162)

$$\boldsymbol{F}\big(x,\eta,\Delta^2\big) = \begin{pmatrix} F^{0(+)} \\ F^{\mathrm{G}} \end{pmatrix}\big(x,\eta,\Delta^2\big).$$

The hard scattering amplitude is given by the row vector

$$\boldsymbol{T}(u,v,\xi) = \left(\tfrac{1}{N_{\mathrm{f}}}{}^{\mathrm{q}}T(u,v) + {}^{\mathrm{pS}}T(u,v) \quad \tfrac{1}{\xi C_{\mathrm{F}}}{}^{\mathrm{G}}T(u,v)\right). \tag{3.256}$$

Therefore, the singlet transition form factor in matrix notation reads

$$\mathcal{F}^{\mathrm{S}}_{\mathrm{V}^0}\big(\xi,\Delta^2,\mathcal{Q}^2\big) = \frac{f_{\mathrm{V}^0}C_{\mathrm{F}}}{\mathcal{Q}N_{\mathrm{c}}}\varphi(v) \overset{v}{\otimes} \boldsymbol{T}\left(\tfrac{\xi+x-i\epsilon}{2(\xi-i\epsilon)},v,\xi\right) \overset{x}{\otimes} \boldsymbol{F}\big(x,\eta,\Delta^2,\mu_{\mathrm{F}}^2\big) \tag{3.257}$$

Hance, we express the initial sum (3.247) of TFF as

$$\mathcal{F}_{\mathrm{V}^0} = \hat{c}^{\mathrm{S}}_{\mathrm{V}^0}\,\mathcal{F}^{\mathrm{S}}_{\mathrm{V}^0} + \mathcal{F}^{\mathrm{NS}}_{\mathrm{V}^0} \quad \text{with} \quad \hat{c}^{\mathrm{S}}_{\mathrm{V}^0} = \hat{c}^{\mathrm{pS}}_{\mathrm{V}^0}. \tag{3.258}$$

3.3.5. Cross section

The factorization theorem for [CFS97] holds for longitudinally polarized virtual photons. Therefore, we have to extract this contribution from the total cross section. To this end, we

introduce the longitudinal polarization vector. The usual normalization and orthogonality conditions for the transverse and longitudinal polarization vectors are

$$\begin{aligned} \epsilon_{\mathrm{T}}^{\mu}(q_1) &= (0, \vec{\epsilon}_{\mathrm{T}})\,, \qquad \vec{q}_1.\vec{\epsilon}_{\mathrm{T}} = 0\,, \qquad \epsilon_{\mathrm{L}}^{\mu}(q_1) = (\epsilon_{\mathrm{L}}^{0}, \vec{\epsilon}_{\mathrm{L}})\,, \\ \vec{q}_1.\vec{\epsilon}_{\mathrm{L}} &= 1\,, \qquad \epsilon_{\mathrm{L}}^{2} = \epsilon_{\mathrm{T}}^{2} = 1\,, \qquad \epsilon_{\mathrm{L}}.\epsilon_{\mathrm{T}} = 0\,. \end{aligned} \tag{3.259}$$

Imposing the orthogonality, we obtain for the longitudinal polarization vector in the laboratory frame

$$\vec{q}_1.\vec{\epsilon}_{\mathrm{L}} = -q_1^z \epsilon_{\mathrm{L}}^z \stackrel{!}{=} 1 \quad \rightarrow \epsilon_{\mathrm{L}}^z = -1/q_1^z\,, \qquad \epsilon_{\mathrm{L}}.\epsilon_{\mathrm{T}} = 0 \rightarrow \epsilon_{\mathrm{L}}^x = \epsilon_{\mathrm{L}}^y = 0\,. \tag{3.260}$$

From the normalization condition, we derive

$$\epsilon_{\mathrm{L}}^2 = \left(\epsilon_{\mathrm{L}}^0\right)^2 - (\epsilon_{\mathrm{L}}^z)^2 \stackrel{!}{=} 1 = \left(\epsilon_{\mathrm{L}}^0\right)^2 - (1/q_1^z)^2 \rightarrow \left(\epsilon_{\mathrm{L}}^0\right)^2 = 1 + \frac{1}{(q_1^z)^2}\,. \tag{3.261}$$

Thus, the components of the longitudinal polarization vector in the laboratory frame are

$$\epsilon_L^{\mu} = \left(-\frac{\sqrt{1+\epsilon^2}}{\epsilon}, 0, 0, \frac{1}{\epsilon}\right)\,. \tag{3.262}$$

Two independent unit vectors spanning the longitudinal subspace are

$$(1,0,0,0) = \frac{1}{M} P_1^{\mu} \qquad (0,0,0,1) = \frac{1}{\sqrt{1+\epsilon^2}} \left(-\frac{\epsilon}{\mathcal{Q}} q_1^{\mu} + \frac{1}{M} P_1^{\mu}\right)\,. \tag{3.263}$$

Hence, the longitudinal vector can be written as

$$\epsilon_{\mathrm{L}}^{\mu}(q_1) = -\frac{1}{\mathcal{Q}\sqrt{1+\epsilon^2}} q_1^{\mu} - \frac{2x_{\mathrm{B}}}{\mathcal{Q}\sqrt{1+\epsilon^2}} P_1^{\mu}\,. \tag{3.264}$$

As in DVCS, we use the Hand's convention [Han63] to obtain the cross section for the photoproduction of a meson from a longitudinally polarized virtual photon. We take off the flux factor $P_1.k_1$, the phase space originated from the outgoing electron and the term from the product of the transition amplitude and the leptonic current. In exchange, we add the photon flux factor and the corresponding Lorentz structure. This leads to the factor

$$\frac{|\epsilon_{\mathrm{L}}.j|^2}{P_1.q_1} \left(e^2 \frac{|L.j|^2}{P_1.k_1} \frac{\mathrm{d}^3 k_2}{(2\pi)^3 2\omega_2}\right)^{-1} = \frac{1}{\alpha_{\mathrm{em}}} \frac{\pi}{1-y} \frac{x_{\mathrm{B}}}{\mathrm{d}x_{\mathrm{B}}} \frac{\mathcal{Q}^2}{\mathrm{d}\mathcal{Q}^2}\,, \tag{3.265}$$

where the individual terms are

$$|\epsilon_{\mathrm{L}}.j|^2 = 4\mathcal{Q}^2\,, \qquad |L.j|^2 = 16\,\frac{1-y}{y^2}\,, \tag{3.266}$$

and as in (3.176)

$$\frac{\mathrm{d}^3 k_2}{2\omega_2} = \frac{\pi y}{2x_{\mathrm{B}}} \mathrm{d}x_{\mathrm{B}} \mathrm{d}\mathcal{Q}^2\,, \qquad P_1.q_1 = \frac{\mathcal{Q}^2}{2x_{\mathrm{B}}}\,, \qquad P_1.k_1 = \frac{\mathcal{Q}^2}{2yx_{\mathrm{B}}}\,.$$

The final cross section reads

$$\mathrm{d}\sigma^{\gamma_\mathrm{L}^* N\to MN'} = \frac{\alpha_\mathrm{em} x_\mathrm{B}^2 y^2}{32\pi \mathcal{Q}^2\sqrt{1+\epsilon^2}} \frac{1}{1-y} \left|L.A_M\right|^2 \mathrm{d}\Delta^2 \mathrm{d}\phi_\mathrm{N} \,. \tag{3.267}$$

The scattering amplitude for longitudinal vector mesons yields

$$\left|L.\mathcal{A}_{\mathrm{V_L}}\right|^2 = \left|L.j\right|^2 \cdot \frac{4\pi^2}{\mathcal{Q}^2} \left(\frac{h^+}{P^+}\mathcal{H} + \frac{e^+}{P^+}\mathcal{E}\right)^2 . \tag{3.268}$$

Whereas for pseudoscalar mesons, we have to replace the vector TFFs by axial-vector TFFs. The summation over the spin of the outgoing nucleon and the evaluation of the nucleon bilinears is equivalent to DVCS. From (3.171) we read off

$$\begin{aligned}
\left(\frac{h^+}{P^+}\mathcal{H} + \frac{e^+}{P^+}\mathcal{E}\right)^2 &= \left(1-\xi^2\right)\mathcal{H}\mathcal{H}^* - \xi^2\left(\mathcal{H}\mathcal{E}^* + \mathcal{E}\mathcal{H}^*\right) - \left(\xi^2 + \frac{\Delta^2}{4M^2}\right)\mathcal{E}\mathcal{E}^* \,, \\
\left(\frac{\tilde{h}^+}{P^+}\widetilde{\mathcal{H}} + \frac{\tilde{e}^+}{P^+}\widetilde{\mathcal{E}}\right)^2 &= \left(1-\xi^2\right)\widetilde{\mathcal{H}}\widetilde{\mathcal{H}}^* - \xi^2\left(\widetilde{\mathcal{H}}\widetilde{\mathcal{E}}^* + \widetilde{\mathcal{E}}\widetilde{\mathcal{H}}^*\right) - \xi^2\frac{\Delta^2}{4M^2}\widetilde{\mathcal{E}}\widetilde{\mathcal{E}}^* \,.
\end{aligned}$$

The replacement of the generalized Bjorken scaling variable ξ by the Bjorken variable is done via (3.81), namely for vector and pseudoscalar mesons

$$\left|L.\mathcal{A}_{\mathrm{V_L}}\right|^2 = \frac{\left|L.j\right|^2}{\left(2-x_\mathrm{B}\right)^2}\left[4\left(1-x_\mathrm{B}\right)\left|\mathcal{H}\right|^2 - x_\mathrm{B}^2\left(\mathcal{H}\mathcal{E}^* + \mathcal{E}\mathcal{H}^*\right) - \left(x_\mathrm{B}^2 + \left(2-x_\mathrm{B}\right)^2\frac{\Delta^2}{4M^2}\right)\left|\mathcal{E}\right|^2\right] , \tag{3.269}$$

$$\left|L.\mathcal{A}_{\mathrm{PS}}\right|^2 = \frac{\left|L.j\right|^2}{\left(2-x_\mathrm{B}\right)^2}\left[4\left(1-x_\mathrm{B}\right)\left|\widetilde{\mathcal{H}}\right|^2 - x_\mathrm{B}^2\left(\widetilde{\mathcal{H}}\widetilde{\mathcal{E}}^* + \widetilde{\mathcal{E}}\widetilde{\mathcal{H}}^*\right) - x_\mathrm{B}^2\frac{\Delta^2}{4M^2}\left|\widetilde{\mathcal{E}}\right|^2\right] . \tag{3.270}$$

Therefore, the cross section of the photoproduction of a longitudinal polarized vector or pseudoscalar meson reads

$$\mathrm{d}\sigma^{\gamma_\mathrm{L}^* N\to MN'} = \frac{2\pi\alpha_\mathrm{em}\, x_\mathrm{B}^2}{\mathcal{Q}^4\sqrt{1+\epsilon^2}} \left[\cdots\right] \mathrm{d}\Delta^2 \mathrm{d}\phi_\mathrm{N} \,, \tag{3.271}$$

where the term in square brackets corresponds to the one in (3.269). In the leading twist-2 approximation, we integrate out the azimuthal angle of the recoiled nucleon. Furthermore, we expand the cross section in x_B in the vicinity of zero. For vector mesons, we obtain

$$\frac{\mathrm{d}\sigma^{\gamma_\mathrm{L}^* N\to MN'}}{\mathrm{d}\Delta^2} = \frac{4\pi^2\alpha_\mathrm{em}\, x_\mathrm{B}^2}{\mathcal{Q}^4}\left(\left|\mathcal{H}\right|^2 - \frac{\Delta^2}{4M^2}\left|\mathcal{E}\right|^2\right) , \tag{3.272}$$

and for pseudoscalar ones the cross section in the small-x_B region reads

$$\frac{\mathrm{d}\sigma^{\gamma^* p\to \mathrm{PS}N}}{\mathrm{d}\Delta^2} = \frac{4\pi^2\alpha_\mathrm{em}\, x_\mathrm{B}^2}{\mathcal{Q}^4}\left|\widetilde{\mathcal{H}}\right|^2 . \tag{3.273}$$

3.3.6. NLO hard scattering amplitudes

For completeness, we repeat the hard scattering amplitudes for the non-singlet (3.216) and gluon (3.238) channel at LO.

$$ {}^{\mathrm{q}}T^{(0)}(u,v) = {}^{\mathrm{G}}T^{(0)}(u,v) = \frac{1}{\bar{u}\bar{v}}\,, \qquad {}^{\mathrm{pS}}T^{(0)}(u,v) = 0\,. \tag{3.274} $$

The NLO corrections to the hard DVMP amplitudes are known in momentum fraction representation. As already mentioned, the flavor non-singlet channel follows from analytic continuation [BM01, DK07] from the diagrammatical results for the pion form factor [MNP99]. As seen in Sec. 3.3.3.1, this finding in the flavor non-singlet channel can be used for all DVMP channels since the two γ_5 matrices, arising from two intrinsic parity odd operators are irrelevant. For DVMP-V_{L}^0, the hard scattering amplitudes to NLO accuracy for the pure singlet and gluon-quark channel were obtained in [ISK04].
In this section, following [MLPKS14], we present the expressions for all the hard scattering amplitudes that are known to NLO accuracy in the momentum fraction representation. We give detailed insights on the analytic structure. We first represent the pure-singlet hard scattering amplitude in the way we consider as the simplest one to outline our reasoning. This is followed the investigation of the general structure and the identification of elementary building blocks. Finally, we present our results of the flavor non-singlet, pure singlet and gluon-quark channels.

3.3.6.1. Analytic structure

The only functions, which appear in the hard scattering amplitudes and possess a cut in the complex plane are the logarithm and the dilogaritm. Their respective cuts in the variable u are

$$ \begin{aligned} \ln(\bar{u}) &\to [1,\infty]\,, \qquad \ln(u) \to [-\infty,0]\,, \\ \mathrm{Li}_2(u) &\to [1,\infty]\,, \qquad \mathrm{Li}_2(\bar{u}) \to [-\infty,0]\,. \end{aligned} \tag{3.275} $$

In addition, we have poles caused by terms like $1/u^n$ or $1/\bar{u}^n$. The same is true for momentum fraction of the distribution amplitude v. Such terms are standard and also appear in the NLO corrections to DVCS. The genuine new feature in DVMP are contributions, that are not separable in u and v. These terms are proportional to

$$ \frac{H(u,v)}{(u-v)^n}\,, \qquad \frac{R(u,v)}{(u-v)^n}\,, \qquad n \in \{1,2\}\,, \tag{3.276} $$

with

$$ H(u,v) = \mathrm{Li}_2(u) - \mathrm{Li}_2(\bar{u}) + \mathrm{Li}_2(\bar{v}) - \mathrm{Li}_2(v) + \ln\bar{u}\ln v - \ln u \ln\bar{v}\,, \tag{3.277} $$

$$ R(u,v) = \bar{v}\ln\bar{u} + v\ln u + \bar{v}\ln\bar{v} + v\ln v\,. \tag{3.278} $$

Note, the function H is obtained from the one in [ISK04] by the conversion of variables[10]. From Eq. 3.277, the analytic structure is not obvious. The cuts in the variable u and v overlap and we have a pole in $u = v$. Applying the identity

$$\mathrm{Li}_2(u) + \mathrm{Li}_2(\bar{u}) + \ln u \ln \bar{u} - \mathrm{Li}_2(1) = 0 \tag{3.279}$$

we can separate the contributions in a way, that we have only cuts along the real axes in $[1, \infty]$ for u and $[-\infty, 0]$ in v. In this way, the cuts in the variables u and v do not overlap. Thus we only allow the functions $\mathrm{Li}_2(u)$, $\ln \bar{u}$ for u and $\mathrm{Li}_2(\bar{v})$, $\ln v$ for v. We introduce a new function $L(u, v)$ for which the cuts are separated

$$L(u, v) = \mathrm{Li}_2(u) + \mathrm{Li}_2(\bar{v}) + \ln \bar{u} \ln v - \zeta(2)\,. \tag{3.280}$$

Employing the identity (3.279), the function H is given by the sum

$$H(u, v) = L(\bar{u}, \bar{v}) - L(u, v)\,. \tag{3.281}$$

We added the term $\zeta(2)$ in the definition of $L(u, v)$ (3.280) for our convenience, and it vanishes in the sum. This has the advantages, that due to

$$L(u, u) = L(v, v) = 0\,, \tag{3.282}$$

the term $L(u, v)/(u - v)^n$ is finite at its own right. It is possible to express the function R by derivatives in u and v acting on H. Therefore, we only have to consider the function L. Its derivatives are given by

$$\begin{aligned} L_u(u, v) &= \frac{\partial}{\partial u} L(u, v) = -\frac{\ln \bar{u}}{u} - \frac{\ln v}{\bar{u}}\,, \\ L_v(u, v) &= \frac{\partial}{\partial v} L(u, v) = \frac{\ln \bar{u}}{v} - \frac{\ln v}{\bar{v}}\,, \\ L_{uv}(u, v) &= \frac{\partial^2}{\partial u \partial v} L(u, v) = -\frac{1}{\bar{u} v}\,. \end{aligned} \tag{3.283}$$

The function $L(u, v)$ is holomorphic in the vicinity of $u = 0$ and $v = 1$. At these points the function takes the values

$$L(u{=}0, v) = \mathrm{Li}_2(\bar{v}) - \zeta(2) \quad \text{and} \quad L(u, v{=}1) = \mathrm{Li}_2(u) - \zeta(2)\,, \tag{3.284}$$

respectively. In addition, with help of the identity (3.279) we write down the two representations

$$\begin{aligned} L(u, v) &= \mathrm{Li}_2(\bar{v}) - \mathrm{Li}_2(\bar{u}) + \ln v \ln \bar{u} - \ln u \ln \bar{u} \\ &= \mathrm{Li}_2(u) - \mathrm{Li}_2(v) + \ln \bar{u} \ln v - \ln \bar{v} \ln v\,. \end{aligned} \tag{3.285}$$

The first representation is the original form in the H function (3.277). By comparison of the two equations above, we obtain the symmetry relation

$$L(v, u) = L(\bar{u}, \bar{v})\,. \tag{3.286}$$

[10] With the replacement rules: $1{+}y \to u$, $-y \to \bar{u}$, $z \to \bar{v}$.

3.3.6.2. Example

As described in the previous section, we reformulate the result of [ISK04] for the hard scattering amplitude of the pure singlet channel introducing the function $L(u,v)$ to separate the cuts in u and v. We first shift our attention to the part that does not factorize in the two momentum fractions.
From Eq. (15) in [ISK04] this part reads in terms of the original variables

$$\frac{1}{z\bar{z}}\left[-\frac{R(1+y,\bar{z})}{y+\bar{z}}+\frac{y(y+1)+(y+\bar{z})^2}{(y+\bar{z})^2}H(1+y,\bar{z})\right]+\{z\to\bar{z}\}\,. \tag{3.287}$$

Note, that we have to change the arguments of the GPD H, due to our definition of the momentum fractions. Transforming the previous equation into our variables leads to

$$\frac{1}{v\bar{v}}\left[-\frac{R(u,v)}{u-v}+\frac{-u\bar{u}+(u-v)^2}{(u-v)^2}H(u,v)\right]+\{v\to\bar{v}\}\,. \tag{3.288}$$

We can employ further symmetries and simplify the expression by using the explicit form of H (3.277) and R (3.278), together with the introduction of L (3.280). We obtain

$$\frac{1}{v\bar{v}}\left[-\frac{\bar{v}\ln\bar{u}+v\ln v}{u-v}+\frac{-u\bar{u}+(u-v)^2}{(u-v)^2}L(u,v)\right]-\{u\to\bar{u}\}+\{v\to\bar{v}\}-\{u\to\bar{u},v\to\bar{v}\}\,. \tag{3.289}$$

Investing this equation closely, we realize, that although the cuts are separated, due to the factors of $1/v$ the pole at $v=0$ lies on the cut of $\ln v$ and $\mathrm{Li}_2(\bar{v})$. We remove this unwanted feature with the two decompositions identities

$$\frac{1}{v(u-v)}=\frac{1}{uv}+\frac{1}{u(u-v)}\,,\qquad \frac{1}{v(u-v)^2}=\frac{1}{u(u-v)^2}+\frac{1}{u^2(u-v)}+\frac{1}{u^2v}\,. \tag{3.290}$$

With theses decompositions (3.289) becomes

$$\begin{aligned}&\frac{u\bar{u}+(u-v)\bar{v}}{u\bar{v}}\frac{L(u,v)}{(u-v)^2}+\frac{\bar{v}\ln\bar{u}+u\ln v}{u\bar{v}(u-v)}+\frac{\mathrm{Li}_2(\bar{v})-\zeta(2)}{uv}+\frac{\mathrm{Li}_2(u)+\ln\bar{u}\ln v}{u\bar{v}}\\&\quad-\frac{2\mathrm{Li}_2(u)}{v\bar{v}}-2\frac{\ln\bar{u}\ln v}{u\bar{v}}+\frac{\ln\bar{u}}{u\bar{v}}+\ln v\frac{\bar{u}-u}{uv\bar{v}}\ln\bar{u}+\{\to\}\,.\end{aligned} \tag{3.291}$$

Here, the symbol $\{\to\}$ stands for the contributions due to the interchange of $u\to\bar{u}$ and $v\to\bar{v}$ as in (3.289). Note, we use this symmetry to obtain terms that have the analytic properties spelled out before. To repeat the special properties of the equation above: we used the symmetry of the original expression to separated the cuts in the variables u and v. In addition, we decomposed the numerators to avoid explicit terms with poles on the remaining cuts. Furthermore, the expression is explicitly finite at the point $u=v$.
The remaining term, which is not proportional to $1/(u-v)^n$ is in the original notation

$$\begin{aligned}&\frac{1}{z\bar{z}}\frac{2y+1}{y(y+1)}\left\{\frac{y}{2}\ln(-y)^2-\frac{y+1}{2}\ln(y+1)^2+\left[\ln\left(\tfrac{\mathcal{Q}^2z}{\mu_F^2}\right)-1\right]\left[y\ln(-y)-(y+1)\ln(y+1)\right]\right\}\\&\quad+\frac{y\ln(-y)+(y+1)\ln(y+1)}{z\bar{z}y(y+1)}+\{z\to\bar{z}\}\,.\end{aligned} \tag{3.292}$$

The straight forward conversion to our variables and the restoration of the symmetry leads to

$$\left[\ln\left(\frac{\mathcal{Q}^2}{\mu_{\mathrm{F}}^2}\right)+\ln\bar{v}+\frac{1}{2}\ln\bar{u}-1\right]\frac{\bar{u}-u}{uv\bar{v}}\ln\bar{u}-\frac{1}{v\bar{v}}\frac{\ln\bar{u}}{u}+\{\to\}\,. \tag{3.293}$$

In that manner, we write the NLO contribution to the hard scattering amplitude ${}^{\mathrm{pS}}T^{(1)}(u,v)$ in terms of a part that factorizes in u and v plus an addendum denoted by $\Delta^{\mathrm{pS}}T^{(1)}(u,v)$. This addenda is now completely free of poles on the cut and is finite at the point $u=v$. The result in the non-symmetric notation (cf. Eq. 3.216 and 3.238) reads:

$$\begin{aligned}{}^{\mathrm{pS}}T^{(1,\mathrm{F})}(u,v) &= \left[\ln\frac{\mathcal{Q}^2}{\mu_{\mathrm{F}}^2}+\frac{1}{2}\ln\bar{u}+\ln(v\bar{v})-1\right]\frac{\bar{u}-u}{uv\bar{v}}\ln\bar{u}-\frac{2\mathrm{Li}_2(u)}{v\bar{v}}\\ &\quad-\left[\frac{1}{2v\bar{v}}+\frac{\ln v}{\bar{v}}+\frac{\ln\bar{v}}{v}\right]\frac{\ln\bar{u}}{u}+\Delta^{\mathrm{pS}}T^{(1)}(u,v)\,, \qquad (3.294a)\\ \Delta^{\mathrm{pS}}T^{(1,\mathrm{F})}(u,v) &= \frac{u\bar{u}+u\bar{v}-v\bar{v}}{u\bar{v}}\frac{L(u,v)}{(u-v)^2}+\frac{\bar{v}\ln\bar{u}+u\ln v}{u\bar{v}(u-v)}+\frac{\mathrm{Li}_2(u)+\ln\bar{u}\ln v}{u\bar{v}}\\ &\quad+\frac{\mathrm{Li}_2(\bar{v})-\zeta(2)}{uv}\,. \qquad (3.294b)\end{aligned}$$

Here, the addendum $\Delta^{\mathrm{pS}}T^{(1,\mathrm{F})}(u,v)$ is defined in such a way, that it does not contain poles due to $1/u$ or $1/\bar{v}$, in order to minimize the complexity of the addendum. Note, that this is the hard scattering amplitudes which does not have definite symmetry with respect to the interchange of $u\to\bar{u}$ and $v\to\bar{v}$.

In addition, we can simplify the expression for the nonfactoriable contribution $\Delta^{\mathrm{pS}}T^{(1)}(u,v)$ that we write it as a derivative acting on

$$\Delta^{\mathrm{pS}}T^{(1)}(u,v)=\frac{1}{v\bar{v}}\frac{\partial}{\partial v}v^2\bar{v}\left[\frac{1}{u}\frac{L(u,v)}{u-v}\right]^{\mathrm{sub}}\,, \tag{3.295}$$

where the subscript sub means, that the singularity at the pole $u=0$ is subtracted. Expanding the subscript reads:

$$\left[\frac{1}{u}\frac{L(u,v)}{u-v}\right]^{\mathrm{sub}}\equiv\frac{L(u,v)}{u(u-v)}+\frac{L(u=0,v)}{uv}\,. \tag{3.296}$$

This representation, will be an advantage, when we switch to conformal space in chapter 4. For now, we stay with this expression in momentum fraction representation. The expressions for the two other parts are obtained complete analogy. Let us first introduce the outlined description in an general form. Afterward we present the result for the flavor non-singlet and gluon-quark channel.

3.3.6.3. Generic structure

In our presentation of the NLO corrections in the channel $A\in\{\mathrm{q},\mathrm{pS},\mathrm{G}\}$. In the momentum fraction representation we write the NLO approximation of the perturbative expansion (3.243)

with the LO coefficient (3.274) as

$$ {}^{A}T(u,v|\cdots) = \alpha_s\, {}^{A}T^{(0)}(u,v) + \frac{\alpha_s^2}{2\pi}\, {}^{A}T^{(1)}(u,v|\cdots) + O(\alpha_s^3)\,. \tag{3.297} $$

We decompose the NLO corrections with respect to their color factors. Schematically, we write

$$ {}^{A}T^{(1)} = \sum_{\rm c} C_{\rm c}\, {}^{A}T^{(1,{\rm c})} \qquad \text{with } C_{\rm c} \in \{C_{\rm F}, C_{\rm A}, C_{\rm G}{=}C_{\rm F} - C_{\rm A}/2, \beta_0\}\,. \tag{3.298} $$

The color factors take the values

$$ C_{\rm F} = \frac{4}{3}\,, \quad C_{\rm A} = 3\,, \quad C_{\rm G}{=}-\frac{1}{6}\,, \quad \text{and } \beta_0 = -11 + \frac{2N_{\rm f}}{3}\,. \tag{3.299} $$

As already demonstrated in section 3.3.6.2, the NLO corrections (3.297) can be decomposed in u and v separable and non-separable contributions,

$$ {}^{A}T^{(1,c)}(u,v) = \sum_{i,j} a_{ij}^c\, f_i(u) f_j(v) + \Delta\, {}^{A}T^{(1,c)}(u,v)\,, \tag{3.300} $$

where $f_i(u)$ are certain single variable functions. $\Delta\, {}^{A}T^{(1,c)}(u,v)$ denotes the non-separable part in channel A with color structure c. We also decompose the non-separable addenda with respect to their color factors into a set of functions $f_i(u,v)$, depending on the two momentum fractions:

$$ \Delta\, {}^{A}T^{(1,c)}(u,v) = \sum_{i} a_i^c\, f_i(u,v)\,. \tag{3.301} $$

In the next two sections we introduce the building blocks for separable and non-separable functions $f_i(u)$ and $f_i(u,v)$, respectively.

3.3.6.4. Building blocks for separable NLO terms

In this section, we introduce the building blocks for separable contributions to the NLO hard scattering amplitudes ordered by their respective degree of singularity.

- *Most singular building blocks.*

The LO coefficients ${}^{A}T^{(0)}(u,v)$ consists of two factorized poles $1/(\bar{u}\bar{v})$ at the cross-over point $u{=}1$, $(x{=}\eta)$, of the GPD and the endpoint $v{=}1$ of the DA. As we have seen in the example 3.3.6.2, Eq. 3.294, they can be accompanied by logarithmic $[1,\infty]$-cuts along the positive real axis at NLO. Such a logarithmic enhancement implies large perturbative corrections in the vicinity of the cross-over point and/or the endpoint region. The most singular term appearing at NLO is proportional to a squared logarithm. As the most singular building blocks, we consider (analogously for $u \to v$)

$$ \frac{1}{\bar{u} - i\epsilon}\,, \quad \frac{\ln(\bar{u} - i\epsilon)}{\bar{u} - i\epsilon}\,, \quad \frac{\ln^2(\bar{u} - i\epsilon)}{\bar{u} - i\epsilon}\,. \tag{3.302} $$

Their values on the cut is governed by the $\bar{u}{-}i\epsilon$-prescription, inherited from Feynman's causality prescription.

- *Building blocks with logarithmical* $[1,\infty]$*-cuts.*

The NLO expressions also contain terms possessing only logarithmic $[1,\infty]$-cuts. In contrast to the most singular building blocks, the LO poles on the cut at $u=1$ (or $v=0$) is absent. Consequently, such terms are rather harmless. The building blocks with logarithmical cuts are (analogously for $u\to v$)

$$\frac{\ln(\bar{u}-i\epsilon)}{u}\,,\quad \frac{\ln^2(\bar{u}-i\epsilon)}{u}\,,\quad \left[\frac{\ln\bar{u}}{u^2}\right]^{\text{sub}}\equiv\frac{\ln(\bar{u}-i\epsilon)+u}{u^2}\,,\quad \frac{\ln^2(\bar{u}-i\epsilon)}{u^2}\,. \tag{3.303}$$

The terms proportional to $1/u^2$ only occur in the gluon-quark channel. Note, the term $\ln(\bar{u}-i\epsilon)/(u-i\epsilon)^2$ possesses also a pole at $u=0$, which is removed in $[\ln(\bar{u}-i\epsilon)+u]/u^2$ by subtraction.

- *Building blocks with dilogarithms.*

Additionally, terms containing the dilogarithm (or Spence) function $\mathrm{Li}_2(u+i\epsilon)$ appear in the NLO hard scattering amplitudes, where causality implies the $u+i\epsilon$-prescription. It has a logarithmical $[1,\infty]$-cut and its asymptotic behavior in the vicinity of $u=0$ is $u+O(u^2)$. The two building blocks with dilogarithms are (analogously for $u\to v$)

$$\frac{\mathrm{Li}_2(u+i\epsilon)}{u}\quad\text{and}\quad\frac{\mathrm{Li}_2(u+i\epsilon)}{u^2}\quad\text{or}\quad\left[\frac{\mathrm{Li}_2(u+i\epsilon)}{u^2}\right]^{\text{sub}}\equiv\frac{\mathrm{Li}_2(u+i\epsilon)-u}{u^2}\,, \tag{3.304}$$

where the single pole in $\mathrm{Li}_2(u)/u^2$ is subtracted. Moreover, dilogarithms appear in connection to poles at the cross-over line $u=1$. Although $u=1$ is a branch point, we subtract these poles that only the most singular building blocks (3.302) contain such poles. Therefore, we introduce the following subtracted building blocks (analogously for $u\to v$)

$$\left[\frac{\mathrm{Li}_2(u)}{\bar{u}}\right]^{\text{sub}}\equiv\frac{\mathrm{Li}_2(u)-\zeta(2)}{\bar{u}}\quad\text{and}\quad\left[\frac{\mathrm{Li}_2(u)}{\bar{u}^2}\right]^{\text{sub}}\equiv\frac{\mathrm{Li}_2(u)-\zeta(2)-\bar{u}\ln\bar{u}+\bar{u}}{\bar{u}^2}\,, \tag{3.305}$$

possessing harmless logarithmical singularities in the vicinity of $u=1$ and approach a constant at $u=0$.

- *Peculiarities at* $u\to\infty$*.*

In the pure singlet quark contribution (3.291) the functions

$$\ln(\bar{u}-i\epsilon)\,,\quad \ln^2(\bar{u}-i\epsilon)\,,\quad\text{and}\quad \mathrm{Li}_2(u+i\epsilon) \tag{3.306}$$

appear, which do not vanish in the limit $u\to\infty$.

- *Exploiting symmetry.*

We can exploit symmetry with respect to the transformations $u\to\bar{u}$ and $v\to\bar{v}$ to express the hard scattering amplitudes by holomorphic function except for discontinuities on the positive

axes. Using the transformation $u \to \bar{u}$, possible terms with poles at $u=0$ and logarithmic $[-\infty, 0]$-cuts along the negative axis, e.g.,

$$\frac{\ln^p u}{u}\,, \quad \frac{\ln^p u}{\bar{u}}\,, \quad \left[\frac{\ln u}{\bar{u}^a}\right]^{\text{sub}}\,, \quad \left[\frac{\text{Li}_2(\bar{u})}{\bar{u}^a}\right]^{\text{sub}}\,, \quad \left[\frac{\text{Li}_2(\bar{u})}{u^a}\right]^{\text{sub}} \tag{3.307}$$

to those in (3.303), having poles at $u=1$ and logarithmic $[1, \infty]$-cuts along the positive axis. As consequence, functions with cuts along the positive and negative axes can be eliminated. The only appearing function of that type in the NLO hard scattering amplitudes is $\ln u \ln \bar{u}$ in connection with a rational function. Utilizing the formula

$$\text{Li}_2(u+i\epsilon)+\text{Li}_2(\bar{u}+i\epsilon)+\ln(u-i\epsilon)\ln(\bar{u}-i\epsilon)-\text{Li}_2(1) \simeq 0 \quad \text{with} \quad \text{Li}_2(1) = \zeta(2)\,, \tag{3.308}$$

where we obtain the identity (3.279) in the limit $\epsilon \to 0$. Consequently, $\ln(u-i\epsilon)\ln(\bar{u}-i\epsilon)$ splits into two terms that are expressed by dilogarithm functions. Note, for $u \geq 1$ ($u<0$) the $u+i\epsilon$ ($\bar{u}+i\epsilon$) prescription in the dilogarithm is consistent with the $\bar{u}-i\epsilon$ ($u-i\epsilon$) one in the logarithm. Afterward, we perform the mapping $u \to \bar{u}$ together with a potential subtraction of $\text{Li}_2(\bar{u})$ and poles at $u=0$.

3.3.6.5. Building blocks for non-separable NLO terms

As we have seen in the example (3.295), the non-separable addenda (3.300) of all channels can be expressed in terms of

$$\frac{1}{u^a \bar{v}^b} \cdot \frac{\text{Li}_2(u) + \text{Li}_2(\bar{v}) + \ln \bar{u} \ln v - \zeta(2)}{u - v} \tag{3.309}$$

and its derivatives with respect to the momentum fraction v. The poles at $u=0$ and $v=1$ are of first and/or second order. In the example (3.295), we had $a=1$, $b=0$. The representation of non-separable terms is not unique, since one might use another combination of dilogarithm and logarithm functions. In addition, due to identities of the type (3.290) the accompanying rational function can be chosen differently, e.g.,

$$\frac{1}{v}\frac{1}{u-v} = \frac{1}{u}\frac{1}{u-v} + \frac{1}{uv}\,.$$

Since the $L(u,v)$-function is holomorphic in the vicinity of $u=0$ and $v=1$, we can straightforwardly subtract the poles in the building blocks (3.309). Let us for example consider the term

$$\frac{1}{\bar{v}}\frac{L(u,v)}{u-v}\,. \tag{3.310}$$

This term has a pole at $v=1$. Besides the prefactor, in the vicinity of the pole we obtain the expression

$$\frac{L(u,v)}{u-v} \overset{v=1}{\to} -\frac{L(u,v=1)}{\bar{u}} = -\frac{\text{Li}_2(u)-\zeta(2)}{\bar{u}}\,. \tag{3.311}$$

Therefore, in the original term (3.310) together with the one above, the pole is subtracted. We use the notation

$$\frac{1}{\bar{v}}\,\frac{L(u,v)}{u-v}+\frac{L(u,v{=}1)}{\bar{u}\bar{v}}\equiv\left[\frac{1}{\bar{v}}\,\frac{L(u,v)}{u-v}\right]^{\text{sub}}. \tag{3.312}$$

The additional term can be expressed by the separable building blocks of dilogarithms (3.305). We will now list the appearing terms for all channels. In the pure singlet quark and gluon-quark channel, we need the subtracted expressions

$$\left[\frac{1}{u\bar{v}}\,\frac{L(u,v)}{u-v}\right]^{\text{sub}}\equiv\frac{L(u,v)}{u\bar{v}(u-v)}+\frac{L(u,v{=}1)}{u\bar{u}\bar{v}}+\frac{L(u{=}0,v)}{uv\bar{v}}-\frac{L(u{=}0,v{=}1)}{u\bar{v}}\,, \tag{3.313a}$$

which is symmetric under $u\leftrightarrow\bar{v}$-reflection. To shorten the notation in the flavor non-singlet channel we also introduce the associated building blocks

$$\left[\frac{1}{\bar{v}}\,\frac{L(u,v)}{u-v}\right]^{\text{sub}}\equiv\frac{L(u,v)}{\bar{v}(u-v)}+\frac{L(u,v{=}1)}{\bar{u}\bar{v}}\,, \tag{3.313b}$$

$$\left[\frac{1}{\bar{v}^2}\,\frac{L(u,v)}{u-v}\right]^{\text{sub}}\equiv\frac{L(u,v)}{\bar{v}^2(u-v)}+\frac{(\bar{u}+\bar{v})L(u,v{=}1)}{\bar{u}^2\bar{v}^2}-\frac{L_v(u,v{=}1)}{\bar{u}\bar{v}}\,, \tag{3.313c}$$

and their $u\leftrightarrow\bar{v}$-reflected analog, see the symmetry relation (3.286),

$$\left[\frac{1}{u}\,\frac{L(u,v)}{u-v}\right]^{\text{sub}}\equiv\frac{L(u,v)}{u(u-v)}+\frac{L(u{=}0,v)}{uv}\,, \tag{3.313d}$$

$$\left[\frac{1}{u^2}\,\frac{L(u,v)}{u-v}\right]^{\text{sub}}\equiv\frac{L(u,v)}{u^2(u-v)}+\frac{(u+v)L(u{=}0,v)}{u^2v^2}+\frac{L_u(u{=}0,v)}{uv}\,. \tag{3.313e}$$

These non-separable building blocks can now be considered as rather harmless, whereas the reshuffled subtraction terms, separable in the u and v variables, contain only one pole in u or v that is accompanied with a rather harmless function in v or u.
Finding such a representation (3.309), where the poles are now subtracted, and the associated differential operator, which we generically call $\vec{\mathcal{D}}^{(p,c)}_{ab}$, labeled by the (negative) powers a and b of the accompanying u and $\bar{v}$ factors for the color structure c in a given channel and the order p in perturbation theory, is now a straightforward algebraic procedure. It leads us to the following simple form of the addenda (3.301)

$$\Delta^A T^{(1,c)}(u,v)=\sum_{a,b}{}^A\vec{\mathcal{D}}^{(1,c)}_{ab}\left[\frac{1}{u^a\,\bar{v}^b}\,\frac{L(u,v)}{u-v}\right]^{\text{sub}}, \tag{3.314}$$

in a given channel. Note that $\vec{\mathcal{D}}^{(p,c)}_{ab}$ can be a second order differential, first order differential, or simply a multiplication operator. In the example (3.295) the corresponding differential operator reads

$${}^{\text{pS}}\vec{\mathcal{D}}^{(1,\text{F})}_{1,0}=\frac{1}{v\bar{v}}\frac{\partial}{\partial v}v^2\bar{v}\,. \tag{3.315}$$

3.3.6.6. Flavor non-singlet channel

The NLO contributions in the flavor non-singlet channel can be read off from [MNP99]. The color factor decomposition of the corresponding coefficient is

$$ {}^{\mathrm{q}}T^{(1)}\left(u,v\middle|\tfrac{\mathcal{Q}^2}{\mu_{\mathrm{F}}^2},\tfrac{\mathcal{Q}^2}{\mu_\varphi^2},\tfrac{\mathcal{Q}^2}{\mu_{\mathrm{R}}^2}\right) = C_{\mathrm{F}}\,{}^{\mathrm{q}}T^{(1,\mathrm{F})}\left(u,v\middle|\tfrac{\mathcal{Q}^2}{\mu_{\mathrm{F}}^2},\tfrac{\mathcal{Q}^2}{\mu_\varphi^2}\right) + \beta_0\,{}^{\mathrm{q}}T^{(1,\beta)}\left(u,v\middle|\tfrac{\mathcal{Q}^2}{\mu_{\mathrm{R}}^2}\right) + C_{\mathrm{G}}\,{}^{\mathrm{q}}T^{(1,\mathrm{G})}(u,v)\,, \tag{3.316}$$

They are symmetric under the exchange of the factorization scales and momentum fractions of the GPD and the DA $(u,\mu_{\mathrm{F}}) \leftrightarrow (v,\mu_\varphi)$. The functions ${}^{\mathrm{q}}T^{(1,\mathrm{F})}(u,v)$ and ${}^{\mathrm{q}}T^{(1,\beta)}(u,v)$ are expressible by separable most singular building blocks (3.302) and the logarithmic ones (3.303). The function ${}^{\mathrm{q}}T^{(1,\mathrm{G})}(u,v)$ on the other hand inherits besides such singularities also logarithmic cuts on the negative u- and v-axis. In addition, it contains a non-separable addendum. Following the subtraction procedure, introduced in Sec. 3.3.6.5 , its explicit reads

$$\begin{aligned}\Delta\,{}^{\mathrm{q}}T^{(1,\mathrm{G})}(u,v) = {}& \left[\frac{\bar u u}{\bar v}+\frac{\bar v v}{\bar u}+\frac{(u-v)^3}{\bar u\bar v}\right]\frac{L(u,v)}{(u-v)^3}+\frac{\bar u\ln v+\bar v^2}{\bar u\bar v^2\,(u-v)}+\frac{2\bar v\ln\bar u+2v\ln v}{\bar v(u-v)^2}\\ & -\frac{\ln\bar u\ln v+\mathrm{Li}_2(\bar v)}{\bar u\bar v^2}-\frac{(\bar u-u)\,[\mathrm{Li}_2(u)-\zeta(2)]+\bar u\ln\bar u}{\bar u^2\bar v}\,.\end{aligned} \tag{3.317}$$

This addendum possesses $1/(u-v)^n$ terms with up to $n=3$, however, it is finite at $u=v$. As desired, $\Delta\,{}^{\mathrm{q}}T^{(1,\mathrm{G})}(u,v)$ has only logarithmic cuts on the positive u- and negative v-axis. We write the terms, which are separable in the color decomposition (3.316) as follows.

$${}^{\mathrm{q}}T^{(1,\mathrm{F})}(u,v) = \left[\ln\frac{\mathcal{Q}^2}{\mu_{\mathrm{F}}^2}+\frac{1}{2}\ln(\bar u\bar v)+1\right]\frac{3+2\ln\bar u}{2\bar u\bar v}-\frac{23}{6\bar u\bar v}-\frac{\ln\bar u}{2u\bar v}+\{\mu_{\mathrm{F}}\to\mu_\varphi, u\leftrightarrow v\}\,, \tag{3.318a}$$

$${}^{\mathrm{q}}T^{(1,\beta)}(u,v) = \left[\frac{1}{2}\ln\frac{\mathcal{Q}^2}{\mu_{\mathrm{R}}^2}+\ln\bar u-\frac{5}{6}\right]\frac{1}{2\bar u\bar v}+\{u\leftrightarrow v\}\,. \tag{3.318b}$$

The term proportional to C_{G} possesses an addendum:

$$\begin{aligned}{}^{\mathrm{q}}T^{(1,\mathrm{G})}(u,v) = {}& \left[\ln\bar u\frac{\ln v}{\bar v}+\ln\bar v-\frac{7}{6}-\zeta(2)+2\mathrm{Li}_2(v)-2\mathrm{Li}_2(\bar v)-\ln u\ln v\right]\frac{1}{\bar u\bar v}\\ & +\left[\frac{\mathrm{Li}_2(\bar v)-\mathrm{Li}_2(v)+\zeta(2)}{\bar v}+\frac{\ln v}{\bar v}-1\right]\frac{1}{\bar u\bar v}+\Delta\,{}^{\mathrm{q}}T^{(1,\mathrm{G})}(u,v)+\{u\leftrightarrow v\}\,.\end{aligned} \tag{3.318c}$$

The addendum $\Delta\,{}^{\mathrm{q}}T^{(1,\mathrm{G})}(u,v)$, see (3.317), can be expressed by means of a differential operator that acts on the non-separable building block (3.313b) and the building block (3.313c),

$$\Delta\,{}^{\mathrm{q}}T^{(1,\mathrm{G})}(u,v) = \left[\frac{\vec\partial^2}{\partial v^2}-\frac{2}{v\bar v}\right]v\bar v\left[\frac{1}{\bar v}\frac{L(u,v)}{u-v}\right]^{\mathrm{sub}}-\frac{\vec\partial}{\partial v}\,\bar v\left[\frac{1}{\bar v}\frac{L(u,v)}{u-v}\right]^{\mathrm{sub}}+\left[\frac{1}{\bar v^2}\,\frac{L(u,v)}{u-v}\right]^{\mathrm{sub}}. \tag{3.318d}$$

Note, to avoid a boundary term in a partial integration, we introduced an oversubtraction for the second order derivative. The $u\leftrightarrow v$-reflected addendum can be conveniently written

in terms of the variables $\bar{v}$ and $\bar{u}$ as

$$\Delta^{\mathrm{q}}T^{(1,\mathrm{G})}(\bar{v},\bar{u}) = \left[\frac{\vec{\partial}^2}{\partial v^2}-\frac{2}{v\bar{v}}\right] v\bar{v}\left[\frac{1}{u}\frac{L(u,v)}{u-v}\right]^{\mathrm{sub}} + \frac{\vec{\partial}}{\partial v}\, v\left[\frac{1}{u}\frac{L(u,v)}{u-v}\right]^{\mathrm{sub}} + \frac{1}{v}\left[\frac{1}{u}\frac{L(u,v)}{u-v}\right]^{\mathrm{sub}} - \frac{\mathrm{Li}_2(u)+\ln\bar{u}+(\ln\bar{u}+u)\ln v}{u^2 v}\,. \tag{3.318e}$$

Here, the last term subtracts the pole contribution at $v=0$.

3.3.6.7. Pure singlet quark channel

We take the pure singlet contribution directly from [ISK04]. As shown in Sec. 3.3.6.2, it is symmetric under $v\to\bar{v}$ and antisymmetric under $u\to\bar{u}$ and $(u,v)\to(\bar{u},\bar{v})$. As mentioned earlier, the contribution of the pure singlet channel is proportional to C_{F}. Thus, we have the decomposition into the color factor as

$${}^{\mathrm{pS}}T^{(1)}\left(u,v\middle|\tfrac{\mathcal{Q}^2}{\mu_{\mathrm{F}}^2},\tfrac{\mathcal{Q}^2}{\mu_{\varphi}^2},\tfrac{\mathcal{Q}^2}{\mu_{\mathrm{R}}^2}\right) = C_{\mathrm{F}}\,{}^{\mathrm{pS}}T^{(1,\mathrm{F})}\left(u,v\middle|\tfrac{\mathcal{Q}^2}{\mu_{\mathrm{F}}^2}\right)\,. \tag{3.319}$$

The non-separate contributions accumulate in the addendum

$$\Delta^{\mathrm{pS}}T^{(1)}(u,v) = \frac{u\bar{u}+u\bar{v}-v\bar{v}}{u\bar{v}}\frac{L(u,v)}{(u-v)^2}+\frac{\bar{v}\ln\bar{u}+u\ln v}{u\bar{v}(u-v)}+\frac{\mathrm{Li}_2(u)+\ln\bar{u}\ln v}{u\bar{v}}+\frac{\mathrm{Li}_2(\bar{v})-\zeta(2)}{uv}. \tag{3.320}$$

As already demonstrated, this function is finite in the point $u=v$ and the pole at $u=0$ is subtracted, while a pole at $v=1$ remains. It can be expressed by the non-separable building block (3.313d), which makes the analytical properties of the addendum obvious. Repeating the final result reads

$${}^{\mathrm{pS}}T^{(1,\mathrm{F})}(u,v) = \left[\ln\frac{\mathcal{Q}^2}{\mu_{\mathrm{F}}^2}+\frac{1}{2}\ln\bar{u}+\ln(v\bar{v})-1\right]\frac{\bar{u}-u}{uv\bar{v}}\ln\bar{u}-\frac{2\mathrm{Li}_2(u)}{v\bar{v}} - \left[\frac{1}{2v\bar{v}}+\frac{\ln v}{\bar{v}}+\frac{\ln\bar{v}}{v}\right]\frac{\ln\bar{u}}{u}+\Delta^{\mathrm{pS}}T^{(1)}(u,v)\,, \tag{3.321a}$$

$$\Delta^{\mathrm{pS}}T^{(1,\mathrm{F})}(u,v) = \frac{1}{v\bar{v}}\frac{\partial}{\partial v}v^2\bar{v}\left[\frac{1}{u}\frac{L(u,v)}{u-v}\right]^{\mathrm{sub}}\,. \tag{3.321b}$$

The first two terms on the right hand side of (3.321a) diverge logarithmically in the limit $u\to\infty$. The terms proportional to $\ln^2\bar{u}$ and $\mathrm{Li}_2(u)$ cancel each other, leaving a constant that vanishes by anti-symmetrization.

3.3.6.8. Gluon-quark channel

For the gluon-quark contribution we take the results from Ref. [ISK04] and rewrite them in a compact form, using symmetry under $u\leftrightarrow\bar{u}$ and $v\leftrightarrow\bar{v}$ (compare Eq. 3.237), in such a manner that the net results have the desired analytic properties[11]. We prefer functions symmetric

[11] To shorter the expression we will allow for one pole contribution at $u=0$.

under $v \leftrightarrow \bar{v}$. The LO contribution ${}^{\mathrm{G}}T^{(0)}(u,v)$ is defined in (3.274). The NLO contribution can be decomposed in terms of its color structure as

$$ {}^{\mathrm{G}}T^{(1)}\left(u,v\middle|\tfrac{\mathcal{Q}^2}{\mu_{\mathrm{F}}^2},\tfrac{\mathcal{Q}^2}{\mu_\varphi^2},\tfrac{\mathcal{Q}^2}{\mu_{\mathrm{R}}^2}\right) = C_{\mathrm{A}}\,{}^{\mathrm{G}}T^{(1,\mathrm{A})}\left(u,v\middle|\tfrac{\mathcal{Q}^2}{\mu_{\mathrm{F}}^2}\right) + C_{\mathrm{F}}\,{}^{\mathrm{G}}T^{(1,\mathrm{F})}\left(u,v\middle|\tfrac{\mathcal{Q}^2}{\mu_{\mathrm{F}}^2},\tfrac{\mathcal{Q}^2}{\mu_\varphi^2}\right) + \frac{\beta_0}{2\bar{u}\bar{v}}\ln\frac{\mu_{\mathrm{F}}^2}{\mu_{\mathrm{R}}^2}\,. \tag{3.322}$$

The term proportional to β_0 is given by $\ln(\mu_{\mathrm{F}}^2/\mu_{\mathrm{R}}^2)$ times the LO amplitude (3.274). We introduce two addenda for the parts proportional to C_{A} and C_{F},

$$\begin{aligned}\Delta^{\mathrm{G}}T^{(1,\mathrm{A})}(u,v) &= \frac{\bar{u}-u}{4v\bar{v}}\left[\frac{L(u,v)}{(u-v)^2}+\frac{u\ln v+\bar{v}\ln\bar{u}}{u\bar{v}(u-v)}\right]+\frac{\mathrm{Li}_2(u)+\ln\bar{u}\ln v+\ln\bar{u}}{2uv}\\ &\quad-\frac{2\mathrm{Li}_2(u)-2\zeta(2)}{4\bar{u}\bar{v}}+\frac{\ln v+1}{2\bar{v}}\frac{\ln\bar{u}}{u}+\frac{\ln v}{2v\bar{v}^2}\,, \qquad (3.323a)\\ \Delta^{\mathrm{G}}T^{(1,\mathrm{F})}(u,v) &= \frac{u\bar{v}-(u-v)^2}{2u\bar{v}}\frac{L(u,v)}{(u-v)^3}+\frac{u\ln v+\bar{v}\ln\bar{u}}{2u\bar{v}(u-v)^2}+\frac{\ln\bar{u}+u}{4uv(u-v)}+\frac{\ln v+\bar{v}}{4\bar{v}^2(u-v)}\\ &\quad-\frac{\mathrm{Li}_2(u)-\zeta(2)}{2u\bar{u}\bar{v}}-\frac{\mathrm{Li}_2(\bar{v})-\bar{v}\zeta(2)}{2uv\bar{v}}\,. \qquad (3.323b)\end{aligned}$$

As before they are finite at $u=v$ possessing only logarithmic cuts on the positive u-axis, and can be expressed by means of differential operators in terms of the non-separable building block (3.313a). Both addenda possess still poles at $v=0$ and/or $v=1$. Their removal is achieved by the conventional method:

$$\begin{aligned}{}^{\mathrm{G}}T^{(1,\mathrm{A})}(u,v) &= \left[\ln\frac{\mathcal{Q}^2}{\mu_{\mathrm{F}}^2}+\frac{\ln\bar{u}}{2}+\frac{3\ln(v\bar{v})}{4}-\frac{3}{2}\right]\left[1+\frac{\bar{u}^2}{u^2}\right]\frac{\ln\bar{u}}{2\bar{u}v\bar{v}}\\ &\quad+\left[\frac{\ln\bar{u}}{2}-\frac{\ln(v\bar{v})}{4}-\frac{3}{2}\right]\frac{\ln\bar{u}}{uv\bar{v}}+\left[1+\zeta(2)-\frac{v^2\ln v+\bar{v}^2\ln\bar{v}}{2v\bar{v}}\right]\frac{1}{4\bar{u}v\bar{v}}\\ &\quad-\left[\frac{(\bar{u}-u)\mathrm{Li}_2(u)+u\,\zeta(2)+\bar{u}\ln^2\bar{u}}{u\bar{u}}+[2+\ln(v\bar{v})]\frac{\ln\bar{u}+u}{4u^2}\right]\frac{1}{2v\bar{v}}\\ &\quad+\Delta^{\mathrm{G}}T^{(1,\mathrm{A})}(u,v)\,. \qquad (3.324a)\end{aligned}$$

The part proportional to C_{F} can be expressed as

$$\begin{aligned}{}^{\mathrm{G}}T^{(1,\mathrm{F})}(u,v) &= \left[\ln\frac{\mathcal{Q}^2}{\mu_{\mathrm{F}}^2}+\frac{\ln\bar{u}}{2}-\frac{1}{\bar{u}}-(1-2v\ln v-2\bar{v}\ln\bar{v})\frac{u}{2\bar{u}}\right]\frac{(-1)\ln\bar{u}}{4u^2v\bar{v}}-\frac{31}{16\bar{u}v\bar{v}}\\ &\quad+\left[\ln\frac{\mathcal{Q}^2}{\mu_\varphi^2}+\frac{\ln\bar{u}}{2u}+\frac{\ln\bar{v}}{2}+\frac{1}{4}\right]\frac{3+2\ln\bar{v}}{2\bar{u}\bar{v}}\\ &\quad+\left[\frac{v^2\ln v+\bar{v}^2\ln\bar{v}}{4v\bar{v}}-\frac{(\bar{v}-v)\left[\mathrm{Li}_2(v)-\mathrm{Li}_2(\bar{v})\right]+\zeta(2)}{2}\right]\frac{1}{2\bar{u}v\bar{v}}\\ &\quad+\Delta^{\mathrm{G}}T^{(1,\mathrm{F})}(u,v)\,. \qquad (3.324b)\end{aligned}$$

Note, that $\ln\bar{u}/u^2$, appearing in the first term on the r.h.s. of (3.324a), contains a pole at $u=0$. The addenda, explicitly given in (3.323), read in terms of the non-separable building

block (3.313a) as

$$\Delta^{\mathrm{G}} T^{(1,\mathrm{A})}(u,v) = \frac{1}{v\bar{v}} \frac{\partial}{\partial v} \frac{v\bar{v}(\bar{v}-v)}{4} \left[\frac{1}{u\bar{v}} \frac{L(u,v)}{u-v} \right]^{\mathrm{sub}} , \tag{3.324c}$$

$$\Delta^{\mathrm{G}} T^{(1,\mathrm{F})}(u,v) = \left[\frac{\partial^2}{\partial v^2} - \frac{2}{v\bar{v}} \right] \frac{v\bar{v}}{4} \left[\frac{1}{u\bar{v}} \frac{L(u,v)}{u-v} \right]^{\mathrm{sub}} . \tag{3.324d}$$

4

Conformal symmetry in QCD

Quantum chromodynamics with massless quarks is invariant under conformal transformations on the classical level. However, the conformal symmetry of a quantum theory requires the vanishing of the β-function, which is not fulfilled in the kinematic region of interest in this thesis. Albeit, conformal symmetry allows to gain new insights such as the reconstruction of the anomalous dimension and evolution kernels at NLO [BM98a, BM99] of the conformal operator product expansion for DVCS [Mül98, BM98b]. For a review see [BKM03, FS10].
In this chapter, we first introduce the conformal group and its collinear subgroup. The operators of interest in this thesis are separated by a light-like distance, hence we present the corresponding conformal operators which form an irreducible representation of the collinear subgroup. Furthermore, we expand the general product of two local conformal operators obtaining the conformal operator product expansion (COPE). Up to this point, we closely follow [BKM03]. As an example, we utilize the COPE to derive the Wilson coefficients of DVCS from the DIS ones [Mül98, BM98b].
In addition, we explain the conformal partial wave expansion of the DA and GPD. Due to the skewness dependence of the GPD, the expansion does not converge. We introduce a Sommerfeld-Watson transformation to achieve a Mellin-Barnes representation of the GPD in terms of its conformal moments [MS06]. This is followed by an exhaustive discussion of the Mellin-Barnes representations of Compton form factors [MS06], and transition form factors [MLPKS14].
The Mellin-Barnes representation of amplitudes grounds on the analytic continuation of the corresponding Wilson coefficients. This was already achieved for DVCS, however for DVMP, the solution was given recently in [MLPKS14]. We present the novel derivation of conformal moments ensuring the analytic continuation. This method is applied to the separable and non-separable building blocks of the hard scattering amplitude in DVMP introduced in Sec 3.3.6. In the end, we give the LO and NLO Wilson coefficients of DVMP in a closed form.

4.1. Conformal group and its collinear subgroup

General coordinate transformations of the 4-dimensional Minkowski space conserve the interval

$$\mathrm{d}s^2 = g_{\mu\nu}(z)\mathrm{d}z^\mu \mathrm{d}z^\nu \,. \tag{4.1}$$

A subclass of such transformations only change the scale of the metric:

$$g'_{\mu\nu}(z') = \omega(z) g'_{\mu\nu}(z)\,. \tag{4.2}$$

Such transformations belong to a generalization of the Poincaré group, under which the metric is unchanged by translations and Lorentz transformations. An example is the dilatation and inversion

$$z^\mu \to z'^\mu = \lambda z^\mu \quad \text{with } \lambda \in \mathbb{R}\,, \qquad z^\mu \to z'^\mu = \frac{z^\mu}{z^2}\,. \tag{4.3}$$

Another example is the conformal transformation

$$z^\mu \to z'^\mu = \frac{z^\mu + a^\mu z^2}{1 + 2a.z + a^2 z^2}\,, \tag{4.4}$$

consisting of the sequential inversion, the translation by an arbitrary constant vector a^μ and the inversion with the same center.
The full conformal algebra in 4 dimensions includes 15 generators [MS69, TJG72]

$\mathbf{P}_\mu$	4 translations
$\mathbf{M}_{\mu\nu}$	6 Lorentz rotations
$\mathbf{D}$	1 dilatation
$\mathbf{K}_\mu$	4 special conformal transformations

where $\mathbf{P}_\mu$ and $\mathbf{M}_{\mu\nu}$ are the generators of the Poincaré group possessing the Lie algebra

$$\begin{aligned}
i\,[\mathbf{P}_\mu, \mathbf{P}_\nu] &= 0\,,\\
i\,[\mathbf{M}_{\alpha\beta}, \mathbf{P}_\mu] &= g_{\alpha\mu}\mathbf{P}_\beta - g_{\beta\mu}\mathbf{P}_\alpha\,,\\
i\,[\mathbf{M}_{\alpha\beta}, \mathbf{M}_{\mu\nu}] &= g_{\alpha\mu}\mathbf{M}_{\beta\nu} - g_{\beta\mu}\mathbf{M}_{\alpha\nu} - g_{\alpha\nu}\mathbf{M}_{\beta\mu} + g_{\beta\nu}\mathbf{M}_{\alpha\mu}\,.
\end{aligned} \tag{4.5}$$

The remaining commutation relations specifying the conformal algebra are

$$\begin{aligned}
i\,[\mathbf{D}, \mathbf{P}_\nu] &= \mathbf{P}_\mu\,,\\
i\,[\mathbf{D}, \mathbf{K}_\nu] &= -\mathbf{K}_\mu\,,\\
i\,[\mathbf{M}_{\alpha\beta}, \mathbf{K}_\mu] &= g_{\alpha\mu}\mathbf{K}_\beta + g_{\beta\mu}\mathbf{K}_\alpha\,,\\
i\,[\mathbf{P}_\mu, \mathbf{K}_\nu] &= -2g_{\mu\nu}\mathbf{D} + 2\mathbf{M}_{\mu\nu}\,,\\
i\,[\mathbf{D}, \mathbf{M}_{\mu\nu}] &= 0\,,\\
i\,[\mathbf{K}_\mu, \mathbf{K}_\nu] &= 0\,.
\end{aligned} \tag{4.6}$$

Infinitesimal transformations of a primary field $\Phi(z)$ with scaling dimension (l) and spin (s) are given by the action of the generators on the primary field. For the four generators we have

$$\begin{aligned}
\delta^P_\mu\,\Phi(z) \equiv i[\mathbf{P}_\mu, \Phi(x)] &= \partial_\mu \Phi(x)\,,\\
\delta^M_{\mu\nu}\Phi(z) \equiv i[\mathbf{M}_{\mu\nu}, \Phi(x)] &= \left(x_\mu\partial_\nu - x^\nu\partial_\mu - \Sigma_{\mu\nu}\right)\Phi(x)\,,\\
\delta^D\,\Phi(z) \equiv i[\mathbf{D}, \Phi(x)] &= (x.\partial + l)\,\Phi(x)\,,\\
\delta^K_\mu\,\Phi(z) \equiv i[\mathbf{K}_\mu, \Phi(x)] &= \left(2x_\mu x.\partial - x^2\partial_\mu + 2lx_\mu - 2x^\nu\Sigma_{\mu\nu}\right)\Phi(x)\,,
\end{aligned} \tag{4.7}$$

where $\Sigma_{\mu\nu}$ is the generator of spin rotations of the primary field $\Phi(z)$, whose action on scalar, spinor and gluon fields yields

$$\Sigma_{\mu\nu}\phi(z) = 0\,, \qquad \Sigma_{\mu\nu}\psi(z) = \frac{i}{2}\sigma_{\mu\nu}\psi(z)\,, \qquad \Sigma_{\mu\nu}A_\alpha(z) = g_{\nu\alpha}A_\mu(z) - g_{\mu\alpha}A_\nu(z)\,, \tag{4.8}$$

respectively. In a free theory, the scaling dimension is equal to the canonical dimension (l^{can}), which is given by the requirement that the action of the theory is dimensionless. In a quantum theory, the scaling dimension is in general different from the canonical dimension. This difference is denoted as anomalous dimension. As we have seen in section 3.2.3, the leading contribution originates from particles that propagate close to the light-cone. Therefore, we introduced the light-cone coordinates in section 3, where the longitudinal and transverse coordinates are separated. For further details, see Sec. B.3.
We now consider the special conformal transformations (4.4), where a is a light-like vector ($a^\mu = a\tilde{n}^\mu$). The transformation of z^- yields

$$z_- \to z'_- = \frac{z_-}{1 + 2az_-}\,. \tag{4.9}$$

In combination with the translation and the dilatation along the same direction

$$z^- \to z^- + a^-\,, \qquad z^- \to az^-\,, \tag{4.10}$$

these transformations form the $SL(2,\mathbb{R})$ group [Lan75]. For the three processes in chapter 3 we considered the operators containing two fields at a light-like separation. We first investigate a single primary field and afterward the product of two primary fields. For a single primary field on the light-ray we introduce the short hand notation

$$\Phi(z) \to \Phi(\alpha n) \equiv \Phi(\alpha)\,. \tag{4.11}$$

Furthermore, we assume, that the primary field is an eigenstate of the spin operator Σ_{+-} with eigenvalue s

$$\Sigma_{+-}\Phi(\alpha) = s\,\Phi(\alpha)\,. \tag{4.12}$$

The leading twist operators in chapter 2 satisfy this condition automatically [Ohr82]. As it is shown later, in the general case, different spin components have to be separated using suitable projection operators.
Moreover, the collinear subgroup acts on the coordinate α as an $SL(2,\mathbb{R})$ transformation

$$\alpha \to \alpha' = \frac{a\alpha + b}{c\alpha + d}\,, \qquad a,b,c,d \in \mathbb{R} \quad ad - bc = 1\,. \tag{4.13}$$

The corresponding action on the collinear field $\Phi(\alpha)$ is given by

$$\Phi(\alpha) \to \Phi'(\alpha) = (c\alpha + d)^{-2j}\Phi\left(\frac{a\alpha + b}{c\alpha + d}\right)\,, \tag{4.14}$$

where

$$j = \frac{l + s}{2}\,. \tag{4.15}$$

The four generators generating the transformations of the collinear subgroup are $\mathbf{P}_+$, $\mathbf{M}_{-+}$, $\mathbf{D}$ and $\mathbf{K}_-$. We introduce the following linear combinations to bring the algebra in the standard from [Ohr82, BDKM99]

$$\begin{aligned}\mathbf{L}_+ &= \mathbf{L}_1 + i\mathbf{L}_2 = -i\mathbf{P}_+\,,\\ \mathbf{L}_- &= \mathbf{L}_1 - i\mathbf{L}_2 = (i/2)\mathbf{K}_-\,,\\ \mathbf{L}_0 &= (i/2)\,(\mathbf{D} + \mathbf{M}_{-+})\,,\\ \mathbf{E} &= (i/2)\,(\mathbf{D} - \mathbf{M}_{-+})\,.\end{aligned} \tag{4.16}$$

The corresponding algebra follows from (4.5) and (4.6). It obeys

$$[\mathbf{L}_0, \mathbf{L}_\pm] = \pm\mathbf{L}_\pm\,, \qquad [\mathbf{L}_-, \mathbf{L}_+] = -2\mathbf{L}_0\,, \tag{4.17}$$

which is the algebra of the group $SL(2,\mathbb{R})$. $\mathbf{E}$ commutes with the generators above. We obtain the action of generators $\mathbf{L}_0$, $\mathbf{L}_\pm$ and $\mathbf{E}$ on the primary field from (4.7) as

$$\begin{aligned}[\mathbf{L}_+, \Phi(\alpha)] &= -\partial_\alpha\,\Phi(\alpha)\,,\\ [\mathbf{L}_-, \Phi(\alpha)] &= (\alpha^2\partial_\alpha + 2j\alpha)\,\Phi(\alpha)\,,\\ [\mathbf{L}_0\,, \Phi(\alpha)] &= (\alpha\partial_\alpha + j)\,\Phi(\alpha)\,,\\ [\mathbf{E}\ \ , \Phi(\alpha)] &= (l-s)/2\;\Phi(\alpha)\,,\end{aligned} \tag{4.18}$$

where $\partial_\alpha = \mathrm{d}/\mathrm{d}\alpha$. Note, the generators with bold letters act on the primary field. We can also introduce operators, that act on the coordinate of a primary field. From the equation above, we define

$$\begin{aligned}L_+\Phi(\alpha) &\equiv -\partial_\alpha\,\Phi(\alpha)\,,\\ L_-\Phi(\alpha) &\equiv (\alpha^2\partial_\alpha + 2j\alpha)\,\Phi(\alpha)\,,\\ L_0\,\Phi(\alpha) &\equiv (\alpha\partial_\alpha + j)\,\Phi(\alpha)\,.\end{aligned} \tag{4.19}$$

These operators have the same algebra as $SL(2)$, namely

$$[L_0, L_\pm] = \mp L_\pm\,, \qquad [L_-, L_+] = 2L_0\,. \tag{4.20}$$

The remaining operator $\mathbf{E}$ in (4.18) counts the collinear twist $t = l - s$ of the primary field $\Phi(\alpha)$ and commits with all $\mathbf{L}_i$. This definition of twist is defined as the "dimension minus the spin projection on the + direction", i.e. (4.12) which differs from the so-called geometric twist referring to the full conformal group [GT71] denoting "dimension minus spin". However, in the leading twist-2 approximation neglecting terms that are suppressed by $M^2/\mathcal{Q}^2$ and $\Delta^2/\mathcal{Q}^2$ the two definitions coincide [JJ92, BBKT98, GL01].
A local primary field $\Phi(\alpha)$ with fixed spin projection s is a eigenstate of the quadratic Casimir operator that commutes with all other generators

$$\sum_{i=0,1,2} [\mathbf{L}_i, [\mathbf{L}_i, \Phi(\alpha)]] = j(j-1)\Phi(\alpha) = L^2\Phi(\alpha)\,. \tag{4.21}$$

The operator L^2 acting on the coordinates of the primary field is defined as

$$L^2 = L_0^2 + L_1^2 + L_2^2 = L_0^2 - L_0 + L_- L_+ \,, \qquad \left[L^2, L_i\right] = 0 \,. \tag{4.22}$$

Consequently, the primary field transforms in a representation of the $SL(2,\mathbb{R})$ group which is specified by the parameter j. We denote this parameter as the conformal spin of the primary field.

4.2. Conformal towers

From (4.18) we conclude, that a primary field at the origin of the light-cone is a eigenstate of $\mathbf{L}_0$ and it is annihilated by $\mathbf{L}_-$:

$$[\mathbf{L}_0, \Phi(0)] = j\ \Phi(0) \,, \qquad [\mathbf{L}_-, \Phi(0)] = 0 \,. \tag{4.23}$$

Therefore, we denote the corresponding eigenvalue by $j = j_0$. Furthermore, $\Phi(0)$ is the highest weight vector in the $SL(2,\mathbb{R})$ representation space. As a consequence, a complete basis on this space is generated by repeated application of the "raising" operator $\mathbf{L}_+$

$$\begin{aligned}
\mathcal{O}_0 &= \Phi(0) \,, \\
\mathcal{O}_1 &= [\mathbf{L}_+, \Phi(0)] = -\partial_+ \Phi(\alpha)|_{\alpha=0} \,, \\
&\vdots \\
\mathcal{O}_k &= [\mathbf{L}_+, \ldots, [\mathbf{L}_+, [\mathbf{L}_+, \Phi(0)]]] = (-\partial_+)^k \Phi(\alpha)\Big|_{\alpha=0} \,.
\end{aligned} \tag{4.24}$$

From the commutation relations in (4.17) we determine the action of the generators $\mathbf{L}_i$ on the operators $\mathcal{O}_k$. The action of $\mathbf{L}_0$ is

$$[\mathbf{L}_0, \mathcal{O}_0] = j\ \mathcal{O}_0 \,, \qquad [\mathbf{L}_0, \mathcal{O}_1] = (j+1)\,\mathcal{O}_1 \,, \qquad [\mathbf{L}_0, \mathcal{O}_{k+1}] = (j+k)\,\mathcal{O}_k \,. \tag{4.25}$$

Moreover, the application of the "lowering" and "raising" operator $\mathbf{L}_\pm$ on the operator $\mathcal{O}_k$ is

$$[\mathbf{L}_+, \mathcal{O}_k] = \mathcal{O}_{k+1} \,, \qquad [\mathbf{L}_-, \mathcal{O}_k] = -k(2j+k-1)\mathcal{O}_{k-1} \,. \tag{4.26}$$

We formally expand the primary field $\Phi(\alpha)$ at an arbitrary position on the light-cone in a Taylor series over local conformal operators

$$\Phi(\alpha) = \sum_{k=0}^{\infty} \frac{(-\alpha)^k}{k!} \left(-\partial_+^k\right) \Phi(\alpha)\Big|_{\alpha=0} = \sum_{k=0}^{\infty} \frac{(-\alpha)^k}{k!} \mathcal{O}_k \,. \tag{4.27}$$

This type of construction is called a conformal tower. The lowest operator $k = 0$ is the highest weight vector in the space of representations. Higher operators $k = 1, 2, \ldots$ are obtained by adding further derivatives. Each of these derivatives increases the conformal spin projection on the "zero" axes by one. For the operator above, we express the derivatives acting on the primary field in (4.27) in terms of polynomials $\mathcal{P}$. For the conformal operator $\mathcal{O}_k$ we have

$$\mathcal{O}_k = \mathcal{P}_k(\partial_\alpha)\Phi(\alpha)|_{\alpha=0} \,, \qquad \text{with} \quad \mathcal{P}_k(u) = (-u)^k \,. \tag{4.28}$$

Instead of the algebra (4.25,4.26), where the generators act on the conformal operators we can introduce differential operators acting on the space of the polynomials. We denote these operators by $\widetilde{L}_i$. They require

$$\begin{aligned}\Big[\widetilde{L}_0\ \mathcal{P}_k(\partial_\alpha)\ \Phi(\alpha)\Big]\Big|_{\alpha=0} &= \mathcal{P}_k(\partial_\alpha)\ \Big[L_0\ \Phi(\alpha)\Big]\Big|_{\alpha=0}\,,\\ \Big[\widetilde{L}_\pm\ \mathcal{P}_k(\partial_\alpha)\ \Phi(\alpha)\Big]\Big|_{\alpha=0} &= \mathcal{P}_k(\partial_\alpha)\ \Big[L_\mp\ \Phi(\alpha)\Big]\Big|_{\alpha=0}\,.\end{aligned} \tag{4.29}$$

Therefore, the action of the "adjoint" representation of the generator on the space of characteristic polynomials is given by

$$\begin{aligned}\widetilde{L}_0\ \mathcal{P}_k(u) &= (u\partial_u + j)\,\mathcal{P}_k(u)\,,\\ \widetilde{L}_+\,\mathcal{P}_k(u) &= \left(u\partial_u^2 + 2j\partial_u\right)\mathcal{P}_k(u)\,,\\ \widetilde{L}_-\,\mathcal{P}_k(u) &= -u\,\mathcal{P}_k(u)\,.\end{aligned} \tag{4.30}$$

Note, in the equations above, the meaning of the plus and minus operators in the basis $\widetilde{L}$ in comparison to $\mathbf{L}$ is changed. The second order derivative in $\widetilde{L}_+$ is avoided by the introduction of a new variable κ instead of u [Ohr82, BDKM99]

$$\frac{u^n}{\Gamma(k+2j)} \to \kappa^k\,, \qquad n = 0, 1, 2, \ldots \tag{4.31}$$

Consequently, the polynomial $\mathcal{P}_k(u)$ is mapped onto the polynomial $\widetilde{\mathcal{P}}_k(\kappa)$. The generators of projective transformations become in this space

$$\begin{aligned}L_0\ \widetilde{\mathcal{P}}_k(\kappa) &= (\kappa\partial_\kappa + j)\,\widetilde{\mathcal{P}}_k(\kappa)\,,\\ L_-\,\widetilde{\mathcal{P}}_k(\kappa) &= -\partial_\kappa\widetilde{\mathcal{P}}_k(u)\,,\\ L_+\,\widetilde{\mathcal{P}}_k(\kappa) &= \left(\kappa^2\partial_\kappa + 2j\kappa\right)\widetilde{\mathcal{P}}_k(u)\,,\end{aligned} \tag{4.32}$$

which are the same differential operators as in (4.19) acting on the field coordinate.
The leading twist operators of interest in this thesis (Cha. 3) all contain two fields at light-like separation. Thus, we consider the product of two primary fields on the light-cone

$$O(\alpha_1, \alpha_2) = \Phi_{j_1}(\alpha_1)\,\Phi_{j_2}(\alpha_2)\ , \qquad \alpha_1 \neq \alpha_2\,, \tag{4.33}$$

where two fields have conformal spin j_1 and j_2. Expanding this product at short distances $|\alpha_1 - \alpha_2| \to 0$ involves the local composite operators

$$\mathcal{O}_n = \mathcal{P}_n(\partial_1, \partial_2)\Phi_{j_1}(\alpha_1)\Phi_{j_2}(\alpha_2)\Big|_{\alpha_1=\alpha_2=0}\,. \tag{4.34}$$

In general, the local operators $\mathcal{O}_n$ do not form an irreducible representation of the collinear subgroup. Hence, following the previous case involving one primary field, we determine a complete basis forming a conformal tower. The group generators for two primary fields are given as the sum of one-particle generators (4.16)

$$\mathbf{L}_a = \mathbf{L}_{1,a} + \mathbf{L}_{2,a}\,, \qquad a \in \{0, 1, 2\} \tag{4.35}$$

Furthermore, the two-particle Casimir operator reads

$$\mathbf{L}^2 = \sum_{a=0,1,2} (\mathbf{L}_{1,a} + \mathbf{L}_{2,a})^2 \,. \tag{4.36}$$

The aim is, to construct a conformal tower with definite conformal spin and spin projection on the light-cone. Let us assume, we have found an operator $\mathbb{O}_n$ which possesses the same transformation properties under the collinear subgroup as the collinear field (4.14). We require equivalently

$$\begin{aligned} \left[\mathbf{L}^2\,, \mathbb{O}_n\right] &= j(j-1)\mathbb{O}_n\,, \\ \left[\mathbf{L}_0\,, \mathbb{O}_n\right] &= (j_1 + j_2 + n)\,\mathbb{O}_n\,, \\ \left[\mathbf{L}_-, \mathbb{O}_n\right] &= 0\,. \end{aligned} \tag{4.37}$$

The operators $\mathbb{O}_n$ is an eigenstate of the quadratic Casimir operator, cf. (4.12), with conformal spin

$$j = j_1 + j_2 + n\,, \tag{4.38}$$

which follows from the second equation in (4.37). According to the third equation the operators $\mathbb{O}_n$ defines the highest weight on the $SL(2,\mathbb{R})$ representation space and has the minimum value of the spin projection.
From this operator, we construct the complete conformal tower by consecutive application of the "raising" operator $\mathbf{L}_+$:

$$\mathbb{O}_{n,n+k} = [\mathbf{L}_+, \ldots, [\mathbf{L}_+, [\mathbf{L}_+, \Phi(0)]]] = (-\partial_+)^k\, \mathbb{O}_n, \qquad \mathbb{O}_{n,n} \equiv \mathbb{O}_n\,, \tag{4.39}$$

where ∂_+ is the total derivative. The remaining task is finding the characteristic polynomial in (4.34). Instead, we go over to the adjoint representation [Ohr82] by introducing the replacement rules analogously to the one-particle case

$$\frac{u_1^{n_1} u_2^{n_2}}{\Gamma(2j_1 + n_1)\,\Gamma(2j_2 + n_2)} \to \kappa_1^{n_1} \kappa_2^{n_2}\,. \tag{4.40}$$

In this space, the characteristic polynomial fulfills

$$\begin{aligned} L_0\ \widetilde{\mathcal{P}}_n(\kappa_1,\kappa_2) &= (\kappa_1\partial_1 + \kappa_2\partial_2 + j_1 + j_2)\,\widetilde{\mathcal{P}}_n(\kappa_1,\kappa_2)\,, \\ L_-\,\widetilde{\mathcal{P}}_n(\kappa_1,\kappa_2) &= -(\partial_1 + \partial_2)\,\widetilde{\mathcal{P}}_n(\kappa_1,\kappa_2)\,, \\ L_+\,\widetilde{\mathcal{P}}_n(\kappa_1,\kappa_2) &= (\kappa_1^2\partial_1 + \kappa_2^2\partial_2 + 2j_1\kappa_1 + j_2\kappa_2)\,\widetilde{\mathcal{P}}_n(\kappa_1,\kappa_2)\,, \end{aligned} \tag{4.41}$$

where the derivatives are $\partial_1 = \partial/\partial\kappa_1$ and $\partial_2 = \partial/\partial\kappa_2$. Let us assume, the characteristic polynomial of a conformal operator is given by $\widetilde{\mathbb{P}}_n(\kappa_1,\kappa_2)$. Consequently, the application of the lowering operator yields

$$L_-\,\widetilde{\mathbb{P}}_n(ka_1,\kappa_2) = -(\partial_1 + \partial_2)\,\widetilde{\mathbb{P}}_n(ka_1,\kappa_2) = 0\,. \tag{4.42}$$

The solution of the relation above is

$$\widetilde{\mathbb{P}}_n(ka_1,\kappa_2) \propto (\kappa_2 - \kappa_2)^n\,, \tag{4.43}$$

where the proportionality is irrelevant. In the original variables u_1 and u_2 the characteristic polynomial reads

$$\mathbb{P}_n^{j_1,j_2}(u_1,u_2) = \sum_{n_1+n_2=n} \binom{n}{n_1} \frac{(-u_1)^{n_1} u_2^{n_2}}{\Gamma(2j_1+n_1)\,\Gamma(2j_2+n_2)} = (u_1+u_2)^n P_n^{(2j_1-1,2j_2-1)}\left(\frac{u_2-u_1}{u_1+u_2}\right) . \tag{4.44}$$

$P_n^{(a,b)}(x)$ are the Jacobi polynomials [AS12], whose coefficients are the Clebsch-Gordon coefficients of the colliner conformal group. The corresponding conformal operator becomes

$$\mathbb{O}_n^{j_1,j_2}(x) = \partial_+^n \left[\Phi_{j_1}(x) P_n^{(2j_1-1,2j_2-1)} \left(\frac{\overrightarrow{\partial}_+ - \overleftarrow{\partial}_+}{\overrightarrow{\partial}_+ + \overleftarrow{\partial}_+} \right) \Phi_{j_2}(x) \right] , \tag{4.45}$$

which was first obtained in [Mak81].
The twist-2 quark operator in Cha. 3 is a nonlocal operator build of a quark and a antiquark field at light-like separation

$$\mathcal{Q}_\mu(\alpha_1,\alpha_2) = \bar\psi(\alpha_1)\gamma_\mu[\alpha_1,\alpha_2]\psi(\alpha_2) , \tag{4.46}$$

where the Wilson line is given by

$$[\alpha_1,\alpha_2] = \mathrm{P}\exp\left[ig \int_{\alpha_2}^{\alpha_1} \mathrm{d}t\, A_+(t) \right] . \tag{4.47}$$

The expansion of the operator $\mathcal{Q}_\mu$ at short distances generates local operators build of the quark and the antiquark field together with covariant derivatives

$$\bar\psi(0)\big(\overleftarrow{D}_+\big)^{n_1}\gamma_\mu\big(\overrightarrow{D}_+\big)^{n_2}\psi(0) . \tag{4.48}$$

As in the general case, our objective is finding the corresponding conformal operator. Since the quark and antiquark fields do not have definite spin projections we introduce the following projection operators

$$\Pi_+ = \frac{1}{2}\gamma_-\gamma_+ , \qquad \Pi_- = \frac{1}{2}\gamma_+\gamma_- , \qquad \Pi_+ + \Pi_- = 1 . \tag{4.49}$$

Therefore, the definite "plus" and "minus" components of quark field are

$$\psi_+ = \Pi_+\psi , \qquad \psi_- = \Pi_-\psi , \qquad \psi = \psi_+ + \psi_- . \tag{4.50}$$

Furthermore, the spin projections of the two components are obtained by utilizing Eq. (4.8)

$$\Sigma_{+-}\psi = \frac{i}{2}\sigma^{+-}\psi = -\frac{1}{2}\left(\Pi_- + \Pi_+\right)\psi = -\frac{1}{2}\psi_- + \frac{1}{2}\psi_- . \tag{4.51}$$

The canonical dimension of a spinor field is $l = 3/2$. Thus, the fields ψ_+ (ψ_-) have conformal spin[1] $j = 1$ ($j = 1/2$) and twist[2] $t = 1$ ($t = 2$), respectively. As a consequence, different

[1] $j = (l+s)/2$
[2] $t = l - s$

Lorentz projections of the operator $\mathcal{Q}_\mu(\alpha_1,\alpha_2)$ correspond to different combinations of quark field components. Each of them has different properties under conformal transformations. For the two particle operator in (4.46) we obtain the following combinations

$$\begin{aligned}
&\text{twist-2:} && \mathcal{Q}_+ = \bar\psi_+\gamma_+\psi_+ && \equiv \mathcal{Q}^{1,1}\,,\\
&\text{twist-3:} && \mathcal{Q}_\perp = \bar\psi_+\gamma_\perp\psi_- + \bar\psi_-\gamma_\perp\psi_+ && \equiv \mathcal{Q}^{1,1/2} + \mathcal{Q}^{1/2,1}\,,\\
&\text{twist-4:} && \mathcal{Q}_- = \bar\psi_-\gamma_-\psi_- && \equiv \mathcal{Q}^{1/2,1/2}\,,
\end{aligned} \tag{4.52}$$

where the superscripts stand for the conformal spin of the quark and antiquark. The corresponding local operators are given by

$$\mathbb{O}_n^{1,1}(x) = \left(i\partial_+\right)^n \left[\bar\psi(x)\,\gamma_+\, C_n^{3/2}\!\left(\overleftrightarrow{D}/\partial_+\right)\psi(x)\right]\,, \tag{4.53}$$

$$\mathbb{O}_n^{1,\frac12}(x) = \left(i\partial_+\right)^n \left[\bar\psi(x)\,\gamma_+\gamma_\perp\gamma_-\, P_n^{(1,0)}\!\left(\overleftrightarrow{D}/\partial_+\right)\psi(x)\right]\,, \tag{4.54}$$

$$\mathbb{O}_n^{\frac12,\frac12}(x) = \left(i\partial_+\right)^n \left[\bar\psi(x)\,\gamma_-\, C_n^{1/2}\!\left(\overleftrightarrow{D}/\partial_+\right)\psi(x)\right]\,, \tag{4.55}$$

where $\overleftrightarrow{D}_+ = \overrightarrow{D}_+ - \overleftarrow{D}_+$ and $\partial_+ = \overrightarrow{D}_+ + \overleftarrow{D}_+$. For equal conformal spin of the quark and antiquark field, the Jacobi polynomials are replaced by Gegenbauer polynomials using the relation (C.4). Note, the twist-2 operator is the one with the highest conformal spin $j=2+n$. For gluons, the $G_{+\perp}$ component of the gluon field strength tensor possesses the spin projection $s=1$. Since the canonical dimension is $l=2$, the conformal spin is $j=3/2$ and the twist is $t=1$. The local conformal operators build from two gluon fields of twist-2 are

$$\mathbb{G}_n^{3/2,3/2}(x) = \left(i\partial_+\right)^n \left[G^a_{+\perp}(x)\gamma_+ C_n^{5/2}\!\left(\overleftrightarrow{D}/\partial_+\right)\psi(x)\right]\,. \tag{4.56}$$

4.3. Conformal operator product expansion

Analogous to the operator product expansion, which was implicitly performed for the phenomenological analysis of DIS, DVCS and DVMP in Ch. 3, the conformal operator product expansion (COPE) reveals new constraints for the Wilson coefficients. Following [FGG71b, FGG71a, FGG72, BST72, CDT85] we present the COPE of the product of two local conformal operators. For a review, see [BKM03, BR05].

The two local conformal operators $A(z)$, $B(0)$ have twist t_A, t_B and spin projection in the plus direction s_A, s_B, respectively. Their product is expanded over a tower of local conformal operators and their derivatives $\mathbb{O}^{j_1,j_2}_{n,n+k}$ in the light-cone limit $z_+, z_\perp \to 0$ and z_- is fixed, i.e., $z^2 \to 0$. In doing so, we assume that the operators form a complete basis. As in the rest of this thesis, we restrict our considerations to the leading twist approximation. Neglecting the unity operator the expansion in a free field theory for dimensional reasons is

$$A(z)B(0) = \sum_{n=0}^{\infty}\left(\frac{1}{z^2}\right)^{\frac{t_A+t_B-t_n}{2}} \sum_{k=0}^{\infty} C_{n,k}\, z_-^{n+k+\Delta}\, \mathbb{O}^{j_1,j_2}_{n,n+k}(0)\,, \tag{4.57}$$

where $C_{n,k}$ are the respective Wilson coefficients. Lorentz invariance fixes $\Delta = s_1 + s_2 - s_A - s_B$, where s_1 and s_2 are the spin projections of the constituent fields in the local operators $\mathbb{O}^{j_1,j_1}_{n,n+k}$. This can be checked by applying the generator $\mathbf{M}_{-+} = -i(\mathbf{L}_0 - \mathbf{E})$ given in (4.16) on both sides of the COPE (4.57). Thereby, the action on the operator is presented in (4.18) and the action on the fields in (4.7). The twist of the conformal operators $\mathbb{O}^{j_1,j_2}_{n,n}$ is

$$t_n = l_n - n - s_1 - s_2 = l_1 + l_2 - s_1 - s_2 \,. \tag{4.58}$$

Furthermore, the singular behavior in the limits $z^2 \to 0$ is governed by the twist of the operators: $t_A + t_B - t_n$. In an interacting theory, the scaling dimension l_n of the operators will be replaced by the anomalous dimensions.
Using conformal symmetry, we obtain the Wilson coefficients $C_{n,k}$ for $k = 1, 2, \ldots$ from the highest operator $C_n \equiv C_{n,k=0}$, which does not involve total derivatives. Applying the "lowering" operator on the right side of the COPE (4.57) we obtain utilizing (4.26)

$$\left[\mathbf{L}_-, \mathbb{O}^{j_1,j_2}_{n,n+k}(0)\right] = -k(k+2j_n-1)\, \mathbb{O}^{j_1,j_2}_{n,n+k-1}(0)\,, \qquad \text{with} \quad j_n = j_1 + j_2 + n\,. \tag{4.59}$$

For the left hand side, we first consider a infinitesimal special conformal transformation of the operator $A(z)$ with conformal spin j_A

$$[\mathbf{L}_-, A(z)] = \left(z_- \, z.\partial - \frac{1}{2} z^2 \tilde{n}.\partial + 2 j_A z_-\right) A(z) + \ldots\,, \tag{4.60}$$

which follows from (4.7)[3]. The ellipsis stands for contributions of higher twists arising in the Sudakov decomposition. Employing the following derivative for generic variables a and b

$$\partial_\mu \left[\left(\frac{1}{z^2}\right)^a (z^-)^b\right] = -2a \left(\frac{1}{z^2}\right)^{a+1} (z^-)^b \, x_\mu + \left(\frac{1}{z^2}\right)^{a+1} b\, (z^-)^b \, \tilde{n}_\mu\,, \tag{4.61}$$

the action of the lowering operator on the right hand side of the conformal operator product expansion becomes

$$[L_-, A(z)B(0)] = \sum_{n=0}^{\infty} \left(\frac{1}{z^2}\right)^{\frac{t_A + t_B - t_n}{2}} \sum_{k=0}^{\infty} (j_A - j_B + j_n + k)\, C_{n,k}\, (z^-)^{n+k+\Delta+1}\, \mathbb{O}^{j_1,j_2}_{n,n+k}(0). \tag{4.62}$$

Comparing the coefficients in (4.59) and in (4.62) we read off the recurrence relation

$$(j_A - j_B + j_n + k)\, C_{n,k} = -(k+1)(k+2j) C_{n,k+1}\,. \tag{4.63}$$

The respective solution is

$$C_{n,k} = (-1)^k \frac{(j_A - j_B + j_n)_k}{k!(2j_n)_k} C_n\,, \qquad C_n \equiv C_{n,0}\,, \tag{4.64}$$

where we used the Pochhammer symbol

$$(a)_k = \frac{\Gamma(a+k)}{\Gamma(a)}\,. \tag{4.65}$$

[3] $\mathbf{L}_- = (i/2)\mathbf{K}_-$.

We are now able to perform the sum over k leading to a hypergeometric function (C.18):

$$\sum_{k=0}^{\infty}(-1)^k\frac{(j_A-j_B+j_n)_k}{k!(2j_n)_k}\,(-z.\partial)^k={}_1F_1\left(\begin{matrix}j_A-j_B+j_n\\2j_n\end{matrix}\,\middle|\,z.\partial\right)\,. \tag{4.66}$$

With the integral representation (C.26) for the hypergeometric function above the COPE in the twist-2 approximation yields

$$\begin{aligned}A(z)B(0)=\sum_{n=0}^{\infty}C_n\left(\frac{1}{z^2}\right)^{\frac{t_A+t_B-t_n}{2}}&\frac{(z^-)^{n+\Delta}}{\mathrm{B}(j_A-j_B+j_n,j_B-j_A+j_n)}\\&\times\int_0^1\mathrm{d}u\;u^{j_A-j_B+j_n-1}\;\bar{u}^{j_B-j_A+j_n-1}\,\mathbb{O}_n^{j_1,j_2}(uz^-)\,,\end{aligned} \tag{4.67}$$

where we employed the identity

$$e^{uz.\partial}\,\mathbb{O}_n(0)=\sum_{k=0}^{\infty}\frac{(uz^-)^k}{k!}\,\partial_\alpha^k\,\mathbb{O}_n(\alpha)\Big|_{\alpha=0}=\mathbb{O}_n(uz^-)\,. \tag{4.68}$$

We utilize the COPE above for the product of two electromagnetic currents, which appears in the Compton tensor (3.94), see Sec. 3.2.3. Conformal symmetry provides the Wilson coefficients for DVCS from the Wilson coefficients for DIS [Mül98, BM98b]. In the leading twist-2 contribution, only the transverse components of the Lorentz indices contribute (3.134). The Compton amplitude imposing the correct Lorentz structure reads

$$T(P,q,\Delta)=i\int\mathrm{d}^4z\,e^{iqz-i\frac{\Delta}{2}z}\langle\mathrm{P}_1|T\{j_\perp(z)j_\perp(0)\}|\mathrm{P}_2\rangle\,. \tag{4.69}$$

The dimension of the electromagnetic current is $3/2$ and its spin projection on the plus direction is zero. Therefore, the twist of the product of the electromagnetic currents is $t_A=t_B=3,\ s_A=s_B=0$. The operator basis consists of the quark operators $\mathbb{Q}^{1,1}_{n,n+k}$ (4.53) with twist $t_n=l_1+l_2-s_1-s_2=2$. Inserting the corresponding parameters into the COPE (4.67) leads to

$$T(P,q,\Delta)=i\int\mathrm{d}^4z\,e^{iqz-i\frac{\Delta}{2}z}\sum_{n=0}^{\infty}C_n\left(\frac{1}{z^2}\right)^{\frac{6-t_n}{2}}\frac{(-iz^-)^{n+1}}{\mathrm{B}(j_n,j_n)}\int_0^1\mathrm{d}u\,(u\bar{u})^{j_n-1}\langle\mathrm{P}_2|\mathbb{Q}_n^{1,1}(uz^-)|\mathrm{P}_1\rangle\,. \tag{4.70}$$

We parametrize the matrix element in the equation above in terms of quark GPDs (2.5), shifting the location of the operator, we get

$$\langle\mathrm{P}_2|\mathbb{Q}_n^{1,1}(uz^-)|\mathrm{P}_1\rangle=e^{iu\eta P.z}P_+^{n+1}\langle\!\langle\mathbb{Q}_n^{1,1}(0)\rangle\!\rangle(\eta,\Delta^2,\mu^2)\,. \tag{4.71}$$

Utilizing the following identity

$$e^{i\left(q-\frac{\Delta}{2}+u\eta P\right).z}(-iP.z)^{n+1}=(-\eta)^{-n-1}\frac{\mathrm{d}^{n+1}}{\mathrm{d}u^{n+1}}e^{i\left(q-\frac{\Delta}{2}+u\eta P\right).z}\,, \tag{4.72}$$

we perform the integration with respect to z. The result of the respective integral reads

$$\int \mathrm{d}^4 z \left(\frac{1}{z^2}\right)^{\frac{6-t_n}{2}} e^{i\left(q-\frac{\Delta}{2}+u\eta P\right).z} = -i2^{t_n-2}\pi^2 \frac{\Gamma\left(2-\frac{6-t_n}{2}\right)}{\Gamma\left(\frac{6-t_n}{2}\right)} \left[\frac{1}{(q-\frac{\Delta}{2}+u\eta P)^2}\right]^{2-\frac{6-t_n}{2}} , \quad (4.73)$$

where we utilized the generic integral

$$\int \mathrm{d}^4 z \frac{e^{iqz}}{(-z^2)^\alpha} = -i2^{4-2\alpha}\pi^2 \frac{\Gamma(2-\alpha)}{\Gamma(\alpha)} \left(\frac{1}{q^2}\right)^{2-\alpha} . \quad (4.74)$$

As already stated, in an interacting theory, the canonical dimensions have to be modified with the anomalous dimensions. Consequently, the twist is given as $t_n = 2+\gamma_n$. The term involving the momentum transfer q becomes

$$\left(q-\frac{\Delta}{2}+u\eta P\right)^2 = q^2\left(1-2u\eta\frac{P.q}{Q^2}+\frac{\Delta.q}{Q^2}\right) = q^2\left[1-(2u-1)\frac{\eta}{\xi}\right] , \quad (4.75)$$

where we neglected contributions proportional to $M^2/\mathcal{Q}^2$, $\Delta^2/\mathcal{Q}^2$, $P.\Delta = 0$. For convenience, we introduce the variable ϑ as the ratio of the skewness and the generalized Bjorken variable. In the next step, we evaluate the derivatives stemming from the identity (4.72), the general expression yields

$$\frac{\mathrm{d}^m}{\mathrm{d}u^m}\left(\frac{1}{1-(2u-1)a}\right)^b = (2a)^m \frac{\Gamma(b+m)}{\Gamma(b)} \left(\frac{1}{1-(2u-1)\vartheta}\right)^{b+m} , \quad (4.76)$$

where m, a and b are generic variables. Taking everything together, the COPE of the Compton amplitude reads

$$\begin{aligned} T(P,q,\Delta) = \sum_{n=0}^{\infty} C_n \left(\frac{\mu^2}{\mathcal{Q}^2}\right)^{\frac{\gamma_n}{2}} \frac{1}{\mathrm{B}(j_n,j_n)} \left(\frac{2\vartheta}{\eta}\right)^{n+1} \frac{\Gamma\left(n+1+\frac{\gamma_n}{2}\right)}{\Gamma\left(2-\frac{\gamma_n}{2}\right)} \\ \times 2^{\gamma_n}\pi^2 \cdot \int_0^1 \mathrm{d}u \, \frac{(u\bar{u})^{j_n-1}}{[1-(2u-1)\vartheta]^{n+1+\frac{\gamma_n}{2}}} \langle\!\langle \mathbb{Q}_n(0) \rangle\!\rangle (\eta,\Delta^2,\mu^2) . \end{aligned} \quad (4.77)$$

The remaining integral is nothing but the integral representation of the Gauss hypergeometric function (C.19), namely

$$\int_0^1 \mathrm{d}u \, \frac{(u\bar{u})^{n+1+\frac{\gamma_n}{2}}}{[1-(2u-1)\vartheta]^{n+1+\frac{\gamma_n}{2}}} = \mathrm{B}\left(n+2+\frac{\gamma_n}{2}, n+2+\frac{\gamma_n}{2}\right) {}_2F_1\left(\begin{matrix}\frac{2n+2+\gamma_n}{4} & \frac{2n+4+\gamma_n}{4} \\ \frac{2n+5+\gamma_n}{2}\end{matrix} \middle| \vartheta^2\right) , \quad (4.78)$$

where we additionally employed the quadratic transformation (C.25). Hence, the COPE in (4.77) becomes

$$\begin{aligned} T(P,q,\Delta) = \sum_{n=0}^{\infty} C_n \left(\frac{\mu^2}{\mathcal{Q}^2}\right)^{\frac{\gamma_n}{2}} \xi^{-n-1} \frac{2^{n+1}2^{\gamma_n}\pi^2\Gamma(n+1+\frac{\gamma_n}{2})}{\Gamma(2-\frac{\gamma_n}{2})} \\ \times {}_2F_1\left(\begin{matrix}\frac{2n+2+\gamma_n}{4} & \frac{2n+4+\gamma_n}{4} \\ \frac{2n+5+\gamma_n}{2}\end{matrix} \middle| \vartheta^2\right) \langle\!\langle \mathbb{O}_n(0) \rangle\!\rangle (\eta,\Delta^2,\mu^2) . \end{aligned} \quad (4.79)$$

In the equation above, everything is known besides the normalization of C_n. The latter is fixed in agreement to the forward case ($\eta=0$). The forward Compton amplitude is given by

$$T(P,q,\Delta=0)=\sum_{n=0}^{\infty}\widetilde{c}_n\left(\frac{\mu^2}{\mathcal{Q}^2}\right)^{\frac{\gamma_n}{2}}x_{\mathrm{B}}^{-n-1}\langle\!\langle\mathbb{O}_n(0)\rangle\!\rangle(x)\,, \tag{4.80}$$

where $\tilde{c}_n$ are the Mellin moments of the corresponding hard scattering amplitudes. Thus, we neglect all prefactors that do not depend on ϑ, since they will be fixed by the correct normalization. Using this normalization, we have

$$T(P,q,\Delta)=\sum_{n=0}^{\infty}\widetilde{c}_n\left(\frac{\mu^2}{\mathcal{Q}^2}\right)^{\frac{\gamma_n}{2}}\xi^{-n-1}{}_2F_1\left(\begin{matrix}\frac{2n+2+\gamma_n}{4} & \frac{2n+4+\gamma_n}{4}\\ \frac{2n+5+\gamma_n}{2}\end{matrix}\,\middle|\,\vartheta^2\right)\langle\!\langle\mathbb{Q}_n(0)\rangle\!\rangle\big(\eta,\Delta^2,\mu^2\big)\,, \tag{4.81}$$

and the conformal moments of the hard scattering amplitudes of DVCS are given by the DIS ones employing the rotation

$$C_n=\widetilde{c}_n\;{}_2F_1\left(\begin{matrix}\frac{2n+2+\gamma_n}{4} & \frac{2n+4+\gamma_n}{4}\\ \frac{2n+5+\gamma_n}{2}\end{matrix}\,\middle|\,\vartheta^2\right)\left(\frac{\mu^2}{\mathcal{Q}^2}\right)^{\frac{\gamma_n}{2}}\,. \tag{4.82}$$

In case of DVCS and DVMP, the skewness and generalized Bjorken variable are approximately equal, see (3.79). The Gauss hypergeometric function reads in this case

$${}_2F_1\left(\begin{matrix}\frac{2n+2+\gamma_n}{4} & \frac{2n+4+\gamma_n}{4}\\ \frac{2n+5+\gamma_n}{2}\end{matrix}\,\middle|\,1\right)=\frac{2^{n+1+\frac{\gamma_n}{2}}\,\Gamma\left(n+\frac{5}{2}+\frac{\gamma_n}{2}\right)}{\Gamma\left(\frac{3}{2}\right)\Gamma\left(n+3+\frac{\gamma_n}{2}\right)}\,. \tag{4.83}$$

Note, the moments $\langle\!\langle\mathbb{Q}_n(0)\rangle\!\rangle\big(\eta,\Delta^2\big)$ are purely conformal Gegenbauer moments, which are not normalized to Mellin moments in the forward case. Thus, we have to add the common factor, cf. (4.98),

$$\frac{\Gamma\left(\frac{3}{2}\right)\Gamma(n+1)}{2^n\Gamma\left(n+\frac{3}{2}\right)}=2^{n+1}\mathrm{B}(n+1,n+2). \tag{4.84}$$

Finally, the COPE for the Compton amplitude becomes

$$T(P,q,\Delta)=\sum_{n=0}^{\infty}\widetilde{c}_n\left(\frac{\mu^2}{\mathcal{Q}^2}\right)^{\frac{\gamma_n}{2}}\xi^{-n-1}\,\frac{2^{n+1+\frac{\gamma_n}{2}}\,\Gamma\left(n+\frac{5}{2}+\frac{\gamma_n}{2}\right)}{\Gamma\left(\frac{3}{2}\right)\Gamma\left(n+3+\frac{\gamma_n}{2}\right)}\langle\!\langle\mathbb{Q}_n(0)\rangle\!\rangle\big(\eta,\Delta^2,\mu^2\big)\,. \tag{4.85}$$

This relation is utilized in [Mül98, BM98b] to determine the Wilson coefficients for DVCS from DIS. For further details, see also [KMPK08].

4.4. Conformal partial wave expansion

In the previous section, we expressed the Compton amplitude as an infinite sum over conformal GPD moments. In this section, our goal is to derive a representation of the GPD in the momentum fraction representation in terms of its conformal moments. This situation is

analog to the inverse Mellin transformation utilized in DIS. The Mellin moments of the quark and gluon PDF are given by (2.44) and (2.47), respectively. They read

$$f_j^q = \int_{-1}^{1} \mathrm{d}x\; x^j f^q(x)\,, \qquad f_j^{\mathrm{G}} = \int_{-1}^{1} \mathrm{d}x\; x^{j-1} f^{\mathrm{G}}(x)\,. \tag{4.86}$$

The inverse Mellin transformation is

$$f^q(x) = \frac{1}{2\pi i}\int_{c-i\infty}^{c+i\infty} \mathrm{d}j\; x^{-j-1} f_j^q\,, \qquad f^{\mathrm{G}}(x) = \frac{1}{2\pi i}\int_{c-i\infty}^{c+i\infty} \mathrm{d}j\; x^{-j} f_j^{\mathrm{G}}\,, \tag{4.87}$$

where contour of integration has to lie to the right of all singularities of f_j^q and f_j^{G}.

4.4.1. Distribution amplitudes

In this section, we analyze the relation between the twist-2 ρ^0-meson distribution amplitude defined in (2.33) and the corresponding matrix elements of the conformal twist-2 quark operator in (4.53). The leading twist DA is defined by

$$\langle 0|\bar{u}(0)\gamma_+ d(z^-)|\mathrm{P}\rangle = P_+ f_{\rho^0}\int_0^1 \mathrm{d}x\; e^{-iuP.z}\varphi(u)\,.$$

Expanding both sides in z^- leads to

$$\langle 0|\bar{u}(0)\gamma_+ (i\overset{\leftrightarrow}{D}_+)^n d(0)|\mathrm{P}\rangle = P_+^{n+1} f_{\rho^0}\int_0^1 \mathrm{d}x\; (2u-1)^n\varphi(u)\,. \tag{4.88}$$

Since we are not restricted to forward matrix elements, we cannot neglect the mixing of these operators with operators containing total derivatives:

$$\mathcal{O}_{n-k,k} = (i\partial_+)^k\, \bar{u}(0)\gamma_+ (i\overset{\leftrightarrow}{D}_+)^{n-k} d(0)\,. \tag{4.89}$$

Operators with less total derivatives mix with operators involving more total derivatives, but not vice versa. For this case, the relevant conformal operators are $\mathbb{Q}_n^{1,1}(z^-)$ defined in (4.53)

$$\mathbb{Q}_n^{1,1}(z) = \big(i\partial_+\big)^n \left[\bar{u}(z)\gamma_+ C_n^{3/2}\Big(\overset{\leftrightarrow}{D}/\partial_+\Big)\, d(z)\right]\,, \tag{4.90}$$

where we adjusted the flavor structure. Comparing (4.90) and (4.88) we realize, that the Gegenbauer moments of the ρ^0-meson DA are given by reduced matrix elements of conformal operators

$$\int_0^1 \mathrm{d}u\; C_n^{3/2}(2u-1)\varphi(u) = \langle\!\langle\, \mathbb{Q}_n^{1,1}\,\rangle\!\rangle\,, \qquad \langle 0|\mathbb{Q}_n^{1,1}(0)|\mathrm{P}\rangle = P_+^{n+1} f_{\rho^0}\,\langle\!\langle\, \mathbb{Q}_n^{1,1}\,\rangle\!\rangle\,. \tag{4.91}$$

The same equation holds for the other DAs defined in Sec. 2.5.
We are able to invert the equation by utilizing the orthogonality of Gegenbauer polynomials (C.3). Including the corresponding weight and normalization, we obtain

$$\varphi(u) = 6u\bar{u} \sum_{n=0}^{\infty} \frac{4(2n+3)}{(n+1)(n+2)} \, C_n^{3/2}(2u-1) \, \langle\!\langle \mathbb{Q}_n^{1,1} \rangle\!\rangle \, . \tag{4.92}$$

This relation can be checked by taking the Gegenbauer moments (4.91) of both sides. In the equation above, the normalization of the DA is chosen to be

$$\int_0^1 \mathrm{d}u \, \varphi(u) = 1 \, . \tag{4.93}$$

For convenience, the conformal moments of a DA are defined in such a way, that they absorb the normalization factor. Thus,

$$\varphi_n = \frac{2(2n+3)}{3(n+1)(n+2)} \, \langle\!\langle \mathbb{Q}_n^{1,1} \rangle\!\rangle \, . \tag{4.94}$$

The final form, first obtained in [ER80, LB79] reads

$$\varphi(u) = 6u\bar{u} \sum_{n=0}^{\infty} C_n^{3/2}(2u-1) \, \varphi_n \, , \tag{4.95}$$

where the normalization condition implies $\varphi_0 = 1$.

4.4.2. GPDs

In this section, we will present the calculation of conformal moments from a given GPD in momentum fraction representation and derive the inverse transformation following [MS06]. The Conformal moments of a quark and gluon GPD read

$$\begin{aligned} F_n^q(\eta, \Delta^2) &= \int_{-1}^{1} \mathrm{d}x \, c_n^{3/2}(x,\eta) F^q(x,\eta,\Delta^2) \, , \\ F_n^{\mathrm{G}}(\eta, \Delta^2) &= \int_{-1}^{1} \mathrm{d}x \, c_{n-1}^{5/2}(x,\eta) F^{\mathrm{G}}(x,\eta,\Delta^2) \, . \end{aligned} \tag{4.96}$$

Furthermore, the corresponding polynomials are given by Gegenbauer polynomials with index 3/2 and 5/2, respectively. Note, the polynomials c_n^λ include a normalization factor which ensures the equality to the common Mellin moments (2.49,2.51) in the forward limit (C.11). They are defined as

$$c_n^\lambda(x,\eta) = \eta^n \frac{\Gamma(\lambda)\,\Gamma(n+1)}{2^n \Gamma(n+\lambda)} C_n^\lambda\left(\frac{x}{\eta}\right) \, , \qquad \lim_{\eta\to 0} c_n^\lambda(x,\eta) = x^n \, . \tag{4.97}$$

For quarks and gluons, the explicit polynomials are given by

$$c_n^{3/2}(x,\eta) = \eta^n \frac{\Gamma\left(\frac{3}{2}\right)\Gamma(n+1)}{2^n \Gamma\left(n+\frac{3}{2}\right)} C_n^{3/2}\left(\tfrac{x}{\eta}\right) \, , \quad c_{n-1}^{5/2}(x,\eta) = \eta^{n-1} \frac{\Gamma\left(\frac{3}{2}\right)\Gamma(n+1)}{2^n \Gamma\left(n+\frac{3}{2}\right)} \frac{3}{n} \, C_{n-1}^{5/2}\left(\tfrac{x}{\eta}\right) \, . \tag{4.98}$$

The gluon GPD possesses a definite symmetry under the transformation $x \to -x$. It is even (odd) for the vector (axial-vector) gluon GPD (2.53), respectively. Due to the symmetry of the Gegenbauer polynomials (C.10), the degree n is odd (even). The quark GPD on the other hand does not possess a definite symmetry under $x \to -x$. Therefore, we introduced the quark GPD with definite charge parity $F^{q(\pm)}$ in (2.15). It is antisymmetric for signature $\sigma = +1$ and symmetric for $\sigma = -1$, see Sec. 2.3. Therefore, the degree n is odd (even) for GPDs with signature $+1$ (-1). Since the singlet quark GPD $F^{0(+)}$ and the gluon GPD mix under evolution, the degree for the gluon polynomials is shifted by the unit of one to have the same odd (even) index n as the singlet quark GPD.
In order to treat both cases simultaneously, we consider the case

$$F_n^A(\eta, \Delta^2) = \int_{-1}^{1} \mathrm{d}x \; c_n^\lambda(x, \eta) F^A(x, \eta, \Delta^2) \;, \tag{4.99}$$

where $\lambda \in \{3/2, 5/2\}$ and $A \in \{q, \mathrm{G}\}$. In addition, for the gluon GPD we employ the transformation $j \to j - 1$.
We decompose the quark GPD into its quark and anti-quark parts [MS06, MLPKS14]

$$F^q(x, \eta, \Delta^2) = q(x, \eta, \Delta^2) - \sigma \bar{q}(-x, \eta, \Delta^2) \,. \tag{4.100}$$

where $-\eta \leq x \leq 1$ and $-1 \leq x \leq \eta$, respectively. The signature is set in correspondence to (2.16). For the gluon GPD, the decomposition reads

$$F^{\mathrm{G}}(x, \eta, \Delta^2) = g(x, \eta, \Delta^2) + \sigma g(-x, \eta, \Delta^2) \,. \tag{4.101}$$

In order to treat the quark and gluon case simultaneously, we introduce the notation

$$F^A(x, \eta, \Delta^2) = f^A(x, \eta, \Delta^2) - \sigma \bar{f}^A(-x, \eta, \Delta^2) \,, \tag{4.102}$$

where we obtain the equations for quarks and gluons by the replacements

$$f^q \to q, \quad \bar{f}^q \to \bar{q}, \quad f^{\mathrm{G}} \to g, \quad \bar{f}^{\mathrm{G}} \to -g \,. \tag{4.103}$$

The conformal moments of the distributions f^a and $\bar{f}^a$ are separately defined as

$$f_j^A(\eta, \Delta^2) = \int_{-\eta}^{1} \mathrm{d}x \; c_j^\lambda(x, \eta) f^A(x, \eta, \Delta^2) \,, \quad \bar{f}_j^A(\eta, \Delta^2) = \int_{-\eta}^{1} \mathrm{d}x \; c_j^\lambda(x, \eta) \bar{f}^A(x, \eta, \Delta^2) \;. \tag{4.104}$$

In this section we reconstruct the GPD from its conformal moments. For this purpose, we take advantage of the fact that the polynomials $c_j^\lambda(x, \eta)$ are orthogonal in the central region $[-\eta, \eta]$. This property stems from the orthogonality of Gegenbauer polynomials with the weight function $(1-x^2)^{\lambda - \frac{1}{2}}$ (C.1). To this end, we define a polynomial including the weight function and the normalization providing the following orthogonality relation

$$\int_{-\eta}^{\eta} \mathrm{d}x \, c_n^\lambda(x, \eta) p_m^\lambda(x, \eta) = (-1)^n \delta_{mn} \,, \tag{4.105}$$

where a factor $(-1)^n$ is included for convenience. Explicitly, expression of the orthogonal polynomials read

$$p_n^\lambda(x,\eta) = \frac{1}{\eta^{n+1}} \frac{2^{n-2\lambda}\Gamma(n+\lambda)}{\Gamma(\lambda)\,\Gamma(n+1)} \frac{1}{N_k^\lambda} C_n^\lambda\left(-\frac{x}{\eta}\right)\left[1-\left(\frac{x}{\eta}\right)^2\right]^{\lambda-\frac{1}{2}} . \tag{4.106}$$

Note, the support is restricted to the central region of the GPD. Let us expand the GPD in terms of the orthogonal polynomials above:

$$f^A\big(x,\eta,\Delta^2\big) = \sum_{n=0}^{\infty}(-1)^n p_n^\lambda(x,\eta) f_n^A\big(\eta,\Delta^2\big)\,, \tag{4.107}$$

which is easy to check by simply inserting the definition of conformal GPD moments and applying the orthogonality relation.
However, this series is divergent as an expansion in terms of polynomials. Even in the central region the coefficients in front of the Gegenbauer polynomials is enhanced by the factor of η^{-n-1}, which diverges for $|\eta| < 0$ at $n \to \infty$. Therefore, it cannot be truncated, but has to be resummed utilizing a Sommerfeld-Watson transformation. We first consider the unphysical region $\eta > 1$ and rewrite the infinite sum (4.107) as a contour integral in the complex plane. In this way, we interpret the formally integer moments labeled by n as a complex continuous variable j

$$f^A\left(x,\eta,\Delta^2\right) = \frac{1}{2i}\oint_{(0)}^{(\infty)} \mathrm{d}j\, \frac{1}{\sin(\pi j)}\, p_j^\lambda(x,\eta)\; f_j^A\left(\eta,\Delta^2\right)\,. \tag{4.108}$$

The factor $1/\sin(\pi j)$ has the residue $(-1)^j/\pi$ for $j \in \mathbb{N}_0$. Thus, in the absence, of any further singularities inside the contour the integral above coincides with the series (4.107).
At this point, the remaining difficulty is finding an the analytic continuation of the polynomial $p_n(x,\eta)$ and the conformal GPD moments $f_j^A(\eta,\Delta^2)$ to obtain the resummation also in the nonphysical region.
The first problem is solved by means of the Schläfli integral:

$$\frac{1}{2\pi i}\oint_{(-1+\epsilon)}^{(1-\epsilon)} \mathrm{d}u\, \frac{\left(u^2-1\right)^{j+\lambda-\frac{1}{2}}}{(x+u\eta)^{j+1}}\,. \tag{4.109}$$

The corresponding contour is a unit circle, where the points -1 and 1 are included. Consequently, the integrand has four branch points in the complex u plane $\{-\infty,-1,-x/\eta,1\}$. We connect these branch points by a single cut on the real axes from $-\infty$ to $\mathrm{Max}(-x/\eta,1)$. For $j \in \mathbb{N}_0$, the Schläfli integral is equivalent to the Rodrigues formula (C.12) for Gegenbauer

polynomials[4]:

$$\begin{aligned}
&\frac{1}{2\pi i}\oint_{(-1+\epsilon)}^{(1-\epsilon)} \mathrm{d}u\, \frac{\left(u^2-1\right)^{j+\lambda-\frac{1}{2}}}{(x+u\eta)^{j+1}} \\
&= \frac{1}{2\pi i}\frac{1}{\eta^{j+1}}\oint \mathrm{d}u\, \frac{\left(u^2-1\right)^{j+\lambda-\frac{1}{2}}}{\left(\frac{x}{\eta}+u\right)^{j+1}} = \mathrm{Res}_{\left(-\frac{x}{\eta}\right)} \frac{1}{2\pi i}\frac{1}{\eta^{j+1}}\oint \mathrm{d}u\, \frac{\left(u^2-1\right)^{j+\lambda-\frac{1}{2}}}{\left(\frac{x}{\eta}+u\right)^{j+1}} \\
&= \frac{1}{j!}\frac{1}{\eta^{j+1}}\frac{\mathrm{d}^j}{\mathrm{d}u^j}\left(u^2-1\right)^{j+\lambda-\frac{1}{2}}\Big|_{u=-\frac{x}{\eta}} = (-1)^{j+\lambda-\frac{1}{2}}\frac{1}{j!}\frac{1}{\eta}\frac{\mathrm{d}^j}{\mathrm{d}x^j}\left[1-\left(\frac{x}{\eta}\right)^2\right]^{j+\lambda-\frac{1}{2}}. \qquad (4.110)
\end{aligned}$$

For integer values of j the integrand only possesses a pole of order $j+1$ situated at $u=-x/\eta$. In case of $|x|<\eta$, the pole is inside the contour and the integral is non-zero. For $|x|>\eta$, the pole lies outside the contour and the integral vanishes. For complex valued j we have the more complex situation described before. With the corresponding normalization the polynomial $p_j^\lambda(x,\eta)$ expressed in terms of the Schläfli integral reads

$$p_j^\lambda(x,\eta) = (-1)^{\lambda-\frac{1}{2}}\frac{\Gamma(j+\lambda+1)}{\Gamma\left(\frac{1}{2}\right)\Gamma\left(j+\lambda+\frac{1}{2}\right)}\cdot\frac{1}{2\pi i}\oint_{(-1+\epsilon)}^{(1-\epsilon)}\mathrm{d}u\,\frac{\left(u^2-1\right)^{j+\lambda-\frac{1}{2}}}{(x+u\eta)^{j+1}}. \qquad (4.111)$$

For $\eta=0$, we need to solve the integral

$$\frac{1}{2\pi i}\oint_{(-1+\epsilon)}^{(1-\epsilon)}\mathrm{d}u\,\left(u^2-1\right)^{j+\lambda-\frac{1}{2}}. \qquad (4.112)$$

The integrand possesses for non-integer j a discontinuity in the interval $-1\le u\le 1$. We safely deform the contour in such a way that the real axes is pinched. For $|\,\Re\mathrm{e}\,u|\le 1$, we pick up a phase factor[5]

$$\begin{aligned}
\frac{1}{2\pi i}\oint_{(-1+\epsilon)}^{(1-\epsilon)}\mathrm{d}u\,\left(u^2-1\right)^{j+\lambda-\frac{1}{2}} &= \frac{1}{2\pi i}\left(1-e^{2\pi i(j+\lambda-\frac{1}{2})}\right)\int_{-1}^{1}\mathrm{d}u\,\left(u^2-1\right)^{j+\lambda-\frac{1}{2}} \\
&= -\frac{\sin\left[\pi\left(j+\lambda-\frac{1}{2}\right)\right]}{\pi}\frac{\Gamma\left(\frac{1}{2}\right)\Gamma\left(j+\lambda+\frac{1}{2}\right)}{\Gamma(j+\lambda+1)}. \qquad (4.113)
\end{aligned}$$

The integration is the beta function (C.20) and the desired polynomial has the form

$$p_j^\lambda(x,\eta=0) = (-1)^{\lambda+\frac{1}{2}}x^{-j-1}\frac{\sin\left[\pi\left(j+\lambda-\frac{1}{2}\right)\right]}{\pi}. \qquad (4.114)$$

For the two cases $\lambda=3/2$ and $\lambda=5/2$, the polynomials read

$$p_j^{3/2}(x,\eta=0) = x^{-j-1}\frac{\sin[\pi(j+1)]}{\pi}, \qquad p_{j-1}^{5/2}(x,\eta=0) = -x^{-j}\frac{\sin[\pi(j+1)]}{\pi}, \qquad (4.115)$$

[4] $\mathrm{Res}_{z_0}\frac{g(z)}{(z-z_0)^k} = \frac{g^{(k-1)}(z_0)}{(k-1)!}$.
[5] See [Jän01], p. 118.

respectively. Besides a prefactor, this is the integral kernel of the inverse Mellin transformation (4.87). Note, the minus sign in the gluon polynomial does not hold any complications, since it cancels in the Sommerfeld-Watson transformation (4.108).
For the GPD on the cross-over line ($\eta=x$), we have to solve the integral

$$\frac{1}{2\pi i}\oint_{(-1+\epsilon)}^{(1-\epsilon)} \mathrm{d}u\, \frac{\left(u^2-1\right)^{j+\lambda-\frac{1}{2}}}{(1+u)^{j+1}}\,. \tag{4.116}$$

The same phase factor as in the previous case appears and the solution is a beta function (C.20), namely

$$\frac{1}{2\pi i}\oint_{(-1+\epsilon)}^{(1-\epsilon)} \mathrm{d}u\, \frac{\left(u^2-1\right)^{j+\lambda-\frac{1}{2}}}{(1+u)^{j+1}} = -\frac{\sin\left[\pi\left(j+\lambda-\frac{1}{2}\right)\right]}{\pi}\, 2^{j+2\lambda-1}\mathrm{B}\left(\lambda-\frac{1}{2}, j+\lambda+\frac{1}{2}\right)\,. \tag{4.117}$$

Thus, the polynomials at the cross-over line $\eta=x$ become

$$p_j^{\lambda}(x,\eta=x) = (-1)^{\lambda+\frac{1}{2}} 2^{j+2\lambda-1} x^{-j-1} \frac{\Gamma\left(\lambda-\frac{1}{2}\right)\Gamma(j+\lambda+1)}{\Gamma\left(\frac{1}{2}\right)\Gamma(j+2\lambda)} \frac{\sin\left[\pi\left(j+\lambda-\frac{1}{2}\right)\right]}{\pi}\,. \tag{4.118}$$

Moreover, the two special cases of interest in this work are given by

$$\begin{aligned} p_j^{3/2}(x,\eta=x) &= \left(\frac{2}{x}\right)^{j+1} \frac{\Gamma\left(j+\frac{5}{2}\right)}{\Gamma\left(\frac{3}{2}\right)\Gamma(j+3)} \frac{\sin[\pi(j+1)]}{\pi}\,, \\ p_{j-1}^{5/2}(x,\eta=x) &= -\left(\frac{2}{x}\right)^{j+1} \frac{2x}{j+3} \frac{\Gamma\left(j+\frac{5}{2}\right)}{\Gamma\left(\frac{3}{2}\right)\Gamma(j+3)} \frac{\sin[\pi(j+1)]}{\pi}\,. \end{aligned} \tag{4.119}$$

With the solution of the two limiting cases, we shift our attention to the general case. Let us repeat the integral once more

$$\oint_{(-1+\epsilon)}^{(1-\epsilon)} \mathrm{d}u\, \frac{\left(u^2-1\right)^{j+\lambda-\frac{1}{2}}}{(x+u\eta)^{j+1}}\,.$$

As mentioned before, η is fixed to be positive. For $x\leq-\eta$, $-x/\eta\geq1$, the pole lies outside the contour and the integral vanishes. In the case $x\geq-\eta$, $-\frac{x}{\eta}\leq1$ the pole is in fact inside the contour and we distinguish two cases: $|x|\leq\eta$, the pole is in the interval $[-x/\eta,1]$ and we can restrict the integration accordingly. For $|x|>\eta$, we cannot restrict the integration. Picking up the phase factors, the integral along the real axis becomes

$$\begin{aligned} p_j^{\lambda}(x,\eta) =& (-1)^{\lambda+\frac{1}{2}} \frac{\Gamma(j+\lambda+1)}{\Gamma\left(\frac{1}{2}\right)\Gamma\left(j+\lambda+\frac{1}{2}\right)} \frac{\sin\left[\pi(j+\lambda-\frac{1}{2})\right]}{\pi} \\ &\times\left[\theta(\eta-|x|)\int_{-x/\eta}^{1}\mathrm{d}u\, \frac{\left(1-u^2\right)^{j+\lambda-\frac{1}{2}}}{(x+u\eta)^{j+1}} + \theta(x-\eta)\int_{-1}^{1}\mathrm{d}u\, \frac{\left(1-u^2\right)^{j+\lambda-\frac{1}{2}}}{(x+u\eta)^{j+1}}\right]\,. \end{aligned} \tag{4.120}$$

To solve the second integral, we employ the transformation $u=2y-1$ and realize, that the integral is nothing else but the integral representation (C.19) of the hypergeometric function ${}_2F_1$:

$$\int_0^1 \mathrm{d}y\, \frac{2}{(x-\eta)^{j+1}} \frac{(4y\bar{y})^{j+\lambda-\frac{1}{2}}}{\left(1-\frac{2\eta}{\eta-x}y\right)^{j+1}} = \frac{2^{2j+2\lambda}}{(x-\eta)^{j+1}} \mathrm{B}\left(j+\lambda+\frac{1}{2}, j+\lambda+\frac{1}{2}\right) {}_2F_1\left(\begin{matrix} j+1 & j+\lambda+\frac{1}{2} \\ 2j+2\lambda+1 \end{matrix} \middle| \frac{2}{1-\frac{x}{\eta}}\right).$$

Using the quadratic transformation (C.25) for the hypergeometric function above, we have

$${}_2F_1\left(\begin{matrix} j+1 & j+\lambda+\frac{1}{2} \\ 2j+2\lambda+1 \end{matrix} \middle| \frac{2}{1-\frac{x}{\eta}}\right) = \left(1-\frac{1}{1-\frac{x}{\eta}}\right)^{-j-1} {}_2F_1\left(\begin{matrix} \frac{j+1}{2} & \frac{j+2}{2} \\ j+\lambda+1 \end{matrix} \middle| \frac{1}{\frac{x^2}{\eta^2}}\right). \tag{4.121}$$

Thus, the result of the second integral becomes

$$2^{2j+2\lambda}\mathrm{B}\left(j+\lambda+\frac{1}{2}, j+\lambda+\frac{1}{2}\right)\left(\frac{x}{\eta}\right)^{-j-1} \eta^{-j-1} {}_2F_1\left(\begin{matrix} \frac{j+1}{2} & \frac{j+2}{2} \\ j+\lambda+1 \end{matrix} \middle| \frac{1}{\frac{x^2}{\eta^2}}\right). \tag{4.122}$$

The respective gamma structure for the polynomial breaks down to

$$\mathrm{B}\left(j+\lambda+\frac{1}{2}, j+\lambda+\frac{1}{2}\right) \frac{\Gamma(j+\lambda+1)}{\Gamma\left(\frac{1}{2}\right)\Gamma\left(j+\lambda+\frac{1}{2}\right)} = 2^{-2j-2\lambda}. \tag{4.123}$$

In order to solve the first integral, we utilize the transformation $u=\frac{x+\eta}{\eta}y-\frac{x}{\eta}$. Its inverse is $y=\frac{x+u\eta}{x+\eta}$. Again, this enables us to write the integral as an integral representation of a Gauss hypergeometric function by applying the transformation

$$1-u^2 \to -\frac{(x+\eta)}{\eta^2}(x-\eta)(1-y)\left(1-\frac{x+\eta}{x-\eta}y\right), \qquad x+u\eta \to y(x+\eta). \tag{4.124}$$

Thus,

$$\begin{aligned} &\int_0^1 \mathrm{d}y\, \eta^{-2j-2\lambda}(\eta-x)^{j+\lambda-\frac{1}{2}}(x+\eta)^{\lambda-\frac{1}{2}} y^{-j-1}\bar{y}^{j+\lambda-\frac{1}{2}} \left(1-\frac{x+\eta}{x-\eta}y\right)^{j+\lambda-\frac{1}{2}} \\ &= \eta^{-2j-2\lambda}(\eta-x)^{j+\lambda-\frac{1}{2}}(x+\eta)^{\lambda-\frac{1}{2}} \mathrm{B}\left(j+\lambda+\frac{1}{2}, -j\right) {}_2F_1\left(\begin{matrix} -j-\lambda+\frac{1}{2} & -j \\ \lambda+\frac{1}{2} \end{matrix} \middle| \frac{x+\eta}{x-\eta}\right). \end{aligned} \tag{4.125}$$

Utilizing the linear transformation (C.24b) for the hypergeometric function, we get

$${}_2F_1\left(\begin{matrix} -j-\lambda+\frac{1}{2} & -j \\ \lambda+\frac{1}{2} \end{matrix} \middle| \frac{x+\eta}{x-\eta}\right) = \left(1-\frac{x+\eta}{x-\eta}\right)^{j+\lambda-\frac{1}{2}} {}_2F_1\left(\begin{matrix} -j-\lambda+\frac{1}{2} & j+\lambda+\frac{1}{2} \\ \lambda+\frac{1}{2} \end{matrix} \middle| \frac{1+\frac{x}{\eta}}{2}\right). \tag{4.126}$$

The complete result for the first integral in (4.120) is

$$2^{j+\lambda-\frac{1}{2}}\eta^{-j-1}\left(1+\frac{x}{\eta}\right)^{\lambda-\frac{1}{2}} \mathrm{B}\left(j+\lambda+\frac{1}{2}, -j\right) {}_2F_1\left(\begin{matrix} -j-\lambda+\frac{1}{2} & j+\lambda+\frac{1}{2} \\ \lambda+\frac{1}{2} \end{matrix} \middle| \frac{1+\frac{x}{\eta}}{2}\right). \tag{4.127}$$

The corresponding gamma structure reads

$$\mathrm{B}\left(j+\lambda+\frac{1}{2},-j\right)\frac{\Gamma(j+\lambda+1)}{\Gamma\left(\frac{1}{2}\right)\Gamma\left(j+\lambda+\frac{1}{2}\right)}=-\frac{\Gamma\left(\frac{1}{2}\right)\Gamma(j+\lambda+1)}{\Gamma(j+1)\Gamma\left(\lambda+\frac{1}{2}\right)\sin(\pi j)}\,, \tag{4.128}$$

where we used the identity

$$\Gamma(1-z)\Gamma(z)=\frac{\pi}{\sin(\pi z)}\quad\rightarrow\quad\Gamma(-z)=-\frac{1}{z}\Gamma(1-z)=-\frac{1}{\Gamma(z+1)}\frac{\pi}{\sin(\pi z)}\,. \tag{4.129}$$

Taking everything together, the analytic continuation of the distribution $p_n^\lambda(x,\eta)$ with respect to conformal spin is given by

$$p_j^\lambda(x,\eta)=\theta(\eta-|x|)\;\eta^{-j-1}\mathcal{P}_j^\lambda\left(\frac{x}{\eta}\right)+\theta(x-\eta)\;\eta^{-j-1}\mathcal{Q}_j^\lambda\left(\frac{x}{\eta}\right)\,, \tag{4.130}$$

where we introduced the two polynomials for the first and second integral

$$\mathcal{P}_j^\lambda(y)=\frac{2^{j+\lambda-\frac{1}{2}}\Gamma(j+\lambda+1)}{\Gamma\left(\frac{1}{2}\right)\Gamma(j+1)\Gamma\left(\lambda+\frac{1}{2}\right)}(1+y)^{\lambda-\frac{1}{2}}\,{}_2F_1\left(\begin{matrix}-j-\lambda+\frac{1}{2} & j+\lambda+\frac{1}{2}\\ \lambda+\frac{1}{2}\end{matrix}\,\middle|\,\frac{1+y}{2}\right)\,, \tag{4.131}$$

$$\mathcal{Q}_j^\lambda(y)=-\frac{\sin(\pi j)}{\pi}y^{-j-1}\,{}_2F_1\left(\begin{matrix}\frac{j+1}{2} & \frac{j+2}{2}\\ j+\lambda+1\end{matrix}\,\middle|\,\frac{1}{y^2}\right)\,. \tag{4.132}$$

In case of $\lambda=3/2$ we get

$$\mathcal{P}_j^{3/2}(y)=\frac{2^{j+1}\Gamma\left(j+\frac{5}{2}\right)}{\Gamma\left(\frac{1}{2}\right)\Gamma(j+1)}(1+y)\,{}_2F_1\left(\begin{matrix}-j-1 & j+2\\ 2\end{matrix}\,\middle|\,\frac{1+y}{2}\right)\,, \tag{4.133}$$

$$\mathcal{Q}_j^{3/2}(y)=-\frac{\sin(\pi j)}{\pi}y^{-j-1}\,{}_2F_1\left(\begin{matrix}\frac{j+1}{2} & \frac{j+2}{2}\\ j+\frac{5}{2}\end{matrix}\,\middle|\,\frac{1}{y^2}\right)\,, \tag{4.134}$$

and for $\lambda=5/2$ the polynomials are

$$\mathcal{P}_{j-1}^{5/2}(y)=\frac{2^j\Gamma\left(j+\frac{5}{2}\right)}{\Gamma\left(\frac{1}{2}\right)\Gamma(j)}(1+y)^2\,{}_2F_1\left(\begin{matrix}-j-1 & j+2\\ 3\end{matrix}\,\middle|\,\frac{1+y}{2}\right)\,, \tag{4.135}$$

$$\mathcal{Q}_{j-1}^{5/2}(y)=\frac{\sin(\pi j)}{\pi}y^{-j}\,{}_2F_1\left(\begin{matrix}\frac{j}{2} & \frac{j+1}{2}\\ j+\frac{5}{2}\end{matrix}\,\middle|\,\frac{1}{y^2}\right)\,. \tag{4.136}$$

Analogous to the Mellin-Barnes representation of PDFs, we improve the contour of the Sommerfeld-Watson transformation in (4.108) to follow a straight vertical line in the complex plane. As depicted in figure 4.1 we safely add two quarter circles in the first and fourth quadrant, whereas the auxiliary arc does not contribute to the integral [MS06]. As a consequence, the Mellin-Barnes integral representation of GPDs reads

$$f^A(x,\eta,\Delta^2)=\frac{i}{2}\int_{c-i\infty}^{c+i\infty}\mathrm{d}j\;\frac{1}{\sin\pi j}p_j^\lambda(x,\eta)\;f_j^A(\eta,\Delta^2)\,, \tag{4.137}$$

where the real constant c is chosen in such that all singularities contained in the conformal moments $f_j^A(\eta,\Delta^2)$ are on the left hand side of the integration path. In order to summarize

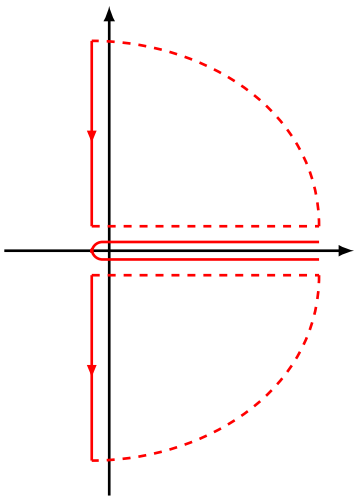

Figure 4.1.: Contour of the Mellin-Barnes representation of the GPD.

our results of the current section, we present the Mellin-Barnes representations of the zero-skewness GPD, the GPD on the cross-over line and the GPD in general.
The Mellin-Barnes representation of the zero-skewness GPD employing the polynomials (4.115) reads

$$\begin{aligned} F^q(x,\eta{=}0,\Delta^2) &= \frac{1}{2\pi i}\int_{c-i\infty}^{c+i\infty} \mathrm{d}j\, x^{-j-1} F_j^q\big(\eta=0,\Delta^2\big)\ , \\ F^{\mathrm{G}}(x,\eta{=}0,\Delta^2) &= \frac{1}{2\pi i}\int_{c-i\infty}^{c+i\infty} \mathrm{d}j\, x^{-j} F_j^{\mathrm{G}}\big(\eta=0,\Delta^2\big)\ . \end{aligned} \tag{4.138}$$

For introducing the GPD evolution, we switch to the evolution basis which solves the quark-gluon mixing problem. In the non-singlet sector, no mixing takes place and the evolution of the GPD in the $\overline{\mathrm{MS}}$ scheme is determined by (D.14). In case of the zero skewness GPD only the diagonal elements of the evolution operator contribute and we have

$$F_j^A(\eta{=}0,\Delta^2,\mu_{\mathrm{F}}^2) = \mathcal{E}_{jj}\,(\mu_{\mathrm{F}},\mu_0;\eta{=}0)\ F_k^A(\eta{=}0,\Delta^2,\mu_0^2)\,, \tag{4.139}$$

with $A \in \{q^{(-)}, 3^{(+)}, 8^{(+)}, 15^{(+)}\}$ and the non singlet evolution operator (D.15). μ_{F} is the factorization scale. Consequently, the evolution of the non-singlet zero skewness GPD is given by

$$F^A(x,\eta{=}0,\Delta^2,\mu_{\mathrm{F}}^2) = \frac{1}{2\pi i}\int_{c-i\infty}^{c+i\infty} \mathrm{d}j\, x^{-j-1}\ {}^{\sigma}\mathcal{E}_{jj}\,(\mu_{\mathrm{F}},\mu_0;0)\ F_j^A\big(\eta=0,\Delta^2,\mu_0^2\big)\ . \tag{4.140}$$

The Mellin-Barnes representation requires the unique analytic continuation of the evolution operator to complex values of j. Therefore, we dressed the evolution operator with a definite signature to hint that all ambiguous factors of $(-1)^j$ contained in the anomalous dimensions have to be replaced by $-\sigma$.
In order to solve the mixing problem of the singlet and gluon GPD, we introduce analogously

to (3.162) in the momentum fraction representation a vector consisting of the conformal moments of the singlet and gluon GPD

$$\boldsymbol{F}_j(\eta,\Delta^2) = \begin{pmatrix} F_j^{0(+)} \\ F_j^{\mathrm{G}} \end{pmatrix}(\eta,\Delta^2)\ . \tag{4.141}$$

Thus, the GPD at the factorization scale μ_{F} evolved from conformal moments at the input scale μ_0 in the Mellin-Barnes representation yields

$$\boldsymbol{F}(x,\eta{=}0,\Delta^2,\mu_{\mathrm{F}}^2) = \frac{1}{2\pi i}\int_c \mathrm{d}j\, x^{-j-1} \begin{pmatrix} 1 & 0 \\ 0 & x \end{pmatrix} {}^{\sigma}\boldsymbol{\mathcal{E}}_{jj}(\mu_{\mathrm{F}},\mu_0;\eta{=}0)\ \boldsymbol{F}_j\big(\eta{=}0,\Delta^2,\mu_0^2\big)\ , \tag{4.142}$$

where the singlet evolution operator $\boldsymbol{\mathcal{E}}$ is given in (D.19) in the $\overline{\mathrm{MS}}$ scheme. To lighten the notation, we employed the abbreviation

$$\int_c \mathrm{d}j \equiv \int_{c-i\infty}^{c+i\infty} \mathrm{d}j\,. \tag{4.143}$$

It is possible to improve the contour of the Mellin-Barnes integral by parametrizing it as

$$j = c + y e^{i\phi}\,, \tag{4.144}$$

where the integration variable is now y. The angle ϕ can be chosen to improve the convergence. Figure 4.2 shows the improved contour. The standard contour is obtained by $\phi = \frac{\pi}{2}$.

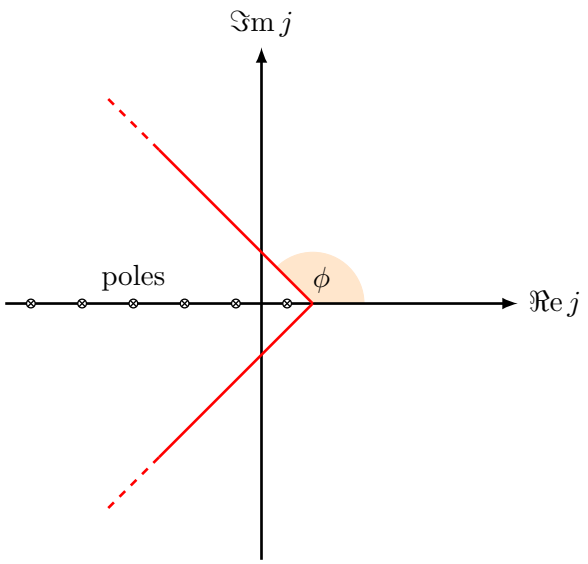

Figure 4.2.: Alternative contour for the Mellin-Barnes integral representation for improved convergence.

Utilizing a value of $\phi > \frac{\pi}{2}$ dampens the integrand due to the factor $x^{y\exp(i\phi)}$ for large values of y. Furthermore, the value of the integral does not depend on c or ϕ as long as no poles

are crossed. In the $\overline{\text{MS}}$-scheme, some caution is necessary in order to avoid poles of the non-diagonal evolution operator.
Note, the Mellin-Barnes representation requires, that the GPD confromal moments have a analytic continuation as well. Troughout this thesis, this is granted by modeling the conformal moments in such a way that this feature is guaranteed. Furthermore, for numerical implementation, we utilize the Schwarz reflection priciple leading to the following representations for the quark and gluon GPD

$$\begin{aligned} F^q(x,\eta{=}0,\Delta^2) &= \frac{1}{\pi}\,\Im\mathrm{m}\, e^{i\phi}\int_0^\infty \mathrm{d}y\, x^{-j-1} F_j^q(\eta,\Delta^2)\,\Big|_{j=c+ye^{i\phi}}\,, \\ F^{\mathrm{G}}(x,\eta{=}0,\Delta^2) &= \frac{1}{\pi}\,\Im\mathrm{m}\, e^{i\phi}\int_0^\infty \mathrm{d}y\, x^{-j} F_j^{\mathrm{G}}(\eta,\Delta^2)\,\Big|_{j=c+ye^{i\phi}}\,, \end{aligned} \tag{4.145}$$

respectively. The inclusion of the evolution operator in the numerical implementation is straight forward. For the GPD on the cross-over line, the corresponding polynomials are given in (4.119). Thus, Mellin-Barnes representations for the quark and gluon GPDs read

$$F^{q^{(\pm)}}(x,\eta{=}x,\Delta^2) = \frac{1}{2\pi i}\int_{c-i\infty}^{c+i\infty}\mathrm{d}j\;\frac{2^{j+1}\Gamma\big(j+\frac{5}{2}\big)}{\Gamma\big(\frac{3}{2}\big)\,\Gamma(j{+}3)}\;x^{-j-1}F_j^{q^{(\pm)}}(\eta,\Delta^2)\;, \tag{4.146}$$

$$F^{\mathrm{G}}(x,\eta{=}x,\Delta^2) = \frac{1}{2\pi i}\int_{c-i\infty}^{c+i\infty}\mathrm{d}j\;\frac{2^{j+2}\Gamma\big(j+\frac{5}{2}\big)}{\Gamma\big(\frac{3}{2}\big)\,\Gamma(j{+}4)}\;x^{-j}F_j^{\mathrm{G}}(\eta,\Delta^2)\;. \tag{4.147}$$

For convenience, we define the following notation for the two prefactors in the previous equations

$$\Gamma_j^{3/2} = \frac{2^{j+1}\Gamma\big(j+\frac{5}{2}\big)}{\Gamma\big(\frac{3}{2}\big)\,\Gamma(j{+}3)}\,, \qquad \Gamma_j^{5/2} = \frac{2^{j+2}\Gamma\big(j+\frac{5}{2}\big)}{\Gamma\big(\frac{3}{2}\big)\,\Gamma(j{+}4)}\,. \tag{4.148}$$

Due to the appearance of the non-diagonal elements of the evolution operator, its inclusion in the Mellin-Barnes representation is intricate. Schematically, omitting unimportant tems, we have for the non-singlet GPDs $A\in\{\mathrm{NS}^{(+)},q^{(-)}\}$

$$\begin{aligned} &\sum_{j=0}^\infty \big[1{-}\sigma(-1)^j\big]\,x^{-j-1}\,\Gamma_j^{3/2}\,F_j^A\big(\eta{=}x,\Delta^2,\mu_{\mathrm{F}}^2\big) \\ &= \sum_{j=0}^\infty \big[1{-}\sigma(-1)^j\big]\,x^{-j-1}\,\Gamma_j^{3/2}\sum_{m=0}^{j}\frac{1{-}\sigma(-1)^m}{2}\,\mathcal{E}_{jm}(\mu_{\mathrm{F}},\mu_0;\eta{=}x)\,F_m^A\big(\eta{=}x,\Delta^2,\mu_0^2\big) \\ &= \sum_{m=0}^\infty\sum_{j=m}^\infty \big[1{-}\sigma(-1)^j\big]\,x^{-j-1}\Gamma_j^{3/2}\,\frac{1{-}\sigma(-1)^m}{2}\,\mathcal{E}_{jm}(\ldots;\eta{=}x)\,F_m^A \\ &= \sum_{j=0}^\infty \big[1{-}\sigma(-1)^j\big]\,x^{-j-1}\left[\sum_{m=j}^\infty\frac{1{-}\sigma(-1)^m}{2}\,\Gamma_m^{3/2}\,\mathcal{E}_{mj}(\ldots;\eta{=}1)\right]F_j^A \\ &= \sum_{j=0}^\infty \big[1{-}\sigma(-1)^j\big]\,x^{-j-1}\left[\sum_{\substack{m=0\\ \text{even}}}^\infty\Gamma_{j+m}^{3/2}\,\mathcal{E}_{j+m,j}(\mu_{\mathrm{F}},\mu_0;1)\right]F_j^A\big(\eta{=}x,\Delta^2,\mu_0^2\big)\;. \end{aligned} \tag{4.149}$$

In the derivation above, we interchanged the indices j and m. Note, the evolution operator is now only convoluted with the prefactor $\Gamma^{3/2}_{j+m}$. Additionally, the evolution operator is at the point $\eta=1$. We define the part including the prefactor and the evolution operator as

$$ {}^{\sigma}\Gamma^{3/2}_{j}(\mu_\mathrm{F},\mu_0) = \Gamma^{3/2}_{j}\,{}^{\sigma}\mathcal{E}_{j,j}(\mu_\mathrm{F},\mu_0;1) + \sum_{\substack{m=0\\ \text{even}}}^{\infty} \Gamma^{3/2}_{j+m+2}\,{}^{\sigma}\mathcal{E}_{j+m+2,j}(\mu_\mathrm{F},\mu_0;1)\;, \tag{4.150} $$

where we decorated the evolution operator with a definite signature to hint, that for the correct analytic continuation the factors of $(-1)^j$ and $(-1)^m$ in the anomalous dimensions have to be replaced by $-\sigma$. Moreover, the remaining sum in the previous equation can be written as a Mellin-Barnes integral [KMPK08]:

$$ {}^{\sigma}\Gamma^{3/2}_{j}(\mu_\mathrm{F},\mu_0) = \Gamma^{3/2}_{j}\,{}^{\sigma}\mathcal{E}_{j,j}(\mu_\mathrm{F},\mu_0;1) - \frac{1}{4i}\int_{d-i\infty}^{d+i\infty} \mathrm{d}m\,\cot\Big(\frac{\pi m}{2}\Big)\,\Gamma^{3/2}_{j+m+2}\,{}^{\sigma}\mathcal{E}_{j+m+2,j}(\mu_\mathrm{F},\mu_0;1)\;. \tag{4.151} $$

Since the only residue of $\cot(\pi m/2)$ is $2/\pi$ for even integer values of m, we chose $-2<d<0$. Taking everything together, the evolution of the non-singlet GPDs on the cross-over line is given by

$$ F^A(x,\eta=0,\Delta^2,\mu_\mathrm{F}^2) = \frac{1}{2\pi i}\int_{c-i\infty}^{c+i\infty} \mathrm{d}j\, x^{-j-1}\;{}^{\sigma}\Gamma^{3/2}_{j}(\mu_\mathrm{F},\mu_0)\;F^A_j\big(\eta=0,\Delta^2,\mu_0^2\big)\;. \tag{4.152} $$

For the mixing in the singlet sector we obtain following the same lines

$$ \boldsymbol{F}(x,\eta=x,\Delta^2,\mu_\mathrm{F}^2) = \frac{1}{2\pi i}\int_{c-i\infty}^{c+i\infty} \mathrm{d}j\, x^{-j-1}\begin{pmatrix}1 & 0\\ 0 & x\end{pmatrix}{}^{\sigma}\boldsymbol{\Gamma}_j(\mu_\mathrm{F},\mu_0)\;\boldsymbol{F}_j\big(\eta=x,\Delta^2,\mu_0^2\big)\;, \tag{4.153} $$

where quark and gluon prefactors and the singlet evolution operator are concentrated in the matrix

$$ {}^{\sigma}\boldsymbol{\Gamma}_j(\mu_\mathrm{F},\mu_0) = \sum_{\substack{m=0\\ \text{even}}}^{\infty}\begin{pmatrix}\Gamma^{3/2}_{j+m} & 0\\ 0 & \Gamma^{5/2}_{j+m}\end{pmatrix}{}^{\sigma}\boldsymbol{\mathcal{E}}_{j+m,j}(\mu_\mathrm{F},\mu_0;\eta=1)\;. \tag{4.154} $$

For the vector singlet GPDs $H^{0(+)}$, $E^{0(+)}$ the signature is $+1$ and for the axial vector singlet GPDs $\tilde{H}^{0(+)}$, $\tilde{E}^{0(+)}$ the signature is -1, cf. Sec. 2.3.
As before, we employ the Schwarz reflection principle to rewrite the Mellin-Barnes representations as

$$ \begin{aligned} F^{q(\pm)}(x,\eta=x,\Delta^2) &= \frac{1}{\pi}\,\Im\mathrm{m}\,e^{i\phi}\int_0^\infty \mathrm{d}y\,\frac{2^{j+1}\Gamma\big(j+\frac{5}{2}\big)}{\Gamma\big(\frac{3}{2}\big)\,\Gamma(j+3)}\,x^{-j-1}F^{q(\pm)}_j\big(\eta=x,\Delta^2\big)\Big|_{j=c+ye^{i\phi}}\,,\\ F^{\mathrm{G}}(x,\eta=x,\Delta^2) &= \frac{1}{\pi}\,\Im\mathrm{m}\,e^{i\phi}\int_0^\infty \mathrm{d}y\,\frac{2^{j+2}\Gamma\big(j+\frac{5}{2}\big)}{\Gamma\big(\frac{3}{2}\big)\,\Gamma(j+4)}\,x^{-j}F^{\mathrm{G}}_j\big(\eta=x,\Delta^2\big)\Big|_{j=c+ye^{i\phi}}\,, \end{aligned} \tag{4.155} $$

for a convenient numerical evaluation. The integration of the evolution in the numeric representation is a straight forward task.

In the general case for arbitrary η, the Mellin-Barnes representation of the quark and gluon GPD reads

$$F^{q(\pm)}(x,\eta,\Delta^2) = \frac{1}{2\pi i}\int_{c-i\infty}^{c+i\infty} \mathrm{d}j\, \frac{p_j^{3/2}(x,\eta)}{\sin(\pi j)}\, F_j^{q(\pm)}(\eta,\Delta^2)\,,$$
$$F^{\mathrm{G}}(x,\eta,\Delta^2) = \frac{1}{2\pi i}\int_{c-i\infty}^{c+i\infty} \mathrm{d}j\, \frac{p_{j-1}^{5/2}(x,\eta)}{\sin(\pi j)}\, F_j^{\mathrm{G}}(\eta,\Delta^2)\,, \tag{4.156}$$

where the polynomials are given in (4.130). Since the representation with a changed contour and the introduction of the evolution operator is almost identical to the GPD on the cross-over line, we do not present the corresponding equation here.

4.5. Mellin-Barnes representation of amplitudes

Next, we study the convolution of a GPD with a given hard scattering amplitude, which is given in DVCS, DVMP and in the forward case for the structure functions. The goal in this section is to utilize the Mellin-Barnes representation for the evaluation of CFFs and TFFs. First, we study the forward case as in instructive example. This is followed by the derivation of the Mellin-Barnes representation of CFFs and TFFs.

4.5.1. Structure functions

We derived the structure functions F_1 and F_2 at LO of perturbation theory in Sec. 3.1.3. The result was

$$F_2(x_{\mathrm{B}}) = 2x_{\mathrm{B}}\, F_1(x_{\mathrm{B}}) = \sum_q Q_q^2\, f^{q(+)}(x_{\mathrm{B}})\,. \tag{4.157}$$

At NLO accuracy, also the gluon PDF contributes. In order to restore the analogy to CFFs and TFFs, we introduce the notation

$$F_l(x_{\mathrm{B}},\mathcal{Q}^2) = \sum_q Q_q^2\, F_l^{q(+)}(x_{\mathrm{B}},\mathcal{Q}^2) + Q_{\mathrm{G}}^2\, F_l^{\mathrm{G}}(x_{\mathrm{B}},\mathcal{Q}^2)\,, \tag{4.158}$$

where $l \in \{1,2\}$ and Q_{G}^2 was defined in (3.153). The corresponding structure functions are defined as

$$F_l^{q(+)}(x_{\mathrm{B}},\mathcal{Q}^2) = \int_{-1}^{1}\frac{\mathrm{d}x}{x}\, {}^{\mathrm{q}}T_l^{\mathrm{V}}\Big(\frac{x_{\mathrm{B}}}{x}\Big|\alpha_{\mathrm{s}}(\mu_{\mathrm{R}}),\tfrac{\mathcal{Q}^2}{\mu_{\mathrm{F}}^2}\Big)\, f^{q(+)}(x,\mu_{\mathrm{F}}^2)\,,$$
$$F_l^{\mathrm{G}}(x_{\mathrm{B}},\mathcal{Q}^2) = \int_{-1}^{1}\frac{\mathrm{d}x}{x}\, {}^{\mathrm{G}}T_l^{\mathrm{V}}\Big(\frac{x_{\mathrm{B}}}{x}\Big|\alpha_{\mathrm{s}}(\mu_{\mathrm{R}}),\tfrac{\mathcal{Q}^2}{\mu_{\mathrm{F}}^2}\Big)\, f^{\mathrm{G}}(x,\mu_{\mathrm{F}}^2)\,. \tag{4.159}$$

The hard scattering amplitude at LO accuracy as derived in Sec. 3.1.3 are

$${}^{\mathrm{q}}T_l^{\mathrm{V}(0)}\Big(\frac{x_{\mathrm{B}}}{x}\Big) = \frac{1}{\pi}\,\Im\mathrm{m}\,\frac{1}{\frac{x_{\mathrm{B}}}{x}-1-i\epsilon} = \delta\Big(\frac{x_{\mathrm{B}}}{x}-1\Big)\,,\qquad {}^{\mathrm{G}}T_l^{\mathrm{V}(0)}\Big(\frac{x_{\mathrm{B}}}{x}\Big) = 0\,. \tag{4.160}$$

Inserting the Mellin-Barnes representation of the quark and gluon PDFs (4.87) we obtain the Mellin-Barnes representation of the structure functions

$$F_l^{q(+)}(x_{\rm B},\mathcal{Q}^2) = \frac{1}{2\pi i}\int_c \mathrm{d}j\, x_{\rm B}^{-j}\ {}^{\rm q}\tilde{c}^{\rm V}_{l,j}\Big(\alpha_{\rm s}(\mu_{\rm R}),\tfrac{\mathcal{Q}^2}{\mu_{\rm F}^2}\Big)\ f_j^{q(+)}(\mu_{\rm F}^2)\,,$$
$$F_l^{\rm G}(x_{\rm B},\mathcal{Q}^2) = \frac{1}{2\pi i}\int_c \mathrm{d}j\, x_{\rm B}^{-j}\ {}^{\rm G}\tilde{c}^{\rm V}_{l,j}\Big(\alpha_{\rm s}(\mu_{\rm R}),\tfrac{\mathcal{Q}^2}{\mu_{\rm F}^2}\Big)\ f_j^{\rm G}(\mu_{\rm F}^2)\,. \tag{4.161}$$

The Mellin moments of the hard scattering amplitude $\tilde{c}$ are at LO of perturbation theory given by

$${}^{\rm q}\tilde{c}^{\rm V(0)}_{1,j} = {}^{\rm q}\tilde{c}^{\rm V(0)}_{2,j} = 1\,,\qquad {}^{\rm q}\tilde{c}^{\rm V(0)}_{1,j} = {}^{\rm q}\tilde{c}^{\rm V(0)}_{1,j} = 0\,. \tag{4.162}$$

In order to solve the mixing problem, we introduce the evolution basis for the structure functions in analogy to the CFFs and TFFs. Namely,

$$F_l(x_{\rm B}) = \sum_A \hat{c}_\gamma^A F_l^A(x_{\rm B})\,,\qquad A\in\{0^{(+)},3^{(+)},8^{(+)},15^{(+)},{\rm G}\}\,, \tag{4.163}$$

where the coefficients $\hat{c}_\gamma^A$ are the same as for the CFF. Thus, the Mellin-Barnes representation of the non-singlet structure functions reads

$$F_l^A(x_{\rm B}) = \frac{1}{2\pi i}\int_c \mathrm{d}j\, x_{\rm B}^{-j}\ {}^{\rm q}\tilde{c}^{\rm V}_{l,j}\Big(\alpha_{\rm s}(\mu_{\rm R}),\tfrac{\mathcal{Q}^2}{\mu_{\rm F}^2}\Big)\ f_j^A(\mu_{\rm F})\,,\qquad A\in\{3^{(+)},8^{(+)},15^{(+)}\}\,. \tag{4.164}$$

The evolution of the non-singlet PDFs can be read of from the evolution of the zero skewness GPD (4.139), namely

$$F_l^A(x_{\rm B}) = \frac{1}{2\pi i}\int_c \mathrm{d}j\, x_{\rm B}^{-j}\ {}^{\rm q}\tilde{c}^{\rm V}_{l,j}\big(\mathcal{Q}^2,\mathcal{Q}_0^2\big)\ f_j^A\big(\mathcal{Q}_0^2\big)\,, \tag{4.165}$$

where we summarized the Mellin moments of the hard scattering amplitude and the evolution operator in

$${}^{\rm q}\tilde{c}^{\rm V}_{l,j}\big(\mathcal{Q}^2,\mathcal{Q}_0^2\big) = {}^{\rm q}\tilde{c}^{\rm V}_{l,j}\Big(\alpha_{\rm s}(\mu_{\rm R}),\tfrac{\mathcal{Q}^2}{\mu_{\rm F}^2}\Big)\ {}^{\sigma}\mathcal{E}_{j,j}(\mu_{\rm F},\mathcal{Q}_0;0)\,. \tag{4.166}$$

On the other hand, in the singlet sector we utilize the forward limit of the vector consisting of the conformal moments of the singlet and gluon GPDs (4.141)

$$\boldsymbol{f}_j = \begin{pmatrix} f_j^{0(+)} \\ f_j^{\rm G}\end{pmatrix}. \tag{4.167}$$

The Mellin-Barnes representation of the singlet structure functions reads

$$F_l^{\rm S}\big(x_{\rm B},\mathcal{Q}^2\big) = \frac{1}{2\pi i}\int_c \mathrm{d}j\, x_{\rm B}^{-j}\ \tilde{\boldsymbol{c}}^{\rm V}_{l,j}\Big(\alpha_{\rm s}(\mu_{\rm R}),\tfrac{\mathcal{Q}^2}{\mu_{\rm F}^2}\Big)\ .\boldsymbol{f}_j\big(\mu_{\rm F}^2\big)\,, \tag{4.168}$$

where the vector of the Mellin moments of the hard scattering amplitudes is given by

$$\tilde{\boldsymbol{c}}^{\rm V}_{l,j} = \begin{pmatrix} {}^{\rm q}\tilde{c}^{\rm V}_{l,j} & {}^{\rm G}\tilde{c}^{\rm V}_{l,j}\end{pmatrix}. \tag{4.169}$$

The evolution of the PDFs can be incorporated easily utilizing the formula for the zero skewness GPD in Sec. 4.4. We obtain

$$F_l^{\mathrm{S}}(x_{\mathrm{B}},\mathcal{Q}^2) = \frac{1}{2\pi i}\int_c \mathrm{d}j\, x_{\mathrm{B}}^{-j}\; \tilde{\boldsymbol{c}}^{\mathrm{V}}_{l,j}(\mathcal{Q}^2,\mathcal{Q}_0^2)\; .\boldsymbol{f}_j(\mu_{\mathrm{F}}^2)\;, \tag{4.170}$$

where we summarized the Mellin moments of the hard scattering amplitude and the singlet evolution operator in

$$\tilde{\boldsymbol{c}}^{\mathrm{V}}_{l,j}(\mathcal{Q}^2,\mathcal{Q}_0^2) = \tilde{\boldsymbol{c}}^{\mathrm{V}}_{l,j}\Big(\alpha_{\mathrm{s}}(\mu_{\mathrm{R}}),\tfrac{\mathcal{Q}^2}{\mu_{\mathrm{F}}^2}\Big)\,\boldsymbol{\mathcal{E}}_{j,j}(\mu_{\mathrm{F}},\mathcal{Q}_0;0)\;. \tag{4.171}$$

4.5.2. Compton form factors

In the last section, we have expanded the GPD in conformal partial waves and derived the reconstruction of the GPD from known conformal moments using the analytic continuation of the respective polynomials. For convenience, we have written the Sommerfeld-Watson transformation as a Mellin-Barnes integral. This technique is very suitable for the evolution of GPDs since the convolution formula in momentum fraction space is replaced by the multiplication of moments.
At LO of perturbation theory, the Compton form factor was defined in (3.142), namely

$$\mathcal{F}^q(\xi,\Delta^2,\mathcal{Q}^2) = \int_{-1}^{1}\mathrm{d}x\,\left[\frac{1}{\xi-x-i\epsilon}\mp\frac{1}{\xi-x-i\epsilon}\right]F^q(x,\eta,\Delta^2,\mathcal{Q}^2)\;, \tag{4.172}$$

where the different signs correspond to the vector and axial-vector CFFs, respectively. We employ the decomposition into quark and antiquark distributions (4.100) and obtain

$$\mathcal{F}^q(\xi,\Delta^2,\mathcal{Q}^2) = \int_{-\xi}^{1}\mathrm{d}x\,\left[\frac{1}{\xi-x-i\epsilon}\mp\frac{1}{\xi-x-i\epsilon}\right]\left[q(x,\eta,\Delta^2,\mathcal{Q}^2)+\bar{q}(x,\eta,\Delta^2,\mathcal{Q}^2)\right]\;. \tag{4.173}$$

At this point, we insert the Mellin-Barnes representation of the GPD (4.156) and perform the integration with respect to the momentum fraction x. The result [MS06] is

$$\mathcal{F}^q(\xi,\Delta^2,\mathcal{Q}^2) = \frac{1}{2i}\int_{c-i\infty}^{c+i\infty}\mathrm{d}j\,\xi^{-j-1}\,\frac{2^{j+1}\Gamma\left(j+\frac{5}{2}\right)}{\Gamma\left(\frac{3}{2}\right)\Gamma(j+3)}\left[i-\frac{\cos(\pi j)\mp 1}{\sin(\pi j)}\right]F_j^q(\eta,\Delta^2,\mathcal{Q}^2)\;. \tag{4.174}$$

Instead of the ratio of trigonometric functions above, it is common to use the equivalent representation

$$i-\frac{\cos(\pi j)\mp 1}{\sin(\pi j)} = i\pm\begin{Bmatrix}\tan\\ \cot\end{Bmatrix}\left(\frac{\pi j}{2}\right)\;. \tag{4.175}$$

The inclusion of higher-order corrections in perturbation theory is straight forward in a conformal subtraction scheme, since they can be written as a convolution of the LO hard-scattering amplitude and certain conformally covariant kernels. At arbitrary order in perturbation theory, we have

$$\mathcal{F}^q(\xi,\Delta^2,\mathcal{Q}^2) = \frac{1}{2i}\int_{c-i\infty}^{c+i\infty}\mathrm{d}j\,\xi^{-j-1}\,\frac{2^{j+1}\Gamma\left(j+\frac{5}{2}\right)}{\Gamma\left(\frac{3}{2}\right)\Gamma(j+3)}\left[i\pm\begin{Bmatrix}\tan\\ \cot\end{Bmatrix}\left(\frac{\pi j}{2}\right)\right]{}^{\mathrm{q}}c_j^{\mathrm{I}}\,F_j^q(\eta,\Delta^2,\mathcal{Q}^2)\;. \tag{4.176}$$

Analogously to the perturbative expansion of the hard scattering amplitude in momentum fraction representation (3.146) the expansion of the Wilson coefficients reads

$$ {}^{\mathrm{q}}c_j^{\mathrm{I}}\Big(\alpha_{\mathrm{s}}(\mu_{\mathrm{R}}), \tfrac{\mathcal{Q}^2}{\mu_{\mathrm{F}}^2}\Big) = {}^{\mathrm{q}}c_j^{\mathrm{I}(0)} + \frac{\alpha_{\mathrm{s}}^2(\mu_{\mathrm{R}})}{2\pi}\, {}^{\mathrm{q}}c_j^{\mathrm{I}(1)}\Big(\alpha_{\mathrm{s}}(\mu_{\mathrm{R}}), \tfrac{\mathcal{Q}^2}{\mu_{\mathrm{F}}^2}\Big) + \mathcal{O}(\alpha_{\mathrm{s}}^2)\,. \tag{4.177} $$

In order to obtain the Mellin-Barnes representation of the quark Compton form factor above, we used the Mellin-Barnes representation of the quark GPDs. Thereby, the analytic continuation of the polynomials $p_n^\lambda(x,\eta)$ in the outer region is already implemented.
Alternatively, the same Mellin-Barnes representation of CFFs follows by utilizing the CPWE in terms of an infinite sum over integer moments n. Since the conformal moments of the GPD do not depend on the momentum fraction x, we perform the convolution of the hard scattering amplitude and the polynomials $p_n^\lambda(x,\eta)$. In the process, we restrict the integration to the central region of the GPD discarding the imaginary part. The result is denoted as the conformal moments of the hard scattering amplitude for integer moments n. The essential extension to the outer region of the GPD is completed by a Sommerfeld-Watson transformation in association with the analytic continuation of the integer moments of the hard scattering amplitude to complex valued ones $n \to j$. The continuation has to be bounded at $j \to \infty$, where the uniqueness is assured by Carlson's theorem [Car14]. In this way, we restore the imaginary part correctly and receive the same Mellin-Barnes representation as before. Let us go through the procedure described above in detail. For the quark and gluon GPDs, the CPWE (4.107) in terms of an infinite sum reads

$$ \begin{aligned} F^q\big(x,\eta,\Delta^2\big) &= \sum_{n=0}^{\infty} p_n^{3/2}\,(x,\eta)\, F_n^{q(+)}\,\big(\eta,\Delta^2\big)\,, \\ F^{\mathrm{G}}\big(x,\eta,\Delta^2\big) &= \sum_{n=0}^{\infty} p_{n-1}^{5/2}(x,\eta)\, F_n^{\mathrm{G}}\,\big(\eta,\Delta^2\big)\,, \end{aligned} \tag{4.178} $$

respectively. Note, in contrast to the original form, we waive the factor $(-1)^n$. The summation goes over odd and even n for the GPDs $\{H^{q(+)}, E^{q(+)}, H^{\mathrm{G}}, E^{\mathrm{G}}\}$ and $\{\widetilde{H}^{q(+)}, \widetilde{E}^{q(+)}, \widetilde{H}^{\mathrm{G}}, \widetilde{E}^{\mathrm{G}}\}$, cf. Tab. 4.1. Inserting the expansion in the previous equation into the CFFs defined in section 3.2.4, Eq. (3.149) leads to

$$ \begin{aligned} \mathcal{F}^{q(+)}(\xi,\Delta^2,\mathcal{Q}^2) &= \int_{-1}^{1}\frac{\mathrm{d}x}{2\xi}\qquad {}^{\mathrm{q}}T^{\mathrm{I}}\Big(\tfrac{\xi+x}{2\xi}\Big|\alpha_{\mathrm{s}}(\mu_{\mathrm{R}}), \tfrac{\mathcal{Q}^2}{\mu_{\mathrm{F}}^2}\Big)\, F^{q(+)}(x,\xi,\Delta^2,\mu_{\mathrm{F}}^2)\,, \\ \mathcal{F}^{\mathrm{G}}\ (\xi,\Delta^2,\mathcal{Q}^2) &= \int_{-1}^{1}\frac{\mathrm{d}x}{2\xi}\,\xi^{-1}\,{}^{\mathrm{G}}T^{\mathrm{I}}\Big(\tfrac{\xi+x}{2\xi}\Big|\alpha_{\mathrm{s}}(\mu_{\mathrm{R}}), \tfrac{\mathcal{Q}^2}{\mu_{\mathrm{F}}^2}\Big)\, F^{\mathrm{G}}\ (x,\xi,\Delta^2,\mu_{\mathrm{F}}^2)\,. \end{aligned} \tag{4.179} $$

Note, for DVCS, only CFFs with even intrinsic parity arise. The perturbative expansion of the hard scattering amplitudes is defined in Sec. 3.2.4. The LO contribution for quarks is given in (3.145), whereas it is zero for gluons. Moreover, the NLO contribution was obtained by rotation from the DIS [Mül98, BM98b] and by diagramatical evaluation in [MPS+98, JO98b,

JO98a]. Inserting the expansion of the GPDs in terms of conformal moments (4.178), we get

$$\begin{aligned}
\mathcal{F}^{q(+)}(\xi,\Delta^2,\mathcal{Q}^2) &= \int_{-1}^{1}\frac{\mathrm{d}x}{2\xi}\qquad {}^{\mathrm{q}}T\left(\tfrac{\xi+x}{2\xi}\right)\sum_{n=0}^{\infty} p_n^{3/2}\,(x,\xi)\;F_n^q\left(\xi,\Delta^2,\mu_{\mathrm{F}}^2\right)\,,\\
\mathcal{F}^{\mathrm{G}}\;(\xi,\Delta^2,\mathcal{Q}^2) &= \int_{-1}^{1}\frac{\mathrm{d}x}{2\xi}\,\xi^{-1}\,{}^{\mathrm{G}}T\left(\tfrac{\xi+x}{2\xi}\right)\sum_{n=0}^{\infty} p_{n-1}^{5/2}(x,\xi)\,F_n^{\mathrm{G}}\left(\xi,\Delta^2,\mu_{\mathrm{F}}^2\right)\,.
\end{aligned}\tag{4.180}$$

For brevity we suppress the scale dependence of the hard scattering amplitudes. The expressions of the polynomials $p_n^\lambda(x,\eta)$ are given in (4.106). We repeat their form for concrete indices $\lambda\in\{3/2,5/2\}$

$$\begin{aligned}
p_n^{3/2}\,(x,\eta) &= \frac{1}{\eta^{n+1}}\,\frac{2^n\Gamma\left(n+\frac{5}{2}\right)}{\Gamma\left(\frac{3}{2}\right)\Gamma(n+3)}\qquad C_n^{3/2}\left(\frac{x}{\eta}\right)\left[1-\left(\frac{x}{\eta}\right)^2\right]\,,\\
p_{n-1}^{5/2}(x,\eta) &= \frac{1}{\eta^{n+1}}\,\frac{2^n\Gamma\left(n+\frac{5}{2}\right)}{\Gamma\left(\frac{3}{2}\right)\Gamma(n+3)}\,\frac{3\eta}{n+3}\,C_{n-1}^{5/2}\left(\frac{x}{\eta}\right)\left[1-\left(\frac{x}{\eta}\right)^2\right]^2\,.
\end{aligned}$$

It is common to write the polynomials in the above form to indicate the possibility to pull out a common prefactor. Inserting the explicit expressions for the polynomials

$$\begin{aligned}
\mathcal{F}^{q(+)}(\xi,\Delta^2,\mathcal{Q}^2) &= \sum_{n=0}^{\infty}\xi^{-n-1}\,\tfrac{2^{n+1}\Gamma\left(n+\frac{5}{2}\right)}{\Gamma\left(\frac{3}{2}\right)\Gamma(n+3)}\int_{-1}^{1}\frac{\mathrm{d}x}{2\xi}\,{}^{\mathrm{q}}T\left(\tfrac{\xi+x}{2\xi}\right)C_n^{3/2}\left(\tfrac{x}{\xi}\right)\frac{1}{2}\left[1-\left(\tfrac{x}{\xi}\right)^2\right]\;F_n^q\left(\xi,\Delta^2,\mu_{\mathrm{F}}^2\right)\,,\\
\mathcal{F}^{\mathrm{G}}\;(\xi,\Delta^2,\mathcal{Q}^2) &= \sum_{n=0}^{\infty}\xi^{-n-1}\,\tfrac{2^{n+2}\Gamma\left(n+\frac{5}{2}\right)}{\Gamma\left(\frac{3}{2}\right)\Gamma(n+4)}\int_{-1}^{1}\frac{\mathrm{d}x}{2\xi}\,{}^{\mathrm{G}}T\left(\tfrac{\xi+x}{2\xi}\right)C_{n-1}^{5/2}\left(\tfrac{x}{\xi}\right)\frac{3}{4}\left[1-\left(\tfrac{x}{\xi}\right)^2\right]^2 F_n^{\mathrm{G}}\left(\xi,\Delta^2,\mu_{\mathrm{F}}^2\right)\,.
\end{aligned}$$

In the previous equations, the same prefactor as in (4.174) emerges for the quark CFF. Additionally, the conformal GPD moments do not depend in the momentum fraction x. Therefore, we define the conformal moments of the hard scattering amplitudes in the quark and gluon channel as

$$\begin{aligned}
{}^{\mathrm{q}}T_n &= \frac{2^{n+1}\Gamma\left(n+\frac{5}{2}\right)}{\Gamma\left(\frac{3}{2}\right)\Gamma(n+3)}\int_{-\xi}^{\xi}\frac{\mathrm{d}x}{2\xi}\;{}^{\mathrm{q}}T\left(\frac{\xi+x}{2\xi}\right)\,C_n^{3/2}\left(\frac{x}{\xi}\right)\frac{1}{2}\left[1-\left(\frac{x}{\xi}\right)^2\right]\,,\\
{}^{\mathrm{G}}T_n &= \frac{2^{n+2}\Gamma\left(n+\frac{5}{2}\right)}{\Gamma\left(\frac{3}{2}\right)\Gamma(n+4)}\int_{-\xi}^{\xi}\frac{\mathrm{d}x}{2\xi}\;{}^{\mathrm{G}}T\left(\frac{\xi+x}{2\xi}\right)\,C_{n-1}^{5/2}\left(\frac{x}{\xi}\right)\frac{3}{4}\left[1-\left(\frac{x}{\xi}\right)^2\right]^2\,.
\end{aligned}\tag{4.181}$$

Note, we already restricted the support to the central region of the GPD. With this definition, we arrive at the following representation for CFFs as an infinite sum over even or odd integer moments

$$\begin{aligned}
\mathcal{F}^{q(+)}(\xi,\Delta^2,\mathcal{Q}^2) &= \sum_{n=0}^{\infty}\xi^{-n-1}\;{}^{\mathrm{q}}T_n\left(\alpha_{\mathrm{s}}(\mu_{\mathrm{R}}),\tfrac{\mathcal{Q}^2}{\mu_{\mathrm{F}}^2}\right)\,F_n^q\left(\xi,\Delta^2,\mu_{\mathrm{F}}^2\right)\,,\\
\mathcal{F}^{\mathrm{G}}\;(\xi,\Delta^2,\mathcal{Q}^2) &= \sum_{n=0}^{\infty}\xi^{-n-1}\;{}^{\mathrm{G}}T_n\left(\alpha_{\mathrm{s}}(\mu_{\mathrm{R}}),\tfrac{\mathcal{Q}^2}{\mu_{\mathrm{F}}^2}\right)F_n^{\mathrm{G}}\left(\xi,\Delta^2,\mu_{\mathrm{F}}^2\right)\,.
\end{aligned}\tag{4.182}$$

This is valid for integer moments in the central GPD region. The remaining task is finding the unique analytic continuation of the conformal moments of the hard scattering amplitudes and expressing the infinite sum over integer moments n by a Sommerfeld-Watson transformation. Before that, let us define a convenient representation for the conformal moments of the hard scattering amplitudes. We employ the variable u, which was already defined in (3.217). The corresponding variable transformation and Jacobian are

$$u = \frac{\xi + x}{2\xi}\,, \qquad \frac{\mathrm{d}u}{\mathrm{d}x} = \frac{1}{2\xi}\,, \qquad x = \xi(2u-1)\,, \qquad (2u-1)^2 = -4u\bar{u} + 1\,. \tag{4.183}$$

With this variable, the conformal moments simplify to

$$\begin{aligned} {}^{\mathrm{q}}T_n &= \frac{2^{n+1}\Gamma\left(n+\frac{5}{2}\right)}{\Gamma\left(\frac{3}{2}\right)\Gamma(n+3)} \int_0^1 \mathrm{d}u\ {}^{\mathrm{q}}T(u)\ \ 2\ \ u\bar{u}\ \ \ C_n^{3/2}\left(2u-1\right)\,, \\ {}^{\mathrm{G}}T_n &= \frac{2^{n+2}\Gamma\left(n+\frac{5}{2}\right)}{\Gamma\left(\frac{3}{2}\right)\Gamma(n+4)} \int_0^1 \mathrm{d}u\ {}^{\mathrm{G}}T(u)\ 12\,(u\bar{u})^2\, C_{n-1}^{5/2}\left(2u-1\right)\,. \end{aligned} \tag{4.184}$$

Taking off the two prefactors we define the auxiliary polynomials

$$\begin{aligned} \hat{p}_n^{3/2}(u) &= \ \ 2\ u\bar{u}\ \ \ C_n^{3/2}\left(2u-1\right)\,, \\ \hat{p}_n^{5/2}(u) &= 12\,(u\bar{u})^2\, C_{n-1}^{5/2}(2u-1)\,. \end{aligned} \tag{4.185}$$

These auxiliary polynomials are actually defined to fulfill the normalization conditions

$$\frac{1}{\bar{u}} \overset{u}{\otimes} \hat{p}_n^{3/2}(u) = 1\,, \qquad \frac{1}{\bar{u}} \overset{u}{\otimes} \hat{p}_n^{5/2}(u) = 1\,, \tag{4.186}$$

which were the reason to include the extra factors in (4.181). The factors for the normalization are for general λ given by the factor

$$\frac{2^{2\lambda-1}\Gamma(\lambda)}{\Gamma\left(\frac{1}{2}\right)\Gamma\left(\lambda-\frac{1}{2}\right)} = \begin{cases} 2 & \lambda = 3/2 \\ 12 & \lambda = 5/2 \end{cases}\,. \tag{4.187}$$

For convenience, we also define conformal moments of the hard scattering amplitude, that are normalized involving the auxiliary polynomials as

$${}^{\mathrm{q}}c_n = {}^{\mathrm{q}}T(u) \overset{u}{\otimes} \hat{p}_n^{3/2}(u)\,, \qquad {}^{\mathrm{G}}c_n = {}^{\mathrm{G}}T(u) \overset{u}{\otimes} \hat{p}_n^{5/2}(u)\,, \tag{4.188}$$

and denote them as auxiliary conformal moments. For quarks, these moments agree with the ones defined in (4.177). Utilizing the auxiliary polynomials, the conformal moments of the hard scattering amplitudes are given by

$${}^{\mathrm{q}}T_n = \frac{2^{n+1}\Gamma\left(n+\frac{5}{2}\right)}{\Gamma\left(\frac{3}{2}\right)\Gamma(n+3)}\ \cdot\ {}^{\mathrm{q}}c_n\,, \qquad {}^{\mathrm{G}}T_n = \frac{2^{n+2}\Gamma\left(n+\frac{5}{2}\right)}{\Gamma\left(\frac{3}{2}\right)\Gamma(n+4)}\ \cdot\ {}^{\mathrm{G}}c_n\,. \tag{4.189}$$

The missing piece is the analytic continuation of the conformal moments above. For this continuation to be unique, we have to introduce a particular symmetry for the hard scattering

amplitudes, which will be expressed by a signature.
Let us first explain the necessity of the signature. The original expression for the quark victor and axial-vector CFF at LO was obtained in (3.142)

$$\mathcal{F}^q\big(\xi,\Delta^2,\mathcal{Q}^2\big) \overset{\text{LO}}{=} \int_{-1}^{1}\frac{\mathrm{d}x}{2\xi}\left[\frac{2(\xi-i\epsilon)}{\xi-x-i\epsilon}\mp\frac{2(\xi-i\epsilon)}{\xi+x-i\epsilon}\right]F^q\big(x,\eta,\Delta^2,\mathcal{Q}^2\big)\,. \tag{4.190}$$

In the next step, we introduce the GPD $F^{q(+)}$ with definite charge parity (2.15) to obtain

$$\mathcal{F}^{q(+)}\big(\xi,\Delta^2,\mathcal{Q}^2\big) \overset{\text{LO}}{=} \int_{-1}^{1}\frac{\mathrm{d}x}{2\xi}\,\frac{2(\xi-i\epsilon)}{\xi-x-i\epsilon}\,F^{q(+)}\big(x,\eta,\Delta^2,\mathcal{Q}^2\big)\,,\quad \mathcal{F}\in\{\mathcal{H},\mathcal{E},\widetilde{\mathcal{H}},\widetilde{\mathcal{E}}\}\,. \tag{4.191}$$

Thereby, we made the arbitrary choice ${}^{\text{q}}T^{\text{I}(0)}(u)=\bar{u}$, whose conformal moments (4.186) possess a unique analytic continuation. On the other hand, we could also define

$$\mathcal{F}^{q(+)}\big(\xi,\Delta^2,\mathcal{Q}^2\big) \overset{\text{LO}}{=} \int_{-1}^{1}\frac{\mathrm{d}x}{2\xi}\,\frac{\mp2(\xi-i\epsilon)}{\xi+x-i\epsilon}\,F^{q(+)}\big(x,\eta,\Delta^2,\mathcal{Q}^2\big)\,,\quad \mathcal{F}\in\{\mathcal{H},\mathcal{E},\widetilde{\mathcal{H}},\widetilde{\mathcal{E}}\}\,, \tag{4.192}$$

with the hard scattering amplitude ${}^{\text{q}}T^{\text{I}(0)}(u)=u$. Its conformal moments follow from the symmetry relation of Gegenbauer polynomials (C.10) as

$$\frac{1}{u}\overset{u}{\otimes}\hat{p}_n^{3/2}(u)=(-1)^n\,\frac{1}{\bar{u}}\overset{u}{\otimes}\hat{p}_n^{3/2}(u)=(-1)^n\,. \tag{4.193}$$

However, these moments do not possess a unique continuation to complex values of $n\to j$ due to the ambiguous factor $(-1)^n$. The way out of this dilemma is to exploit the symmetry of the GPD. The GPD $F^{q(+)}$ is antisymmetric for vector operators and symmetric for axial-vector operators. Hence, their conformal moments are odd and even, respectively. Taking the definite symmetry of the GPD into account, we safely make the replacement

$$(-1)^n\to-\sigma\,. \tag{4.194}$$

In that way, the two possibilities to define the hard scattering amplitude lead to the same Mellin-Barnes representation of the CFF. Consequently, we will always utilize the corresponding symmetry with respect to the transformation $u\to\bar{u}$ to obtain the unique analytic continuation of the conformal moments. In table 4.1 we summarize the occurring GPDs for DVCS and their properties. To ensure the uniqueness of the analytic continuation, we introduce the hard scattering amplitude in the quark channel with a definite signature

$${}^{\text{q}}T_j\to{}^{\sigma}T_j\,. \tag{4.195}$$

This can be seen as a replacement of all occurring factors of $(-1)^n$ by $-\sigma$ depending on the signature factor of the quark GPD. Equally well, we define the conformal moments with definite signature factor as

$${}^{\sigma}T_j=\frac{1-\sigma(-1)^j}{2}\,{}^{\text{q}}T_j\,, \tag{4.196}$$

GPD	C	σ	moments	MBR
$H^{q(+)}$, $E^{q(+)}$	$+$	$+$	odd	tan
H^{G}, E^{G}	$+$			
$\widetilde{H}^{q(+)}$, $\widetilde{E}^{q(+)}$	$+$	$-$	even	cot
$\widetilde{H}^{\mathrm{G}}$, $\widetilde{E}^{\mathrm{G}}$	$-$			

Table 4.1.: Charge parity and signature for all occurring GPDs for the twist-2 approximation in DVCS. We also include the correct term in the Mellin-Barnes representation (MBR).

which then automatically takes care of all factors $(-1)^j$. The introduction of a hard scattering amplitude with a definite signature is always possible by

$$ {}^{\sigma}T(u) = \frac{1}{2}\left[{}^{\mathrm{q}}T(u) - \sigma\, {}^{\mathrm{q}}T(\bar{u})\right] , \qquad {}^{\pm}T(u) = \frac{1}{2}\left[{}^{\mathrm{q}}T(u) \mp {}^{\mathrm{q}}T(\bar{u})\right] . \tag{4.197} $$

Taking everything together, we obtain the the vector and axial-vector quark CFFs, as an infinite sum over the integer conformal moments of the hard scattering amplitude and the GPD

$$ \begin{aligned} \mathcal{F}^{q(+)}\big(\xi,\Delta^2,\mathcal{Q}^2\big) &= \sum_{\substack{n=0\\ \text{odd}}}^{\infty} \xi^{-n-1}\, {}^{+}T^{\mathrm{I}}_n\left(\alpha_{\mathrm{s}}(\mu_{\mathrm{R}}), \tfrac{\mathcal{Q}^2}{\mu_{\mathrm{F}}^2}\right) F_n^{q(+)}\big(\xi,\Delta^2,\mu_{\mathrm{F}}^2\big) , \quad \mathcal{F}\in\{\mathcal{H},\mathcal{E}\} , \\ \mathcal{F}^{q(+)}\big(\xi,\Delta^2,\mathcal{Q}^2\big) &= \sum_{\substack{n=0\\ \text{even}}}^{\infty} \xi^{-n-1}\, {}^{-}T^{\mathrm{I}}_n\left(\alpha_{\mathrm{s}}(\mu_{\mathrm{R}}), \tfrac{\mathcal{Q}^2}{\mu_{\mathrm{F}}^2}\right) F_n^{q(+)}\big(\xi,\Delta^2,\mu_{\mathrm{F}}^2\big) , \quad \mathcal{F}\in\{\widetilde{\mathcal{H}},\widetilde{\mathcal{E}}\} , \end{aligned} \tag{4.198} $$

respectively. The corresponding signature factor for the quark CFFs can be read off from Tab. 4.1. For the gluon GPD, we do not have to introduce a signature explicitly, since they already have definite symmetry with respect to $x\to -x$ or $u\to\bar{u}$. Note, in DVCS, we are able to avoid introducing the signature explicitely, since we use the label $\mathrm{I}\in\{\mathrm{V},\mathrm{A}\}$ instead. However, we will use it heavily for DVMP and it is introductory here, where we do not have the additional complication of the DA. From now on, we dispense with the signature for DVCS. Under the assumption, that we obtained the correct analytic continuation of the hard scattering amplitudes, we rewrite the summation as a Mellin-Barnes integral using a Summerfeld-Watson transformation. Intuitively, we make the replacement

$$ \sum_{\substack{n=0\\ \text{odd/even}}}^{\infty} T_n F_n \to \frac{1}{2i}\int_{c-i\infty}^{c+i\infty} \mathrm{d}j\, \frac{\sigma - e^{-i\pi j}}{\sin(\pi j)} T_j\, F_j = \frac{1}{2i}\int_{c-i\infty}^{c+i\infty} \mathrm{d}j \left[i\pm\begin{Bmatrix}\tan\\ \cot\end{Bmatrix}\left(\frac{\pi j}{2}\right)\right] T_j\, F_j . \tag{4.199} $$

Finally, the Mellin-Barnes representation for the vector and axial-vector CFFs reads

$$ \mathcal{F}^{q(+)}\big(\xi,\Delta^2,\mathcal{Q}^2\big) = \frac{1}{2i}\int_{c-i\infty}^{c+i\infty} \mathrm{d}j\, \xi^{-j-1}\left[i\pm\begin{Bmatrix}\tan\\ \cot\end{Bmatrix}\left(\frac{\pi j}{2}\right)\right] {}^{\mathrm{q}}T^{\mathrm{I}}_j\left(\tfrac{\mathcal{Q}^2}{\mu_{\mathrm{F}}^2}\right) F_j^{q(+)}\big(\xi,\Delta^2,\mu_{\mathrm{F}}^2\big) . \tag{4.200} $$

As we already known from the investigation of the perturbative expansion of the CFFs in Sec. 3.2.4.2, the singlet CFF mixes with the gluon CFF. Analogously to momentum fraction

representation, we introduce the evolution basis (Sec. 3.2.4.3) where we split the CFFs in a non-singlet and a singlet contribution.
Expanding the CFFs in terms of SU(4) multiplets, we have (3.156)

$$\mathcal{F}_\gamma = \sum_A \hat{c}_\gamma^A \, \mathcal{F}_\gamma^A \,, \qquad A \in \{0^{(+)}, 3^{(+)}, 8^{(+)}, 15^{(+)}, \mathrm{G}\} \,.$$

In the non-singlet sector, no mixing appears. Thus, the Mellin-Barnes representation of the non-singlet CFFs reads

$$\mathcal{F}^A\big(\xi, \Delta^2, \mathcal{Q}^2\big) = \frac{1}{2i} \int_{c-i\infty}^{c+i\infty} \mathrm{d}j \, \xi^{-j-1} \left[i \pm \begin{Bmatrix} \tan \\ \cot \end{Bmatrix} \left(\frac{\pi j}{2} \right) \right] T_j^{\mathrm{I}} \left(\tfrac{\mathcal{Q}^2}{\mu_{\mathrm{F}}^2} \right) F_j^A\big(\xi, \Delta^2, \mu_{\mathrm{F}}^2\big) \,, \tag{4.201}$$

where $A \in \{3^{(+)}, 8^{(+)}, 15^{(+)}\}$. The corresponding signature factor is clear from the index $\mathrm{I} \in \{\mathrm{V}, \mathrm{A}\}$.
On the other hand, in the singlet sector we have to solve the mixing problem. As for the GPD in Sec. 4.4.2, we utilize the vector (4.141) of the conformal moments of the singlet and gluon GPD. Furthermore, as in the momentum fraction representation (3.163), the conformal moments of the hard scattering amplitude are summarized in the row vector

$$\boldsymbol{T}_j^{\mathrm{I}} = \frac{2^{n+1} \Gamma\big(n+\frac{5}{2}\big)}{\Gamma\big(\frac{3}{2}\big) \, \Gamma(n+3)} \left({}^{\mathrm{q}}c_j^{\mathrm{I}} \quad \tfrac{2}{j+3} \, {}^{\mathrm{G}}c_j^{\mathrm{I}} \right) \,, \tag{4.202}$$

where we pulled out a common prefactor and utilized the auxiliary conformal moments, see (4.189). The conformal moments of the hard scattering amplitude at LO in perturbation theory are

$${}^{\mathrm{q}}c_j^{\mathrm{V}(0)} = {}^{\mathrm{q}}c_j^{\mathrm{A}(0)} = 1 \,, \qquad {}^{\mathrm{G}}c_j^{(0)} = 0 \,. \tag{4.203}$$

We present the NLO correction later in this chapter. Finally, the Mellin-Barnes representation of the singlet CFF is

$$\mathcal{F}^{\mathrm{S}}\big(\xi, \Delta^2, \mathcal{Q}^2\big) = \frac{1}{2i} \int_{c-i\infty}^{c+i\infty} \mathrm{d}j \, \xi^{-j-1} \left[i \pm \begin{Bmatrix} \tan \\ \cot \end{Bmatrix} \left(\frac{\pi j}{2} \right) \right] \boldsymbol{T}_j^{\mathrm{I}} \left(\tfrac{\mathcal{Q}^2}{\mu_{\mathrm{F}}^2} \right) . \boldsymbol{F}_j\big(x, \xi, \Delta^2, \mu_{\mathrm{F}}^2\big) \,. \tag{4.204}$$

The corresponding expression for the vector and axial-vector case follows from the signature, that is presented in Tab. 4.1.
With the definition of the non-singlet and singlet CFFs, we have everything at hand, to include the evolution of the GPDs. As presented in Sec. D.1, the evolution of the non-singlet GPDs ($A \in \{NS^{(+)}, q^{(-)}\}$) is governed by the non-singlet evolution operator:

$$F_j^A\big(\eta, \Delta^2, \mu_{\mathrm{F}}^2\big) = \sum_{m=0}^{j} {}^{\sigma}\mathcal{E}_{jm}\big(\mu_{\mathrm{F}}, \mu_0; \eta\big) \, F_m^A\big(\eta, \Delta^2, \mu_0^2\big) \,, \tag{4.205}$$

where we have to include a definite signature for the same reasons as before (4.197). In case of the singlet GPD moments (4.141) the evolution operator is a 2×2-matrix

$$\boldsymbol{F}_j\big(\eta, \Delta^2, \mu_{\mathrm{F}}^2\big) = \sum_{m=0}^{j} {}^{\sigma}\boldsymbol{\mathcal{E}}_{jm}(\mu_{\mathrm{F}}, \mu_0; \eta) \boldsymbol{F}_m\big(\eta, \Delta^2, \mu_0^2\big) \,. \tag{4.206}$$

To include the evolution operator in the Mellin-Barnes representation, we go back to the representation as an infinite sum over integer moments. Schematically, inserting the non-sinlget GPD evolution (4.205) into (4.198) ommitting the unimportant terms, we have

$$\begin{aligned}
&\sum_{j=0}^{\infty} \xi^{-j-1}\ {}^{\sigma}T_j\Big(\tfrac{\mathcal{Q}^2}{\mu_{\rm F}^2}\Big)\ F_j^A\big(\xi,\Delta^2,\mu_{\rm F}^2\big) \\
&= \sum_{j=0}^{\infty} \xi^{-j-1}\ {}^{\sigma}T_j\Big(\tfrac{\mathcal{Q}^2}{\mu_{\rm F}^2}\Big)\ \sum_{m=0}^{j} {}^{\sigma}\mathcal{E}_{jm}\big(\mu_{\rm F},\mu_0;\xi\big)\ F_m^A\big(\xi,\Delta^2,\mu_0^2\big) \\
&= \sum_{m=0}^{\infty}\sum_{j=m}^{\infty} \xi^{-j-1}\ {}^{\sigma}T_j\ {}^{\sigma}\mathcal{E}_{jm}\big(\ldots;\xi\big)\ F_m^A \\
&= \sum_{j=0}^{\infty} \xi^{-j-1} \left[\sum_{m=j}^{\infty} {}^{\sigma}T_m\ {}^{\sigma}\mathcal{E}_{mj}\big(\ldots;\xi=1\big)\right] F_j^A \\
&= \sum_{j=0}^{\infty} \xi^{-j-1} \left[\sum_{\substack{m=0\\ \text{even}}}^{\infty} {}^{\sigma}T_{j+m}\Big(\tfrac{\mathcal{Q}^2}{\mu_{\rm F}^2}\Big)\ {}^{\sigma}\mathcal{E}_{j+m,j}\big(\mu_{\rm F},\mu_0;\xi=1\big)\right] F_j^A\big(\xi,\Delta^2,\mu_0^2\big)\ ,
\end{aligned} \tag{4.207}$$

where we interchanged the indices $j \leftrightarrow m$ and applied the shift $m \to j+m$. Independent of the signature, the second sum is restricted to even moments m. Moreover, we define the convolution of the hard scattering amplitude and the evolution operator as

$${}^{\sigma}T_j^{\rm I}\big(\mathcal{Q}^2,\mathcal{Q}_0^2\big) = {}^{\sigma}T_{j+m}^{\rm I}\Big(\alpha_{\rm s}(\mu_{\rm R}),\tfrac{\mathcal{Q}^2}{\mu_{\rm F}^2}\Big) \overset{m}{\underset{\text{even}}{\oplus}} {}^{\sigma}\mathcal{E}_{j+m,j}\big(\mu_{\rm F},\mathcal{Q}_0\big)\ , \tag{4.208}$$

where we utilized the abbreviation

$$\overset{m}{\oplus} \equiv \sum_{m=0}^{\infty}\ . \tag{4.209}$$

In the convolution above, it is convenient to seperate the diagonal and non-diagonal parts of the evolution operator and represent the remaining summation over even m as Mellin-Barnes integral [KMPK08]:

$$\begin{aligned}
{}^{\sigma}T_j^{\rm I}\big(\mathcal{Q}^2,\mathcal{Q}_0^2\big) &= \sum_{m=0}^{\infty} {}^{\sigma}T_{j+m}^{\rm I}\ {}^{\sigma}\mathcal{E}_{j+m,j} = {}^{\sigma}T_j^{\rm I}\ {}^{\sigma}\mathcal{E}_{jj} + \sum_{m=0}^{\infty} {}^{\sigma}T_{j+m+2}^{\rm I}\ {}^{\sigma}\mathcal{E}_{j+m+2,j} \\
&= {}^{\sigma}T_j^{\rm I}\ {}^{\sigma}\mathcal{E}_{jj} - \frac{1}{4i}\int_{d-i\infty}^{d+i\infty} {\rm d}m\ \cot\Big(\frac{\pi m}{2}\Big)\ {}^{\sigma}T_{j+m+2}^{\rm I}\ {}^{\sigma}\mathcal{E}_{j+m+2,j}\ .
\end{aligned} \tag{4.210}$$

Since the only residue of $\cot(\pi m/2)$ is $2/\pi$ for even integer values of m, we chose $-2<d<0$. The convolution of the hard scattering amplitude and the evolution operator in the singlet follows along the same lines. The result yields

$$\boldsymbol{T}_j^{\rm I}\big(\mathcal{Q}^2,\mathcal{Q}_0^2\big) = \boldsymbol{T}_{j+m}^{\rm I}\Big(\alpha_{\rm s}(\mu_{\rm R}),\tfrac{\mathcal{Q}^2}{\mu_{\rm F}^2}\Big) \overset{m}{\underset{\text{even}}{\oplus}} {}^{\sigma}\boldsymbol{\mathcal{E}}_{j+m,j}\big(\mu_{\rm F},\mathcal{Q}_0\big)\ . \tag{4.211}$$

The remaining sum over j can be written as a Mellin-Barnes integral as well. Finally, the non-singlet and singlet CFFs including the evolution operator are given by

$$\begin{aligned}\mathcal{F}^{A}(\xi,\Delta^2,\mathcal{Q}^2) &= \frac{1}{2i}\int_{c-i\infty}^{c+i\infty} \mathrm{d}j\, \xi^{-j-1}\left[i\pm\begin{Bmatrix}\tan\\ \cot\end{Bmatrix}\left(\frac{\pi j}{2}\right)\right] {}^{\sigma}T_j^{\mathrm{I}}(\mathcal{Q}^2,\mathcal{Q}_0^2)\, F_j^{A}(\xi,\Delta^2,\mathcal{Q}_0^2)\,,\\ \mathcal{F}^{\mathrm{S}}(\xi,\Delta^2,\mathcal{Q}^2) &= \frac{1}{2i}\int_{c-i\infty}^{c+i\infty} \mathrm{d}j\, \xi^{-j-1}\left[i\pm\begin{Bmatrix}\tan\\ \cot\end{Bmatrix}\left(\frac{\pi j}{2}\right)\right] \boldsymbol{T}_j^{\mathrm{I}}(\mathcal{Q}^2,\mathcal{Q}_0^2)\, \boldsymbol{F}_j(\xi,\Delta^2,\mathcal{Q}_0^2)\,. \end{aligned} \tag{4.212}$$

This is the final form of the CFFs which is used in the data analysis later in this thesis. To simplify the notation, we introduce the abbreviation

$$\begin{bmatrix}\tan\\ \cot\end{bmatrix} \equiv \left[i\pm\begin{Bmatrix}\tan\\ \cot\end{Bmatrix}\left(\frac{\pi j}{2}\right)\right]\,. \tag{4.213}$$

4.5.3. Transition form factor

Following the considerations in the previous section, we now derive the Mellin-Barnes representation of TFFs. The additional complication stems from the treatment of the DA. The quark and gluon TFFs are defined in Sec. 3.3.4. They read in the momentum fraction representation

$$\begin{aligned}\mathcal{F}^{q(\pm)}(\xi,\Delta^2,\mathcal{Q}^2) &= \frac{fC_{\mathrm{F}}}{\mathcal{Q}N_{\mathrm{c}}}\,\varphi(v)\overset{v}{\otimes} {}^{\mathrm{q}}T\left(\tfrac{\xi+x}{2\xi},v\middle|\tfrac{\mathcal{Q}^2}{\mu_{\mathrm{F}}^2},\tfrac{\mathcal{Q}^2}{\mu_{\varphi}^2},\tfrac{\mathcal{Q}^2}{\mu_{\mathrm{R}}^2}\right)\overset{x}{\otimes} F^{q(\pm)}(x,\eta,\Delta^2,\mu_{\mathrm{F}}^2)\,,\\ \mathcal{F}^{\mathrm{G}}\ (\xi,\Delta^2,\mathcal{Q}^2) &= \frac{fC_{\mathrm{F}}}{\mathcal{Q}N_{\mathrm{c}}}\,\varphi(v)\overset{v}{\otimes}\frac{1}{C_{\mathrm{F}}\xi}{}^{\mathrm{G}}T\left(\tfrac{\xi+x}{2\xi},v\middle|\tfrac{\mathcal{Q}^2}{\mu_{\mathrm{F}}^2},\tfrac{\mathcal{Q}^2}{\mu_{\varphi}^2},\tfrac{\mathcal{Q}^2}{\mu_{\mathrm{R}}^2}\right)\overset{x}{\otimes} F^{\mathrm{G}}\ (x,\eta,\Delta^2,\mu_{\mathrm{F}}^2)\,, \end{aligned} \tag{4.214}$$

where we suppressed the dependence of the hard scattering amplitudes on the strong coupling for brevity. The conformal partial wave expansion of the DA was introduced in Sec. 4.4.1, Eq. 4.95:

$$\varphi(v) = 6v\bar{v}\sum_{\substack{k=0\\ \text{even}}}^{\infty} C_k^{3/2}(2v-1)\,\varphi_n\,, \qquad \varphi_0 = 1\,.$$

Together with the CPWE of the GPD we can introduce the conformal moments of the hard scattering amplitudes analogously to (4.181) for CFFs. Thus, the quark and gluon TFFs as an infinite sum over the conformal moments of the GPD and DA reads

$$\begin{aligned}\mathcal{F}^{q(\pm)}(\xi,\Delta^2,\mathcal{Q}^2) &= \frac{fC_{\mathrm{F}}}{\mathcal{Q}N_{\mathrm{c}}}\sum_{n,k=0}^{\infty}\xi^{-n-1}\,\varphi_k(\mu_{\varphi}^2)\ {}^{\mathrm{q}}T_{nk}\left(\tfrac{\mathcal{Q}^2}{\mu_{\mathrm{F}}^2},\tfrac{\mathcal{Q}^2}{\mu_{\varphi}^2},\tfrac{\mathcal{Q}^2}{\mu_{\mathrm{R}}^2}\right)F_n^{q(\pm)}(\xi,\Delta^2,\mu_{\mathrm{F}}^2)\,,\\ \mathcal{F}^{\mathrm{G}}\ (\xi,\Delta^2,\mathcal{Q}^2) &= \frac{f}{\mathcal{Q}N_{\mathrm{c}}}\sum_{n,k=0}^{\infty}\xi^{-n-1}\,\varphi_k(\mu_{\varphi}^2)\ {}^{\mathrm{G}}T_{nk}\left(\tfrac{\mathcal{Q}^2}{\mu_{\mathrm{F}}^2},\tfrac{\mathcal{Q}^2}{\mu_{\varphi}^2},\tfrac{\mathcal{Q}^2}{\mu_{\mathrm{R}}^2}\right)\ F_n^{\mathrm{G}}(\xi,\Delta^2,\mu_{\mathrm{F}}^2)\,, \end{aligned} \tag{4.215}$$

where the sum over the conformal moments of the DA runs over even k for the vector meson DAs in Tab. 3.2. The index n is either even or odd, depending on the symmetry of the GPD. Table 4.2 shows the correct symmetry for the occurring GPDs. The integer conformal

GPD	C	σ	moments	MBR
$H^{q(C)}$, $E^{q(C)}$	+	+	odd	tan
	−	−	even	cot
H^{G},E^{G}	+	+	odd	tan
$\widetilde{H}^{q(C)}$, $\widetilde{E}^{q(C)}$	+	−	even	cot
	−	+	even	tan
$\widetilde{H}^{\mathrm{G}}$,$\widetilde{E}^{\mathrm{G}}$	−	−	odd	cot

Table 4.2.: Charge parity and signature for all occurring GPDs for DVMP. We also include the correct term in the Mellin-Barnes representation (MBR).

moments of the hard scattering amplitudes are defined in terms of the variable u analogously to (4.184) as

$$
\begin{aligned}
{}^{\mathrm{q}}T_{nk} &= \frac{2^{n+1}\Gamma\left(n+\frac{5}{2}\right)}{\Gamma\left(\frac{3}{2}\right)\Gamma(n+3)} \cdot 3 \cdot \ 2\ u\bar{u} \quad C_n^{3/2}(2u-1) \overset{u}{\otimes} {}^{\mathrm{q}}T(u,v) \overset{v}{\otimes} 2v\bar{v}\, C_k^{3/2}(2v-1)\,, \\
{}^{\mathrm{G}}T_{nk} &= \frac{2^{n+2}\Gamma\left(n+\frac{5}{2}\right)}{\Gamma\left(\frac{3}{2}\right)\Gamma(n+4)} \cdot 3 \cdot 12(u\bar{u})^2\, C_{n-1}^{5/2}(2u-1) \overset{u}{\otimes} {}^{\mathrm{G}}T(u,v) \overset{v}{\otimes} 2v\bar{v}\, C_k^{3/2}(2v-1)\,.
\end{aligned}
\tag{4.216}
$$

The factor 3 stems from the different normalization of the DA, cf. Eq. 4.95. Furthermore, the moments are already written in a way that is suitable for the introduction of the auxiliary polynomials (4.185). Hence, the auxiliary conformal moments are given by

$$
{}^{\mathrm{q}}c_{nk} = \hat{p}_n^{3/2}(u) \overset{u}{\otimes} {}^{\mathrm{q}}T(u,v) \overset{v}{\otimes} \hat{p}_n^{3/2}(v)\,, \qquad {}^{\mathrm{G}}c_{nk} = \hat{p}_n^{5/2}(u) \overset{u}{\otimes} {}^{\mathrm{G}}T(u,v) \overset{v}{\otimes} \hat{p}_n^{3/2}(v)\,. \tag{4.217}
$$

Employing the auxiliary conformal moments above, the conformal moments of the hard scattering amplitude read

$$
{}^{\mathrm{q}}T_{nk} = \frac{2^{n+1}\Gamma\left(n+\frac{5}{2}\right)}{\Gamma\left(\frac{3}{2}\right)\Gamma(n+3)} \cdot 3 \cdot {}^{\mathrm{q}}c_{nk}\,, \qquad {}^{\mathrm{G}}T_{nk} = \frac{2^{n+2}\Gamma\left(n+\frac{5}{2}\right)}{\Gamma\left(\frac{3}{2}\right)\Gamma(n+4)} \cdot 3 \cdot {}^{\mathrm{G}}c_{nk}\,. \tag{4.218}
$$

As in case of the CFFs, our goal is the Mellin-Barnes representation of TFFs. Therefore, we have to find the analytic continuation of the conformal moments above. To this end, we introduce a signature as in the previous section. Such a symbol is unavoidable, because TFFs with even and odd intrinsic parity contribute. Furthermore, the hard scattering amplitudes for vector and pseudoscalar mesons are not labeled by a distinctive index. The only difference between the mesons is the composition of TFFs, see Tab. 3.2 for a collection of mesons and the contributing TFFs/GPDs.
In analogy to the Mellin-Barnes representation of CFFs, the introduction of a signature in the flavor non-singlet allows the analytic continuation $n \to j$ of even and odd conformal moments separately. The corresponding signature of the occurring GPDs for DVMP is given in Tab. 4.2. As for the Wilson coefficients of DVCS, we introduce the signature by the replacement

$$
{}^{\mathrm{q}}T_{nk} \to {}^{\sigma}T_{nk}\,. \tag{4.219}
$$

Hence, the quark TFFs read

$$\mathcal{F}^{q(\pm)}(\xi,\Delta^2,\mathcal{Q}^2) = \frac{fC_\mathrm{F}}{\mathcal{Q}N_\mathrm{c}} \sum_{n,k=0}^{\infty} \xi^{-n-1}\, \varphi_k(\mu_\varphi^2)\; {}^{\sigma}T_{nk}\, F_n^{q(\pm)}\left(\xi,\Delta^2,\mu_\mathrm{F}^2\right) , \tag{4.220}$$

where the conformal moments of the DA are always even for the DAs considered in this thesis. Under the assumption that we found the unique analytic continuation from integer moments n to complex valued j, the Mellin-Barnes representation of the quark TFFs utilizing (4.199) reads

$$\mathcal{F}^{q(\pm)}(\xi,\Delta^2,\mathcal{Q}^2) = \frac{fC_\mathrm{F}}{\mathcal{Q}N_\mathrm{c}} \frac{1}{2i} \int_c \mathrm{d}j\, \xi^{-j-1} \begin{bmatrix}\tan\\ \cot\end{bmatrix} \varphi_k(\mu_\varphi^2) \underset{\text{even}}{\overset{k}{\oplus}} {}^{\sigma}T_{jk}\, F_j^{q(\pm)}(\xi,\Delta^2,\mu_\mathrm{F}^2) , \tag{4.221}$$

where we suppressed the scale dependence of Wilson coefficients for brevity. The corresponding signature is given in Tab. 4.2. For clarity, we present all possibilities for the TFFs $\mathcal{H}$ and $\widetilde{\mathcal{H}}$

$$\begin{aligned}
\mathcal{H}^{q(+)}(\xi,\Delta^2,\mathcal{Q}^2) &= \frac{fC_\mathrm{F}}{\mathcal{Q}N_\mathrm{c}} \frac{1}{2i} \int_c \mathrm{d}j\, \xi^{-j-1}\, [\tan]\, \varphi_k(\mu_\varphi^2) \overset{k}{\otimes} {}^{+}T_{jk}\left(\tfrac{\mathcal{Q}^2}{\mu_\mathrm{F}^2},\tfrac{\mathcal{Q}^2}{\mu_\varphi^2},\tfrac{\mathcal{Q}^2}{\mu_\mathrm{R}^2}\right) H_j^{q(+)}(\xi,\Delta^2,\mu_\mathrm{F}^2) ,\\
\mathcal{H}^{q(-)}(\xi,\Delta^2,\mathcal{Q}^2) &= \frac{fC_\mathrm{F}}{\mathcal{Q}N_\mathrm{c}} \frac{1}{2i} \int_c \mathrm{d}j\, \xi^{-j-1}\, [\cot]\, \varphi_k(\mu_\varphi^2) \overset{k}{\otimes} {}^{-}T_{jk}\left(\tfrac{\mathcal{Q}^2}{\mu_\mathrm{F}^2},\tfrac{\mathcal{Q}^2}{\mu_\varphi^2},\tfrac{\mathcal{Q}^2}{\mu_\mathrm{R}^2}\right) H_j^{q(-)}(\xi,\Delta^2,\mu_\mathrm{F}^2) ,\\
\widetilde{\mathcal{H}}^{q(+)}(\xi,\Delta^2,\mathcal{Q}^2) &= \frac{fC_\mathrm{F}}{\mathcal{Q}N_\mathrm{c}} \frac{1}{2i} \int_c \mathrm{d}j\, \xi^{-j-1}\, [\cot]\, \varphi_k(\mu_\varphi^2) \overset{k}{\otimes} {}^{-}T_{jk}\left(\tfrac{\mathcal{Q}^2}{\mu_\mathrm{F}^2},\tfrac{\mathcal{Q}^2}{\mu_\varphi^2},\tfrac{\mathcal{Q}^2}{\mu_\mathrm{R}^2}\right) H_j^{q(+)}(\xi,\Delta^2,\mu_\mathrm{F}^2) ,\\
\widetilde{\mathcal{H}}^{q(-)}(\xi,\Delta^2,\mathcal{Q}^2) &= \frac{fC_\mathrm{F}}{\mathcal{Q}N_\mathrm{c}} \frac{1}{2i} \int_c \mathrm{d}j\, \xi^{-j-1}\, [\tan]\, \varphi_k(\mu_\varphi^2) \overset{k}{\otimes} {}^{+}T_{jk}\left(\tfrac{\mathcal{Q}^2}{\mu_\mathrm{F}^2},\tfrac{\mathcal{Q}^2}{\mu_\varphi^2},\tfrac{\mathcal{Q}^2}{\mu_\mathrm{R}^2}\right) H_j^{q(-)}(\xi,\Delta^2,\mu_\mathrm{F}^2) .
\end{aligned}$$

Furthermore, the respective expressions for the TFFs $\mathcal{E}$ and $\widetilde{\mathcal{E}}$ follow by the replacement $\{\mathcal{H},H\}\to\{\mathcal{E},E\}$ in the vector and axial-vector case, respectively.
At this point, we are able to include the evolution of the DA and GPD. Let us switch to the evolution basis like in the momentum fraction representation in Sec. 3.3.4.2:

$$\mathcal{F}_M = \sum_A \hat{c}_M^A\, \mathcal{F}_M^A , \qquad A \in \{0^{(\pm)}, 3^{(\pm)}, 8^{(\pm)}, 15^{(\pm)}, \mathrm{pS}, \mathrm{G}\} . \tag{4.222}$$

Since only the TFFs with even intrinsic parity mix with the gluon TFF, the non-singlet contribution consists of the TFFs

$$A \in \{q^{(-)}, 3^{(+)}, 8^{(+)}, 15^{(+)}\} . \tag{4.223}$$

The Mellin-Barnes representation of the non-singlet TFFs above reads

$$\mathcal{F}^{A}(\xi,\Delta^2,\mathcal{Q}^2) = \frac{fC_\mathrm{F}}{\mathcal{Q}N_\mathrm{c}} \frac{1}{2i} \int_c \mathrm{d}j\, \xi^{-j-1} \begin{bmatrix}\tan\\ \cot\end{bmatrix} \varphi_k(\mu_\varphi^2) \overset{k}{\oplus} {}^{\sigma}T_{jk}\left(\tfrac{\mathcal{Q}^2}{\mu_\mathrm{F}^2},\tfrac{\mathcal{Q}^2}{\mu_\varphi^2},\tfrac{\mathcal{Q}^2}{\mu_\mathrm{R}^2}\right) F_j^{A}(\xi,\Delta^2,\mu_\mathrm{F}^2) , \tag{4.224}$$

where correct signature is given in Tab. 4.2.
As we have seen in Sec. 3.3.1, e.g., Tab. 3.2, only the neutral vector mesons incorporate a contribution of the gluon GPD. Therefore, we define the singlet TFF exclusively for the TFFs $\mathcal{H}^{q(+)}$ and $\mathcal{E}^{q(+)}$ possessing a definite signature (Tab. 4.2). We summarize the conformal

moment of the singlet GPD and the gluon GPD in the vector $\boldsymbol{F}_j(\eta,\Delta^2)$ (4.141). The Wilson coefficients were defined in (4.218) by

$$ {}^{\mathrm{q}}T_{nk} = \frac{2^{n+1}\Gamma\left(n+\frac{5}{2}\right)}{\Gamma\left(\frac{3}{2}\right)\Gamma(n+3)} \cdot 3 \cdot {}^{\mathrm{q}}c_{nk}\,, \qquad {}^{\mathrm{G}}T_{nk} = \frac{2^{n+2}\Gamma\left(n+\frac{5}{2}\right)}{\Gamma\left(\frac{3}{2}\right)\Gamma(n+4)} \cdot 3 \cdot {}^{\mathrm{G}}c_{nk}\,. $$

Pulling out the common prefactor, we define a row vector analogously to the momentum fraction representation (3.256) as

$$ \boldsymbol{T}_{jk} = \frac{2^{n+1}\Gamma\left(n+\frac{5}{2}\right)}{\Gamma\left(\frac{3}{2}\right)\Gamma(n+3)} \cdot 3 \cdot \left(\tfrac{1}{N_{\mathrm{f}}}\, {}^{+}c_{jk} + {}^{\mathrm{pS}}c_{jk} \qquad \tfrac{1}{C_{\mathrm{F}}}\tfrac{2}{j+3}\, {}^{\mathrm{G}}c_{jk} \right) . \tag{4.225} $$

As already argued, the signature is uniquely defined in the singlet sector. Therefore, the Mellin-Barnes representation of the singlet TFF for neutral vector mesons becomes

$$ \mathcal{F}^{\mathrm{S}}_{\mathrm{V}^0}(\xi,\Delta^2,\mathcal{Q}^2) = \frac{C_{\mathrm{F}} f_{\mathrm{V}^0}}{N_{\mathrm{c}}\mathcal{Q}} \frac{1}{2i} \int_c \mathrm{d}j\, \xi^{-j-1} \begin{bmatrix} \tan \\ \cot \end{bmatrix} \varphi_k(\mu_\varphi^2) \bigoplus_{\text{even}}^{k} \boldsymbol{T}_{jk}\, \boldsymbol{F}_j(x,\xi,\Delta^2,\mu_{\mathrm{F}}^2)\,. \tag{4.226} $$

For mesons without a gluon contribution, we directly employ the Mellin-Barnes representation (4.224) with the non-singlet evolution operator. We neglected the dependence on the factorization scales and the renormalization scale. The full form in (4.226) actually reads

$$ \varphi_k(\mu_\varphi^2) \bigoplus_{\text{even}}^{k} \boldsymbol{T}_{jk}\left(\alpha_{\mathrm{s}}(\mu_{\mathrm{R}}), \tfrac{\mathcal{Q}^2}{\mu_{\mathrm{F}}^2}, \tfrac{\mathcal{Q}^2}{\mu_\varphi^2}, \tfrac{\mathcal{Q}^2}{\mu_{\mathrm{R}}^2}\right) \boldsymbol{F}_j(x,\xi,\Delta^2,\mu_{\mathrm{F}}^2)\,. \tag{4.227} $$

As we determined the Mellin-Barnes representations of the non-singlet and singlet GPD, we are ready to include the evolution of the GPD and DA. In addition to the evolution of CFFs, we also have to consider the DA, which is evolved by the non-singlet evolution operator (D.15)[6]:

$$ \varphi_k(\mu_\varphi^2) = \sum_{l=0}^{k} \mathcal{E}_{kl}(\mu_\varphi,\mu_0)\varphi_l(\mu_0^2)\,, \tag{4.228} $$

where a signature is not necessary, since the conformal moments of the DAs in this thesis are even. Analogously to the cases before, we achieve the inclusion of the evolution operator by going back to the representation of the TFFs through infinite sums over the conformal moments of the GPD and DA (4.215). Schematically, the non-singlet TFFs ($A\in\{\mathrm{NS}^{(+)}, q^{(-)}\}$) become[7]

$$ \begin{aligned} &\sum_{j,k=0}^{\infty} \xi^{-j-1}\, \varphi_l(\mu_\varphi^2)\, {}^{\sigma}T_{jk}\left(\alpha_{\mathrm{s}}(\mu_{\mathrm{R}}), \tfrac{\mathcal{Q}^2}{\mu_{\mathrm{F}}^2}, \tfrac{\mathcal{Q}^2}{\mu_\varphi^2}, \tfrac{\mathcal{Q}^2}{\mu_{\mathrm{R}}^2}\right) F_j^A(\xi,\Delta^2,\mu_{\mathrm{F}}^2) \\ &= \sum_{j=0}^{\infty} \sum_{\substack{k=0 \\ \text{even}}}^{\infty} \sum_{m=0}^{j} \sum_{l=0}^{k} \xi^{-j-1}\, \varphi_l(\mu_\varphi^2)\; \mathcal{E}_{kl}(\mu_\varphi,\mu_0)\; {}^{\sigma}T_{jk}\; {}^{\sigma}\mathcal{E}_{jm}(\mu_{\mathrm{F}},\mu_0;\xi)\, F_m^A(\xi,\Delta^2,\mu_{\mathrm{F}}^2) \\ &= \sum_{j=0}^{\infty} \sum_{\substack{k=0 \\ \text{even}}}^{\infty} \sum_{m,l=0}^{\infty} \xi^{-j-1}\, \varphi_k(\mu_\varphi^2)\; E_{k+l,k}(\mu_\varphi,\mu_0;1)\; {}^{\sigma}T_{j+m,k+l}\; {}^{\sigma}E_{j+m,j}(\mu_{\mathrm{F}},\mu_0)\; F_j^A(\xi,\Delta^2,\mu_{\mathrm{F}}^2)\,. \end{aligned} \tag{4.229} $$

[6] We set $\eta = 1$.
[7] For CFFs see (4.207).

The convolution of the hard scattering amplitude and the two evolution operators is in the case of TFFs defined as

$$ {}^{\sigma}T_{jk}\left(\mathcal{Q}^2,\mathcal{Q}_0^2\right)=\sum_{m,l=0}^{\infty}\mathcal{E}_{k+l,k}\left(\mu_\varphi,\mathcal{Q}_0\right){}^{\sigma}T_{j+m,k+l}\left(\alpha_{\mathrm{s}}(\mu_{\mathrm{R}}),\tfrac{\mathcal{Q}^2}{\mu_{\mathrm{F}}^2},\tfrac{\mathcal{Q}^2}{\mu_\varphi^2},\tfrac{\mathcal{Q}^2}{\mu_{\mathrm{R}}^2}\right){}^{\sigma}\mathcal{E}_{j+m,j}\left(\mu_{\mathrm{F}},\mathcal{Q}_0\right). \quad (4.230) $$

As in DVCS (4.210), the remaining summations over l and m can be written in terms of a Mellin-Barnes integral. Including the evolution, the non-singlet TFFs (4.224) become

$$ \mathcal{F}^A\left(\xi,\Delta^2,\mathcal{Q}^2\right)=\frac{fC_{\mathrm{F}}}{\mathcal{Q}N_{\mathrm{c}}}\frac{1}{2i}\int_c \mathrm{d}j\,\xi^{-j-1}\begin{bmatrix}\tan\\ \cot\end{bmatrix}\varphi_k\left(\mathcal{Q}_0^2\right)\bigoplus_{\text{even}}^{k}{}^{\sigma}T_{jk}\left(\mathcal{Q}^2,\mathcal{Q}_0^2\right)F_j^A\left(\xi,\Delta^2,\mathcal{Q}_0^2\right). \quad (4.231) $$

In case of an asymptotic distribution amplitude $\varphi_{n>0}=0$ only the diagonal part of the evolution operator contributes and the convolution of the hard scattering amplitude and the evolution operators (4.230) simplifies to

$$ {}^{\sigma}T_{j0}\left(\mathcal{Q}^2,\mathcal{Q}_0^2\right)=\sum_{m=0}^{\infty}\mathcal{E}_{0,0}\left(\mu_\varphi,\mathcal{Q}_0\right){}^{\sigma}T_{j+m,0}\left(\alpha_{\mathrm{s}}(\mu_{\mathrm{R}}),\tfrac{\mathcal{Q}^2}{\mu_{\mathrm{F}}^2},\tfrac{\mathcal{Q}^2}{\mu_\varphi^2},\tfrac{\mathcal{Q}^2}{\mu_{\mathrm{R}}^2}\right){}^{\sigma}\mathcal{E}_{j+m,j}\left(\mu_{\mathrm{F}},\mathcal{Q}_0\right). \quad (4.232) $$

Moreover, the LO and NLO evolution operator of the DA is given by

$$ \mathcal{E}_{0,0}^{(0)}(\mu_\varphi,\mu_0)=1\,,\qquad \mathcal{E}_{0,0}^{(1)}(\mu_\varphi,\mu_0)=\frac{1}{\beta_0}\left[\frac{\beta_1}{\beta_0}{}^{\mathrm{NS}}\gamma_0^{(0)}-{}^{\mathrm{NS}}\gamma_0^{(1)}\right]. \quad (4.233) $$

The most suitable form for a DA with a finite number of conformal moments is easily obtained from the previous equations. From the considerations in the non-singlet sector, the convolution of the Wilson coefficients and the evolution operators in the singlet sector reads

$$ \boldsymbol{T}_{jk}\left(\mathcal{Q}^2,\mathcal{Q}_0^2\right)=\sum_{m,l=0}^{\infty}E_{k+l,k}\left(\mu_\varphi,\mathcal{Q}_0\right)\boldsymbol{T}_{j+m,k+l}\left(\alpha_{\mathrm{s}}(\mu_{\mathrm{R}}),\tfrac{\mathcal{Q}^2}{\mu_{\mathrm{F}}^2},\tfrac{\mathcal{Q}^2}{\mu_\varphi^2},\tfrac{\mathcal{Q}^2}{\mu_{\mathrm{R}}^2}\right)\boldsymbol{\mathcal{E}}_{j+m,j}\left(\mu_{\mathrm{F}},\mathcal{Q}_0\right), \quad (4.234) $$

where we dispense with the signature factor in the singlet case, because it is uniquely defined. The corresponding singlet TFF becomes

$$ \mathcal{F}_{\mathrm{V}^0}^{\mathrm{S}}\left(\xi,\Delta^2,\mathcal{Q}^2\right)=\frac{C_{\mathrm{F}}f_{\mathrm{V}^0}}{N_{\mathrm{c}}\mathcal{Q}}\frac{1}{2i}\int_c \mathrm{d}j\,\xi^{-j-1}\begin{bmatrix}\tan\\ \cot\end{bmatrix}\varphi_k\left(\mathcal{Q}_0^2\right)\bigoplus_{\text{even}}^{k}\boldsymbol{T}_{jk}\left(\mathcal{Q}^2,\mathcal{Q}_0^2\right)\boldsymbol{F}_j\left(\xi,\Delta^2,\mathcal{Q}_0^2\right). \quad (4.235) $$

4.6. Conformal moments of hard scattering amplitudes

In the last section we derived the Mellin-Barnes representation of CFFs and TFFs under the premise that we know the analytic continuation for the conformal moments of the hard scattering amplitudes from integer n to complex j. In [MLPKS14] a novel method for the calculation of continuable conformal moments was introduced, based on the imaginary part ensuring the correct analytic continuation. We will outline the method in the following.

Suppose, we want to derive the conformal moments of a function $G(u)$, which only has a pole at $u=1$ and/or a cut in $[1,\infty]$. For example, we consider functions like

$$G(u)=\frac{1}{\bar{u}}\,,\qquad G(u)=\frac{\ln\bar{u}}{\bar{u}}\,,\qquad G(u)=\frac{\ln\bar{u}}{u}\,.$$

This type of functions are the only ones occurring in the NLO corrections of DVMP, since functions with a cut in $[-\infty,0]$ can be mapped by the transformation $u\to\bar{u}$ introducing an appropriate signature. Applying the auxiliary polynomials (4.185), we define the notation for conformal moments with arbitrary index λ

$$\big\langle G(u)\big\rangle_n^\lambda = G(u)\overset{u}{\otimes}\hat{p}_n^\lambda(u)\,. \tag{4.236}$$

In order to treat the cases $\lambda=3/2$ and $\lambda=5/2$ simultaneously, we utilize the general normalization (4.187) and define

$$\big\langle\!\big\langle G(u)\big\rangle\!\big\rangle_n^\lambda = \frac{2^{2\lambda-1}\Gamma(\lambda)}{\Gamma\big(\frac{1}{2}\big)\,\Gamma\big(\lambda-\frac{1}{2}\big)}\int_0^1 \mathrm{d}u\; G(u)\,(u\bar{u})^{\lambda-\frac{1}{2}}C_n^\lambda(2u-1)\,. \tag{4.237}$$

Note, we introduced the double bracket notation to indicate, that for gluons ($\lambda=5/2$) we have to apply the shift $n\to n-1$. Hence,

$$\big\langle G(u)\big\rangle_n^{3/2}=\big\langle\!\big\langle G(u)\big\rangle\!\big\rangle_n^{3/2}\,,\qquad \big\langle G(u)\big\rangle_n^{5/2}=\big\langle\!\big\langle G(u)\big\rangle\!\big\rangle_{n-1}^{5/2}\,. \tag{4.238}$$

For the Mellin-Barnes integral, we require the analytic continuation of the integer conformal moments to complex valued ones $k\to j$ in such a way, that they are bounded in the limit $j\to\infty$. Moreover, the uniqueness is ensured by Carlson's theorem [Car14]. Using the Cauchy formula we write the function $G(u)$ in terms of its imaginary part as

$$G(u)=\frac{1}{\pi}\int_1^\infty \mathrm{d}u'\;\frac{\Im\mathrm{m}\,G(u')}{u'-u}\,. \tag{4.239}$$

To NLO accuracy, there are no subtractions needed as can be checked explicitly. We change the integration limits by using the transformation $u'=1/y$. Therefore,

$$G(u)=\frac{1}{\pi}\int_0^1 \frac{\mathrm{d}y}{y}\,\frac{\Im\mathrm{m}\,G(1/y)}{1-uy}\,. \tag{4.240}$$

In order to obtain the conformal moments (4.237), we have to perform the convolution with the auxiliary polynomial. Employing the Rodrigues formula for Gegenbauer polynomials (C.13), we get

$$\big\langle\!\big\langle G(u)\big\rangle\!\big\rangle_n^\lambda = \frac{(-1)^n}{\Gamma(n+1)}\,\frac{1}{\mathrm{B}\big(n+\lambda+\frac{1}{2},\lambda-\frac{1}{2}\big)}\,\frac{1}{\pi}\int_0^1\mathrm{d}u\left[\frac{\mathrm{d}^n}{\mathrm{d}u^n}(u\bar{u})^{n+\lambda-\frac{1}{2}}\right]\int_0^1\frac{\mathrm{d}y}{y}\,\frac{\Im\mathrm{m}\,G(1/y)}{1-uy}\,, \tag{4.241}$$

where the beta function stems from the coefficient of the Rodrigues formula and the normalization coefficient for arbitrary λ (4.187). Since the dependence in u is separated from the

function G altogether, we ensure the correct analytic continuation from integer n to complex j. By partial integration, we obtain

$$\langle\!\langle G(u)\rangle\!\rangle_n^\lambda = \frac{1}{\mathrm{B}\left(n+\lambda+\frac{1}{2},\lambda-\frac{1}{2}\right)}\frac{1}{\pi}\int_0^1 \mathrm{d}u\,(u\bar{u})^{\lambda-\frac{1}{2}}\int_0^1\frac{\mathrm{d}y}{y}\left(\frac{yu\bar{u}}{1-uy}\right)^n \frac{\Im\mathrm{m}\,G(1/y)}{1-uy}\,, \tag{4.242}$$

where we utilized the derivative

$$\frac{\mathrm{d}^n}{\mathrm{d}u^n}\frac{1}{1-uy} = \frac{n!\,y^n}{(1-uy)^{n+1}}\,. \tag{4.243}$$

Consequently, the conformal moments are given by

$$\langle\!\langle G(u)\rangle\!\rangle_j^\lambda = \widetilde{p}_j^\lambda(y)\overset{y}{\otimes}\frac{1}{\pi y}\,\Im\mathrm{m}\,G(1/y)\,, \tag{4.244}$$

where the polynomials $\widetilde{p}_j^\lambda(y)$ are defined by the integral representation

$$\widetilde{p}_j^\lambda(y) = \frac{1}{\mathrm{B}\left(j+\lambda+\frac{1}{2},\lambda-\frac{1}{2}\right)}\,y^j\int_0^1\mathrm{d}u\,\frac{(u\bar{u})^{j+\lambda-\frac{1}{2}}}{(1-uy)^{j+1}}\,. \tag{4.245}$$

The integral is given by a Gauss hypergeometric function (C.19), namely

$$\widetilde{p}_j^\lambda(y) = \frac{\Gamma(j+2\lambda)\,\Gamma\left(j+\lambda+\frac{1}{2}\right)}{\Gamma\left(\lambda-\frac{1}{2}\right)\Gamma(2j+2\lambda+1)}\,y^j\,{}_2F_1\left(\begin{matrix}j+1 & j+\lambda+\frac{1}{2}\\ 2j+2\lambda+1\end{matrix}\,\middle|\,y\right)\,. \tag{4.246}$$

Since the gamma function and the hypergeometric function are analytically continuable, the conformal moments obtained by (4.244) are sufficient for numerical evaluation.
We can make further simplifications by introducing the variable w instead of y

$$w = \frac{yu\bar{u}}{1-uy}\,,\qquad y = \frac{w}{u(\bar{u}+w)}\,,\qquad \frac{\mathrm{d}y}{\mathrm{d}w} = \frac{\bar{u}}{u(\bar{u}+w)^2}\,. \tag{4.247}$$

Hence, the conformal moments become

$$\langle\!\langle G(u)\rangle\!\rangle_j^\lambda = \frac{1}{\mathrm{B}\left(j+\lambda+\frac{1}{2},\lambda-\frac{1}{2}\right)}\frac{1}{\pi}\int_0^1\mathrm{d}u\,(u\bar{u})^{\lambda-\frac{1}{2}}\int_0^u\mathrm{d}w\frac{1}{w}w^j\,\Im\mathrm{m}\,G\left(\frac{u(\bar{u}+w)}{w}\right)\,. \tag{4.248}$$

Interchanging the order of integration, we obtain

$$\langle\!\langle G(u)\rangle\!\rangle_j^\lambda = \frac{1}{\mathrm{B}\left(j+\lambda+\frac{1}{2},\lambda-\frac{1}{2}\right)}\int_0^1\mathrm{d}w\,w^j\int_w^1\mathrm{d}u\,(u\bar{u})^{\lambda-\frac{1}{2}}\frac{1}{w}\frac{1}{\pi}\,\Im\mathrm{m}\,G\left(\frac{u(\bar{u}+w)}{w}\right)\,. \tag{4.249}$$

The result now is written as a Mellin transformation. Note, additionally the transformation $u=u'+w$ is convenient for a analytic derivation

$$\begin{aligned}\langle\!\langle G(u)\rangle\!\rangle_j^\lambda = {}& \frac{1}{\mathrm{B}\left(j+\lambda+\frac{1}{2},\lambda-\frac{1}{2}\right)}\int_0^1\mathrm{d}w\,w^j\\ &\times\int_0^{1-w}\mathrm{d}u'\,\left[(u'+w)(\bar{u}'-w)\right]^{\lambda-\frac{1}{2}}\frac{1}{w}\frac{1}{\pi}\,\Im\mathrm{m}\,G\left(\frac{(u'-w)(\bar{u}'-w)}{w}\right)\,.\end{aligned} \tag{4.250}$$

In the previous two solutions, the conformal moments are given by a common Mellin transformation.
For convenience, we exploit the general structure of the imaginary part of the functions of interest. To this aim, we introduce the variable

$$r = \frac{\xi}{x}\,, \qquad 0 \leq r \leq 1\,, \tag{4.251}$$

which is restricted to this interval, because the imaginary part arises only in the outer region of the GPD, e.g. $u>1$ or $x>\eta$. Moreover, we do not consider the region $x<-\eta$ due to the analytic structure of $G(u)$. Expressing the variables u and $y=1/u$ by r, we have

$$u = \frac{\xi+x}{2\xi} = \frac{x}{2\xi}\left(\frac{\xi}{x}+1\right) = \frac{r+1}{2r}\,, \qquad r = \frac{1}{2\frac{1}{y}-1} = \frac{y}{2-y}\,. \tag{4.252}$$

Typically, the involved imaginary parts look in terms of the variables u, y and r as

$$\begin{aligned} \Im\mathrm{m}\,\frac{1}{\bar{u}} &= \pi\delta(\bar{u}) = \pi y\,\delta(y-1) = 2\pi r\,\delta(1-r)\,, \\ \Im\mathrm{m}\,\frac{\ln\bar{u}}{u} &= -\pi\frac{\theta(-\bar{u})}{u} = -\pi y\,\theta(1-y) = \frac{2\pi r\,\theta(r)}{r+1}\,. \end{aligned} \tag{4.253}$$

As we will realize later on, all imaginary parts will be accompanied by a factor of $2\pi r$. To simplify the notation, we reformulate (4.244) anticipating the factor in terms of the variable y

$$\langle\!\langle G(u)\rangle\!\rangle_j^\lambda = \tilde{p}_j^\lambda(y) \overset{y}{\otimes} \frac{1}{y}\frac{2y}{2-y}\left[\frac{2-y}{2\pi y}\,\Im\mathrm{m}\,G(1/y)\right]\,. \tag{4.254}$$

In order to simplify the notation of the imaginary part, we express the term in square brackets in terms of r and introduce a new function, namely

$$\frac{2-y}{2\pi y}\,\Im\mathrm{m}\,G(1/y) = \frac{1}{2\pi r}\,\Im\mathrm{m}\,G\left(\frac{r+1}{2r}\right) = g(r)\,. \tag{4.255}$$

Therefore, the conformal moments utilizing the new function become

$$\langle\!\langle G(u)\rangle\!\rangle_j^\lambda = \widetilde{p}_j^\lambda(y) \overset{y}{\otimes} \frac{2\,g\left(\frac{y}{2-y}\right)}{2-y}\,. \tag{4.256}$$

The conformal moments in terms of Mellin moments (4.249) are given by

$$\langle\!\langle G(u)\rangle\!\rangle_j^\lambda = \frac{1}{\mathrm{B}\left(j+\lambda+\frac{1}{2},\lambda-\frac{1}{2}\right)}\int_0^1 \mathrm{d}w\,w^j \int_w^1 \mathrm{d}u\,\frac{2(u\bar{u})^{\lambda-\frac{1}{2}}}{2u\bar{u}+w(u-\bar{u})}\,g\left(\frac{w}{2u\bar{u}+w(u-\bar{u})}\right)\,. \tag{4.257}$$

From the considerations above, the calculation of the conformal moments of the hard scattering amplitude is straight forward. Utilizing (4.244) the auxiliary conformal moments for DVCS and DVMP are for complex j and integer k

$${}^A c_j = \widetilde{p}_j^\lambda(y) \overset{y}{\otimes} \frac{2}{2-y}\,{}^A t\left(\frac{y}{2-y}\right)\,, \tag{4.258}$$

$${}^A c_{jk} = \widetilde{p}_j^\lambda(y) \overset{y}{\otimes} \frac{2}{2-y}\,{}^A t\left(\frac{y}{2-y},v\right) \overset{v}{\oplus} \hat{p}_k^{3/2}(v)\,, \tag{4.259}$$

where $A \in \{+,-,\mathrm{pS},\mathrm{G}\}$. The index λ has to be chosen accordingly. Using the definition (4.255) the imaginary parts of the hard scattering amplitudes developing in the region $\Re\mathrm{e}\, u \geq 1$ are given by

$$ {}^{A}t\left(\frac{\xi}{x}\right) = \frac{x}{2\pi\xi}\,\Im\mathrm{m}\,{}^{A}T\left(\frac{\xi+x-i\epsilon}{2(\xi-i\epsilon)}\right), \quad {}^{A}t\left(\frac{\xi}{x},v\right) = \frac{x}{2\pi\xi}\,\Im\mathrm{m}\,{}^{A}T\left(\frac{\xi+x-i\epsilon}{2(\xi-i\epsilon)},v\right). \tag{4.260}$$

Before introducing the explicit expressions for the conformal moments of the hard scattering amplitudes in DVCS and DVMP, we consider first two examples.
The LO hard scattering amplitude is $1/\bar{u}$. As we already know, its conformal moments will be 1, since they present the normalization condition. The corresponding imaginary part is given by

$$\Im\mathrm{m}\,\frac{1}{\bar{u}} = \pi\,\delta(1-u) = y\pi\,\delta(1-y) = 2\pi r\,\delta(1-r)\,. \tag{4.261}$$

Inserting the imaginary part into (4.242), we obtain

$$\begin{aligned}\langle\!\langle 1/\bar{u}\rangle\!\rangle_k^\lambda &= \frac{1}{\mathrm{B}\big(k+\lambda+\frac{1}{2},\lambda-\frac{1}{2}\big)}\int_0^1 \mathrm{d}u\,(u\bar{u})^{\lambda-\frac{1}{2}}\int_0^1\frac{\mathrm{d}y}{y}\left(\frac{yu\bar{u}}{1-uy}\right)^k\frac{y\,\delta(1-y)}{1-uy}\\ &= \frac{1}{\mathrm{B}\big(k+\lambda+\frac{1}{2},\lambda-\frac{1}{2}\big)}\int_0^1 \mathrm{d}u\,u^{k+\lambda-\frac{1}{2}}\bar{u}^{\lambda-\frac{3}{2}} = 1\,.\end{aligned} \tag{4.262}$$

The integral is the integral representation of the beta function. In terms of Mellin moments (4.249), we have

$$\begin{aligned}\langle\!\langle 1/\bar{u}\rangle\!\rangle_j^\lambda &= \frac{1}{\mathrm{B}\big(j+\lambda+\frac{1}{2},\lambda-\frac{1}{2}\big)}\int_0^1 \mathrm{d}w\,w^j\int_w^1 \mathrm{d}u\,(u\bar{u})^{\lambda-\frac{1}{2}}\delta[-\bar{u}(u-w)]\\ &= \frac{1}{\mathrm{B}\big(j+\lambda+\frac{1}{2},\lambda-\frac{1}{2}\big)}\int_0^1 \mathrm{d}w\,w^j\,w^{j+\lambda-\frac{1}{2}}\bar{w}^{\lambda-\frac{3}{2}}\,,\end{aligned} \tag{4.263}$$

leads to the same result as above.
As a second example we consider

$$\Im\mathrm{m}\,\frac{\ln\bar{u}}{u} = -\pi\frac{\theta(-\bar{u})}{u} = \frac{2\pi r}{r+1}\,. \tag{4.264}$$

Inserting the imaginary part into (4.250) and performing the integration with respect to u', we obtain for $\lambda\in\{3/2,5/2\}$

$$\begin{aligned}\langle\!\langle \ln\bar{u}/u\rangle\!\rangle_j^{3/2} &= (k+2)\int_0^1 \mathrm{d}w\,w^j(-\bar{w}-w\ln w) = \frac{-1}{(1+k)_2}\,,\\ \langle\!\langle \ln\bar{u}/u\rangle\!\rangle_j^{5/2} &= (k+4)(k+3)\int_0^1 \mathrm{d}w\,w^j\frac{1}{6}\left[-1+3w+9w^2-11w^3+6w^2(1+w)\ln w\right]\\ &= \frac{-2(j+2)_2-2}{(j+1)_2}\,.\end{aligned} \tag{4.265}$$

Note, we used the Pochhammer symbol (4.65). The conformal moments for quarks and gluons follow from (4.238).
At this point, we have all tools at hand, to derive the Wilson coefficients including their analytic continuation from a given hard scattering amplitude in the momentum fraction representation. In the rest of this chapter, we present the LO and NLO Wilson coefficients for DIS, DVCS and DVMP.

4.6.1. DIS

In this section, we present the Mellin moments of the hard scattering amplitudes for deeply inelastic scattering up to NLO order in perturbation theory. The perturbative expansions in the quark and gluon channel are

$$\begin{aligned} {}^{\mathrm{q}}\tilde{c}^{\mathrm{I}}_{l,j}(\alpha_{\mathrm{s}}(\mu_{\mathrm{R}})) &= {}^{\mathrm{q}}\tilde{c}^{\mathrm{I}}_{l,j} + \frac{\alpha_{\mathrm{s}}(\mu_{\mathrm{R}})}{2\pi}\, {}^{\mathrm{q}}\tilde{c}^{\mathrm{I}(1)}_{l,j} + \mathcal{O}(\alpha_{\mathrm{s}}^3)\,, \\ {}^{\mathrm{G}}\tilde{c}^{\mathrm{I}}_{l,j}(\alpha_{\mathrm{s}}(\mu_{\mathrm{R}})) &= {}^{\mathrm{G}}\tilde{c}^{\mathrm{I}}_{l,j} + \frac{\alpha_{\mathrm{s}}(\mu_{\mathrm{R}})}{2\pi}\, {}^{\mathrm{G}}\tilde{c}^{\mathrm{I}(1)}_{l,j} + \mathcal{O}(\alpha_{\mathrm{s}}^3)\,. \end{aligned} \tag{4.266}$$

At LO accuracy the Mellin moments are

$${}^{\mathrm{q}}\tilde{c}^{\mathrm{V}(0)}_{l,j} = 1\,, \qquad {}^{\mathrm{G}}\tilde{c}^{\mathrm{V}(0)}_{l,j} = 0\,, \qquad l \in \{1,2\}\,. \tag{4.267}$$

Note, the index $l=1$ denotes the Wilson coefficients of the structure function F_1. For the structure functions F_2 with index $l=2$ the Wilson coefficients coincide. At NLO accuracy, the Mellin moments of the hard scattering amplitude in the non-singlet channel [BBDM78] for the scale setting $\mu_{\mathrm{F}}=\mu_{\mathrm{R}}=\mathcal{Q}$ are

$${}^{\mathrm{q}}\tilde{c}^{\mathrm{V}(1)}_{1,j} = C_{\mathrm{F}}\left[S_1^2(j+1) + \frac{3}{2}S_1(j+2) - \frac{9}{2} + \frac{5-2S_1(j)}{2(j+1)_2} - S_2(j+1)\right]. \tag{4.268}$$

And for gluonic structure functions the Wilson coefficients read

$${}^{\mathrm{G}}\tilde{c}^{\mathrm{V}(1)}_{1,j} = -N_{\mathrm{f}}\frac{(j^2+3j+4)S_1(j)+j^2+3j+2}{(j+1)_3}\,. \tag{4.269}$$

In addition, for F_2 we have the Mellin moments

$${}^{\mathrm{q}}\tilde{c}^{\mathrm{V}(1)}_{2,j} = 2\,{}^{\mathrm{q}}\tilde{c}^{\mathrm{V}(1)}_{1,j} + \frac{4C_{\mathrm{F}}}{2+j}\,, \qquad {}^{\mathrm{G}}\tilde{c}^{\mathrm{V}(1)}_{2,j} = 2\,{}^{\mathrm{G}}\tilde{c}^{\mathrm{V}(1)}_{1,j} + \frac{8N_{\mathrm{f}}}{(2+j)(3+j)}\,. \tag{4.270}$$

In the literature[8], instead of labeling the quark hard scattering amplitudes, one utilizes the singlet and non-singlet Wilson coefficients and a pure singlet contribution arising at NNLO. In order to hold the similarity to DVCS and DVMP, we stay with the labels above.

[8] For a review see [Blu13].

4.6.2. DVCS

The radiative corrections for DVCS are known to NLO in the $\overline{\text{MS}}$ scheme. They have been obtained by rotation from the conformal prediction [Mül98, BM98b] and by diagrammatical evaluation in [MPS+98, JO98b, JO98a]. The perturbative expansion in the quark and gluon channel utilizing the auxiliary conformal moments (4.181) are

$$
\begin{aligned}
{}^{\text{q}}T_j^{\text{I}}\left(\alpha_{\text{s}}(\mu_{\text{R}}),\tfrac{\mathcal{Q}^2}{\mu_{\text{F}}^2}\right) &= \frac{2^{n+1}\Gamma\left(n+\frac{5}{2}\right)}{\Gamma\left(\frac{3}{2}\right)\Gamma(n+3)}\left[{}^{\text{q}}c_j^{\text{I}(0)} + \frac{\alpha_{\text{s}}^2(\mu_{\text{R}})}{2\pi}\,{}^{\text{q}}c_j^{\text{I}(1)}\left(\tfrac{\mathcal{Q}^2}{\mu_{\text{F}}^2}\right) + \mathcal{O}\left(\alpha_{\text{s}}^3\right)\right],\\
{}^{\text{G}}T_j^{\text{I}}\left(\alpha_{\text{s}}(\mu_{\text{R}}),\tfrac{\mathcal{Q}^2}{\mu_{\text{F}}^2}\right) &= \frac{2^{n+2}\Gamma\left(n+\frac{5}{2}\right)}{\Gamma\left(\frac{3}{2}\right)\Gamma(n+4)}\left[{}^{\text{G}}c_j^{\text{I}(0)} + \frac{\alpha_{\text{s}}^2(\mu_{\text{R}})}{2\pi}\,{}^{\text{G}}c_j^{\text{I}(1)}\left(\tfrac{\mathcal{Q}^2}{\mu_{\text{F}}^2}\right) + \mathcal{O}\left(\alpha_{\text{s}}^3\right)\right].
\end{aligned}
\tag{4.271}
$$

See also the perturbative expansion in the momentum fraction representation in Sec. 3.2.4.2. The conformal moments follow by utilizing the method in Sec. 4.6. A summary of the hard scattering amplitudes in momentum fraction representation is given in [BMNS00]. We already know the LO coefficients:

$$
{}^{\text{q}}c_j^{\text{V}(0)} = {}^{\text{q}}c_j^{\text{A}(0)} = 1\,, \qquad {}^{\text{G}}c_j^{\text{V}(0)} = {}^{\text{G}}c_j^{\text{A}(0)} = 0\,. \tag{4.272}
$$

At NLO of perturbation theory the result [KMPK08] in the quark channel reads

$$
{}^{\text{q}}c_j^{\text{V}(1)}\left(\frac{\mathcal{Q}^2}{\mu_{\text{F}}^2}\right) = C_{\text{F}}\left[2S_1^2(j+1) - \frac{9}{2} + \frac{5-4S_1(j+1)}{2(j+1)(j+2)} + \frac{1}{(j+1)^2(j+2)^2}\right] + \frac{1}{2}\ln\frac{\mathcal{Q}^2}{\mu_{\text{F}}^2}\,\gamma_j^{(0)}\,, \tag{4.273}
$$

$$
{}^{\text{q}}c_j^{\text{A}(1)}\left(\frac{\mathcal{Q}^2}{\mu_{\text{F}}^2}\right) = C_{\text{F}}\left[2S_1^2(j+1) - \frac{9}{2} + \frac{3-4S_1(j+1)}{2(j+1)(j+2)} + \frac{1}{(j+1)^2(j+2)^2}\right] + \frac{1}{2}\ln\frac{\mathcal{Q}^2}{\mu_{\text{F}}^2}\,\gamma_j^{(0)}\,, \tag{4.274}
$$

and in the gluon channel

$$
{}^{\text{G}}c_j^{\text{V}(1)}\left(\frac{\mathcal{Q}^2}{\mu_{\text{F}}^2}\right) = -N_{\text{f}}\frac{(j^2+3j+4)[S_1(j)+S_1(j+2)]+j^2+3j+2}{(j+1)_3} + \frac{1}{2}\ln\frac{\mathcal{Q}^2}{\mu_{\text{F}}^2}\,{}^{\Sigma\text{G}}\gamma_j^{\text{V}(0)}\,, \tag{4.275}
$$

$$
{}^{\text{G}}c_j^{\text{A}(1)}\left(\frac{\mathcal{Q}^2}{\mu_{\text{F}}^2}\right) = -N_{\text{f}}\frac{j\,[1+S_1(j)+S_1(j+2)]}{(j+1)_2} + \frac{1}{2}\ln\frac{\mathcal{Q}^2}{\mu_{\text{F}}^2}\,{}^{\Sigma\text{G}}\gamma_j^{\text{A}(0)}\,. \tag{4.276}
$$

The anomalous dimensions are summarized in Sec. D.1. Furthermore, the Mellin-Barnes representation of the non-singlet and singlet CFFs is given in Sec. 4.5.2.

4.6.3. DVMP

The hard scattering amplitudes at NLO approximation in perturbation theory for DVMP are known in momentum fraction representation since one decade. However, it was not in a suitable form for the Mellin-Barnes representation of TFFs. The main reason was the treatment of the conformal moments of the non-separable terms which was recently solved in [MLPKS14]. As presented in Sec. 3.3.6 the NLO corrections were organized in such a way, that we only have cuts along $[1,\infty]$ in the variable u and cuts along $[-\infty,0]$ in the momentum fraction v of the distribution amplitude. Additionally, we subtract all poles in

$G(u)$	$\frac{1}{2\pi r}\,\Im\mathrm{m}G\left(\frac{r+1}{2r}\right)$	$\langle G(u)\rangle_j^\lambda$
$\frac{1}{\bar{u}}$	$\delta(1-r)$	1
		1
$\frac{\ln\bar{u}}{\bar{u}}$	$\left\{\frac{1}{1-r}\right\}_+$	$-2S_1(j+1)+\frac{1}{(j+1)_2}$
		$-2S_1(j+1)+1+\frac{4(j+1)_2-2}{(j)_4}$
$\frac{\ln^2\bar{u}}{\bar{u}}$	$\left\{\frac{2\ln\frac{1-r}{2r}}{1-r}\right\}_+$	$\left[2S_1(j+1)-\frac{1}{(j+1)_2}\right]^2+\frac{2(j+1)_2+1}{[(j+1)_2]^2}$
		$\left[2S_1(j+1)-1-\frac{4(j+1)_2-2}{(j)_4}\right]^2-1+\frac{2j(j+3)+9}{[j(j+3)]^2}+\frac{2(j+1)_2+1}{[(j+1)_2]^2}$

Table 4.3.: Imaginary parts and conformal moments of the most singular building blocks for quarks (upper lines) and gluons (lower lines).

$u=0$ and $v=1$. Therefore, the derivation of the conformal moments of the non-separable terms is not unnecessarily complicated. Furthermore, this ensures the numerical smallness of the non-separable contributions.
In this section, we present the conformal moments of the separable and non-separable building blocks (See Sec. 3.3.6) utilizing the method outlined in Sec. 4.6 based on the imaginary part. The result is applied to determine the conformal moments of the hard scattering amplitudes for DVMP in NLO of perturbation theory. For the flavor non-singlet quark channel, we utilize a definite signature to ensure the uniqueness of the analytic continuation.

4.6.4. Separable building blocks

We introduced the NLO corrections to the hard scattering amplitude in momentum fraction representation in section 3.3.6 and identified the elementary separable building blocks in Sec. 3.3.6.4. In this section, we present the corresponding imaginary parts and evaluate their conformal moments.

- *Most singular building blocks.*

In Eq. 3.302 we identified the three most singular building blocks, namely

$$\frac{1}{\bar{u}-i\epsilon}\,,\qquad \frac{\ln(\bar{u}-i\epsilon)}{\bar{u}-i\epsilon}\,,\qquad \frac{\ln^2(\bar{u}-i\epsilon)}{\bar{u}-i\epsilon}\,.$$

The corresponding imaginary parts, which are necessary for the determination of the conformal moments (see Sec. 4.6), are obtained by expressing the building blocks in terms of a derivative acting on a logarithm to the power p

$$\frac{\mathrm{d}}{\mathrm{d}u}\ln^p(\bar{u})=\frac{p\,\ln^p(\bar{u})}{-\bar{u}}\,. \tag{4.277}$$

For the cases of interest $p\in\{0,1,2\}$, we receive the three most singular building blocks above

$$\frac{\mathrm{d}}{\mathrm{d}u}\ln(\bar{u})=-\frac{1}{\bar{u}}\,,\qquad \frac{\mathrm{d}}{\mathrm{d}u}\ln^2(\bar{u})=-2\frac{\ln(\bar{u})}{\bar{u}}\,,\qquad \frac{\mathrm{d}}{\mathrm{d}u}\ln^3(\bar{u})=-3\frac{\ln^2(\bar{u})}{\bar{u}}\,. \tag{4.278}$$

The real and imaginary part of a logarithm to power p reads

$$\ln^p(\bar{u} - i\epsilon) = [\ln(-\bar{u}) - i\pi\theta(-\bar{u})]^p \,. \tag{4.279}$$

For the cases of interest, the imaginary parts are

$$\begin{aligned} \Im\mathrm{m} \ln\,(\bar{u}) &= -\,\pi\theta(-\bar{u})\,, \\ \Im\mathrm{m} \ln^2(\bar{u}) &= -2\pi\theta(-\bar{u}) \ln\,(-\bar{u})\,, \\ \Im\mathrm{m} \ln^3(\bar{u}) &= -3\pi\theta(-\bar{u}) \ln^2(-\bar{u}) + \pi^3\theta(\bar{u})\,. \end{aligned} \tag{4.280}$$

For the general case, we utilize the binomial formula

$$\Im\mathrm{m} \ln^p(\bar{u}) = -\pi\theta(-\bar{u}) \sum_{\substack{m=1 \\ \text{odd}}}^{p} \binom{p}{m} \ln^{p-m}(-\bar{u})(i\pi)^{m-1}\,. \tag{4.281}$$

Consequently, the imaginary parts of all building blocks follow by differentiation. E.g., for $p = 1$

$$\Im\mathrm{m} \frac{1}{\bar{u}} = -\frac{\mathrm{d}}{\mathrm{d}u} \Im\mathrm{m} \ln(\bar{u}) = \pi \frac{\mathrm{d}}{\mathrm{d}u}\theta(-\bar{u}) = \pi\delta(\bar{u})\,, \tag{4.282}$$

and in case of $p=2$

$$\Im\mathrm{m} \frac{\ln \bar{u}}{\bar{u}} = -\frac{1}{2}\frac{\mathrm{d}}{\mathrm{d}u} \Im\mathrm{m} \ln^2(\bar{u}) = \pi \frac{\mathrm{d}}{\mathrm{d}u} \left[\theta(-\bar{u}) \ln(-\bar{u})\right] \,. \tag{4.283}$$

Performing the differentiation, the two arising terms are not finite in the limit $u \to 1$ individually. Therefore, we regularize obtaining two finite terms. We introduce the notation

$$\frac{\mathrm{d}}{\mathrm{d}u} \left[\theta(-\bar{u})G(u)\right] \equiv \left[\!\!\left[\theta(-\bar{u}) \frac{\mathrm{d}G(u)}{\mathrm{d}u}\right]\!\!\right]_+ \,, \tag{4.284}$$

for a general function $G(u)$ as in Sec. 4.6. In the definition above, the regularization is achieved by

$$\left[\!\!\left[\theta(-\bar{u})G'(u)\right]\!\!\right]_+ = \lim_{\epsilon \to 0} \left[\theta(-\bar{u})G'(u+\epsilon) + \delta(\bar{u})G(1+\epsilon)\right] \,, \tag{4.285}$$

where the (infinite) constant is regularized by ϵ and can be represented by

$$G(1+\epsilon) = -\int_1^{u_1} \mathrm{d}u\, G'(u+\epsilon) + G(u_1)\,. \tag{4.286}$$

The term above cancels the singularity at $u = 1$ in the integral containing $G'(u)$. Moreover, the upper integration limit u_1 can be fixed freely. Thus, the imaginary part for $p=2$ reads

$$\Im\mathrm{m} \frac{\ln \bar{u}}{\bar{u}} = \pi \left[\!\!\left[\frac{\theta(-\bar{u})}{-\bar{u}}\right]\!\!\right]_+ \,. \tag{4.287}$$

Furthermore, the imaginary part for the case $p=3$ becomes

$$\begin{aligned}\Im\mathrm{m}\,\frac{\ln^2\bar{u}}{\bar{u}} &= -\frac{1}{3}\frac{\mathrm{d}}{\mathrm{d}u}\,\Im\mathrm{m}\ln^3(\bar{u}) = \pi\frac{\mathrm{d}}{\mathrm{d}u}\left[\theta(-\bar{u})\ln^2(-\bar{u})\right] - 2\zeta(2)\delta(\bar{u}) \\ &= \pi\left[\!\!\left[\theta(-\bar{u})\frac{2\ln(-\bar{u})}{-\bar{u}}\right]\!\!\right]_+ - 2\zeta(2)\delta(\bar{u})\,. \end{aligned} \tag{4.288}$$

For a convenient representation of the imaginary parts, we express the imaginary parts taking off the factor $2\pi r$. The imaginary part in (4.283) becomes

$$\frac{1}{2r}\left[\!\!\left[\frac{\theta(-\bar{u})}{-\bar{u}}\right]\!\!\right]_+ = \left[\!\!\left[\frac{\theta(1-r)}{1-r}\right]\!\!\right]_+ = \left\{\frac{1}{1-r}\right\}_+, \tag{4.289}$$

where the $\{\ldots\}_+$ prescription is defined without the factor $2\pi r$ and in addition, we omit the theta function since r is in the interval $[0,1]$. Utilizing the regularization, the numerical evaluation (4.244) of the conformal moments of most singular building blocks containing a logarithm read

$$\begin{aligned}\langle\!\langle \ln\bar{u}/\bar{u}\rangle\!\rangle_j^\lambda &= \int_0^1 \mathrm{d}y\,\left[\widetilde{p}_j^\lambda(y)-\widetilde{p}_j^\lambda(1)\right]\frac{1}{y}\frac{-1}{-1+\frac{1}{y}}\,, \\ \langle\!\langle \ln^2\bar{u}/\bar{u}\rangle\!\rangle_j^\lambda &= \int_0^1 \mathrm{d}y\,\left[\widetilde{p}_j^\lambda(y)-\widetilde{p}_j^\lambda(1)\right]\frac{1}{y}\frac{-2\ln\left(-1+\frac{1}{y}\right)}{-1+\frac{1}{y}}\,, \end{aligned} \tag{4.290}$$

where the integrand is finite at the point $y=1$.
The conformal moments of the three most singular building blocks have been already obtained in [Mül99], App. B, by utilizing the identity

$$\frac{\ln^p\bar{u}}{\bar{u}} = \lim_{\epsilon\to 0}\left(\frac{\partial^p}{\partial\epsilon^p}\bar{u}^{\epsilon-1}\right)\,. \tag{4.291}$$

We have already derived the conformal moments of the LO amplitude $1/\bar{u}$ as an example in Sec. 4.6. The imaginary part and the conformal moments of the most singular building blocks are given in Tab. 4.3. For $p\geq 1$, harmonic sums arise, see App. C.5. The logarithmic enhancement of the pole situated at $u=1$ is reflected in the logarithmical growth of the conformal moments at large values of j, since the asymptotic behavior of the harmonic sum is

$$S_1(j+1) = \ln(j+1) + \gamma_E + O\left(\tfrac{1}{j+1}\right)\,, \tag{4.292}$$

where γ_E is the Euler-Mascheroni constant.

- *Building blocks with logarithmic $[1,\infty]$-cuts.*

In (3.303) we introduced the building blocks involving logarithmical cuts, we had

$$\frac{\ln(\bar{u}-i\epsilon)}{u}\,,\quad \frac{\ln^2(\bar{u}-i\epsilon)}{u}\,,\quad \left[\frac{\ln\bar{u}}{u^2}\right]^{\mathrm{sub}} \equiv \frac{\ln(\bar{u}-i\epsilon)+u}{u^2}\,,\quad \frac{\ln^2(\bar{u}-i\epsilon)}{u^2}\,.$$

$G(u)$	$\frac{1}{2\pi r}\,\Im\mathrm{m}\,G\left(\frac{r+1}{2r}\right)$	$\langle G(u)\rangle_j^\lambda$
$\frac{\ln\bar{u}}{u}$	$-\frac{1}{1+r}$	$\frac{-1}{(j+1)_2}$
		$\frac{-2(j+1)_2-2}{(j)_4}$
$\frac{\ln^2\bar{u}}{u}$	$-\frac{2}{1+r}\ln\frac{1-r}{2r}$	$\frac{4S_1(j+1)}{(j+1)_2}-\frac{(j+1)_2+1}{[(j+1)_2]^2}$
		$\frac{8\,[j(j+3)+3]\,S_1(j+1)-6j(j+3)-22}{(j)_4}-\frac{8\,[j(j+3)+3]\,[2j(j+3)+3]}{[(j)_4]^2}$
$\frac{\ln\bar{u}+u}{u^2}$	$-\frac{2r}{(1+r)^2}$	$\frac{(j+1)_2}{2}\left[S_2\left(\frac{j+1}{2}\right)-S_2\left(\frac{j}{2}\right)\right]-1$
		$-\frac{2}{(j+1)_2}$
$\frac{\ln^2\bar{u}}{u^2}$	$-\frac{4r}{(1+r)^2}\ln\frac{1-r}{2r}$	$--$
		$\frac{8\,S_1(j+1)-6}{(j+1)_2}-\frac{4}{[(j+1)_2]^2}$

Table 4.4.: Imaginary parts and conformal moments of the separable building blocks with logarithmical $[1,\infty]$-cuts for quarks (upper lines) and gluons (lower lines).

Since all poles are removed, the imaginary part is completely determined by the logarithmical cut. As before, we are only interested in the imaginary part of $\ln^{p+1}(\bar{u}-i\epsilon)$, with $p\in\{0,1\}$. Thus, from the imaginary part of the logarithm to power p in (4.281), we get

$$\Im\mathrm{m}\left[\frac{\ln^p(\bar{u})}{u^a}\right]^{\mathrm{sub}} = -\pi\theta(-\bar{u})\sum_{m=1,\mathrm{odd}}^{p}\binom{p}{m}\frac{\ln^{p-m}(-\bar{u})}{u^a}(i\pi)^{m-1}\,. \tag{4.293}$$

For the relevant cases $p\in\{1,2\}$ the sum over the binomial coefficient drops, since only the case $m=1$ contributes. Hence,

$$\Im\mathrm{m}\left[\frac{\ln^p(\bar{u})}{u^a}\right]^{\mathrm{sub}} = -\pi\theta(-\bar{u})\frac{p\ln^{p-1}(-\bar{u})}{u^a}\,. \tag{4.294}$$

Note, the subtraction is only needed in case of $\{a=1,p=1\}$.
The conformal moments are obtained for quarks in [MMPK03], App. C, and for gluons in [KMPK08], App. C.1. The definition of conformal moments therein is different. Therefore, we have to neglect the factors

$$2N_j^{3/2}\,,\qquad 12N_{j-1}^{5/2}\,, \tag{4.295}$$

which in our case are already included in the definition of conformal moments (4.185). Furthermore, the conformal moments of the subtracted building block is given in [Mül99] in terms of a hypergeometric function ${}_3F_2$. Using the procedure outlined in Sec. 4.6, we can present them in terms of harmonic sums. In terms of Mellin moments (4.249), we obtain

$$\begin{aligned}\left[\frac{\ln\bar{u}}{u^2}\right]^{\mathrm{sub}}\overset{u}{\otimes}\hat{p}_j^{3/2}(u) &= (j+2)\int_0^1 \mathrm{d}w\,w^{j+1}\left[\frac{1-w}{1+w}+\frac{2\ln w}{(1+w)^2}\right]\\ &= \frac{(j+1)_2}{2}\left[S_2\left(\frac{j+1}{2}\right)-S_2\left(\frac{j}{2}\right)\right]-1\,.\end{aligned} \tag{4.296}$$

The solution of the integral is given by harmonic sums, see Sec. C.5. The function $\ln \bar{u}/u$ was treated as an example in Sec. 4.6.
In principle, the harmonic sums with half integer arguments can be reduced to harmonic sums with negative index utilizing the identity

$$S_n\left(\frac{z+1}{2}\right) - S_n\left(\frac{z}{2}\right) = (-1)^{z+1} 2^n \left[S_{-n}(z+1) + (1-2^{1-n})\zeta(n)\right] \equiv \Delta S_n\left(\frac{z+1}{2}\right) . \quad (4.297)$$

However, introducing $S_{-n}(z)$ leads to an ambiguity of the analytic continuation and requires a definite signature. In order to circumvent this unnecessary complication, we omit the harmonic sums with negative arguments.
In table 4.4 we present the logarithmical building blocks, their imaginary parts and the respective conformal moments. Moreover, the conformal moments vanish in the limit $j \to \infty$ as $1/j^2$ or $\ln j/j^2$.

- *Building blocks with dilogarithms.*

$G(u)$	$\frac{1}{2\pi r}\,\Im\mathrm{m} G\left(\frac{r+1}{2r}\right)$	$\langle G(u)\rangle_j^\lambda$
$\frac{\mathrm{Li}_2(u)}{u}$	$\frac{\ln\frac{1+r}{2r}}{1+r}$	$-\frac{1}{2}\left[S_2\left(\frac{j+1}{2}\right) - S_2\left(\frac{j}{2}\right)\right] + \frac{(j+1)_2+1}{[(j+1)_2]^2}$
		$\frac{1}{2}\left[S_2\left(\frac{j+1}{2}\right) - S_2\left(\frac{j}{2}\right)\right] + \frac{18-j(j+3)}{2j^2(j+3)^2} - \frac{2+(j+1)_2}{2[(j+1)_2]^2}$
$\frac{\mathrm{Li}_2(u)-u}{u^2}$	$\frac{2r\ln\frac{1+r}{2r}}{(1+r)^2}$	$1 + (j+1)_2\Big\{\frac{1}{4}\left[S_3\left(\frac{j+1}{2}\right) - S_3\left(\frac{j}{2}\right)\right] + \left[S_2\left(\frac{j+1}{2}\right) - S_2\left(\frac{j}{2}\right)\right]$
		$\times\left[S_1(j+1) - \frac{1}{2}\right] + 4(-1)^j\left[S_{-2,1}(j+1) + \frac{5\zeta(3)}{8}\right]\Big\}$
		$\frac{j(j+3)}{2}\left[S_2\left(\frac{j+1}{2}\right) - S_2\left(\frac{j}{2}\right)\right] + \frac{2+3(j+1)_2}{[(j+1)_2]^2} - 1$
$\frac{\mathrm{Li}_2(u)-\zeta(2)}{\bar{u}}$	$-\frac{\ln\frac{1+r}{2r}}{1-r}$	$-\frac{(j+1)_2+1}{[(j+1)_2]^2}$
		$-\frac{18-j(j+3)}{2j^2(j+3)^2} - \frac{2+5(j+1)_2}{2[(j+1)_2]^2}$
$\frac{\mathrm{Li}_2(u)-\zeta(2)-\bar{u}\ln\bar{u}+\bar{u}}{\bar{u}^2}$	$\frac{2r\ln\frac{1+r}{2r}-1+r}{(1-r)^2}$	$2(j+1)_2\left[S_3(j+1) - \zeta(3)\right] + 1 - \frac{1}{(j+1)_2}$
		$--$

Table 4.5.: Imaginary parts and conformal moments of the building blocks with dilogarithms for quarks (upper lines) and gluon (lower lines).

The four building blocks involving dilogarithms were given in (3.304) and with additional subtracted $u=1$ poles in (3.305):

$$\frac{\mathrm{Li}_2(u+i\epsilon)}{u}, \qquad \left[\frac{\mathrm{Li}_2(u+i\epsilon)}{u^2}\right]^{\mathrm{sub}}, \qquad \left[\frac{\mathrm{Li}_2(u)}{\bar{u}}\right]^{\mathrm{sub}}, \qquad \left[\frac{\mathrm{Li}_2(u)}{\bar{u}^2}\right]^{\mathrm{sub}}.$$

The imaginary part of the dilogarithm is given by

$$\Im\mathrm{m}\,\mathrm{Li}_2(u+i\epsilon) = \pi\theta(-\bar{u})\ln(u)\,. \quad (4.298)$$

Since no pole in $u=0$ is present, the imaginary part of the building blocks proportional to $1/u$ is

$$\Im\mathrm{m}\left[\frac{\mathrm{Li}_2(u)}{u^a}\right]^{\mathrm{sub}} = \pi\theta(-\bar{u})\frac{\ln(u)}{u^a}\,. \tag{4.299}$$

For the terms with subtracted $u=1$ poles, we obtain

$$\Im\mathrm{m}\left[\frac{\mathrm{Li}_2(u)}{\bar{u}}\right]^{\mathrm{sub}} = \frac{\pi\theta(-\bar{u})\ln(u)}{\bar{u}} = -\frac{\pi\theta(1-r)2r\ln\left(\frac{r+1}{2r}\right)}{1-r}\,, \tag{4.300}$$

$$\Im\mathrm{m}\left[\frac{\mathrm{Li}_2(u)}{\bar{u}^2}\right]^{\mathrm{sub}} = \frac{\pi\theta(-\bar{u})\left[\ln(u)-\bar{u}\right]}{\bar{u}^2} = \frac{\pi\theta(1-r)2r}{(1-r)^2}\left[2r\ln\left(\frac{r+1}{2r}\right)+r-1\right]\,. \tag{4.301}$$

The conformal moments of the first and third building block for quarks have been determined in [MMPK03], App. C,

$$\begin{aligned}
\left[\frac{\mathrm{Li}_2(u)}{u^2}\right]^{\mathrm{sub}} \overset{u}{\otimes} \hat{p}_j^{3/2}(u) &= 1+2(j+1)_2\int_0^1 \mathrm{d}w\, w^{j+1}\,\frac{\left[1-\frac{1}{2}\ln w+\ln(w+1)\right]\ln w+2\mathrm{Li}_2(-w)+\zeta(2)}{1+w}\\
\left[\frac{\mathrm{Li}_2(u)}{\bar{u}^2}\right]^{\mathrm{sub}} \overset{u}{\otimes} \hat{p}_j^{3/2}(u) &= 1-\frac{1}{(j+1)_2}+(j+1)_2\int_0^1 \mathrm{d}w\, w^{j+1}\,\frac{\ln^2 w}{1-w}\,.
\end{aligned} \tag{4.302}$$

In terms of harmonic sums, the second integral is

$$\int \mathrm{d}w\, w^{j+1}\,\frac{\ln^2 w}{1-w} = -2S_3(j+1)+2\zeta(3)\,. \tag{4.303}$$

The first integral follows from from [BK99, Ver99], we get

$$(-1)^{j+1}\left\{S_{-3}(j+1)+\frac{3\zeta(3)}{4}+\left[2S_1(j+1)-1\right]\left[S_{-2}(j+1)+\frac{\zeta(2)}{2}\right]-2\left[S_{-2,1}(j+1)+\frac{5\zeta(3)}{8}\right]\right\}.$$

The conformal moments for gluons are obtained analogously. Table 4.5 summarizes the result including the imaginary parts. Unlike the logarithmical building blocks, they are rather harmless, since they only contain logarithmical $[1,\infty]$-cuts and the imaginary parts are constant at the point $r=1$. The conformal moments vanish in the limit $j\to\infty$.

- *Peculiarities at $u\to\infty$.*

In the pure singlet quark contribution the separable building blocks (3.306)

$$\ln(\bar{u}-i\epsilon)\,,\quad \ln^2(\bar{u}-i\epsilon)\,,\quad \text{and}\quad \mathrm{Li}_2(u+i\epsilon)$$

appeared.
The imaginary part follows directly from the imaginary part of the logarithm (4.294) with $a=0$ and from the imaginary part of the dilogarithm (4.298).

$G(u)$	$\frac{1}{2\pi r}\,\Im\mathrm{m}\,G\big(\frac{r+1}{2r}\big)$	$\langle G(u)\rangle_j^{3/2}$
$\frac{\bar u-u}{u}\ln\bar u$	$\frac{1}{r(1+r)}$	$-\frac{\mathrm{G}\Sigma\gamma_j^{(0,\mathrm{F})}}{2(j+3)}$
$\frac{\bar u-u}{2u}\ln^2\bar u-2\mathrm{Li}_2(u)$	$\frac{\ln\frac{1-r}{1+r}}{r(1+r)}-\frac{\ln\frac{1+r}{2r}}{1+r}$	$[S_1(j+1)-1]\,\frac{\mathrm{G}\Sigma\gamma_j^{(0,\mathrm{F})}}{j+3}-\frac{(j+1)_2+1}{[(j+1)_2]^2}$

Table 4.6.: Combinations of Peculiarities at $u\to\infty$ as found in the pure-singlet quark channel.

Utilizing Rodrigues formula (C.13) we obtain the conformal moments for $n\geq 1$

$$\begin{aligned}
\ln\bar u\overset{u}{\otimes}\hat p_j^{3/2}(u)&=\frac{-1}{j(j+3)}\,,\\
\ln^2\bar u\overset{u}{\otimes}\hat p_j^{3/2}(u)&=\frac{6}{j(j+3)^2}+\frac{S_1(j+3)+3}{j(j+3)}+\frac{1}{(j+1)_2}\,,\\
\mathrm{Li}_2(u)\overset{u}{\otimes}\hat p_j^{3/2}(u)&=\frac{2(j+1)_2+2}{((j)_2)^2}\,.
\end{aligned}\tag{4.304}$$

For $n=0$, the conformal moments are finite as well, however, they do not integrate in the closed expressions above. Since for the pure singlet quark channel, the conformal GPD moments are odd, this is negligible. The second order pole at $j=0$ cancels in the final expression for the hard scattering amplitude, as it is also the case in the gluon quark channel. In table 4.6 we present the terms involving the peculiarities such that the $j=0$ pole cancels.

- *Exploiting symmetry.*

The conformal moments of terms with poles at $u=0$ and logarithmical $[-\infty,0]$-cuts, e.g. (3.307), follow from the ones with poles at $u=1$ and logarithmical $[1,\infty]$-cuts by decoration with a factor $(-1)^j$. This factor is replaced in the flavor non-singlet and quark-gluon channel by $-\sigma$ and σ, respectively. On the other hand, conformal moments stemming from terms that depend on v are decorated with a factor $(-1)^k$ that is replaced by $+1$ and -1 for symmetric and anti-symmetric DAs.

4.6.5. Non-separable building blocks

We recall from section 3.3.6.3, that we are able to separate the separable and non-separable terms in the hard scattering amplitudes. The non-separable terms are written as an addenda, where all poles in u have been removed. In Sec. 3.3.6.5, the addenda are expressed by a differential operator acting on certain building blocks. The general expression for the NLO addenda was given in (3.314) as

$$\Delta^A T^{(1,c)}(u,v)=\sum_{a,b}{}^A\vec{\mathcal{D}}_{a,b}^{(1,c)}\left[\frac{1}{u^a\bar v^b}\,\frac{L(u,v)}{u-v}\right]^{\mathrm{sub}}\,,$$

where the function $L(u,v)$ is defined in (3.280). It only includes cuts along $[1,\infty]$ for the variable u and cuts along $[-\infty,0]$ for the momentum fraction v of the DA. Moreover, all poles at $u=0$ or $v=1$ are subtracted.
In the following, we utilize the notation

$$[a,b] \equiv \left[\frac{1}{u^a\bar{v}^b}\,\frac{L(u,v)}{u-v}\right]^{\text{sub}} \tag{4.305}$$

for the subtracted non-separable building blocks. The flavor non-singlet channel (Sec. 4.6.6.1) contained the blocks $[0,1]$ and $[0,2]$. The pure singlet channel (Sec. 4.6.6.2) contains only $[1,0]$ whereas the gluon-quark channel (Sec. 4.6.6.3) contains the building block $[1,1]$.
Since in the non-separable building blocks poles are absent, the imaginary part is solely given by the logarithm and the dilogarithm. As we already know from (4.294) and (4.298), their imaginary parts are

$$\begin{aligned}\Im\mathrm{m}\ln(\bar{u}-i\epsilon) &= -\pi\theta(u-1) = -\pi\theta(r)\,,\\ \Im\mathrm{m}\,\mathrm{Li}_2(u+i\epsilon) &= \pi\theta(u-1)\ln u = \pi\theta(r)\ln\left(\frac{r+1}{2r}\right)\,,\end{aligned}$$

respectively. Consequently, the imaginary part of $L(u,v)$ reads

$$\Im\mathrm{m}\,\frac{L(u,v)}{u-v} = \frac{\pi\theta(u-1)\ln\left(\frac{u}{v}\right)}{u-v} = 2\pi r\cdot\frac{\theta(r)\ln\left(\frac{r+1}{2rv}\right)}{r+1-2rv}\,. \tag{4.306}$$

From the imaginary part above, we evaluate the imaginary part of the general building block $[a,b]$ by

$$\begin{aligned}\Im\mathrm{m}\left[\frac{1}{u^a\bar{v}^b}\,\frac{L(u,v)}{u-v}\right]^{\text{sub}} \Rightarrow \left[\frac{(2r)^a}{(r+1)^a\bar{v}^b}\,\frac{\theta(r)\ln\left(\frac{r+1}{2rv}\right)}{r+1-2rv}\right]^{\text{sub}}\\ = \frac{\theta(r)(2r)^a}{(r+1)^a\bar{v}^b}\left[\frac{\ln\left(\frac{r+1}{2rv}\right)}{r+1-2rv} - \sum_{i=0}^{b-1}\frac{(-\bar{v})^i}{i!}\frac{\partial^i}{\partial v^i}\,\frac{\ln\left(\frac{r+1}{2rv}\right)}{r+1-2rv}\bigg|_{v=1}\right]\,,\end{aligned} \tag{4.307}$$

where we do not need a subtraction for $b=0$. Note, we introduce the symbol $\Rightarrow$ to hint that the factor $2\pi r$ was taken off. The interesting subtractions ($b\in\{1,2\}$) follow for $i\in\{0,1\}$. The corresponding subtraction terms are

$$\frac{\ln\left(\frac{r+1}{2rv}\right)}{r+1-2rv}\bigg|_{v=1} = \frac{\ln\left(\frac{r+1}{2r}\right)}{1-r}\,,\qquad -\bar{v}\,\frac{\partial}{\partial v}\,\frac{\ln\left(\frac{r+1}{2rv}\right)}{r+1-2rv}\bigg|_{v=1} = \frac{2r\ln\left(\frac{r+1}{2r}\right)-1+r}{(1-r)^2}\,. \tag{4.308}$$

The auxiliary conformal moments of the addenda are given by a sum of different non-separable building blocks(cf. 3.314):

$$\Delta^A c_{jk}^{(o,c)} = \sum_{a,b}\Delta^A c_{jk}^{(o,c),ab}\,. \tag{4.309}$$

The integer conformal moments of the individual terms above in terms of the auxiliary polynomials (4.185) read

$$\Delta^A c_{jk}^{(o,c),ab} = \hat{p}_j^{\lambda}(u) \overset{u}{\otimes} {}^A\vec{\mathcal{D}}_{a,b}^{(o,c)} \left[\frac{1}{u^a \bar{v}^b} \frac{L(u,v)}{u-v}\right]^{\text{sub}} \overset{v}{\otimes} \hat{p}_k^{3/2}(v)\,, \tag{4.310}$$

where in case of $A \in \{\pm, \text{pS}\}$ the index is $\lambda = 3/2$ and for $A = \text{G}$ we set $\lambda = 5/2$. By partial integration, we shift the differentiation operator from the building block $[a,b]$ to the auxiliary polynomial $\hat{p}_k^{3/2}(v)$. Therefore,

$$\Delta^A c_{jk}^{(o,c),ab} = \hat{p}_j^{\lambda}(u) \overset{u}{\otimes} \left[\frac{1}{u^a \bar{v}^b} \frac{L(u,v)}{u-v}\right]^{\text{sub}} \overset{v}{\otimes} {}^A\vec{\mathcal{D}}_{a,b}^{\dagger(o,c)} \hat{p}_k^{3/2}(v)\,, \tag{4.311}$$

where ${}^A\vec{\mathcal{D}}_{a,b}^{\dagger(o,c)}$ denotes the adjoint differential operator. For fixed integer values of k, we utilize the imaginary part (4.307) to evaluate the conformal moments numerically by (4.244)

$$\Delta^A c_{jk}^{(o,c),ab} = \widetilde{p}_j^{\lambda}(y) \overset{y}{\otimes} \frac{y^a}{\bar{v}^b} \left[\frac{-\ln(yv)}{1-yv} - \sum_{i=0}^{b-1} \frac{(-\bar{v})^i}{i!} \frac{\partial^i}{\partial v^i} \frac{-\ln(yv)}{1-yv}\bigg|_{v=1}\right] \overset{v}{\otimes} {}^A\vec{\mathcal{D}}_{a,b}^{\dagger(o,c)} \hat{p}_k^{3/2}(v)\,. \tag{4.312}$$

In the rest of this section, we find a analytic solution. From the defining differential equation for Gegenbauer polynomials with index 3/2 given in (C.8) we determine the following differential relation for the auxiliary polynomials (4.185)

$$v\bar{v} \frac{\mathrm{d}^2}{\mathrm{d}v^2} \hat{p}_k^{3/2}(v) = -(k+1)_2\, \hat{p}_k^{3/2}(v)\,. \tag{4.313}$$

In order to express the adjoint differential operator acting on the auxiliary polynomials in (4.185), we use the identities

$$v\bar{v} \frac{\mathrm{d}}{\mathrm{d}v} \hat{p}_k^{3/2}(v) = \frac{(k+1)_2}{2(2k+3)} \hat{p}_{k-1}^{3/2}(v) - \frac{(k+1)_2}{2(2k+3)} \hat{p}_{k+1}^{3/2}(v)\,, \tag{4.314}$$

$$(v\bar{v})^2 \frac{\mathrm{d}}{\mathrm{d}v} \frac{1}{v\bar{v}} \hat{p}_k^{3/2}(v) = \frac{(k+2)_2}{2(2k+3)} \hat{p}_{k-1}^{3/2}(v) - \frac{(k)_2}{2(2k+3)} \hat{p}_{k+1}^{3/2}(v)\,, \tag{4.315}$$

$$(v-\bar{v})v\bar{v} \frac{\mathrm{d}}{\mathrm{d}v} \frac{1}{v\bar{v}} \hat{p}_k^{3/2}(v) = 2k\, \hat{p}_{k-1}^{3/2}(v) + \sum_{l=0}^{k-1} \left[1 + (-1)^{k-l}\right] (2l+3)\, \hat{p}_l^{3/2}(v)\,. \tag{4.316}$$

Applying the previous four identities, we are able to express the differential operator in (4.312) by a finite sum over Gegenbauer polynomials. Therefore, we only need to evaluate the following conformal moments:

$$L_{nk}^{\lambda,a,b} = \hat{p}_n^{\lambda}(u) \overset{u}{\otimes} \left[\frac{1}{u^a \bar{v}^b} \frac{L(u,v)}{u-v}\right]^{\text{sub}} \overset{v}{\otimes} \hat{p}_k^{3/2}(v)\,. \tag{4.317}$$

We can further simplify the considerations, by decomposing the auxiliary polynomial for gluons in terms of quark ones, namely from (4.315)

$$\hat{p}_n^{5/2}(u) = (v\bar{v})^2 \frac{\mathrm{d}}{\mathrm{d}v} \frac{1}{v\bar{v}} \hat{p}_k^{3/2}(v) = \frac{(n+2)_2}{2(2n+3)} \hat{p}_{n-1}^{3/2}(u) - \frac{(n)_2}{2(2n+3)} \hat{p}_{n+1}^{3/2}(u)\,. \tag{4.318}$$

Thus, we reduce the gluonic conformal moments of the non-separable building block $[1,1]$ to quark ones by the identity

$$L_{nk}^{5/2,a,b} = \frac{(n+2)_2}{2(2n+3)} L_{n-1,k}^{3/2,a,b} - \frac{(n)_2}{2(2n+3)} L_{n+1,k}^{3/2,a,b} \,. \tag{4.319}$$

In the next steps, we effectively reduce the number of functions to the building block $[1,1]$. At first, we reduce $[0,1]$ by the identity

$$\left[\frac{1}{\bar{v}} \frac{L(u,v)}{u-v}\right]^{\text{sub}} = v \left[\frac{1}{u\bar{v}} \frac{L(u,v)}{u-v}\right]^{\text{sub}} + \frac{\text{Li}_2(u) - u\zeta(2)}{u\bar{u}} + \frac{\ln \bar{u} \ln v}{u\bar{v}} \,, \tag{4.320}$$

which stems follows from partial faction decomposition. We avoid the extra factor of v by the recurrence relation

$$v\, \hat{p}_k^{\lambda}(v) = \frac{k+1}{2(2k+3)} \hat{p}_{k+1}^{\lambda}(v) + \frac{1}{2} \hat{p}_k^{\lambda}(v) + \frac{k+2}{2(2k+3)} \hat{p}_{k-1}^{\lambda}(v) \,. \tag{4.321}$$

Thus, the corresponding conformal moments are given by the sum

$$L_{jk}^{3/2,0,1} = \frac{k+1}{2(2k+3)} L_{j+1,k}^{3/2,1,1} + \frac{1}{2} L_{jk}^{3/2,1,1} + \frac{k+2}{2(2k+3)} L_{j-1,k}^{3/2,1,1} + \frac{(-1)^k}{(j+1)_2 (k+1)_2} \,. \tag{4.322}$$

Next, we transform the non-separable building block $[0,2]$ to $[1,1]$ by employing the identity

$$\left[\frac{1}{\bar{v}^2} \frac{L(u,v)}{u-v}\right]^{\text{sub}} = \frac{1}{\bar{v}} \left[\frac{1}{u\bar{v}} \frac{L(u,v)}{u-v}\right]^{\text{sub}} - \left[\frac{1}{u\bar{v}} \frac{L(u,v)}{u-v}\right]^{\text{sub}} + \frac{\text{Li}_2(u) - u\zeta(2)}{u\bar{u}\bar{v}} + \frac{\ln \bar{u} \ln v}{u\bar{v}^2} \,. \tag{4.323}$$

The factor $\bar{v}$ is avoided by the finite sum

$$\frac{1}{\bar{v}} \hat{p}_k^{3/2}(v) = 2v C_k^{3/2}(1) + \sum_{l=0}^{k} (2l+3) \frac{(l+1)_2 - (k+1)_2}{(l+1)_2} \hat{p}_l^{3/2}(v) \,. \tag{4.324}$$

As before, we are able to evaluate the conformal moments in terms of the $[1,1]$ ones:

$$\begin{aligned} L_{nk}^{\frac{3}{2},0,2} = &- \sum_{l=0}^{k} (2l+3) \frac{(k-l)(k+l+3)}{(l+1)_2} L_{nl}^{\frac{3}{2},1,1} - L_{nk}^{\frac{3}{2},1,1} - \frac{(j-k)(j+k+3)\Delta S_2\left(\frac{j+1}{2}\right)}{2(j+1)_2} + \frac{1+(-1)^k}{(j+1)_2} \\ &- (k+1)_2 \left[2S_3(j+1) - 2\zeta(3) - \frac{\Delta S_2\left(\frac{j+1}{2}\right)}{2} + (-1)^k \frac{\Delta S_2\left(\frac{k+1}{2}\right)}{2(j+1)_2} + \frac{\zeta(2)}{(1+j)(2+j)}\right] \,. \end{aligned} \tag{4.325}$$

The third case $[1,0]$ can be obtained from the case $[0,1]$. For $\lambda = 3/2$, we utilize the symmetry with respect to the interchange $u \leftrightarrow \bar{v}$. For conformal moments this reflects in the interchange of a and b. From the definition of $L(u,v)$ (3.280) we obtain

$$L_{nk}^{\frac{3}{2},a,b} = (-1)^{n-k} L_{nk}^{\frac{3}{2},b,a} \,. \tag{4.326}$$

The only task still due is the evaluation of the conformal moments $L_{jk}^{3/2,1,1}$ in terms of harmonic sums. The moments were defined in (4.317) as

$$L_{nk}^{\frac{3}{2},1,1} = \hat{p}_n^{3/2}(u) \overset{u}{\otimes} \left[\frac{1}{u\bar{v}} \frac{L(u,v)}{u-v}\right]^{\text{sub}} \overset{v}{\otimes} \hat{p}_k^{3/2}(v)\,.$$

As explained in Sec. 4.6, the unique analytic continuation is ensured by utilizing its imaginary part in (4.256):

$$L_{jk}^{\frac{3}{2},1,1} = \widetilde{p}_j^{3/2}(y) \overset{y}{\otimes} \frac{2}{2-y} \left[\frac{2r}{(1+r)\bar{v}} \frac{\ln\left(\frac{1+r}{2rv}\right)}{1+r-2rv}\right]_{r=\frac{y}{2-y}}^{\text{sub}} \overset{v}{\otimes} \hat{p}_k^{3/2}(v)\,. \tag{4.327}$$

We first solve the integration with respect to v. Therefore, we define the function

$$L_k^{(1,1)}(r) = \int_0^1 \mathrm{d}v \left[\frac{2r}{(1+r)\bar{v}} \frac{\ln\left(\frac{1+r}{2r}\right)}{1+r-2rv}\right]^{\text{sub}} 2v\bar{v}\, C_k^{3/2}(2v-1)\,. \tag{4.328}$$

It is given as a linear combination of subtracted polylogarithms[9]

$$L_k^{(1,1)}(r) = \frac{2-y}{y} \sum_{l=0}^{k} \frac{(-1)^{k-l}\Gamma(k+l+3)}{l!(l+1)!\Gamma(k-l+1)} \left[\frac{\mathrm{Li}_2(\bar{y})}{y^{l+1}}\right]_{y=\frac{2r}{1+r}}^{\text{sub}}\,. \tag{4.329}$$

The remaining step is the evaluation of

$$L_{jk}^{\frac{3}{2},1,1} = \widetilde{p}_j^{3/2}(y) \overset{y}{\otimes} \frac{2}{2-y} L_k^{(1,1)}\left(\frac{y}{2-y}\right)\,. \tag{4.330}$$

With the help of the Mellin moments (4.249), the result reads

$$L_{jk}^{\frac{3}{2},1,1} = -(-1)^k \frac{(j+1)_2\, \Delta S_2\left(\frac{j+1}{2}\right) - (k+1)_2\, \Delta S_2\left(\frac{k+1}{2}\right)}{2(j-k)(j+k+3)}\,, \tag{4.331}$$

where we utilized (4.297). This formula is valid also for complex valued k and it is finite at the point $j=k$. Due to the fact, that the conformal moments of the addenda stem from subtracted contributions, they are numerically less important. In the limit $j\to\infty$ or $k\to\infty$ they have the asymptotic behavior $1/j^2$ or $1/k^2$, respectively.
We are now in the position to express the building block $[0,2]$ in terms of $[1,1]$. Thereby, the finite sum over l in (4.325) simplifies to

$$\sum_{l=0}^{k} \frac{(-1)^l(2l+1)\left[\Delta S_2\left(\frac{j+1}{2}\right) - \Delta S_2\left(\frac{l}{2}\right)\right]}{4(j-l+1)(j+l+2)}\,. \tag{4.332}$$

[9] We used $\ln(yv) = \lim_{\epsilon\to 0} \frac{\mathrm{d}}{\mathrm{d}\epsilon}(yv)^\epsilon$.

Furthermore, the case $[2,0]$ follows from the symmetry relation (4.326). The respective sum with upper limit n is transformed in one with upper limit k by employing the identity

$$\begin{aligned}(-1)^n\left[S_3(k+1)-\zeta(3)\right]-(-1)^n\sum_{l=0}^{n}\frac{(-1)^l(2l+1)\left[\Delta S_2\left(\frac{k+1}{2}\right)-\Delta S_2\left(\frac{l}{2}\right)\right]}{4(k-l+1)(k+l+2)} \\ =\frac{\left[S_2\left(\frac{n+1}{2}\right)-S_2\left(\frac{n}{2}\right)\right]\left[S_1(n+1)-S_1(k+1)\right]+4(-1)^n\left[S_{-2,1}(n+1)+\frac{5\zeta(3)}{8}\right]}{2} \\ +\frac{S_3\left(\frac{n+1}{2}\right)-S_3\left(\frac{n}{2}\right)}{8}-\sum_{l=0}^{k}\frac{(2l+1)\left[\Delta S_2\left(\frac{n+1}{2}\right)-\Delta S_2\left(\frac{l}{2}\right)\right]}{4(n-l+1)(n+l+2)}+\frac{\Delta S_2\left(\frac{k+1}{2}\right)-\Delta S_2\left(\frac{n+1}{2}\right)}{4(n-k)}\,.\end{aligned} \tag{4.333}$$

The conformal moments for gluons follow from (4.319). We summarize the imaginary parts and conformal moments of the non-separable building blocks in table 4.7. To shorten the notation, we introduce the following notations for harmonic sums:

$$\Delta S_2\left(\frac{j+1}{2},\frac{k+1}{2}\right)=\frac{\Delta S_2\left(\frac{j+1}{2}\right)-\Delta S_2\left(\frac{k+1}{2}\right)}{2(j-k)(j+k+3)}\,,\quad \Delta S_2\left(\frac{j+1}{2},\frac{j+1}{2}\right)=-\frac{\Delta S_3\left(\frac{j+1}{2}\right)}{2j+3}\,. \tag{4.334}$$

$G(u)$	$\frac{1}{2\pi r}\Im\mathrm{m}G\left(\frac{r+1}{2r}\right)$	$\langle G(u)\rangle_j^\lambda$
$\left[\frac{1}{u\bar v}\,\frac{L(u,v)}{u-v}\right]^{\text{sub}}$	$\frac{-2r}{1+r}\,\frac{\frac{2r}{1-r}\ln\frac{1+r}{2r}+\frac{\ln v}{\bar v}}{1+r-2rv}$	$-(-1)^k(k+1)_2\,\Delta S_2\left(\frac{j+1}{2},\frac{k+1}{2}\right)-\frac{(-1)^k}{2}\Delta S_2\left(\frac{j+1}{2}\right)$ $\frac{(-1)^k(k+1)_2}{2}\left[\frac{(j)_2}{2j+3}\Delta S_2\left(\frac{j+2}{2},\frac{k+1}{2}\right)-\frac{(j+2)_2}{2j+3}\Delta S_2\left(\frac{j}{2},\frac{k+1}{2}\right)\right]$ $+\frac{(-1)^k}{2}\Delta S_2\left(\frac{j+1}{2}\right)-(-1)^k\,\frac{3(j+1)_2+2}{[(j+1)_2]^2}$
$\left[\frac{1}{\bar v}\,\frac{L(u,v)}{u-v}\right]^{\text{sub}}$	$-\frac{\frac{2r}{1-r}\ln\frac{1+r}{2r}+\frac{\ln v}{\bar v}}{1+r-2rv}$	$\frac{(-1)^k(k+1)_2}{2}\left[\frac{-k-3}{2k+3}\Delta S_2\left(\frac{j+1}{2},\frac{k+2}{2}\right)+\frac{-k}{2k+3}\Delta S_2\left(\frac{j+1}{2},\frac{k}{2}\right)\right.$ $\left.+\Delta S_2\left(\frac{j+1}{2},\frac{k+1}{2}\right)\right]+\frac{(-1)^k}{(j+1)_2(k+1)_2}$
$\left[\frac{1}{\bar v^2}\,\frac{L(u,v)}{u-v}\right]^{\text{sub}}$	$\frac{\frac{2r}{1-r}\left[\frac{2r}{1-r}\ln\frac{1+r}{2r}-1\right]-\frac{\ln v+\bar v}{\bar v^2}}{1+r-2vr}$	$a_{jk}\left[S_3(j+1)-\zeta(3)-\sum_{l=0}^{k}\frac{(-1)^l(2l+1)}{2}\Delta S_2\left(\frac{j+1}{2},\frac{l}{2}\right)\right]$ $-\frac{(-1)^k(k+1)_2}{2}\left[2\Delta S_2\left(\frac{j+1}{2},\frac{k+1}{2}\right)-\frac{\Delta S_2\left(\frac{j+1}{2}\right)-\Delta S_2\left(\frac{k+1}{2}\right)}{k+2}\right.$ $\left.-\frac{(j+1)_2-1}{(j+1)_2}\left(\Delta S_2\left(\frac{k+1}{2}\right)-\frac{2}{(k+1)_2}\right)\right]$

Table 4.7.: Imaginary parts of the subtracted non-separable building blocks for quarks (upper lines) and gluons (lower lines). We use the notation (4.334) with $a_{jk}=2[(j+1)_2-(k+1)_2]$.

4.6.6. NLO corrections

The hard scattering amplitudes for DVMP in LO approximation of perturbation theory were introduced in Sec. 3.3.6 in momentum fraction representation. The result was organized to suit the derivation of corresponding imaginary parts and its conformal moments. Utilizing the method of Sec. 4.6, we ensure the unique analytic continuation from integer n to complex

valued moments j. This replaces the established procedures for the conformal moments of separable building blocks and permits the derivation of the non-separable ones (Sec. 4.6.5). The occurrence of such moments is a genuine feature of DVMP, which was not present in the already established DVCS analysis.
In this section, we present the imaginary parts of the NLO hard scattering amplitudes through the variable r and the corresponding conformal moments.

4.6.6.1. Flavor non-singlet channel

In the flavor non-singlet channel, we had to introduce a signature to ensure the unique analytic continuation of the conformal moments. Consequently, the momentum fraction is $x \geq \xi$ and the terms only possess poles at $u=1$ and u-cuts along $[1,\infty]$. Utilizing the result from this section, the imaginary parts of the flavor non-singlet channel (3.318) are

$$\begin{aligned}
{}^{\mathrm{q}}t^{(1,\mathrm{F})}(r,v) &= \left[\ln\frac{\mathcal{Q}^2}{\mu_{\mathrm{F}}^2}+\frac{1}{2}\ln\bar{v}+1\right]\left[\frac{3}{2}\delta(1-r)+\left\{\frac{1}{1-r}\right\}_+\right]\frac{1}{\bar{v}}+\left\{\frac{\frac{3}{4}+\ln\frac{1-r}{2r}}{1-r}\right\}_+\frac{1}{\bar{v}} \\
&\quad+\left[\left(\ln\frac{\mathcal{Q}^2}{\mu_{\varphi}^2}+\frac{1}{2}\ln\bar{v}+1\right)\delta(1-r)+\frac{1}{2}\left\{\frac{1}{1-r}\right\}_+\right]\frac{3+2\ln\bar{v}}{2\bar{v}} \\
&\quad-\left[\frac{23}{3}+\frac{\bar{v}}{2v}\ln\bar{v}\right]\frac{\delta(1-r)}{\bar{v}}+\frac{1}{1+r}\,\frac{1}{2\bar{v}}\,, \qquad (4.335a)\\
{}^{\mathrm{q}}t^{(1,\beta)}(r,v) &= \left[\ln\frac{\mathcal{Q}^2}{\mu_{\mathrm{R}}^2}-\frac{5}{3}+\ln\bar{v}\right]\frac{\delta(1-r)}{2\bar{v}}+\left\{\frac{1}{1-r}\right\}_+\frac{1}{2\bar{v}}\,, \qquad (4.335b)\\
{}^{\mathrm{q}}t^{(1,\mathrm{G})}(r,v) &= \left\{\frac{1}{1-r}\right\}_+\frac{\ln v}{\bar{v}^2}-\frac{2\ln\frac{1+r}{2r}-1+r}{(1-r)^2\,\bar{v}} \qquad (4.335c)\\
&\quad+\left[2\zeta(2)-\frac{7}{3}+\frac{v-\bar{v}}{\bar{v}}\left[\mathrm{Li}_2(\bar{v})-\mathrm{Li}_2(v)+\zeta(2)\right]+\frac{\ln v-\bar{v}}{\bar{v}}\right]\frac{\delta(1-r)}{\bar{v}}+\Delta^{\mathrm{q}}t^{(1,\mathrm{G})}(r,v)\,.
\end{aligned}$$

The imaginary part of the addendum (3.318d) can be written in a compact form as

$$\Delta^{\mathrm{q}}t^{(1,\mathrm{G})}(r,v)=-\left[\frac{v-\bar{v}}{\bar{v}^2}+\frac{\partial}{\partial v}\frac{v\,\partial}{\partial v}\right]\left[\frac{2r\bar{v}\ln\frac{1+r}{2r}+(1-r)\ln v}{(1-r)(1+r-2rv)}\right]+\frac{2r\ln\frac{1+r}{2r}-1+r}{(1-r)^2\bar{v}}. \qquad (4.335d)$$

With the imaginary parts, we are able to determine the conformal moments of (3.318) as

$$
\begin{aligned}
{}^{\mathrm{q}}c_{jk}^{(1,\mathrm{F})} &= \left[-\ln\frac{\mathcal{Q}^2}{\mu_{\mathrm{F}}^2} + S_1(j+1) + S_1(k+1) - 1 - \frac{1}{2(j+1)_2} - \frac{1}{2(k+1)_2}\right]\frac{\gamma_j^{(0,\mathrm{F})}}{2} \\
&\quad - \frac{23}{6} + \frac{3(j+1)_2+1}{2[(j+1)_2]^2} + \{j \leftrightarrow k, \mu_{\mathrm{F}} \to \mu_\varphi\}\,, \qquad (4.336a)\\
{}^{\mathrm{q}}c_{jk}^{(1,\beta)} &= \frac{1}{4}\ln\frac{\mathcal{Q}^2}{\mu_{\mathrm{R}}^2} - S_1(j+1) - \frac{5}{12} + \frac{1}{2(j+1)_2} + \{j \leftrightarrow k\}\,, \qquad (4.336b)\\
{}^{\mathrm{q}}c_{jk}^{(1,\mathrm{G})} &= \left[2S_1(j+1) - \frac{1}{(j+1)_2}\right]\left[1 + (-1)^k - (-1)^k(k+1)_2\frac{\Delta S_2\left(\frac{k+1}{2}\right)}{2}\right] + \zeta(2) - \frac{7}{6} \\
&\quad + \left[(-1)^k\,\mathbb{S}_3(k+1) + \frac{(-1)^k\,\Delta S_2\left(\frac{k+1}{2}\right)}{2(k+1)_2} - S_3(k+1) + \zeta(3) - \frac{(k+1)_2 - 1}{2[(k+1)_2]^2}\right]2(k+1)_2 \\
&\quad - \frac{2\left[1+(-1)^k\right]\left[(k+1)_2+1\right]}{\left[(k+1)_2\right]^2} - \frac{(-1)^{j+k}}{(j+1)_2(k+1)_2} + \Delta^{\mathrm{q}}c_{jk}^{(1,\mathrm{G})} + \{j \leftrightarrow k\}\,, \qquad (4.336c)
\end{aligned}
$$

where

$$
\gamma_j^{(0,F)} = 4S_1(j+1) - 3 - \frac{2}{(j+1)_2} \qquad (4.336d)
$$

is apart from the color factor the anomalous dimension (D.24). We employed the shorthand notation

$$
\mathbb{S}_3(n) = \frac{S_3\left(\frac{n}{2}\right) - S_3\left(\frac{n-1}{2}\right)}{8} + \frac{\left[S_2\left(\frac{n}{2}\right) - S_2\left(\frac{n-1}{2}\right)\right]S_1(n)}{2} - 2(-1)^n\left[S_{-2,1}(n) + \frac{5\zeta(3)}{8}\right]\,. \qquad (4.336e)
$$

The function above is finite for $n=0$ and behaves asymptotically $1/n^4$ for $n\to\infty$. The conformal moments of the addendum (3.318d) read for complex j and non-negative integer k as

$$
\begin{aligned}
\Delta^{\mathrm{q}}c_{jk}^{(1,\mathrm{G})} &= a_{jk}\left[S_3(j+1) - \zeta(3) + \frac{(-1)^k(k+1)\Delta S_2\left(\frac{j+1}{2},\frac{k+1}{2}\right)}{2} - \sum_{l=0}^{k}\frac{(2l+1)(-1)^l\Delta S_2\left(\frac{j+1}{2},\frac{l}{2}\right)}{2}\right] \\
&\quad + \frac{(-1)^k(k+1)_2}{2}\sum_{b=0}^{2}\frac{(-1)^b(2k+3b)\left[4+3b(3-b)+2kb+2(k+1)^2\right]\Delta S_2\left(\frac{j+1}{2},\frac{k+b}{2}\right)}{[3+(-1)^b](2k+3)} \\
&\quad + \frac{(-1)^k\left[(j+1)_2 - 1\right]\left[(k+1)_2\,\Delta S_2\left(\frac{k+1}{2}\right) - 2\right]}{2(j+1)_2} - \frac{2(-1)^k}{(j+1)_2(k+1)_2}\,, \qquad (4.336f)
\end{aligned}
$$

where we use the abbreviation $a_{jk} = 2(j-k)(j+k+3)$. For the addendum with interchanged $j \leftrightarrow k$ we employ identity (4.333) and obtain

$$\begin{aligned}\Delta^{\mathrm{q}}c_{kj}^{(1,\mathrm{G})} = a_{kj}(-1)^j \Bigg[\mathbb{S}_3(j+1) - \frac{S_1(k+1)\Delta S_2\left(\frac{j+1}{2}\right)}{2} - \sum_{l=0}^{k} \frac{(2l+1)\Delta S_2\left(\frac{j+1}{2}, \frac{l}{2}\right)}{2} \Bigg] \\ - \frac{(-1)^j (k+1)_2}{2} \sum_{b=0}^{2} \frac{(2k+3b)\left[4+3b(3-b)+2kb+2(k+1)^2\right]\Delta S_2\left(\frac{j+1}{2}, \frac{k+b}{2}\right)}{[3+(-1)^b](2k+3)} \\ - \left[(k+1)^2+2+\frac{(j+1)_2}{(k+1)_2}\right]\frac{(-1)^j \Delta S_2\left(\frac{j+1}{2}\right)}{2} - \frac{(-1)^j (k+1)\Delta S_2\left(\frac{k+1}{2}\right)}{2} + \frac{(-1)^j}{(k+1)_2}\,.\end{aligned} \tag{4.336g}$$

The conformal moments ${}^{\mathrm{q}}c_{jk}^{(1,\mathrm{F})}$, ${}^{\mathrm{q}}c_{jk}^{(1,\beta)}$, and $\Delta^{\mathrm{q}}c_{jk}^{(1,\mathrm{G})}$ do not inherit a signature, whereas the $(-1)^j$ factors for complex valued j in ${}^{\mathrm{q}}c_{jk}^{(1,\mathrm{G})}$ and $\Delta^{\mathrm{q}}c_{kj}^{(1,\mathrm{G})}$ must be replaced by $-\sigma$, to ensure the uniqueness of the analytic continuation.

4.6.6.2. Pure singlet quark channel

The hard scattering amplitudes at NLO of perturbation theory are introduced in Sec. 3.3.6.7. Since the pure singlet contribution is antisymmetric under the transformations $u \to \bar{u}$ and $\{u \to \bar{u},\, v \to \bar{v}\}$ and symmetric under $v \to \bar{v}$, the introduction of a signature factor is not necessary. Therefore, the conformal moments of the GPD and DA are odd and even, respectively. The imaginary parts of (3.321) are

$$\begin{aligned}{}^{\mathrm{pS}}t^{(1,\mathrm{F})}\Big(r, v\Big|\tfrac{\mathcal{Q}^2}{\mu_{\mathrm{F}}^2}\Big) &= \left[\ln\frac{\mathcal{Q}^2}{\mu_{\mathrm{F}}^2} + \ln(v\bar{v}) + \ln\frac{1-r}{1+r} - 1\right]\frac{1}{r(1+r)v\bar{v}} - \frac{\ln\frac{1+r}{2r}}{(1+r)v\bar{v}} \\ &\quad + \left[\frac{1}{2v\bar{v}} + \frac{\ln v}{\bar{v}} + \frac{\ln\bar{v}}{v}\right]\frac{1}{1+r} + \Delta^{\mathrm{pS}}t^{(1,\mathrm{F})}(r,v)\,,\end{aligned} \tag{4.337a}$$

$$\Delta^{\mathrm{pS}}t^{(1,\mathrm{F})}(r,v) = \frac{1}{v\bar{v}}\frac{\partial}{\partial v}v\bar{v}\left[\frac{2rv}{1+r}\,\frac{\ln\frac{1+r}{2rv}}{1+r-2rv}\right]. \tag{4.337b}$$

The corresponding conformal moments are

$$\begin{aligned}{}^{\mathrm{pS}}c_{jk}^{(1,\mathrm{F})} &= \left[-\ln\frac{\mathcal{Q}^2}{\mu_{\mathrm{F}}^2} + 2S_1(j+1) + 2S_1(k+1) - 1\right]\frac{{}^{\mathrm{G}\Sigma}\gamma_j^{(0,\mathrm{F})}}{j+3} \\ &\quad - \left[\frac{1}{2} + \frac{1}{(j+1)_2} + \frac{1}{(k+1)_2}\right]\frac{2}{(j+1)_2} + \Delta^{\mathrm{pS}}c_{jk}^{(1,\mathrm{F})}\,,\end{aligned} \tag{4.338a}$$

$$\Delta^{\mathrm{pS}}c_{jk}^{(1,\mathrm{F})} = \frac{(k)_4\left[\Delta S_2\left(\frac{j+1}{2}, \frac{k}{2}\right) - \Delta S_2\left(\frac{j+1}{2}, \frac{k+2}{2}\right)\right]}{2(2k+3)}, \tag{4.338b}$$

where we extracted the color factor from the anomalous dimension (D.25c)

$$\frac{{}^{\mathrm{G}\Sigma}\gamma_j^{(0,\mathrm{F})}}{j+3} = -\frac{4+2(j+1)_2}{(j)_4}, \tag{4.338c}$$

in the gluon-quark channel. Expressing the addendum (3.321b) in terms of the non-separable building block $[1,1]$ in (3.313a) we use the identity for the adjoint differential operator (4.315) and the conformal moments in table 4.7. An artificial δ_{k0} term drops out in the final expression.

4.6.6.3. Gluon-quark channel

As the hard scattering amplitude of the pure singlet quark channel, also the gluon-quark channel has a definite symmetry. Therefore, we abstain from the introduction of a signature. The imaginary part of the part proportional to C_A (3.324a) is

$$\begin{aligned}
{}^{\mathrm{G}}t^{(1,\mathrm{A})}(r,v) = {}& \left[\ln\frac{\mathcal{Q}^2}{\mu_\mathrm{F}^2} + \frac{3\ln(v\bar v)}{4} - \frac{3}{2}\right]\left[\left\{\frac{1}{1-r}\right\}_+ - \delta(1-r) + \frac{1-r}{(1+r)^2}\right]\frac{1}{2v\bar v} \\
&+ \left[\left\{\frac{\ln\frac{1-r}{2r}}{1-r}\right\}_+ - \frac{(1+3r)\ln\frac{1-r}{2r}}{(1+r)^2} + \frac{3}{1+r} + \frac{\ln(v\bar v)}{2(1+r)}\right]\frac{1}{2v\bar v} \\
&+ \left[\frac{2\ln\frac{1-r}{1+r}}{1+r} - \frac{2r\ln\frac{1+r}{2r}}{1-r^2} + [2+\ln(v\bar v)]\,\frac{r}{2(1+r)^2}\right]\frac{1}{2v\bar v} \\
&+ \left[1+\zeta(2) - \frac{v^2\ln v + \bar v^2\ln\bar v}{2v\bar v}\right]\frac{\delta(1-r)}{4v\bar v} + \Delta^{\mathrm{G}}t^{(1,\mathrm{A})}(r,v)\,,
\end{aligned} \tag{4.339a}$$

and the one of the part proportional to C_F (3.324b) is

$$\begin{aligned}
{}^{\mathrm{G}}t^{(1,\mathrm{F})}(r,v) = {}& \left[\ln\frac{\mathcal{Q}^2}{\mu_\mathrm{F}^2}\delta(1-r) + \ln\frac{\mathcal{Q}^2}{\mu_\mathrm{F}^2}\,\frac{2r}{(1+r)^2} + \frac{3-2v\ln v - 2\bar v\ln\bar v}{2}\right. \\
&\left.\times\left(\left\{\frac{1}{1-r}\right\}_+ - \frac{1}{1+r}\right) - \frac{35}{4}\delta(1-r) + \frac{2r\ln\frac{1-r}{2r} - 2r}{(1+r)^2}\right]\frac{1}{4v\bar v} \\
&+ \left[\ln\frac{\mathcal{Q}^2}{\mu_\varphi^2}\delta(1-r) + \frac{1}{2}\left\{\frac{1}{1-r}\right\}_+ + \frac{1+2\ln\bar v}{4}\delta(1-r) - \frac{1}{2(1+r)}\right]\frac{3+2\ln\bar v}{2\bar v} \\
&+ \left[\frac{v^2\ln v + \bar v^2\ln\bar v}{4v\bar v} - \frac{(\bar v - v)\,[\mathrm{Li}_2(v) - \mathrm{Li}_2(\bar v)] + \zeta(2)}{2}\right]\frac{\delta(1-r)}{2v\bar v} + \Delta^{\mathrm{G}}t^{(1,\mathrm{F})}(r,v)\,.
\end{aligned} \tag{4.339b}$$

We employed the symmetry under $r \to -r$ (or $u \to \bar u$) to express the Dirac function $\delta(1+r)$ originating from the remaining $u = 0$ pole,

$$\frac{\ln\bar u}{u^2} \quad\Rightarrow\quad -\frac{2r}{(1+r)^2} - \delta(1+r) \quad\Rightarrow\quad -\frac{2r}{(1+r)^2} - \delta(1-r)\,.$$

The imaginary parts of the addenda (3.323a) and (3.323b) are

$$\Delta^{\mathrm{G}}t^{(1,\mathrm{A})}(r,v) = \frac{1}{4v\bar v}\frac{\partial}{\partial v}\frac{2rv(\bar v - v)}{1+r}\left[\frac{\ln\frac{1+r}{2rv}}{1+r-2rv} - \frac{\ln\frac{1+r}{2r}}{1-r}\right], \tag{4.339c}$$

$$\Delta^{\mathrm{G}}t^{(1,\mathrm{F})}(r,v) = \frac{1}{2}\left[\frac{\partial^2}{\partial v^2} - \frac{2}{v\bar v}\right]\frac{rv}{1+r}\left[\frac{\ln\frac{1+r}{2rv}}{1+r-2vr} - \frac{\ln\frac{1+r}{2r}}{1-r}\right], \tag{4.339d}$$

respectively. The corresponding conformal moments read

$$
\begin{aligned}
{}^{\mathrm{G}}c_{jk}^{(1,\mathrm{A})} &= \left[-\ln\frac{\mathcal{Q}^2}{\mu_{\mathrm{F}}^2} + S_1(j+1) + \frac{3}{2}S_1(k+1) + \frac{1}{2} + \frac{1}{(j+1)_2}\right]\frac{{}^{\mathrm{GG}}\gamma_j^{(0,\mathrm{A})}}{2} \\
&\quad - \frac{3\left[2S_1(j+1) + S_1(k+1) - 6\right]}{j(j+3)} + \frac{8 + 4\zeta(2) - (k+1)_2\,\Delta S_2\left(\frac{k+1}{2}\right)}{8} \\
&\quad - \frac{\Delta S_2\left(\frac{j+1}{2}\right)}{2} - \frac{10(j+1)_2 + 4}{[(j+1)_2]^2} + \Delta^{\mathrm{G}}c_{jk}^{(1,\mathrm{A})}\,, \qquad (4.340a) \\
{}^{\mathrm{G}}c_{jk}^{(1,\mathrm{F})} &= \left[-\ln\frac{\mathcal{Q}^2}{\mu_\varphi^2} + S_1(j+1) + S_1(k+1) - \frac{3}{4} - \frac{1}{2(k+1)_2} - \frac{1}{(j+1)_2}\right]\frac{\gamma_k^{(0,\mathrm{F})}}{2} \\
&\quad + \left[-\ln\frac{\mathcal{Q}^2}{\mu_{\mathrm{F}}^2} + 3S_1(j+1) - \frac{1}{2} + \frac{2S_1(j+1) - 1}{(k+1)_2} - \frac{1}{(j+1)_2}\right]\frac{j+3}{2}\,\frac{{}^{\Sigma\mathrm{G}}\gamma_j^{(0,n_f)}}{2} \\
&\quad - \left[35 - [(k+1)_2 + 2]\,\Delta S_2\Big(\frac{k+1}{2}\Big) - \frac{4}{[(k+1)_2]^2}\right]\frac{1}{8} \\
&\quad + \left[\frac{[(k+1)_2 + 2]\,S_1(j+1)}{(k+1)_2} + 1\right]\frac{1}{(j+1)_2} + \Delta^{\mathrm{G}}c_{jk}^{(1,\mathrm{F})}\,, \qquad (4.340b)
\end{aligned}
$$

where $\gamma_k^{(0,\mathrm{F})}$ is defined in (D.24). Moreover,

$$
{}^{\Sigma\mathrm{G}}\gamma_j^{(0,N_{\mathrm{f}})} = -\frac{4 + 2(j+1)_2}{(j+1)_3} \qquad (4.340c)
$$

can be read off from (D.25b), and

$$
{}^{\mathrm{GG}}\gamma_j^{(0,\mathrm{A})} = 4S_1(j+1) + \frac{4}{(j+1)_2} - \frac{12}{j(j+3)} \qquad (4.340d)
$$

is the C_{A} proportional part of the anomalous dimension (D.25d) in the gluon channel. The conformal moments of the addenda follow from their imaginary parts (4.339c,4.339d), namely

$$
\begin{aligned}
\Delta^{\mathrm{G}}c_{jk}^{(1,\mathrm{A})} &= \left[-\frac{\Delta S_2\left(\frac{j+1}{2}\right)}{2(k+1)_2} - \frac{(k-1)\Delta S_2\left(\frac{j+1}{2},\frac{k}{2}\right) + (k+4)\,\Delta S_2\left(\frac{j+1}{2},\frac{k+2}{2}\right)}{2k+3}\right]\frac{(k)_4}{4} \\
&\quad + \frac{(k+1)_2\,S_1(k+1) - 2}{(j+1)_2(k+1)_2}\,, \qquad (4.340e) \\
\Delta^{\mathrm{G}}c_{jk}^{(1,\mathrm{F})} &= \left[\frac{\Delta S_2\left(\frac{j+1}{2}\right)}{2(k+1)_2} - \frac{(k-1)_2\,\Delta S_2\left(\frac{j+1}{2},\frac{k}{2}\right) - (k+3)_2\,\Delta S_2\left(\frac{j+1}{2},\frac{k+2}{2}\right)}{2(2k+3)}\right]\frac{(k+1)_2[(k+1)_2+2]}{4} \\
&\quad - \frac{(k+1)_2 + 2}{2(j+1)_2(k+1)_2}\,, \qquad (4.340f)
\end{aligned}
$$

where we eliminated the finite sum originating from the identity (4.316) in $\Delta^{\mathrm{G}}c_{jk}^{(1,\mathrm{A})}$.

5

Probability theory as extended logic

The aim of physics is to describe phenomena observed in nature using mathematical models. We distinguish between models and theories. While the latter are based on a few fundamental axioms, the former allows for many variations to study phenomenology. To test, we calculate on the one hand new theoretical predictions and design experiments to test them. On the other side, we try to explain new observations applying the established theory. This interaction between theory and experiment is the essence of physics. With the growing number of observations a theory describes, our confidence in the theory increases.
The measurement of a certain quantity can not be performed with arbitrary precision. Therefore, we need to employ probability theory to connect experiment and theory. In general, the theory contains free parameters, which have to be estimated by experiments. When calculating predictions, we want to propagate these uncertainties. Especially in the rise of a physical theory, there are several concurring models and we have to evaluate the best model. These are the main problems in physics, where probability theory is needed: Parameter estimation, error propagation and hypothesis test.
For these three tasks, there are well known simplified procedures. To estimate parameters there is maximum likelihood and minimum χ^2 criterion. The parameter uncertainties are given by the Hesse matrix. For error propagation, the covariance matrix together with model linearization is used. To compare two models the minimal value of χ^2 divided by the number of degrees of freedom or p-values are popular. However, all these methods are only valid under certain conditions, or their result is similar to the correct result by coincidence. This also explains their popularity. In simple cases they give similar results and in addition, they are easy to implement.
Since probability theory is such an essential part of physics, it deserves a detailed study, in order to replace the ad hoc procedures by the correct result. The advantage of the approach of probability theory in this work is, that all problems are solved starting from basic principles and the assumptions in the derivations are clearly stated.
As we are going to show, the parameter estimation problem in this work does not meet the conditions to allow the ad hoc procedures. Using probability theory always leads to the correct result. Nonetheless, the ad hoc procedures are special cases of probability theory. In the derivation of these cases, we clearly see the assumptions that are necessary for these procedures and reveal logical inconsistencies.
In this chapter, we give a detailed introduction to probability theory. We first derive the sum and product rule, which are sufficient to solve all problems in probability theory. In the following, we will calculate the solutions to the three main problems stated above.

The Gaussian distribution plays an important role in the analysis of experimental data, therefore we explain in detail its properties and the consequence of its use. Using this results, we solve four examples. Finally, we give a detailed derivation of the ad hoc procedures and their assumptions in the appendix.
This chapter contains general knowledge given on various references. For the derivation of the sum and product rule, we follow the original work in [Cox61]. The way of introducing probability theory is analogous to the work in [Jay03]. However, we altered it, to be closer to physics. The basic examples are well known problems, solved in uncountable variations. The rest of the chapter is a compilation of [Jay03, Gre05, D'A03]. The way the solutions are presented perfectly fits to the parameter estimation problem. In all cases, we present more detailed calculations and give the basic ideas, in a way, that cannot be found in any of these books. The advanced examples besides the comparison of two means are original work.

5.1. Deductive and plausible reasoning

In order to develop probability theory, we take a close look on the type of reasoning, that leads to scientific discoveries. We make certain observations in nature and search for common causes of these phenomena to formulate a model. Let us take Newton's first law as an example: "If no force affects an object, it stays at rest or moves with constant velocity". The law consists of the two propositions:

$$A \equiv \text{"No force affects the object."}$$
$$B \equiv \text{"The object moves with constant velocity."}$$

Knowing, that one of the propositions is true, the other one is equally true. If no force affects the object ($A = \text{true}$), then it moves with constant velocity ($B = \text{true}$). The inverse statement is: If the object does not move with constant velocity ($B = \text{false}$), then a force affects the object ($A = \text{false}$).
Reasoning of this type is called a strong syllogism. The major premise is Newton's first law. Then a minor premise is proposed and under the consideration of the major premise, we reach a conclusion. Following this notation, the first reasoning reads:

$$\begin{array}{ll} \text{major premise:} & \text{if } A \text{ is true, then } B \text{ is true} \\ \text{minor premise:} & A \text{ is true} \\ \text{conclusion:} & B \text{ is true} \end{array} \tag{5.1}$$

The second reasoning is the inverse statement

$$\begin{array}{ll} \text{major premise:} & \text{if } A \text{ is true, then } B \text{ is true} \\ \text{minor premise:} & B \text{ is false} \\ \text{conclusion:} & A \text{ is false} \end{array} \tag{5.2}$$

This deductive reasoning is the preferred type of reasoning.
However, the strong syllogism is not always possible and we have to fall back on a weaker

form. In the process of discovering that law, Newton had to realize, that he had to consider an object that moves without any friction. The ideal situation of the law is not the most frequent observation in nature. Therefore, in the beginning, Newton had only evidence for a weaker syllogism of the following type: If the object moves with a constant velocity, it is more plausible, that no force affects the object. In order to turn this into the strong syllogism, he had to make sure, that no force compensates for the friction. In the notation in terms of syllogisms, we have

major premise:	if A is true, then B is true	
minor premise:	B is true	
conclusion:	A becomes more plausible	(5.3)

Another weak syllogism is: If a force affects the object, it becomes less plausible that the object moves with constant velocity. We write

major premise:	if A is true, then B is true	
minor premise:	A is false	
conclusion:	B becomes less plausible	(5.4)

This weak syllogism is the starting point of all discoveries [Pól45, Pól54]. Intuition tells us there is a strong syllogism, but we have only evidence for the weak form.
Only after further reasoning and the evaluation of new evidence, we might be able to prove the strong form of the syllogism. For Newton's first law, we have to prove, that if B is true, then A has to be true. Thus, we perform an experiment, in which the friction between the object and the ground is reduced as much as possible. A series of such experiments will increase our knowledge and prove the validity of Newton's law to a certain accuracy depending on the type of experiment. In order to compare the new evidence with the situation before the experiment, we need to evaluate the degree of plausibility.

5.2. Rules of plausible reasoning

In this section, we develop probability theory to evaluate the degree of plausibility of propositions. After a short recapitulation of the Boolean algebra we propose a series of desiderata, the theory has to fulfill. These desiderata directly lead to two quantitative rules, which are sufficient to solve all problems in probability theory.

5.2.1. Symbolic logic

The mathematical language to deal with propositions is symbolic logic, or Boolean algebra. A proposition A can only have the two possible true values: "true" (T) or "false" (F). Several

propositions can be connected by three basic logical operations. The denial of a proposition A, indicated by a bar:

$$\overline{A} = A \text{ is false.} \tag{5.5}$$

The proposition that both A and B are true is called logical product, conjunction, or AND. It is represented by the symbol

$$AB \equiv \text{“both } A \text{ and } B \text{ are true”}. \tag{5.6}$$

The logical sum, disjunction, or OR denotes the proposition that at least one of the propositions A and B is true:

$$A + B \equiv \text{“}A \text{ or } B \text{ is true or both a true”}. \tag{5.7}$$

Instead of considering the logical sum and product, we might also consider its inverse operations $\overline{A + B}$ and $\overline{AB}$. The following truth table contains the true values of the inverse operations and the operations with inverted propositions:

A, B	T,T	T,F	F,T	F,F
$\overline{A + B}$	F	F	F	T
$\overline{AB}$	F	T	T	T
$\overline{A} + \overline{B}$	F	T	T	T
$\overline{A}\,\overline{B}$	F	F	F	T

The propositions with the same true values are equal. Therefore, we deduce the two identities

$$\overline{AB} = \overline{A} + \overline{B}, \qquad \overline{A + B} = \overline{A}\,\overline{B}. \tag{5.8}$$

The logical product and sum of a proposition with itself is

$$\begin{aligned} AA &= A, \\ A + A &= A. \end{aligned} \tag{5.9}$$

The complete Boolean algebra is defined by the following identities:

Idempotence:	$AA = A$ $A + A = A$
Commutativity:	$AB = BA$ $A + B = B + A$
Associativity:	$A(BC) = (AB)C$ $A + (B + C) = (A + B) + C$
Distributivity:	$A(B + C) = AB + AC$ $A + BC = (A + B)(A + C)$
Duality:	$\overline{AB} = \overline{A} + \overline{B}$ $\overline{A + B} = \overline{A}\,\overline{B}$

Table 5.1.: The Boolean algebra.

We have defined three logical operations, the denial, the logical product and sum. Two of these operations are sufficient to generate all possible logical operations as shown in appendix E.1. It is even possible to reduce it to one operation, either NAND or NOR.
Before proposing the desiderata of the theory, we first introduce a convenient notation for the weak syllogism. We denote the major premise with the symbol C. The first one (5.3) reads: "If B is true, then A becomes more plausible". For the plausibility of A given B and the major premise C we define the notation

$$A|BC. \tag{5.10}$$

Using this conditional plausibility, the syllogism is written as

$$A|BC > A|C. \tag{5.11}$$

The second weak syllogism (5.4) reads

$$B|\overline{A}C < B|C. \tag{5.12}$$

Probability theory evaluates the degree of these conditional plausibilities.

5.2.2. Basic desiderata

Probability theory has to solve two different problems. First, it has to represent the degree of plausibility. The only possible ansatz is to represent the degree of plausibility by real numbers. The second problem is how to evaluate from given degrees of plausibilities the degree of plausibility for other propositions. This evaluation has to follow certain guidelines. An infinitesimal change in the plausibility of a proposition corresponds to an infinitesimal change of the degree of plausibility. By convention, one often used that an infinitesimal

greater plausibility corresponds to an infinitesimal greater number. Let us assume, we have the plausibility $A|B$, and we obtain new information B' in a way that

$$A|B < A|B' . \tag{5.13}$$

Consequently, the plausibility of the inverse proposition $\overline{A}$ becomes less plausible:

$$\overline{A}|B > \overline{A}|B' . \tag{5.14}$$

We summarize requirements of this type in the desideratum "Qualitative correspondence with common sense".
Since in our approach, probability theory is based on symbolic logic, the desiderata have to reflect the properties of the Boolean algebra. Therefore, we have to assign an equal degree of plausibility to equivalent propositions:

$$\overline{AB}|C = \left(\overline{A} + \overline{B}\right)|C . \tag{5.15}$$

Relations of this type fall under the desideratum of consistency. Following [Jay03] the three basic desiderata are

I Degrees of plausibility are represented by real numbers

II Qualitative correspondence with common sense

III Consistency

- a If a conclusion can be reaached in more than one way, then every possible way must lead to the same result.
- b All available information is used. All conclusions are completely non-ideological.
- c Equivalent states of knowledge are represented by equivalent plausibility assignments.

Considering these desiderata, we are able to derive two quantitative rules to evaluate the degree of plausibility.

5.2.3. Product rule

The logical sum and product are sufficient for symbolic logic. In order to build a theory to evaluate the degree of plausibility, we need to find quantitative rules which allow the evaluation of the plausibility of logical functions from the plausibility of their elementary propositions. These rules have to be in agreement with the basic desiderata of the previous section.
At first, we want to relate the plausibility of the logical product $AB|D$ to the plausibility of A and B separately. There are two equivalent ways to decide whether AB is true. First, we declare A is true. Knowing that A is true, we decide B is true. Symbolically, the two plausibilities are written as $A|D$ and $B|AD$, respectively. Due to the commutativity of the logical product starting with proposition B leads to the same plausibility according to

desideratum IIIa. Therefore, the plausibility of the logical product is given by the functional form

$$AB|D = F\big(A|D, B|AD\big) = F\big(B|D, A|BD\big). \tag{5.16}$$

Considering the propositions A and B to be exclusive, shows that F is symmetric in its arguments. We can derive further properties using desideratum I. Let us assume, we have acquired new information D', such that B becomes more plausible, but the plausibility of A does not change:

$$B|D' > B|D, \qquad A|BD' = A|BD. \tag{5.17}$$

Therefore, employing the new information D', the logical product $AB|D'$ is more plausible

$$AB|D' \geq AB|D. \tag{5.18}$$

Since degrees of plausibility have to be represented by real numbers (desideratum I), an infinitesimal increase in the plausibility for $B|D$ requires an infinitesimal increase in the plausibility of $AB|D$. Consequently, the function F is a continuous monotonic function in the first argument. It can be either increasing or decreasing. Due to its symmetry the same applies for the second argument.
We determine the functional form of F demanding the associativity of the Boolean algebra. In order to examine this, we apply (5.16) to the plausibility $ABC|D$. Considering AB as a single proposition leads to

$$ABC|D = F\big(AB|D, C|ABD\big) = F\Big[F\big(B|D, A|BD\big), C|ABD\Big]. \tag{5.19}$$

Taking AC as a single proposition we obtain

$$ABC|D = F\big(B|D, AC|BD\big) = F\Big[B|D, F\big(A|BD, C|ABD\big)\Big]. \tag{5.20}$$

Using the abbreviations

$$x \equiv B|D, \qquad y \equiv A|BD, \qquad z \equiv C|ABD, \tag{5.21}$$

the combination of (5.19) and (5.20) provides the functional equation

$$F\left[x, F(y, z)\right] = F\left[F(x, y), z\right]. \tag{5.22}$$

We introduce the following notation for the first order derivatives with respect to the first and second argument, respectively:

$$F_1(x, y) \equiv \frac{\partial F(x, y)}{\partial x}, \qquad F_2(x, y) \equiv \frac{\partial F(x, y)}{\partial y}. \tag{5.23}$$

The differentiation of the functional equation (5.22) with respect to x and y leads to

$$F_1\left[x, F(y, z)\right] = F_1\left[F(x, y), z\right] F_1(x, y), \tag{5.24}$$

$$F_2\left[x, F(y, z)\right] F_1(y, z) = F_1\left[F(x, y), z\right] F_2(x, y). \tag{5.25}$$

Elimination $F_1\left[F(x,y),z\right]$ results in two differential equations

$$(5.25)/(5.24): \quad G\left[x,F(y,z)\right]F_1(y,z) = G(x,y), \tag{5.26}$$
$$(5.24)/(5.25): \quad G\left[x,F(y,z)\right]F_2(y,z) = G(x,y)G(y,z), \tag{5.27}$$

where we used the abbreviation

$$G(x,y) \equiv \frac{F_2(x,y)}{F_1(x,y)}. \tag{5.28}$$

In order to obtain a condition for G, we differentiate (5.26) and (5.27) with respect to z and y, respectively:

$$\begin{aligned}\frac{\partial}{\partial z}(5.26) &= G_2\left[x,F(y,z)\right]F_2(y,z)F_1(y,z) + G\left[x,F(y,z)\right]F_{12}(y,z),\\ \frac{\partial}{\partial y}(5.27) &= G_2\left[x,F(y,z)\right]F_1(y,z)F_2(y,z) + G\left[x,F(y,z)\right]F_{21}(y,z).\end{aligned} \tag{5.29}$$

Thus

$$\frac{\partial}{\partial y}G(x,y)G(y,z) = \frac{\partial}{\partial z}G(x,y) = 0. \tag{5.30}$$

Therefore, the product $G(x,y)G(y,z)$ does not depend on y. The general solution satisfying this constraint is

$$G(x,y) = a\frac{H(x)}{H(y)}, \tag{5.31}$$

where $a > 0$ is an arbitrary constant and the function H does not change sign. Inserting this solution, (5.26) and (5.27) become

$$F_1(y,z) = \frac{H\left[F(y,z)\right]}{H(y)}, \qquad F_2(y,z) = a\frac{H\left[F(y,z)\right]}{H(z)}. \tag{5.32}$$

Inserting the above equations into the total differential

$$\mathrm{d}F(y,z) = F_1(y,z)\mathrm{d}y + F_2(y,z)\mathrm{d}z, \tag{5.33}$$

we obtain the differential equation

$$\frac{\mathrm{d}F(y,z)}{H\left[F(y,z)\right]} = \frac{\mathrm{d}y}{H(y)} + a\frac{\mathrm{d}z}{H(z)}. \tag{5.34}$$

On integration and taking the exponent

$$kw\left[F(y,z)\right] = w(y)w^a(z), \tag{5.35}$$

where w is defined as

$$\ln w(u) = \int^u \frac{\mathrm{d}u'}{H\left(u'\right)}. \tag{5.36}$$

The absence of a lower limit gives rise to the integration constant. Equation 5.22 determines the parameter a:

$$w(x)w^a(y)w^{2a}(z) = w(x)w^a(y)w^a(z), \tag{5.37}$$

which only has a solution for $a = 1$. Finally, for the initial equation 5.16, we get

$$kw(AB|C) = w(A|C)\, w(B|AC) = w(B|C)\, w(A|BC)\,. \tag{5.38}$$

The integration constant k is given by the plausibility for the certain proposition. We consider the rule (5.38) with A being the certain proposition:

$$kw\left[\left(A+\overline{A}\right)B|C\right] = w\left[\left(A+\overline{A}\right)|C\right] w\left[B|\left(A+\overline{A}\right)C\right]\,. \tag{5.39}$$

This becomes

$$kw(B|C) = w\left[\left(A+\overline{A}\right)|C\right] w(B|C)\,. \tag{5.40}$$

Therefore, k is the degree of plausibility of the certain proposition

$$k = w\left[\left(A+\overline{A}\right)|C\right]. \tag{5.41}$$

In general, k can be any finite positive real number except zero. The common choice is $k = 1$, albeit there is no difference to $k = 16$ for example. Next, we determine the value of the function $w(\cdots)$, which represents the impossible proposition. For the impossible proposition $A\overline{A}$ we have

$$kw\big(A\overline{A}B\big|C\big) = w(B|C)\, w\big(A\overline{A}\big|BC\big)\,. \tag{5.42}$$

This equation must be valid independent of the plausibility of B. The plausibility of the two impossible propositions are equal

$$w\big(A\overline{A}B\big|C\big) = w\big(A\overline{A}\big|BC\big) = w\big(A\overline{A}\big|C\big) = l. \tag{5.43}$$

With this abbreviation, (5.42) becomes

$$kl = lw(B|C)\,. \tag{5.44}$$

Thus, l has to be zero or plus infinity. Both choices are equally valid. In total, $w(x)$ is a positive continuous monotonic function. It can be increasing in the interval $[0, 1]$ or decreasing in $[1, \infty[$. From now on, we use the first choice. In order to summarize the results from this section, we determined the function $F(x, y)$ as

$$F(x, y) = w^{-1}\left[w(x)w(y)\right], \tag{5.45}$$

and the plausibility of the proposition AB is determined by

$$w(AB|D) = w(A|D)\, w(B|AD) = w(B|D)\, w(A|BD)\,, \tag{5.46}$$

where $0 \leq w(\cdots) \leq 1$ by convention. To our surprise, the solution depends on the function w. In the end of the next section, we examine the meaning of that function and show, that it does not lead to any conceptual difficulties.

5.2.4. Sum rule

In the analysis of the product rule, we had to introduce the function w. Thus, also the sum rule depends on this function. The plausibility of the denial must depend on the plausibility of the proposition A:

$$w(A|C) = f\left[w\left(\overline{A}\middle|C\right)\right] \tag{5.47}$$

The self-reciprocal nature of the denial[1] imposes the condition

$$f\left[f(x)\right] = x, \qquad x \equiv w(A|C)\,. \tag{5.48}$$

Desideratum II (Sec. 5.2.2) requires, that an infinitesimal increase in the plausibility of A causes an infinitesimal decrease of the plausibility of its denial. Therefore, $f(x)$ is a monotonic decreasing function in the interval $x \in [0,1]$. In the case, where x represents the certain proposition $f(1) = 0$, whereas for the impossible proposition $f(0) = 1$. Analogous to the previous section, we determine the functional form of f by demanding consistency with the Boolean algebra. Using duality, the denial of the logical sum $A + B$ reads

$$f\left[w(A+B|C)\right] = w\left(\overline{A}\;\overline{B}\middle|C\right). \tag{5.49}$$

In order to find a relation allowing the determination of f, we eliminate all inverted plausibilities using only the definition of f and the product rule (5.46). For the previous equation, we write

$$w\left(\overline{A}\;\overline{B}\middle|C\right) = w\left(\overline{A}\middle|C\right) w\left(\overline{B}\middle|\overline{A}C\right) = f\left[w(A|C)\right] f\left[w\left(B\middle|\overline{A}C\right)\right]. \tag{5.50}$$

We transform the argument in the last factor into

$$w\left(B\middle|\overline{A}C\right) = \frac{w\left(\overline{A}B\middle|C\right)}{w\left(\overline{A}\middle|C\right)} = \frac{w\left(\overline{A}B\middle|C\right)}{f\left[w(A|C)\right]}. \tag{5.51}$$

The denominator turns into

$$\begin{aligned} w\left(\overline{A}B\middle|C\right) &= w(B|C)\, w\left(\overline{A}\middle|BC\right) = w(B|C)\, f\left[w(A|BC)\right] \\ &= w(B|C)\, f\left[\frac{w(AB|C)}{w(B|C)}\right]. \end{aligned} \tag{5.52}$$

Putting everything together and applying f on both sides leads to

$$f\left[w(A|C)\right] f\left[\frac{f\left[w(A+B|C)\right]}{f\left[w(A|C)\right]}\right] = w(B|C)\, f\left[\frac{w(AB|C)}{w(B|C)}\right]. \tag{5.53}$$

In order to solve this functional equation we use the substitution

$$A = DE, \qquad B = D + E. \tag{5.54}$$

[1] $\overline{\overline{A}} = A$.

Thus,

$$\begin{aligned} AB &= DE(D+E) = DE = A, \\ A+B &= DE + D + E = D + E = B. \end{aligned} \tag{5.55}$$

Therefore, we write (5.53) as

$$f\left[w(A|C)\right] f\left[\frac{f\left[w(B|C)\right]}{f\left[w(A|C)\right]}\right] = w(B|C)\, f\left[\frac{w(A|C)}{w(B|C)}\right]. \tag{5.56}$$

With the substitutions

$$x \equiv f\left[w(A|C)\right], \qquad y = w(B|C), \tag{5.57}$$

we bring it into a more convenient form:

$$xf\left[\frac{f(y)}{x}\right] = yf\left[\frac{f(x)}{y}\right]. \tag{5.58}$$

Following our argument in the beginning of the section, f is a differentiable function. We obtain a system of differential equations, by differentiating with respect to x, y and to x and y:

$$xf(u) = yf(v), \tag{5.59}$$
$$f(u) - uf'(u) = f'(v)f'(x), \tag{5.60}$$
$$f'(u)f'(y) = f(v) - vf'(v), \tag{5.61}$$
$$\frac{u}{x}f''(u)f'(y) = \frac{v}{y}f''(v)f'(x), \tag{5.62}$$

where we employed the abbreviations

$$u \equiv \frac{f(y)}{x}, \qquad v \equiv \frac{f(x)}{y}. \tag{5.63}$$

The first and second order derivative of f are denoted by f' and f''. Multiplying the first (5.59) and last (5.62) equation eliminates x and y. Thus,

$$uf''(u)f(u)f'(y) = vf''(v)f(v)f'(x). \tag{5.64}$$

By inserting the second (5.60) and third (5.61) equation, we eliminate the first order derivatives. We obtain

$$\frac{uf''(u)f(u)}{f'(u)\left[f(u) - uf'(u)\right]} = \frac{vf''(v)f(v)}{f'(v)\left[f(v) - vf'(v)\right]}. \tag{5.65}$$

The right hand side is independent of u, so the left hand side has to be independent as well and both sides are equal to a constant k. The resulting second order differential equation is

$$uf''(u)f(u) = k\left[f(u) - uf'(u)\right] f'(u). \tag{5.66}$$

After multiplication with $\mathrm{d}u/\left[uf(u)f'(u)\right]$ we get

$$\frac{\mathrm{d}f'(u)}{f'(u)} = k\left[\frac{\mathrm{d}u}{u} - \frac{\mathrm{d}f(u)}{f(u)}\right]. \tag{5.67}$$

A single integration gives us

$$\ln f'(u) = k\left[\ln u - \ln f(u)\right] + A, \tag{5.68}$$

where A is the integration constant. Taking the exponent and redefining A leads to

$$f'(u) = A\left[\frac{u}{f(u)}\right]^k. \tag{5.69}$$

Another integration together with the substitution $r = k + 1$ gives us the solution

$$f^r(u) = Au^r + B. \tag{5.70}$$

It has to fulfill the self-reciprocal relation (5.48) resulting in the condition

$$\left(A^2x^r + AB + B\right)^{\frac{1}{r}} = x\,, \tag{5.71}$$

which gives us the two conditions

$$A^2 = \pm 1 \quad \text{and} \quad AB + B = 0. \tag{5.72}$$

In addition, we have to satisfy the primary equation (5.65):

$$A^2y^r + AB + Bz^r = A^2z^r + AB + By^r. \tag{5.73}$$

Considering these two conditions, we conclude $B = A^2$ and $A = -1$. Therefore, the solution is

$$f^r(x) = 1 - x^r\,, \qquad x^r + f^r(x) = 1\,. \tag{5.74}$$

Consequently, the initial problem (5.47) reads

$$w^r(A|C) + w^r\left(\overline{A}\middle|C\right) = 1\,. \tag{5.75}$$

The condition for r is $0 < r < \infty$. Analogous to the previous equation, we write the product rule in the form

$$w^r(AB|C) = w^r(B|C)\,w^r(A|BC)\,. \tag{5.76}$$

The actual value of r is irrelevant. The function w is an arbitrary monotonic increasing function in the interval $[0, 1]$. Going from $w(x)$ to $w^r(x)$ does not introduce any freedom, which we did not have before in the choice of w. From now one, we define

$$P(A|C) = w^r(A|B)\,, \qquad 0 \leq P(A|C) \leq 1, \tag{5.77}$$

and we will call $P(A|C)$ the probability of the proposition A assuming that the proposition C is true. The final product and sum rule are

$$\boxed{\begin{gathered} P(AB|C) = P(A|C)\,P(B|AC) = P(B|C)\,P(A|BC)\,, \\ P(A|C) + P\big(\overline{A}\big|C\big) = 1. \end{gathered}} \tag{5.78}$$

Before we analyze the meaning of the functions w and P, we recall our finding up to this point. The start of the product rule was to relate the plausibility of$(AB|C)$ to the plausibility of its elementary proposition. The solution

$$w(AB|C) = w(A|C)\,w(B|AC) \tag{5.79}$$

required an monotonic increasing function w. According to our desiderata, we call this function the degree of plausibility. In the derivation of the product rule, we obtained the relation of the degree of plausibility of a denied proposition to the degree of plausibility of the proposition. The obtained sum rule is

$$w^r(A|C) + w^r\big(\overline{A}\big|C\big) = 1, \tag{5.80}$$

where r is a positive real number greater than zero. After bringing the product rule in the same form, we introduced the term probability P defined as

$$P(A|C) = w^r(A|C)\,. \tag{5.81}$$

This result raises two issues. It seems, that we did not find one rule for probability theory, but an infinite amount of rules depending on the choice of the monotonic increasing function w^r. The second problem is the definition of plausibility. In our derivation, it is only an abstract term. We will resolve this problems in the next section and see, that we have indeed found unique rules for probability theory.

5.2.5. Unique rules

Assume, we have three propositions A_i, with $i \in \{1,2,3\}$ and we want to evaluate the probability of their logical sum $P(A_1 + A_2 + A_3|B)$. The rule for the logical sum of two propositions is

$$\begin{aligned} P(A+B|C) &= 1 - P\big(\overline{A}\;\overline{B}\big|C\big) = 1 - P\big(\overline{A}\big|C\big)\,P\big(\overline{B}\big|\overline{A}C\big) \\ &= 1 - P\big(\overline{A}\big|C\big)\,\big[1 - P\big(B\big|\overline{A}C\big)\big] \\ &= P(A|C) + P\big(\overline{A}\big|C\big)\,P\big(B\big|\overline{A}C\big) \\ &= P(A|C) + P\big(\overline{A}B\big|C\big) \\ &= P(A|C) + P(B|C)\,P\big(\overline{A}\big|BC\big) \\ &= P(A|C) + P(B|C)\,[1 - P(A|BC)] \\ &= P(A|C) + P(B|C) - P(AB|C)\,, \end{aligned} \tag{5.82}$$

which is called the extended sum rule. In the case of $B = \overline{A}$, we obtain the original sum rule (5.78). Iterative application of the extended sum rule leads to

$$\begin{aligned} P(A_1 + A_2 + A_3|B) =& P(A_1 + A_2|B) + P(A_3|B) - P(A_1A_3 + A_2A_3|B) \\ =& P(A_1|B) + P(A_2|B) + P(A_3|B) \\ & - P(A_1A_2|B) - P(A_1A_3|B) - P(A_2A_3|B) \\ & + P(A_1A_2A_3|B)\,. \end{aligned} \tag{5.83}$$

In the case of mutually exclusive proposition, we obtain

$$P(A_iA_j|B) = P(A_i|B)\,P(A_j|A_iB) = P(A_i|B)\,\delta_{ij}. \tag{5.84}$$

Therefore, the expression for the probability that at least one of the propositions is true simplifies to

$$P(A_1 + A_2 + A_3|B) = P(A_1|B) + P(A_2|B) + P(A_3|B)\,. \tag{5.85}$$

And the general expression for N mutually exclusive propositions is

$$P(A_1 + \cdots + A_N|B) = \sum_{i=1}^{N} P(A_i|B)\ . \tag{5.86}$$

In addition, we consider the proposition B such that only one of the propositions A_i is true. The propositions A_i are exhaustive assuming B is true. Therefore, we have the normalization condition

$$\sum_{i=1}^{n} P(A_i|B) = 1. \tag{5.87}$$

This result directly follows from the sum and product rule and was not an axiom of our theory. With this equation, we still do not know what values to assign to the individual probabilities $P(A_i|B)$.
Let us for example consider the tossing of a coin. For one coin, two possible propositions are heads (H) and tails (T). Albeit, the assignment of the names heads and tails are arbitrary. Therefore, the probabilities $P(H|B)$ and $P(T|B)$ are equal and we assign

$$P(H|B) = P(T|B) = 0.5. \tag{5.88}$$

The assignment of numerical values does not depend on the specific choice of the function P, rather all choices lead to the same probability of 0.5.
We also realize, that the plausibility of heads and tails is irrelevant, and the only thing that matters is the probability P.

5.2.6. Marginalization

We can use the result in the previous section to derive an important procedure. Let us assume, we have N mutually exclusive and exhaustive propositions $A_1, \ldots, A_N$ under B. The only

available information are the conditional probabilities $P(A_iB|C)$, but we are interested in the probability of B. Extending the normalization condition in (5.87) to our situation, we have

$$\sum_{i=1}^{N} P(A_i|BC) = 1. \tag{5.89}$$

Therefore, the probability of B is given by

$$P(B|C) = P(B|C)\sum_{i=1}^{N} P(A_i|BC) = \sum_{i=1}^{N} P(B|I)\,P(A_i|BC) = \sum_{i=1}^{N} P(A_iB|C)\,. \tag{5.90}$$

This procedure is called marginalization. We will see several applications throughout this thesis.

5.3. Basic examples

Employing our current knowledge, we are able to solve basic problems in probability theory. The problems all break down to using given conditional probabilities and evaluating the desired probability applying the sum and product rule. The demanding task is rather the formulation of the problem in the language of probability theory than the calculation of the solution.

5.3.1. False positive test

Mammography is a test for breast cancer. Like every test, it is not free of uncertainty. In [KGB+96] 1000 women were tested. 8 women had breast cancer, whereas only 7 of them were diagnosed. On the other hand, 63 women were tested positive, albeit they did not have cancer. We want to evaluate the probability of not having breast cancer, when tested positive. We define the following propositions:

$$\begin{aligned} R &\equiv \text{“Positive test result”},\\ C &\equiv \text{“Breast cancer”},\\ I &\equiv \text{“Prior information”}. \end{aligned} \tag{5.91}$$

From the study, we have the following information:

$$P(R|CI) = \frac{7}{8} = 0.875, \quad P\big(R\big|\overline{C}I\big) = \frac{63}{992} \approx 0.063, \quad P(C|I) = \frac{8}{1000} = 0.008. \tag{5.92}$$

We are interested in the probability $P\big(\overline{C}\big|RI\big)$. By the sum and product rule, we have

$$P\big(\overline{C}\big|RI\big) = \frac{P\big(\overline{C}R|I\big)}{P(R|I)} = \frac{P\big(\overline{C}|I\big)\,P\big(R|\overline{C}I\big)}{P(R|I)}\,. \tag{5.93}$$

The denominator can be written as

$$P(R|I) = P(CR|I) + P\big(\overline{C}R\big|I\big) = P(C|I)\,P(R|CI) + P\big(\overline{C}\big|I\big)\,P\big(R\big|\overline{C}I\big)\,. \tag{5.94}$$

The final result is

$$\begin{aligned} P\big(\overline{C}\big|RI\big) &= \frac{P\big(\overline{C}\big|I\big)\,P\big(R\big|\overline{C}I\big)}{P(C|I)\,P(R|CI) + P\big(\overline{C}\big|I\big)\,P\big(R\big|\overline{C}I\big)} \\ &= \frac{(1-0.008)\cdot 0.063}{0.008\cdot 0.875 + (1-0.008)\cdot 0.063} \approx 0.90. \end{aligned} \tag{5.95}$$

The probability of not having breast cancer, if tested positive is 90 %. Intuitively, one may have expected, that the probability is $P\big(R\big|\overline{C}I\big) = 0.063$. Our rules clearly show

$$P\big(R\big|\overline{C}I\big) \neq P\big(\overline{C}\big|RI\big)\,. \tag{5.96}$$

5.3.2. Zonk

There is a famous TV show, with world wide variations. The scheme is the following: there are three doors, but only behind one of them is a prize. In the German version, behind the other two doors is a stuffed animal called Zonk. The candidate of the show has to chose one door. After that, the show master opens one of the other two doors containing a Zonk. After that, he offers the candidate to change the selected door. Is it an advantage to change the door? We define the propositions:

$$\begin{aligned} A &\equiv \text{“The prize is behind door 1.”} \\ B &\equiv \text{“The prize is behind door 2.”} \\ C &\equiv \text{“The prize is behind door 3.”} \end{aligned} \tag{5.97}$$

Let us assume, the candidate decides initially on the first door. We know, that the show master will provide the information, that behind the second or the third door is a Zonk. Thus, the probability that the price is behind the first door, under the condition that a Zonk is behind the second or the third door is represented by $P\big(A\big|(\overline{B}+\overline{C})I\big)$. Using the sum and product rule we get

$$\begin{aligned} P\big(A\big|(\overline{B}+\overline{C})I\big) &= \frac{P\big(A(\overline{B}+\overline{C})\big|I\big)}{P\big(\overline{B}+\overline{C}\big|I\big)} = \frac{P\big(A\overline{B}\big|I\big) + P\big(A\overline{C}\big|I\big) - P\big(A\overline{B}\overline{C}\big|I\big)}{P\big(\overline{B}\big|I\big) + P\big(\overline{C}\big|I\big) - P\big(\overline{B}\,\overline{C}\big|I\big)} \\ &= \frac{P(A|I) + P(A|I) - P(A|I)}{P\big(\overline{B}\big|I\big) + P\big(\overline{C}\big|I\big) - P(A|I)} \\ &= \frac{\frac{1}{3}}{\frac{2}{3}+\frac{2}{3}-\frac{1}{3}} = \frac{1}{3}, \end{aligned} \tag{5.98}$$

where we used

$$P\big(\overline{B}\,\overline{C}\big|I\big) = P\big(\overline{B+C}\big|I\big) = 1 - P(B+C|I) = \frac{1}{3}. \tag{5.99}$$

The probability stays 1/3, if we do not change the door. On the other hand, the probability if we change the door is given by

$$P\big(\overline{A}\big|(\overline{B}+\overline{C})I\big) = \frac{2}{3}. \tag{5.100}$$

In this case, it is easy to obtain the solution by going trough all cases. However, the intricate part is the formulation of the problem by conditional probabilities.

5.4. Hypothesis tests

In this section, we solve the first of the three basic problems of probability theory: The hypothesis test. Let us first recall the product and sum rule, (5.78) which are sufficient to solve all problems in probability theory:

$$\begin{aligned} P(AB|C) &= P(A|C)\,P(B|AC) \\ P\big(\overline{A}\big|C\big) &= 1 - P(A|C) \end{aligned}$$

We have given two competing hypotheses H_1 and H_2, which are exclusive and exhaustive. The aim is to evaluate the probability, that the hypothesis H_1 is true given some data D. In our notation, this probability is given by $P(H_1|DI)$. It is called the posterior probability. The symbol I denotes any prior information about the hypotheses. Using the product rule twice, we obtain

$$P(H_1|DI) = \frac{P(H_1D|I)}{P(D|I)} = \frac{P(H_1|I)\,P(D|H_1I)}{P(D|I)}. \tag{5.101}$$

This consequence of the product rule is called Bayes theorem. The probability $P(H_1|I)$ is called prior and denotes all knowledge, we have about the hypothesis without considering the data. If there is no prior information favoring one of the hypotheses, we will assign

$$P(H_1|I) = P(H_2|I)\,. \tag{5.102}$$

The second term in the numerator $P(D|H_1I)$ is the likelihood. It is the probability for obtaining the data D, if the hypothesis H_1 and the prior information I are true. The term in the denominator $P(D|I)$ is the normalization factor. Applying marginalization, we write

$$\begin{aligned} P(D|I) &= P(H_1D|I) + P(H_2D|I) \\ &= P(H_1|I)\,P(D|H_1I) + P(H_2|I)\,P(D|H_2I)\,. \end{aligned} \tag{5.103}$$

Therefore, the posterior probability for the first hypothesis gets

$$P(H_1|DI) = \frac{P(H_1|I)\,P(D|H_1I)}{P(H_1|I)\,P(D|H_1I) + P(H_2|I)\,P(D|H_2I)} = \frac{1}{1+\frac{P(H_2|I)P(D|H_2I)}{P(H_1|I)P(D|H_1I)}}. \tag{5.104}$$

We may introduce the odds ratio of the two posterior probabilities, defined as

$$O_{12} = \frac{P(H_1|D\ I)}{P(H_2|D\ I)} = \frac{P(H_1|I)}{P(H_2|I)} \cdot \frac{P(D|H_1\ I)}{P(D|H_2\ I)}, \tag{5.105}$$

which is the product of prior odds and the likelihood ratio, respectively. Using the odds ratio, the posterior probability is given as

$$P(H_1|DI) = \frac{1}{1 + \frac{1}{O_{12}}}. \tag{5.106}$$

Since the two hypotheses are exclusive and exhaustive, the sum rule

$$P(H_1|D\ I) + P(H_2|D\ I) = 1 \tag{5.107}$$

allows the calculation of the posterior probability of the second hypothesis. In the general case of N hypotheses, the normalization condition is

$$\sum_{i=1}^{N} P(H_i|D\ I) = 1. \tag{5.108}$$

The posterior probability for the ith hypothesis is given by the generalization of (5.104):

$$P(H_i|DI) = \frac{1}{\sum_{j=1}^{N} O_{ji}}. \tag{5.109}$$

The important lesson is, that it is only possible to compare hypotheses. There is now way to estimate the quality of a hypothesis without comparing it to other hypotheses.
Up to this point, we have exclusively considered discrete propositions and hypotheses. We will now consider a continuous space of hypotheses of the kind

$$H_x \equiv \text{The numerical value of the quantity is } x, \tag{5.110}$$

with $x \in [a, b]$. As we go from the formula for discrete hypotheses to continuous ones, we have to replace the summation by integration:

$$P(H_i|DI) = \frac{P(H_i|I)\, P(D|H_i I)}{\sum_i P(H_i|I)\, P(D|H_i I)} \to P(H_x|DI) = \frac{P(H_x|I)\, P(D|H_x I)}{\int_a^b \mathrm{d}x\ P(H_x|I)\, P(D|H_x I)} \tag{5.111}$$

This formula allows the estimation of a parameter x from the data D. In the next section, we will show in detail how to extend probability theory to continuous parameters.

5.5. Probability distribution functions

The product and sum rule are only valid for a discrete space of propositions. However, if we measure the length L of an object and determine the uncertainty of L, we consider L to be a

continuous variable. Let us assume, we want to determine, whether the length is greater or less than a certain value x. We are dealing with the two exclusive propositions

$$A \equiv (L \leq x)\,, \qquad \overline{A} \equiv (L > x)\,. \tag{5.112}$$

For an arbitrary $x \geq 0$, we define

$$F(x|I) = P(A|I)\,, \tag{5.113}$$

which evaluates the probability that the length of the object is smaller than x. Furthermore, we are interested in the possibility that the length is in a certain interval $[a, b]$. We consider the propositions

$$A \equiv (L \leq a)\,, \qquad B \equiv (L \leq b)\,, \qquad C \equiv (a < L \leq b)\,. \tag{5.114}$$

The proposition B is the logical sum of the propositions A and C (see Fig. 5.1). The

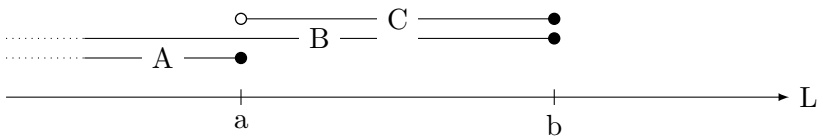

Figure 5.1.: Propositions in order to determine the probability for the length of an object to be in a certain interval. Hollow circles denote excluded points, whereas full ones denote included points.

probability of B is

$$P(B|I) = P(A + C|I) = P(A|I) + P(C|I)\,. \tag{5.115}$$

Using the function $F(x|I)$, we get

$$P(a < L \leq b|I) = P(C|I) = F(b|I) - F(a|I)\,. \tag{5.116}$$

Due to its definition, $F(x|I)$ is continuous and differentiable, thus we use

$$P(a < L \leq b|I) = \int_a^b \mathrm{d}x\; f(x|D)\,, \tag{5.117}$$

where $f(x|I) = F'(x|I)$ is the derivative of $F(x|I)$. Its general term is probability distribution function or probability density function (pdf). For convenience, we also use the term distribution with the same meaning. The integral $F(x)$ is the cumulative distribution function (cdf) .
In case of the length L of a object, $f(x|I)\,\mathrm{d}x$ is the probability, that the length of the object is within the interval $[x, x + \mathrm{d}x]$ and $f(x|I)$ is the probability distribution for L. The pdf is normalized, because it is certain, that the object has a certain length:

$$P(0 \leq L < \infty|I) = \int_0^\infty \mathrm{d}x\; f(x|I) = 1. \tag{5.118}$$

With the help of this analysis, we understand the precise meaning of the ad hoc formula (5.111). It estimates the probability, that a parameter is in a certain interval. The formula was

$$P(H_x|DI) = \frac{P(H_x|I)\,P(D|H_xI)}{P(D|I)}$$

For the interval $[x, x + \mathrm{d}x]$ we employ the probability distribution functions:

$$P(H_x|DI) = f(x|DI)\,\mathrm{d}x, \qquad P(H_x|I) = f(x|I)\,\mathrm{d}x. \tag{5.119}$$

Therefore, the solution of the hypothesis test becomes

$$f(x|DI) = \frac{f(x|I)\,P(D|H_xI)}{P(D|I)}. \tag{5.120}$$

The normalization is given by

$$P(D|I) = \int \mathrm{d}x\; f(x|I)\,P(D|H_xI) \tag{5.121}$$

For simplicity, we will frequently use the abbreviation $P(D|H_xI) \equiv P(D|xI)$. The above formula for a continuous hypothesis test can be identified as a parameter estimation as well. We estimate a parameter x from the data.
All information about continuous hypotheses or parameters are contained in the posterior probability distribution function. As we will see later in this section, there are generic pdfs. Therefore, instead of giving the complete pdf, it is in some particular cases sufficient to report only certain characteristics.

5.5.1. General characteristics

In practice, an estimated probability distribution function has a shape similar to the one in figure 5.2. It has only one peak and it is symmetric. In such a case, it is common practice, not to report the complete pdf, but some information, that is obtained from the pdf. Unfortunately, there is no standard procedure. Therefore, we give some examples in this section.

5.5.1.1. Moments

One way is to report only certain moments of a pdf. The ath moment of a continuous probability distribution function is defined as

$$\left\langle x^a \right\rangle = \int \mathrm{d}x\; x^a f(x|I) \tag{5.122}$$

By knowing all the moments, we can reconstruct the full pdf. Since a pdf is always normalized, the zeroth moment $\left\langle x^0 \right\rangle$ is one. Intuitively, an important information is the point with the

Figure 5.2.: Generic probability distribution function.

highest density. For a symmetric, single peaked pdf, this point is equal to the first moment, also called mean value of the pdf.
In addition, the width of the distribution contains important information. For this purpose, central moments

$$\left\langle \left(x - \langle x \rangle\right)^a \right\rangle = \int \mathrm{d}x \ \left(x - \langle x \rangle\right)^a f(x|I) \tag{5.123}$$

are used. The first central moment is by definition always zero. For a symmetric, single peaked pdf the second central moment is a well suited characteristic for the width of the pdf. Hence, it has a special name, the variance. It is given by

$$\begin{aligned} \mathrm{var}(x) &= \left\langle \left(x - \langle x \rangle\right)^2 \right\rangle = \left\langle x^2 - 2\langle x \rangle x + \langle x \rangle^2 \right\rangle = \left\langle x^2 \right\rangle - 2\langle x \rangle^2 + \langle x \rangle^2 \\ &= \left\langle x^2 \right\rangle - \langle x \rangle^2. \end{aligned} \tag{5.124}$$

With a given mean value and variance, it is common practice to report the information about a quantity x as

$$x = \langle x \rangle \pm \sqrt{\mathrm{var}(x)}. \tag{5.125}$$

Instead of variance, one frequently uses the square of the standard deviation[2] σ:

$$\mathrm{var}(x) = \sigma^2. \tag{5.126}$$

The third central moment ($a = 3$), the skewness is a measure for the asymmetry of a pdf. For a symmetric distribution, it is zero, as well as all other odd central moments. The fourth

[2] Compare with Gaussian distribution in section 5.5.2.1.

central moment is called kurtosis. It is a measure of the flatness of a distribution near its peak. Knowing the mean value and the variance is sufficient to qualitatively describe a single peaked symmetric pdf as shown in figure 5.3(a). However, for a asymmetric pdf as in figure 5.3(b), two values are not at all sufficient to reproduce the displayed pdf.

5.5.1.2. Credible regions

Instead of reporting moments of a pdf, it is quite popular to report intervals of a certain probability. We will call a interval of such type a credible region. Analogous to the moments, these intervals are uniquely defined only for a symmetric single peaked pdf. Figure 5.3(a) shows three different credible regions with 20 % probability.
For an asymmetric distribution (see Fig. 5.3(b)) it is not obvious, whether we should choose the maximum or the mean value as the center of the interval. In such cases, we have to report

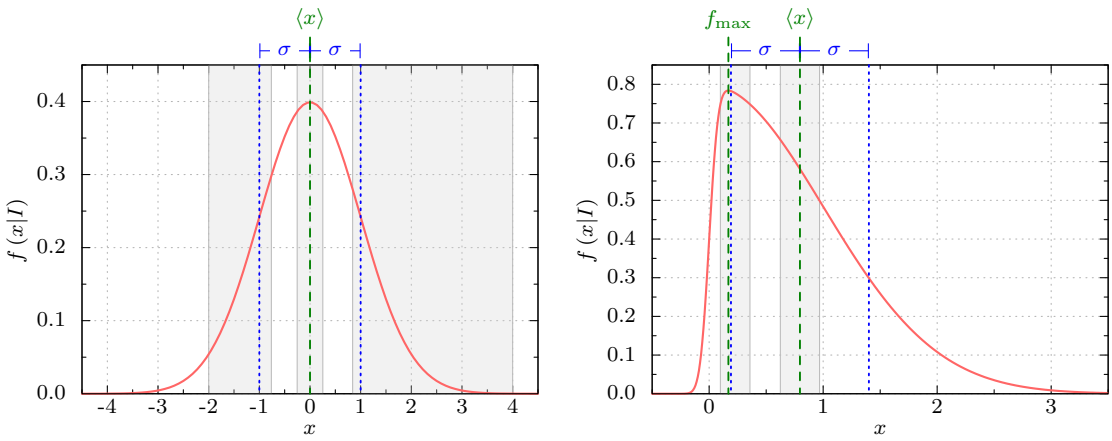

(a) symmetric pdf (b) asymmetric pdf

Figure 5.3.: A genuine symmetric and asymmetric probability distribution function. The gray areas show different credible regions of 20 %. In addition we have drawn the standard variation σ in blue and the expectation value in green. For the asymmetric distribution the mean and the maximum of the pdf are in general different.

the complete probability distribution function. None the less, in most cases, it is useful to present a single value as an estimate for the parameter.

5.5.1.3. Best estimate

We have evaluated the posterior pdf for a parameter μ. This parameter has a true value, but we are not able to determine it, due to limited precision. Albeit the pdf perfectly describes our knowledge about the parameter, we want to give a numerical value, that we belief is closest to the true value. We intend to give an estimate μ^*. For the relation between the true value and the estimate we may write

$$\mu^* = \mu + e, \tag{5.127}$$

where e is the error. According to Gauss and Legendre, the best estimate is given by minimizing the expected square of the error e:

$$\left\langle e^2 \right\rangle = \left\langle \left(\mu^* - \mu\right)^2 \right\rangle = \left\langle \mu^2 \right\rangle - 2\mu^* \left\langle \mu \right\rangle + \mu^{*2} = \left(\left\langle \mu \right\rangle - \mu^*\right)^2 + \left\langle \mu^2 \right\rangle - \left\langle \mu \right\rangle^2. \tag{5.128}$$

By choosing the mean value for the estimate, the expected square of the error takes its minimal value. Therefore, the variance is the smallest possible error. Minimization of the expected square of the error is called least squares. The drawback is, that an error twice as large is considered four times as serious. Thus, using the mean value tries to avoid the very large, but unlikely errors. Thus, it is very sensitive to the tail region of the pdf.
Laplace suggested to use the minimum of the expected absolute value of the error to define an estimate:

$$\left\langle |\mu^* - \mu| \right\rangle = \int_{-\infty}^{\mu^*} \mathrm{d}\mu \ \left(\mu^* - \mu\right) f(\mu|DI) + \int_{\mu^*}^{\infty} \mathrm{d}\mu \ \left(\mu - \mu^*\right) f(\mu|DI) \tag{5.129}$$

The minimum is given by

$$\frac{\mathrm{d}}{\mathrm{d}\mu^*} \left\langle |\mu^* - \mu| \right\rangle = \int_{-\infty}^{\mu^*} \mathrm{d}\mu \ f(\mu|DI) - \int_{\mu^*}^{\infty} \mathrm{d}\mu \ f(\mu|DI) = 0 \tag{5.130}$$

Or in other words, we have to choose the estimate by the criterion

$$P(\mu < \mu^*|DI) = \frac{1}{2}\,. \tag{5.131}$$

This estimator is called median.

5.5.2. Generic distributions

As it was previously mentioned, an experimental apparatus is not able to measure a quantity with arbitrary precision. Even the measurement of the length of an object is a complicated procedure. The length of a ruler varies with the temperature, the scale is not perfect and the experimenter is not able to read off the result without uncertainties. Effects like these contribute to the total uncertainty in the measurement. However, due to the intrinsic nature of even the simplest measurement, we do not attempt to describe all the little effects that contribute to the uncertainty. Instead, we use probability theory to describe the uncertainty. It was realized, that one can categorize the uncertainties in different classes. In each class, the measured values are distributed with a certain pdf. In this section, we introduce two classes, that are of importance in this work.

5.5.2.1. Gaussian distribution

In 1941 Vernon D. Landon observed, that the electrical noise voltage of an electrical circuit at a certain time always had the same properties independent of the actual value of the voltage. He realized, that it is not possible, to trace back the sources of the noise, rather he suggested

to describe the noise voltage theoretically using probability distribution functions.
We assume, that the present noise can be described by the pdf $g(x|\sigma)$, characterized by the mean value and the width of the distribution. To parametrize the width, we use the standard deviation (Sec. 5.5.1.1). We increment the present noise voltage by a small additional contribution ϵ distributed with $q(\epsilon)$. The updated noise voltage is

$$x' = x + \epsilon. \tag{5.132}$$

Applying the product and sum rule, the pdf of the updated noise voltage is

$$\begin{aligned} f(x') &= \int \mathrm{d}x\mathrm{d}\epsilon\, f(x'x\epsilon) = \int \mathrm{d}x\mathrm{d}\epsilon\, f(x\epsilon)\, P(x'|x\epsilon) \\ &= \int \mathrm{d}x\mathrm{d}\epsilon\, f(x)\, f(\epsilon)\, \delta(x+\epsilon-x') = \int \mathrm{d}\epsilon\, f(x'-\epsilon)\, f(\epsilon)\,. \end{aligned} \tag{5.133}$$

Note, that this equation is written in an abstract notation, where f denotes an arbitrary pdf, in the same way that $P(A)$ denotes a real number. Identifying with the actual functional form, we write

$$g(x'|\sigma') = \int \mathrm{d}\epsilon\, g(x'-\epsilon|\sigma)\, q(\epsilon)\,. \tag{5.134}$$

The expansion of $g(x = x' - \epsilon|\sigma)$ in the vicinity of x' reads

$$g(x'-\epsilon|\sigma) = g(x'|\sigma) + \left.\frac{\partial g(x|\sigma)}{\partial x}\right|_{x=x'} (x-x') + \frac{1}{2}\left.\frac{\partial^2 g(x|\sigma)}{\partial x^2}\right|_{x=x'} (x-x')^2 + \dots\,. \tag{5.135}$$

Putting the expansions back into (5.134) leads to

$$g(x'|\sigma') = g(x'|\sigma) - \frac{\partial g(x'|\sigma)}{\partial x'} \int \mathrm{d}\epsilon\, \epsilon q(\epsilon) + \frac{1}{2}\frac{\partial^2 g(x'|\sigma)}{\partial x'^2} \int \mathrm{d}\epsilon\, \epsilon^2 q(\epsilon) + \dots\,. \tag{5.136}$$

The mean value of the pdf $q(\epsilon)$ is zero. Hence,

$$g(x'|\sigma') = g(x'|\sigma) + \frac{1}{2}\langle\epsilon^2\rangle \frac{\partial^2 g(x'|\sigma)}{\partial x'^2} + \dots\,. \tag{5.137}$$

On the other hand, we can also expand the pdf $g(x'|\sigma')$ in the standard deviation. For this purpose we calculate the variance σ'^2 of the updated distribution. The mean value is

$$\begin{aligned} \langle x'\rangle &= \int \mathrm{d}x'\, x' \cdot g(x'|\sigma') = \int \mathrm{d}x'\, x' \cdot \int \mathrm{d}\epsilon\, g(x'-\epsilon|\sigma)\, q(\epsilon) \\ &= \int \mathrm{d}x\mathrm{d}\epsilon\, (x+\epsilon)\, g(x|\sigma)\, q(\epsilon) = \langle x\rangle + \langle\epsilon\rangle. \end{aligned} \tag{5.138}$$

The second moment is given by

$$\begin{aligned} \langle x'^2\rangle &= \int \mathrm{d}x'\, x'^2 \cdot g(x'|\sigma') = \int \mathrm{d}x'\, x'^2 \cdot \int \mathrm{d}\epsilon\, g(x'-\epsilon|\sigma)\, q(\epsilon) \\ &= \int \mathrm{d}x\mathrm{d}\epsilon\, (x+\epsilon)^2\, g(x|\sigma)\, q(\epsilon) = \langle x^2\rangle + \langle\epsilon^2\rangle + 2\langle x\rangle\langle\epsilon\rangle. \end{aligned} \tag{5.139}$$

Therefore, the standard deviation squared of the updated distribution is obtained as

$$\begin{aligned}\sigma'^2 &= \langle x^2\rangle - \langle x\rangle^2 + \langle \epsilon^2\rangle - \langle \epsilon\rangle^2 \\ &= \sigma^2 + \langle \epsilon^2\rangle. \end{aligned} \tag{5.140}$$

Employing this result we write

$$\begin{aligned} g(x'|\sigma') &= g(x'|\sigma) + \left.\frac{\partial g(x'|\sigma')}{\partial\left(\sigma'^2\right)}\right|_{\sigma'=\sigma}\left(\sigma'^2-\sigma^2\right)+\dots \\ &= g(x'|\sigma) + \langle\epsilon^2\rangle\frac{\partial g(x'|\sigma)}{\partial\left(\sigma^2\right)}+\dots . \end{aligned} \tag{5.141}$$

Comparing the equations (5.137) and (5.141), we obtain the following differential equation:

$$\frac{1}{2}\frac{\partial^2 g(x'|\sigma)}{\partial x'^2} = \frac{\partial g(x'|\sigma)}{\partial\left(\sigma^2\right)}. \tag{5.142}$$

With the initial condition $g(x|\sigma=0)=\delta(x)$, the solution is the Gaussian distribution

$$g(x|\sigma) = \frac{1}{\sqrt{2\pi\sigma^2}}\, e^{-\frac{x^2}{2\sigma^2}}. \tag{5.143}$$

Strictly speaking, this derivation is only valid up to second order in the expansion. By adding more and more variations so that the updated quantity is given by $x' = x + n\epsilon$, the derivation becomes exact[3]. In general, the additive noises can have different origins. The Gaussian distribution is often denoted by $\mathcal{N}(\mu,\sigma^2)$. In the following, we utilize the notation

$$x \sim \mathcal{N}(\mu,\sigma^2) \tag{5.144}$$

to state that the quantity x is distributed as a Gaussian distribution with mean value μ and standard deviation σ. Hence, its probability distribution function reads

$$f(x|I) = \frac{1}{\sqrt{2\pi}\sigma}\exp\left[-\frac{1}{2}\left(\frac{\mu-x}{\sigma}\right)^2\right] \equiv g(x,\mu,\sigma)\,. \tag{5.145}$$

To avoid confusion in the terminology, we recall some features of the Gaussian pdf. Figure 5.4 shows a Gaussian distribution with standard deviation $\sigma = 1$. The variance is given by

$$\mathrm{var}(x) = \sigma^2. \tag{5.146}$$

Due to this result, the term variance and standard deviation are almost used as synonyms, although the equality is only valid for the Gaussian distribution. The probability for the interval $[\mu-\sigma, \mu+\sigma]$ is

$$P(-\sigma \le x \le \sigma) = \int_{-\sigma}^{\sigma} \mathrm{d}x\; g(x,\mu,\sigma) \approx 0.683. \tag{5.147}$$

This value is so well known that unfortunately, a probability of 0.683 is always called "one sigma" regardless the actual distribution. Analogue misinterpretations hold for higher "sigmas". A detailed look in this topic is given in appendix E.3.3.

[3] This is an example of the central limit theorem introduced in section 5.8.3. We start from a delta function and by adding more and more noise, we obtain a Gaussian distribution.

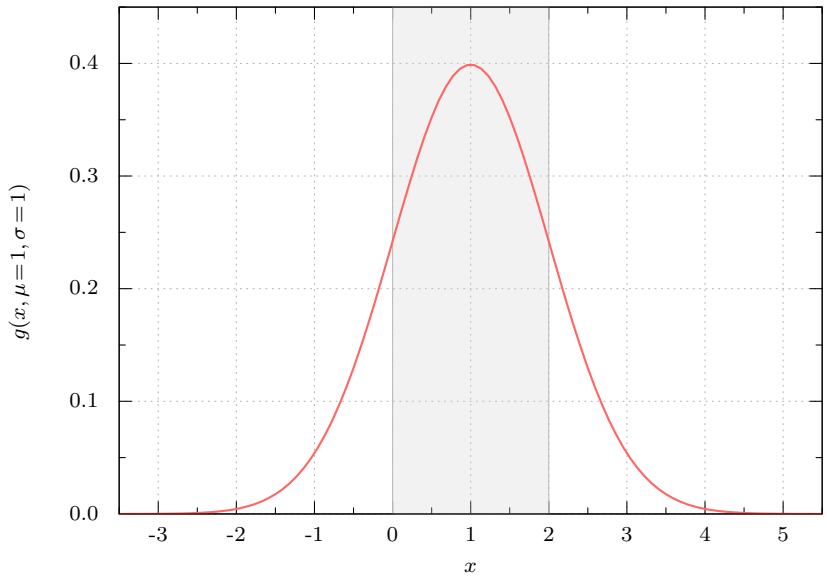

Figure 5.4.: Gaussian probability distribution function $g(x, \mu=1, \sigma=1)$ with mean value one and variance one. The width of the gray area centered of the mean value is $2 \cdot \mathrm{var}(x)$.

5.5.2.2. Log-normal distribution

In the previous section, we have seen, that additive uncertainties from different sources are described by a Gaussian distribution. This distribution is most commonly used for experimental quantities. However, we can not use it for positive quantities, where the additional noise value is proportional to the current value. An example is the normalization of a cross section (see Sec. 5.7) in collider experiments or the life expectation of a cancer patient. Following the derivation in the previous section, the updated noise value with a small additive noise is

$$x' = x + x\epsilon. \tag{5.148}$$

Taking the logarithm and expanding around $\epsilon = 0$, we write

$$\ln x' = \ln x + \epsilon + \cdots . \tag{5.149}$$

With the substitution $y = \ln x$, we get the same equation as for the derivation of the Gaussian distribution (5.132). By re-substitution, we obtain

$$f(x|\sigma) = \frac{1}{x\sqrt{2\pi\sigma^2}} e^{-\frac{\ln^2 x}{2\sigma^2}}, \tag{5.150}$$

where we added a factor x in the denominator to normalize the distribution. We use the symbol $\mathcal{L}(\mu, \sigma^2)$ for the log-normal distribution. Its probability distribution function is denoted by

$$l(x, \mu, \sigma) \equiv \frac{1}{x\sqrt{2\pi\sigma^2}} e^{-\frac{(\mu - \ln x)^2}{2\sigma^2}}, \tag{5.151}$$

where we added a parameter for a variable location. Figure 5.5 shows an example of a log-normal distribution. In contrast to the Gaussian distribution, the mean value and variance

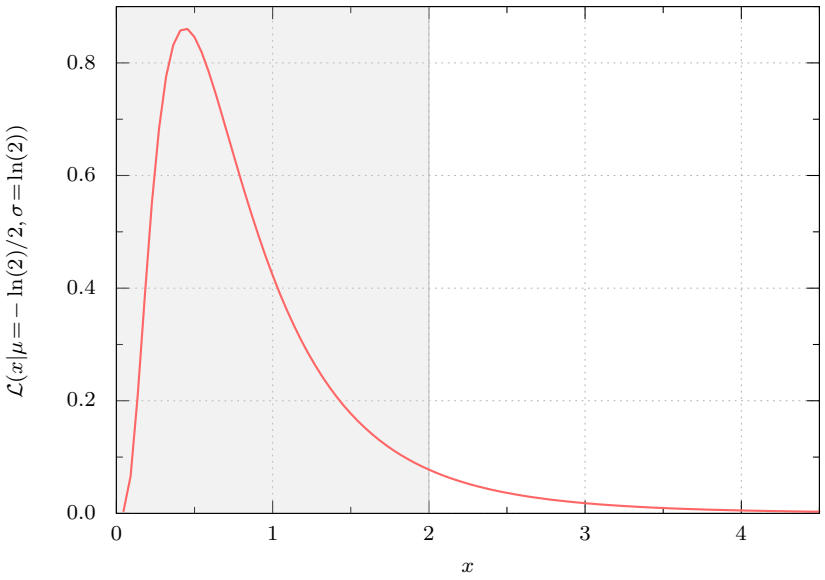

Figure 5.5.: Log-normal probability distribution function $\mathcal{L}(x|\mu = -\ln 2/2, \sigma = \ln(2))$ with mean value 1 and variance 1. The width of gray area centered in the mean value is $2\mathrm{var}(x)$.

are more complicated:

$$\langle x \rangle = e^{\mu + \frac{\sigma^2}{2}}, \qquad \mathrm{var}(x) = \left(e^{\sigma^2} - 1\right) e^{2\mu + \sigma^2}. \tag{5.152}$$

Inverting these formulas leads to

$$\mu = \ln\left(\langle x \rangle\right) - \frac{1}{2} \ln\left(1 + \frac{\mathrm{var}(x)}{\langle x \rangle^2}\right) = \ln\left(\langle x \rangle\right) - \frac{\sigma^2}{2}, \qquad \sigma^2 = \ln\left(1 + \frac{\mathrm{var}(x)}{\langle x \rangle^2}\right). \tag{5.153}$$

The probability for a parameter to be within the variance of a log-normal distribution always depends on the mean value. Thus, stating such probabilities is not unique.

5.5.3. Prior distributions

By this point, we have realized, that priors are an essential compound of probability theory, see Sec. 5.4. The likelihood itself has no probabilistic interpretation, only in connection with priors and the normalization we obtain normalized posterior probabilities. In the case of a discrete hypothesis test, the prior probabilities will be real numbers in the interval $[0, 1]$ (see examples in section 5.3). In this section, we will introduce prior probability distribution functions, that represent our prior state of knowledge in the case of continuous parameters. One might argue, that the inclusion of a prior is not objective, because it alters the result in comparison to the data. It was shown by [Jef39], that for a prior, smooth in the region of the

highest density of the likelihood, the result for the posterior will not depend on the choice of the prior. For a significant contribution to the posterior distribution, the prior has to modify the likelihood in the region of its highest density and not the tail of the likelihood. A prior that seems perfect for this demand is the uniform prior.

5.5.3.1. Uniform prior distribution

Let us assume, we want to estimate a parameter $\theta \in \mathbb{R}$ and the only prior knowledge we have is, that it is contained in a certain interval $\theta \in [a, b]$. To represent the present state of knowledge, the probability in the interval has to be uniform, whereas it vanishes outside of the interval. The uniform prior distribution is

$$f(\theta|I) = u(\theta, a, b) \equiv \begin{cases} \frac{1}{b-a} & a \leq \theta \leq b \\ 0 & \text{else} \end{cases}. \tag{5.154}$$

In the following we use the notation $\mathcal{U}(a, b)$. At first glance, the uniform priors seems to be the most objective choice. However, if the interval becomes large, we will discover a problem. For example, we consider a parameter in the interval $\theta \in [1, 100]$ stretching over two decades. The probability for θ to be in the second decade is 10 times larger than to be in the first one:

$$\frac{\int_{10}^{100} \mathrm{d}\theta\, \mathcal{U}(\theta|100-1)}{\int_{1}^{10} \mathrm{d}\theta\, \mathcal{U}(\theta|100-1)} = \frac{100-10}{10-1} = 10 \tag{5.155}$$

This is the typical situation for a scale parameter. In case where we are not sure about the order of magnitude of the parameter, we use the Jeffrey‘s prior.

5.5.3.2. Jeffrey's prior distribution

Jeffrey‘s prior ensures equal probability per decade in a prior for a real parameter θ in the interval $\theta \in [a, b]$. The functional form is

$$f(\theta|I) = j(\theta, a, b) \equiv \frac{1}{\theta \ln\left(\frac{b}{a}\right)}, \tag{5.156}$$

and we denote it by the symbol $\mathcal{J}(a, b)$. With this prior distribution, we have equal probability for every decade

$$\frac{\int_{10}^{100} \mathrm{d}\theta\; f(\theta|I)}{\int_{1}^{10} \mathrm{d}\theta\; f(\theta|I)} = \frac{\ln(100/10)}{\ln(10/1)} = 1. \tag{5.157}$$

In order to avoid the singularity, we have to truncate the lower bound. In some models, we can choose x or $y = x^2$ as a parameter. Assigning a uniform prior to x and y is not equal. By error propagation, the pdf for y using a uniform prior for x is

$$f(y) = \int \mathrm{d}x\; \delta\left(y - x^2\right) \mathcal{U}(x|b-a) = \frac{1}{2\sqrt{y} \ln\left(\frac{b}{a}\right)}, \tag{5.158}$$

in the interval $\left[a^2, b^2\right]$. However, for Jeffrey‘s prior, the two distributions have the same functional form.

5.5.3.3. Gaussian prior distribution

We might also use a Gaussian distribution as a prior, to express, that we approximately know the mean value and the range of the parameter, but we do not want to exclude the outer region as strictly as with the uniform prior.

5.6. Error propagation

An important aspect of probability theory is error propagation. Suppose, we estimated the posterior probability function $f(\theta|I)$ of several parameters θ. Ultimately, we are interested in the uncertainty of a parameter α that is given as a function g of the estimated parameters θ, namely

$$\alpha = g(\theta)\,. \tag{5.159}$$

The pdf for the parameter α is given by

$$f(\alpha|I) = \int \mathrm{d}\theta\; f(\alpha\theta|I) = \int \mathrm{d}\theta\; f(\theta|I)\, P(\alpha|\theta I)\;. \tag{5.160}$$

Since the probability $P(\alpha|\theta I)$ relates two true values, we employ the delta function

$$P(\alpha|\theta I) = \delta\left[\alpha - g(\theta)\right]. \tag{5.161}$$

The general formula for error propagation becomes

$$f(\alpha|I) = \int \mathrm{d}\theta\; \delta\left[\alpha - g(\theta)\right]\;\; f(\theta|I)\,. \tag{5.162}$$

In numerical applications, we use a distribution with a final width as a representation for the delta function [CSI00]. In fact, error propagation is nothing more than the application of the product rule. Consider a further quantity β with distribution $f(\beta|I)$. Now the new parameter α is given by

$$\alpha = g(\theta, \beta). \tag{5.163}$$

Again, the corresponding pdf is

$$\begin{aligned} f(\alpha|I) &= \int \mathrm{d}\theta\mathrm{d}\beta\; f(\alpha\beta\theta|I) = \int \mathrm{d}\theta\mathrm{d}\beta\; f(\theta|I)\, f(\beta|I)\, P(\alpha|\theta\beta I) \\ &= \int \mathrm{d}\theta\mathrm{d}\beta\; \delta\left[\alpha - g(\theta,\beta)\right]\;\; f(\theta|I)\, f(\beta|I)\,. \end{aligned} \tag{5.164}$$

5.7. Parameter estimation

At this stage, we have completed all preparatory work for the treatment of parameter estimation. Starting from the sum and product rule, we have extended the applicability to continuous hypotheses. We used this result to derive generic probability distributions that appear in measurements. Toward describing the experiments, we use models involving free parameters.
For parameter estimation in general, the model F relates the quantity y to the quantities u, v, w, x, ... using M parameters $\theta = \{\theta_1, \ldots, \theta_M\}$. The relation between the true values of the quantities is

$$y = F(x, w, v, u, \ldots, \theta). \tag{5.165}$$

We will restrict our considerations to the dependence on one quantity x due to simplicity. The extension to the general case is straight forward.
To estimate the unknown parameters, we need to measure the quantity y in dependence of the quantity x. Due to the limited precision of our measurement, it is not possible to measure the true values of the quantities in our model. Instead, we will measure values furnished with an error. Thus, an experiment will provide a number of N measured values (x_i', y_i'). These measured values are related to their true values (x_i, y_i) by probability distribution functions. Without specifying the distribution, we may write

$$f\left(y_i'|y_i I\right), \quad f\left(x_i'|x_i I\right). \tag{5.166}$$

In the literature, also the following notation for the relation of measured and true values is used:

$$y_i' = y_i + a_i, \quad x_i' = x_i + b_i. \tag{5.167}$$

Where the difference between the true value and the measured on is given by the errors a and b. Using the formula for error propagation (5.162), the pdfs of the experimental values and the errors are related by

$$g(a_i|y_i I) = f(a_i + y_i|y_i I). \tag{5.168}$$

Consequently, by knowing the distribution of the errors, we also know the distribution of the measured values and vice versa.

5.7.1. Direct measurement

For didactic reasons, we first treat the case, where the model does not depend on the quantity x. We analyze a direct measurement of the parameters. The dependence of the true values on the parameters for all data points simplifies to

$$y_i = F(\theta) = \mu. \tag{5.169}$$

Without loss of generality, we estimate only one parameter μ. The three quantities in our analysis are y_i', μ and y_i. The dependence of the true values y_i and the parameter μ is given by the model. Whereas, the dependence of the true values and the experimental values are given by probability distributions. Figure 5.6 shows the corresponding dependencies in a Bayesian network. The aim is to calculate the posterior distribution function $f(\mu|y'I)$ for μ given the

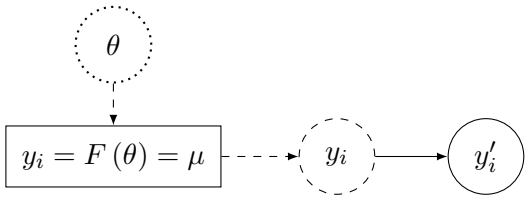

Figure 5.6.: Bayesian network for the direct measurement of a parameter. The dashed line symbolizes dependence via the model, whereas the solid lines represent the dependence by probability distribution functions. The parameters of the models are in the dotted node. The measured values and the true ones are in the solid and dashed nodes, respectively.

data y_i'. In the first step, we write down the joint probability distribution function for the quantities given in our problem. We use the sum rule to factor out the prior probability of the data:

$$f\left(yy'\mu\middle|I\right) = P\left(y'\middle|I\right) f\left(y\mu\middle|y'I\right). \tag{5.170}$$

A quantity without the index i symbolizes the logical product of all N actual quantities. Expanding the symbol, the above equation reads

$$f\left(y_1 \cdots y_N \cdot y_1' \cdots y_N' \cdot \mu\middle|I\right) = P\left(y_1' \cdots y_N'\middle|I\right) f\left(y_1 \cdots y_N \cdot \mu\middle|y_1' \cdots y_N' \cdot I\right).$$

The true values of the measured quantities are not known, and we are not interested in them. Consequently, we obtain the posterior distribution from the second term on the right hand side of (5.170), by marginalizing over all true values y_i

$$f\left(\mu\middle|y'I\right) = \int \mathrm{d}y_1 \cdots \mathrm{d}y_N \; f\left(y\mu\middle|y'I\right). \tag{5.171}$$

Inserting (5.170) into the equation for the joint pdf (5.170), the posterior pdf is given by

$$f\left(\mu\middle|y'I\right) = \int \mathrm{d}y \; \frac{f(yy'\mu|I)}{P(y'|I)}. \tag{5.172}$$

Recursive use of the sum rule factorizes the numerator into three terms reflecting the dependencies of the quantities shown in figure 5.6. The result is

$$f\left(yy'\mu\middle|I\right) = f(\mu|I)\, f(y|\mu I)\, P\left(y'\middle|y\mu I\right), \tag{5.173}$$

where the first term is the prior probability of the parameter. Note, the above expression will always contain probability distribution functions connecting the true values to the measured

ones, and pdfs connecting the true values via the model. In the case of N independent measurements, we may write these as

$$P(y'|y\mu I) = P(y'|yI) = \prod_{i=1}^{N} P(y_i'|y_i I)\,,$$
$$f(y|\mu I) = \prod_{i=1}^{N} f(y_i|yI) = \delta\left(y_i - \mu\right). \tag{5.174}$$

Inserting the factorization from above into (5.172) we obtain the desired posterior distribution[4]:

$$\begin{aligned} f(\mu|y'I) &= \int \mathrm{d}y_1 \cdots \mathrm{d}y_N \, \frac{f(\mu|I)\,\delta\left(y_i - \mu\right) \prod_i P(y_i'|y_i I)}{P(y'|I)} \\ &= \frac{f(\mu|I) \prod_i P(y_i'|\mu I)}{P(y'|I)} = \frac{f(\mu|I)\, P(y'|\mu I)}{P(y'|I)}\,. \end{aligned} \tag{5.175}$$

The normalization of the posterior pdf is calculated by integrating the prior and the likelihood over the whole parameter space:

$$P(y'|I) = \int \mathrm{d}\mu \; f(y'\mu|I) = \int \mathrm{d}\mu \; f(\mu|I)\, P(y'|\mu I)\;. \tag{5.176}$$

In most of the practical applications, a Gaussian distribution is used for the distribution of the experimental values. The corresponding likelihood, for N independent measurements reads

$$P(y'|\mu I) = \prod_{i=1}^{N} g(y_i', \mu, \sigma)\;. \tag{5.177}$$

In the problem of direct measurement of a parameter it is possible to find an analytic solution for the posterior pdf.
We consider the tree cases: All the data points have a Gaussian distribution and

1. the same known standard deviation σ,
2. the same unknown standard deviation σ,
3. different known standard deviations σ_i.

The detailed calculation is given in the appendix and we only present the results here. In the first case, the mean value and the variance of the parameter (see appendix E.2.1) are

$$\langle \mu \rangle = \overline{y} = \frac{1}{N} \sum_{i=1}^{N} y_i', \qquad \mathrm{var}(\mu) = \frac{\sigma^2}{N}. \tag{5.178}$$

[4] This is exactly the same result as obtained in (5.120), but we gained a detailed understanding of parameter estimation and the derivation is directly applicable to complex situations.

It is well known, that the mean value is given by the arithmetic mean and the variance shrinks with the square root of the number of measurements. This result is an important consequence of the Gaussian distribution. A detailed analysis of the consequences of using a Gaussian for the distribution of the measured values is given in section 5.8.
In the second case, also the variance is unknown. The corresponding posterior distribution function is

$$f\left(\mu\sigma\middle|y'I\right) = \frac{f(\mu|I)\, f(\sigma|I)\, P(y'|\mu I)}{P(y'|I)}. \tag{5.179}$$

As demonstrated in appendix E.2.2, we obtain the posterior pdf for the parameter μ by marginalization. The resulting mean value and the variance are

$$\langle\mu\rangle = \overline{y}, \qquad \mathrm{var}(\mu) = \frac{1}{N(N-3)} \sum_{i=1}^{N} \left(\overline{y} - y_i'\right)^2. \tag{5.180}$$

The mean value of the standard deviation squared is given by

$$\langle\sigma^2\rangle = \frac{1}{N-1} \sum_{i=1}^{N} \left(\overline{y} - y_i'\right)^2. \tag{5.181}$$

Quite frequently, instead of the variance of the parameter, the mean value of the standard deviation is used to express the uncertainty in the parameter. In fact, the estimate (5.180) is more accurate.
In the third case (appendix E.2.3), where the standard deviation of all measured values is known, the mean value is given by the weighted arithmetic mean:

$$\langle\mu\rangle = \overline{y}_w = \frac{\sum_{i=1}^{N} w_i y_i'}{\sum_{i=1}^{N} w_i}, \qquad \mathrm{var}(\mu) = \frac{1}{\sum_{i=1}^{N} w_i}, \qquad w_i = \frac{1}{\sigma_i^2}. \tag{5.182}$$

In case of equal weights, we obtain the second case.

5.7.2. Indirect measurement

In the case of an indirect measurement of the model parameters, where the model depends on the quantity x, it is no longer possible to find an analytical solution for an arbitrary model. However, there are numerical procedures to evaluate the posterior pdf. The dependence of the true values on the parameter is

$$y = F(x, \theta). \tag{5.183}$$

To derive the posterior pdf for the parameters, we follow the same steps as in the previous section. The unknown quantities are

$$x, y, \quad x', y', \quad \theta. \tag{5.184}$$

Figure 5.7 shows the corresponding Bayesian network. Using the sum rule, we write the joint

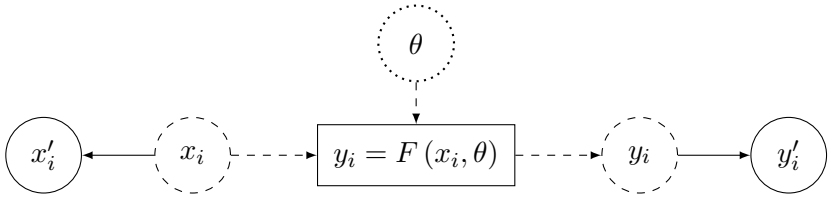

Figure 5.7.: Bayesian network for a general parameter estimation. For the meaning of the symbols see figure 5.6.

probability distribution function as

$$f\big(xyx'y'\theta\big|I\big) = P\big(x'y'\big|I\big)\, f\big(xy\theta\big|x'y'I\big)\,. \tag{5.185}$$

The posterior pdf is given via marginalization by the last term in the previous equation

$$f\big(\theta\big|x'y'I\big) = \int \mathrm{d}x\mathrm{d}y\; f\big(xy\theta\big|x'y'I\big)\;. \tag{5.186}$$

Combining the two previous equations, we may write

$$f\big(\theta\big|x'y'I\big) = \int \mathrm{d}x\mathrm{d}y\; \frac{f(xyx'y'\theta|I)}{P(x'y'|I)}. \tag{5.187}$$

Factorization into the two types of dependencies leads to

$$f\big(xyx'y'\theta\big|I\big) = f(\theta|I)\, f(x|\theta I)\, f(y|x\theta I)\, P\big(y'\big|xy\theta I\big)\, P\big(x'\big|y'xy\theta I\big)\,. \tag{5.188}$$

Identifying of the last term in the equation above with the corresponding distributions, we write

$$\begin{aligned}
P\big(x'\big|y'xy\theta I\big) &= P\big(x'\big|xI\big) = \prod_i P\big(x'_i\big|x_iI\big)\,,\\
P\big(y'\big|xy\theta I\big) &= P\big(y'\big|yI\big) = \prod_i P\big(y'_i\big|y_iI\big)\,,\\
f(y|x\theta I) &= \prod_i f(y_i|x_i\theta I) = \prod_i \delta\left[y_i - F\left(x_i,\theta\right)\right],\\
f(x|\theta I) &= 1.
\end{aligned} \tag{5.189}$$

Besides the normalization, the posterior pdf is proportional to

$$f\big(\theta\big|x'y'I\big) \propto \int \mathrm{d}x\mathrm{d}y\; \prod_i P\big(x'_i\big|x_iI\big)\, P\big(y'_i\big|y_iI\big)\, \delta\left[y_i - F\left(x_i,\theta\right)\right] f(\theta|I)\,. \tag{5.190}$$

We are able to perform the marginalization over the true values y_i:

$$f\big(\theta\big|x'y'I\big) \propto \int \mathrm{d}x\; \prod_i\; P\big(x'_i\big|x_iI\big)\, P\big(y'_i\big|F\left(x_i,\theta\right)I\big)\, f(\theta|I)\;. \tag{5.191}$$

If the pdf of the measured values x_i' follows a specific pdf, we will be left with N integrals or we use a linear approximation for the model to perform the integration analytically. In practice, it is common, that the error on the values x_i' is not known, or it is neglected. We express this knowledge by a delta function:

$$P\left(x_i'\middle|x_i I\right) = \delta\left(x_i' - x_i\right). \tag{5.192}$$

Consequently, the posterior pdf including the normalization is

$$\boxed{f\left(\theta\middle|x'y'I\right) = \frac{f(\theta|I)\, P[y'|F\left(x',\theta\right) I]}{\int \mathrm{d}\theta\; f(\theta|I)\, P[y'|F\left(x',\theta\right) I]}.} \tag{5.193}$$

To simplify the notation, we collapsed the independent measurement values. It is common practice, to use the abbreviations

$$P\left(y'\middle|\theta I\right) \equiv P\left[y'\middle|F\left(x',\theta\right) I\right] \tag{5.194}$$

for the likelihood. For convenience, sometimes the measured values are represented by the symbol D. In most situations we use a Gaussian distribution for the measured values, the corresponding likelihood function is

$$P\left(y_i'\middle|\, F\left(x_i',\theta\right) I\right) = \prod_i g\left(y_i', F\left(x_i',\theta\right), \sigma_i\right), \tag{5.195}$$

where σ_i denotes the standard deviations of the measured values. Once we have understood the steps of the derivation, we are able to extend it to any possible situation.
For high energy physics, it is experimentally difficult to determine the normalization of the experimental data. Therefore, we consider the normalization as an additional parameter. In the end, we are always able to marginalize over the normalization parameter. The correct treatment of the normalization error is especially important when analyzing data from different experiments. We will briefly derive the posterior pdf for the parameters including a normalization uncertainty. The model is

$$y = \nu \cdot F(x,\theta), \tag{5.196}$$

including the normalization ν. The modified Bayesian network is displayed in figure 5.8. Repeating the previous calculation for the new model leads to

$$f\left(\theta\nu\middle|x'y'I\right) = \frac{f(\theta|I)\, f(\nu|I)\, P[y'|\nu \cdot F\left(x',\theta\right) I]\, P(\nu'|\nu)}{\int \mathrm{d}\theta \mathrm{d}a\; f(\theta|I)\, f(\nu|I)\, P[y'|\nu \cdot F\left(x',\theta\right) I]\, P(\nu'|\nu)}. \tag{5.197}$$

Since the normalization is a positive real number, the probability distribution function of the measured values follows the log-normal distribution with mean value one introduced in section 5.5.2.2. However, for small errors in the normalization, it is equivalent to a Gaussian distribution.
This concludes our analysis on parameter estimation. The only unclear topic is, why we use a Gaussian distribution in most of the practical applications.

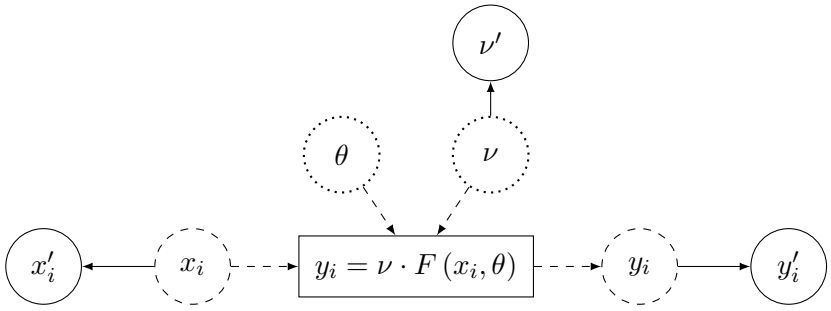

Figure 5.8.: Bayesian network for parameter estimation with a normalization uncertainty. For the meaning of the symbols see figure 5.6.

5.8. Consequences of the Gaussian distribution

In practice, the Gaussian distribution is the one, that is most frequently used. The derivation of Gauss (1809) proved, that it is the only distribution which leads to the arithmetic mean as mean value of the posterior pdf (Sec. 5.7.1). Yet, it is often argued, that employing a Gaussian distribution for the measured values does not reflect the true distribution of the measured values.
To clarify the situation, we analyze the consequences of a Gaussian distribution for the estimated parameters. We start with deriving the actual information content in our estimates, that is transferred by a Gaussian distribution. This is followed by studying the accuracy of the estimates depending on different distributions. Finally, we derive the central limit theorem, showing that if a measured value is given by the sum of a large number of contributions, the value will follow a Gaussian distribution, independent of the distribution of the single contributions.

5.8.1. Best sampling distribution

In section 5.7.1 we analyzed the direct measurement of a parameter μ. The corresponding dependence of the true values is

$$y_i = \mu.$$

We derived the mean value and the variance for the parameter using N measured values y_i' following a Gaussian distribution. The result for a known standard deviation of the measured values is

$$\langle \mu \rangle = \overline{y} = \frac{1}{N} \sum_{i=1}^{N} y_i', \qquad \mathrm{var}(\mu) = \frac{\sigma}{\sqrt{N}}.$$

In case of an unknown standard deviation for all measured values we can estimate the deviation as well:

$$\langle \mu \rangle = \overline{y}, \qquad \mathrm{var}(\mu) = \frac{\sum_{i=1}^{N} (\overline{y} - y_i')^2}{N(N-3)}, \qquad \langle \sigma^2 \rangle = \frac{\sum_{i=1}^{N} (\overline{y} - y_i')^2}{N-3}.$$

In the third case, we assume different, known standard deviations for all measured values. Hence, the estimates of the parameter are

$$\langle \mu \rangle = \overline{y}_w = \frac{\sum_{i=1}^{N} w_i y_i'}{\sum_{i=1}^{N} w_i}, \qquad \mathrm{var}(\mu) = \frac{1}{\sum_{i=1}^{N} w_i}, \qquad w_i = \frac{1}{\sigma_i^2}.$$

In every case, the estimates only depend on the first and second moment of the distribution for the measured values.
This is exactly, what the Gaussian distribution does. If we use a Gaussian distribution for the measured values, our estimate will only use the first and second moment of the distribution for the measured values. Therefore, in a situation, where we only know these two moments, a Gaussian distribution perfectly describes our knowledge. If the true distribution of the measured values is in fact Gaussian or not is irrelevant, because we do not know it anyway. So, only in cases where more information is known, we assign a different distribution.
These arguments also hold for the indirect measurement of parameters (Sec. 5.7.2), albeit, we can not derive a closed form of the posterior pdf for an arbitrary model.

5.8.2. Most accurate estimates

Additionally, we compare the accuracy of our estimates, using a Gaussian distribution for the measured values, to all other distributions. For this purpose, we reanalyze the case of the direct measurement of a parameter (Sec. 5.7.1) using N measured values y_i'. We assume, that the data is independent and follows a single peaked distribution. The posterior pdf for the parameter μ is proportional to the likelihood function

$$f(\mu|y'I) \propto \prod_{i=1}^{N} P(y_i'|\mu I)\,. \tag{5.198}$$

In case of a constant prior in the region of high probability, the mean value of the posterior pdf will coincide with the maximum of the likelihood. For convenience, we apply the logarithm

$$\ln f(\mu|y'I) = C + \sum_{i=1}^{N} \ln P(y_i'|\mu I)\,. \tag{5.199}$$

Using the abbreviation

$$\ln P(y_i'|\mu I) = g(y_i' - \mu)\,, \tag{5.200}$$

we find the maximum via the derivative

$$\frac{\mathrm{d}}{\mathrm{d}\mu} \ln f(\mu|y'I) \stackrel{!}{=} 0 = \sum_{i=1}^{N} \frac{\mathrm{d}}{\mathrm{d}\mu} g(y_i' - \mu)\,. \tag{5.201}$$

We assume, that the parameter μ is close to the data values y_i' and expand every term separately in the vicinity of zero:

$$\sum_{i=1}^{N} \frac{\mathrm{d}^2}{\mathrm{d}^2\mu} g(y_i' - \mu)\Big|_{\mu=y_i'} (\mu - y_i') = 0. \tag{5.202}$$

We denote the second order derivatives at the specific points by the weights w_i:

$$\sum_{i=1}^{N} w_i(\mu - y_i') = 0\,. \tag{5.203}$$

Hence, we estimate the parameter by a weighted arithmetic mean:

$$\langle \mu \rangle = \sum_{i=1}^{N} w_i' y_i', \qquad w_i' = \frac{w_i}{\sum_{i=1}^{N} w_i}. \tag{5.204}$$

The variance of our estimate is

$$\begin{aligned} \mathrm{var}(\mu) &= \langle\, (\mu - \langle \mu \rangle))^2 \rangle = \langle \left[\sum_{i=1}^{N} w_i' \left(\mu - y_i'\right) \right]^2 \rangle \\ &= \langle \sum_{i,j=1}^{N} w_i' w_j' e_i e_j \rangle = \sum_{i,j=1}^{N} w_i' w_j' \langle e_i e_j \rangle = \sigma^2 \sum_{i=1}^{N} w_i'^2, \end{aligned} \tag{5.205}$$

where we used that the errors are independent and have the same standard deviation σ, $\langle e_i e_j \rangle = \sigma^2 \delta_{ij}$. Note, that this variance is the variance of an arbitrary single peaked distribution and not necessarily of a Gaussian distribution.
In case of a Gaussian distribution, the weights would be given by the standard deviation $w_i = 1/\sigma_i$ and the normalized ones would be $w_i' = 1/N$. In order to investigate the deviation from a Gaussian distribution, we write the weights as

$$w_i' = \frac{1}{N} + q_i \tag{5.206}$$

Hence, the variance reads as

$$\mathrm{var}(y) = \sigma^2 \sum_{i=1}^{N} \left(\frac{1}{N^2} + \frac{2q_i}{N} + q_i^2 \right) = \sigma^2 \left(\frac{1}{N} + \sum_{i=1}^{N} q_i^2 \right) \tag{5.207}$$

Therefore, using a Gaussian distribution leads to the smallest variance and the most accurate estimate, in comparison to all other distributions.

5.8.3. Central limit theorem

The central limit theorem states, that the distribution of a quantity y given as the sum of N quantities x_i, as N goes to infinity is a Gaussian, regardless of the distribution of the x_i. An example application is the Landon derivation of the Gaussian distribution in section 5.5.2.1. If a quantity is the sum of a large number of effects, this quantity will follow a Gaussian distribution, independent of the individual distributions of each effect.

In this section, we found three reasons to use a Gaussian distribution for measured values. In most of the cases, the measured value is a result of a large number of additive contributions.

According to the central limit theorem, this value follows a Gaussian distribution, regardless of the distribution of the single contributions. Even if we do not know the true distribution of the measured values, using a Gaussian distribution perfectly describes our state of knowledge if we only know the first two moments. As a consequence, the Gaussian distribution will lead to the most accurate estimates.

5.9. Advanced examples

5.9.1. Comparison of two measurements

In this example, we solve a common problem in the analysis of a direct parameter measurement (see section 5.7.1). We measure a quantity employing method 1. For an experiment that is precise and easy to perform. After some time, it is realized, that method 1 does not actually measure the interesting quantity, but rather the sum of two effects. A second experiment using method 2 is designed to isolate the interesting quantity. However, the method is much more difficult and has a larger uncertainty.
In the present example, we analyze two data sets, D_1 and D_2 with 20 and 10 points, respectively. Figure 5.9 shows the two data sets, whereas the numerical values are given in table 5.2. Since we do not have further knowledge of the data, we use a Gaussian distribution for

Nr.	data 1	data 2
1	-0.1981	1.0371
2	-0.0496	0.5779
3	-0.0879	-0.1340
4	-0.2172	-0.3498
5	-0.0935	0.4451
6	0.0008	0.2094
7	-0.0225	0.4886
8	0.1109	-0.4455
9	-0.1488	0.5950
10	0.2368	-0.0593
11	-0.3099	
12	0.0028	
13	-0.1399	
14	0.0629	
15	0.2426	
16	0.0119	
17	0.1875	
18	0.0853	
19	0.2097	
20	-0.0741	

Table 5.2.: Data from the measurements via method 1 and method 2.

the measured values.

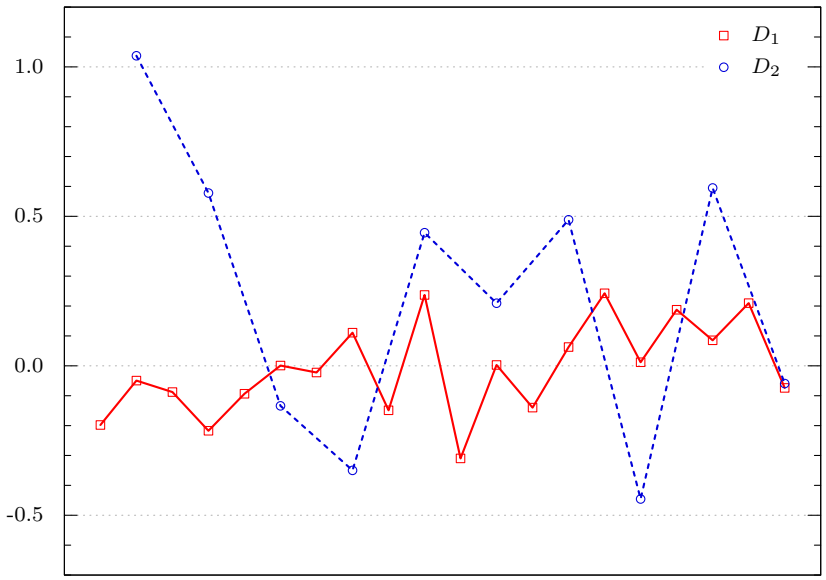

Figure 5.9.: Data from the measurements via method 1 and method 2. For clarity, we connected the measurements with lines.

First, we want to determine the posterior pdf for the parameter μ and the standard variation σ from each data set individually. The posterior (5.179) for one data set is given by

$$f(\mu\sigma|y'I) = \frac{f(\mu|I)\, f(\sigma|I)\, P(y'|\mu\sigma I)}{P(y'|I)}.$$

The likelihood for the independent measurements is

$$P(y'|\mu\sigma I) = \prod_{i=1}^{N} g(y'_i, \mu, \sigma) \ . \tag{5.208}$$

We choose an uniform prior distribution in the interval $[-2, 2]$ for the parameter μ. For σ, we have to use a Jeffrey's prior distribution, because we can consider σ or σ^2 as parameters (Sec. 5.5.3.2). The priors are

$$f(\mu|I) = u(\mu, -2, 2), \qquad f(\sigma|I) = j(\sigma, 0.001, 2)\,. \tag{5.209}$$

By marginalization, we evaluate the normalization constant as

$$P(y'|I) = \int \mathrm{d}\mu\mathrm{d}\sigma f(\mu\sigma y'|I) = \int \mathrm{d}\mu\mathrm{d}\sigma f(\mu|I)\, f(\sigma|I)\, P(y'|\mu\sigma I)\,. \tag{5.210}$$

Finally, the posterior pdf for the parameters is

$$f(\mu\sigma|y'I) = \frac{\frac{1}{\sigma}\prod_{i=1}^{N} g(y'_i, \mu, \sigma)}{\int \mathrm{d}\mu\mathrm{d}\sigma \frac{1}{\sigma}\prod_{i=1}^{N} g(y'_i, \mu, \sigma)}\,. \tag{5.211}$$

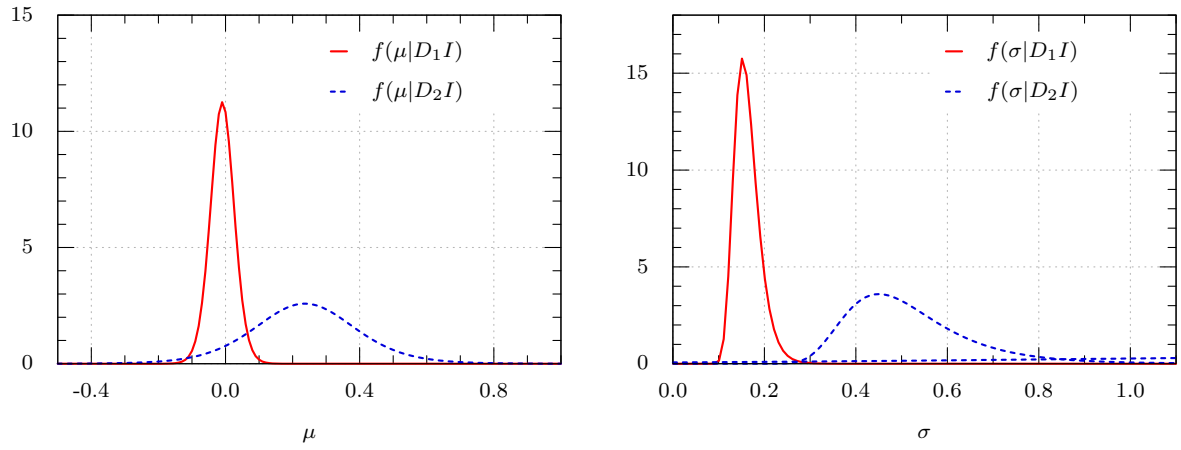

Figure 5.10.: Probability distribution functions for the parameter μ and σ for the two data sets.

Having obtained the posterior pdf, we calculate the posterior pdf of each parameter:

$$f(\mu|y'I) = \int \mathrm{d}\sigma f(\mu\sigma|y'I)\,, \qquad f(\sigma|y'I) = \int \mathrm{d}\mu f(\mu\sigma|y'I)\,. \tag{5.212}$$

The result is shown in figure 5.10. The corresponding mean values and variances of the parameters are

$$\begin{aligned} \mu_1 &= -0.0095 \pm 0.0370, \qquad & \sigma_1 &= 0.1630 \pm 0.0281, \\ \mu_2 &= 0.2364 \pm 0.1701, \qquad & \sigma_2 &= 0.5193 \pm 0.140, \end{aligned} \tag{5.213}$$

where the index denotes the data set. The mean values are different and the standard deviation in the second data set is larger.
However, the only way to systematically compare the estimates obtained from the two data sets is a hypotheses test (Sec. 5.4). We consider the two propositions

$$\begin{aligned} M &\equiv \text{“The mean values are equal: } \mu_1 = \mu_2\text{”}, \\ S &\equiv \text{“The standard deviations are equal: } \sigma_1 = \sigma_2\text{”}. \end{aligned} \tag{5.214}$$

Thus, the complete space of hypotheses contains four propositions: MS, $M\overline{S}$, $\overline{M}S$ and $\overline{M}\,\overline{S}$. The probability of the first one is

$$\begin{aligned} P(MS|D_1D_2I) &= \int \mathrm{d}\mu_1\mathrm{d}\mu_2\mathrm{d}\sigma_1\mathrm{d}\sigma_2\; f(MS\mu_1\mu_2\sigma_1\sigma_2|D_1D_2I) \\ &= \int \mathrm{d}\mu_1\mathrm{d}\mu_2\mathrm{d}\sigma_1\mathrm{d}\sigma_2\; \frac{f(MS\mu_1\mu_2\sigma_1\sigma_2D_1D_2|I)}{P(D_1D_2|I)} \\ &= \int \mathrm{d}\mu_1\mathrm{d}\mu_2\mathrm{d}\sigma_1\mathrm{d}\sigma_2\; \frac{f(MS\mu_1\mu_2\sigma_1\sigma_2|I)\,P(D_1D_2|MS\mu_1\mu_2\sigma_1\sigma_2I)}{P(D_1D_2|I)} \\ &= \int \mathrm{d}\mu\mathrm{d}\sigma\; \frac{f(\mu\sigma|I)\,P(D_1D_2|\mu\sigma I)}{P(D_1D_2|I)}. \end{aligned} \tag{5.215}$$

By modification of the last step, the probabilities for the other hypotheses follow. Besides the normalization constant, they read

$$\begin{aligned}
P\big(M\overline{S}\big|D_1D_2I\big) &\propto \int \mathrm{d}\mu\mathrm{d}\sigma_1\mathrm{d}\sigma_2 \qquad f(\mu\sigma_1|D_1I)\; f(\mu\sigma_2|D_2I)\,,\\
P\big(\overline{M}S\big|D_1D_2I\big) &\propto \int \mathrm{d}\mu_1\mathrm{d}\mu_2\mathrm{d}\sigma \qquad f(\mu_1\sigma|D_1I)\; f(\mu_2\sigma|D_2I)\,,\\
P\big(\overline{M}\;\overline{S}\big|D_1D_2I\big) &\propto \int \mathrm{d}\mu_1\mathrm{d}\mu_2\mathrm{d}\sigma_1\mathrm{d}\sigma_2\; f(\mu_1\sigma_1|D_1I)\; f(\mu_2\sigma_2|D_2I)\,.
\end{aligned} \tag{5.216}$$

We calculate the normalization constant using the condition, that at least one of the four hypotheses H_i, $i = 1, \ldots, 4$, must be true:

$$\begin{aligned}
P(D_1D_2|I) &= \sum_i f(H_iD_1D_2|I)\\
&= \sum_i \int \mathrm{d}\mu_1\mathrm{d}\mu_2\mathrm{d}\sigma_1\mathrm{d}\sigma_2\; f(H_i\mu_1\mu_2\sigma_1\sigma_2D_1D_2|I)\\
&= \sum_i \int \mathrm{d}\mu_1\mathrm{d}\mu_2\mathrm{d}\sigma_1\mathrm{d}\sigma_2\; f(H_i\mu_1\mu_2\sigma_1\sigma_2|I)\, P(D_1D_2|H_i\mu_1\mu_2\sigma_1\sigma_2I)\\
&= \int \mathrm{d}\mu\mathrm{d}\sigma\; f(\mu\sigma|I)\, P(D_1D_2|\mu\sigma I) + \int \mathrm{d}\mu\mathrm{d}\sigma_1\mathrm{d}\sigma_2\; f(\mu\sigma_1|D_1I)\, f(\mu\sigma_2|D_2I)\\
&\quad + \int \mathrm{d}\mu_1\mathrm{d}\mu_2\mathrm{d}\sigma\; f(\mu_1\sigma|D_1I)\, f(\mu_2\sigma|D_2I)\\
&\quad + \int \mathrm{d}\mu_1\mathrm{d}\mu_2\mathrm{d}\sigma_1\mathrm{d}\sigma_2\; f(\mu_1\sigma_1|D_1I)\, f(\mu_2\sigma_2|D_2I)\;.
\end{aligned} \tag{5.217}$$

The resulting probabilities for all four hypotheses are

$$\begin{aligned}
P(MS|D_1D_2I) &= 0.0008,\\
P\big(M\overline{S}\big|D_1D_2I\big) &= 0.4217,\\
P\big(\overline{M}S\big|D_1D_2I\big) &= 0.0008,\\
P\big(\overline{M}\;\overline{S}\big|D_1D_2I\big) &= 0.5777.
\end{aligned} \tag{5.218}$$

Finally, the probability, that the two mean values are different is

$$P\big(\overline{M}S\big|D_1D_2I\big) + P\big(\overline{M}\;\overline{S}\big|D_1D_2I\big) = 0.5785. \tag{5.219}$$

We are not considering this probability as enough evidence to prove that the method 2 successfully disentangled the two contributions. Albeit, we are sure by almost 100 %, that the standard deviation is different.

5.9.2. Nonlinear model

As a second example, we estimate the parameters a and b of the model

$$h(x, a, b) = x^a(1 - x)^b \tag{5.220}$$

Nr.	x'_i	y'_i	σ_i
1	0.1	0.005	0.011
2	0.8	0.113	0.009
3	0.9	0.077	0.011

Table 5.3.: Data generated from $h(x, a = 2, b = 1)$ with a Gaussian error.

from given data. The data contains three points (see Tab. 5.3), that have been generated from $h(x, a=2, b=1)$ by adding a Gaussian error. Let us recall the formula for the posterior distribution function for an indirect measurement given in (5.197):

$$f(ab|DI) = \frac{f(a|I)\, f(b|I)\, P(D|abI)}{P(D|I)}. \tag{5.221}$$

For this problem, we use a uniform prior (Sec. 5.5.3.1) in the interval $[0, 6]$ for both of the parameters:

$$f(a|I) = u(a, 0, 6)\,, \qquad f(b|I) = u(b, 0, 6)\,. \tag{5.222}$$

The likelihood for the four independent data points is

$$P(D|abI) = \prod_{i=1}^{3} g\big(y'_i, h(x'_i, a, b), \sigma_i\big)\ . \tag{5.223}$$

For the normalization we write

$$P(D|I) = \int_0^6 \mathrm{d}a\mathrm{d}b\ f(abD|I) = \int_0^6 \mathrm{d}a\mathrm{d}b\ f(ab|I)\, P(D|abI)\,. \tag{5.224}$$

Finally, the posterior pdf is evaluated as

$$f(ab|I) = \frac{\prod_i g(y'_i, h(x'_i, a, b), \sigma_i)}{\int_0^6 \mathrm{d}a\mathrm{d}b\ \prod_i g(y'_i, h(x'_i, a, b), \sigma_i)}. \tag{5.225}$$

Where the uniform priors drop out. By marginalization, the mean value and the variance of the parameters are:

$$\begin{aligned} \big\langle a \big\rangle &= 2.777, \qquad & \mathrm{var}(a) &= 0.471, \\ \big\langle b \big\rangle &= 0.984, \qquad & \mathrm{var}(b) &= 0.006. \end{aligned} \tag{5.226}$$

Figure 5.11 shows the probability distribution functions for the parameters. Knowing the posterior distribution function of the parameter, we are able to calculate all interesting quantities. In Figure 5.12 we show the pdf for the quantity $c = h(x = 0.5, a, b)$. The mean value and variance are

$$\big\langle c \big\rangle = 0.080, \qquad \mathrm{var}(c) = 9.739 \cdot 10^{-4}. \tag{5.227}$$

In order to demonstrate the accuracy of the estimate (see Fig. 5.13), we plot an error band given by the mean value and the square root of the variance of the function h. For comparison, we also show the mean value separately and the function $h(x, a = 2, b = 1)$ from which we generated the data. From the figure, it is obvious, that almost all information about the parameters is obtained from reproducing the decreasing slope.

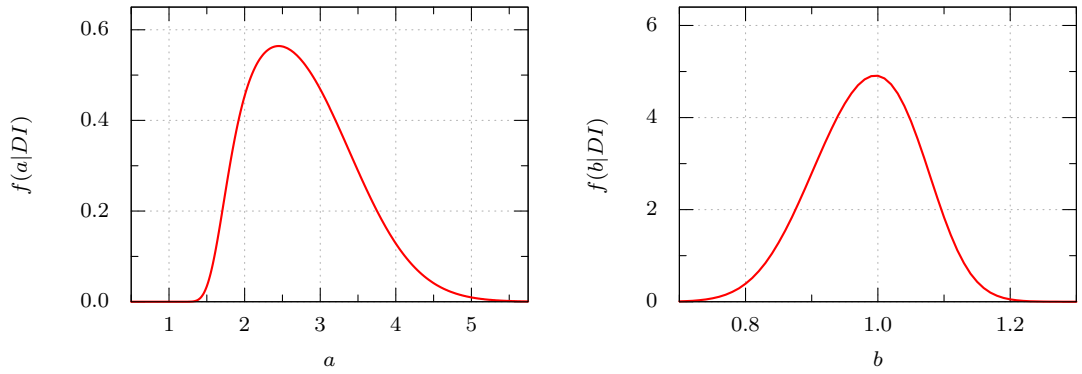

Figure 5.11.: Probability distribution functions for the parameters a and b.

5.9.3. Higgs boson

The Higgs boson is predicted from the standard model of particle physics. Until recently, it was not confirmed experimentally. In this example, we reanalyze the data on the Higgs boson decaying into two photons published by the ATLAS collaboration [A+12]. In a plot of the number of events versus the invariant mass of the two photons, the Higgs boson would show up as a bump standing out of the background (compare figure 5.14(a)).
The measured range is $110\,\text{GeV} \leq m \leq 150\,\text{GeV}$ with an integrated luminosity of $4.9\,\text{fb}^{-1}$ and a center of mass energy of $\sqrt{s} = 7\,\text{TeV}$. For convenience, we consider the events with a subtracted background shown in figure 5.14(b).
As model for the excess, we use a Gaussian, with the mass m, the amplitude A and the standard deviation σ as parameters:

$$h(x) = A \cdot \exp\left[-\frac{1}{2}\left(\frac{x-m}{\sigma}\right)^2\right]. \tag{5.228}$$

The posterior pdf for the parameters (5.193) is given by

$$f\left(Am\sigma|y'I\right) = \frac{f(Am\sigma|I)\,P(y'|Am\sigma I)}{P(y'|I)}. \tag{5.229}$$

For the likelihood, we use a Gaussian distribution instead of a Poisson distribution, because they are equivalent for the given number of events:

$$P\left(y'\middle|Am\sigma I\right) = \prod_i g\left(y_i', h(x_i), \sigma_i\right)\ . \tag{5.230}$$

For the mass and the amplitude we employ a uniform prior. The mass outside of 110-150 GeV is already excluded and we expect the amplitude to be non zero only in the interval [0,150]. The value $A = 0$ encodes that no event is present. The obvious prior for the standard deviation is a Jeffrey‘s prior (Sec. 5.5.3.2), because it is the only prior, which gives the same result no matter whether we consider σ or σ^2 as a parameter. We cut off the Jeffrey’s prior for σ at $\sigma = 0.5$, because if we use a smaller lower bound, the estimate will be sensitive to

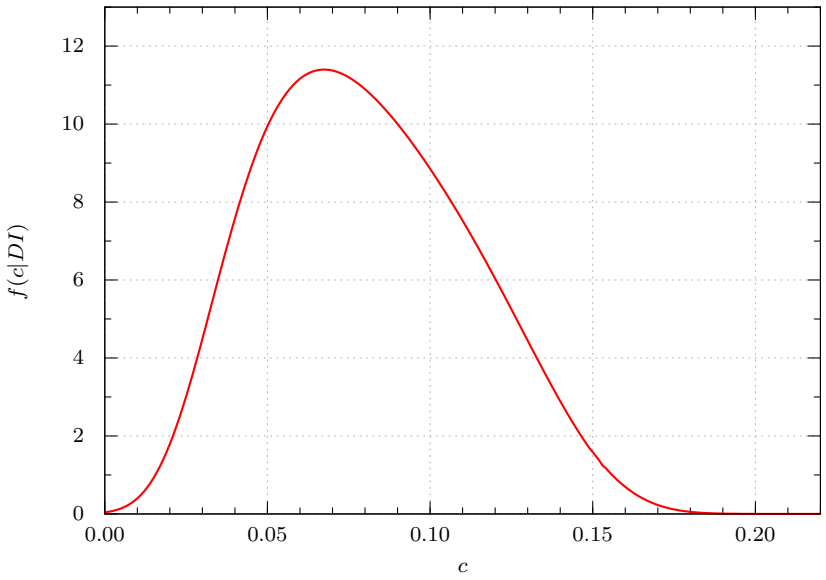

Figure 5.12.: Probability distribution function for $c = h(x = 0.5, a, b)$ derived from the posterior pdf.

resonances between the data points. This is equivalent to the assumption, that the resolution of the experiment is sufficiently good to resolve the excess. To summarize our prior knowledge, we have

$$f(A|I) = u(A, 0, 150)\ , \quad f(m|I) = u(m, 110, 150)\ , \quad f(\sigma|I) = j(\sigma, 0.5, 3)\ . \tag{5.231}$$

Thus, the normalization of the posterior distribution is

$$P(D|I) = \int_0^{150} \mathrm{d}A \int_{110}^{150} \mathrm{d}m \int_{0.5}^{3} \mathrm{d}\sigma\ \frac{1}{\sigma} P(D|Am\sigma I)\,, \tag{5.232}$$

where we neglected the constant terms in the prior distributions, because they drop out in the posterior pdf. Marginalization over the posterior pdf for the parameters leads to the pdfs of each of the three parameters as shown in figure 5.15. The mean value and square root of the standard deviation of the parameter pdfs are:

$$A = 38.14 \pm 23.23, \qquad m = 126.31 \pm 5.37, \qquad \sigma = 0.99 \pm 0.51. \tag{5.233}$$

The pdf of the invariant mass m is not a Gaussian. The probability for the mass to be in the range set by the square root of the variance is $\approx 80\,\%$, as for a Gaussian it should be $\approx 68.3\,\%$.
We have found an estimate for the mass of the Higgs like particle, however, we did not evaluate the significance of the excess. For this task, we perform a hypotheses test (see 5.4) comparing the two hypotheses

$$\begin{aligned} H &\equiv \text{Excess with mass M,} \\ \overline{H} &\equiv \text{No excess, the signal is zero.} \end{aligned} \tag{5.234}$$

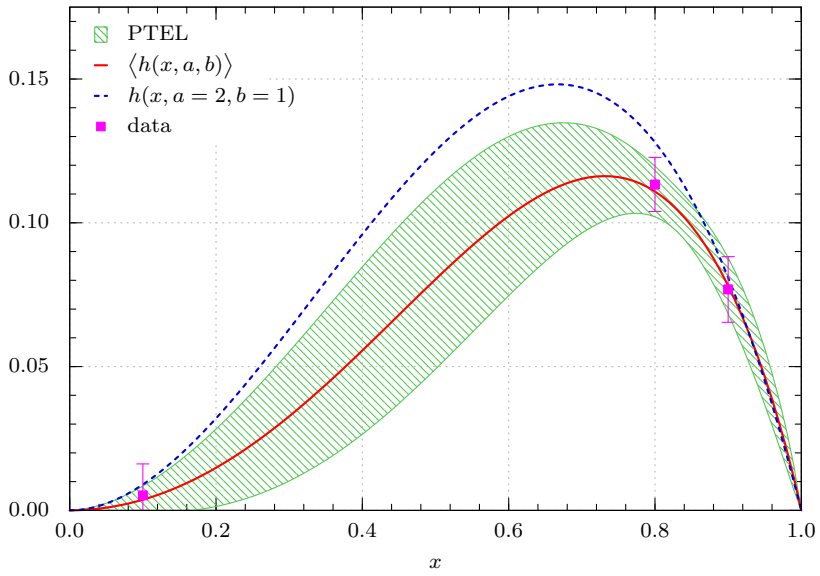

Figure 5.13.: Estimate for $h(x,a,b)$. The area corresponds to the square root of the variance at each point x.

Consequently, we are not interested in the Amplitude or the width. we obtain our hypothesis by marginalization of the posterior. In addition, we do not have any prior information about the hypotheses at hand, so the prior odds is one. The odds ratio is given as

$$O_{12} = \frac{P(H|D\ I)}{P(\overline{H}|D\ I)}. \tag{5.235}$$

By marginalization, the probability for H reads

$$\begin{aligned} P(H|DI) &= \int \mathrm{d}A\mathrm{d}m\mathrm{d}\sigma\ f(HAm\sigma|DI) = C\int \mathrm{d}A\mathrm{d}m\mathrm{d}\sigma\ f(HAm\sigma D|I) \\ &= C\int \mathrm{d}A\mathrm{d}m\mathrm{d}\sigma\ f(HAm\sigma|I)\, P(D|HAm\sigma I) \\ &= C\int \mathrm{d}A\mathrm{d}m\mathrm{d}\sigma\ f(Am\sigma|I)\, P(H|Am\sigma I)\, P(D|HAm\sigma I)\,, \end{aligned} \tag{5.236}$$

with the abbreviation for the normalization $C = 1/P(D|I)$. Employing our hypothesis, we write

$$P(H|Am\sigma I) = P(H|mI) = \delta(m-M). \tag{5.237}$$

Thus, we have the probability

$$P(H|DI) = C\int \mathrm{d}A\mathrm{d}\sigma\ \frac{1}{150}\frac{1}{40}\frac{1}{\sigma\ln\left(\frac{3}{0.5}\right)}P(D|AM\sigma I)\,, \tag{5.238}$$

where the likelihood is given by equation (5.230). For $\overline{H}$, we employ the equivalent derivation as in (5.236), albeit

$$P(\overline{H}|Am\sigma I) = P(\overline{H}|AI) = \delta(A). \tag{5.239}$$

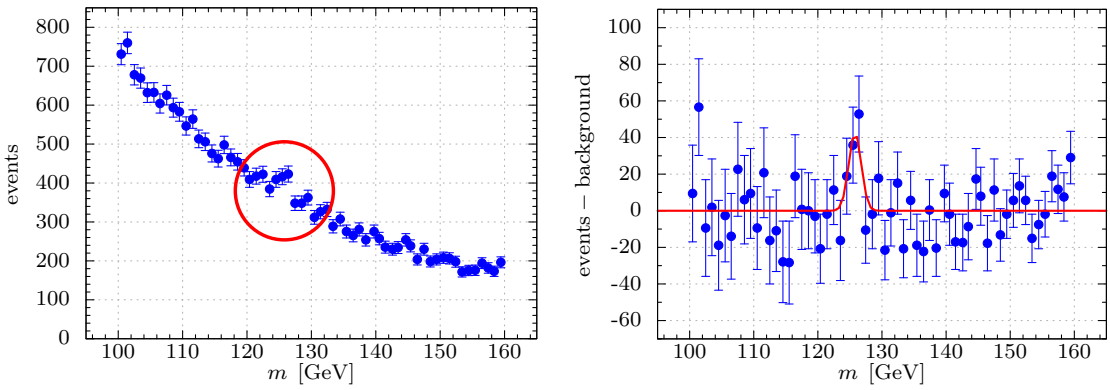

Figure 5.14.: Higgs signal without and with subtracted background. The red line is the estimated model.

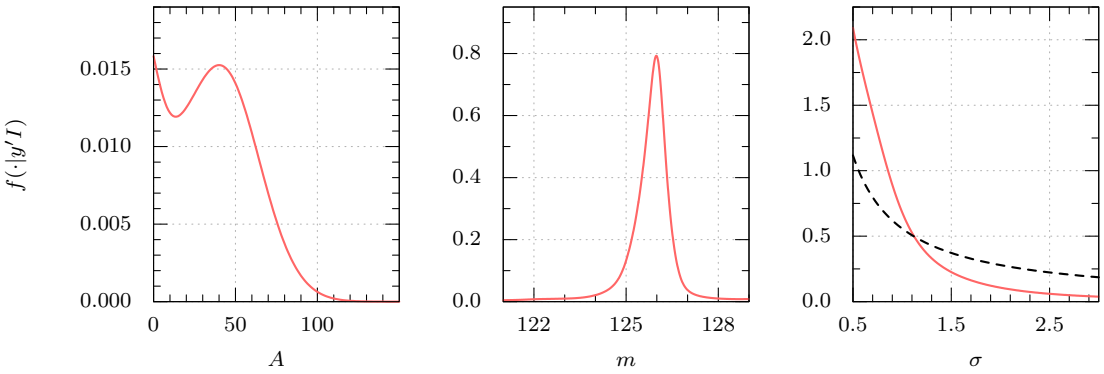

Figure 5.15.: Probability distribution functions for the parameters of the Higgs boson analysis. The dashed line is the applied Jeffries prior.

Hence, the probability for the inverse hypothesis is

$$P\left(\overline{H}\middle|DI\right) = CP(D|(A=0)I)\,. \tag{5.240}$$

For the final result, the constant C cancels in the odds ratio. This derivation seems unnecessarily lengthy and difficult, but the interpretation is very important. From (5.238) we realize, that we have to include the prior distribution for the parameter m. This look-elsewhere-effect drastically reduces the probability for our hypothesis and its origin is easy to understand in our approach.
Note, that the prior distributions in (5.236) act as penalty terms in favor of the model with less parameters. This feature is known under the term Ockham's razor and it is a immediate consequence of the sum and product rule.
Figure 5.16 shows the probability to find an excess with mass M. The shaded intervals mark regions, where the probability for the background model $\overline{H}$ is larger than 95 %. We chose this probability as evidence, that there is no excess in this regions. The highest probability for the hypothesis $H \sim 93\,\%$ is obtained for a mass of 125.98 GeV. In [A+12] the regions 113-115 GeV and 134.5-136 GeV are excluded. Our analysis gives a similar result, albeit the

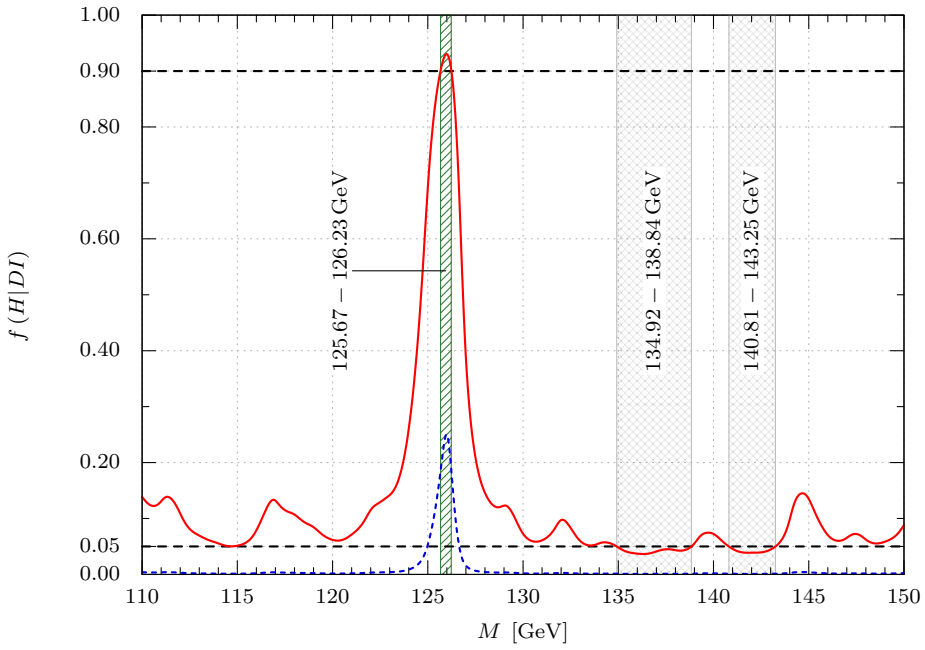

Figure 5.16.: Probability for the discovery of the Higgs boson (hypothesis H) for different masses. The mass ranges filled with the gray cross pattern show the excluded intervals. The blue dashed curve includes the prior for the parameter m (look-elsewhere-effect) and the mass range with the green diagonal pattern marks the area with a probability above 95 % without considering the look-elsewhere-effect.

first region only barely touches the 5 % level and the second region is larger and we find an additional region above 140 GeV. However, including the look-elsewhere-effect, the excess has no significance. The probability for the hypothesis H is 25 % at its maximum, and the background only hypothesis is always preferred. Although our analysis is a simplified version of the original one, we obtain the essential results and reach similar conclusions.

5.9.4. Asymmetric uncertainties

The last example [D'A04] presents a possible solution to deal with the situation, in which more than the first and second moment of the measured values are available. Quite frequently, experimental results for a quantity y are reported in the following scheme

$$y'^{\Delta^+}_{\Delta^-}. \tag{5.241}$$

Quite obviously, the result stems from an asymmetric distribution $a(y)$. The present information is not sufficient to reconstruct the true asymmetric distribution. Therefore, we will still use a Gaussian distribution. In order to determine the corresponding mean value and standard deviation, we analyze the reasons for an asymmetric distribution. There are two possible causes. One is the misuse of the $\Delta\chi^2$ procedure to estimate the uncertainty (Sec. E.3.1.2).

The other one is an asymmetric pdf, due to systematic effects. For example, the errors are larger in a certain direction, or the measured quantity depends non linearly on input quantities of the measurement. To resolve the situation, we consider the asymmetric distribution of the parameter y as a result of nonlinear propagation via the function $F(x)$ from a symmetric distribution $s(x)$ with mean value μ and standard deviation σ. By error propagation (5.162), the asymmetric distribution reads

$$a(y) = \int \mathrm{d}x \; \delta\left[y - F(x)\right] s(x). \tag{5.242}$$

We further assume, that the asymmetric errors are obtained as

$$\Delta^+ = F(\mu + \sigma) - F(\mu), \qquad \Delta^- = F(\mu) - F(\mu - \sigma). \tag{5.243}$$

The aim is to express the mean value and the variance of the distribution a by the asymmetric errors Δ^+ and Δ^-. Expanding the function $F(x)$ around the mean value μ of the symmetric distribution leads to

$$F(x) \approx F(\mu) + F'(\mu)(x - \mu) + \frac{1}{2}F''(\mu)(x - \mu)^2 + \ldots. \tag{5.244}$$

Therefore, the mean value of the asymmetric distribution using (5.242) with the previous expansion (5.244) is

$$\begin{aligned}
\left\langle y \right\rangle &= \int \mathrm{d}y \; y \; a(y) \\
&= \int \mathrm{d}y\mathrm{d}x \; y \; \delta\left[y - F(x)\right] s(x) = \int \mathrm{d}x \; F(x) \; s(x) \\
&\approx \int \mathrm{d}x \; \left[F(\mu) + F'(\mu)(x - \mu) + \frac{1}{2}F''(\mu)(y - \mu)^2\right] \; s(x) \\
&\approx F(\mu) + \frac{1}{2}F''(\mu)\sigma^2.
\end{aligned} \tag{5.245}$$

In the same manner, we obtain the variance

$$\begin{aligned}
\mathrm{var}(y) &\approx \int \mathrm{d}x \; \left[F(\mu) + F'(\mu)(x - \mu) + \frac{1}{2}F''(\mu)(y - \mu)^2\right]^2 \; s(x) \\
&\approx F^2(\mu) + \left(F'(\mu)\right)^2 \sigma^2.
\end{aligned} \tag{5.246}$$

For the first and second order derivatives, we use the approximations [BSMM00]

$$\left.\frac{\mathrm{d}F(x)}{\mathrm{d}x}\right|_{x=\mu} = \frac{F(\mu + \sigma) - F(\mu - \sigma)}{2\sigma} = \frac{\Delta^+ + \Delta^-}{2\sigma}, \tag{5.247}$$

$$\left.\frac{\mathrm{d}^2F(x)}{\mathrm{d}x^2}\right|_{x=\mu} = \frac{F(\mu + \sigma) - 2F(\mu) + F(\mu - \sigma)}{\sigma^2} = \frac{\Delta^+ - \Delta^-}{\sigma^2}. \tag{5.248}$$

Hence, the mean value and variance in terms of the asymmetric uncertainties are

$$\left\langle y \right\rangle = F(\mu) + \frac{\Delta^+ - \Delta^-}{2}, \qquad \mathrm{var}(y) = \left(\frac{\Delta^+ + \Delta^-}{2}\right)^2. \tag{5.249}$$

Thus, the probability distribution, that represents our knowledge best is

$$P(y'|yI) = g\left(y', y + \frac{\Delta^+ - \Delta^-}{2}, \frac{\Delta^+ + \Delta^-}{2}\right) . \tag{5.250}$$

5.10. Summary

In this chapter, we have developed probability theory as an extension of logic from basic desiderata. Applying the resulting sum and product rule, we solve the three main problems in probability theory: hypothesis tests, error propagation and parameter estimation. Foremost, the first issue is treated for discrete hypotheses. Extending the formalism to continuous propositions leads to the solution of the latter two problems involving probability distribution functions. We derived certain probability distribution functions that theoretically describe the noise of experimental data. Finally, we gave a detailed solution to parameter estimation using prior information as a crucial ingredient. In the end, we analyzed the consequences of a Gaussian distribution for measured values.
The presented approach to probability theory has certain advantages over the procedures of orthodox statistics. As demonstrated in appendix E.3, the procedures are only valid in special cases, or their logical meaning is inconsistent.
To estimate a parameter, orthodox statistics knows the minimization of χ^2 or maximization of the likelihood. The resulting parameter values will agree with the mean value of the posterior distribution, if the prior is constant in the region of the highest density of the likelihood. For a posterior of complicated shape, the estimates will differ in general. In addition, orthodox statistics strongly concentrates on the large error in the data (Sec. 5.5.1.3), where as the result of probability theory is the complete posterior pdf.
Estimating the uncertainties of the parameters using the covariance matrix is only an approximation to the case of a multivariate Gaussian posterior distribution. In high dimensional problems with nonlinear models, we are not able to check whether this condition is fulfilled. Also the application of the $\Delta\chi^2$-rule is not advisable. For the estimate of a single parameter with a Gaussian posterior distribution it coincides with probability theory. In all other cases the logical meaning differs with the definition of the variance.
Using the covariance matrix and linearization to propagate the parameter uncertainties to a function is questionable, because in addition to the problems induced by the covariance matrix we are dealing with an approximation of the corresponding function.
Performing a hypothesis test by comparison of p-values suffers from the implicit comparison to future data sets, that are not obtained, yet. Whereas in probability theory, it is only possible to compare at least two hypotheses with each other.
In addition an important and intuitive feature as marginalization does not possess a counterpart in orthodox statistics.
Considering the facts in this chapter, we conclude, that orthodox statistics is not applicable for the parameter estimation in this work, because the considered model is highly nonlinear. It is not possible to check if the posterior distribution is a multivariate Gaussian distribution, moreover the comparison with previous results will show that it is not a Gaussian. In addition, the present approach allows the inclusion of important prior information about the

parameters, which greatly improves the stability of the parameter estimation. In any case, we will obtain the full posterior probability distribution function and we are able to correctly propagate the parameter uncertainties to any function of interest.

6 Parametrization

The Mellin-Barnes representation of amplitudes (Sec. 4.5) requires a realistic ansatz for the conformal moments of GPDs. As in [KMPK08, KM10] we utilize the expansion of conformal GPD moments in terms of SO(3)-PWs. This has the advantage, that the analytic continuation of the conformal moments is achieved by the utilized model itself. Furthermore, it leads to a flexible GPD parametrization which is the key to a phenomenological study of GPDs.
In this chapter, we introduce the parametrization in terms of SO(3)-PWs following [KMPK08, KM10]. Furthermore, we discuss the equality to the forward limit and its implication for the parametrization of conformal GPD moments. This is followed by the introduction of the relevant models and their respective parameters. The chapter concludes with a listing of the available prior information for the parameters.

6.1. SO(3)-PW expansion

The Mellin-Barnes representations of the basic non-perturbative objects, CFFs and TFFs require a unique analytic continuation of the conformal GPD moments. In [Pol99], the conformal moments of meson GPDs were decomposed into irreducible SO(3) representations, which are given in terms of Legendre polynomials labeled by the angular momentum quantum number. This basis has been adapted in [GT06] for the conformal moments of nucleon GPDs. Following [KMPK08, KM10], the decomposition reads

$$F_j(\eta,t) = \sum_{\substack{J=J_{\min}\\ \text{even}}}^{j+1} F_j^J(t)\,\eta^{j+1-J}\,\hat{d}^J_{\alpha,\beta}(\eta)\,, \qquad J = j{+}1,\, j{-}1,\, j{-}3,\, j{-}5,\,\ldots\,, \tag{6.1}$$

where the quantum number J denotes the total angular momentum. $\hat{d}^J_{\alpha,\beta}(\eta)$ is the crossed version of the Wigner matrix, where the rotation matrix of the spinor bilineras is taken off. They are given by Gegenbauer polynomials with the index $1/2$ ($\alpha=0$, $\beta=0$) or $3/2$ ($\alpha=0$, $\beta=1$) for GPDs with even and odd charge parity [Die03], respectively. For the case $J_{\min}=0$ they read

$$\hat{d}^J_{0,0}(\eta) = \frac{\Gamma\left(\frac{1}{2}\right)\Gamma(J{+}1)}{2^J\Gamma\left(J{+}\frac{1}{2}\right)}\,\eta^J C_J^{1/2}\left(\frac{1}{\eta}\right) = \frac{\Gamma\left(\frac{1}{2}\right)\Gamma(J{+}1)}{2^J\Gamma\left(J{+}\frac{1}{2}\right)}\,\eta^J\;\; {}_2F_1\left(\begin{matrix}-J & J+1\\ 1\end{matrix}\,\middle|\,\frac{\eta-1}{2\eta}\right)\,, \tag{6.2}$$

and for $J_{\min}=2$ with Gegenbauer polynomials of index $\nu=3/2$ we have

$$\hat{d}^J_{0,1}(\eta) = \frac{\Gamma\left(\frac{1}{2}\right)\Gamma(J)}{2^J\Gamma\left(J+\frac{1}{2}\right)}\,\eta^{J-1}C^{3/2}_{J-1}\left(\frac{1}{\eta}\right) = \frac{\Gamma\left(\frac{3}{2}\right)\Gamma(J+1)}{2^J\Gamma\left(J+\frac{1}{2}\right)}\,\eta^{J-1}\,{}_2F_1\left(\begin{matrix}-J+1 & J+2\\ & 2\end{matrix}\,\middle|\,\frac{\eta-1}{2\eta}\right), \tag{6.3}$$

where we used the identity (C.15) to express the Gegenbauer polynomials in terms of hypergeometric functions, also providing the analytic continuation to complex valued j. Note, it is also common to employ the representation provided by the identity (C.24), see [MLPKS14].

6.2. Partonic basis

For the analysis of GPDs, it is common to utilize the decomposition into sea and valence quark distributions, see Eq. 2.27 for PDFs. The same decomposition applies for GPDs. The dominant contribution at small-x_{B} arises from sea quarks and gluons. We define the light quark sea contribution as

$$S_u = S_d = \frac{2}{5}S\,, \qquad S_s = \frac{1}{5}\,. \tag{6.4}$$

The parameters S_q are the sea quark asymmetry parameters as used in [MRST98]. In addition, we equate the sea quark and the anti-quark distribution. The quark distribution itself is decomposed into the valence quark distribution and the sea quark distribution:

$$q = q^{\mathrm{val}} + q^{\mathrm{sea}}\,. \tag{6.5}$$

Therefore, for GPDs with even charge parity we have

$$F^{q^{(+)}} = F^{q_{\mathrm{val}}} + F^{q_{\mathrm{sea}}} + F^{\bar{q}} = F^{q_{\mathrm{val}}} + \frac{2}{5}F^{\mathrm{sea}}\,, \qquad q\in\{u,d\}\,, \tag{6.6}$$

$$F^{s^{(+)}} = F^{s_{\mathrm{sea}}} + F^{\bar{s}} \qquad = \frac{1}{5}F^{\mathrm{sea}}\,. \tag{6.7}$$

GPDs with odd charge parity do not possess a sea quark contribution, hence

$$F^{q^{(-)}} = F^{q_{\mathrm{val}}}\,, \qquad q\in\{u,d,s,c,\dots\}\,. \tag{6.8}$$

For DVCS and DVMP on protons, it is sufficient to model the valence GPD for the up and down quarks, sea quark and gluon GPD. Therefore, we define the partonic basis as the vector

$$\left(F^{u_{\mathrm{val}}} \quad F^{d_{\mathrm{val}}} \quad F^{\mathrm{sea}} \quad F^{\mathrm{G}}\right). \tag{6.9}$$

We recall, that the cross sections in chapter 3 are presented in the so called flavor basis. With the intention of solving the mixing problem, we introduced the evolution basis for CFFs and TFFs in the sections 3.2.4.3 and 3.3.4.2, respectively. The corresponding transformations were given in Sec. 2.7. Connecting the partonic basis to the evolution basis is achieved by

utilizing suitable transformation matrices. The singlet GPD as defined in (2.54) in terms of the partonic degrees of freedom (6.6) reads

$$F^{0(+)} = \sum_q F^{q(+)} = F^{u_{\text{val}}} + F^{d_{\text{val}}} + F^{\text{sea}} \,. \tag{6.10}$$

Thus, the transformation of the vector singlet GPD (3.162) and the partonic basis is achieved by

$$\begin{pmatrix} F^{0(+)} \\ F^{\text{G}} \end{pmatrix} = \begin{pmatrix} 1 & 1 & 1 & 0 \\ 0 & 0 & 0 & 1 \end{pmatrix} \begin{pmatrix} F^{u_{\text{val}}} \\ F^{d_{\text{val}}} \\ F^{\text{sea}} \\ F^{\text{G}} \end{pmatrix} . \tag{6.11}$$

In addition, the non-singlet contributions with even charge parity are given by the following transformation

$$\begin{pmatrix} F^{3(+)} \\ F^{8(+)} \\ F^{15(+)} \end{pmatrix} = \begin{pmatrix} 1 & -1 & 0 & 0 \\ 1 & 1 & 2/5 & 0 \\ 1 & 1 & 1 & 0 \end{pmatrix} \begin{pmatrix} F^{u_{\text{val}}} \\ F^{d_{\text{val}}} \\ F^{\text{sea}} \\ F^{\text{G}} \end{pmatrix} . \tag{6.12}$$

For GPDs with odd charge parity $F^{q(-)}$, there is only the valence contribution and no mixing with the gluon GPD takes place, cf. (6.8). In contrast to DVCS, DVMP in some cases involves GPD with odd charge parity (Tab. 3.2). However, in this thesis, we only include the singlet contribution and neutral vector mesons.

6.3. Functional form

In order to determine the functional form of the conformal GPD moments, we employ the equality to Mellin moments of PDFs in the foreward case. As seen in section 2.4 we have the relation

$$\lim_{\eta \to 0} H_j^q(\eta, \Delta^2) = f_j^q(\Delta^2) \,. \tag{6.13}$$

From the expansion in terms of SO(3)-PWs in (6.1) only the term with angular momentum $J = j+1$ remains after taking the limit $\eta \to 0$. This term $F_j^{j+1}(t)$ is denoted as the conformal moments of the zero-skewness GPD. In general, the PDF does not depend on the transverse momentum transfer Δ^2, since its dependence vanished in the forward limit. For conformal moments, this statement does not hold any longer. Therefore, we will adapt the common functional form of the sea quark and gluon PDFs and introduce a t-dependence.
In the momentum fraction space the quark PDF is parametrized as

$$q(x) = N \frac{x^{-\alpha}(1-x)^{\beta}}{\text{B}(2-\alpha, \beta+1)} \,, \tag{6.14}$$

where α is the Regge intercept of an effective "pomeron trajectory"and β parametrizes the large-x behavior. The ansatz is normalized to the momentum fraction average N

$$\int_0^1 \mathrm{d}x\, x\, q(x) = N\,. \tag{6.15}$$

The Mellin moments of the parametrization in (6.14) yield

$$q_j = N\frac{\mathrm{B}(1-\alpha+j,\beta+1)}{\mathrm{B}(2-\alpha,\beta+1)}\,. \tag{6.16}$$

We utilize this parametrization for the sea quark and gluon PDFs as well.
It is standard in Regge phenomenology that the t-dependence is modeled by an exponential ansatz. However, it is not clear, whether the polynomiality of GPDs can be incorporated with such an ansatz [MMPR03]. The analysis of a spectator quark model [HM08] shows that at small-x, the x- and t-dependence factorize and a power-like behavior arises. To obtain a statistically valid comparison, we study both cases in this thesis:

$$\beta(t) = e^{Bt}, \qquad \beta(t) = \left(1-\frac{t}{M^2}\right)^{-p}\,. \tag{6.17}$$

A possible dependence of the slope parameter B or the cut-off mass M on the conformal moment j will be neglected, since such a dependence cannot be constrained by data in the small-x_B region [KM10].
In addition, we decorate the PDF Mellin moments with a t-dependence. Extending the Regge intercept α to a linear trajectory leads to

$$\alpha \to \alpha(t) = \alpha + \alpha' t\,, \tag{6.18}$$

where we only introduced the leading pole. The parameter α' is denoted as the Regge slope. Moreover, the partial wave amplitudes contain an impact form factor to describe the interaction with the target and a propagator $1/(m^2(J)-t) \propto 1/(J-\alpha(t))$ of the exchanged particle [KMPK08]. These form factors will be modeled by a monopole with a J-dependent cut-off mass.
Taking everything together, we obtain the following model for the conformal moments of the zero-skewness GPD

$$H_j^a(\eta=0,t) = N^a\frac{\mathrm{B}(1-\alpha^a+j,\beta^a+1)}{\mathrm{B}(2-\alpha^a,\beta^a+1)}\cdot\frac{\beta(t)}{1-\frac{t}{\left(m_j^a\right)^2}}\,, \qquad \left(m_j^a\right)^2 = \frac{1+j-\alpha^a}{\alpha'^a}\,, \tag{6.19}$$

where $a \in \{\mathrm{sea},\mathrm{G}\}$. For the parametrization of the conformal moments of valence quarks see [BM09]. The generic value for the Regge intercept of valence quarks is $\alpha \sim 1/2$, whereas it is $\alpha \sim 1$ for sea quarks and gluons. Therefore, the valence quarks are suppressed in the small-x_B region and can be neglected.
As already stated, we employ the parametrization in (6.19) for the conformal moments of the sea quark and gluon GPD. However, the parameters are different. Thus, by only modeling the conformal moments of the zero-skewness GPD we have $2\times5=10$ parameters

$$N^a, \alpha^a, \alpha'^a, \beta^a, \{B^a \vee M^a\}\,. \tag{6.20}$$

The functional form of the higher PWs is completely unknown. Therefore, we apply the same functional form as for the conformal moments of the zero-skewness GPD, but with different parameters for each PW. In principle, we have to take into account all terms in the SO(3)-PW expansion, which have to be resummed as well. Instead, we propose an effective parametrization with a fixed number of PWs. In this thesis, we utilize at most three partial waves. The corresponding effective parametrization reads

$$F_j(\eta, \Delta^2) = F_j^{j+1}(t)\, \hat{d}_{\alpha,\beta}^{j+1}(\eta) + F_j^{j-1}(t)\, \eta^2 \hat{d}_{\alpha,\beta}^{j-1}(\eta) + F_j^{j-3}(t)\, \eta^4 \hat{d}_{\alpha,\beta}^{j-3}(\eta) \tag{6.21}$$

Unfortunately, the functional form of the higher PWs is not constrained by the forward case. Therefore, we utilize the same functional form as for the l-PW, where only the index j is shifted. For a closed notation, we introduce the simplification

$$F_j^J(t) \to F_{J-1}^{j+1-J}(t)\,, \tag{6.22}$$

where the upper index just labels the partial waves and the lower one denotes the conformal moment j. Thus, the conformal moments including three PWs read

$$F_j(\eta, t) = F_j^0(t)\, \hat{d}_{\alpha,\beta}^{j+1}(\eta) + F_{j-2}^2(t)\, \eta^2 \hat{d}_{\alpha,\beta}^{j-1}(\eta) + F_{j-4}^4(t)\, \eta^4 \hat{d}_{\alpha,\beta}^{j-3}(\eta)\,. \tag{6.23}$$

The general expansion for an arbitrary number of PWs becomes

$$F_j(\eta, t) = \sum_\nu F_{j-2\nu}^{2\nu}(t)\, \eta^{2\nu}\, \hat{d}_{\alpha,\beta}^{j+1-2\nu}(\eta)\,, \qquad \nu = 0, 1, 2, \dots\,, \tag{6.24}$$

where the index $\nu = (j+1-J)/2 = 0, 1, 2, \dots$ labels the PWs, which are denoted as leading-PW (l-PW), next-to-leading-PW (nl-PW) and next-to-next-to-leading-PW (nnl-PW). Since the higher-PWs possess in general different parameters than the leading one, we introduce the following notation for the parameters

$$N_\nu^a,\ \alpha_\nu^a,\ \alpha_\nu'^a,\ \beta_\nu^a,\ \{B_\nu^a \vee \{M_\nu^a,\ p_\nu^a\}\}\,, \quad a \in \{u_{\text{val}},\ d_{\text{val}},\ \text{sea},\ \text{G}\}\,. \tag{6.25}$$

As a result, a model with three partial waves including sea quark and gluon GPDs contains $2 \times 5 \times 3 = 30$ parameters. To shorten the notation, we sometimes drop the index ν. In this case, we always consider parameters of the l-PW.

6.4. Reduced model

The expansion of conformal GPD moments in terms of SO(3)-PWs in completely general. We utilized the forward limit to parametrize the l-PW. Furthermore, we made the assumption, that the functional form of the higher PWs is equal to the l-PW. At this point, we will start denoting the resulting conformal GPD moments as a model. In the following, we will discuss the possible types of models that arise from (6.24).
The analysis in this thesis, will focus on the small-x_{B} region. Thus, we will not be able to constrain the parameters β^a. We know beforehand, that the cross section at small-x_{B} will

not be sensitive to this parameters, and an analysis of small-x_B data will always reveal the corresponding prior distribution. Therefore, we fix their values to

$$\beta^{\text{sea}} = 8, \qquad \beta^{\text{G}} = 6, \tag{6.26}$$

which is slightly larger than the canonical values to compensate for the increase with resolution scale [KMPK08, KM10].
Since the two parameters of the power-like t-dependence (6.17) will obviously be highly correlated, we fix the exponent p^a to

$$p^{\text{sea}} = p^{\text{G}} = 2\,, \tag{6.27}$$

allowing a possible comparison of our result to the characteristic size of a nucleon, given by the cut-off mass in the dipole parametrization of the Sachs form factors.
In previous analysis of DIS and DVCS data [KMPK08, KM10], it was sufficient to use a simplified version of the model in (6.24). In such a reduced model the parameters of the higher PWs are equal to the l-PW ones. In addition, the higher partial waves were modified multiplicatively by the skewness parameters, leading to the following effective model

$$F_j(\eta, t) = \sum_\nu s_\nu F^0_{j-2\nu}(t)\ \eta^{2\nu}\ \hat{d}^{j+1-2\nu}_{\alpha,\beta}(\eta)\,, \qquad s_0 = 1\,. \tag{6.28}$$

This model was successful in the description of DVCS and DIS data. Equivalently, in this work, we will use the normalization of the higher PWs N_ν instead of the skewness parameters s_ν. Thus, in comparison to [KM10], we have the relation

$$N_\nu = s_\nu N_0\,. \tag{6.29}$$

Consequently, the reduced model possesses the following parameters

$$N^a_0,\ \alpha^a_0,\ \alpha'^a_0,\ \{B^a_0 \vee M^a_0\}, \quad N^a_2, \quad N^a_4\,. \tag{6.30}$$

Thus, the higher PWs differ from the l-PW only by their normalization. This results in the small-x_B region in $2\times 6 = 12$ parameters for the sea quark and gluon GPD.

6.5. Full model

In addition to the reduced model, in the full model we do not equate the parameters of the higher PWs. We only apply one restriction: Since the α' was hard to constrain in [KM10], we will employ the same parameter for the Regge slope of all PWs:

$$\alpha'^a_\nu = \alpha'^a\,. \tag{6.31}$$

Taking everything together, the full model possesses the following parameters

$$N^a_\nu,\ \alpha^a_\nu,\ \alpha'^a,\ \{B^a_\nu \vee M^a_\nu\}\ . \tag{6.32}$$

This model sums up to $2\times(3\times 3+1) = 20$ parameters. At first glance, this seems a large number. However, our main interest is to verify whether the full parametrization is suitable for a global GPD analysis. Utilizing the advantages of probability theory, we are able to determine the unnecessary parameters, which effectively reduces the number of parameters.

6.6. Prior information

As we have seen in Chap. 5, priors are an essential part in the parameter estimation. Since the likelihood itself has no probabilistic interpretation, only in connection with priors, we obtain the posterior probability distribution function, which is normalized.
In situations with very detailed and precise data, the likelihood will possess a region with a high probability density. Utilizing a prior which is constant in this region does not influence the result, since the constant cancels with the normalization (seen in Sec. E.2.1). However, in actual applications, the data does not correspond to the preferred situation described before. In almost all cases, we are able to present a rough interval for each of the parameters. Consequently, this knowledge goes into the prior distributions. In order to influence the estimate as little as possible, we utilize wide prior distributions, that smooth out the tails of the likelihood, but are constant in the region of the highest probability density.
As a remark, adding prior information is often used implicitly in χ^2 minimization and likelihood maximization. For the minimization algorithm, a starting position has to be specified. Especially with limited data quality, the parameter set maximizing the likelihood strongly depends on the starting position. In case a parameter value is not in the desired interval, it is common to slightly alter the starting position. This procedure is repeated until a satisfying parameter set is obtained. As a consequence, prior information is in fact utilized after the actual parameter estimation. With the use of priors in PTEL, we employ this information up front. This has several advantages. First, we are completely objective. The exact prior information is known and the reader is able to judge himself whether it is reasonable. Second, priors improve the convergence of the Markov chain and greatly reduce the sensitivity to the starting point.
A further advantage of PTEL is the access to the degree of interference of a certain parameter by the data through the comparison of the posterior pdf and the corresponding prior distribution. In case the data does not contain information about a certain parameter, its posterior pdf will be equal to its prior pdf. If by coincidence the data holds exactly the same information as the prior, the posterior pdf will be narrower, since the posterior pdf is the combined estimate from two equal contributions. E.g. if the prior and the likelihood are a Gaussian with standard deviation σ, the posterior distribution follows according to (5.178).
We introduced three different prior distributions in Sec. 5.5.3. In this thesis, we employ Gaussian prior distributions, which have the advantage, that they are congruent to the likelihood and improve the convergence of the Markov chain.
The origin of prior information can be extremely versatile. We might use experimental data or theoretical considerations like SVZ sum rules for the higher moments of the DAs. Furthermore, we exploit the equality of GPDs and PDFs in the forward case by first estimating the corresponding PDF parameters from data on DIS. This problem is easily studied in comparison to a GPD estimate since the parameter space and the data is reduced. The mean value of the resulting parameter pdf will be utilized in future estimates as central value for the prior distribution. However, we increase the standard deviation until the point, where the DIS estimate is no longer influenced by the prior information. Note, we do not employ the posterior pdfs of the parameter as prior distribution, as they do not incorporate the correlations of the parameters. This has the effect, that we smooth the tails of the likelihood,

but leave the region of the highest probability density unchanged. Note, a two step fit, as employed in [KM10] neglects the correlations between the PDF parameters itself and GPD parameters leading to a false estimate for both the mean values of the parameters and their variances.
From the analysis of DIS data, we realize, that the normalization of the sea quark GPD N_0^{sea} is around 0.17. To lighten the notation, we drop the index $\nu = 0$ for the l-PW. In order to reflect the prior knowledge, we use a Gaussian prior distribution with standard deviation 0.02:

$$N^{\text{sea}} \sim \mathcal{N}\left(0.17, 0.02^2\right) . \tag{6.33}$$

The normalization of the gluon GPD N^G is constrained by the momentum sum rule

$$N^{\text{val}} + N^{\text{sea}} + N^{\text{G}} = 1 , \qquad N^{\text{val}} = \frac{1}{2} N^{u_{\text{val}}} = N^{d_{\text{val}}} . \tag{6.34}$$

In [KMPK08, KM10] the normalization of the valence GPD was determined as $N^{\text{val}} = 0.4$. Note, the difference to the PDF estimate in [MSTW09] originates in the respective value of N^{val}. Since in this work, we only analyze data in the small-x_{B} region, we are not able to constrain valence GPDs. Therefore, we utilize the momentum sum rule not exactly, but use a narrow Gaussian distribution with standard deviation 0.01 to test for the compatibility of the choice $N^{\text{val}} = 0.4$:

$$N^{\text{G}} \sim \mathcal{N}\left(0.6 - N^{\text{sea}}, 0.01^2\right) . \tag{6.35}$$

Direct implementation of the momentum sum rule to constrain N^{G} makes only sense if data sensitive to the valence region is added.
For the Regge intercepts and Regge slopes we utilize results from elastic J/ψ production. This process is dominated by the two-gluon t-channel exchange [FKS96]. From an analysis of measurements of the differential cross section [A$^+$00b, C$^+$02, C$^+$04, A$^+$06] the pomeron trajectory was extracted [A$^+$06]

$$\alpha(t) = 1.224 \pm 0.01 \pm 0.012 + (0.015 \pm 0.028 + 0.030)\, t\,/\text{GeV}^2 . \tag{6.36}$$

Utilizing these findings as a guideline, we define the following prior distributions for the Regge intercept and slope

$$\alpha_0^a \sim \mathcal{N}\left(1.2, 0.05^2\right) , \qquad \alpha_\nu'^a \cdot \text{GeV}^2 \sim \mathcal{N}\left(0.15, 0.05^2\right) , \tag{6.37}$$

respectively.
In this thesis we employ for the first time different parameters for higher PWs. In case the Regge intercepts α of the higher partial waves become much larger than the ones of the l-PW they will dominate the GPD. Hence, an agreement with DIS data would be artificial. Therefore, we use a Gaussian prior distribution with the Regge intercept of the l-PW as the mean value and demand that the Regge intercepts of the higher partial waves have to be smaller than the one of leading partial wave. The corresponding prior distribution reads

$$\alpha_\nu^a \sim \mathcal{N}_-\left(\alpha_0^a, 0.05^2\right) , \qquad \nu \in \{1, 2\} . \tag{6.38}$$

The simplest model for a GPD is a PDF decorated with a t-dependence. Therefore, we use a Gaussian prior distribution with mean value zero and standard deviation 0.5 for the normalization of the higher partial waves

$$N_\nu^a \sim \mathcal{N}\big(0, 0.5^2\big) \,, \qquad \nu \in \{1, 2\} \,, \tag{6.39}$$

allowing for a very broad range.
Last, we have the parameters for the dipole and exponential ansatz for the t-dependence. Their prior distributions follow from from elastic J/ψ production. The residual t-slope was extracted using an exponential ansatz [A+06]

$$2B = 4.630 \pm 0.060^{+0.043}_{-0.163} / \mathrm{GeV}^2 \,. \tag{6.40}$$

Utilizing this as a guideline, we employ the following priors distributions

$$B_\nu^a \cdot \mathrm{GeV}^2 \sim \mathcal{N}(2, 1) \,, \qquad M_\nu^{2,a} \cdot \mathrm{GeV}^{-2} \sim \mathcal{N}\big(0.7, 0.2^2\big) \,, \qquad \nu \in \{0, 1, 2\} \,, \tag{6.41}$$

where the findings from the exponential ansatz were transferred to the dipole ansatz.
All this prior distributions above are chosen in a way that they guide the estimation, but their impact on the result including error propagation is minimal. Table 6.1 summarizes our prior distributions. Note, in [LMS13] the prior distributions are very narrow and the result

parameter	$\nu = 0$	$\nu \in \{1, 2\}$
N^{sea}	$\mathcal{N}\big(0.17, 0.02^2\big)$	$\mathcal{N}\big(0, 0.5^2\big)$
N^{G}	$\mathcal{N}\big(0.6 - N_0^{\mathrm{sea}}, 0.01^2\big)$	$\mathcal{N}\big(0, 0.5^2\big)$
α_ν^a	$\mathcal{N}\big(1.20, 0.05^2\big)$	$\mathcal{N}_-\big(\alpha_0, 0.05^2\big)$
$\alpha_\nu'^{,a}$	$\mathcal{N}\big(0.15, 0.05^2\big)$	
$M_\nu^{2,a}$	$\mathcal{N}\big(0.70, 0.20^2\big)$	-
B_ν^a	$\mathcal{N}(2.00, 1.00)$	-

Table 6.1.: Summary of the prior distributions for all parameters.

is influenced by the choice of priors. Therefore, we use very wide priors in this thesis.

7 Estimation

A GPD estimate from data on DIS and DVCS was performed in [KMPK08, KM10, KMM13]. However, for DVMP only the LO estimates for π^+ [BM09] and light vector mesons [MM14] within the perturbative framework are available. Furthermore, a GPD inspired hand-bag model was utilized in [GK05, GK08, GK10] to link GPD models to DVMP measurements. In this thesis, we fully stay in the perturbative framework. The first global GPD estimate was performed in [LMS13], which is similar to the analysis in this thesis. We spell out the differences in the text.
For a systematic analysis, we first introduce a nomenclature, that can be used to denote the models and also the estimate that results from utilizing the model on the data. The notation in this thesis is

$$\text{M - PW - T - D - P}\,. \tag{7.1}$$

The symbol M stands for the complexity of the model, it is ether "reduced" (R) or "full" (F), compare Sec. 6.4 and Sec. 6.5, respectively. PW denotes the number of partial waves, which is l, nl or nnl. In addition, T is the ansatz for the t-dependence, which can be either exponential (Et) or dipole-like (Dt). Furthermore, we also add symbols specifying the crucial features for parameter estimation. D denotes the analyzed data. We perform three different scenarios: A pure DIS estimation (A), a DIS and DVCS estimation (B) and a global estimate including DIS, DVCS and DVMP data (C). A detailed discussion on the available data is given in the following section. Furthermore, P stands for the order of perturbation theory. Taking everything together, we have the possibilities

$$\text{M}\in\{\text{R, F}\}\,,\quad \text{PW}\in\{\text{l, nl, nnl}\}\,,\quad \text{T}\in\{\text{Dt, Et}\}\,,\quad \text{D}\in\{\text{A,B,C}\}\,,\quad \text{P}\in\{\text{LO, NLO}\}\,. \tag{7.2}$$

However, not all combinations are useful. Estimating the parameters of the model R-nnl solely on DIS data will certainly not constrain the parameters of the higher PWs.
In this chapter, we have a detailed look on the available data and present the useful data. This is followed by the estimation of the longitudinal cross section from the total one. Next, we perform the three different analyses mentioned before. First, we undertake a pure DIS analysis showing the uses of PTEL and also a comparison with the orthodox statistics. Second, we carry out a DIS and DVCS analysis using PTEL. We reproduce the results of [KMPK08, KM10]. In addition, we realize, what value the use of PTEL brings to the data analysis, gaining knowledge that was not obvious before. These insights are then used to

extend the analysis to include data on DVMP, which is one of the main objectives of this thesis.
For all our estimates we sample the posterior distribution utilizing the Metropolis-Hastings [Has70] algorithm. The properties of the resulting Markov chains are presented in appendix F.

7.1. Experimental data

Since the GPDs are equal to the PDF in the forward case, we could in principle add all processes allowing phenomenological access to PDFs. However, our aim is to estimate GPDs. Thus, in order to avoid unnecessary complications, we only use the limited data from the H1 collaboration [A$^+$96a]. The inclusion of the combined H1 and ZEUS data set [A$^+$10a] with our parametrization for PDFs (6.14) in the small-x_B region is a straight forward task.
The DVCS cross section was extracted by the H1 [A$^+$01, A$^+$05, A$^+$08a, A$^+$09a] and ZEUS [C$^+$03,C$^+$09] collaborations from the unpolarized electroproduction one subtracting the Bethe-Heitler one. Azimuthal angular integration suppresses the interference term while the longitudinal-to-transverse photon helicity flip part is power suppressed, and the transverse-to-transverse photon helicity flip part is expected to be numerically suppressed. In our GPD analysis we use only the cross section data from [A$^+$05, A$^+$09a, C$^+$09] that can be considered as statistically independent.
Exclusive electroproduction of light mesons has been measured extensively in the past. The production of vector mesons was measured in both collider and fixed target kinematics at H1 [A$^+$96b, A$^+$97b, A$^+$10b, A$^+$00a], ZEUS [B$^+$99, B$^+$00, C$^+$05, C$^+$07], HERMES [A$^+$00c, A$^+$09b], E665 [A$^+$97a], NMC [A$^+$94], COMPASS [AAA$^+$12], CLAS [H$^+$05, M$^+$05, M$^+$09, S$^+$08] and CORNELL [CAB$^+$81]. Data on pseudoscalar meson production in fixed target kinematics are given by HERMES [A$^+$08b, A$^+$10c], CLAS [DM$^+$08, B$^+$12a] and HALL-C [B$^+$08]. An overview of the available data is found in Tab. 7.1.
This thesis focuses on the unpolarized hard exclusive vector meson production. Unfortunately, the data on DVMP-ω in [B$^+$00] contains only four data points above the input scale $\mathcal{Q}_0 = 2\,\mathrm{GeV}$. Moreover, the R-ratio has not been measured and consequently, we neglect data. Furthermore, the data in [A$^+$96b] and [A$^+$00a] is contained in [A$^+$10b]. However, additional data is published in [A$^+$00a], which we use in the analysis of the corresponding R-ratio, see Sec. 7.2. We also neglect the data in [B$^+$99] with an integrated luminosity of $6\,\mathrm{pb}^{-1}$ in comparison to [C$^+$07] with $118.9\,\mathrm{pb}^{-1}$. Also the data in [A$^+$97b] is not considered in comparison to [A$^+$10b] with integrated luminosities of $2.8\,\mathrm{pb}^{-1}$ and $51\,\mathrm{pb}^{-1}$, respectively. We also neglect all data which contains very few points above the input scale $\mathcal{Q}_0$, due to numerical reasons for the evolution of GPDs. An overview of the data analyzed in this thesis is found in Tab. 7.2.
Note, we also give the normalization errors of the data sets if available. Considering the normalization of the data sets as free parameters increases the compatibility of the data and is recommended in the combination of data from different sources and experiments.
As mentioned in Sec. 3.3, the factorization theorem for DVMP is only valid for longitudinally polarized virtual photons. On the other hand, the experiments measure the total cross section. In addition, they provide data on the ratio of the longitudinal to the transverse cross

reference	collaboration	year	mesons	comment	analysis
[A$^+$96b]	H1	1996	ρ^0, J/ψ	contained in [A$^+$10b]	
[A$^+$97b]	H1	1997	ρ^0, ϕ	insignificant	
[A$^+$10b]	H1	2009	ρ^0, ϕ		✓
[A$^+$00a]	H1	1999	ρ^0	contained in [A$^+$10b]	
[B$^+$99]	ZEUS	1998	ρ^0, J/ψ	insignificant	
[B$^+$00]	ZEUS	2000	ω	insignificant	
[C$^+$05]	ZEUS	2005	ϕ		✓
[C$^+$07]	ZEUS	2007	ρ^0		✓
[A$^+$00c]	HERMES	2000	ρ^0	$0.7 \leq \mathcal{Q}^2 \leq 4.0$	
[A$^+$09b]	HERMES	2009	ρ^0	polarized target	
[A$^+$08b]	HERMES	2008	π^+	$1 \leq \mathcal{Q}^2 \leq 11$	
[A$^+$10c]	HERMES	2000	π^+	polarized target	
[A$^+$97a]	E665	1997	ρ^0	$0.17 \leq \mathcal{Q}^2 \leq 7.51$	
[A$^+$94]	NMC	1994	ρ^0, ϕ	D,C,Ca-target	
[AAA$^+$12]	COMPASS	2012	ρ^0	polarized target	
[H$^+$05]	CLAS	2004	ρ^0	$1.5 \leq \mathcal{Q}^2 \leq 3.0$	
[M$^+$05]	CLAS	2005	ω	$1.7 \leq \mathcal{Q}^2 \leq 4.8$	
[M$^+$09]	CLAS	2009	ρ^0	$1.6 \leq \mathcal{Q}^2 \leq 5.6$	
[S$^+$08]	CLAS	2008	ϕ	$1.4 \leq \mathcal{Q}^2 \leq 3.8$	
[DM$^+$08]	CLAS	2008	π^0	polarized target	
[B$^+$12a]	CLAS	2012	π^0	$1.0 \leq \mathcal{Q}^2 \leq 4.6$	
[CAB$^+$81]	CORNELL	1981	ρ^0, ω, ϕ	$0.7 \leq \mathcal{Q}^2 \leq 4.0$	
[B$^+$08]	HALL-C	1981	π^+	$0.60 \leq \mathcal{Q}^2 \leq 2.45$	

Table 7.1.: Experimental data used in our global GPD analysis of electroproduction collider data.

section. Therefore, we model the ratio in the next section to extract the longitudinal cross section. For consistency, we only use the information on the ratio that is provided in the data sets that are considered in this work.
To conclude the section, we present a overview of the data including number of points and range of x_B in table 7.3. As a consequence, we more than double the number of data points where the GPDs are directly involved in comparison to previous analyses solely on DIS and DVCS data.
All the parameter estimations in this chapter are performed utilizing a Markov chain Monte Carlo. Since the experimental collaborations only publish the mean value and the corresponding error, we will always utilize a Gaussian distribution for the likelihood function. Strictly speaking, the normalization errors follow a log-normal distribution, however for the present experimental uncertainties it is equivalent to a Gaussian distribution. Following the considerations in the example in Sec. 5.9.4 we correct for asymmetric errors in the data.

collaboration	year	process	R	analysis	σ_ν	abbreviation	reference	data set
H1	1996	$\gamma^* p \to X$		✓	0.039	H1-96	[A$^+$96a]	A, B, C
H1	2001	$\gamma^* p \to \gamma p$				H1-01	[A$^+$01]	
H1	2005	$\gamma^* p \to \gamma p$		✓		H1-05	[A$^+$05]	B, C
H1	2007	$\gamma^* p \to \gamma p$				H1-07	[A$^+$08a]	
H1	2009	$\gamma^* p \to \gamma p$		✓		H1-09	[A$^+$09a]	B, C
ZEUS	2003	$\gamma^* p \to \gamma p$				ZEUS-03	[C$^+$03]	
ZEUS	2008	$\gamma^* p \to \gamma p$		✓		ZEUS-08	[C$^+$09]	B, C
H1	1999	$\gamma^* p \to \rho^0 p$	✓			H1-99	[A$^+$00a]	
H1	2009	$\gamma^* p \to \rho^0 p$ $\gamma^* p \to \phi p$	✓	✓	0.039 0.047	H1-09	[A$^+$10b]	C
ZEUS	2005	$\gamma^* p \to \phi p$	✓	✓	0.053	ZEUS-05	[C$^+$05]	C
ZEUS	2007	$\gamma^* p \to \rho^0 p$	✓	✓	0.060	ZEUS-07	[C$^+$07]	C

Table 7.2.: Experimental data used in our global GPD analysis of electroproduction collider data.

process	x_B-range	# points ($\mathcal{Q}^2 \geq 4\,\mathrm{GeV}^2$)	# points
$\gamma^* p \to X$	$8 \cdot 10^{-5} < x_B < 0.032$	102	111
$\gamma^* p \to \gamma p$	$1 \cdot 10^{-4} < x_B < 0.012$	78	95
$\gamma^* p \to \rho^0 p$	$2 \cdot 10^{-4} < x_B < 0.0.012$	124	157
$\gamma^* p \to \phi p$	$2 \cdot 10^{-4} < x_B < 0.006$	71	110

Table 7.3.: x_B-range and number of data points of the data analyzed in this thesis from Tab. 7.2.

7.2. Extraction of the longitudinal cross section

In DVMP of neutral vector mesons the H1 and ZEUS collaborations extracted in first place the (t-differential) photoproduction cross section stemming from both transversely and longitudinally polarized photons

$$\frac{\mathrm{d}\sigma}{\mathrm{d}t} = \frac{\mathrm{d}\sigma_\mathrm{T}}{\mathrm{d}t} + \varepsilon(W, \mathcal{Q}^2)\, \frac{\mathrm{d}\sigma_\mathrm{L}}{\mathrm{d}t}\,, \qquad \varepsilon\big(W, \mathcal{Q}^2\big) \approx \frac{1-y}{1-y+\frac{1}{2}y^2}\,, \tag{7.3}$$

where the flux ratio $\varepsilon(y)$ of longitudinal to transverse photons is with the electron energy loss (3.4) $y = (W^2 + \mathcal{Q}^2 - M^2)/(s - M^2)$ a function of W, $\mathcal{Q}^2$ and the center-of-mass energy s (3.69) that is fixed. In the following we take the measurements for the ρ^0 and ϕ channels [C$^+$05, C$^+$07, A$^+$10b] and ignore the statistically less important data from the ω channel, which we use as a test later in this thesis.
In addition, relying on the hypothesis of s-channel helicity conservation, the H1 and ZEUS

collaboration were able to measure the ratio of the longitudinal and transverse cross section

$$R(W,\mathcal{Q}^2,) = \frac{\sigma_{\mathrm{L}}(W,\mathcal{Q}^2)}{\sigma_{\mathrm{T}}(\langle W\rangle,\mathcal{Q}^2)}\,, \tag{7.4}$$

as function of $\mathcal{Q}^2$ for the means $\langle W\rangle \sim 75\,\mathrm{GeV}$, integrated over $0 \lesssim -t \lesssim 0.5\,\mathrm{GeV}^2$. To access twist-two GPDs we only need the longitudinal cross section and to include the complete set of data, we employ the relation

$$\frac{\mathrm{d}\sigma_{\mathrm{L}}}{\mathrm{d}t} = \frac{1}{R^{-1}(\mathcal{Q}^2,W)+\varepsilon(W,\mathcal{Q}^2)}\,\frac{\mathrm{d}\sigma}{\mathrm{d}t}\,. \tag{7.5}$$

Experimentally, the W-dependence of the R-ratio cannot be resolved. Hence, we neglect this dependence and parametrize the ratio as [MM14]

$$R(\mathcal{Q}^2) = \frac{\mathcal{Q}^2}{m_{\mathrm{V}}^2}\left(1+a\frac{\mathcal{Q}^2}{m_{\mathrm{V}}^2}\right)^{-p}\,, \tag{7.6}$$

where the expectations of dimensional counting for the large-$\mathcal{Q}^2$ asymptotic is modified to be $\mathcal{Q}^{2+2p}$.

We estimate the parameters a and p separately for DVMP-ρ^0 and ϕ utilizing probability theory (PTEL) introduced in Ch. 5. The prior distributions for the parameters are

$$a \sim \mathcal{H}_+(0,50)\,, \qquad p \sim \mathcal{H}_+(0,1)\,. \tag{7.7}$$

A Gaussian distribution was utilized for the experimental uncertainties. All quantities of interest follow directly from the posterior pdf $f(ap|DI)$, where D stands for the data on the R-ratio, cf. Tab. 7.2. In figure 7.1 we show the pdfs for both parameters, which we obtain by marginalization together with their prior distributions. The parameters for the R-ratio

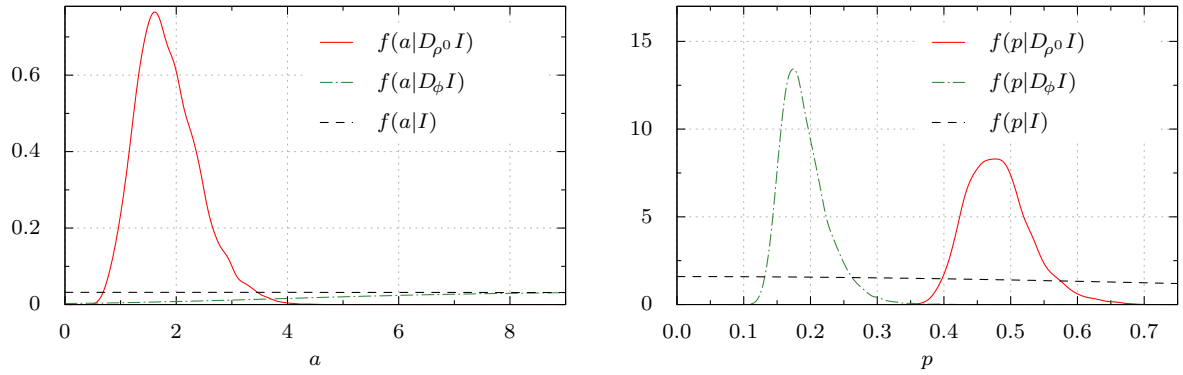

Figure 7.1.: Probability distribution functions of the parameters a and p together with the respective prior distributions,

of DVMP-ρ^0 are well constrained by the available data, thus the posterior pdf surmounts the prior distribution. This is also true for the parameter p for the R-ratio of DVMP-ϕ. However, we realize, that due to the missing data above $\mathcal{Q}^2 \sim 20\,\mathrm{GeV}^2$ the posterior pdf for

the parameter a is restricted by the prior and can not be determined accurately. In order to report the posterior pdfs for the parameters we present the mean values and the square root of the variances in the usual notation (5.125)

$$\begin{aligned} a_{\rho^0} &= 10.453 \pm 10.070\,, & p_{\rho^0} &= 0.336 \pm 0.057\,, \\ a_{\phi} &= 57.755 \pm 34.986\,, & p_{\phi} &= 0.160 \pm 0.027\,, \end{aligned} \tag{7.8}$$

where the meson masses are $m_{\rho^0} = 0.776 \pm 0.00035\,\text{GeV}$ and $m_{\phi} = 1.020 \pm 0.00002\,\text{GeV}$ [B+12b]. Our estimate (hatched error band) is displayed together with the one from a conventional least square estimate (dashed lines surround the error band obtained via the covariance matrix) and experimental measurements in Fig. 7.1 for DVMP-ρ^0 (left) and DVMP-ϕ (right).

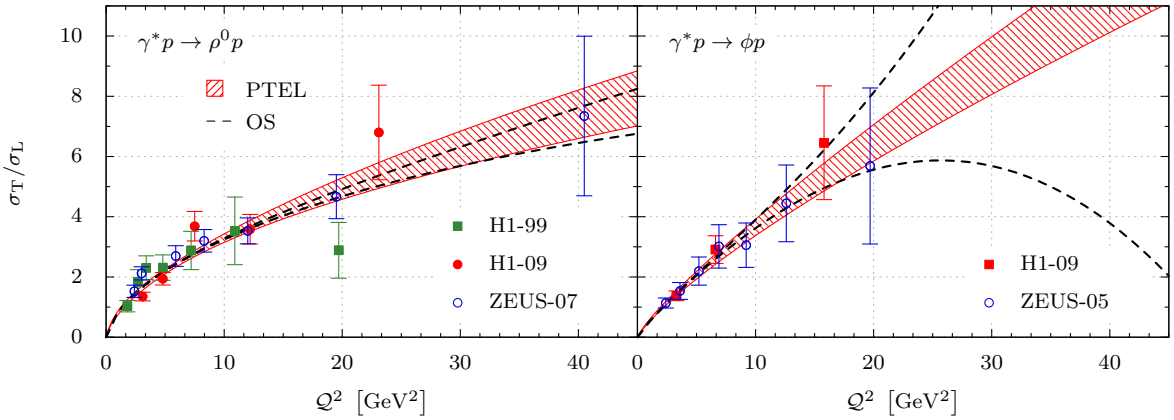

Figure 7.2.: Estimate for the R-ratio of DVMP-ρ^0 and DVMP-ϕ. The experimental data of the ratio of the transverse and longitudinal cross section from [A+00a, A+10b, C+07] and [A+10b, C+05] for ρ^0- and ϕ-production in the left and right panel, respectively. The hatched area corresponds to the square root of the variance of the R-ratio, while the dashed lines show the same quantity from a conventional least square estimate and the covariance matrix for error propagation.

Employing the R-ratio, we are able to extract the longitudinal cross section from the total one (7.5). For a fixed kinematic point, the pdf for the R-ratio $r = R\left(\mathcal{Q}^2\right)$ is given by (5.162):

$$f(r|DI) = \int \mathrm{d}a\,\mathrm{d}p\,\mathrm{d}m\;\delta\big(r - R\left(\mathcal{Q}^2\right)\big)\, f(a\,p\,m|DI)\;. \tag{7.9}$$

Hence, we derive the pdf for the longitudinal cross section from the data D' for the total one by

$$f\big(\sigma_\mathrm{L}\big|DD'I\big) = \int \mathrm{d}\sigma\mathrm{d}r\;\delta\left(\sigma_\mathrm{L} - \frac{1}{r^{-1}+\varepsilon}\sigma\right)\; f(r|DI)\, f\big(\sigma\big|D'I\big)\;. \tag{7.10}$$

To avoid confusion in the formula above, we assume that each point of the total cross section was measured as $\sigma_i \pm e_i$. Assuming a Gaussian distribution for the experimental errors, the pdf of the total cross section reads

$$f\big(\sigma\big|D'I\big) = g\big(\sigma, \sigma_i, e_i^2\big)\;. \tag{7.11}$$

In addition, we also need the inverted formula to obtain the pdf for the total cross section from the pdf for the longitudinal one. This formula follows analogously and will not be presented here.

7.3. Setting the scene

Due to the complicated and intricate nature of the given estimation problem, we introduce the numerical values of several constants in this section. We also summarize the formula for the physical observables in terms of the GPD parameters.

7.3.1. Numerical values

The electromagnetic fine structure constants is given by

$$\alpha_{\text{em}} = 1/137\,. \tag{7.12}$$

Moreover, the phenomenological values of the running coupling constant at the input scale $\mathcal{Q}_0 = 2\,\text{GeV}$ are

$$\alpha_{\text{s}}^{\text{LO}}(\mathcal{Q}_0) = 0.3404\,, \qquad \alpha_{\text{s}}^{\text{NLO}}(\mathcal{Q}_0) = 0.2914\,, \tag{7.13}$$

which correspond to the phenomenological value $\alpha_{\text{s}}(m_{Z^0}) = 0.114$ at the mass of the Z^0-boson with $m_{Z^0} = 91.18\,\text{GeV}$ using the standard evolution prescription [CKS00]. However, we perform forward evolution over the $\mathcal{Q}^2$ range of interest with keeping the number of active quarks N_{f} fixed. In this thesis, we choose

$$N_{\text{f}} = 4\,. \tag{7.14}$$

Furthermore, we use the following scale setting prescription

$$\mu_{\text{F}} = \mu_{\text{R}} = \mu_{\varphi} = \mathcal{Q}\,. \tag{7.15}$$

The decay constants of the neutral vector mesons investigated in this thesis are

$$f_{\rho 0} = 209\,\text{MeV}\,, \qquad f_{\omega} = 195\,\text{MeV}\,, \qquad f_{\phi} = 221\,\text{MeV}\,, \tag{7.16}$$

where we only use an asymptotic distribution amplitude, namely

$$\varphi_0 = 1\,, \qquad \varphi_k = 0 \qquad \forall k \in \{2, 4, 6, \dots\}\,. \tag{7.17}$$

On the more technical side, the Mellin-Barnes representation of amplitude requires the fixing of the vertical line of integration c and the angle ϕ, see Sec. 4.5.3. The rightmost singularity of the conformal moments of the sea quark and gluon GPD arises due to the gamma function $\Gamma(1-\alpha+j)$. Hence, the real part of j has to fulfill $j > \alpha - 1$. With the generic value of the Regge intercept $\alpha = 1.2$ we set the constant c and the standard angle ϕ

$$c = 0.35\,, \qquad \phi = \pi/2\,. \tag{7.18}$$

The convergence with the angle $\phi = \pi/2$ is sufficient. Furthermore, the integral representation of the NLO evolution operator and the hard scattering amplitude (4.210,4.230) requires the constant d, which we set to

$$d = -0.25\,. \tag{7.19}$$

7.3.2. DIS

In the parameter estimation we utilize data on the structure function $F_2\big(x_{\mathrm{B}}, \mathcal{Q}^2\big)$. Following the derivation in Sec. 4.5 and taking only the singlet contribution, the structure function reads

$$F_2(x_{\mathrm{B}}, \mathcal{Q}^2) = \frac{1}{N_{\mathrm{f}}} \sum_q Q_q^2 F_2^{\mathrm{S}}(x_{\mathrm{B}}, \mathcal{Q}^2)\,. \tag{7.20}$$

The corresponding Mellin-Barnes representation yields

$$F_2^{\mathrm{S}}(x_{\mathrm{B}}, \mathcal{Q}^2) = \frac{1}{2\pi i} \int_c \mathrm{d}j\; x_{\mathrm{B}}^{-j}\; \tilde{\boldsymbol{c}}_{2,j}^{\mathrm{V}}\big(\mathcal{Q}^2, \mathcal{Q}_0^2\big)\,.\boldsymbol{f}_j\big(\mathcal{Q}_0^2\big)\;. \tag{7.21}$$

The convolution of the hard scattering amplitude and the evolution operator $\tilde{\boldsymbol{c}}_{2,j}^{\mathrm{V}}\big(\mathcal{Q}^2, \mathcal{Q}_0^2\big)$ is given in Sec. 4.5.1, Eq. 4.171. Furthermore, the Mellin moments of the hard scattering at LO and NLO of perturbation theory are presented in Sec. 4.6.1.

7.3.3. DVCS

We derived the cross section of deeply virtual Compton scattering in Sec. 3.2. The final form was given in (3.180), namely

$$\frac{\mathrm{d}\sigma^{\gamma^* N \to \gamma N}}{\mathrm{d}\Delta^2} \approx \frac{\pi \alpha_{\mathrm{em}}^2}{\big(W^2 + \mathcal{Q}^2\big)^2} |\mathcal{H}|^2\,, \tag{7.22}$$

where we disregarded the contribution proportional axial-vector CFF $\widetilde{\mathcal{H}}$ and the helicity flip CFF $\mathcal{E}$. The leading Regge trajectory in the GPD $\widetilde{\mathcal{H}}$ arises from mesons with the generic intercept $\alpha(0) \approx 1/2$. Thus, we neglect this contribution in comparison to the GPD $\mathcal{H}$ with the generic intercept of $\alpha(0) \approx 1$. In addition, the mean value of the transverse momentum transfer is $\big\langle \Delta^2 \big\rangle = -0.17\,\mathrm{GeV}^2$ as measured in [A$^+$05] for $|\Delta^2| < 1\,\mathrm{GeV}^2$. Therefore, the helicity flip contribution is in the Δ^2 integrated cross section kinematically suppressed by a factor of

$$-\frac{\big\langle \Delta^2 \big\rangle}{4M^2} \sim 5 \cdot 10^{-2}\,. \tag{7.23}$$

Hence, we neglect the squared CFF $|\mathcal{E}|^2$ in the kinematical region considered in this thesis. However, in the differential cross section at larger values of $-\Delta^2$ it might contribute. The present data does not allow a separation of the CFF $\mathcal{H}$ and $\mathcal{E}$ contributions [KM10].

The Compton form factor $\mathcal{H}(\xi, \Delta^2, \mathcal{Q}^2)$ and its properties were extensively studied in Sec. 3.2.4. The contribution from the flavor nonsinglet sector generally do not exceed the 10 % level [KM10]. We neglect the non-singlet contribution to simplify the analysis. The CFF $\mathcal{H}$ taking only the singlet contribution in (3.165) reads

$$\mathcal{H}(\xi, \Delta^2, \mathcal{Q}^2) = \frac{1}{N_\mathrm{f}} \sum_q Q_q^2 \, \mathcal{H}^\mathrm{S}(\xi, \Delta^2, \mathcal{Q}^2) \; . \tag{7.24}$$

The corresponding Mellin-Barnes representation (Sec. 4.5.3, Eq. 4.212) yields

$$\mathcal{H}^\mathrm{S}(\xi, \Delta^2, \mathcal{Q}^2) = \frac{1}{2i} \int_c \mathrm{d}j \, \xi^{-j-1} \begin{bmatrix} \tan \\ \cot \end{bmatrix}^+ \boldsymbol{T}_j^\mathrm{V}(\mathcal{Q}^2, \mathcal{Q}_0^2) \, \boldsymbol{H}_j(\xi, \Delta^2, \mathcal{Q}_0^2) \; . \tag{7.25}$$

The conformal moments of the hard scattering amplitude $\boldsymbol{T}_j^\mathrm{V}$ were defined in (4.202), where the signature for the GPD H is $\sigma = +1$. Its explicit expressions at LO and NLO of perturbation theory are presented in Sec. 4.6.2. Moreover, the convolution of the hard scattering amplitude and the evolution operator $\boldsymbol{T}_j^\mathrm{V}(\mathcal{Q}^2, \mathcal{Q}_0^2)$ is given in Sec. 4.5.2, Eq. 4.211.

7.3.4. DVMP

The cross section for the deeply virtual meson production was derived in Sec. 3.3.5, Eq. 3.272. In this thesis, we only study the electroproduction of neutral vector mesons. Neglecting the TFF $\mathcal{E}$ due to the same reasons as in the previous section, the differential cross section reads

$$\frac{\mathrm{d}\sigma^{\gamma_\mathrm{L}^* N \to \mathrm{V}_\mathrm{L}^0 N'}}{\mathrm{d}\Delta^2} \approx \frac{4\pi^2 \alpha_\mathrm{em} \, x_\mathrm{B}^2}{\mathcal{Q}^4} \, |\mathcal{H}|^2 \, . \tag{7.26}$$

The TFF $\mathcal{H}$ and its properties were studied in Sec. 3.3.4. Considering only the singlet contribution, we have (3.258)

$$\mathcal{H}_{\mathrm{V}^0} = \hat{c}_{\mathrm{V}^0}^\mathrm{S} \, \mathcal{H}_{\mathrm{V}^0}^\mathrm{S} \, , \quad \text{with} \quad \hat{c}_{\mathrm{V}^0}^\mathrm{S} = \hat{c}_{\mathrm{V}^0}^\mathrm{pS} \, , \tag{7.27}$$

where the coefficients in general depending on the outgoing meson are given in (3.248a). The Mellin-Barnes representation (Sec. 3.3.4, Eq. 4.235) of the TFF $\mathcal{H}$ of neutral vector mesons reads

$$\mathcal{H}_{\mathrm{V}^0}^\mathrm{S}(\xi, \Delta^2, \mathcal{Q}^2) = \frac{C_\mathrm{F} f_{\mathrm{V}^0}}{N_\mathrm{c} \mathcal{Q}} \frac{1}{2i} \int_c \mathrm{d}j \, \xi^{-j-1} \begin{bmatrix} \tan \\ \cot \end{bmatrix} \varphi_k(\mathcal{Q}_0^2) \bigoplus_{\text{even}}^k \boldsymbol{T}_{jk}(\mathcal{Q}^2, \mathcal{Q}_0^2) \, \boldsymbol{H}_j(\xi, \Delta^2, \mathcal{Q}_0^2) \; . \tag{7.28}$$

The conformal moments of the hard scattering amplitude $\boldsymbol{T}_{jk}$ were defined in (4.225), whose explicit expressions at LO and NLO of perturbation theory are presented in Sec. 4.6.6. Moreover, the convolution of the hard scattering amplitude and the evolution operator $\boldsymbol{T}_{jk}(\mathcal{Q}^2, \mathcal{Q}_0^2)$ is given in Sec. 4.5.3, Eq. 4.234.

Consequently, we have reduced the observables of interest to the point, where the unknown quantity is the singlet GPD vector $\boldsymbol{H}_j(\xi, \Delta^2, \mathcal{Q}_0^2)$, which is given in terms of the partonic basis (6.11) as

$$\boldsymbol{H}_j(\eta, \Delta^2) = \begin{pmatrix} H_j^{0(+)} \\ H_j^\mathrm{G} \end{pmatrix}(\eta, \Delta^2) = \begin{pmatrix} H_j^\mathrm{sea} \\ H_j^\mathrm{G} \end{pmatrix}(\eta, \Delta^2) \; , \tag{7.29}$$

where we neglected the valence contribution. The respective parametrization is given in (6.19).

7.4. Analysis of data on DIS

In this section, we analyze the data on the structure function $F_2(x_\mathrm{B}, \mathcal{Q}^2)$ as presented in [A+96a], see also the overview of experimental data in Tab. 7.2. We only include points with a higher value of $\mathcal{Q}^2$ than the input scale of $\mathcal{Q}_0^2 = 4\,\mathrm{GeV}^2$, which leaves 102 data points. Note, our final task is to obtain a GPD estimate, therefore, we do not attempt to incorporate a global PDF analysis in the lines of [MSTW09]. This task is left for future publications. Additionally, we will abstain from including the normalization uncertainty for the present analysis, since we only consider a single data set.
We utilize the model R-l, described in Sec. 6.4 possessing the following parameters

$$N^\mathrm{sea},\ \alpha^\mathrm{sea},\ N^\mathrm{G},\ \alpha^\mathrm{G}\,. \tag{7.30}$$

The respective prior distributions are summarized in Tab. 6.1.
For instructive purposes and a comparison with orthodox statistics, we also study the model R*-l, which is the same as R-l, but the momentum average of the gluon PDF N^G is exactly given by the momentum sum rule $N^\mathrm{G} = 1 - N^\mathrm{sea} - 0.4$. Thus, N^G is no longer a free parameter.
In the present section, we present a model comparison of R-l and R*-l at LO and NLO of perturbation theory and show the resulting description of the data. This is followed by the pdfs of the estimated parameters and our estimate for the sea quark and gluon PDFs and the size of the perturbative corrections. Finally, we oppose the estimate from orthodox statistics (Sec. E.3) and PTEL to convince the reader once more that PTEL is indispensable for the given parameter estimation problem of this thesis.

7.4.1. Model comparison

The comparison of models is nothing else than a hypothesis test introduced already in Sec. 5.4. Let us shortly repeat the main findings here. We consider a finite set of models/hypotheses $\{H_1, H_2, \ldots, H_k\}$. The probability for the hypothesis i was derived in the example in Sec. 5.9.3. In the general case, we have

$$\begin{aligned} P(M_i|DI) &= \int \mathrm{d}\theta_i\ f(M_i\theta_i|DI) = C \int \mathrm{d}\theta_i\ f(M_i\theta_i D|I) = C \int \mathrm{d}\theta_i\ f(M_i\theta_i|I)\, P(D|M_i\theta_i I) \\ &= C \int \mathrm{d}\theta_i\ f(\theta_i|I)\, f(M_i|\theta_i I)\, P(D|M_i\theta_i I) = C \int \mathrm{d}\theta_i\ f(\theta_i|I)\, P(D|M_i\theta_i I)\ , \end{aligned} \tag{7.31}$$

with the constant $C = P(D|I)$. Note, The probability distribution function $f(M_i|\theta_i I)$ is in general utilized to specify the respective model. As a consequence, the probability of a model follows from the normalization constant of the posterior distribution function. The probability of a hypothesis i (5.109) yields

$$P(H_i|DI) = \frac{1}{\sum_{j=1}^{N} O_{ji}}\,, \tag{7.32}$$

where the odds ratio O_{ji} (5.105) is given by

$$O_{ij} = \frac{\int \mathrm{d}\theta_i \; f(\theta_i|I)\, P(D|\theta_i I)}{\int \mathrm{d}\theta_j \; f(\theta_j|I)\, P(D|\theta_j I)} \,. \tag{7.33}$$

The normalization constants can be obtained from the output of the Metropolis-Hastings algorithms as outlined in [CJ01]. Table 7.7 shows the logarithm of the marginalized posterior pdf and the logarithm of the maximum of the posterior pdf. As the reader realizes, the best

model	order	Max $\ln f(\theta\|DI)$	$\ln P(D\|I)$	$P(M\|DI)$
R-l	LO	-21.277	-35.576	0.091
	NLO	-23.740	-39.193	0.002
R*-l	LO	-21.347	-33.389	0.810
	NLO	-23.807	-35.520	0.096

Table 7.4.: The logarithm of the maximum of the posterior pdf $\ln f_{\max}$ and the normalization constant of the posterior pdf $\ln f_{\mathrm{marg}}$.

estimate is achieved by the model R*-l at LO of perturbation theory. Due to the fact that at LO gluons only contribute through evolution, the meaning of the difference between the LO and NLO estimate is not clear. On the other side, the model comparison of R-l and R*-l at a fixed order of perturbation theory behaves as expected.
The model R*-l has one parameter more than R-l resulting in a slightly higher maximum value of the likelihood. However, additional parameters are penalized by Bayes' theorem. A complicated model has to be justified by the description of the data. This concept is called Occam's razor (Sec. 5.9.3). Indeed, the complication induced by the additional parameter is not worth the gain in the description of the data, as becomes clear by comparison of the marginalized posterior pdf values.[1] For the reasons outlined in the previous chapter, we present our findings only for the model R-l.

7.4.2. Description of data

Figure 7.3 shows the $\mathcal{Q}^2$ dependence of the structure function $F_2(x_{\mathrm{B}}, \mathcal{Q}^2)$ for selected values of the Bjorken scaling variable x_{B} together with the corresponding data of (cf. table 7.2).
Both the LO and NLO estimates for the model R-l reproduce the data very well and it is impossible to judge the quality of the description with the naked eye. The only noticeable feature is the increased steepness of the $\mathcal{Q}^2$-dependence of the structure function at NLO of perturbation theory.

7.4.3. Parameters

After the comparison of the models and proving that the experimental data is well described, we investigate the estimated parameters. Figure 7.4 shows the posterior pdfs for the para-

[1] Comparing the maximum of the posterior pdf is equivalent to the comparison of the χ^2/d.o.f. values.

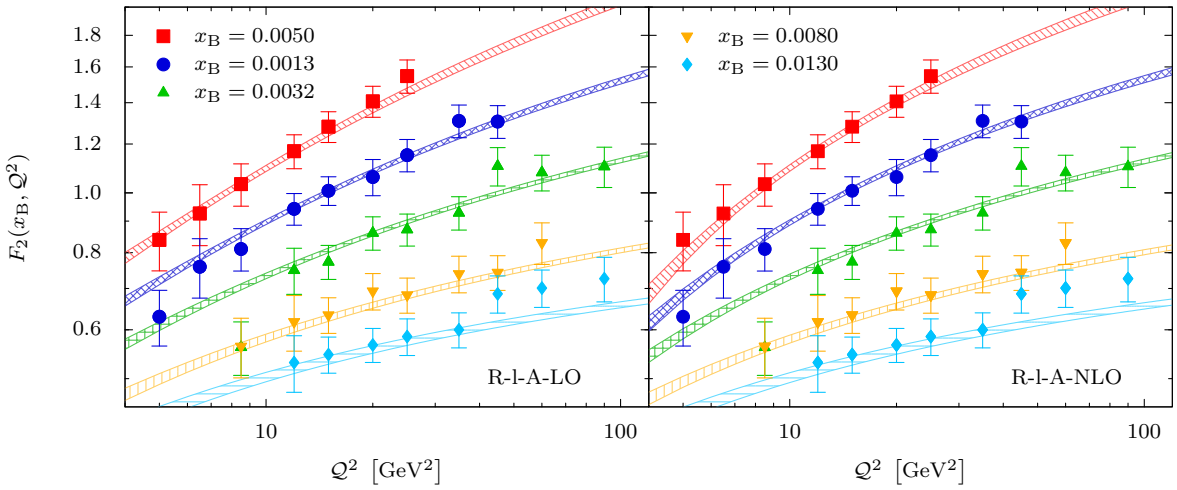

Figure 7.3.: Dependence on the momentum transfer $\mathcal{Q}^2$ of the structure function $F_2(x_B, \mathcal{Q}^2)$ for selected values of x_B at LO (left panel) and NLO (right panel) of perturbation theory.

meters of the model R-l together with the respective prior distributions.

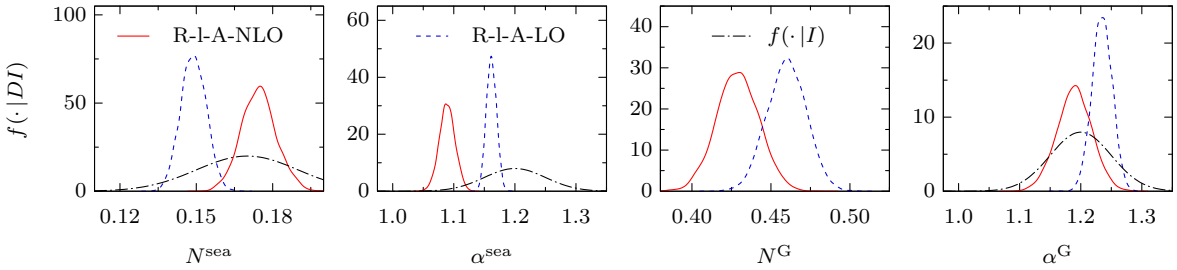

Figure 7.4.: Posterior pdfs for the parameters of the estimate R-l-A-LO (blue, dashed) and R-l-A-NLO (red, solid) together with the respective prior distributions (black, dashed-dotted).

The momentum fraction average of the sea quark GPD N^{sea} of the NLO estimate is larger than the LO estimate. This coincides with the findings in [KMPK08, KM10]. In both cases, the posterior pdfs are much more defined than the corresponding prior distributions. Thus, the available data on the structure function F_2 constrains this parameter well and the estimate is only mildly influenced by the given prior information. The estimate for the momentum average of the gluon GPD is exactly the utilized prior distribution. A fact, that was already expected in the model comparison in Sec. 7.4.1. Consequently the choice $N^{sea}+N^G+0.4=1$ is consistent with the given data.

The Regge intercepts are different from the employed prior information both at LO and NLO of perturbation theory. Additionally, the NLO estimate is smaller and its pdf is wider for both sea quark and gluon PDFs. This is a remainder of the different contributions of the gluon PDF at LO and NLO. At LO, they only contribute via evolution, thus the information of the data transferred to the parameters for the gluon PDF is limited. This results in narrow pdfs

of the sea quark parameters. At NLO, more information is transferred to the gluon GPD, thus less information is left for the sea quark PDF parameters resulting in wider pdfs for the estimate R-l-A-NLO.
In Table 7.5, we summarize the numerical values of the parameter pdfs. The uncertainties are

parameter	LO	NLO
N^{sea}	0.1489 ± 0.0049	0.1746 ± 0.0068
α^{sea}	1.1617 ± 0.0082	1.0892 ± 0.0128
N^{G}	0.4599 ± 0.0123	0.4290 ± 0.0133
α^{G}	1.2350 ± 0.0163	1.1900 ± 0.0283

Table 7.5.: Mean and square root of the variance of the parameter pdfs for the estimates of the model R-l at LO and NLO of perturbation theory in the common notation.

given by the square root of the variance (5.125). We remind the reader, that these moments are just a convenient way to report the actual information content in the parameter pdfs as discussed in Sec. 5.5.1.1.

7.4.4. Parton distribution functions

The estimates for the sea quark and gluon PDFs are presented in Fig. 7.5. Our estimate is in good agreement with the one in [Ale03], which used approximately the same data set and model. The PDF estimate of [MSTW09] is different. This can be tracked down to the fixing of the momentum fraction average of the valence quarks N^{val}. Adjusting this parameter, we can obtain the same PDFs, which also describe the data. We stay with our choice, since our goal is to estimate GPDs, and it was already shown, that the our data set cannot distinguish different values of N^{val}. It would certainly be interesting to also include more data, but this is not the topic of this thesis.

7.4.5. Error estimate from the covariance matrix

In this section, we use the DIS estimate for the model R*-l[2] at NLO of perturbation theory, to confront orthodox statistics with PTEL. We remind the reader of the opposing example in Sec. E.3.4. As already discussed in Sec. E.3, the parameter values are given by maximizing the likelihood with respect to the parameters.
Let us first compare the likelihood with the unnormalized posterior pdf separately for each parameter, where the other parameters are fixed to the values that maximize the likelihood. We show both in figure 7.8. The prior distributions do not alter the shape of the likelihood and we expect a very weak influence of the priors on the estimate. This finding agrees with the comparison of the prior distributions and the corresponding posterior pdfs of the parameters

[2] We do not utilize the model R-l, since the concept of prior information on the parameter is unknown to orthodox statistics. In this way, we achieve a fair comparison.

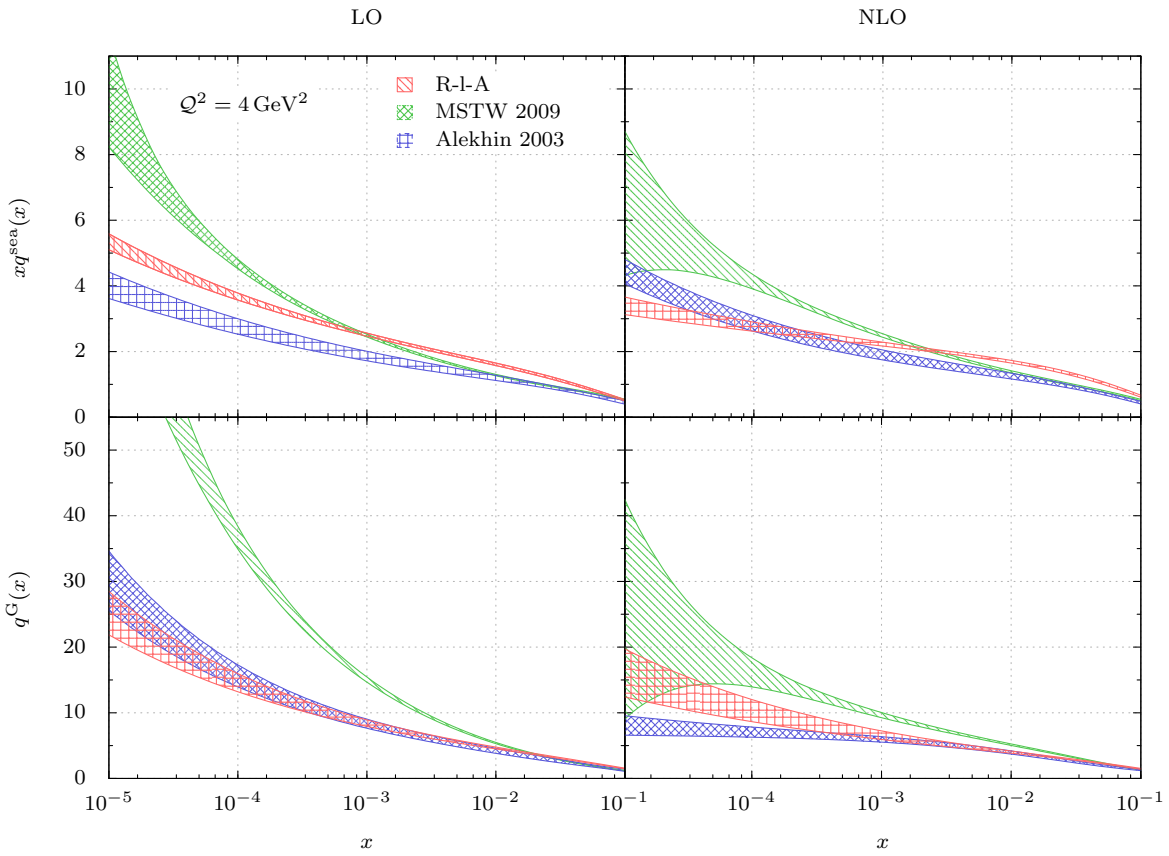

Figure 7.5.: Estimate for the sea quark and Gluon PDFs at the input scale $\mathcal{Q}^2 = 4\,\mathrm{GeV}^2$ from data A on the structure function F_2 at small-x_{B} together with the estimates of Alekhin 2003 [Ale03] and MSTW 2009 [MSTW09]. The error bands of our estimate are given by the mean value and the square root of the variance.

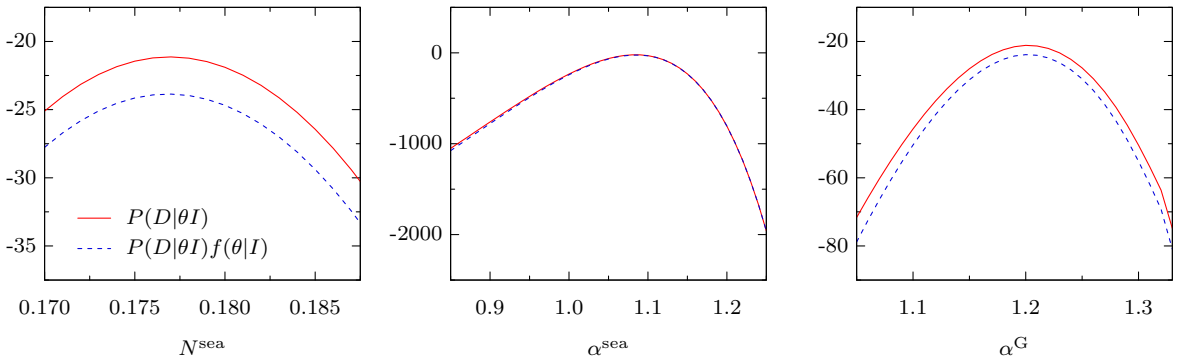

Figure 7.6.: Comparison of the unnormalized posterior distribution and the likelihood.

in Sec. 7.4.1.

Furthermore, the covariance matrix is employed for the estimate of parameter errors and the performance of error propagation. From the necessary assumptions, we already realized, that these methods are not reliable to estimate GPDs or PDFs. The covariance matrix is given by the inverse Hesse matrix ψ (E.40). For our model, it reads

$$\psi^{-1} = \begin{pmatrix} 0.0000466 & -0.0000835 & 0.0001108 \\ -0.0000835 & 0.0001910 & -0.0003330 \\ 0.0001108 & -0.0003330 & 0.0008820 \end{pmatrix}, \qquad \theta = \begin{pmatrix} N^{\text{sea}} \\ \alpha^{\text{sea}} \\ \alpha^{\text{G}} \end{pmatrix}. \tag{7.34}$$

The parameter uncertainties follow from the diagonal entries of the covariance matrix, cf. (E.49). In table 7.6, we present the resulting estimates for the parameters. In PTEL, the

parameter	orthodox statistics	PTEL
N^{sea}	0.1765 ± 0.0068	0.1754 ± 0.0061
α^{sea}	1.0845 ± 0.0138	1.0885 ± 0.0123
α^{G}	1.2016 ± 0.0297	1.1940 ± 0.0259

Table 7.6.: Estimate for the parameters for the model R*-l at NLO of perturbation theory from orthodox statistics and PTEL.

uncertainties are given as the square root of the variance. On a first look, the mean values and the uncertainties are similar. Moreover, in figure 7.7 we compare the pdfs for the parameters. They are all similar but do not agree exactly.

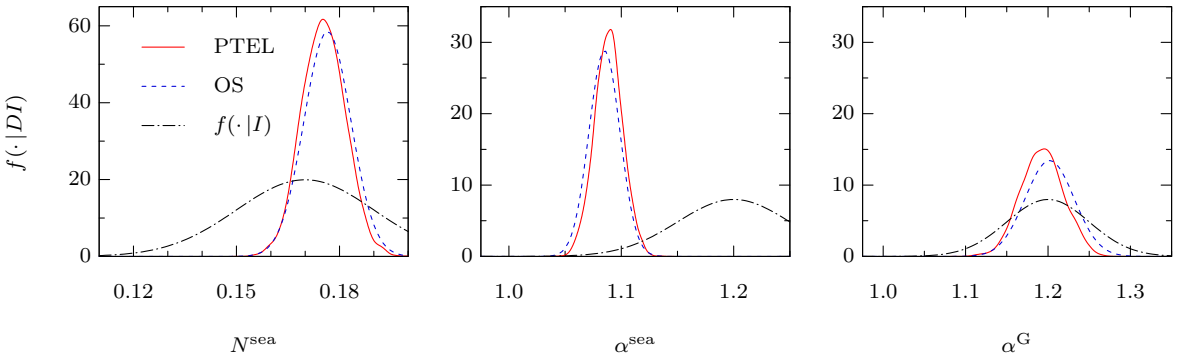

Figure 7.7.: Comparison of the estimated parameter pdfs for the model R*-l from PTEL and from orthodox statistics.

Comparing the parameter pdfs is only the first step. Of particular interest is the propagation of the uncertainty to functions like the PDFs in our case. This propagation was discussed for orthodox statistics in detail in Sec. E.3.2. The outlined approach utilized a Taylor expansion of a function F around the values maximizing the likelihood. Thus, the expectation value is given by the function itself at the maximum. Furthermore, the variance is given by the derivatives of F with respect to the parameters (E.58). This can be expressed by employing

the covariance matrix (E.59). As a consequence, one assumes that the function F can be approximated linearly. Let us compare the estimate for the sea quark and gluon PDF at the input scale, as shown in figure 7.8. There is a difference due to the fact that the model can

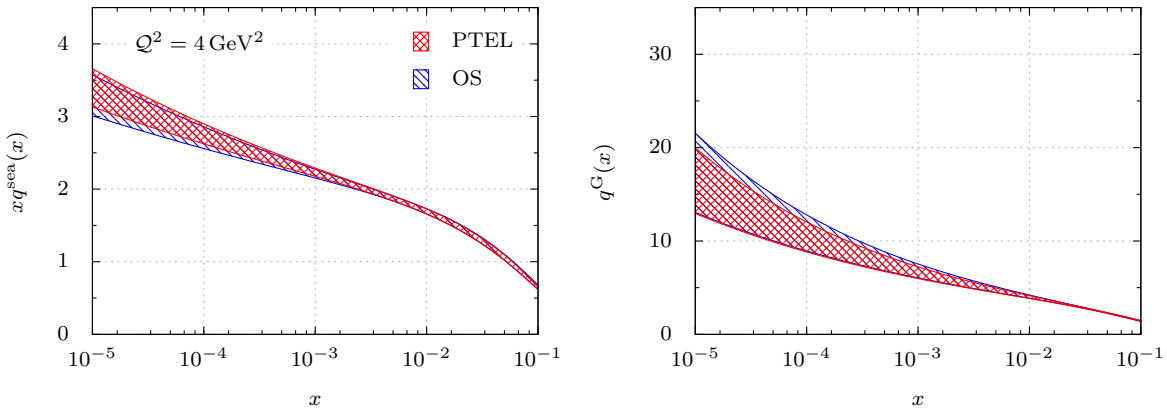

Figure 7.8.: Comparison of the estimated posterior distribution functions for the sea quark and gluon PDFs from PTEL and orthodox statistics.

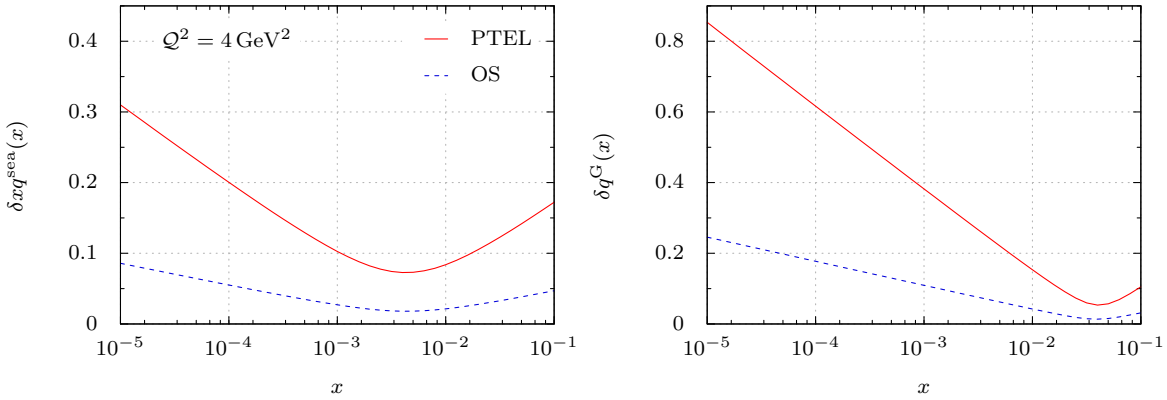

Figure 7.9.: Comparison of the relative PDF uncertainties from PTEL and orthodox statistics.

not be linearly approximated. To quantify the difference, we investigate the relative errors

$$\delta xq^{\mathrm{sea}}(x) = \frac{\sqrt{\mathrm{var}(xq^{\mathrm{sea}}(x))}}{xq^{\mathrm{sea}}(x)}\,, \qquad \delta q^{\mathrm{G}}(x) = \frac{\sqrt{\mathrm{var}(q^{\mathrm{G}}(x))}}{q^{\mathrm{G}}(x)}\,, \tag{7.35}$$

as shown in figure 7.9. The error is underestimated by a factor of ~ 2 for the sea quark PDF and ~ 3 for the gluon PDF in the x-region of the data. As a result, utilizing the covariance matrix underestimates the uncertainties drastically.

7.5. Analysis of data on DIS and DVCS

In this thesis, we study all 12 resulting parametrizations and thus present the first complete study of GPD models within a rigorous statistical analysis. We use PTEL and sample the posterior pdf of the respective parameters with the Metropolis-Hastings algorithm, see appendix E.4. The description of the data within the R-l parametrization at LO in perturbation theory is not possible neither with a exponential nor a power-like t-dependence. Additionally, the R-nnl model has too many parameters which are unconstrained by the data. This makes it hardly possible to optimize the parameters of the Metropolis-Hastings algorithm. As a consequence, the obtained Markov chain does not fulfill the criteria mentioned in appendix F. Certainly, we could improve the situation by utilizing narrower prior distributions. However, the essence will be the same: the model R-nnl parametrization has too many parameters. Therefore, we consider the model R-nnl parametrization as over complicated.
We also add a detailed comparison with the findings in [KM10]. In this work, the same data was analyzed utilizing the model R-nl with some restrictions. The momentum sum rule was employed strictly for the momentum average of the gluon GPD, the Regge slope for both sea quarks and gluons was fixed to $\alpha' = 0.15/\mathrm{GeV}^2$. Furthermore, the parameters for the t-dependence of the gluon GPD were fixed to the values $M^2 = 0.7\,\mathrm{GeV}^2$ and $B = 2.32/\mathrm{GeV}^2$.

7.5.1. Model comparison

The aim of this section is to present a extensive model study for the GPD estimation from DIS and DVCS data. Furthermore, we determine the necessary number of effective SO(3)-PWs to describe the data and investigate the preferred t-dependence. Fur this purposes, we employ a model comparison in the usual manner, compare Sec. 7.4.1. The marginalized posterior pdf and the maximum value of the unnormalized posterior distribution are given in Tab. 7.7.
From comparing the marginal posterior pdf values, we realize, that for the analysis of DIS and DVCS data, the LO estimate is for all models superior to the NLO estimate as already found in [KM10] by comparing the respective χ^2/d.o.f. values. Furthermore, if we only consider the achieved maximal value of the posterior distribution, which transfers to the minimal value of the logarithmical posterior pdf, the model R-nnl describes the data best. However, the additional parameters cause extra complication. Taking into account the marginalized posterior pdf the R-nl model describes the data best. Note, with the exponential t-dependence, the R-l-Et model is the most probable model. However, due to the fact that a LO estimate is not possible, we still consider the model R-nl-Et as the most probable one. In the language of PTEL, this view point would manifest in a low prior probability for R-l as a consequence of the missing LO estimate.
As we have already discussed in Sec. 7.4.1, we do not directly compare the LO and NLO estimate due to the different roles of the gluon GPD.
Let us now compare the exponential and dipole-like t-dependence for the R-nl model. The maximum values of the posterior pdf are almost equal. Albeit, from the marginalized posterior pdf values the exponential dependence has the highest probability. It is unclear, if this difference is due to the different prior information.
From the considerations in this section, we conclude that for the present DVCS data, the

model	order	Max $\ln f(\theta\|DI)$	$\ln f(D\|I)$
R-l-Dt	LO	-	-
	NLO	-84.754	-127.915
R-l-Et	LO	-	-
	NLO	-74.543	-113.579
R-nl-Dt	LO	-60.542	-109.138
	NLO	-65.164	-123.600
R-nl-Et	LO	-60.103	-105.123
	NLO	-65.681	-117.157
R-nnl-Dt	LO	-51.777	-123.470
	NLO	-56.770	-128.366
R-nnl-Et	LO	-46.483	-109.231
	NLO	-49.210	-118.645

Table 7.7.: The logarithm of the maximum of the posterior pdf $\ln f_{\max}$ and the normalization constant of the posterior pdf $\ln f_{\text{marg}}$.

model R-nnl is superfluous and we consider the model R-nl as the best choice. In addition, the exponential t-dependence describes the data best. However, we do not exclude the dipole like model. The model with one PW is excluded due to the missing LO estimate.

7.5.2. Description of the data

In figure 7.10 we show the dependence of the total DVCS cross section on the momentum transfer $\mathcal{Q}^2$ and on W as well as the t-dependence of the differential DVCS cross section. For simplicity, we only show the estimate for R-nl-Et at NLO of perturbation theory, since the results for the other models are not distinguishable by the naked eye. The description of the data on structure function F_2 is equal to the one in figure 7.3. Note, we always integrate the normalization uncertainty in the respective data points itself in order to avoid giving different estimates for the data of different collaborations with unequal normalizations. The data is very well described by the R-nl model.

7.5.3. Parameters

In section 7.5.1 we concluded by model comparison, that the preferable model is the R-nl one, where we obtain a reliable estimate at LO and NLO of perturbation theory. Let us now have a closer at look the estimated parameters. Figure 7.11 displays the posterior probability distribution functions of the common parameters. In addition, the parameters for the t-dependence are shown in Fig. 7.12. Furthermore, the numerical values are presented in

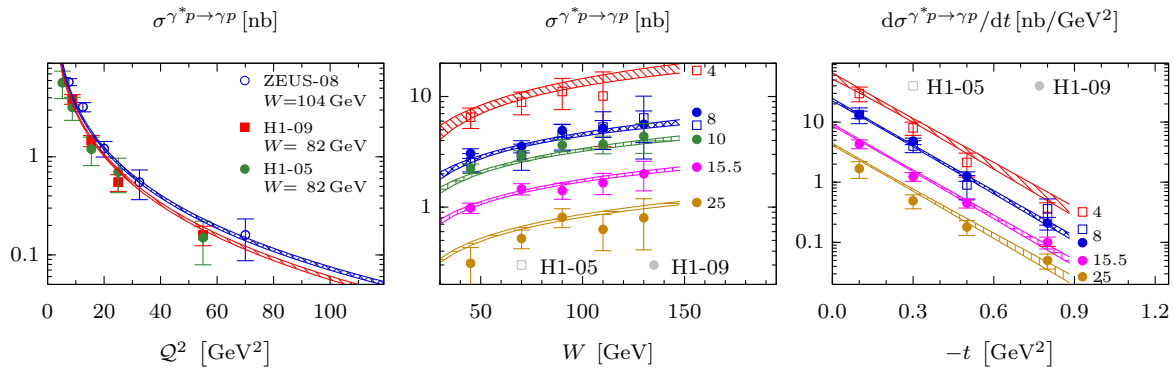

Figure 7.10.: Estimate of the $\mathcal{Q}^2$, W^2 and t dependence of the total and differential DVCS cross sections at NLO of perturbation theory from the model R-nl-Et, respectively. The small numbers behind the estimates in the W and t dependence correspond to the respective value of $\mathcal{Q}^2$.

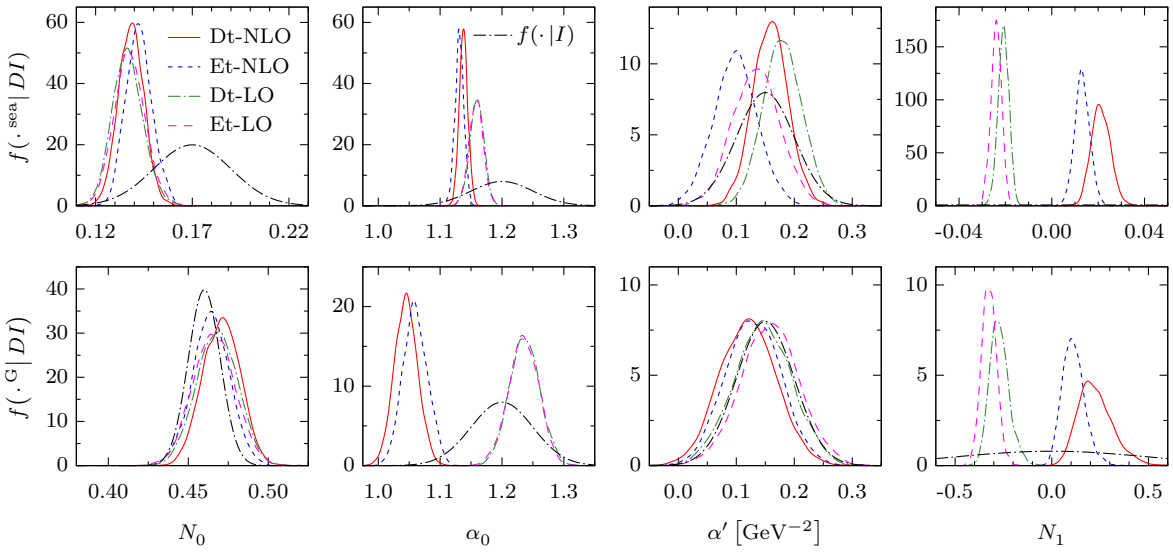

Figure 7.11.: Probability distribution functions for the common parameters of all R-nl models at LO and NLO of perturbation theory including the corresponding prior information.

Tab. 7.8.
The momentum fraction average of the sea quark GPD of all four estimates are approximately equal. However, the two estimates at NLO in perturbation theory are slightly increased. In comparison to the utilized prior information the pdf is much higher and narrower. Therefore, we conclude, that the prior information affects the estimates only weakly. Our estimate is in agreement with the one in [KM10][3], albeit it is smaller due to the additional variability of the momentum fraction average of the gluon GPD. The corresponding pdf is equal to the

[3] $N_0^{\mathrm{sea}\ \mathrm{LO}} = 0.152$, $N_0^{\mathrm{sea}\ \mathrm{NLO}} = 0.168$.

parameter	R-nl-Dt		R-nl-Et	
	LO	NLO	LO	NLO
N_0^{sea}	0.1366 ± 0.0079	0.1384 ± 0.0066	0.1377 ± 0.0079	0.1424 ± 0.0067
α_0^{sea}	1.1593 ± 0.0113	1.1379 ± 0.0070	1.1581 ± 0.0112	1.1313 ± 0.0072
$\alpha_0'^{,\text{sea}}$	0.1797 ± 0.0334	0.1589 ± 0.0303	0.1347 ± 0.0400	0.0983 ± 0.0371
$M_0^{2,\text{sea}}$	0.6585 ± 0.0857	0.5593 ± 0.0592		
B_0^{sea}			2.0642 ± 0.2076	2.5361 ± 0.1861
N_1^{sea}	-0.0208 ± 0.0024	0.0212 ± 0.0041	-0.0239 ± 0.0023	0.0131 ± 0.0032
N_0^{G}	0.4679 ± 0.0126	0.4707 ± 0.0114	0.4659 ± 0.0129	0.4643 ± 0.0114
α_0^{G}	1.2366 ± 0.0241	1.0449 ± 0.0186	1.2349 ± 0.0241	1.0598 ± 0.0197
$\alpha_0'^{,\text{G}}$	0.1456 ± 0.0501	0.1204 ± 0.0480	0.1578 ± 0.0496	0.1293 ± 0.0467
$M_0^{2,\text{G}}$	0.3564 ± 0.0755	0.4663 ± 0.1020		
B_0^{G}			3.6973 ± 0.5390	2.6077 ± 0.3590
N_1^{G}	-0.2704 ± 0.0511	0.2270 ± 0.0905	-0.3243 ± 0.0388	0.1124 ± 0.0572
ν_X^{H}	1.0570 ± 0.0300	1.0880 ± 0.0274	1.0569 ± 0.0299	1.0802 ± 0.0273

Table 7.8.: Numerical values of the parameters of the R-nl model extracted from DIS and DVCS.

prior distribution and does not differ significantly within the four estimates and we conclude, that the assumption of N^{val} [KMPK08, KM10] was a reasonable choice, since the data does not allow the extraction of such information.
The Regge intercepts of the sea quark GPDs at LO and NLO differ significantly from the prior distribution: they are peaked and very narrow. The estimates of the R-nl-Et-B and R-nl-Dt-B model agree, whereas the NLO estimate is slightly smaller, which is was also found in [KM10][4]. On the other hand, the Regge intercept of the gluon GPD is less defined, but again the R-nl-Dt and R-nl-Et model have equal values at the same order of perturbation theory. As the estimate in [KM10][5] the NLO order mean value is higher than the LO one and the numerical values agree with ours. Due to the absence of gluons at the input scale in LO of perturbation theory, their contribution to the cross section is limited. However at NLO they contribute. Thus, due to the free parameter for the t-dependence (M^{G}, B^{G}), it is slightly smaller then the value in [KM10].
The pdfs for the Regge slope confirm the assumption [KM10], namely that the data does not hold any information about that parameters on a statistically rigorous ground. For the sea quarks GPD the data contains some information and the posterior pdf is different than the prior distribution. In contrast, For the gluon GPD, we almost get the prior distribution. Therefore, we conclude, that the analyzed DVCS data contains almost no information on the

[4] $\alpha_0^{\text{sea}} \overset{\text{LO}}{=} 1.158$, $\alpha_0^{\text{sea}} \overset{\text{NLO}}{=} 1.128$.
[5] $\alpha_0^{\text{G}} \overset{\text{LO}}{=} 1.247$, $\alpha_0^{\text{G}} \overset{\text{NLO}}{=} 1.099$.

Regge slope.
The skewness parameters for the two models R-nl-Et and R-nl-Dt roughly agree. There is a noticeable difference of R-Et to R-Dt at NLO of perturbation theory. In addition, the uncertainty for the gluon GPD is larger than for the sea quark GPD. Our estimates are consistent with the values of [KM10][6], including the positive and negative values at NLO and LO, respectively. Note, we transformed the skewness parameters into our conventions (6.29).
Let us first see the R-nl-Dt model for the t-dependence. The respective parameter pdfs are

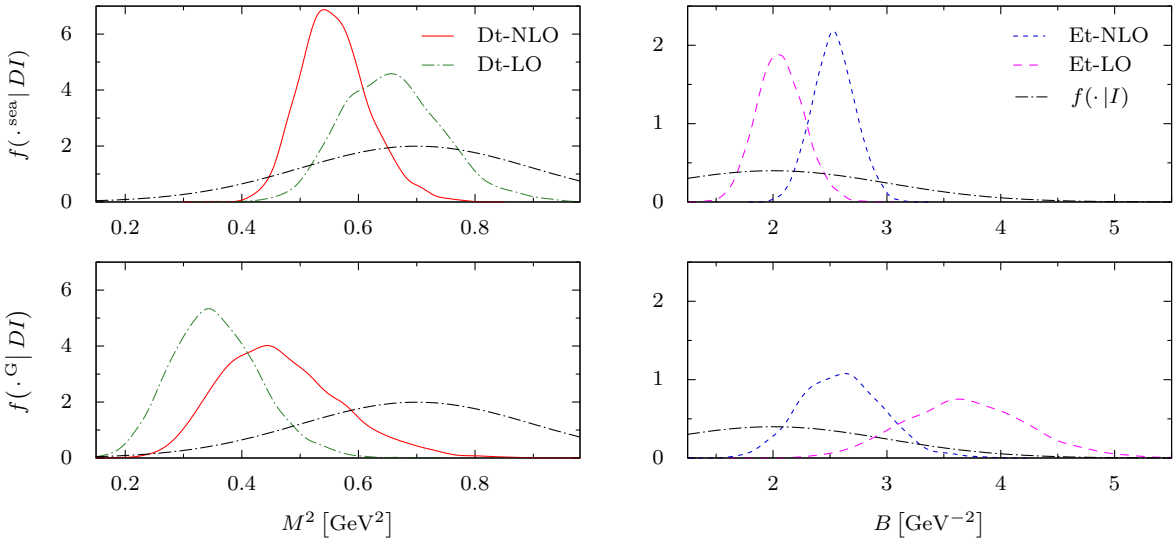

Figure 7.12.: Probability distribution functions for the parameters of the t-dependence of the model R-nl at LO and NLO of perturbation theory together with the corresponding prior distributions.

shown in Fig. 7.12. At NLO, the estimate of M^2 for the sea quark GPD is different from the prior distribution in both its mean value and variance. At LO it is only slightly different from the prior information and its mean value is larger than the NLO one. For gluons, in LO and NLO the pdfs are wide and the corresponding parameters cannot be well constrained. For the R-nl-Et model, the same statements hold. Thus, we conclude, that there is information about such parameters an LO and NLO for both sea quarks and gluons, in contrast to the claim in [KM10][7].
As previously mentioned, the normalization ν_X^{H} of the DIS data is a free parameter. In Figure 7.13 we present the corresponding pdfs for all models. The normalization completely agrees for all models at LO of perturbation theory and has a moderate mean value. At NLO, the estimates for the two different t-dependencies are slightly different and also the mean value increases.
We add the general remark, that if the information in the data is very weak, which is certainly the case for the analyzed DIS and DVCS data, PTEL plays its strengths. Due to the utiliza-

[6] $N_1^{\mathrm{sea}} \overset{\mathrm{LO}}{=} -0.02508$, $N_1^{\mathrm{sea}} \overset{\mathrm{NLO}}{=} 0.00672$, $N_1^{\mathrm{G}} \overset{\mathrm{LO}}{=} -0.37408$, $N_1^{\mathrm{G}} \overset{\mathrm{NLO}}{=} 0.00864$.
[7] $M_0^{2,\mathrm{sea}} \overset{\mathrm{LO}}{=} 0.48$, $M_0^{2,\mathrm{sea}} \overset{\mathrm{NLO}}{=} 0.59$, $B^{\mathrm{sea}} \overset{\mathrm{LO}}{=} 4.8$, $B^{\mathrm{sea}} \overset{\mathrm{NLO}}{=} 4$.

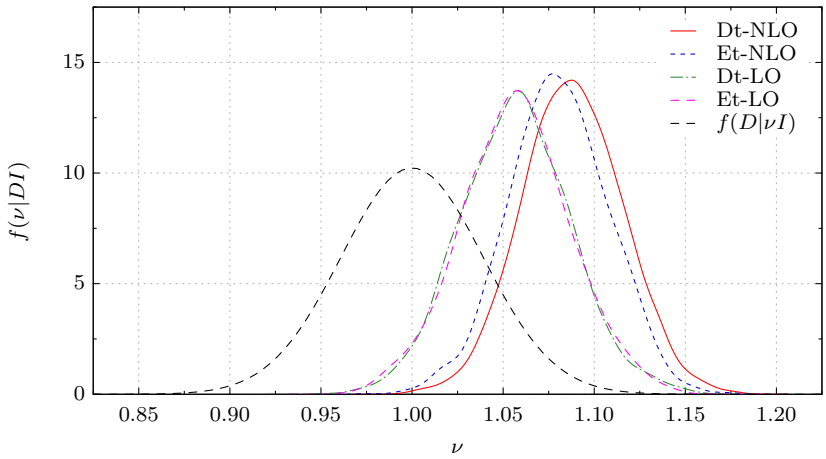

Figure 7.13.: Posterior probability distribution for the normalization of the DIS data from the estimate of the nl-T models at LO and NLO of perturbation theory.

tion of priors information the knowledge is improved in a objective way without influencing the parameter estimate. This exactly corresponds to the given situation.

7.5.4. Generalized parton distributions

In addition to the parameters, we also present the estimates for the GPD from the R-nl-Et model. As it became already clear in the analysis of the respective parameters in the previous section, the models R-nl-Et and R-nl-Dt are equivalent and our findings hold for R-nl-Dt as well. Figures 7.15 and 7.14 show the dependence on the momentum fraction x (upper row) and the transverse momentum t (lower row) of the GPD on the cross-over line and the PDF at LO and NLO of perturbation theory, respectively. Note, we have removed the momentum average N^a. The error bands are given by the mean value and the square root of the variance of the respective pdf.
At NLO, the GPD is well constrained by the data. The sea quark GPD on the cross-over line and the PDF are different, whereas they are similar in the gluonic case. This agrees with the findings in [KM10] and is typical for the utilized models.
At LO, the sea quark GPD on the cross-over line is similar to the sea quark PDF possessing approximately the same statistical uncertainty. For the gluon GPD, we first notice the negative values for the GPD on the cross-over line. Solely from this type of figure, we would conclude, that the gluon GPD is in fact negative. However, this is a situation as mentioned in Sec. 5.5.1.2, where the given type of figure does not represent the actual state of knowledge in a sufficient manner. Thanks to PTEL, we have direct access to the pdf, not just the mean value and a number corresponding to the uncertainty. In Fig. 7.16 we present the pdf of the gluon GPD on the cross-over line at the kinematical points $x = 10^{-3}$ and $t = 0$. By inspection of this pdf, we notice that the actual state of knowledge is in fact very different from the one displayed in Fig. 7.15. The pdf is very wide and we are only able to conclude, that the gluon GPD on the cross-over line is in the interval $[-15, 5]$. This is an example of a pdf, where the

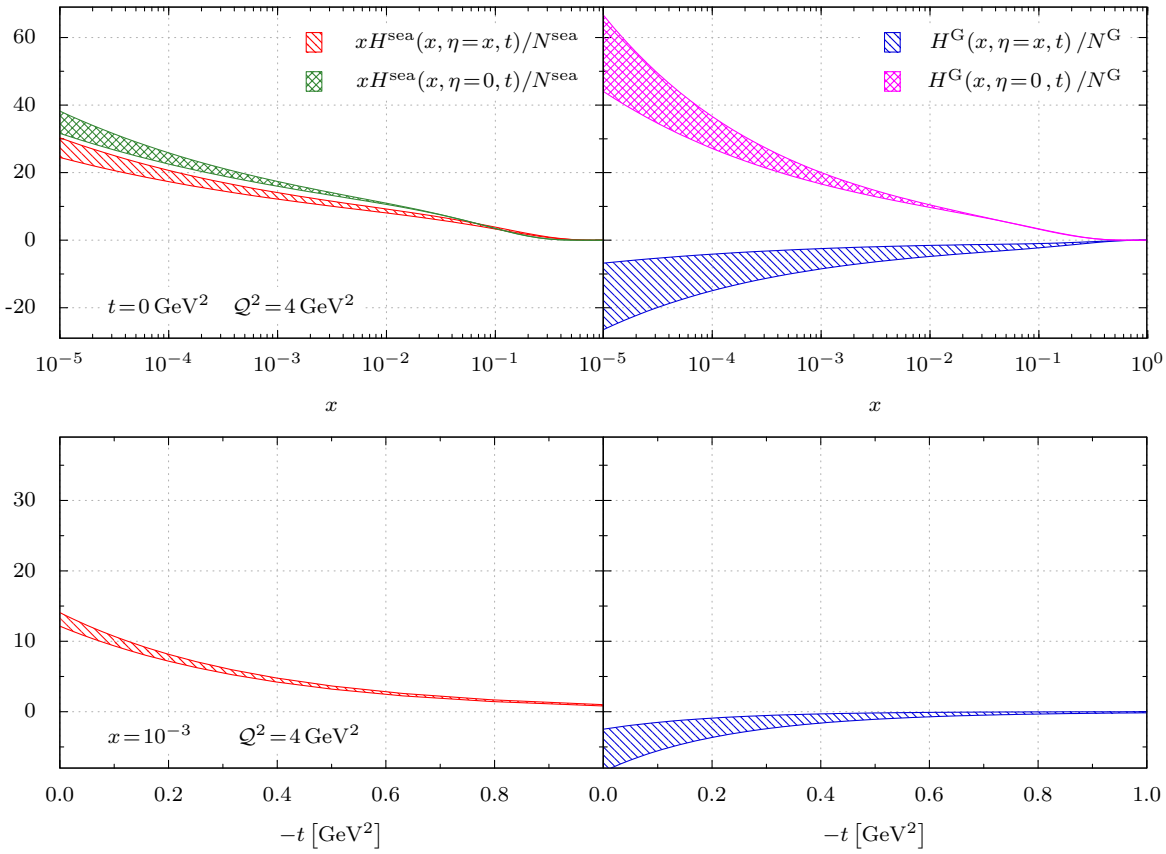

Figure 7.14.: Estimate R-nl-Et-B-LO for the dependence on the momentum fraction x and the transverse momentum t of the GPD on the cross-over line divided by the momentum fraction average and the corresponding PDF.

mean value and the variance are not enough information to report a pdf (cf. Sec. 5.5.1.1). Utilizing very narrow priors, we are able to force the gluon GPD on the cross-over line to positive values. As a consequence, the negative value is mainly induced by the free parameter of the t-dependence. Fixing the values ($M^{\rm G}$, $B^{\rm G}$) as in [KM10] the gluon GPD on the cross-over line is in the interval [-15,20]. Therefore, the gluon GPD is not constrained by the data at LO.
The Et model at NLO is a little smaller than the Dt model, but qualitatively it is the same. We saw, that a LO analysis of present DVCS data is not sufficient to determine the gluon GPD. This all goes down to the fact, that at LO the gluon GPD takes only part via evolution. On the other hand, at NLO, we are able to determine the gluon GPD with satisfying precision. We also realize, that the sea quark GPD is now less determined, due to a different information transport.

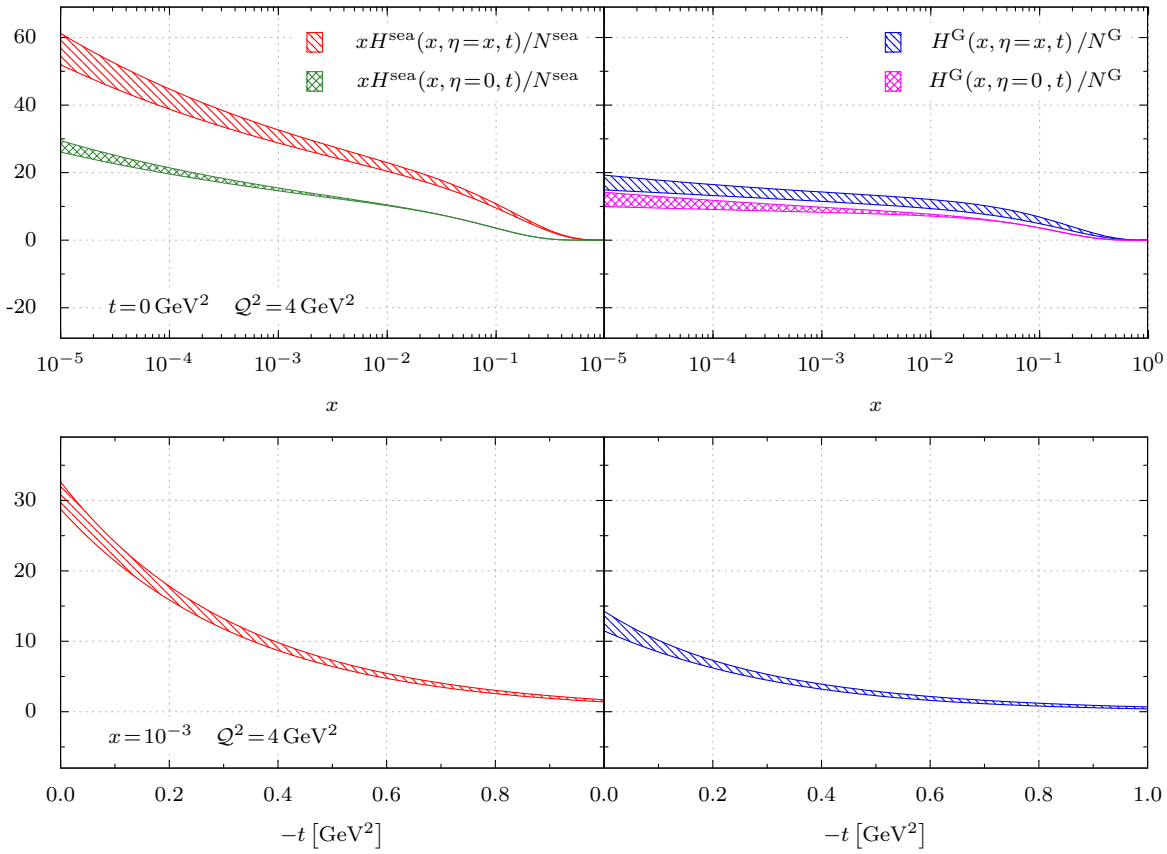

Figure 7.15.: Estimate R-nl-Et-B-NLO for the dependence on the momentum fraction x and the transverse momentum t of the GPD on the cross-over line divided by the momentum fraction average and the corresponding PDF.

7.5.5. Skewness ratio

An important characteristic of a GPD model is the ratio of the GPD on the cross-over line to the corresponding PDF. This skewness ratio is for small-x mostly independent of x. For the sea quark and gluon GPD it reads

$$r^A(\mathcal{Q}^2) = \frac{H^A(x,\eta=x,t=0,\mathcal{Q}^2)}{H^A(x,\eta=0,t=0,\mathcal{Q}^2)}\,, \qquad A\in\{\text{sea},\text{G}\}\,. \tag{7.36}$$

At LO of perturbation theory, the sea quark skewness ratio is given as the ratio of the imaginary part of the CFF $\Im\mathrm{m}\,\mathcal{H}(x,t=0,\mathcal{Q}^2)/\pi$ and the transverse unpolarized DIS structure function $F_{\rm T}(x,\mathcal{Q}^2)/x$. Thus, it can almost be directly measured. Assuming an exponential t-dependence, the skewness effect is revealed by employing the total DVCS cross section [A+08a]

$$R(W,\mathcal{Q}^2) = \frac{\sqrt{16\pi\sigma(\gamma^*p\to\gamma p)b(\mathcal{Q}^2)/(1+\rho^2)}}{\sigma_{\rm T}(\gamma^*p\to X)} \overset{\rm LO}{=} \frac{H^{\rm sea}(x,\eta=x,t=0,\mathcal{Q}^2)}{H^{\rm sea}(X,\eta=0,t=0,\mathcal{Q}^2)}\bigg|_{X=2x/(2-x)}\,, \tag{7.37}$$

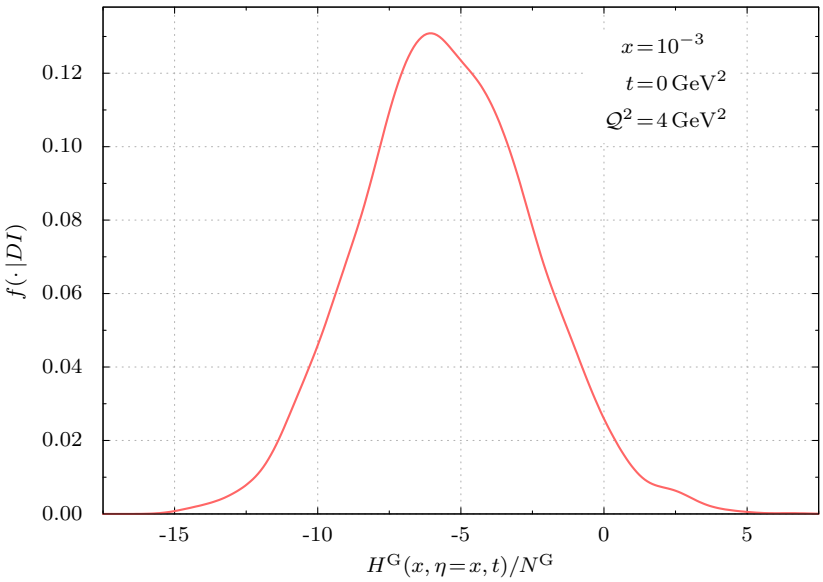

Figure 7.16.: Probability distribution function of the gluon GPD on the cross-over line divided by the momentum average N^{G} for $x = 10^{-3}$, $t = 0\,\mathrm{GeV}^2$ and $\mathcal{Q}^2 = 4\,\mathrm{GeV}^2$.

where the t-slope $b(\mathcal{Q}^2)$ has been estimated under the assumption $\alpha' = 0$ [A+08a],

$$b(\mathcal{Q}^2) = A\left[1 - B\ln\left(\frac{\mathcal{Q}^2}{2\mathrm{GeV}^2}\right)\right], \quad A = 6.98 \pm 0.54\,\mathrm{GeV}^{-2}, \quad B = 0.12 \pm 0.03, \tag{7.38}$$

and the ratio of the real and imaginary part of the DVCS amplitude is set to $\rho = \cot(\alpha(\mathcal{Q}^2)\pi/2)$. In Fig. 7.17 we display the skewness ratio of the sea quark and gluon GPD at LO and NLO of perturbation theory. Averaging over the displayed range of $\mathcal{Q}^2$, we obtain the following values at LO of perturbation theory

$$\langle r^{\mathrm{sea}} \rangle = 0.986 \pm 0.106, \qquad \langle r^{\mathrm{G}} \rangle = 0.967 \pm 0.201, \tag{7.39}$$

which is consistent with the claim in [KM10], that the sea quark skewness ratio at LO is ~ 1. This was utilized to predict correctly the DVCS cross section. In figure 7.18 we show the skewness effect (7.37), which is consistent with the experimental data in [A+05, A+08a]. On the other hand, the skewness ratio increases at NLO to the values

$$\langle r^{\mathrm{sea}} \rangle = 1.996 \pm 0.068, \qquad \langle r^{\mathrm{G}} \rangle = 1.166 \pm 0.089, \tag{7.40}$$

which is also consistent with the findings in [KM10]. The negative skewness ratio for gluons is a result of the limited prior information as already discussed in the previous section.

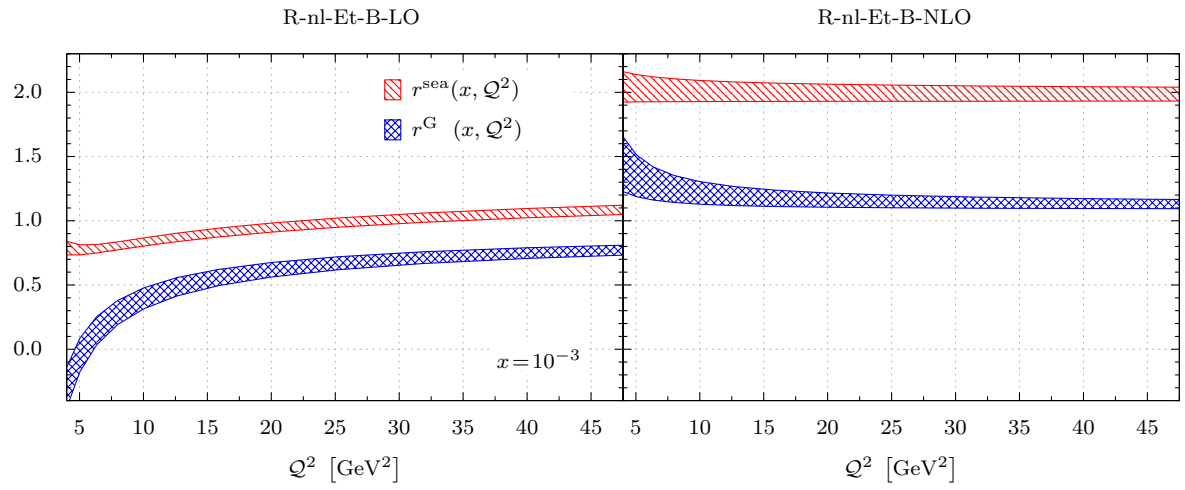

Figure 7.17.: Skewness ratio of the estimate for the model R-nl-Et at LO and NLO of perturbation theory.

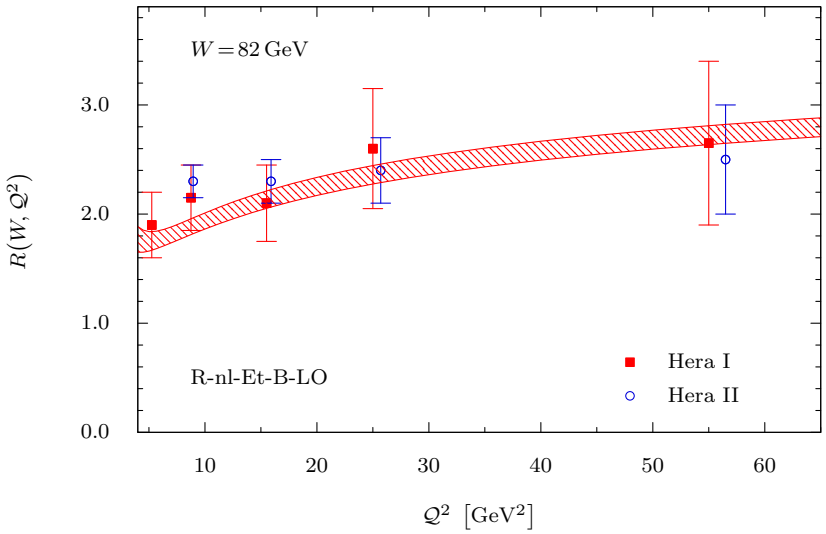

Figure 7.18.: Experimental skewness ratio $R(W,\mathcal{Q}^2)$ for $W = 82\,\mathrm{GeV}$ together with the experimental data of Hera I [A+05] and Hera II [A+08a].

7.5.6. Size of NLO corrections

In order to investigate the convergence of the perturbative series, we utilize the ratio of the CFF at NLO to the one at LO, namely [KMPK08]

$$\frac{\mathcal{H}^{\mathrm{NLO}}}{\mathcal{H}^{\mathrm{LO}}}\left(\xi,\Delta^2,\mathcal{Q}^2\right) \equiv K\left(\xi,\Delta^2,\mathcal{Q}^2\right)\exp\left[i\delta\varphi\left(\xi,\Delta^2,\mathcal{Q}^2\right)\right]\,. \tag{7.41}$$

If convergence holds, the ratio of the moduli

$$K = \frac{\left|\mathcal{H}^{\mathrm{NLO}}\right|}{\left|\mathcal{H}^{\mathrm{LO}}\right|}\,, \qquad \delta K = K - 1\,, \tag{7.42}$$

becomes one. The phase difference

$$\delta\varphi(\xi, \Delta^2, \mathcal{Q}^2) = \arg\left(\frac{\mathcal{H}^{\mathrm{NLO}}}{\mathcal{H}^{\mathrm{LO}}}\right) \tag{7.43}$$

is formally of order $\alpha_\mathrm{s}/(2\pi)$ and diminishes at higher orders, if convergence holds.
Fig. 7.19 displays the relative NLO corrections (7.42) and (7.43) at the input scale $\mathcal{Q}_0^2 = 4\,\mathrm{GeV}^2$ for the momentum transfer squared $t = 0$ and $t = -1\,\mathrm{GeV}^2$. The phase is very

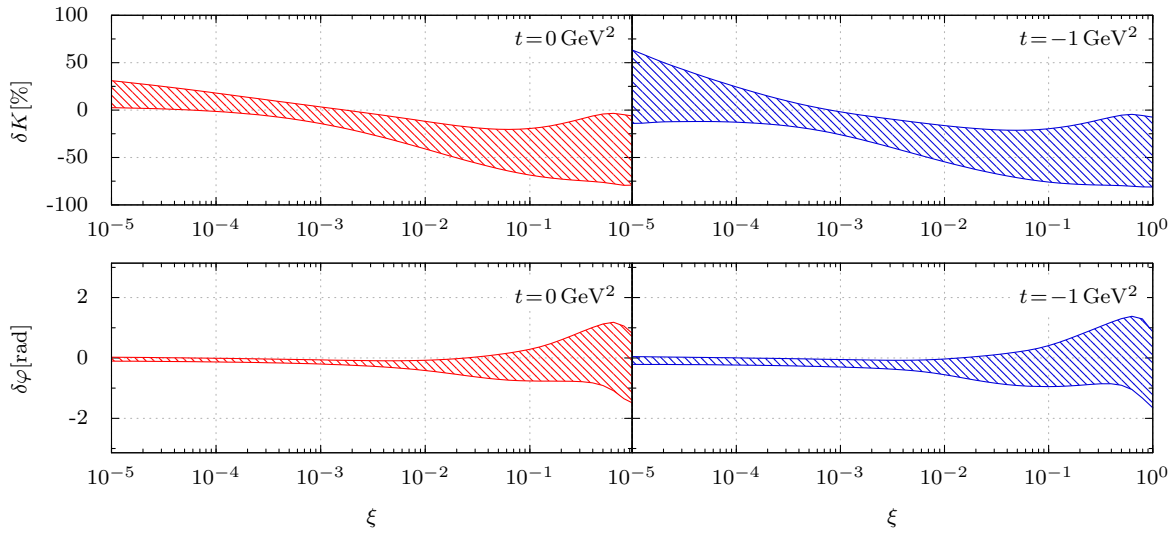

Figure 7.19.: Ratio of the moduli δK and the phase difference $\delta\varphi$ in dependence of the skewness variable ξ for different values of the momentum transfer t for the quantification of the size of the perturbative corrections.

small in the region of the experimental data $10^{-4} \leq \xi \leq 10^{-2}$ and increases in the valence region. This finding holds for both values of the momentum transfer t, whereas it is larger for $t = -1\,\mathrm{GeV}^2$. This agrees with the results in [KMPK08]. Also in [BMNS00, FM02] moderate NLO corrections were found. The NLO corrections to the moduli are about 20 % for $t = 0$ and slightly larger for $t = -1\,\mathrm{GeV}^2$. Therefore, we obtain rather small perturbative corrections. This is the first time perturbative corrections were quantified with error propagation, which shows the advantage of PTEL, where the pdfs of all interesting quantities directly follow from the posterior pdf of the parameters.

7.5.7. Transverse distribution of partons

The analysis of the t-dependence of the DIS and DVCS data can be utilized to present a partonic picture of the nucleon. In the infinite momentum frame, the proton might be viewed

as a disc with radius [Bur03]

$$\sqrt{4\frac{\mathrm{d}}{\mathrm{d}t}\ln F_1(t)\Big|_{t=0}} \approx 0.6\,\mathrm{fm}\,, \tag{7.44}$$

arising from the dipole parametrization of the Dirac form factor. The transverse width of parton distributions, the average distance $\sqrt{\langle \vec{b}^2 \rangle}$ of the struck parton from the proton center is given by the t-slope of the zero-skewness GPD

$$\langle \vec{b}^2 \rangle = 4\frac{\mathrm{d}}{\mathrm{d}t}\ln H(x, \eta{=}0, t, \mathcal{Q}^2)\Big|_{t=0}\,. \tag{7.45}$$

The transverse width for the sea quark and the gluon GPD at LO and NLO of perturbation theory are displayed in Fig. 7.31. In table 7.9 we show the numerical values of the transverse

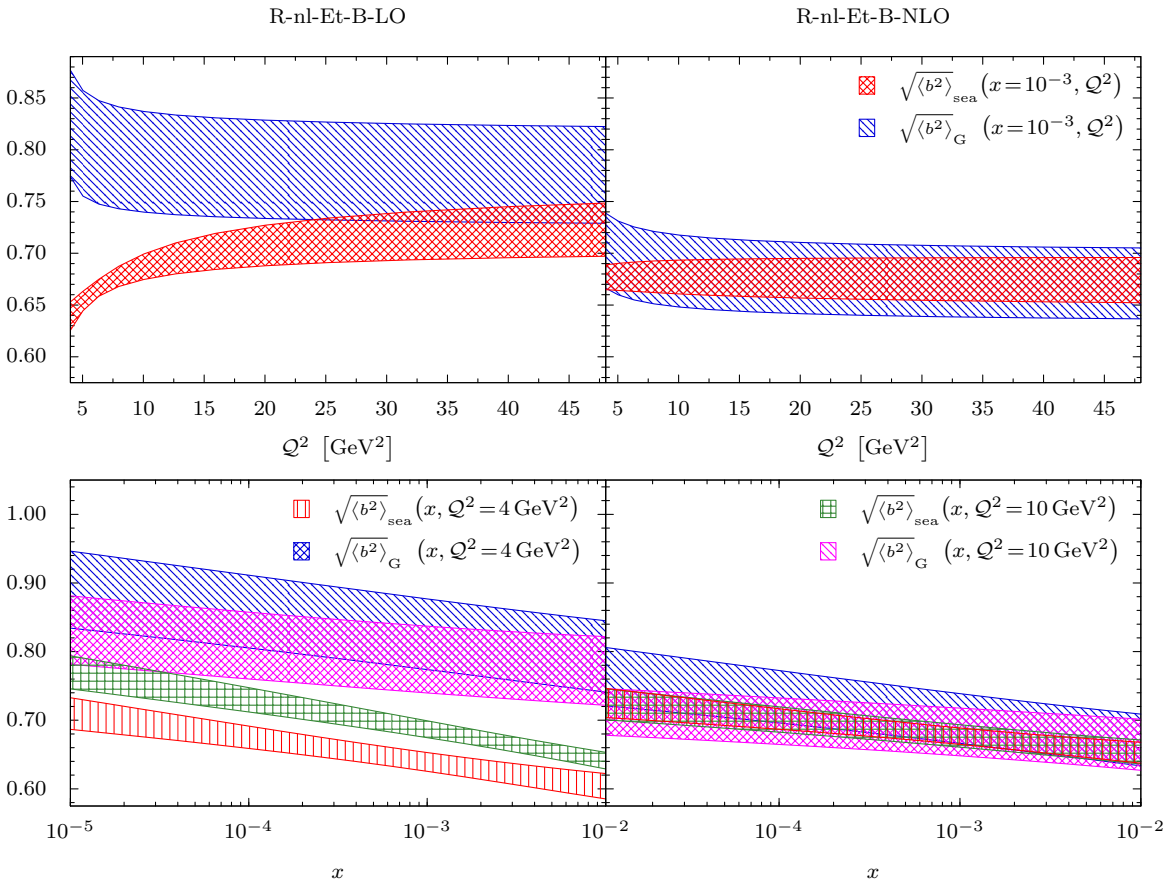

Figure 7.20.: Transverse width $\sqrt{\langle \vec{b}^2 \rangle}$ of sea quark and gluon GPDs at LO and NLO of perturbation theory.

width at the input scale and at $x = 10^{-3}$.
At LO, the transverse width of sea quarks is smaller than the one of gluons. However,

model	$\mathcal{Q}^2$ [GeV^2]	order	$\sqrt{\langle b^2\rangle_{\text{sea}}}$ [fm]	$\sqrt{\langle b^2\rangle_{\text{G}}}$ [fm]
R-nl-Dt	4	LO	0.761 ± 0.028	0.971 ± 0.085
		NLO	0.800 ± 0.026	0.859 ± 0.072
	10	LO	0.818 ± 0.023	0.939 ± 0.082
		NLO	0.808 ± 0.033	0.841 ± 0.071
R-nl-Et	4	LO	0.639 ± 0.014	0.825 ± 0.051
		NLO	0.677 ± 0.012	0.703 ± 0.036
	10	LO	0.687 ± 0.012	0.788 ± 0.049
		NLO	0.677 ± 0.016	0.683 ± 0.035

Table 7.9.: Transverse width at the input scale $\mathcal{Q}_0^2 = 4\,\text{GeV}^2$ and $x = 10^{-3}$.

we always see the characteristic x-dependence, which is related to the partonic shrinkage effect. In contrast to the findings in [KM10], gluons are not more centralized than sea quarks. This probably is a consequence of the fact that the parameters are no longer fixed by J/ψ-production, but are constrained only by the data. See also Sec. 6.6 about the employed prior information.
Comparing the transverse width at the input scale of $\mathcal{Q}_0^2 = 4\,\text{GeV}^2$ with the one at $\mathcal{Q}^2 = 10\,\text{GeV}^2$, we realize, that they slightly differ for the sea quark GPD and agree for the gluon GPD within the given uncertainties. Also the partonic shrinkage effect is present at the higher scale. The uncertainties for the gluon GPD are larger.
Comparing the estimate for the dipol-like and exponential t-dependence, we see, that the dipol-like ansatz leads to a larger estimate, which was already pointed out by the authors in [KM10]. Additionally, the uncertainties are slightly increased and the difference of the transverse width for the sea quark GPD at the input scales and at the scale $\mathcal{Q}^2 = 10\,\text{GeV}^2$ is no longer present.
In a realistic GPD model, the t-dependence vanishes in the limit $x \to 1$ [H$^+$08] and the partons are entirely concentrated in the central region. This feature can be implemented by dressing the cut-off or the exponential slope parameter with a j-dependence.
At NLO, the picture changes. In Fig. 7.31 we show the transverse width for NLO. The interesting thing is, that the sea quark and gluon width are equal. However, the gluon width has a larger uncertainty. This also holds at higher scales. The characteristic behavior with x is clearly visible. Again, the estimate for the dipole-like t-dependence is larger and has a higher uncertainty.
Consequently, utilizing a flexible skewness ratio and the same functional form for sea quarks and gluons we obtain the same transverse width at NLO, whereas at LO, the sea quark width is slightly smaller. This is in agreement with the findings in [FSW05] of 0.65 fm. At LO, we obtain a different value, due to the large uncertainty of the gluon GPD.

In addition, we also show the normalized transverse profile function

$$\rho^A(b,x,\mathcal{Q}^2) = \frac{\int_{-\infty}^{\infty} \mathrm{d}^2\vec{\Delta}\, e^{i\vec{\Delta}\vec{b}} H^A(x,\eta=0,t=-\vec{\Delta}^2,\mathcal{Q}^2)}{\int_{-\infty}^{\infty} \mathrm{d}^2\vec{\Delta} \qquad H^A(x,\eta=0,t=-\vec{\Delta}^2,\mathcal{Q}^2)}\,. \tag{7.46}$$

The corresponding estimate is given in Fig. 7.21. For the model R-nl-Dt the LO and NLO

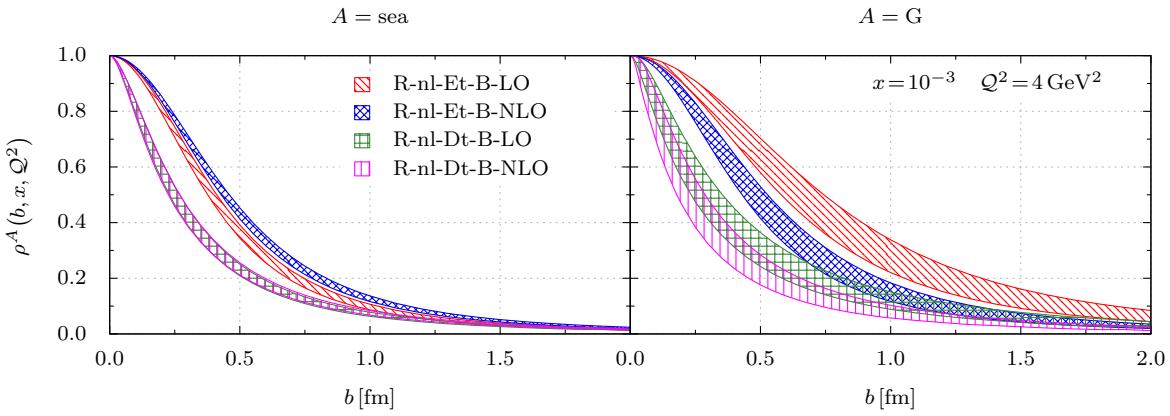

Figure 7.21.: Transverse profile function for the model R-nl-Et at LO and NLO of perturbation theory.

estimate are equal within the given uncertainties. On the other hand, for the model R-nl-Et there is a slight difference of the two estimates from different order of perturbation theory. In contrast to [KM10] we see a significant difference of the dipole and exponential ansatz not only in the tail region.

7.6. Analysis of data on DIS, DVCS and DVMP

At this point, we have repeated the analysis of GPDs in the perturbative framework in the last decade. We have verified the previous findings utilizing PTEL and gained new important insights, which have not been possible before. Next, we employ the same tools to further extend the analysis incorporating DVMP data as well. This task is much more demanding than the previous estimates.

7.6.1. LO estimate

The difficulty of a LO analysis is the description of the DIS data. Utilizing the model R-nnl, the Regge intercept for the gluon GPD becomes very soft [MM14] and the description of the DIS data is insufficient. Employing the model F-nnl improves the situation. Albeit, the W-dependence of the cross section below $\mathcal{Q}^2 \approx 10\,\mathrm{GeV}^2$ is not described with sufficient accuracy, see figure 7.24. Note, we actually show the result for the narrow priors as in [LMS13].

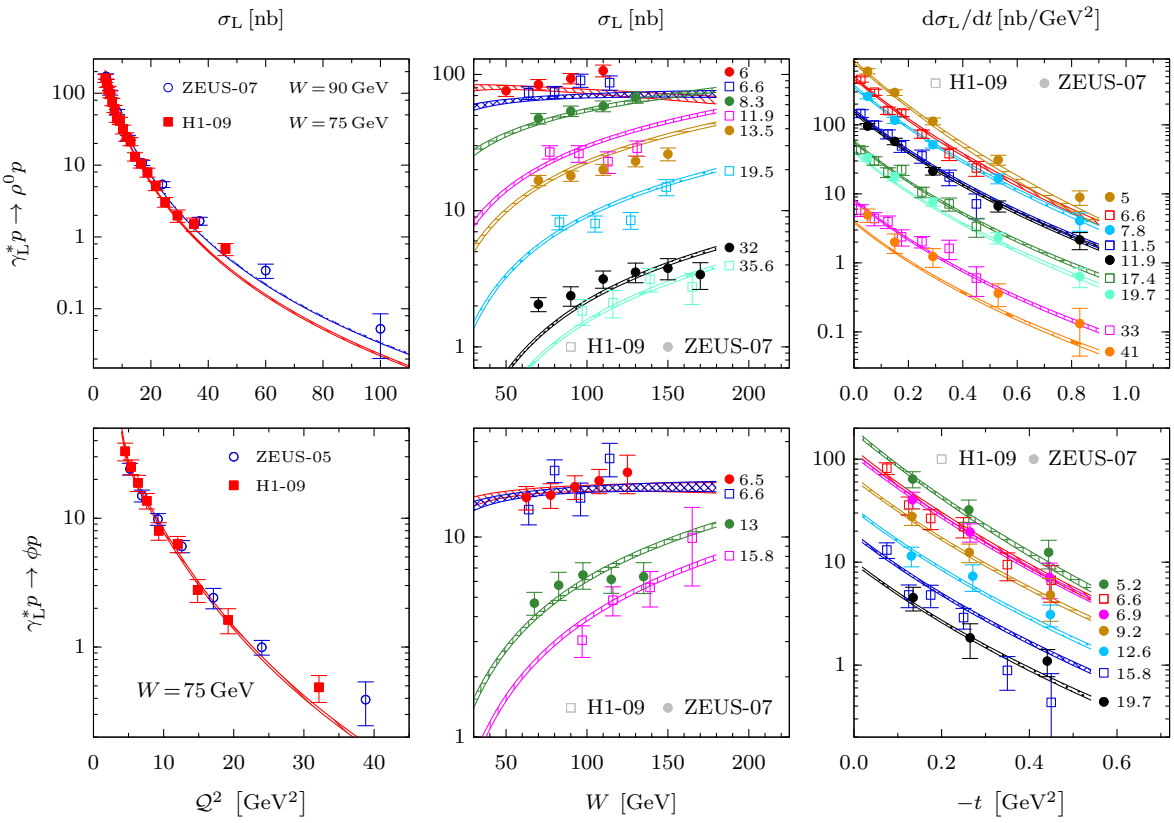

Figure 7.22.: The estimate for the model F-nnl-Dt with the narrow priors from [LMS13] at LO of perturbation theory for the $\mathcal{Q}^2$, W^2 and t dependence of the total and differential longitudinal DVCS cross sections, respectively. The small numbers behind the estimates in the W and t dependence correspond to the respective value of $\mathcal{Q}^2$.

Unfortunately, broadening the prior distributions does not improve the estimate. Furthermore, including additional parameters for the nl- and nnl-PW of the distribution amplitudes does not remove the incident. As a consequence, a LO estimate remains an open problem.

7.6.2. Description of the data

At NLO of perturbation theory, the model F-nnl-Dt describes the DIS, DVCS and DVMP data very well. We disclaim on showing the description of the DIS data, since it is of the same quality as in Fig. 7.3. Figure 7.23 displays our estimate for the cross section data of DVCS. We obtain a very good description. Additionally, in figure 7.24 we present the description of the data on DVMP-ρ^0 and DVMP-ϕ. Note, we show the longitudinal cross section for simplicity. Rescaling the estimate to the total cross section is straight forward utilizing the results of Sec. 7.2.

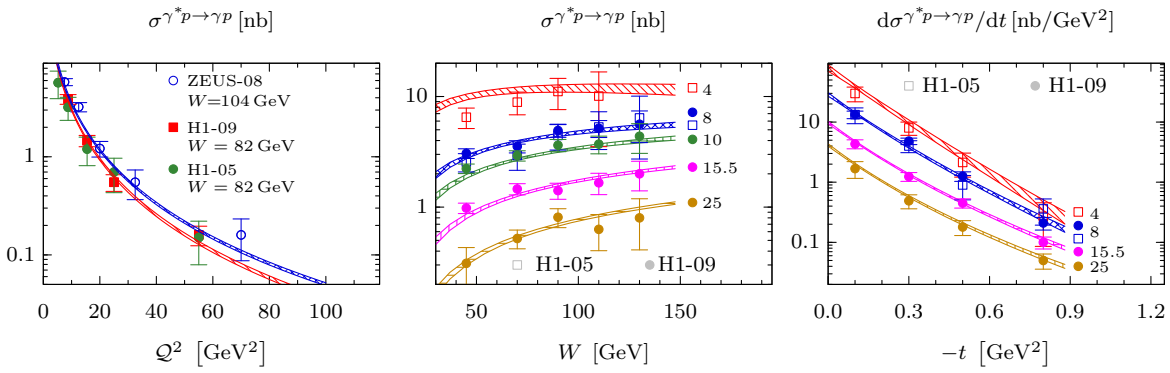

Figure 7.23.: The estimate for the model F-nnl-Dt at NLO of perturbation theory for the $\mathcal{Q}^2$, W^2 and t dependence of the total and differential DVCS cross sections, respectively. The small numbers behind the estimates in the W and t dependence correspond to the respective value of $\mathcal{Q}^2$.

7.6.3. Parameters

In figure 7.25 we show the parameter pdfs of the estimate F-nnl-Dt-C-NLO. Table 7.10 gives the mean value and the square root of the variance of the corresponding parameter pdfs.

Parameter	$\langle\cdot\rangle \pm \sqrt{\text{var}(\cdot)}$	Parameter	$\langle\cdot\rangle \pm \sqrt{\text{var}(\cdot)}$	Parameter	$\langle\cdot\rangle \pm \sqrt{\text{var}(\cdot)}$
N_0^{sea}	0.1833 ± 0.0076	N_0^{G}	0.3979 ± 0.0108	ν_X^{H}	0.9840 ± 0.0229
α_0^{sea}	1.0910 ± 0.0075	α_0^{G}	1.2151 ± 0.0102	$\nu_{\rho^0}^{\text{H}}$	1.0288 ± 0.0275
$\alpha'^{,\text{sea}}$	0.1236 ± 0.0302	$\alpha'^{,\text{G}}$	0.0265 ± 0.0288	$\nu_{\rho^0}^{\text{Z}}$	1.0824 ± 0.0295
$M_0^{2,\text{sea}}$	0.8024 ± 0.1101	$M_0^{2,\text{G}}$	0.4530 ± 0.0391	ν_{ϕ}^{H}	0.7284 ± 0.0256
N_1^{sea}	-0.1421 ± 0.0204	N_1^{G}	-0.3078 ± 0.0366	ν_{ϕ}^{Z}	0.9362 ± 0.0298
α_1^{sea}	0.9568 ± 0.0206	α_1^{G}	1.1067 ± 0.0232		
$M_1^{2,\text{sea}}$	0.9255 ± 0.1414	$M_1^{2,\text{G}}$	0.4981 ± 0.1087		
N_2^{sea}	0.0257 ± 0.0038	N_2^{G}	0.0698 ± 0.0099		
α_2^{sea}	1.0840 ± 0.0095	α_2^{G}	1.1950 ± 0.0142		
$M_2^{2,\text{sea}}$	0.7037 ± 0.0908	$M_2^{2,\text{G}}$	0.5434 ± 0.1218		

Table 7.10.: Numerical values of the parameters of the estimate F-nnl-Dt-C-NLO from DIS, DVCS and DVMP data.

The pdf for the momentum fraction average of the sea quark GPD N^{sea} clearly overwhelms its prior distribution. In comparison to the estimate R-nl-Et-B-NLO, it is higher, which is due to the different number of PWs, which was also found in [KM10]. For the gluonic momentum fraction average N^{G} we almost obtain the prior distribution.
The normalization parameters for the nl-PW N_1^a are negative, which is already known from

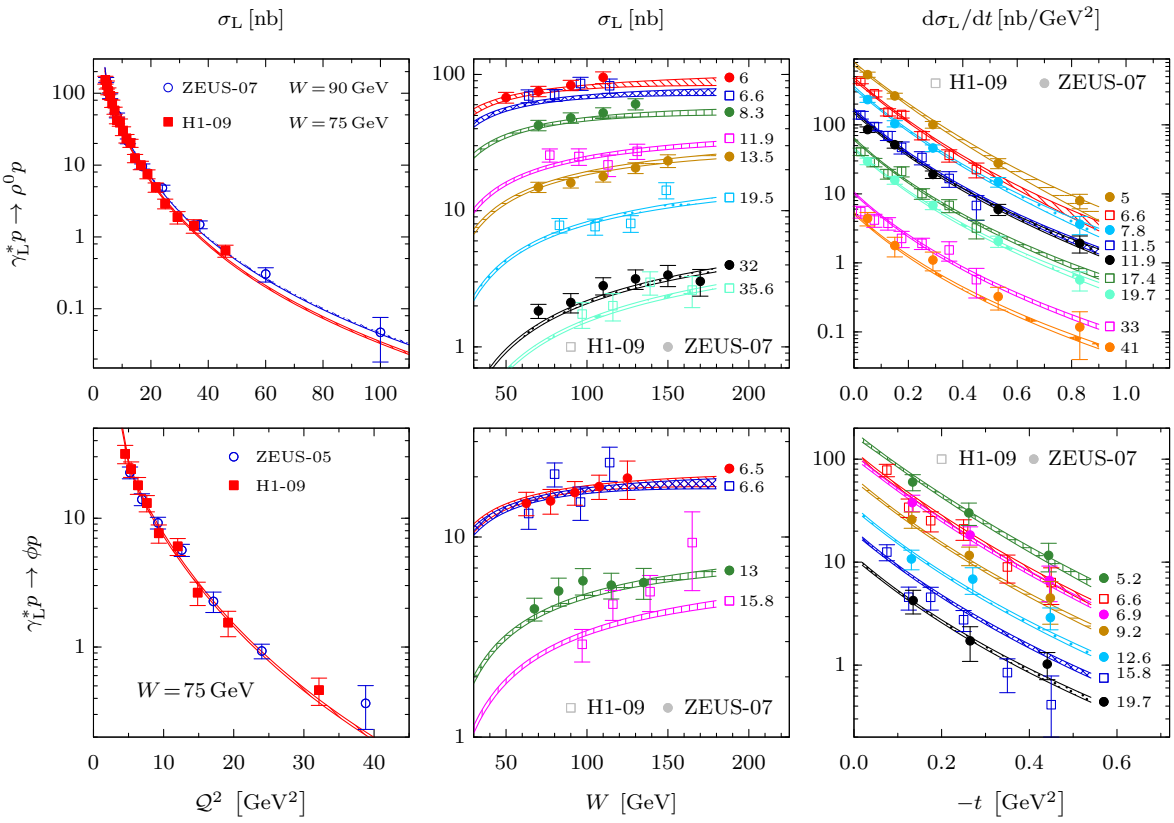

Figure 7.24.: The estimate for the model F-nnl-Dt at NLO of perturbation theory for the $\mathcal{Q}^2$, W^2 and t dependence of the total and differential longitudinal DVMP cross sections, respectively. The small numbers behind the estimates in the W and t dependence correspond to the respective value of $\mathcal{Q}^2$.

estimates from DIS and DVCS [KM10]. N_1^{G} is smaller than N_1^{sea}. For the nnl-PW normalization N_2^a, they are much narrower than N_1^a and both are positive. We again stress here, that the fact that the normalization of the nnl-PWs is close to zero does not mean that they are unimportant. We only have a effective parametrization, thus reducing the number of PWs in an existing estimation does not simply reduce the accuracy. Quite the contrary, these parameters have a significant influence.

The Regge intercepts α are hard and we are in full agreement with the DIS data. The intercept for the nl-PW is smaller than the l-PW one, for both gluons and sea quarks. The nnl-PW parameter agrees with the l-PW one with a small discrepancy for the gluon GPD. For all cases, the pdfs dominate their respective prior distribution. In comparison to our DIS and DVCS analysis, the gluonic parameter is significantly larger as an effect of the different parametrization of the higher PWs.

We realized in the DIS and DVCS analysis before, that the data contains only little information about the Regge slopes α', cf. Fig. 7.11. Incorporating data on DVMP, we are now able to constrain such parameters. The sea quark parameter is less constrained than the gluonic

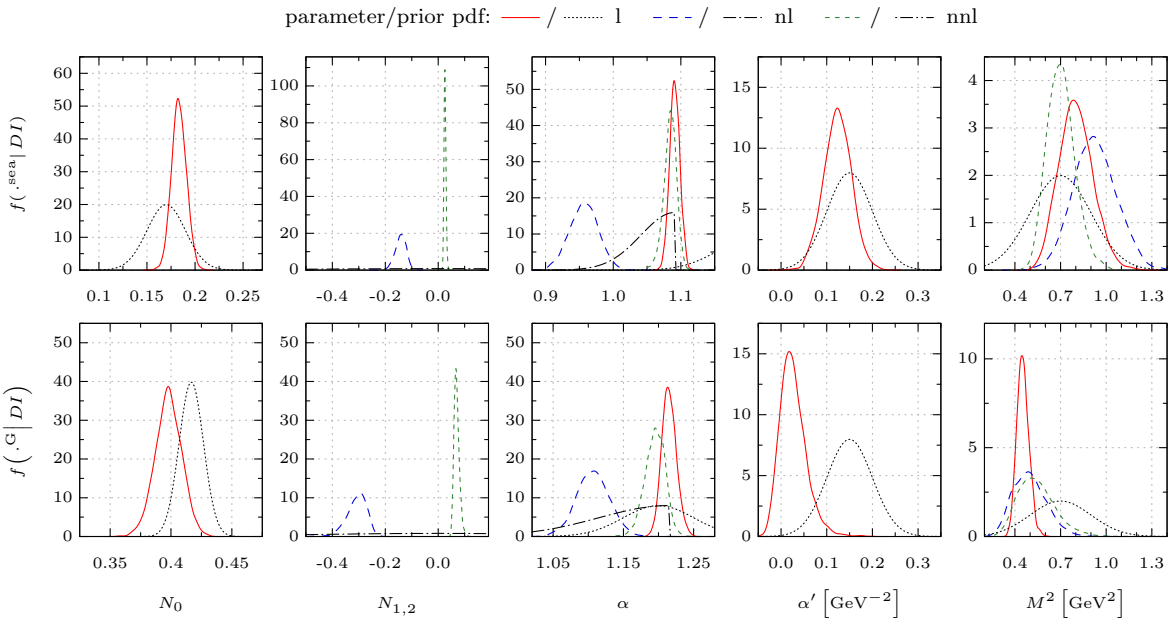

Figure 7.25.: Estimated parameters for the model F-nnl-Dt from a global data analysis at NLO accuracy of perturbation theory. The line style for prior distributions is black. The PWs are l: red solid, black dotted nl: blue dashed, black dash dotted nnl: green loosely dashed, black dash dot doted.

one, which is close to $0\,\mathrm{GeV}^{-2}$.
The cut-off mass parameters M^2 are almost equal for all PWs. In case of the sea quark GPD they are compatible with the prior distribution (6.41) peaking at $0.7\,\mathrm{GeV}^2$. In case of the gluon GPD, the value is much smaller than the prior, but again, all PWs are compatible with one another, whereas the higher PWs are less constrained. As a consequence, we realize, that the data does not support different cut-off mass parameters for the higher partial waves. A model with only two parameters would lead to an equal description of the data without the unnecessary complication.
Figure 7.26 shows the pdfs for the normalization parameters ν. The normalization of the DVMP-ρ^0 and DVMP-ϕ data from the ZEUS experiment is slightly higher than for the H1 measurements. This difference is not biased by our assumptions, whereas the low mean value of the DVMP-ϕ normalization could be compensated by the shape of the DAs for ρ^0 and ϕ mesons and/or a different sea quark flavor decomposition. We also note, that the normalization of the DIS data is here very close to one, in contrast to the analysis of solely DIS and DVCS data in Sec. 7.5.
In the discussion of the parameter pdfs, we directly saw the improvement of the knowledge in comparison to a pure DIS and DVCS analysis. In addition, we realized, that the cut-off parameters M^2 can be the same for all PWs. For the Regge intercepts, the one for the nl-PW is essential, whereas the nnl-PW parameters are basically equal to the prior distribution.

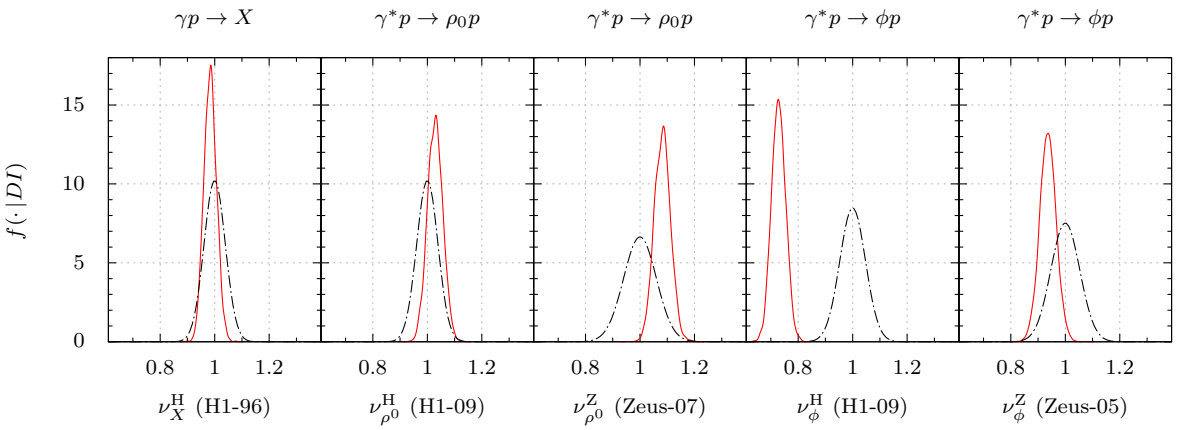

Figure 7.26.: Estimate F-nnl-Dt-C-NLO for the normalization parameters of the experimental data sets (solid red) together with the experimental pdfs (dash-dotted black).

7.6.4. Generalized parton distributions

We first compare the estimate for the sea quark and gluon PDFs of the estimate F-nnl-Dt-C-NLO to the estimate R-nl-T-B-NLO at NLO of perturbation theory. The resulting PDFs of the first estimate are displayed in figure 7.27. We are in particular interested in the com-

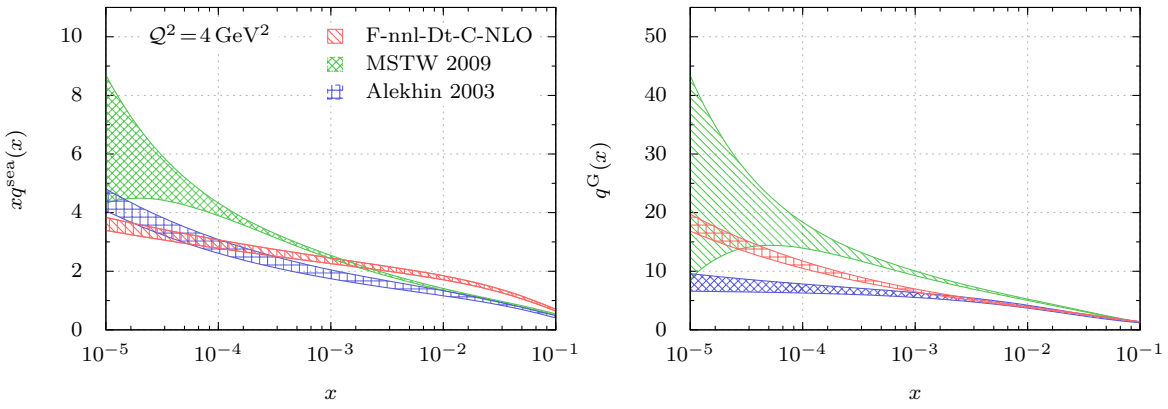

Figure 7.27.: Estimate F-nnl-Dt-C-NLO for the sea quark and Gluon PDFs at the input scale $\mathcal{Q}^2 = 4\,\mathrm{GeV}^2$ together with the estimates of Alekhin 2003 [Ale03] and MSTW 2009 [MSTW09]. The error bands of our estimate are given by the mean value and the square root of the variance.

parison of the estimated PDFs from the three different data sets A, B and C. In this way, we are able to judge, how much information is used to constrain the parameters appearing in a pure DIS analysis and weather the estimate is improved by DVMP and DVCS data. For this purpose, we compare sea quark and gluon PDFs from the estimates R-l-A-NLO, R-nl-Et-B-NLO and F-nnl-Dt-C-NLO at the kinematical point $\mathcal{Q}^2 = \mathcal{Q}_0^2$ and $x = 10^{-3}$, as depicted in figure 7.28. For the sea quark PDF, all three estimates are consistent. Moreover,

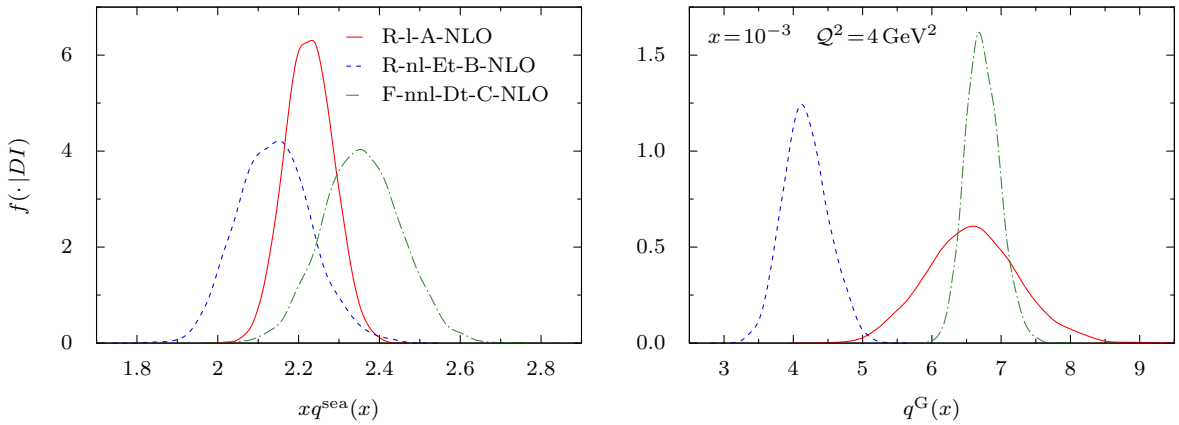

Figure 7.28.: Probability distribution functions for the sea quark and gluon PDF for $x=10^{-3}$ and $\mathcal{Q}^2=4\,\mathrm{GeV}^2$ from the estimates R-l-A-NLO, R-nl-Et-B-NLO and F-nnl-Dt-C-NLO.

the estimate F-nnl-Dt-C-NLO is in fact less precise than the pure DIS estimate R-l-A-NLO. The pdf for the gluon PDF from the estimate R-l-A-NLO is very broad. This uncertainty decreases by incorporating data on DVCS or both DVCS and DVMP. The broader pdf of F-nnl-Dt-C-NLO for the sea quark PDF could be caused by a more precise estimate of the gluon PDF. However, it is not possible to track the information flow from the data to the single parameters or PDFs.
The GPD is now very different from the estimate in Sec. 7.5.4. We first notice the steep fall off of the sea quark GPD on the cross-over line which is close to zero for large values of x. Note, the small values actually lie outside of the range of the available data and with the given uncertainty, non zero values are also possible. Moreover, the steepness is decreased in comparison to the estimate of [LMS13], due to the wider priors in this thesis. In the gluon case, the GPD on the cross-over line is approximately of the same size as the corresponding PDF. Furthermore, the t-dependence shows the typical behavior.

7.6.5. Skewness ratio

The estimate F-nnl-Dt-C-NLO for the $\mathcal{Q}^2$-dependence of the skewness ratio (7.36) is displayed in figure 7.30. At the input scale $\mathcal{Q}_0$ and for $x=10^{-3}$ we obtain the following numerical values:

$$\begin{aligned} r^{\mathrm{sea}}\left(x=10^{-3},\,\mathcal{Q}^2=4\,\mathrm{GeV}^2\right) &= 1.717\pm 0.082\,, \\ r^{\mathrm{G}}\left(x=10^{-3},\,\mathcal{Q}^2=4\,\mathrm{GeV}^2\right) &= 0.856\pm 0.033\,. \end{aligned} \tag{7.47}$$

This is consistent with the findings in [KM10], namely $r^{\mathrm{sea}}\approx 1.6$ and $r^{\mathrm{G}}\approx 1$ relying on fixed parameters for the gluon GPD. In the DVCS estimate in Sec. 7.5.5 the skewness ratio was slightly higher as a consequence of the unconstrained parameters. Moreover, the narrow priors in [LMS13] lead to the same skewness ratio, but decreased uncertainty.

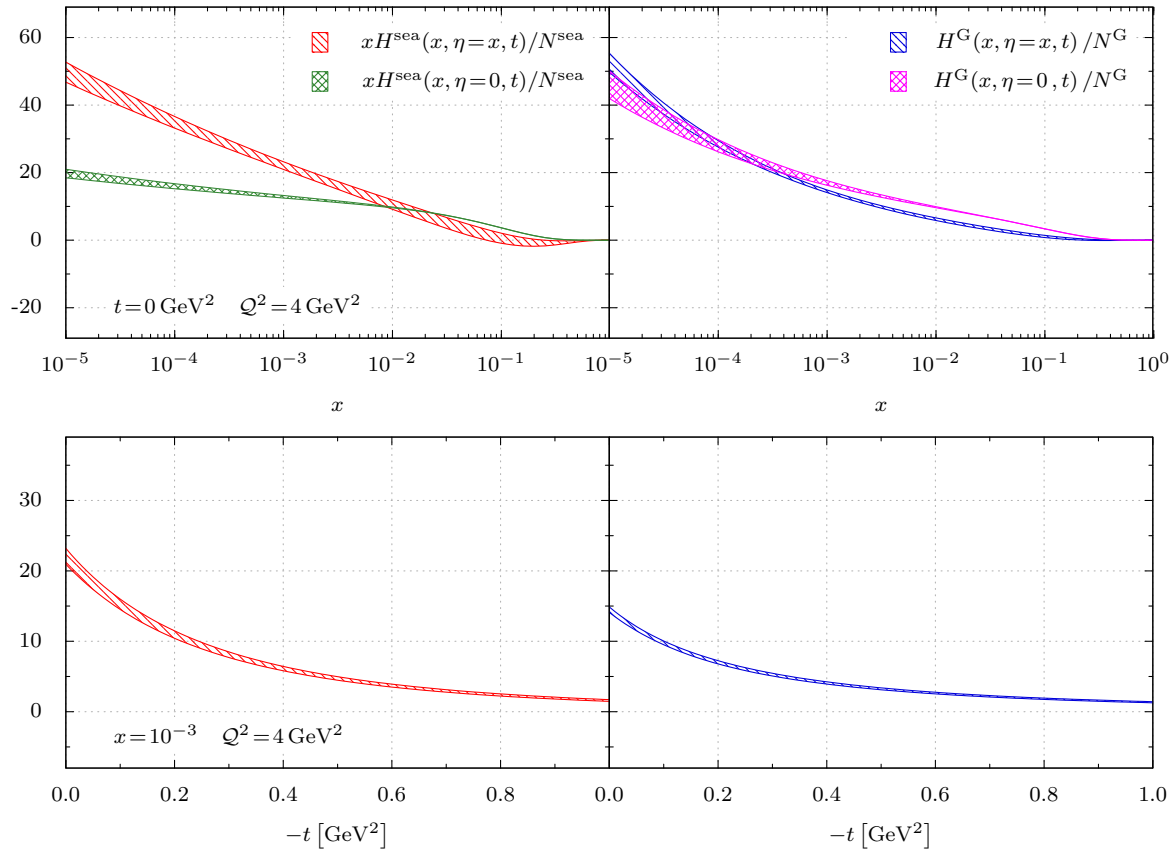

Figure 7.29.: Estimate F-nnl-Dt-C-LO for the dependence on the momentum fraction x and the transverse momentum t of the GPD on the cross-over line divided by the momentum fraction average and the corresponding PDF.

7.6.6. Transverse distribution of partons

The transverse width of partons is given in (7.45). As in the previous analysis of DIS and DVCS, we investigate its $\mathcal{Q}^2$- and x-dependence. The results are shown in Fig. 7.31. In comparison to the estimate R-nl-Et-B-NLO, the transverse width of the gluon GPD is slightly higher than the one of the sea quark GPD. Again, the values are stable with $\mathcal{Q}^2$ and x. We now compare the values at the fixed point $\mathcal{Q}^2 = 4\,{\rm GeV}^2$ and $x = 10^{-3}$. The numerical values are shown in Tab. 7.11, which are slightly lower than the values from the estimate R-nl-Dt-B-NLO.

estimate	$\mathcal{Q}^2$ [GeV^2]	$\sqrt{\langle b^2\rangle_{\rm sea}}$ [fm]	$\sqrt{\langle b^2\rangle_{\rm G}}$ [fm]
F-nnl-Dt-C-NLO	4	0.708 ± 0.041	0.822 ± 0.026
	10	0.735 ± 0.026	0.804 ± 0.019

Table 7.11.: Transverse width at the input scale $\mathcal{Q}_0^2 = 4\,{\rm GeV}^2$ and $x = 10^{-3}$.

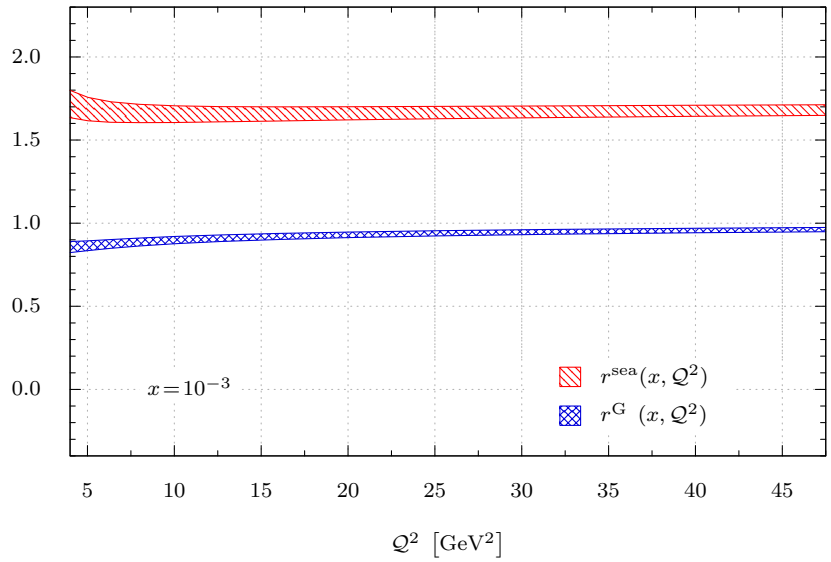

Figure 7.30.: Estimate F-nnl-Dt-C-NLO for $\mathcal{Q}^2$-dependence of the skewness ratio at $x = 10^{-3}$.

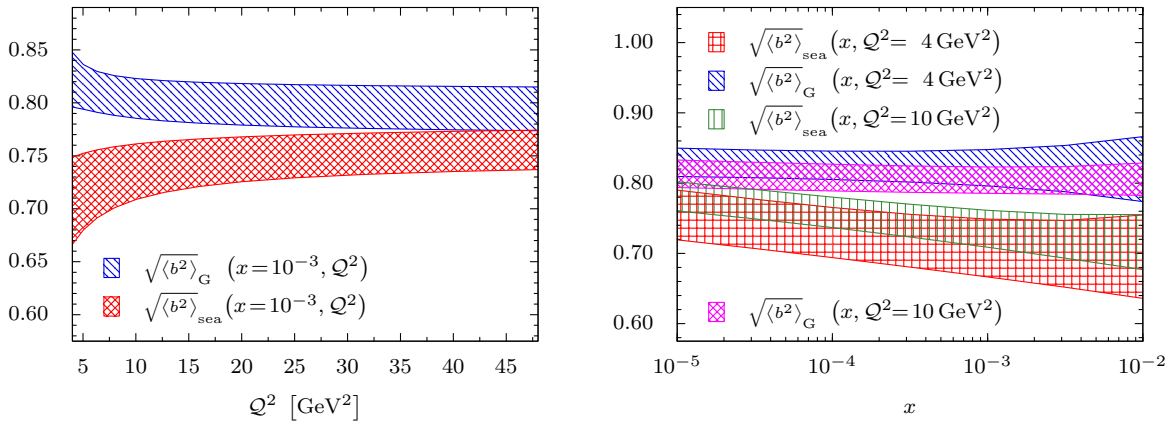

Figure 7.31.: Transverse width $\sqrt{\langle \vec{b}^2 \rangle}$ of sea quark and gluon GPDs at LO and NLO of perturbation theory.

At the input scale, the transverse width of sea quarks is smaller than the one of gluons in contrast to the estimate R-nl-Et-B-NLO. Additionally, we see the characteristic x-dependence as in the previous estimate for DIS and DVCS data, whereas the transverse width for gluons does not decrease with increasing momentum fraction x. In contrast to the estimate R-nl-Et-B-NLO, the transverse width is slightly larger and we see a clear separation, which is also visible at higher scales.
Comparing the transverse width at the input scale $\mathcal{Q}_0^2$ and at the scale $\mathcal{Q}^2 = 10\,\text{GeV}$, we realize, that they are equal in the sea quark and gluon case. However, in contrast to the estimate R-nl-Et-B-NLO, the transverse width of sea quarks is now smaller than the one of gluons.

As before, we also present the transverse profile function (7.46) in figure 7.32. The fall off

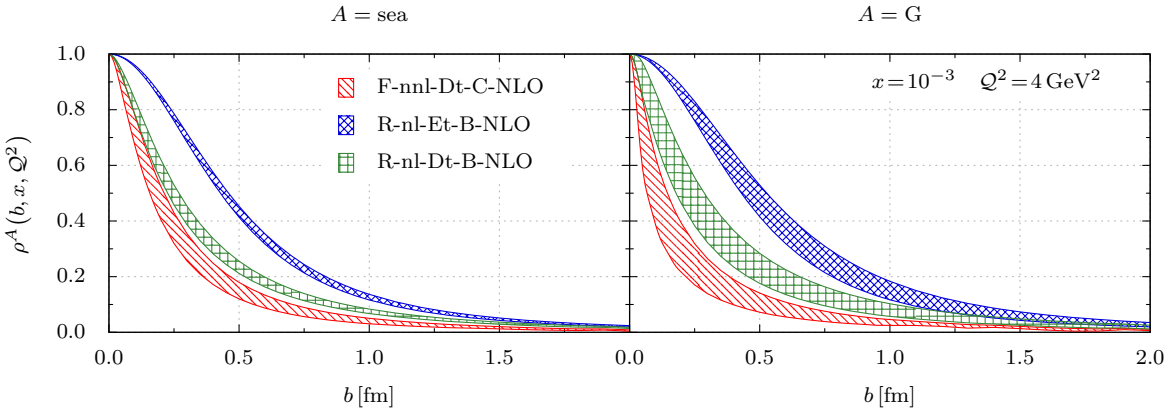

Figure 7.32.: The normalized profile function of the estimates R-nl-Dt-B-NLO, R-nl-Et-B-NLO and F-nnl-Dt-C-NLO at the kinematical point $x = 10^{-3}$ and $\mathcal{Q}^2 = 4\,\mathrm{GeV}^2$.

of the transverse profile function from the estimate F-nnl-Dt-C-NLO is slightly larger than the one of the DIS and DVCS estimate R-nl-Dt-B-NLO. Moreover, the uncertainty of the estimate F-nnl-Dt-C-NLO is increased in contrast to the other estimates.

7.6.7. Prediction for DVMP of ω mesons

As previously mentioned in the introduction of the available experimental data in Sec. 7.1, we only have four data points of the total DVMP-ω cross section above the input scale $\mathcal{Q}_0$. In principle, it is possible to utilize this data and the estimate F-nnl-Dt-C-NLO for the longitudinal cross section of DVMP-ω to estimate the corresponding R-ratio (7.4). However, such a analysis shows, that the four available points are not sufficient to estimate the parameters of the R-ratio. Therefore, at this point, we give the estimate of the longitudinal cross section in figure 7.33. The estimate has the same qualitative properties as the estimates for DVMP-ρ^0 and DVMP-ϕ. Note, a future comparison of the given estimate with a measurement requires the analysis of the R-ratio as well as the normalization of the data.

7.6.8. Cross section ratios

The experimental collaborations also publish the ratio of the total cross sections of different mesons. From quark charge counting the ratios are $\rho^0 : \omega : \phi = 9 : 1 : 2$.
Let us first give the estimate of the $\phi : \rho^0$ ratio. Note, the published ratios of the H1 and ZEUS collaboration include the normalization uncertainty. As we realized in Sec. 7.6.3, their actual numerical values are quite different from one, cf. Fig. 7.26. Consequently, we correct the measured ratios by the estimated normalization.
We denote the originally measured cross section ratio $\phi : \rho^0$ by R, where the corresponding pdf

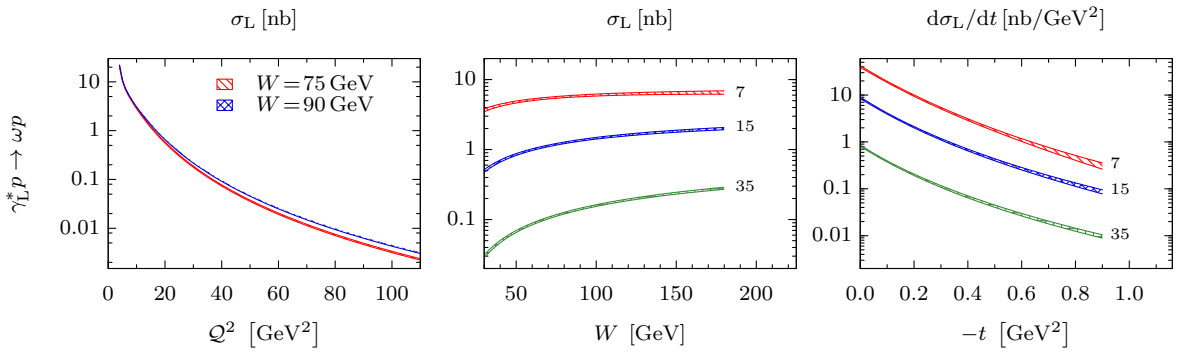

Figure 7.33.: Prediction for the longitudinal DVMP-ω cross section from the estimate F-nnl-Dt-C-NLO. The small numbers behind the estimates in the W and t dependence correspond to the respective value of $\mathcal{Q}^2$.

$f(R|D'I)$ is evaluated from the data D' (H1-99, H1-09). Hence, the probability distribution function of the corrected ratio R_ν reads

$$f\big(R_\nu\big|D'\,D\,I\big) = \int \mathrm{d}R\;\mathrm{d}\nu_{\rho^0}\;\mathrm{d}\nu_\phi\;\frac{\nu_{\rho^0}}{\nu_\phi}\;R\;f\big(\nu_{\rho^0}\big|DI\big)\;\;f(\nu_\phi|DI)\,f\big(R\big|D'I\big)\;, \tag{7.48}$$

where D denotes the data set C for the estimate F-nnl-Dt-C-NLO. It is crucial, that the model itself is multiplied with the normalization uncertainty as explained in Sec. 5.7.2, Eq. 5.196. Since the normalization is shifted to the data, we apply the fraction of the normalization parameters as in the previous equation.
Correcting the originally published value of 0.182 ± 0.082 in [B$^+$00] at the kinematical point $Q^2 = 7\,\mathrm{GeV}^2$ and $W = 70\,\mathrm{GeV}$ for the normalization uncertainty leads to

$$\frac{\sigma^{\gamma^* p\to\phi p}}{\sigma^{\gamma^* p\to\rho^0 p}} = 0.211 \pm 0.095\,. \tag{7.49}$$

Our estimate from F-nnl-Dt-C-NLO at the same kinematical points reads

$$\frac{\sigma^{\gamma^* p\to\phi p'}}{\sigma^{\gamma^* p\to\rho^0 p'}} = 0.248 \pm 0.010\,, \tag{7.50}$$

which roughly agrees with the values of the ZEUS collaboration within the uncertainties and is close to the result $2:9$ from quark charge counting. Furthermore, the H1 collaboration also measured the $\mathcal{Q}^2$ dependence as depicted in figure 7.34. Including the correction for the normalization uncertainty, we exactly reproduce the measured constant $\mathcal{Q}^2$-behavior.
All possible estimates for DVMP-ω is plagued by the missing R-ratio. Therefore, we present only the ratios of the longitudinal cross section. At the kinematical point of [B$^+$00] our numerical values are

$$\frac{\sigma^{\gamma_L^* p\to\omega p}}{\sigma^{\gamma_L^* p\to\rho^0 p}} = 0.097 \pm 0.004\,, \qquad \frac{\sigma^{\gamma_L^* p\to\omega p}}{\sigma^{\gamma_L^* p\to\phi p}} = 0.390 \pm 0.016\,, \tag{7.51}$$

which are fairly close to the values from quark charge counting.

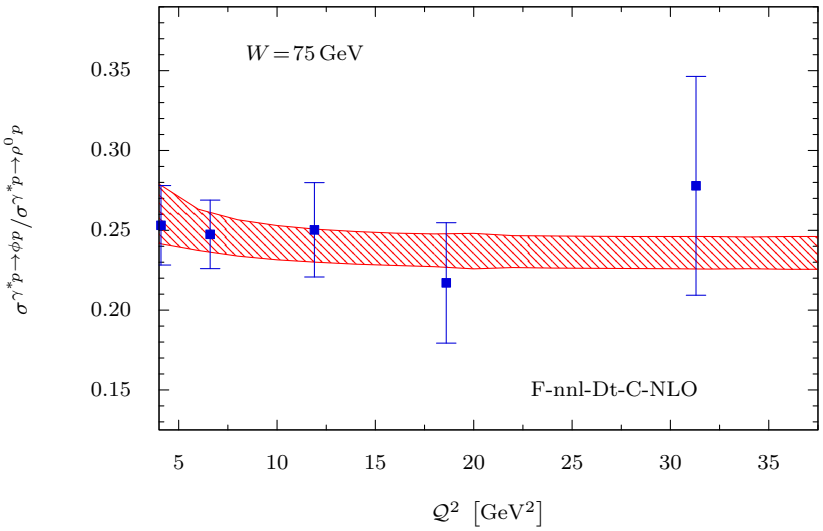

Figure 7.34.: $\mathcal{Q}^2$-dependence of the cross section ratio ϕ:ρ^0 together with the measurement of [A$^+$10b], which was corrected for the normalization uncertainties.

8

Summary and outlook

In thus thesis, we gave an extensive review of the phenomenology of GPD analysis utilizing the perturbative framework. Starting from basic principles, we derived the differential cross sections of deeply virtual Compton scattering and deeply virtual meson production in the twist-2 approximation involving GPDs as non-perturbative objects. Since GPDs are equal to PDFs in the forward limit, we also derived the structure functions F_1 and F_2. In these processes, we have identified the structure functions, Compton form factors and transition form factors as the basic impartible objects and all observables are presented in terms of these objects. We also presented the evolution of DAs, PDFs and GPDs up to NLO in our conventions. To show the separation of the non-perturbative objects and the hard scattering amplitude, we derived the differential cross section at LO. A special focus lied on the hard scattering amplitudes of DVMP at NLO perturbation theory. We completely organized the formulae and identified the most singular terms allowing an easy implementation of radiative corrections.
The framework for the global analysis of GPDs relies on the uses of conformal symmetry. We gave a short introduction to this topic. This lead to the Mellin-Barnes representation of the basic non-perturbative objects involving the conformal moments of the GPD. For this purpose, the conformal moments of the hard scattering amplitudes and their analytic continuation are essential. As this is already solved in case of DIS and DVCS, up to the work in [MLPKS14] the solution for DVMP remained an open question. We derived the imaginary parts of the NLO hard scattering amplitudes of DVMP and analytic expressions for the conformal moments in terms of rational functions and harmonic sums. The method also allows a numerical evaluation of the conformal moments ensuring the analytic properties as well. The expressions are completely general such that different models for the DA can be implemented easily. As the main result, we extended the framework of [KMPK08] to DVMP opening the door for a global GPD analysis.
Such estimates for GPDs and PDFs in general based on orthodox statistics. We showed that its methods are not justified for the given interference problem and we present a extensive introduction to probability theory as extended logic. In the course, we covered all topics relevant for a GPD analysis. All methods were derived from the product and sum rule to ensure the conceptual understanding. In the corresponding appendix, we derived several methods of orthodox statistics resulting in a detailed list of assumptions, that go into their derivations. This gives the reader a clear picture of the statistical methods utilized in high energy physics. The chapter was accompanied by several introductory examples. Among

them is the analysis of the data on the Higgs particle performed at the large hadron collider, presenting a clear picture of the utilized statistical methods.
With PTEL at hand, we repeated the DIS and DVCS analysis of [KMPK08, KM10] showing the advantage of PTEL and gaining new insights in the parameter estimation. This was possible due to the utilization of prior information, which allows to deduce the amount of information for a parameter delivered by the data. Employing asymptotic DAs we were able to extend the previous analysis to include data on DVMP-ρ^0 and DVMP-ϕ at NLO of perturbation theory as well. Therefore, we succeeded in a global GPD estimate, claimed more or less impossible a few years ago.
An open question remains the LO analysis. This requires the analysis of the correlations of the GPD and DA. For light vector meson DAs we have only SVZ sum rule [BB96, BBKT98] results and and AdS/QCD model predictions [BdT04] available. Furthermore, as we neglected the contribution of the GPD E its incorporation would be an interesting venture. For such a task, PTEL will prove very useful, since it allows to judge whether it is possible to constrain the GPD E. Moreover, the analysis could be extended beyond the small-x_{B} region including valence quark GPDs as well.

A

Perturbative QCD

A.1. Propagators

The massless quark propagator in momentum space is given by

$$\overbrace{\psi^a_\alpha(x)\bar{\psi}^b_\beta}(y) = \delta^{ab}\int \frac{\mathrm{d}^4k}{(2\pi)^4}\, e^{-ik(x-y)}\frac{i\not{k}_{\alpha\beta}}{k^2+i\epsilon}. \tag{A.1}$$

In coordinate space it is given by

$$\overbrace{\psi^a_\alpha(x)\bar{\psi}^b_\beta}(y) = \frac{\delta^{ab}\,\Gamma\left(\frac{d}{2}\right)}{2\pi^{\frac{d}{2}}}\frac{i(\not{x}-\not{y})_{\alpha\beta}}{\left[-(x-y)^2+i\epsilon\right]^{\frac{d}{2}}}, \tag{A.2}$$

where d ($d=4$) is the dimension. The gluon propagator reads in momentum space

$$\overbrace{A^A_\mu(x)A^B_\nu}(y) = \delta^{AB}\int \frac{d^dk}{(2\pi)^d}\left(\frac{-ig_{\mu\nu}}{k^2+i\epsilon}\right)e^{-ik(x-y)}, \tag{A.3}$$

and in coordinate space

$$\overbrace{A^A_\mu(x)A^B_\nu}(y) = \frac{-g_{\mu\nu}\delta^{AB}}{4\pi^{\frac{d}{2}}}\frac{\Gamma\left(\frac{d}{2}-1\right)}{\left[-(x-y)^2+i\epsilon\right]^{\frac{d}{2}-1}}. \tag{A.4}$$

The photon propagator is given by

$$\overbrace{A_\mu(x)A_\nu}(y) = \int \frac{d^dk}{(2\pi)^d}\left(\frac{-ig_{\mu\nu}}{k^2+i\epsilon}\right)e^{-ik(x-y)}. \tag{A.5}$$

B

Processes

B.1. Three-body phase space

In this section, we derive the three-body Lorentz invariant phase space, that is needed for the kinematic of DVCS (Sec. 3.2.2) and DVMP (Sec. 3.3.2). The general form of the LIPS for the Compton amplitude reads

$$\mathrm{d}\Pi_3 = (2\pi)^4 \delta^{(4)}\left(k_1+P_1-k_2-q_2-P_2\right) \frac{\mathrm{d}^3 k_2}{2(2\pi)^3\omega_2} \frac{\mathrm{d}^3 q_2}{2(2\pi)^3\nu_2} \frac{\mathrm{d}^3 P_2}{2(2\pi)^3 E_2}\,, \tag{B.1}$$

with the nomenclature of the particle momenta is introduced in Sec. 3.2.1. As we recall from Eq. 3.84, the components of the particle momenta in the laboratory frame are

$$\begin{aligned} P_1^\mu &= (M, \vec{0})\,, & P_2^\mu &= (E_2, \vec{P}_2)\,, \\ k_1^\mu &= (\omega_1, \vec{k}_1)\,, & k_2^\mu &= (\omega_2, \vec{k}_2)\,, \\ q_1^\mu &= (\nu_1, 0, 0, -q_1^z)\,, & q_2^\mu &= (\nu_2, \vec{q}_2)\,. \end{aligned}$$

As already argued in Sec. 3.2.2, there are four independent variables in the process. We chose the energy and the scattering angle of the outgoing electron and the energy and azimuthal angle of the recoiling nucleon (3.100)

$$\omega_2,\ \theta \text{ and } E_2,\ \phi_N\,. \tag{B.2}$$

For an illustration of the relevant angles and momenta, see figure 3.7 in the laboratory frame. The goal is to express the momenta in the LIPS above by these four variables. The integration with respect to the photon momentum q_2 yields

$$\int \frac{\mathrm{d}^3 q_2}{2\nu_2} \delta^{(4)}\left(k_1+P_1-k_2-q_2-P_2\right) = \delta\left[(k_1+P_1-k_2-P_2)^2-m^2\right]\,, \tag{B.3}$$

where m is the meson mass, which is neglected in our case. To obtain the equation above, we used

$$\int \frac{\mathrm{d}^3 k}{2k_0} = \int \mathrm{d}^4 k\, \delta_+(k^2-m^2), \qquad \delta_+(k^2-m^2) = \delta(k^2-m^2)\Theta(k_0)\,. \tag{B.4}$$

Thus, the LIPS becomes

$$\mathrm{d}\Pi_3 = \frac{1}{(2\pi)^5}\delta\left[(k_1+P_1-k_2-P_2)^2\right]\frac{\mathrm{d}^3k_2}{2\omega_2}\frac{\mathrm{d}^3P_2}{2E_2}\,. \tag{B.5}$$

Expressing the two remaining differentials in terms of its components, we get

$$\begin{aligned}\mathrm{d}^3k_2 &= |\vec{k}_2|^2\mathrm{d}|\vec{k}_2|\mathrm{d}(\cos\theta)\mathrm{d}\phi_2 = 2\pi\,\omega_2^2\mathrm{d}\omega_2\mathrm{d}(\cos\theta)\,,\\ \mathrm{d}^3P_2 &= |\vec{P}_2|^2\mathrm{d}|\vec{P}_2|\mathrm{d}(\cos\theta_\mathrm{N})\mathrm{d}\phi = |\vec{P}_2|E_2\mathrm{d}E_2\mathrm{d}(\cos\theta_\mathrm{N})\mathrm{d}\phi_\mathrm{N}\,,\end{aligned} \tag{B.6}$$

where we integrated out the azimuthal angle of the electron ϕ_2. The polar angle of the recoiling nucleon is denoted by θ_N. The next step is the integration with respect to θ_N utilizing the δ-function. Its argument reads

$$(k_1+P_1-k_2-P_2)^2 = s+M^2-2\left[(\nu_1+M)E_2+|\vec{q}_1||\vec{P}_2|\cos\vartheta_\mathrm{N}\right]\,, \tag{B.7}$$

where s is the invariant mass of the embedded virtual photon-nucleon system. Note, in our choice of coordinates, the virtual photon moves in the negative z direction. Hence, the relation to the polar angle of the scattered nucleon is $\vartheta_\mathrm{N} = \pi - \theta_\mathrm{N}$. With the help of the identities

$$\delta(\alpha x) = \frac{1}{|\alpha|}\,\delta(x)\,, \qquad \delta\left[g(x)\right] = \sum_i \frac{1}{|g'(x_i)|}\,\delta(x-x_i)\,, \tag{B.8}$$

of the δ-function, resulting in a factor of $2|\vec{q}_1||\vec{P}_2|$ in the nominator, we obtain the following phase space

$$\mathrm{d}\Pi_3 = \frac{1}{8(2\pi)^4}\frac{\omega_2}{|\vec{q}_1|}\cdot\mathrm{d}\omega_2\;\mathrm{d}(\cos\theta)\cdot\mathrm{d}E_2\;\mathrm{d}\phi_\mathrm{N}\,. \tag{B.9}$$

The absolute values of the particle three-momenta are given by

$$|\vec{P}_2| = \sqrt{E_2^2-M^2}\,, \qquad |\vec{q}_1| = \frac{\mathcal{Q}^2}{\epsilon}\sqrt{1+\epsilon^2} \quad \text{with } \epsilon = \frac{2x_\mathrm{B}M}{\mathcal{Q}}\,. \tag{B.10}$$

To derive the last equation, we used

$$x_\mathrm{B} = \frac{\mathcal{Q}^2}{2P_1.q_1} = \frac{\mathcal{Q}^2}{2\nu_1 M} \quad \text{and} \quad |\vec{q}_1| = q_1^z = \sqrt{\nu_1^2-q_1^2}\,. \tag{B.11}$$

The last step is to express the phase space in terms of the variables $x_\mathrm{B}, y, \Delta^2$ and ϕ_N. In terms of the present variables, they read:

$$\begin{aligned}x_\mathrm{B} &= \frac{2\omega_1\omega_2(1-\cos\theta_2)}{2M(\omega_1-\omega)}\,,\\ y &= \frac{P_1,q_1}{P_1.k_1} = \frac{\omega_1-\omega_2}{\omega_1}\,,\\ \Delta^2 &= (P_2-P_1)^2 = 2M^2-2ME_2\,.\end{aligned} \tag{B.12}$$

Employing the two Jacobians

$$\left|\frac{\partial(x_{\mathrm{B}},y)}{\partial(\omega_2,\cos\theta)}\right| = -\frac{\omega_2}{yM\omega_1}\,, \qquad \left|\frac{\mathrm{d}\Delta^2}{\mathrm{d}E_2}\right| = -\frac{1}{2M}\,, \tag{B.13}$$

the phase space reads

$$\mathrm{d}\Pi_3 = \frac{1}{8(2\pi)^4}\frac{\omega_2 2Mx_{\mathrm{B}}}{\mathcal{Q}^2\sqrt{1+\epsilon^2}}\cdot\frac{yM\omega_1}{\omega_2}\cdot\frac{1}{2M}\cdot\mathrm{d}x_{\mathrm{B}}\mathrm{d}y\mathrm{d}\Delta^2\mathrm{d}\phi_{\mathrm{N}} = \frac{1}{16(2\pi)^4}\frac{\mathrm{d}x_{\mathrm{B}}\mathrm{d}y\mathrm{d}\Delta^2\mathrm{d}\phi_{\mathrm{N}}}{\sqrt{1+\epsilon^2}}\,. \tag{B.14}$$

At this point, we give further relations between momentum components and the experimental quantities. The polar angle of the nucleon is given by

$$\cos\vartheta_{\mathrm{N}} = -\cos\theta_{\mathrm{N}} = \frac{\left(\mathcal{Q}^2-t\right)\epsilon^2 - 2x_{\mathrm{B}}t}{4Mx_{\mathrm{B}}|\vec{P}_2|\sqrt{1+\epsilon^2}}\,. \tag{B.15}$$

Neglecting the electron masses, from the conditions $k_2^2 = 0$[1] and $k_1^2 = 0$ we derive the polar angles of the incoming and outgoing electrons

$$\cos\theta_1 = -\frac{1+\frac{y\epsilon^2}{2}}{\sqrt{1+\epsilon^2}}\,, \qquad \cos\theta_2 = \frac{1-\frac{y\epsilon^2}{2\bar{y}}}{\sqrt{1+\epsilon^2}}\,, \tag{B.16}$$

respectively.

B.2. Symmetric variables

In this section, we give the variables for the description of the Compton amplitude as introduced in section 3.2.1 for the analysis of DVCS and DVMP. We use the three symmetric Lorentz scalars

$$q^2 = -Q^2\,, \qquad \xi = \frac{Q^2}{P.q}\,, \qquad \eta = -\frac{\Delta.q}{P.q}\,, \tag{B.17}$$

in (3.72). Experimentally, it is convenient to use the variables (3.74)

$$\mathcal{Q}^2 = -q_1^2\,, \qquad q_2^2\,, \qquad x_{\mathrm{B}} = \frac{\mathcal{Q}^2}{2P_1.q_1}\,. \tag{B.18}$$

For the analysis of DVMP, we neglect the meson mass $q_2^2 = 0$, thus the variables are equal to DVCS. In addition we restrict our considerations to cases, where the target and recoiled nucleon have equal masses. This manifests in $P.\Delta = 0$. For academic reasons, we waive these assumptions and derive the conversions for the general case.
To obtain the theoretical variables in terms of the experimental ones, we need the Lorentz scalars $P.q$, Q^2 and $\Delta.q$. The first one is using the explicit form in (3.70, 3.71)

$$2P.q = \frac{2-x_{\mathrm{B}}}{x_{\mathrm{B}}}\mathcal{Q}^2 - q_2^2 + \Delta^2 - \Delta.P\,. \tag{B.19}$$

[1] $k_2^2 = 0 = (k_1 - k_2 - k_1)^2 = \ldots$

The second and third Lorentz scalars are

$$Q^2 = \frac{1}{2}\left(\mathcal{Q}^2 - q_2^2 + \frac{\Delta^2}{2}\right) \quad \text{and} \quad \Delta.q = -\frac{1}{2}\left(\mathcal{Q}^2 + q_2^2\right), \tag{B.20}$$

respectively. From the combination of the last three equations, we obtain the theoretical variables in terms of the experimental ones, namely

$$Q^2 = \frac{1}{2}\left(\mathcal{Q}^2 - q_2^2 + \frac{\Delta^2}{2}\right), \quad \eta = \frac{\mathcal{Q}^2 + q_2^2}{\frac{2-x_\mathrm{B}}{x_\mathrm{B}}\mathcal{Q}^2 - q_2^2 + \Delta^2 - \Delta.P}, \quad \xi = \frac{\mathcal{Q}^2 - q_2^2 + \frac{\Delta^2}{2}}{\frac{2-x_\mathrm{B}}{x_\mathrm{B}}\mathcal{Q}^2 - q_2^2 + \Delta^2 - \Delta.P}. \tag{B.21}$$

For the inverse transformation, we first derive the ratio of the two scaling variables

$$\frac{\eta}{\xi} = \frac{\mathcal{Q}^2 + q_2^2}{\mathcal{Q}^2 - q_2^2 + \frac{\Delta^2}{2}}. \tag{B.22}$$

In addition, we have

$$\left(1 + \frac{\eta}{\xi}\right) Q^2 = \mathcal{Q}^2 + \frac{\Delta^2}{4}, \qquad \left(1 - \frac{\eta}{\xi}\right) Q^2 = -q_2^2 + \frac{\Delta^2}{4}. \tag{B.23}$$

Together with

$$2P_1.q_1 = \frac{1+\eta}{\xi} Q^2 - \frac{\Delta^2}{2} + \frac{\Delta.P}{2}, \tag{B.24}$$

the inverse transformations are

$$\mathcal{Q}^2 = \left(1+\frac{\eta}{\xi}\right) Q^2 - \frac{\Delta^2}{4}, \quad q_2^2 = -\left(1-\frac{\eta}{\xi}\right) Q^2 + \frac{\Delta^2}{4}, \quad x_\mathrm{B} = \frac{(\xi+\eta)\, Q^2 - \xi\Delta^2/4}{(1+\eta)\, Q^2 - \xi\Delta^2/2 + \xi\Delta.P/2}. \tag{B.25}$$

With the special cases $\Delta.P = P_2^2 - P_1^2 = 0$ and $q_2^2 = 0$ we receive the expressions for DVCS and DVMP as presented in section 3.2.1.

B.3. Light-cone coordinates

We start by defining two independent light-like vectors n and $\tilde{n}$, $n^2 = \tilde{n}^2 = 0$. For convenience, we further set $n.\tilde{n} = 1$. We decompose an arbitrary vector a^μ in terms of its light-like components as

$$a^\mu = a^+ \tilde{n}^\mu + a^- n^\mu + a_\perp^\mu, \qquad \text{with} \quad a^+ = a.n,\ a^- = a.\tilde{n}\,. \tag{B.26}$$

The decomposition above is denoted as Sudakov decomposition. The two components a^+ and a^- are called the plus and minus components. The scalar product of two four-vectors is

$$a.b = a_\mu b^\mu = a^+ b^- + a^- b^+ - a_\perp.b_\perp\,. \tag{B.27}$$

The metric in the transverse subspace is defined as

$$g^{\perp}_{\mu\nu} = g_{\mu\nu} - n_\mu \tilde{n}_\nu - \tilde{n}_\mu n_\nu \,. \tag{B.28}$$

The transverse projection of the totally antisymmetric tensor is

$$\epsilon^{\perp}_{\mu\nu} = \epsilon_{\mu\nu-+} \,. \tag{B.29}$$

In addition, the corresponding Sudakov decomposition is

$$\begin{aligned}\epsilon^{\mu\nu\alpha\beta} = &-(n^\mu\tilde{n}^\nu - \tilde{n}^\mu n^\nu)\,\epsilon_\perp^{\alpha\beta} + (n^\mu\tilde{n}^\alpha - \tilde{n}^\mu n^\alpha)\,\epsilon_\perp^{\nu\beta} - (n^\mu\tilde{n}^\beta - \tilde{n}^\mu n^\beta)\epsilon_\perp^{\nu\alpha} \\ &-(n^\nu\tilde{n}^\alpha - \tilde{n}^\nu n^\alpha)\,\epsilon_\perp^{\mu\beta} + (n^\nu\tilde{n}^\beta - \tilde{n}^\nu n^\beta)\epsilon_\perp^{\mu\alpha} - (n^\alpha\tilde{n}^\beta - \tilde{n}^\alpha n^\beta)\epsilon_\perp^{\mu\nu} \,.\end{aligned} \tag{B.30}$$

The two light-like vectors are invariant under boosts along the z-axes. Thus, we are able to rescale the two light-like vectors

$$\tilde{n}_\mu \to \rho\tilde{n}_\mu \,, \qquad n_\mu \to \rho^{-1} n_\mu \,, \tag{B.31}$$

whereas their scalar product remains invariant.

B.4. Frames

The light-like vectors (see Sec. B.3) are used to perform the twist decomposition of the operators and observables in chapter 3. For this purpose, we express the symmetric variables of the Compton amplitude (3.70) in terms of the two light-like vectors. Note that, due to the selected reference frame, the momenta P and q do not have transverse components. First, we will project the summed nucleon momentum P. In the process, we will provide all expressions including a plus component P^+, which we fix in the end by (B.31). For the symmetric nucleon momentum squared, the Sudakov decomposition (B.27) reads

$$P^2 = 2P^+P^- = 4M^2 - \Delta^2 \qquad \text{with} \quad M_1 = M_2 = M, \qquad P^\mu_\perp = 0 \,. \tag{B.32}$$

Thus, the minus components is given by

$$P^- = \frac{4M^2 - \Delta^2}{2P^+} = \frac{2Q^2\delta^2}{P^+} \,, \qquad \delta^2 = \frac{M^2 - \frac{1}{4}\Delta^2}{Q^2} \,. \tag{B.33}$$

Therefore, the vector P^μ reads

$$P^\mu = P^+\tilde{n}^\mu + \frac{2Q^2\delta^2}{P^+} n^\mu \,. \tag{B.34}$$

Employing the same procedure for q^μ, we obtain

$$q^2 = 2q^+q^- = -Q^2 \qquad \to q^- = -\frac{Q^2}{2q^+} \,. \tag{B.35}$$

To determine its "plus" component, we use the relation

$$P.q = P^+q^- + P^-q^+ = -\frac{Q^2P^+}{2q^+} + \frac{2Q^2\delta^2}{P^+}q^+ = \frac{Q^2}{\xi}\,, \tag{B.36}$$

to obtain the quadratic equation

$$\frac{2\delta^2}{P^+}\left(q^+\right)^2 - \frac{q^+}{\xi} - \frac{P^+}{2} = 0\,. \tag{B.37}$$

Its solution is given by

$$q^+ = \frac{\frac{1}{\xi} - \sqrt{\frac{1}{\xi^2} + 4\frac{2\delta^2}{P^+}\frac{P^+}{2}}}{2\frac{2\delta^2}{P^+}} = P^+\frac{1-\sqrt{1+4\xi^2\delta^2}}{4\xi\delta^2}\,. \tag{B.38}$$

Thus, q^μ in terms of the two light-like vectors is

$$q^\mu = -\frac{\xi P^+}{1+\sqrt{1+4\xi^2\delta^2}}\tilde{n}^\mu - \frac{1}{P^+}\frac{2\xi Q^2\delta^2}{1-\sqrt{1+4\xi^2\delta^2}}n^\mu\,. \tag{B.39}$$

The light-like vectors n and $\tilde{n}$ are only auxiliary vectors. In the end, we re-express them in terms of symmetric particle momenta. From the sum of (B.34) and (B.39) we get n, namely

$$n^\mu = -\frac{P^+}{4Q^2\delta^2}\,\frac{1-\sqrt{1+4\xi^2\delta^2}}{\sqrt{1+4\xi^2\delta^2}}\,P^\mu + \frac{\xi P^+}{Q^2\sqrt{1+4\xi^2\delta^2}}\,q^\mu\,. \tag{B.40}$$

The second light-like vector $\tilde{n}$ follows in the same manner

$$\tilde{n}^\mu = \frac{1+\sqrt{1+4\xi^2\delta^2}}{2P^+\sqrt{1+4\xi^2\delta^2}}P^\mu + \frac{2\delta^2\xi}{P^+\sqrt{1+4\xi^2\delta^2}}q^\mu\,. \tag{B.41}$$

In addition, we derive the Sudakov decomposition of the transverse momentum transfer Δ. Equating the nucleon masses, its minus component reads

$$\Delta.P = \Delta^+P^- + \Delta^-P^+ = \Delta^+\frac{2Q^2\delta^2}{P^+} = 0\,, \qquad \to \Delta^- = -\frac{2Q^2\delta^2}{(P^+)^2}\Delta^+\,. \tag{B.42}$$

On the other hand, the plus component follows from

$$\Delta.q = \Delta^+q^- + \Delta^-q^+ = -\eta P.q = -\eta\frac{Q^2}{\xi} = \Delta^+\frac{Q^2}{P^+}\frac{\sqrt{1+4\xi^2\delta^2}}{\xi}\,, \tag{B.43}$$

which is obtained by a straight forward insertion of the known light-like components of q and Δ. Thus,

$$\Delta^+ = -\frac{\eta P^+}{\sqrt{1+4\xi^2\delta^2}} \tag{B.44}$$

and the desired Sudakov decomposition reads

$$\Delta^\mu = -\frac{\eta P^+}{\sqrt{1+4\xi^2\delta^2}}\,\tilde{n}^\mu - \frac{2\eta Q^2\delta^2}{P^+\sqrt{1+4\xi^2\delta^2}}\,n^\mu + \Delta_\perp^\mu\,. \tag{B.45}$$

At this point, it is trivial to obtain the momenta of the Compton amplitude utilizing (3.71). The nucleon momenta are

$$\begin{aligned} P_1^\mu &= \frac{P^+}{2}\left(1+\tfrac{\eta}{\sqrt{1+4\xi^2\delta^2}}\right)\tilde{n}^\mu + \frac{Q^2\delta^2}{P^+}\left(1+\tfrac{\eta}{\sqrt{1+4\xi^2\delta^2}}\right)n^\mu - \frac{1}{2}\Delta_\perp^\mu\,,\\ P_2^\mu &= \frac{P^+}{2}\left(1-\tfrac{\eta}{\sqrt{1+4\xi^2\delta^2}}\right)\tilde{n}^\mu + \frac{Q^2\delta^2}{P^+}\left(1-\tfrac{\eta}{\sqrt{1+4\xi^2\delta^2}}\right)n^\mu + \frac{1}{2}\Delta_\perp^\mu\,. \end{aligned} \tag{B.46}$$

The momenta of the real and virtual photons are

$$\begin{aligned} q_1^\mu &= -\frac{P^+}{2}\left(\tfrac{2\xi}{1+\sqrt{1+4\xi^2\delta^2}}+\tfrac{\eta}{\sqrt{1+4\xi^2\delta^2}}\right)\tilde{n}^\mu - \frac{Q^2\delta^2}{P^+}\left(\tfrac{2\xi}{1-\sqrt{1+4\xi^2\delta^2}}-\tfrac{\eta}{\sqrt{1+4\xi^2\delta^2}}\right)n^\mu + \frac{1}{2}\Delta_\perp^\mu\,,\\ q_2^\mu &= -\frac{P^+}{2}\left(\tfrac{2\xi}{1+\sqrt{1+4\xi^2\delta^2}}-\tfrac{\eta}{\sqrt{1+4\xi^2\delta^2}}\right)\tilde{n}^\mu - \frac{Q^2\delta^2}{P^+}\left(\tfrac{2\xi}{1-\sqrt{1+4\xi^2\delta^2}}+\tfrac{\eta}{\sqrt{1+4\xi^2\delta^2}}\right)n^\mu - \frac{1}{2}\Delta_\perp^\mu\,. \end{aligned} \tag{B.47}$$

The results above are more precise, than we actually need in the analysis of the processes in chapter 3, where we neglect contributions proportional to $M^2/\mathcal{Q}^2$ and $\Delta^2/\mathcal{Q}^2$. Therefore, we expand the result in terms δ^2 (B.33) in the vicinity of zero. The leading contribution of the three appearing terms are

$$\frac{1}{\sqrt{1+4\xi^2\delta^2}} \approx 1\,, \qquad \frac{1}{1+\sqrt{1+4\xi^2\delta^2}} \approx \frac{1}{2}\,, \qquad \frac{\delta^2}{1-\sqrt{1+4\xi^2\delta^2}} \approx -\frac{1}{2\xi^2}\,. \tag{B.48}$$

Within this approximation, the symmetric momenta read

$$P^\mu = P^+\tilde{n}^\mu\,, \qquad q^\mu = -\frac{\xi P^+}{2}\tilde{n}^\mu + \frac{1}{P^+}\frac{Q^2}{\xi}n^\mu\,, \qquad \Delta^\mu = -\eta P^+\,\tilde{n}^\mu + \Delta_\perp^\mu\,. \tag{B.49}$$

The particle momenta become

$$\begin{aligned} P_1^\mu &= \frac{(1+\eta)\,P^+}{2}\tilde{n}^\mu - \frac{1}{2}\Delta_\perp^\mu\,, & q_1^\mu &= -\frac{P^+}{2}\,(\xi+\eta)\,\tilde{n}^\mu + \frac{Q^2}{\xi P^+}n^\mu + \frac{1}{2}\Delta_\perp^\mu\,,\\ P_2^\mu &= \frac{(1-\eta)\,P^+}{2}\tilde{n}^\mu + \frac{1}{2}\Delta_\perp^\mu\,, & q_2^\mu &= -\frac{P^+}{2}\,(\xi-\eta)\,\tilde{n}^\mu + \frac{Q^2}{\xi P^+}n^\mu - \frac{1}{2}\Delta_\perp^\mu\,. \end{aligned} \tag{B.50}$$

The light-like vectors on the other hand are

$$n^\mu = \frac{\xi P^+}{2Q^2}\,(2q^\mu + \xi P^\mu)\,, \qquad \tilde{n}^\mu = \frac{1}{P^+}P^\mu\,. \tag{B.51}$$

B.4.1. Compton frame

In this work, we employ the Compton frame as described in section 3.2.1. The system is boost invariant along this axes and the average momenta P and q are collinear to the two light-like

vectors and thus, do not possess transverse components. Due to the boost invariance (B.31) we can always change the definition of the light-like vectors by a constant factor. Thus, the actual value for P^+ is actually irrelevant for the discussion. A convenient choice is

$$P^+ = 2\,. \tag{B.52}$$

Listing the results from above with this convention, we obtain the symmetric momenta

$$P^\mu = 2\tilde{n}^\mu\,, \qquad q^\mu = -\xi\tilde{n}^\mu + \frac{Q^2}{2\xi}n^\mu\,, \qquad \Delta^\mu = -2\eta\,\tilde{n}^\mu + \Delta_\perp^\mu\,, \tag{B.53}$$

and the particle momenta

$$\begin{aligned} P_1^\mu &= (1+\eta)\,\tilde{n}^\mu - \frac{1}{2}\Delta_\perp^\mu\,, & q_1^\mu &= -(\xi+\eta)\,\tilde{n}^\mu + \frac{Q^2}{2\xi}n^\mu + \frac{1}{2}\Delta_\perp^\mu\,, \\ P_2^\mu &= (1-\eta)\,\tilde{n}^\mu + \frac{1}{2}\Delta_\perp^\mu\,, & q_2^\mu &= -(\xi-\eta)\,\tilde{n}^\mu + \frac{Q^2}{2\xi}n^\mu - \frac{1}{2}\Delta_\perp^\mu\,, \end{aligned} \tag{B.54}$$

as well as the two light-like vectors

$$n^\mu = \frac{\xi}{Q^2}\left(2q^\mu + \xi P^\mu\right)\,, \qquad \tilde{n}^\mu = \frac{1}{2}P^\mu\,. \tag{B.55}$$

in the Compton frame. Whereas it is often practical to use the relations with the replacement $P.q = Q^2/\xi$.

B.4.2. Breit frame

In the Breit frame, the incoming virtual photon has zero energy and moves along the z-axes. The initial-state proton moves counter-along the z-axes directly into the photon. As one notices, the results in Sec. B.4 we obtained neglecting the transverse components of P and q. Whereas this is exactly valid in the Compton frame, it is only approximately valid in the Breit frame. The momentum of the virtual photon in such a frame is given by

$$q_1^\mu = (0,0,0,q_1^3)\,, \qquad \to q_1^+ \sim q_1^3 = -q_1^-\,. \tag{B.56}$$

For the plus component we evaluate

$$q_1^2 = 2q_1^+q_1^- = -2\left(q_1^+\right)^2 = \mathcal{Q}^2\,, \qquad \to q_1^+ = -\frac{\mathcal{Q}}{\sqrt{2}}\,. \tag{B.57}$$

The complete Sudakov decomposition reads

$$q_1^\mu = -\frac{\mathcal{Q}}{\sqrt{2}}n^\mu + \frac{\mathcal{Q}}{\sqrt{2}}\tilde{n}^\mu\,. \tag{B.58}$$

From this equation, we directly read of the corresponding P^+

$$\frac{\mathcal{Q}}{\sqrt{2}} = -\frac{P^+}{2}\left(\xi+\eta\right)\,, \qquad \to P^+ = -\frac{\sqrt{2}\mathcal{Q}}{\xi+\eta}\,. \tag{B.59}$$

Thus, for the particle momenta in the Breit frame, we find

$$P_1^\mu = -\frac{1+\eta}{\xi+\eta}\frac{\mathcal{Q}}{\sqrt{2}}n^\mu\,,$$
$$P_2^\mu = -\frac{1-\eta}{\xi+\eta}\frac{\mathcal{Q}}{\sqrt{2}}n^\mu\,. \tag{B.60}$$

The momentum of the outgoing photon/meson becomes

$$q_2^\mu = \frac{\mathcal{Q}}{\sqrt{2}}\frac{\xi-\eta}{\xi+\eta}\,\tilde{n}^\mu - \frac{\mathcal{Q}}{\sqrt{2}}\,n^\mu\,. \tag{B.61}$$

C

Special functions

C.1. Gegenbauer polynomials

Gegenbauer polynomials or ultraspherical polynomials $C_n^\lambda(z)$ are orthogonal polynomials in the interval $[-1,1]$ with respect to the weight function $(1-x^2)^{\lambda-\frac{1}{2}}$. Moreover, $n\in\mathbb{N}$ denotes the degree of the polynomial and the index λ, where $\lambda>\frac{1}{2}$ and $\lambda\neq 0$. The corresponding orthogonality relation reads

$$\int_{-1}^{1}\mathrm{d}x\; C_k^\lambda(x)C_l^\lambda(x)\left(1-x^2\right)^{\lambda-\frac{1}{2}}=\delta_{kl}\frac{\pi 2^{1-2\lambda}\Gamma(k+2\lambda)}{k!(k+\lambda)\Gamma^2(\lambda)}=\delta_{kl}2^{2\lambda}N_k^\lambda\,. \tag{C.1}$$

It is quite common to apply the variable transformation

$$x=2u-1\,,\qquad \frac{\mathrm{d}x}{\mathrm{d}u}=2\,,\qquad x^2=4u^2-4u+1=-4u\bar{u}+1\,,\qquad \bar{u}=1-u\,, \tag{C.2}$$

which maps the Gegenbauer polynomials into the interval $[0,1]$. Furthermore, the orthogonality relations become

$$\int_0^1\mathrm{d}u\, C_k^\lambda(2u-1)C_l^\lambda(2u-1)\,(u\bar{u})^{\lambda-\frac{1}{2}}=\delta_{kl}N_k^\lambda\,. \tag{C.3}$$

The Gegenbauer polynomials are a special case of the Jacobi polynomials, namely

$$P_n^{(\lambda-\frac{1}{2},\lambda-\frac{1}{2})}(x)=\frac{\Gamma(2\lambda)\,\Gamma\left(n+\lambda+\frac{1}{2}\right)}{\Gamma(n+2\lambda)\,\Gamma\left(\lambda+\frac{1}{2}\right)}\,C_n^\lambda(x)\,. \tag{C.4}$$

In addition, they are the solutions to the Gegenbauer differential equation

$$\left(1-x^2\right)\frac{\mathrm{d}^2}{\mathrm{d}x^2}C_n^\lambda(x)-(2\lambda+1)x\frac{\mathrm{d}}{\mathrm{d}x}C_n^\lambda(x)+n(n+2\lambda)C_n^\lambda(x)=0\,. \tag{C.5}$$

In the special case $\lambda=1/2$, the equation above is the Legendre equation and the Gegenbauer polynomials reduce to the Legendre polynomials. Utilizing the variable u, the differential equation yields

$$u\bar{u}\frac{\mathrm{d}^2}{\mathrm{d}u^2}C_n^\lambda(2u-1)-\frac{1}{2}(2\lambda+1)(2u-1)\frac{\mathrm{d}}{\mathrm{d}u}C_n^\lambda(2u-1)+n(n+2\lambda)C_n^\lambda(2u-1)=0\,. \tag{C.6}$$

It is also possible to include the weight function, we get

$$\left(1-x^2\right)\frac{\mathrm{d}^2}{\mathrm{d}x^2}\left(1-x^2\right)^{\lambda-\frac{1}{2}}C_n^\lambda(x)+(2\lambda-3)x\frac{\mathrm{d}}{\mathrm{d}x}\left(1-x^2\right)^{\lambda-\frac{1}{2}}C_n^\lambda(x)$$
$$+(n+1)(n+2\lambda-1)\left(1-x^2\right)^{\lambda-\frac{1}{2}}C_n^\lambda(x)=0\,. \tag{C.7}$$

Preforming the transformation to the variable u, the equation above with $\lambda=3/2$ turns into

$$u\bar{u}\frac{\mathrm{d}^2}{\mathrm{d}u^2}\,u\bar{u}\,C_n^{3/2}(2u-1)+(n+1)(n+2)\,u\bar{u}\,C_n^{3/2}(2u-1)=0\,. \tag{C.8}$$

The general derivative of Gegenbauer polynomials is given by

$$\frac{\mathrm{d}^m}{\mathrm{d}z^m}C_n^\lambda(z)=2^m(\lambda)_m C_{n-m}^{m+\lambda}(z)\,. \tag{C.9}$$

Furthermore, they posses the following symmetry property under $x\to-x$

$$C_n^\lambda(-x)=(-1)^n C_n^\lambda(x)\,, \tag{C.10}$$

and the asymptotic behavior at infinity

$$C_n^\lambda(x)\overset{x\to\infty}{=}\frac{2^n\Gamma(n+\lambda)}{\Gamma(\lambda)\,\Gamma(n+1)}x^n\,. \tag{C.11}$$

Moreover, the Rodrigues formula reads in the interval $[-1,1]$ and $[0,1]$

$$\left(1-x^2\right)^{\lambda-\frac{1}{2}}C_k^\lambda(x)=\frac{(-1)^k2^{2k+\lambda-\frac{5}{2}}}{k!}\frac{\Gamma(k+\lambda)\Gamma(k+2\lambda)}{\Gamma(\lambda)\Gamma(2k+2\lambda)}\frac{\mathrm{d}^k}{\mathrm{d}x^k}\left(1-x^2\right)^{k+\lambda-\frac{1}{2}}\,, \tag{C.12}$$

$$(u\bar{u})^{\lambda-\frac{1}{2}}C_n^\lambda(2u-1)=\frac{(-1)^n4^n}{n!}\frac{\Gamma(n+\lambda)\Gamma(n+2\lambda)}{\Gamma(\lambda)\Gamma(2n+2\lambda)}\frac{\mathrm{d}^k}{\mathrm{d}u^k}\left(u\bar{u}\right)^{n+\lambda-\frac{1}{2}}\,, \tag{C.13}$$

respectively. In Chap. 4, we utilize the Rodrigues formula for the variable

$$\left[1-\left(\frac{x}{\eta}\right)^2\right]^{\lambda-\frac{1}{2}}C_k^\lambda(x)=\frac{(-1)^k2^k}{k!}\frac{\Gamma(k+\lambda)\Gamma(k+2\lambda)}{\Gamma(\lambda)\Gamma(2k+2\lambda)}\eta^n\frac{\mathrm{d}^k}{\mathrm{d}x^k}\left[1-\left(\frac{x}{\eta}\right)^2\right]^{k+\lambda-\frac{1}{2}}\,. \tag{C.14}$$

The Gegenbauer polynomials can be represented by a Gauss hypergeometric function (see Sec. C.2) as

$$C_n^\lambda(z)=\frac{\Gamma(n+2\lambda)}{\Gamma(n+1)\Gamma(2\lambda)}\,{}_2F_1\left(\begin{matrix}-n & n+2\lambda\\ \frac{1}{2}+\lambda\end{matrix}\,\middle|\,\frac{1-z}{2}\right)\,,\quad -\lambda-\frac{1}{2}\notin\mathbb{N}\,. \tag{C.15}$$

In the two special cases $\lambda\in\{1/2,3/2\}$ we have

$$C_n^{1/2}(z)={}_2F_1\left(\begin{matrix}-n & n+1\\ 1\end{matrix}\,\middle|\,\frac{1-z}{2}\right)\,,$$
$$C_n^{3/2}(z)=\frac{n+1}{2}\,{}_2F_1\left(\begin{matrix}-n & n+3\\ 2\end{matrix}\,\middle|\,\frac{1-z}{2}\right)\,. \tag{C.16}$$

In addition, we have the following recurrence relations with respect to the degree n

$$C_n^\lambda(z)=\frac{2(n+\lambda+1)z}{n+2\lambda}C_{n+1}^\lambda(z)-\frac{n+2}{n+2\lambda}C_{n+2}^\lambda(z)\,,$$
$$C_n^\lambda(z)=\frac{2(n+\lambda-1)z}{n}C_{n-1}^\lambda(z)-\frac{n+2\lambda-2}{n}C_{n-2}^\lambda(z)\,. \tag{C.17}$$

C.2. Hypergeometric functions

The generalized hypergeometric function can be written as the following series

$$ {}_pF_q\left(\begin{matrix} a_1 & a_2 & \dots & a_p \\ b_1 & b_2 & \dots & b_q \end{matrix}\middle| z\right) = \sum_{n=0}^{\infty} \frac{(a_1)_n (a_2)_n \cdots (a_p)_n}{(b_1)_n (b_2)_n \cdots (b_q)_n} \frac{z^n}{n!} \,. \tag{C.18} $$

The most occurring case in this thesis Gaussian hypergeometric function, where $p = 2$ and $q = 1$. It can be represented by the following integral

$$ {}_2F_1\left(\begin{matrix} a & b \\ c \end{matrix}\middle| z\right) = \frac{\Gamma(c)}{\Gamma(b)\,\Gamma(c-b)} \int_0^1 \mathrm{d}t\; t^{b-1}(1-t)^{c-b-1}(1-tz)^{-a} \,. \tag{C.19} $$

Therefore, from the integral representation of the beta function

$$ \mathrm{B}(x,y) = \int_0^1 \mathrm{d}t\, t^{x-1}(1-t)^{y-1} = 2^{1-x-y} \int_{-1}^1 \mathrm{d}w\, (1+y)^{x-1}(1-y)^{y-1} \,, \tag{C.20} $$

where

$$ \mathrm{B}(x,y) = \frac{\Gamma(x)\,\Gamma(y)}{\Gamma(x+y)} \,, \tag{C.21} $$

we read of the hypergeometric function for $z = 1$

$$ {}_2F_1\left(\begin{matrix} a & b \\ c \end{matrix}\middle| 1\right) = \frac{\Gamma(c)\,\Gamma(c-a-b)}{\Gamma(c-a)\,\Gamma(c-b)} \,. \tag{C.22} $$

Other special values are

$$ {}_2F_1\left(\begin{matrix} a & b \\ c \end{matrix}\middle| 0\right) = 1 \,. \tag{C.23} $$

Further identities can be found in [PBEoNR53, AS12]. Let us present a small selection, which is of importance in this thesis. The Gaussian hypergeometric function fulfills the following linear transformations

$$ {}_2F_1\left(\begin{matrix} a & b \\ c \end{matrix}\middle| z\right) = (1-z)^{-a-b+c}\, {}_2F_1\left(\begin{matrix} c-a & c-b \\ c \end{matrix}\middle| z\right) \tag{C.24a} $$

$$ = (1-z)^{-a}\, {}_2F_1\left(\begin{matrix} a & c-b \\ c \end{matrix}\middle| \frac{z}{1-z}\right) \tag{C.24b} $$

$$ = (1-z)^{-b}\, {}_2F_1\left(\begin{matrix} c-a & b \\ c \end{matrix}\middle| \frac{z}{1-z}\right) \,. \tag{C.24c} $$

Moreover, we make use of the quadratic transforation

$$ {}_2F_1\left(\begin{matrix} a & b \\ 2b \end{matrix}\middle| z\right) = \left(1-\frac{z}{2}\right)^{-a}\, {}_2F_1\left(\begin{matrix} \frac{a}{2} & \frac{a+1}{2} \\ b+\frac{1}{2} \end{matrix}\middle| \frac{z^2}{(2-z)^2}\right) \,. \tag{C.25} $$

Additionally, we also employ the confluent hypergeometric function ($p = q = 1$). Its integral representation reads

$$ {}_1F_1\left(\begin{matrix} a \\ b \end{matrix}\middle| z\right) = \frac{\Gamma(b)}{\Gamma(a)\Gamma(b-a)} \int_0^1 \mathrm{d}u\; e^{zu}\, u^{a-1}\bar{u}^{b-a-1} \,, \quad \Re\mathrm{e}\, b > \Re\mathrm{e}\, a > 0 \,. \tag{C.26} $$

C.3. Polylogarithm function

The polylogarithm function of order s is defined by the infinite sum

$$\mathrm{Li}_s(z) = \sum_{k=1}^{\infty} \frac{z^k}{k^s}\,, \qquad |z| < 1\,. \tag{C.27}$$

In the special case $s = 1$ the polylogarithm function reduces to the logarithm $\mathrm{Li}_1(z) = -\ln(1-z)$. Furthermore, the case $s = 2$ is called dilogarithm or Spence's function. In addition, it reduces to the Riemann zeta function for $z = 1$, $\mathrm{Li}_s(1) = \zeta(s)$. We frequently utilize the identity

$$\mathrm{Li}_2(z) + \mathrm{Li}_2(1-z) = -\ln(z)\ln(1-z) + \zeta(2)\,. \tag{C.28}$$

C.4. Polygamma function

The polygamma function is defined as the $m+1$-th derivative of the logarithm of the gamma function

$$\psi_n(z) = \frac{\mathrm{d}^{n+1}}{\mathrm{d}z^{n+1}} \ln\Gamma(z)\,. \tag{C.29}$$

It is holomorphic in $\mathbb{C}$ besides the poles of order $m+1$ at negative integer arguments. The case $\psi_0(z) \equiv \psi(z)$ is called digamma function. Furthermore, it satisfies the recurrence relation

$$\psi_n(z+1) = \psi_n(z) + (-1)^n \frac{n!}{z^{n+1}}\,. \tag{C.30}$$

In case of $n \in \{0, 1\}$ the previous equation yields

$$\psi_0(z+1) = \psi_0(z) + \frac{1}{z}\,, \qquad \psi_1(z+1) = \psi_1(z) - \frac{1}{z^2}\,. \tag{C.31}$$

At the points $z = 1$, its value is given by the Riemann zeta function ζ

$$\psi_n(1) = (-1)^{n+1} n! \zeta(n+1) \quad n = 1, 2, 3, \ldots\,. \tag{C.32}$$

The value of the digamma function is given by the Euler-Mascheroni constant

$$\psi_0(1) = -\gamma_{\mathrm{E}}\,, \tag{C.33}$$

where

$$\gamma_{\mathrm{E}} = 0.5772156649\ldots\,. \tag{C.34}$$

For a collection of identities, see [AS12] Sec. 6.4.

C.5. Harmonic sums

Harmonic sums are defined as

$$S_m(n) = \sum_{i=1}^{n} \frac{1}{i^m}\,, \qquad S_{-m}(n) = \sum_{i=1}^{n} \frac{(-1)^i}{i^m}\,, \qquad m > 0\,, \tag{C.35}$$

for $n, m \in \mathbb{N}$, $n, m > 0$. The case $m = 1$ corresponds to the n-th partial sum of the diverging harmonic series. It is denoted as the n-th harmonic number

$$H_n \equiv S_1(n) = \sum_{i=1}^{n} \frac{1}{i}\,. \tag{C.36}$$

Higher harmonic sums are defined as

$$S_{m,a,b,c,\ldots}(n) = \sum_{i=1}^{n} \frac{1}{i^m}\, S_{a,b,c,\ldots}(i)\,, \qquad S_{-m,a,b,c,\ldots}(n) = \sum_{i=1}^{n} \frac{(-1)^m}{i^m}\, S_{a,b,c,\ldots}(i)\,. \tag{C.37}$$

The harmonic sums can be analytically continued to complex arguments $n \to z$ utilizing polygamma functions, namely

$$S_m(z) = \frac{(-1)^{m-1}}{(m-1)!}\left[\psi_{m-1}(z+1) - \psi_{m-1}(1)\right]\,, \quad m \in \mathbb{N},\ m > 0\,. \tag{C.38}$$

Furthermore, the harmonic sums with a negative index can be expressed with harmonic sums of positive index by the identity

$$S_{-m}(z+1) = \frac{(-1)^{z+1}}{2^m}\left[S_m\left(\frac{z+1}{2}\right) - S_m\left(\frac{z}{2}\right)\right] + \left(2^{1-m}\right)\zeta(m)\,. \tag{C.39}$$

In terms of Polygamma functions, the relation above reads

$$S_{-m}(z) = \frac{(-1)^z}{2^{m-1}}\frac{(-1)^{m-1}}{(m-1)!}\left[\psi_{m-1}\left(\frac{z+2}{2}\right) - \psi_{m-1}\left(\frac{z+1}{2}\right)\right] + \mathrm{Li}_m(-1)\,. \tag{C.40}$$

For example for positive indices, we have

$$\begin{aligned} S_1(z) &= \psi_0(z+1) + \gamma\,, \\ S_2(z) &= -\psi_1(z+1) + \zeta(2)\,, \\ S_3(z) &= \tfrac{1}{2}\psi_2(z+1) + \zeta(3)\,, \end{aligned} \tag{C.41}$$

and for negative indices

$$\begin{aligned} S_{-1}(z) &= \frac{(-1)^z}{2}\left[\psi_0\left(\frac{z+2}{2}\right) - \psi_0\left(\frac{z+1}{2}\right)\right] - \ln 2\,, \\ S_{-2}(z) &= \frac{(-1)^{z+1}}{4}\left[\psi_1\left(\frac{z+2}{2}\right) - \psi_1\left(\frac{z+1}{2}\right)\right] - \frac{1}{2}\zeta(2)\,, \\ S_{-3}(z) &= \frac{(-1)^z}{16}\left[\psi_2\left(\frac{z+2}{2}\right) - \psi_2\left(\frac{z+1}{2}\right)\right] - \frac{3}{4}\zeta(3)\,. \end{aligned} \tag{C.42}$$

In this thesis, we only need the harmonic sums with positive indices, where the analytic continuation is ensured through the representation of polygamma function. Albeit, there is one exception, in the flavor-non-singlet channel, the higher harmonic sum $S_{-2,1}(z)$ arises. For its analytic continuation, we use the integral representation

$$S_{-2,1}(z) = -\frac{5\zeta(3)}{8} + (-1)^z \int_0^1 \mathrm{d}w \, \frac{\zeta(2) - \mathrm{Li}_2(w)}{1+w} \, w^z \,, \tag{C.43}$$

where the factor $(-1)^z$ has to be fixed. For a collection of identities see [BK99, Ver99].

D

Conformal QCD

D.1. GPD evolution

In order to present a exhaustive introduction to the Mellin-Barnes representation of structure functions, Compton form factors and transition form factors (Sec. 4.5) we introduce in this section the GPD evolution within our conventions in conformal space following the collection in [KMPK08].

D.1.1. $\overline{\text{CS}}$ scheme

The renormalization group equation for the conformal moments of the flavor non-singlet GPD in the $\overline{\text{CS}}$ scheme [KMPK08] reads

$$\mu\frac{\mathrm{d}}{\mathrm{d}\mu}F_j\left(\eta,\Delta^2,\mu_\mathrm{F}^2\right) = -\gamma_j(\alpha_\mathrm{s}(\mu))\; F_j\left(\eta,\Delta^2,\mu_\mathrm{F}^2\right) - \frac{\beta(\alpha_\mathrm{s}(\mu))}{g(\mu)}\sum_{k=0}^{j-2}\eta^{j-k}\Delta_{jk}(\alpha_\mathrm{s}(\mu))\; F_k\left(\eta,\Delta^2,\mu_\mathrm{F}^2\right).$$

The mixing term appears starting from NNLO accuracy, due to the breaking of the conformal symmetry. The analysis in this thesis is up to NLO accuracy, thus mixing effects can be neglected at least in the $\overline{\text{CS}}$ scheme. With the perturbative expansion of the anomalous dimension we have

$$\mu\frac{\mathrm{d}}{\mathrm{d}\mu}F_j\left(\eta,\Delta^2,\mu_\mathrm{F}^2\right) = -\left[\frac{\alpha_\mathrm{s}(\mu)}{2\pi}\gamma_j^{(0)} + \frac{\alpha_\mathrm{s}^2(\mu)}{(2\pi)^2}\gamma_j^{(1)} + \mathcal{O}\left(\alpha_\mathrm{s}^3\right)\right] F_j\left(\eta,\Delta^2,\mu_\mathrm{F}^2\right). \tag{D.1}$$

The solution of the renormalization group equation is given by the path ordered exponential:

$$F_j\left(\eta,\Delta^2,\mu_\mathrm{F}^2\right) = \mathcal{E}_j(\mu,\mu_0)F_j\left(\eta,\Delta^2,\mu_0^2\right), \qquad \mathcal{E}_j(\mu,\mu_0) = \exp\left[-\int_{\mu_0}^{\mu}\frac{\mathrm{d}\mu'}{\mu'}\gamma_j(\mu')\right]. \tag{D.2}$$

For the numerical analysis, we utilize the result of [MMPK03], where only the leading logarithms are resumed and the non-leading ones are expanded. Hence, the evolution operator in NLO accuracy yields

$$\mathcal{E}_j(\mu,\mu_0) = \left[1+\frac{\alpha_\mathrm{s}(\mu)}{2\pi}\mathcal{A}_j^{(1)}(\mu,\mu_0)+O(\alpha_\mathrm{s}^2)\right]\left[\frac{\alpha_\mathrm{s}(\mu)}{\alpha_\mathrm{s}(\mu_0)}\right]^{-\frac{\gamma^{(0)}{}_j}{\beta_0}}, \tag{D.3}$$

where

$$\mathcal{A}_j^{(1)}(\mu,\mu_0) = \left[1 - \frac{\alpha_s(\mu)}{\alpha_s(\mu_0)}\right]\left[\frac{\beta_1}{2\beta_0}\frac{{}^{\rm NS}\gamma_j^{(0)}}{\beta_0} - \frac{{}^{\rm NS}\gamma_j^{(1)}}{\beta_0}\right]. \tag{D.4}$$

Moreover, the expansion coefficients of the β function read

$$\beta_0 = \frac{2}{3}N_f - 11\,, \qquad \beta_1 = \frac{38}{3}N_f - 102\,. \tag{D.5}$$

The solution of the renormalization in the flavor singlet sector is

$$\boldsymbol{F}_j\big(\eta,\Delta^2,\mu_F^2\big) = \boldsymbol{\mathcal{E}}_j(\mu,\mu_0)\boldsymbol{F}_j\big(\eta,\Delta^2,\mu_0\big)\ , \tag{D.6}$$

where the vector of the conformal moments of the singlet and gluon GPD is defined in (4.141). The evolution operator is given by

$$\boldsymbol{\mathcal{E}}_j(\mu,\mu_0) = \mathcal{P}\exp\left\{-\int_{\mu_0}^{\mu}\frac{\mathrm{d}\mu'}{\mu'}\,\boldsymbol{\gamma}_j\big(\alpha_s(\mu')\big)\right\}. \tag{D.7}$$

The Expansion of the evolution operator resuming the leading logarithms and expanding the non-leading ones [KMPK08] yields

$$\boldsymbol{\mathcal{E}}_j(\mu,\mu_0) = \sum_{a,b=\pm}\left[\delta_{ab}\,{}^a\boldsymbol{P}_j + \frac{\alpha_s(\mu)}{2\pi}\,{}^{ab}\boldsymbol{\mathcal{A}}_j^{(1)} + \mathcal{O}(\alpha_s^2)\right]\left[\frac{\alpha_s(\mu)}{\alpha_s(\mu_0)}\right]^{-\frac{{}^b\lambda_k}{\beta_0}}, \tag{D.8}$$

where $ab \in \{++,+-,-+,--\}$. The projectors are given by

$${}^{\pm}\boldsymbol{P}_j = \frac{\pm 1}{{}^{+}\lambda_j - {}^{-}\lambda_j}\left(\boldsymbol{\gamma}_j^{(0)} - {}^{\mp}\lambda_j\mathbf{1}\right). \tag{D.9}$$

Furthermore, the eigenvalues ${}^{\pm}\lambda_j$ are

$${}^{\pm}\lambda_j = \frac{1}{2}\left[{}^{\Sigma\Sigma}\gamma_j^{(0)} + {}^{\rm GG}\gamma_j^{(0)} \mp \left({}^{\Sigma\Sigma}\gamma_j^{(0)} - {}^{\rm GG}\gamma_j^{(0)}\right)\left(\frac{4\,{}^{\Sigma\rm G}\gamma_j^{(0)}\,{}^{\rm G\Sigma}\gamma_j^{(0)}}{\left({}^{\Sigma\Sigma}\gamma_j^{(0)} - {}^{\rm GG}\gamma_j^{(0)}\right)^2}\right)^{\frac{1}{2}}\right]. \tag{D.10}$$

The matrix valued coefficient ${}^{ab}\boldsymbol{\mathcal{A}}_j^{(1)}$ reads

$${}^{ab}\boldsymbol{\mathcal{A}}_j^{(1)} = {}^{ab}R_{jj}(\mu,\mu_0\,|1)\;{}^a\boldsymbol{P}_j\left[\frac{\beta_1}{2\beta_0}\boldsymbol{\gamma}_j^{(0)} - \boldsymbol{\gamma}_j^{(1)}\right]{}^b\boldsymbol{P}_j\,, \tag{D.11}$$

where the function involving the scale dependence is defined as

$${}^{ab}R_{jk}(\mu,\mu_0\,|n) = \frac{1}{n\beta_0 + {}^a\lambda_j - {}^b\lambda_k}\left[1 - \left(\frac{\alpha_s(\mu_0)}{\alpha_s(\mu)}\right)^{\frac{n\beta_0 + {}^a\lambda_j - {}^b\lambda_k}{\beta_0}}\right]. \tag{D.12}$$

D.1.2. $\overline{\text{MS}}$ scheme

In the $\overline{\text{MS}}$ scheme, the mixing already starts at NLO accuracy. The corresponding renormalization group equation for the flavor non-singlet conformal moments is

$$\mu\frac{\mathrm{d}}{\mathrm{d}\mu}F_j\big(\eta,\Delta^2,\mu_{\text{F}}^2\big)=-\sum_{k=0}^{\infty}\gamma_{jk}\,\eta^{j-k}\,F_k\big(\eta,\Delta^2,\mu_{\text{F}}^2\big)\;. \tag{D.13}$$

The diagonal anomalous dimensions $\gamma_j=\gamma_{jj}$ are already known from DIS and given in App. D.2. The non-diagonal ones are known to two loop accuracy [Mül94, BM98a, BM99]. For integer conformal moments, the solution of the renormalization group equation reads

$$F_j^A\big(\eta,\Delta^2,\mu_{\text{F}}^2\big)=\sum_{k=0}^{j}\frac{1-\sigma(-1)^k}{2}\,\mathcal{E}_{jk}(\mu_{\text{F}},\mu_0;\eta)F_k^A\big(\eta,\Delta^2,\mu_0^2\big)\;. \tag{D.14}$$

Note that we switched to GPDs with a definite charge parity (Sec. 2.3). In the non-singlet case, we have $A\in\{q^{(-)},3^{(+)},8^{(+)},15^{(+)}\}$. The expansion of the evolution operator to NLO accuracy yields

$$\mathcal{E}_{jk}(\mu,\mu_0;\eta)=\left[\delta_{jk}+\frac{\alpha_{\text{s}}(\mu)}{2\pi}\Big(\mathcal{A}_j^{(1)}\delta_{jk}+\mathcal{B}_{jk}^{(1)}\eta^{j-k}\Big)(\mu,\mu_0)+O(\alpha_{\text{s}}^2)\right]\left[\frac{\alpha_{\text{s}}(\mu)}{\alpha_{\text{s}}(\mu_0)}\right]^{-\frac{{}^{\text{NS}}\gamma_k^{(0)}}{\beta_0}}\;. \tag{D.15}$$

where $\mathcal{A}_j^{(1)}$ is defined in D.4 and the term $\mathcal{B}_{jk}^{(1)}$ reads

$$\mathcal{B}_{jk}^{(1)}(\mu,\mu_0)=-{}^{ab}R_{jk}(\mu,\mu_0|1)\Big({}^{\text{NS}}\gamma_j^{(0)}-{}^{\text{NS}}\gamma_k^{(0)}\Big)\Big[\Big(\beta_0-{}^{\text{NS}}\gamma_k^{(0)}\Big){}^{\text{NS}}d_{jk}\;+{}^{\text{NS}}g_{jk}\Big]\;, \tag{D.16}$$

and ${}^{ab}R_{jk}(\mu,\mu_0|1)$ was presented in (D.12). The coefficients ${}^{\text{NS}}d_{jk}$ and ${}^{\text{NS}}g_{jk}$ are given in [BMNS99]:

$$\begin{aligned}{}^{\text{NS}}d_{jk}&=-\frac{2^k\Gamma(j+1)\,\Gamma\big(k+\frac{3}{2}\big)}{2^j\Gamma(k+1)\,\Gamma\big(j+\frac{3}{2}\big)}\frac{2k+3}{(j-k)(j+k+3)}\,,\\ {}^{\text{NS}}g_{jk}&=\frac{2^k\Gamma(j+1)\,\Gamma\big(k+\frac{3}{2}\big)}{2^j\Gamma(k+1)\,\Gamma\big(j+\frac{3}{2}\big)}{}^{\Sigma\Sigma}g_{jk}\,,\end{aligned} \tag{D.17}$$

where ${}^{\Sigma\Sigma}g_{jk}$ is presented in (D.23).
The solution of the renormalization group equation for the flavor singlet conformal moments becomes

$$\boldsymbol{F}_j\big(\eta,\Delta^2,\mu_{\text{F}}^2\big)=\sum_{k=0}^{j}\frac{1\mp(-1)^k}{2}\boldsymbol{\mathcal{E}}_{jk}(\mu_{\text{F}},\mu_0;\eta)\boldsymbol{F}_k\big(\eta,\Delta^2,\mu_0^2\big)\;, \tag{D.18}$$

where the evolution operator to NLO accuracy is expanded as

$$\boldsymbol{\mathcal{E}}_{jk}(\mu,\mu_0;\eta)=\sum_{a,b=\pm}\left[\delta_{ab}{}^{a}\boldsymbol{P}_j\delta_{jk}+\frac{\alpha_{\text{s}}(\mu)}{2\pi}\Big({}^{ab}\boldsymbol{\mathcal{A}}_j^{(1)}\delta_{jk}+{}^{ab}\boldsymbol{\mathcal{B}}_{jk}^{(1)}\eta^{j-k}\Big)(\mu,\mu_0)+O(\alpha_{\text{s}}^2)\right]\left[\frac{\alpha_{\text{s}}(\mu)}{\alpha_{\text{s}}(\mu_0)}\right]^{-\frac{{}^{b}\lambda_k}{\beta_0}}\;. \tag{D.19}$$

The matrix valued coefficient ${}^{ab}\boldsymbol{\mathcal{A}}_j^{(1)}$ is given in (D.11). Furthermore, the coefficient is matrix valued as well, it reads [BMNS99]

$$ {}^{ab}\boldsymbol{\mathcal{B}}_{jk}^{(1)} = -{}^{ab}R_{jk}(\mu,\mu_0|1)\left({}^{a}\lambda_j - {}^{b}\lambda_k\right)\left[\left(\beta_0 - {}^{b}\lambda_k\right){}^{a}\boldsymbol{P}_j\boldsymbol{d}_{jk}{}^{b}\boldsymbol{P}_k + {}^{a}\boldsymbol{P}_j\boldsymbol{g}_{jk}{}^{b}\boldsymbol{P}_k\right], \tag{D.20}$$

where the matrices $\boldsymbol{d}_{jk}$ and $\boldsymbol{g}_{jk}$ can be read of from the results in [BMNS99]. They read

$$ \boldsymbol{d}_{jk} = -\frac{2^k\Gamma(j+1)\,\Gamma\left(k+\frac{3}{2}\right)}{2^j\Gamma(k+1)\,\Gamma\left(j+\frac{3}{2}\right)}\frac{2k+3}{(j-k)(j+k+3)}\begin{pmatrix}1 & 0\\ 0 & \frac{k}{j}\end{pmatrix} \tag{D.21}$$

and

$$ \boldsymbol{g}_{jk} = \frac{2^k\Gamma(j+1)\,\Gamma\left(k+\frac{3}{2}\right)}{2^j\Gamma(k+1)\,\Gamma\left(j+\frac{3}{2}\right)}\begin{pmatrix}{}^{\Sigma\Sigma}g_{jk} & \frac{k}{6}{}^{\Sigma G}g_{jk}\\ \frac{6}{j}{}^{G\Sigma}g_{jk} & \frac{k}{j}{}^{GG}g_{jk}\end{pmatrix}. \tag{D.22}$$

The matrix elements in the previous equation are

$$\begin{aligned}
{}^{\Sigma\Sigma}g_{jk} &= -C_F\frac{4(2k+3)}{(j-k)(j+k+3)}\left\{\left(1+\frac{(j-k)(j+k+3)}{2(k+1)(k+2)}\right)\left[S_1\left(\tfrac{j+k+2}{2}\right)+S_1\left(\tfrac{j-k-1}{2}\right)+\ln(4)\right]\right.\\
&\qquad\left.-\left(1+\frac{(j-k)(j+k+3)}{(k+1)(k+2)}\right)S_1(j+1)\right\},\\
{}^{\Sigma G}g_{jk} &= 0\,,\\
{}^{G\Sigma}g_{jk} &= -C_F\frac{(3+2k)}{3(k+1)(k+2)}\,,\\
{}^{GG}g_{jk} &= -C_A\frac{4(2k+3)}{(j-k)(j+k+3)}\left\{\frac{1}{2}\left(1+\frac{(j)_4}{(k)_4}\right)\left[S_1\left(\tfrac{j+k+2}{2}\right)+S_1\left(\tfrac{j-k-1}{2}\right)+\ln(4)\right]\right.\\
&\qquad\left.-\frac{(j)_4}{(k)_4}S_1(j+1)+\frac{(j-k)(j+k+3)}{(k)_4}\right\}.
\end{aligned} \tag{D.23}$$

D.2. Anomalous dimensions

In this section, we list the anomalous dimensions for the GPD evolution in conformal space.

D.2.1. LO

The LO anomalous dimension was derived in [GP74, GW74]. Taking the equation 2.79a in [Bur80] and applying the shift $n\to j+1$ we have

$$ {}^{NS}\gamma_j^{(0)} = -C_F\left[3+\frac{2}{(j+1)_2}-4S_1(j+1)\right]. \tag{D.24}$$

The LO anomalous dimensions in the singlet sector for the vector GPD [Bur80], Eq. 2.79a yield

$$
\begin{aligned}
{}^{\Sigma\Sigma}\gamma_j^{\mathrm{V}(0)} &= {}^{\mathrm{NS}}\gamma_j^{(0)}\,, && \text{(D.25a)}\\
{}^{\Sigma\mathrm{G}}\gamma_j^{\mathrm{V}(0)} &= -4N_\mathrm{f}T_\mathrm{F}\frac{4+3j+j^2}{(j+1)_3}\,, && \text{(D.25b)}\\
{}^{\mathrm{G}\Sigma}\gamma_j^{\mathrm{V}(0)} &= -2C_\mathrm{F}\frac{4+3j+j^2}{(j)_3}\,, && \text{(D.25c)}\\
{}^{\mathrm{GG}}\gamma_j^{\mathrm{V}(0)} &= -C_\mathrm{A}\left[-\frac{4}{(j+1)_2}+\frac{12}{j(j+3)}-4S_1(j+1)\right]+\beta_0\,. && \text{(D.25d)}
\end{aligned}
$$

The LO anomalous dimensions in the singlet sector for the axial-vector GPD from [GRSV96] with the transformation $n\to j+1$ read

$$
\begin{aligned}
{}^{\Sigma\Sigma}\gamma_j^{\mathrm{A}(0)} &= {}^{\mathrm{NS}}\gamma_j^{(0)}\,, && \text{(D.26a)}\\
{}^{\Sigma\mathrm{G}}\gamma_j^{\mathrm{A}(0)} &= -4N_\mathrm{f}T_\mathrm{F}\frac{j}{(j+1)_2}\,, && \text{(D.26b)}\\
{}^{\mathrm{G}\Sigma}\gamma_j^{\mathrm{A}(0)} &= -2C_\mathrm{F}\frac{j+3}{(j+1)_2}\,, && \text{(D.26c)}\\
{}^{\mathrm{GG}}\gamma_j^{\mathrm{A}(0)} &= -C_\mathrm{A}\left[\frac{8}{(j+1)_2}-4S_1(j+1)\right]+\beta_0\,. && \text{(D.26d)}
\end{aligned}
$$

D.2.2. NLO

The anomalous dimensions in the non-singlet sector are given in [CFP80, GRV90]. In order to transfer the expression to our conventions, we applied the transformation $N\to j+1$ and added a factor of $1/4$, to compensate the perturbative expansion with respect to $\alpha_\mathrm{s}/(4\pi)$ instead of $\alpha_\mathrm{s}/(2\pi)$. We get

$$
\begin{aligned}
{}^{\mathrm{NS}}\gamma_j^{\sigma(1)} = {}& \frac{C_\mathrm{F}\,N_\mathrm{f}\,T_\mathrm{F}}{3}\left\{1+\frac{4}{3}\frac{13+27j+11j^2}{(j+1)_2^2}-\frac{40}{3}S_1(j+1)+8S_2(j+1)\right\}\\
&+\frac{C_\mathrm{F}C_\mathrm{A}}{4}\left\{-\frac{43}{6}-\frac{4}{9}\frac{523+1590j+1792j^2+867j^3+151j^4}{(j+1)_2^3}+\left[\frac{536}{9}+\frac{8(2j+3)}{(j+1)_2^2}\right]S_1(j+1)\right.\\
&\left.+\left[\frac{8}{(j+1)_2}-\frac{52}{3}\right]S_2(j+1)-16S_1(j+1)S_2(j+1)\right\}\\
&+C_\mathrm{F}C_\mathrm{G}\left\{-\frac{3}{4}-2\frac{3+11j+10j^2+3j^3}{(j+1)_2^3}+4(-1)^j\frac{5+6j+2j^2}{(j+1)_2^3}+4\frac{(2j+3)S_1(j+1)}{(j+1)_2^2}\right.\\
&+16S_{-2,1}(j+1)+6S_2(j+1)\\
&+4\left[2S_1(j+1)-\frac{1}{(1+j)_2}\right]\left[S_2(j+1)-\frac{1-(-1)^j}{2}S_2\left(\frac{j+1}{2}\right)-\frac{1+(-1)^j}{2}S_2\left(\frac{j}{2}\right)\right]\\
&\left.-2\left[\frac{1-(-1)^j}{2}S_3\left(\frac{j+1}{2}\right)+\frac{1+(-1)^j}{2}S_3\left(\frac{j}{2}\right)\right]\right\}, \qquad \text{(D.27)}
\end{aligned}
$$

where we utilized the Pochhammer symbol (4.65) leading to the definition

$$(j)_k^p \equiv [(j)_k]^p \ . \tag{D.28}$$

We dressed the anomalous dimension with the signature σ to indicate, that for the utilization in the Mellin-Barnes representation, we have to replace the factors of $(-1)^j$ by $-\sigma$ to ensure the correct analytic continuation, see Sec. 4.5.2 for more details. In DVCS, exclusively the GPDs $F^{q(+)}$ contribute, cf. 4.1. Thus, in the vector case, we make the replacement $(-1)^j \to -1$ and in the axial-vector case, we apply $(-1)^j \to 1$. Note that the definition of the harmonic sum $S_{-2,1}(z)$ (C.43) involves a factor of $(-1)^z$ as well, which has to be fixed accordingly. To stress the necessary choice of the signature, we dress the evolution operator and also the non-singlet anomalous dimension with the symbol σ.
In the singlet sector, the anomalous dimensions are given in [FKL81]. Again, we apply the transformation $N \to j+1$ and include a factor of $1/4$ to obtain

$${}^{\Sigma\Sigma}\gamma_j^{\mathrm{V}(1)} = {}^{\mathrm{NS}}\gamma_j^{+(1)} - 4C_{\mathrm{F}}N_{\mathrm{f}}T_{\mathrm{F}}\frac{160+404j+427j^2+227j^3+57j^4+5j^5}{j(j+1)_2(j+1)_3^2}\,, \tag{D.29a}$$

$$\begin{aligned}
{}^{\Sigma\mathrm{G}}\gamma_j^{\mathrm{V}(1)} = {}& -2C_{\mathrm{A}}\,N_{\mathrm{f}}\,T_{\mathrm{F}}\Bigg\{\left[-2S_1^2(j+1)+2S_2(j+1)-\left(1-(-1)^j\right)S_2\left(\frac{j+1}{2}\right)-\left(1+(-1)^j\right)S_2\left(\frac{j}{2}\right)\right]\\
&\times\frac{j^2+3j+4}{(j+1)_3}+\frac{8S_1(j+1)(2j+5)}{(j+2)_2^2}\\
&+2\frac{480+1488j+2252j^2+2273j^3+1711j^4+963j^5+382j^6+99j^7+15j^8+j^9}{j(j+1)_3^3}\Bigg\}\\
&-2C_{\mathrm{F}}\,N_{\mathrm{f}}\,T_{\mathrm{F}}\Bigg\{\frac{\left(2S_1^2(j+1)-2S_2(j+1)+5\right)\left(j^2+3j+4\right)}{(j+1)_3}-\frac{4S_1^2(j+1)}{(j+1)^2}\\
&+\frac{64+160j+159j^2+70j^3+11j^4}{(j+1)_3^3}\Bigg\}\,,
\end{aligned} \tag{D.29b}$$

$$\begin{aligned}
{}^{\mathrm{G}\Sigma}\gamma_j^{\mathrm{V}(1)} = {}& -C_{\mathrm{F}}^2\Bigg\{\frac{\left(-2S_1^2(j+1)+10S_1(j+1)-2S_2(j+1)\right)\left(4+3j+j^2\right)}{j(1+j)(2+j)}-\frac{4S_1(j+1)}{(j+2)^2}\\
&-\frac{96+464j+821j^2+740j^3+373j^4+102j^5+12j^6}{j(1+j)^3(2+j)^3}\Bigg\}\\
&-2C_{\mathrm{F}}C_{\mathrm{A}}\Bigg\{\frac{\left(S_1^2(j+1)+S_2(j+1)-\frac{1-(-1)^j}{2}S_2\left(\frac{j+1}{2}\right)-\frac{1+(-1)^j}{2}S_2\left(\frac{j}{2}\right)\right)\left(4+3j+j^2\right)}{j(1+j)(2+j)}\\
&-S_1(j+1)\frac{24+128j+143j^2+68j^3+17j^4}{3j^2(1+j)^2(2+j)}\\
&+\frac{2592+21384j+72582j^2+128014j^3+133818j^4+88673j^5+38022j^6+10292j^7+1602j^8+109j^9}{9j^2(1+j)^3(2+j)^3(3+j)^2}\Bigg\}\\
&-\frac{8}{3}C_{\mathrm{F}}N_{\mathrm{f}}T_{\mathrm{F}}\left(\frac{\left(S_1(j+1)-\frac{8}{3}\right)\left(4+3j+j^2\right)}{j(1+j)(2+j)}+\frac{1}{(j+2)^2}\right)\,,
\end{aligned} \tag{D.29c}$$

$$
\begin{aligned}
{}^{\mathrm{GG}}\gamma_j^{\mathrm{V}(1)} &= C_{\mathrm{A}}\, N_{\mathrm{f}}\, T_{\mathrm{F}} \left\{ -\frac{40}{9} S_1(j+1) + \frac{8}{3} + \frac{8}{9} \frac{138 + 312j + 275j^2 + 114j^3 + 19j^4}{j(1+j)^2(2+j)^2(3+j)} \right\} \\
&+ C_{\mathrm{F}}\, N_{\mathrm{f}}\, T_{\mathrm{F}} \left\{ 2 + 4 \frac{-16 - 8j + 41j^2 + 74j^3 + 51j^4 + 16j^5 + 2j^6}{j(1+j)^3(2+j)^3(3+j)} \right\} \\
&+ C_{\mathrm{A}}^2 \left\{ \frac{134}{9} S_1(j+1) + 16 S_1(j+1) \frac{18 + 66j + 81j^2 + 48j^3 + 15j^4 + 2j^5}{j^2(1+j)^2(2+j)^2(3+j)^2} \right. \\
&\quad - \frac{16}{3} + 8 \frac{\left[\frac{1-(-1)^j}{2} S_2\left(\frac{j+1}{2}\right) + \frac{1+(-1)^j}{2} S_2\left(\frac{j}{2}\right) \right] \left(3 + 3j + j^2\right)}{j(1+j)(2+j)(3+j)} - 4 S_1(j+1) \left[\frac{1-(-1)^j}{2} S_2\left(\frac{j+1}{2}\right) + \frac{1+(-1)^j}{2} S_2\left(\frac{j}{2}\right) \right] \\
&\quad + 8 S_{-2,1}(j+1) - \frac{1-(-1)^j}{2} S_3\left(\frac{j+1}{2}\right) - \frac{1+(-1)^j}{2} S_3\left(\frac{j}{2}\right) \\
&\quad \left. - \frac{1}{9} \frac{15552 + 101088j + 308808j^2 + 529962j^3 + 557883j^4 + 376129j^5 + 163542j^6 + 44428j^7 + 6855j^8 + 457j^9}{j^2(1+j)^3(2+j)^3(3+j)^3} \right\},
\end{aligned}
\tag{D.29d}
$$

The anomalous dimensions in the axial-vector case at NLO of perturbation theory were originally derived in [MvN96, Vog96]. Taking the expressions in [GRSV96] (A.2-A.6) and employing the transformation $n \to j+1$ leads to

$$
{}^{\Sigma\Sigma}\gamma_j^{\mathrm{A}(1)} = {}^{\mathrm{NS}}\gamma_j^{-(1)} + 4 C_{\mathrm{F}} N_{\mathrm{f}} T_{\mathrm{F}} \frac{12 + 19j + 14j^2 + 6j^3 + j^4}{(1+j)^3(2+j)^3}\,,
\tag{D.30a}
$$

$$
\begin{aligned}
{}^{\Sigma\mathrm{G}}\gamma_j^{\mathrm{A}(1)} &= 2 C_{\mathrm{F}} N_{\mathrm{f}} T_{\mathrm{F}} j \left\{ \frac{2 S_2(j+1) - 2 S_1^2(j+1)}{(1+j)(j+2)} + \frac{4 S_1(j+1)}{(1+j)^2(j+2)} - \frac{16 + 49j + 60j^2 + 30j^3 + 5j^4}{(1+j)^3(2+j)^3} \right\} \\
&+ 4 C_{\mathrm{A}} N_{\mathrm{f}} T_{\mathrm{F}} \left\{ \frac{j \left(-S_2(j+1) + \frac{1-(-1)^j}{2} S_2\left(\frac{j+1}{2}\right) + \frac{1+(-1)^j}{2} S_2\left(\frac{j}{2}\right) + S_1^2(j+1) \right)}{(1+j)(j+2)} - \frac{4 S_1(j+1)}{(1+j)(j+2)^2} \right. \\
&\quad \left. - \frac{-8 - 4j + 7j^2 + 10j^3 + 6j^4 + j^5}{(1+j)^3(2+j)^3} \right\},
\end{aligned}
\tag{D.30b}
$$

$$
\begin{aligned}
{}^{\mathrm{G}\Sigma}\gamma_j^{\mathrm{A}(1)} &= 8 C_{\mathrm{F}} N_{\mathrm{f}} T_{\mathrm{F}} \left(-\frac{(j+3) S_1(j+1)}{3(1+j)(j+2)} + \frac{21 + 22j + 5j^2}{9(1+j)(2+j)^2} \right) \\
&+ C_{\mathrm{F}}^2 \left(\frac{2(j+3)\left[S_2(j+1) + S_1^2(j+1) \right]}{(1+j)(j+2)} - \frac{2\left(12 + 13j + 3j^2\right) S_1(j+1)}{(1+j)(j+2)^2} + \frac{36 + 207j + 335j^2 + 234j^3 + 75j^4 + 9j^5}{(1+j)^3(2+j)^3} \right) \\
&+ 2 C_{\mathrm{F}} C_{\mathrm{A}} \left\{ \frac{(j+3)\left[-S_2(j+1) + \frac{1-(-1)^j}{2} S_2\left(\frac{j+1}{2}\right) + \frac{1+(-1)^j}{2} S_2\left(\frac{j}{2}\right) - S_1^2(j+1) \right]}{(1+j)(j+2)} + \frac{\left(45 + 44j + 11j^2\right) S_1(j+1)}{3(1+j)^2(j+2)} \right. \\
&\quad \left. - \frac{750 + 2380j + 3189j^2 + 2098j^3 + 651j^4 + 76j^5}{9(1+j)^3(2+j)^3} \right\},
\end{aligned}
\tag{D.30c}
$$

$$
\begin{aligned}
{}^{\mathrm{GG}}\gamma_j^{\mathrm{A}(1)} &= 2 C_{\mathrm{F}} N_{\mathrm{f}} T_{\mathrm{F}} \frac{8 + 30j + 70j^2 + 71j^3 + 35j^4 + 9j^5 + j^6}{(1+j)^3(2+j)^3} + 8 C_{\mathrm{A}} N_{\mathrm{f}} T_{\mathrm{F}} \left(-\frac{5}{9} S_1(j+1) + \frac{35 + 75j + 52j^2 + 18j^3 + 3j^4}{9(1+j)^2(2+j)^2} \right) \\
&+ C_{\mathrm{A}}^2 \left\{ -\frac{1-(-1)^j}{2} S_3\left(\frac{j+1}{2}\right) - \frac{1+(-1)^j}{2} S_3\left(\frac{j}{2}\right) - 4 S_1(j+1) \left[\frac{1-(-1)^j}{2} S_2\left(\frac{j+1}{2}\right) + \frac{1+(-1)^j}{2} S_2\left(\frac{j}{2}\right) \right] \right. \\
&\quad + 8 S_{-2,1}(j+1) + 8 \frac{\frac{1-(-1)^j}{2} S_2\left(\frac{j+1}{2}\right) + \frac{1+(-1)^j}{2} S_2\left(\frac{j}{2}\right)}{(1+j)(j+2)} + \frac{2 S_1(j+1)}{9} \frac{484 + 948j + 871j^2 + 402j^3 + 67j^4}{(1+j)^2(j+2)^2} \\
&\quad \left. - \frac{1768 + 5250j + 7075j^2 + 4974j^3 + 1909j^4 + 432j^5 + 48j^6}{9(1+j)^3(2+j)^3} \right\}.
\end{aligned}
\tag{D.30d}
$$

We avoided a the signature here to lighten the notation albeit the factors of $(-1)^j$ have to be fixed ensuring the correct analytic continuation. Summarizing the LO and NLO anomalous dimensions in the singlet sector, we have up to NLO of perturbation theory

$$\begin{aligned}\boldsymbol{\gamma}_j &= \frac{\alpha_\mathrm{s}}{2\pi}\boldsymbol{\gamma}_j^{(0)} + \frac{\alpha_\mathrm{s}^2}{(2\pi)^2}\boldsymbol{\gamma}_j^{(1)} + O(\alpha_\mathrm{s}^3) \\ &= \frac{\alpha_\mathrm{s}}{2\pi}\begin{pmatrix} {}^{\Sigma\Sigma}\gamma_j^{(0)} & {}^{\Sigma\mathrm{G}}\gamma_j^{(0)} \\ {}^{\mathrm{G}\Sigma}\gamma_j^{(0)} & {}^{\mathrm{GG}}\gamma_j^{(0)} \end{pmatrix} + \frac{\alpha_\mathrm{s}^2}{(2\pi)^2}\begin{pmatrix} {}^{\Sigma\Sigma}\gamma_j^{(1)} & {}^{\Sigma\mathrm{G}}\gamma_j^{(1)} \\ {}^{\mathrm{G}\Sigma}\gamma_j^{(1)} & {}^{\mathrm{GG}}\gamma_j^{(1)} \end{pmatrix} + O(\alpha_\mathrm{s}^3)\,. \end{aligned} \tag{D.31}$$

E

Additional remarks about probability theory

E.1. Set of operations

In general we are dealing with n propositions A_n. On the basis of these propositions, we might construct further ones like $B = f(A_1, \ldots, A_n)$. As A_n can take two true values, the function f is defined on a space S with dimension $\dim(S) = 2^n$ and there are $2^{\dim(S)}$ possible functions.
For a single proposition A, the space S of f has dimension two and there are four functions. The complete truth table is

A	T	F
$f_1(A)$	T	T
$f_2(A)$	T	F
$f_3(A)$	F	T
$f_4(A)$	F	F

The four possible functions include the logical sum, inversion and the logical product are

$$\begin{aligned} f_1(A) &= A + \overline{A}, \\ f_2(A) &= A, \\ f_3(A) &= \overline{A}, \\ f_4(A) &= A\overline{A}, \end{aligned} \tag{E.1}$$

where f_1 denotes the certain proposition, which is always true regardless the true value of A. The fourth function is the contradiction.
For $n = 2$, the functional space has four points and sixteen possible functions. The truth table for the four functions, which are true only on one point of S is

A, B	T,T	T,F	F,T	F,F
$f_1(A,B)$	T	F	F	F
$f_2(A,B)$	F	T	F	F
$f_3(A,B)$	F	F	T	F
$f_4(A,B)$	F	F	F	T

The corresponding operations built with the logical product and inversion are

$$\begin{aligned} f_1(A,B) &= AB, \\ f_2(A,B) &= A\overline{B}, \\ f_3(A,B) &= \overline{A}B, \\ f_4(A,B) &= \overline{A}\,\overline{B}. \end{aligned} \tag{E.2}$$

The remaining eleven functions, true in at least two points of S, are expressed by the logical sum of the basic conjunctions in (E.2). First, we consider the six functions being true in two points

A, B	T,T	T,F	FT,	F,F
$f_5(A,B) = A$	T	T	F	F
$f_6(A,B) = B$	T	F	T	F
$f_7(A,B) = AB + \overline{A}\,\overline{B}$	T	F	F	T
$f_8(A,B) = A\overline{B} + \overline{A}B$	F	T	T	F
$f_9(A,B) = \overline{B}$	F	T	F	T
$f_{10}(A,B) = \overline{A}$	F	F	T	T

For example, f_5 is a combination of f_1 and f_2

$$f_5(A,B) = f_1(A,B) + f_2(A,B) = AB + A\overline{B} = A(B + \overline{B}) = A. \tag{E.3}$$

The functions which are true in at least three points of S are

A, B	T,T	T,F	FT,	F,F
$f_{11}(A,B) = A + B$	T	T	T	F
$f_{12}(A,B) = A + \overline{B}$	T	T	F	T
$f_{13}(A,B) = \overline{A} + B$	T	F	T	T
$f_{14}(A,B) = \overline{A} + \overline{B}$	F	T	T	T
$f_{15}(A,B) = A + \overline{A}$	T	T	T	T

The missing function is the one, returning false in all cases. For this we choose the contradiction $A\overline{A}$. This method is equally valid for arbitrary n. We have seen, that two operations out of NOT, AND and OR are sufficient for plausible reasoning.
In fact, we are able to combine NOT with AND or OR to have only one operation. We define the operation NAND as

$$A \uparrow B \equiv \overline{AB} = \overline{A} + \overline{B}. \tag{E.4}$$

The three logical operations in terms of NAND are:

$$\begin{aligned} \overline{A} &= \overline{A} + \overline{A} = A \uparrow A, \\ AB &= \overline{\overline{A} + \overline{B}} = \left(\overline{A} + \overline{B}\right) \uparrow \left(\overline{A} + \overline{B}\right) = (A \uparrow B) \uparrow (A \uparrow B), \\ A + B &= \overline{\overline{A}\,\overline{B}} = \overline{A} \uparrow \overline{B} = (A \uparrow A) \uparrow (B \uparrow B). \end{aligned} \tag{E.5}$$

Due to duality, there is a second operation called NOR, which is built from the inverted propositions and inverted NAND:

$$A \downarrow B = \overline{\overline{A}\,\overline{B}} = \overline{A + B} = \overline{A}\,\overline{B}. \tag{E.6}$$

Expressing the three basic operations in terms of NOR reads to

$$\begin{aligned} \overline{A} &= \overline{A}\,\overline{A} = A \downarrow A, \\ AB &= \overline{\overline{A} + \overline{B}} = \left(\overline{A} + \overline{B}\right) \downarrow \left(\overline{A} + \overline{B}\right) = (A \downarrow B) \downarrow (A \downarrow B), \\ A + B &= \overline{\overline{A}\,\overline{B}} = \overline{A} \downarrow \overline{B} = (A \downarrow A) \downarrow (B \downarrow B). \end{aligned} \tag{E.7}$$

As already stated in the text in section 5.2.1, the logical sum and the logical product are sufficient for symbolic logic. On that basis, we developed the sum and product rule of probability theory.

E.2. Solutions to parameter estimation

For the sake of clarity, we placed the derivation of the solution of the parameter estimation in the case of a direct measurement (Sec. 5.7.1) in the appendix. We analyze N measured values, that follow a Gaussian distribution and estimate the parameter μ. We consider the three situations: First, all measured values have the same known variance. Second, the variances are equal, but they are unknown. Therefore, we derive also the posterior pdf for the variance of the data. And third, the variances are unequal, but they are known.

E.2.1. Equal and known variances

Let us assume, we estimate a parameter μ from N measured values y_i with known standard deviation σ. The posterior pdf (5.175) for the parameter μ reads

$$f(\mu|y'I) = \frac{f(\mu|I)\, P(y'|\mu I)}{P(y'|I)}. \tag{E.8}$$

Employing a Gaussian distribution for the measured values leads to

$$P(y'|yI) = \prod_{i=1}^{N} \frac{1}{\sqrt{2\pi}\sigma} \exp\left[-\frac{1}{2}\left(\frac{y_i' - \mu}{\sigma}\right)^2\right]$$
$$= \left(2\pi\sigma^2\right)^{\frac{N}{2}} \exp\left[-\frac{1}{2}\frac{\sum_i (y_i' - \mu)^2}{\sigma^2}\right]. \tag{E.9}$$

We may write the term in the exponent as

$$Q = \sum_{i=1}^{N} \left(y_i' - \mu\right)^2 = \sum_i y_i'^2 - 2N\mu\overline{y} + N\mu^2 = N\left(\mu - \overline{y}\right)^2 + N\overline{y^2} - N\overline{y}^2$$
$$= N\left[(y - \overline{y})^2 + s^2\right], \tag{E.10}$$

using the abbreviations

$$\overline{y} = \frac{1}{N}\sum_{i=1}^{N} y_i', \qquad \overline{y^2} = \frac{1}{N}\sum_{i=1}^{N} y_i'^2, \qquad s^2 = \overline{y^2} - \overline{y}^2. \tag{E.11}$$

For a uniform prior $N_y = u(y, a, b)$ for the parameter, the posterior pdf is

$$P(y|y'I) = \frac{N_y \left(2\pi\sigma^2\right)^{-\frac{N}{2}} \exp\left[-\frac{1}{2}\frac{(y-\overline{y})^2 + s^2}{\sigma^2/N}\right]}{\int_a^b \mathrm{d}y\; N_y \left(2\pi\sigma^2\right)^{-\frac{N}{2}} \exp\left[-\frac{1}{2}\frac{\left(y-\overline{d}\right)^2 + s^2}{\sigma^2/N}\right]}$$
$$= \frac{1}{\sqrt{2\pi\sigma^2/N}} \exp\left[-\frac{1}{2}\frac{(y - \overline{y})^2}{\sigma^2/N}\right]. \tag{E.12}$$

Hence, the posterior for the parameter is a Gaussian distribution and its mean value is the arithmetic mean.

E.2.2. Unequal and unknown variances

Instead of the previous case, it is more frequent, that the standard deviation of the measured values is unknown. With the results from section 5.7.1, we can also estimate the posterior pdf for the variance of the data. The joint posterior pdf of the parameter and the standard deviation is (5.179)

$$f(\mu\sigma|y'I) = \frac{f(\mu|I)\, f(\sigma|I)\, P(y'|\mu I)}{P(y'|I)}.$$

We use the same uniform prior as in the previous case for the parameter μ and a Jeffrey's prior for the standard deviation. By marginalization, the posterior pdf for μ is

$$f(\mu|y'I) = \int \mathrm{d}\sigma\; f(\mu\sigma|y'I)\,. \tag{E.13}$$

With the abbreviation Q (E.10), the likelihood is given by

$$P\left(y'\middle|\mu\sigma I\right) = (2\pi)^{-\frac{N}{2}}\sigma^{-N}\exp\left(-\frac{Q}{2\sigma^2}\right). \tag{E.14}$$

Hence, the final form of the posterior reads

$$f\left(\mu\middle|y'I\right) = \frac{\int \quad \mathrm{d}\sigma\ \sigma^{-(N+1)}\exp\left(-\frac{Q}{2\sigma^2}\right)}{\int \mathrm{d}\mu\mathrm{d}\sigma\ \sigma^{-(N+1)}\exp\left(-\frac{Q}{2\sigma^2}\right)}, \tag{E.15}$$

where the constant terms of the priors and the likelihood cancel. To solve the integrals, we apply the substitution

$$\rho = \frac{Q}{2\sigma^2}. \tag{E.16}$$

The posterior pdf becomes

$$f\left(\mu\middle|y'I\right) = \frac{\int \quad \mathrm{d}\rho\ Q^{-\frac{N}{2}}\rho^{\frac{N}{2}-1}e^{-\rho}}{\int \mathrm{d}\mu\mathrm{d}\rho\ Q^{-\frac{N}{2}}\rho^{\frac{N}{2}-1}e^{-\rho}}. \tag{E.17}$$

We can perform the integration with respect to ρ employing the incomplete gamma function. The result is not just a constant, but it depends on μ. However, using the appropriate bounds for the integration the mean value μ is approximately independent:

$$\sigma_{min} \ll s^2, \qquad \sigma_{max} \gg s^2. \tag{E.18}$$

The boundaries make use of the asymptotic behavior of the incomplete gamma function. Consequently, the posterior without the constant term reads

$$P\left(\mu\middle|y'I\right) \propto \frac{Q^{-\frac{N}{2}}}{\int \mathrm{d}\mu\ Q^{-\frac{N}{2}}}. \tag{E.19}$$

Substituting the expression (E.10) for Q we obtain

$$f\left(\mu\middle|y'I\right) \propto \left[1+\frac{(\mu-\overline{y})^2}{s^2}\right]^{-\frac{N}{2}}. \tag{E.20}$$

This particular probability distribution function is called Student's-t-distribution. Its general form is

$$f(t|\nu) = \frac{\Gamma\left(\frac{\nu+1}{2}\right)}{\sqrt{\pi\nu}\Gamma\left(\frac{\nu}{2}\right)}\left(1+\frac{t^2}{\nu}\right)^{-\frac{\nu+1}{2}}, \tag{E.21}$$

with the mean value and variance

$$\left\langle t\right\rangle = 0, \qquad \mathrm{var}(t) = \frac{\nu}{\nu-2}. \tag{E.22}$$

Making the identification

$$\nu = N - 1, \qquad \frac{t^2}{\nu} = \frac{(\mu - \overline{y})^2}{s^2}, \tag{E.23}$$

the normalized posterior pdf for μ reads

$$f(\mu|y'I) = \frac{\Gamma\left(\frac{N}{2}\right)}{\sqrt{\pi}s\Gamma\left(\frac{N+1}{2}\right)}\left[1 + \frac{(\mu - \overline{y})^2}{s^2}\right]^{-\frac{N}{2}}. \tag{E.24}$$

Thus, the mean value and variance are

$$\langle\mu\rangle = \overline{y}, \qquad \mathrm{var}(\mu) = \frac{s^2}{N-3}. \tag{E.25}$$

In addition, we are able to marginalize over μ in order to obtain the posterior pdf for the standard deviation. Analogous to (E.15), we write

$$\begin{aligned} f(\sigma|y'I) &= \frac{\int \mathrm{d}\mu \quad \sigma^{-(N+1)} \exp\left(-\frac{Q}{2\sigma^2}\right)}{\int \mathrm{d}\mu \mathrm{d}\sigma\ \sigma^{-(N+1)} \exp\left(-\frac{Q}{2\sigma^2}\right)} \\ &= \frac{\int \mathrm{d}\mu \quad \sigma^{-(N+1)} \exp\left[-\frac{N(\mu-\overline{y})^2 + Ns^2}{2\sigma^2}\right]}{\int \mathrm{d}\mu \mathrm{d}\sigma\ \sigma^{-(N+1)} \exp\left(-\frac{Q}{2\sigma^2}\right)} \\ &= \frac{\int \mathrm{d}\mu \quad \sigma^{-(N+1)} \exp\left(-\frac{Ns^2}{2\sigma^2}\right) \exp\left[-\frac{N(\mu-\overline{y})^2}{2\sigma^2}\right]}{\int \mathrm{d}\mu \mathrm{d}\sigma\ \sigma^{-(N+1)} \exp\left(-\frac{Ns^2}{2\sigma^2}\right) \exp\left[-\frac{N(\mu-\overline{y})^2}{2\sigma^2}\right]} \\ &= \frac{\sigma^{-N} \exp\left(-\frac{Ns^2}{2\sigma^2}\right)}{\int \mathrm{d}\sigma\ \sigma^{-N} \exp\left(-\frac{Ns^2}{2\sigma^2}\right)}. \end{aligned} \tag{E.26}$$

By using the definition of the gamma function, we obtain the normalization

$$\int \mathrm{d}\sigma\ \sigma^{-N} \exp\left(-\frac{Ns^2}{2\sigma^2}\right) = \frac{1}{2}\left(\frac{Ns^2}{2}\right)^{-\frac{N-1}{2}} \Gamma\left(\frac{N-1}{2}\right). \tag{E.27}$$

The resulting mean value of the standard deviation is

$$\langle\sigma\rangle = \int_0^\infty \mathrm{d}\sigma\ \sigma f(\sigma|y'I) = \sqrt{\frac{N}{2}} s \frac{\Gamma\left(\frac{N-2}{2}\right)}{\Gamma\left(\frac{N-1}{2}\right)}. \tag{E.28}$$

The mean value of the standard deviation squared is

$$\langle\sigma^2\rangle = \int_0^\infty \mathrm{d}\sigma\ \sigma^2 f(\sigma|y'I) = \frac{Ns^2}{N-3} = \frac{1}{N-3}\sum_{i=1}^{N}\left(y_i' - \overline{y}\right)^2. \tag{E.29}$$

It is quite common to use the latter two quantities to express the uncertainty in the parameter μ, although logically, this is information about the data and not the parameter μ. In fact, we are allowed to give the precise estimate (E.25).

E.2.3. Variances unequal and known

In the case of unequal but known variances, the posterior pdf (5.175) for a direct measurement is

$$f(\mu|y'I) = \frac{f(\mu|I)\, P(y'|\mu I)}{P(y'|I)}.$$

The likelihood in the given case is

$$\begin{aligned} f(y'|\mu I) &= \prod_{i=1}^{N} \frac{1}{\sqrt{2\pi\sigma_i^2}} \exp\left[-\frac{1}{2}\left(\frac{y_i' - \mu}{\sigma_i}\right)^2\right] \\ &= \left(\prod_{i=1}^{N} \frac{1}{\sigma_i}\right)\left(\frac{1}{2\pi}\right)^{\frac{N}{2}} \exp\left[-\frac{1}{2}\sum_{i=1}^{N}\left(\frac{y_i' - \mu}{\sigma_i}\right)^2\right]. \end{aligned} \tag{E.30}$$

By applying the abbreviation $w_i = 1/\sigma_i^2$ the sum in the exponent reads

$$\begin{aligned} \sum_{i=1}^{N} w_i \left(y_i' - \mu\right)^2 &= \sum \left(w_i y_i'^2 - 2\mu w_i y_i' + w_i \mu^2\right) \\ &= \left(\sum w_i\right)\left(\frac{\sum w_i y_i'^2}{\sum w_i} - 2\mu\frac{\sum w_i y_i'}{\sum w_i} + \mu^2\right) \\ &= \left(\sum w_i\right)\left(\mu - \frac{\sum w_i y_i'}{\sum w_i}\right)^2 - \frac{\left(\sum w_i y_i'\right)^2}{\sum w_i} + \sum w_i y_i'^2 \\ &= \left(\frac{\mu - \overline{y}_w}{\sigma_w}\right)^2 + C, \end{aligned} \tag{E.31}$$

where we used the definitions

$$\overline{y}_w = \frac{\sum w_i y_i'}{\sum w_i}, \qquad \sigma_w^2 = \frac{1}{\sum w_i}, \tag{E.32}$$

and a constant term C in the last step. Hence, the posterior is proportional to

$$f(\mu|y'I) \propto f(\mu|I)\left(\prod_{i=1}^{N} \frac{1}{\sigma_i}\right)(2\pi)^{-\frac{N}{2}} \exp\left[-\frac{1}{2}\left(\frac{\mu - \overline{y}_w}{\sigma_w}\right)^2\right]. \tag{E.33}$$

The normalization constant $P(D|I)$ is given by

$$f(D|I) = \int \mathrm{d}\mu\; f(\mu|I)\, P\left(y'|\mu I\right). \tag{E.34}$$

For a uniform prior in the interval $[a, b]$, we may write

$$f(\mu|y'I) = \frac{\exp\left[-\frac{1}{2}\left(\frac{\mu - \overline{y}_w}{\sigma_w}\right)^2\right]}{\int_a^b \mathrm{d}\mu\; \exp\left[-\frac{1}{2}\left(\frac{\mu - \overline{y}_w}{\sigma_w}\right)^2\right]}. \tag{E.35}$$

The posterior distribution is a Gaussian with the known mean value and variance

$$\langle \mu \rangle = \overline{y}_w, \qquad \mathrm{var}(\mu) = \sigma_w^2. \tag{E.36}$$

In order to obtain the case with equal and known variances, we set $\sigma_i = \sigma$ and obtain the same result as in section E.2.1.

E.3. Orthodox statistics

Orthodox statistics only provides the same result as probability theory for certain cases. In this section, we derive the most common procedures of orthodox statistics that are used in parameter estimation as limiting cases of probability theory. This analysis provides a detailed insight into these methods, which is not provided in most of the literature of orthodox statistics. These results allow us to apply the simple and fast procedure of orthodox statistics, when their application is justified. In all other situations, we have probability theory at hand. We start with the derivation of the uncertainties of parameters using the covariance matrix and the $\Delta\chi^2$-rule. This is followed by error propagation. In order to evaluate the quality of our estimates, we introduce the distribution of χ^2. In the end of the introduction of each procedure, we state the assumptions that went into its derivation. We also compare the results of orthodox statistics and probability theory by reanalyzing the example in section 5.9.2 comparing both methods.

E.3.1. Parameter estimation

In orthodox statistics, the mean value of the parameters are determined my maximizing the likelihood or minimizing χ^2. In the case of priors, that are constant in the regions of the highest density of the likelihood, this is equivalent to evaluating the mean values from the posterior pdf [Jef39]. However, if we have important prior information, we can not use it in orthodox statistics, because the concept of priors is completely rejected. Instead, the important object is the likelihood or χ^2. As we have seen, the likelihood itself does not possess a probabilistic interpretation. And therefore, the procedures restore interpretation by various assumptions. Unfortunately, due to the simplicity of the procedures they are implemented in almost all software for data analysis, accounting for inconsiderate use in unsuitable situations.

E.3.1.1. Covariance matrix

After determining the parameter values $\hat{\theta}$ by maximizing the likelihood or minimizing χ^2 employing a suitable numerical algorithm, we are interested in its uncertainties. The posterior pdf in the general situation derived in section 5.7.2 is

$$f\left(\theta \middle| x'y'I\right) = \frac{f(\theta|I)\, P(x'y'|\theta I)}{P(x'y'|I)}.$$

In case of a Gaussian distribution for the measured values y_i the χ^2 is given as

$$\chi^2 = \sum_{i=1}^{N} \left(\frac{y_i' - f(x_i', \theta)}{\sigma_i} \right)^2 . \tag{E.37}$$

Note, that the dependence on the parameters is not shown explicitly. Thus, for uniform priors the posterior reads

$$f\big(\theta \big| x'y'I\big) = C \cdot e^{-\frac{1}{2}\chi^2}, \tag{E.38}$$

where C is the normalization. We expand χ^2 in the vicinity of its minimum:

$$\begin{aligned} \chi^2 &= \chi^2_{\min} + \frac{1}{2} \sum_{\alpha\beta} \left. \frac{\partial^2 \chi^2}{\partial\theta_\alpha \partial\theta_\beta} \right|_{\theta=\hat{\theta}} \delta\theta_\alpha \delta\theta_\beta + \dots \\ &= \chi^2_{\min} + \Delta\chi^2 + \dots , \end{aligned} \tag{E.39}$$

using the abbreviation $\delta\theta = \theta - \hat{\theta}$. In matrix notation, we write

$$\Delta\chi^2 = \delta\theta^{\mathrm{T}} . \psi . \delta\theta, \qquad \psi_{\alpha\beta} = \frac{1}{2} \left. \frac{\partial^2 \chi^2}{\partial\theta_\alpha \partial\theta_\beta} \right|_{\theta=\hat{\theta}} . \tag{E.40}$$

Hence, the resulting posterior pdf of the parameters is

$$f\big(\theta \big| x'y'I\big) = C' e^{-\frac{1}{2}\Delta\chi^2}, \tag{E.41}$$

with the constant C' absorbing the constant term in the expansion of χ^2. In case of multivariate Gaussian distribution, the above relation is exact, because its functional form is completely determined by the first and second moment.
By marginalization, we obtain the pdf for each parameter. In order to determine the parameter errors, we have to marginalize over all other parameters. Marginalizing over the first of all M parameters leads to

$$f\big(\theta_2 \cdots \theta_M \big| x'y'I\big) = C' \int \mathrm{d}\theta_1 \; e^{-\frac{1}{2}\Delta\chi^2}. \tag{E.42}$$

In order to separate the dependence on the first parameter, we rewrite

$$\begin{aligned} \Delta\chi^2 &= \sum_{\alpha,\beta=1}^{M} \delta\theta_\alpha \psi_{\alpha\beta} \delta\theta_\beta = \psi_{11} \left(\delta\theta_1\right)^2 + 2\delta\theta_1 \sum_{\beta=2}^{M} \psi_{1\beta}\delta\theta_\beta + \sum_{\alpha,\beta=2}^{M} \delta\theta_\alpha \psi_{\alpha\beta} \delta\theta_\beta \\ &= \psi_{11} \left(\delta\theta_1 + \psi_{11}^{-1} \sum_{\beta=2}^{M} \psi_{1\beta}\delta\theta_\beta \right)^2 - \frac{1}{\psi_{11}} \left(\sum_{\beta=2}^{M} \psi_{1\beta}\delta\theta_\beta \right)^2 + \sum_{\alpha,\beta=2}^{M} \delta\theta_\alpha \psi_{\alpha\beta} \delta\theta_\beta . \end{aligned} \tag{E.43}$$

Therefore, the integration with respect to θ_1 gives a Gaussian. Using a large prior range, it is independent from the other parameters and we can absorb it into the normalization. The term for the remaining parameters in the exponential of the posterior is

$$-\frac{1}{\psi_{11}} \left(\sum_{\beta=2}^{M} \psi_{1\beta}\delta\theta_\beta \right)^2 + \sum_{\alpha,\beta=2}^{M} \delta\theta_\alpha \psi_{\alpha\beta} \delta\theta_\beta . \tag{E.44}$$

In the case of two parameters ($M = 2$) we may write

$$-\frac{1}{\psi_{11}}\left(\psi_{12}\delta\theta_2\right)^2 + \delta\theta_2\psi_{22}\delta\theta_2 = \left(\delta\theta_2\right)^2 \frac{\psi_{11}\psi_{22} - \psi_{12}^2}{\psi_{11}}. \tag{E.45}$$

Thus, the posterior distribution for the parameter θ_2 is a Gaussian

$$f\left(\theta_2 \middle| x'y'I\right) = C'' e^{-\frac{1}{2}(\delta\theta_2)^2 \frac{\psi_{11}\psi_{22}-\psi_{12}^2}{\psi_{11}}}, \tag{E.46}$$

with known mean value and variance

$$\mathrm{var}(\theta_2) = \frac{\psi_{11}}{\psi_{11}\psi_{22} - \psi_{12}^2}. \tag{E.47}$$

Repeating the procedure for the parameter θ_1, we obtain the variance

$$\mathrm{var}(\theta_1) = \frac{\psi_{11}}{\psi_{22}\psi_{22} - \psi_{12}^2}\,. \tag{E.48}$$

Hence, for M parameters, the variance for the θ_α is given by the diagonal matrix elements

$$\mathrm{var}(\theta_\alpha) = \left(\psi^{-1}\right)_{\alpha\alpha}. \tag{E.49}$$

The inverse of ψ is denoted as the covariance matrix. In probability theory, the variance of the parameters is the second central moment (5.124). Extending this definition to incorporate the non-diagonal elements of the covariance matrix, we define

$$\left(\psi^{-1}\right)_{\alpha\beta} = \left\langle \left(\theta_\alpha - \hat{\theta}_\alpha\right)\left(\theta_\beta - \hat{\theta}_\beta\right) \right\rangle = \int \mathrm{d}\theta \, \left(\theta_\alpha - \hat{\theta}_\alpha\right)\left(\theta_\beta - \hat{\theta}_\beta\right) f\left(\theta \middle| x'y'I\right). \tag{E.50}$$

For $\beta = \alpha$, we obtain the variance of the parameters. The non-diagonal entries contain information about the correlation of the parameters.
In the course of the derivation of the parameter uncertainties using the covariance matrix, we expanded χ^2 up to second order. Consequently, the result is exact only for a Gaussian posterior distribution. If not, the covariance matrix will only be an approximation for the parameter uncertainties with unknown accuracy.

E.3.1.2. $\Delta\chi^2$-rule

In addition to the covariance matrix, there is a second method defining probability intervals to estimate the parameter uncertainties. Employing the expansion of χ^2 with constant priors, the posterior (E.41) is

$$f\left(\theta \middle| x'y'I\right) = C' \exp\left(-\frac{1}{2}\Delta\chi^2\right), \qquad \Delta\chi^2 = \delta\theta^{\mathrm{T}}.\psi.\delta\theta.$$

We consider $\delta\theta$ as the new parameters. By integration of the posterior pdf with respect to $\delta\theta$ from zero to a fixed upper limit, we slightly increase the probability until we reach 1.

With increasing the distance to the minimum, we also increase $\Delta\chi^2$ to a critical upper bound denoted by $\Delta\chi^2_{\text{crit}}$. The corresponding probability is given by

$$P = \int\limits_{\Delta\chi^2<\Delta\chi^2_{\text{crit}}} \mathrm{d}\theta \; f\left(\theta\middle|x'y'I\right). \tag{E.51}$$

Using the incomplete gamma function, we have

$$P = 1 - \frac{\gamma\left(\frac{M}{2}, \frac{\Delta\chi^2_{\text{crit}}}{2}\right)}{\Gamma\left(\frac{M}{2}\right)}. \tag{E.52}$$

The idea is to fix a probability P and evaluate boundaries for the parameters by the condition

$$\delta\theta^{\mathrm{T}}.\psi.\delta\theta = \Delta\chi^2_{\text{crit}}. \tag{E.53}$$

Since the conventional applied probability is 0.683, we give the numerical solution of (E.52) in table E.1 for different numbers of parameters. Again, the procedure suffers from the ex-

M	1	2	3	4	5	6	7	8	9	10
$\Delta\chi^2_{\text{crit}}$	1.0	2.30	3.53	4.72	5.89	7.04	8.18	9.31	10.43	11.54

Table E.1.: Critical χ^2-values for P=0.683 at various degrees of freedom.

pansion of χ^2 up to second order. The solution (E.52) is only valid for a Gaussian posterior distribution. However, this problem is negligible considering the misinterpretation of the parameter intervals. To investigate this, we first consider the estimation of only one parameter. Condition (E.53) becomes

$$\frac{(\theta-\hat{\theta})^2}{\sigma^2} = 1. \tag{E.54}$$

Hence, the by plotting χ^2, we can read off the variance of the parameter as shown in figure E.1 for a Gaussian posterior with mean value zero and variance one. Since the distribution is symmetric, and Gaussian, the value at $\Delta\chi^2_{\text{crit}} = 1$ is equal to the standard deviation. However, in case of an asymmetric pdf, this procedure results in asymmetric uncertainties for the parameters as mentioned in section 5.9.4. In addition, we do not know the normalization of the distribution. Therefore, the correspondence of $\Delta\chi^2_{\text{crit}} = 1$ to a probability of 0.683 is lost. A consequence is, that the value of $\Delta\chi^2_{\text{crit}}$ is arbitrarily increased, to give a believable uncertainty. For details compare the listing in table E.1 from [D'A03]. It shows the values of the strong coupling constant α_{s} estimated by three different collaborations. Although their values of $\Delta\chi^2_{\text{crit}}$ highly differ, they obtain roughly the same uncertainty.
For two parameters and a diagonal matrix ψ, the condition (E.53) reads

$$\frac{(\theta_1-\hat{\theta}_1)^2}{\sigma_1^2} + \frac{(\theta_2-\hat{\theta}_2)^2}{\sigma_2^2} = 2.3. \tag{E.55}$$

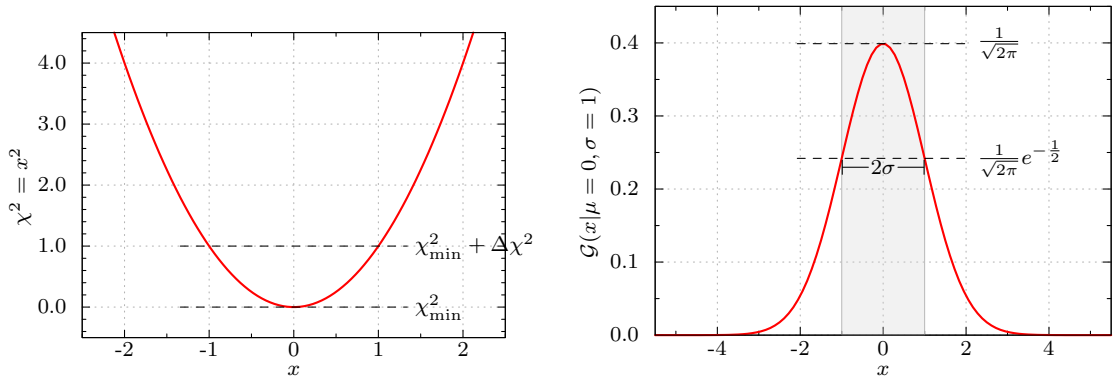

Figure E.1.: Estimate of the parameter uncertainty using the $\Delta\chi^2$-Rule for a Gaussian posterior distribution. For a single parameter $\Delta\chi^2_{\text{crit}} = 1$, the uncertainty coincides with the variance. The left panel shows χ^2 and the right one the corresponding posterior distribution.

collaboration	$\Delta\chi^2_{\text{crit}}$	$\alpha_{\text{s}}(m_{Z^0})$
CTEQ6	100	0.1165 ± 0.0065
ZEUS	50	0.1166 ± 0.0052
MRST	20	0.1190 ± 0.0036
H1	1	0.1150 ± 0.0086

Table E.2.: Numerical values for the strong coupling constant α_{s} obtained by different collaborations and their chosen values for $\Delta\chi^2_{\text{crit}}$.

Thus, the uncertainties of the parameters are provided by the major and minor semi-axes of an ellipse. The probability defined in this way is completely different than the one obtained from integration of the posterior within the interval $[\hat{\theta} - \sqrt{\text{var}(\theta)}, \hat{\theta} + \sqrt{\text{var}(\theta)}]$. As a consequence, the estimated uncertainties will have no logical connection to the variances of the posterior pdf.

E.3.2. Error propagation

The solution to error propagation is the simple formula introduced in section 5.6, as a consequence of the product rule. In orthodox statistics, the covariance matrix is also employed for error propagation. Assume, we want to evaluate the pdf for a quantity $c = F(\theta)$ from the posterior pdf $f(\theta|DI)$. According to probability theory, the result is

$$f(c|DI) = \int \mathrm{d}\theta \; \delta[c - F(\theta)] f(\theta|DI) \,.$$

To obtain the orthodox solution, we expand F to first order in every parameter θ_α:

$$F(\theta) = F(\hat{\theta}) + \sum_{\alpha}^{M} \frac{\partial F\left(\hat{\theta}\right)}{\partial \theta_\alpha}(\theta - \hat{\theta})_\alpha + \dots . \tag{E.56}$$

Using this expansion and neglecting the higher order terms, the mean value of the distribution $f(c|DI)$ is given by

$$\langle c \rangle = F(\hat{\theta}). \tag{E.57}$$

The second central moment is

$$\langle c^2 \rangle = F^2(\hat{\theta}) + \sum_{\alpha}^{M}\sum_{\beta}^{M} \frac{\partial^2 F(\hat{\theta})}{\partial \theta_\alpha \partial \theta_\beta} \langle (\theta - \hat{\theta})_\alpha (\theta - \hat{\theta})_\beta \rangle. \tag{E.58}$$

Hence, the variance of the function F deduced from the uncertainties in the parameters using the covariance matrix (E.50) is

$$\mathrm{var}(c) = J^{\mathrm{T}}.\left(\psi^{-1}\right).J, \tag{E.59}$$

where we used the Jacobian J of the function F for a compact notation. This is the most common formula for error propagation. Let us recall the assumptions for this formula.
In addition to the complications of expanding χ^2, we are only considering the first order expansion of F. This further limits the range of applicability.

E.3.3. Hypothesis test

For the purpose of testing hypotheses or evaluating the goodness-of-fit, orthodox statistics applies the χ^2 statistic. From (E.37), χ^2 is defined as

$$\chi^2 = \sum_{i=1}^{N} \left(\frac{y_i - f(x_i, \theta)}{\sigma_i} \right)^2 .$$

We will now evaluate the distribution of the obtained χ^2 values from a parameter estimation. If the measured values follow a Gaussian distribution, also the quantity

$$z = \frac{y - f(x)}{\sigma} \tag{E.60}$$

will have a Gaussian distribution. In order to obtain the desired distribution of the χ^2 values we consider the quantity

$$v = \left(\frac{y - f(x, \theta)}{\sigma} \right)^2 = z^2. \tag{E.61}$$

Thus, the corresponding pdf is given by

$$f(v) = \int \mathrm{d}z\, \delta\left(v - z^2\right) \frac{1}{\sqrt{2\pi}} e^{-\frac{z^2}{2}} = \frac{1}{\sqrt{2\pi}} v^{-\frac{1}{2}} e^{-\frac{v}{2}}. \tag{E.62}$$

This is the χ^2-distribution for $N = 1$. For an arbitrary number of experimental values the general form is

$$\mathcal{X}(u|\nu) = \frac{1}{\Gamma\left(\frac{\nu}{2}\right) 2^{\frac{\nu}{2}}} u^{\frac{\nu}{2}-1} e^{-\frac{u}{2}}, \tag{E.63}$$

with mean value and variance

$$\left\langle x \right\rangle = \nu\,, \qquad \mathrm{var}(x) = 2\nu\,. \tag{E.64}$$

The quantity ν denotes the degrees of freedom. In the expression above, we have to set $\nu = N - 1$. However, we did not consider the distribution of the parameters in the model. Choosing the M parameters in a way, that they eliminate M experimental values, we have $\nu = N - M$ degrees of freedom.
Applying the statistics allows us to evaluate how far in the tail region of the χ^2-distribution the observed value value χ^2_{obs} lies. To characterize this, we evaluate the probability also denoted as p-value by

$$\text{p-value} = P\left(\chi^2_{\mathrm{obs}} \leq \chi^2\right) = \int\limits_{\chi^2_{\mathrm{obs}}}^{\infty} \mathrm{d}x\, \mathcal{X}(x|N-M)\,. \tag{E.65}$$

Strictly speaking, this is the probability to obtain a χ^2-value larger that the current one in a new conduction of the same experiment. Therefore, the probability is a statement about future experiments, which are not done or never will be done. Furthermore, this probability is used to evaluate the validity of the hypothesis by the probability (1 − p-value).
Analogously to the meaning of (E.65), this is the probability to obtain χ^2-values smaller than the observed one in an identical repetition of the experiment. Logically, we are not allowed to state that the probability to accept the hypothesis is equal to (1 − p-value). As seen in section 5.4, we are only able to evaluate the probability for a hypothesis in comparison to at least one concurring hypothesis.
Since the expectation value of the χ^2 distribution is equal to the degree of freedom (d.o.f.), frequently, the quantity

$$\frac{\chi^2}{\text{d.o.f.}} \tag{E.66}$$

is used to characterize the goodness of a parameter estimation. If the value is far below one, the model is considered too complicated for the data, whereas a large value leads to the rejection of the model. However, the exact values for rejection are unknown. For example, we consider the example about the Higgs boson in section 5.9.3. For the model H with the peak, we have $\chi^2/\text{d.o.f.} = 0.74$ and for the background only model $\overline{H}$ it is $\chi^2/\text{d.o.f.} = 0.88$. Therefore, the first model is slightly better, but it is unclear how to quantify the correct one. The corresponding p-values are 0.95 and 0.73 for the hypotheses H and $\overline{H}$, respectively. Using this approach, it is very demanding to introduce the look-elsewhere effect, that is a natural consequence of probability theory.

E.3.4. Opposing example

In this section, we reanalyze the example of a nonlinear model in section 5.9.2 using both orthodox statistics and probability theory to work out the differences. From the posterior distribution, we derived the estimates of the parameters as

$$a = 2.777 \pm 0.686, \qquad b = 0.984 \pm 0.077, \tag{E.67}$$

written in the notation introduced in section 5.5.1.1. On the other hand, by maximizing the likelihood and evaluating the parameter uncertainties by the covariance matrix, we obtain

$$a = 2.467 \pm 0.856, \qquad b = 1.007 \pm 0.100. \tag{E.68}$$

The final estimates do not seem to differ that much. However, the posterior pdfs (fig. E.2) differ significantly. Especially, the pdf for the parameter a is very different from a Gaussian

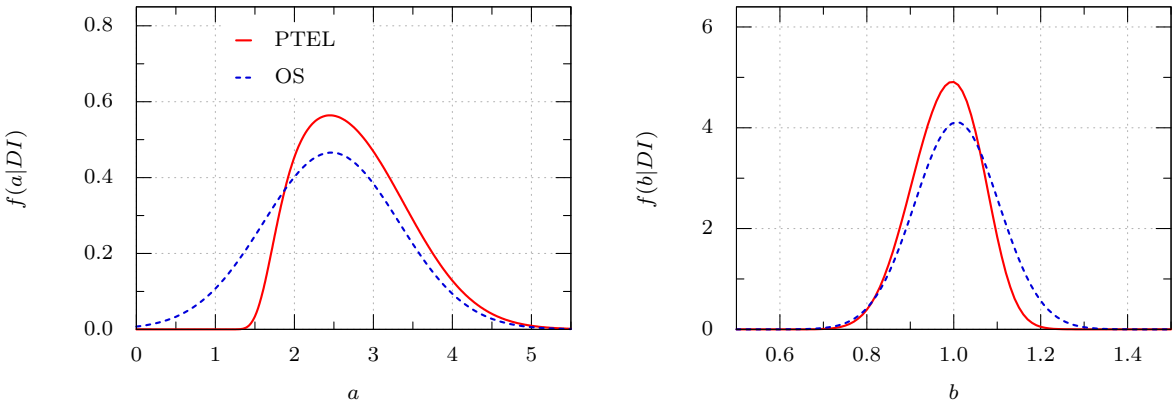

Figure E.2.: Probability distribution function for the parameters a and b obtained from orthodox statistics and probability theory.

distribution.
Finally, we consider the error propagation from the posterior pdf to the model h itself. As in the example, we evaluate the pdf for the quantity $c = h(x = 0.5, a, b)$. By probability theory, the estimate is

$$c = 0.080 \pm 0.031. \tag{E.69}$$

Whereas, orthodox statistics estimates it as

$$c = 0.090 \pm 0.048. \tag{E.70}$$

Figure E.3 shows the corresponding distributions, which are quite different.
To compare the accuracy of both results, we plot the function h with propagated uncertainties in figure E.4. The crossed area corresponds to the interval bounded by the mean value and the square root of the variance. This example was generated in a way to show the difference of the two approaches. Equally well, we could have constructed an example without any difference in the result or where the differences are even more dramatic. Using probability theory, we are always save, since we obtain the full posterior distribution.

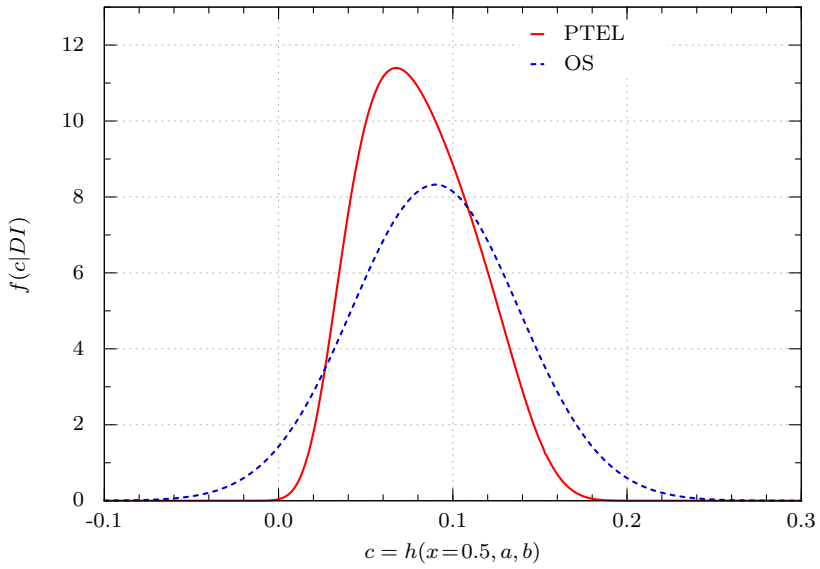

Figure E.3.: Probability distribution function for $h(x = 0.5, a, b)$ obtained from orthodox statistics and probability theory.

E.4. Markov chain Monte Carlo

In this thesis, we employ a Markov chain Monte Carlo in particular the Metropolis-Hastings algorithm [Has70] to sample the posterior distribution $f(\theta|DI)$, where θ is a vector representation of the parameters of the respective model. Let us outline the algorithm in the following. First, we have to set a initialization values of the parameters. The initial values are denoted as θ^0. Note, that the upper Greek index denotes a individual item of the Markov chain, whereas a lower roman index denotes a component of the parameter vector. The new sample ι is generated from the proposal distribution $f(\iota|\theta^\alpha)$. The acceptance of the new sample is given by the Metropolis ratio

$$r = \frac{f(\iota|DI)}{f(\theta^\alpha|DI)}\,, \tag{E.71}$$

where we assumed that we utilize a symmetric proposal distribution. If $r \geq 1$, the new sample is accepted $\theta^{\alpha+1} = \iota$. If $r < 1$, the sample ι is accepted by drawing a random variable u from a uniform distribution in the interval $[0, 1]$. If $u \leq r$ the sample is accepted $\theta^{\alpha+1} = \iota$ otherwise we draw a new sample ι from the proposal distribution $f(\iota|\theta^\alpha)$. In general, the second step is summarized in the acceptance probability

$$\alpha\left(\theta^\alpha, \iota\right) = \min(1, r)\,. \tag{E.72}$$

The finding of an optimal proposal distribution as very intricate. In this thesis, we utilize a Gaussian proposal distributions for all parameters. Therefore, we have to optimize the corresponding standard deviations. The samples of the resulting Markov chain are in general

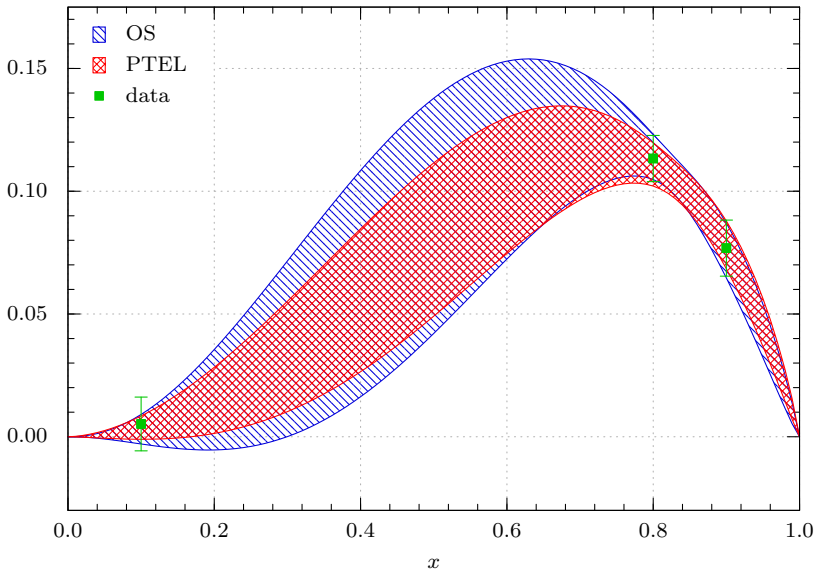

Figure E.4.: Probability distribution function for $h(x, a, b)$ obtained from orthodox statistics and probability theory.

correlated. A measure for the correlations is the autocorrelation function of the parameter θ_i

$$\rho(\beta) = \frac{\sum_{\alpha=1}^{N-\beta} \left(\theta^{\alpha} - \mu_i\right)\left(\theta_i^{\alpha+\beta} - \mu_i\right)}{\sqrt{\sum_{\alpha=1}^{N-\beta} \left(\theta_i^{\alpha} - \mu_i\right)^2} \cdot \sqrt{\sum_{\alpha=1}^{N-\beta} \left(\theta_i^{\alpha+\beta} - \mu_i\right)^2}}, \tag{E.73}$$

where the argument β is denoted as lag and N is the length of the Markov chain. μ_i is the arithmetic mean of all samples of the Markov chain for the parameter θ_i. A introduction to the use of a the Markov chain Monte Carlo in PTEL is for example found in [Gre05].

F

Markov chains

In this chapter, we list the properties of the utilized Markov chains in this thesis to ensure the reproducibility of the estimates. As pointed out in Sec. E.4 the Metropolis-Hastings algorithm requires the proposal distribution and the starting position. We utilize a Gaussian distribution for the proposal distribution. Thus, we have to adjust the respective standard deviations individually for each parameter. The adjustment of the standard deviations is the crucial part, especially with a large amount of parameters. For all Markov chains, we give the generic starting position, the starting position to cut off the burn in phase and the standard deviations of the Gaussian proposal distributions to obtain a new sample.
It is of utter importance to control the properties of the resulting Markov chain, to evaluate if the result is trustworthy. In this thesis, we utilize the autocorrelation of the parameters and the the convergence of the mean value of the parameters with increasing length of the parameters. The autocorrelation (E.73) has to fall off to zero as fast as possible. Due to the large amount of parameters and the strong correlations, this requirement is the hardest to meet. For all Markov chains, we require the autocorrelations of the parameters to fall off to zero within the lag 10. We disclaim on showing the convergence of the parameter mean values, albeit the length of ~ 3000 samples of each individual Markov chains ensures the convergence.

F.1. Estimates for data set A

For the DIS estimate in Sec. 7.4 we analyze in total three scenarios. The estimates were denoted as

$$\text{R-l-A-LO}\,, \qquad \text{R-l-A-NLO}\,, \qquad \text{R}^*\text{-l-A-LO}\,, \qquad \text{R}^*\text{-l-A-NLO}\,,$$

where we utilize the nomenclature introduced in (7.1). The Markov chain parameters of the three DIS estimates are given in the tables F.1, F.2, F.3 and F.4, respectively. The autocorrelations of the parameters are shown in Fig. F.1.

parameter	generic start	burn in start	σ
N^{sea}	0.17	0.148689	0.00388004
N^{G}	0.43	0.460155	0.00976808
α^{sea}	1.2	1.162310	0.00670465
α^{G}	1.2	1.234630	0.01314340

Table F.1.: Generic start, burn in start and standard deviation of the Gaussian proposal distribution for all parameters of the estimate R-l-A-LO.

parameter	generic start	burn in start	σ
N^{sea}	0.17	0.174348	0.00458778
N^{G}	0.43	0.429345	0.00948346
α^{sea}	1.2	1.08956	0.00879991
α^{G}	1.2	1.18893	0.0196156

Table F.2.: Generic start, burn in start and standard deviation of the Gaussian proposal distribution for all parameters of the estimate R-l-A-NLO.

parameter	generic start	burn in start	σ
N^{sea}	0.17	0.154668	0.00391536
α^{sea}	1.2	1.13862	0.00864402
α^{G}	1.2	1.28242	0.0152018

Table F.3.: Generic start, burn in start and standard deviation of the Gaussian proposal distribution for all parameters of the estimate R*-l-A-LO.

parameter	generic start	burn in start	σ
N^{sea}	0.17	0.174348	0.00458778
α^{sea}	1.2	1.08956	0.00879991
α^{G}	1.2	1.18893	0.0196156

Table F.4.: Generic start, burn in start and standard deviation of the Gaussian proposal distribution for all parameters of the estimate R*-l-A-NLO.

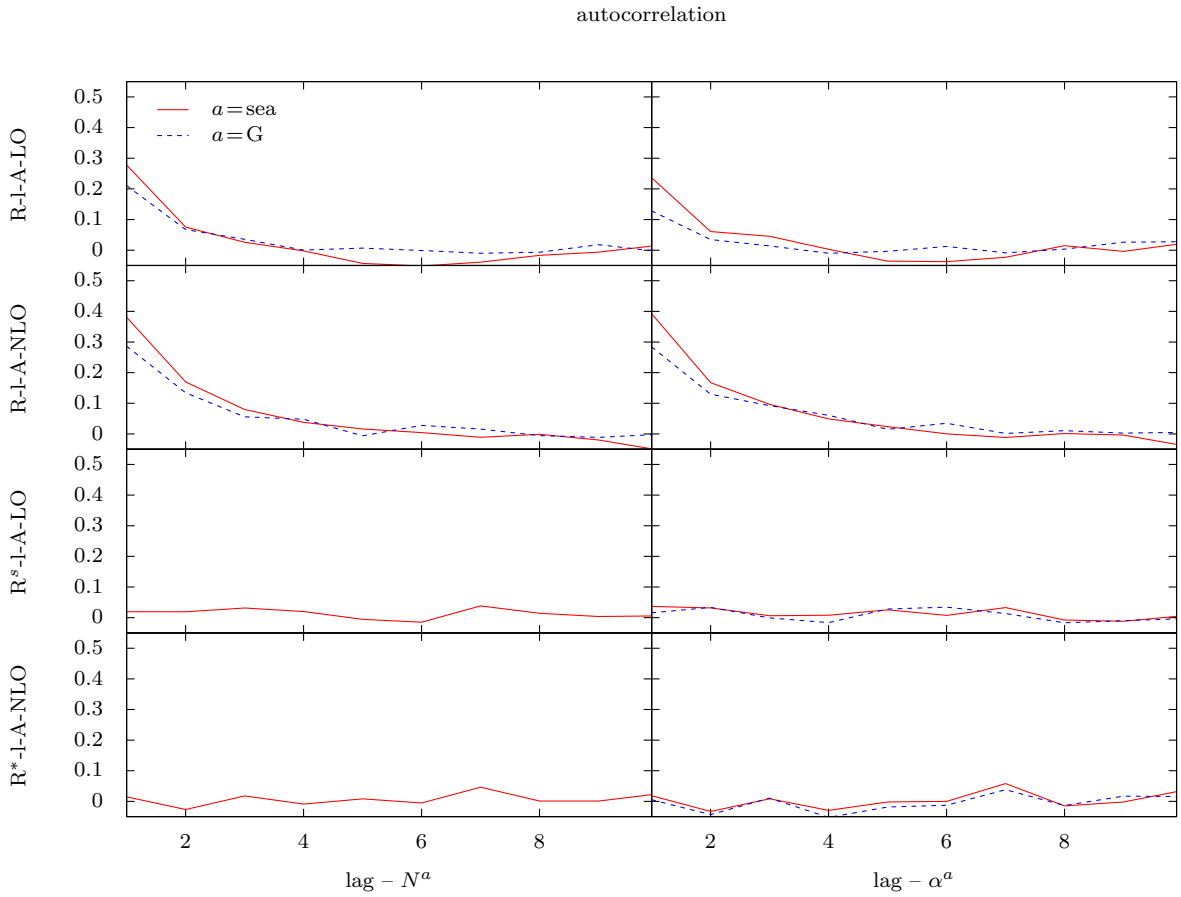

Figure F.1.: Autocorrelations of the parameters of the estimates for the data set A.

F.2. Estimates for data set B

The estimate of the DIS and DVCS data set B in Sec. 7.5 are

R-nl-Et-B-LO , R-nl-Et-B-NLO , R-nl-Dt-B-LO , R-nl-Dt-B-NLO .

The parameters of the respective Markov chains are given in the tables F.5, F.6, F.7 and F.8. The autocorrelations of the parameters are shown in Fig. F.2.

parameter	generic start	burn in start	σ
N^{sea}	0.17	0.136671	0.00165599
N^{G}	0.43	0.466149	0.00251744
α^{sea}	1.2	1.16054	0.00219274
α^{G}	1.2	1.23093	0.00504098
$\alpha'^{,\mathrm{sea}}$	0.15	0.138288	0.00738642
$\alpha'^{,\mathrm{G}}$	0.15	0.153525	0.00953638
B^{sea}	2	2.02935	0.0373226
B^{G}	2	3.76255	0.106067
N_1^{sea}	0	-0.0240987	0.000469334
N_1^{G}	0	-0.315128	0.00789062
ν_X^{H}	1	1.05998	0.0062061

Table F.5.: Generic start, burn in start and standard deviation of the Gaussian proposal distribution for all parameters of the estimate R-nl-Et-B-LO.

parameter	generic start	burn in start	σ
N^{sea}	0.17	0.142174	0.00113298
N^{G}	0.43	0.464237	0.00216682
α^{sea}	1.2	1.13175	0.00141886
α^{G}	1.2	1.06075	0.0037534
$\alpha'^{,\mathrm{sea}}$	0.15	0.104627	0.00711436
$\alpha'^{,\mathrm{G}}$	0.15	0.132649	0.00958896
B^{sea}	2	2.49813	0.0381988
B^{G}	2	2.57218	0.0715324
N_1^{sea}	0	0.0128424	0.00058331
N_1^{G}	0	0.105169	0.0101253
ν_X^{H}	1	1.07973	0.00496088

Table F.6.: Generic start, burn in start and standard deviation of the Gaussian proposal distribution for all parameters of the estimate R-nl-Et-B-NLO.

parameter	generic start	burn in start	σ
N^{sea}	0.17	0.138031	0.00168611
N^{G}	0.43	0.465442	0.00260904
α^{sea}	1.2	1.15728	0.00229992
α^{G}	1.2	1.24026	0.00499264
$\alpha'^{,\text{sea}}$	0.15	0.177181	0.00662886
$\alpha'^{,\text{G}}$	0.15	0.141191	0.0093687
$M^{2,\text{sea}}$	0.7	0.655927	0.016313
$M^{2,\text{G}}$	0.7	0.346512	0.0131062
N_1^{sea}	0	-0.0211774	0.000460932
N_1^{G}	0	-0.265992	0.00947816
ν_X^{H}	1	1.05353	0.00604512

Table F.7.: Generic start, burn in start and standard deviation of the Gaussian proposal distribution for all parameters of the estimate R-nl-Dt-B-LO.

parameter	generic start	burn in start	σ
N^{sea}	0.17	0.138244	0.000977568
N^{G}	0.43	0.47139	0.00173722
α^{sea}	1.2	1.13748	0.00104262
α^{G}	1.2	1.04458	0.00292014
$\alpha'^{,\text{sea}}$	0.15	0.160316	0.00472457
$\alpha'^{,\text{G}}$	0.15	0.116541	0.00698287
$M^{2,\text{sea}}$	0.7	0.554092	0.00892728
$M^{2,\text{G}}$	0.7	0.444315	0.0151809
N_1^{sea}	0	0.0220089	0.00065668
N_1^{G}	0	0.246382	0.0164396
ν_X^{H}	1	1.08882	0.0044403

Table F.8.: Generic start, burn in start and standard deviation of the Gaussian proposal distribution for all parameters of the estimate R-nl-Dt-B-NLO.

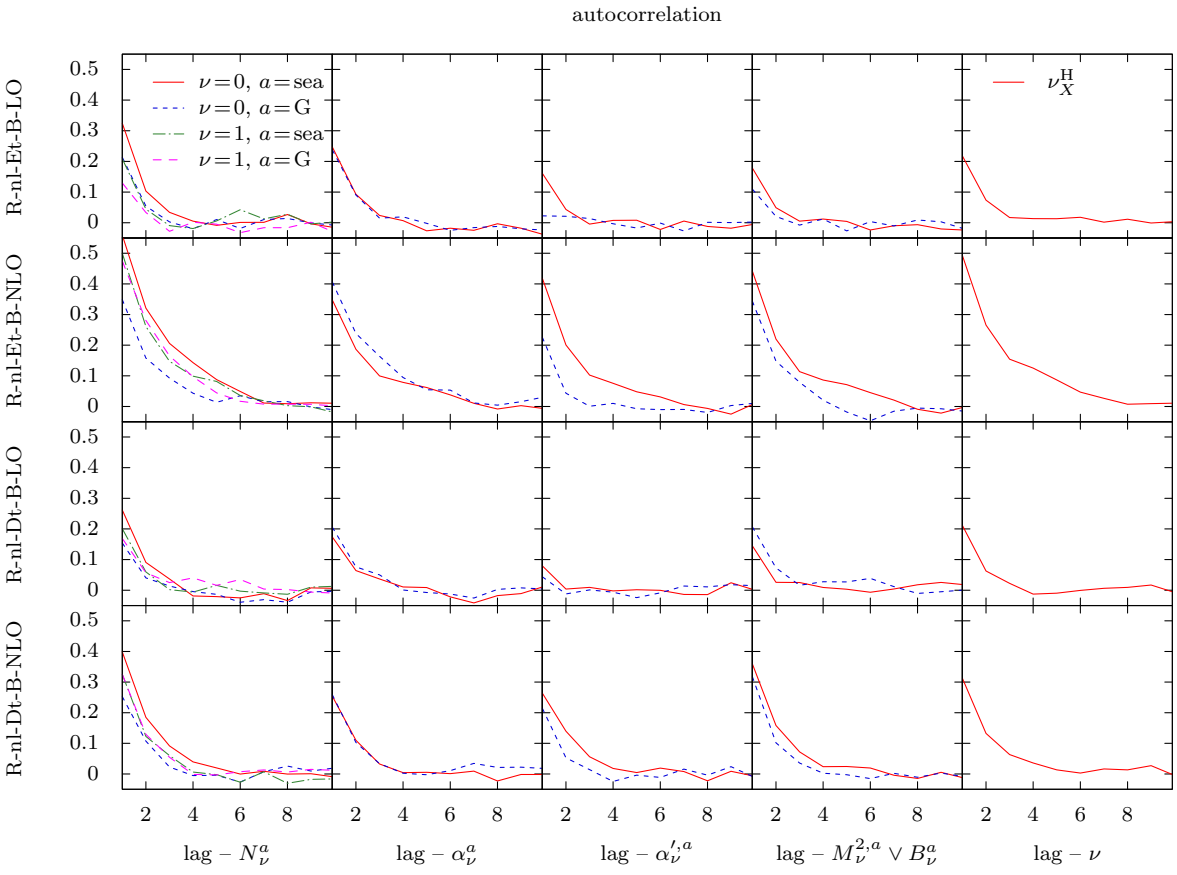

Figure F.2.: Autocorrelations of the parameters of the estimates for the data set B.

F.3. Estimates for data set C

The estimate of the DIS, DVCS and DVMP data set C in Sec. 7.6 is

F-nnl-Dt-C-NLO .

The parameters of the respective Markov chains are given in table F.9. The autocorrelations of the parameters are shown in Fig. F.3.

parameter	generic start	burn in start	σ
N_0^{sea}	0.17	0.183132	0.000140946
N_0^{G}	0.43	0.394101	0.000198819
α_0^{sea}	1.2	1.09112	0.0001261
α_0^{G}	1.2	1.2155	0.000180174
$\alpha'^{,\mathrm{sea}}$	0.15	0.12866	0.000524996
$\alpha'^{,\mathrm{G}}$	0.15	0.0560238	0.000543521
$M_0^{2,\mathrm{sea}}$	0.7	0.77714	0.00183751
$M_0^{2,\mathrm{G}}$	0.7	0.50211	0.000639303
$M_1^{2,\mathrm{sea}}$	0.7	0.873051	0.00244398
$M_1^{2,\mathrm{G}}$	0.7	0.652112	0.00124814
N_1^{sea}	0	-0.148904	0.000341933
N_1^{G}	0	-0.288602	0.000552088
α_1^{sea}	1.2	0.957386	0.00038308
α_1^{G}	1.2	1.10742	0.000371722
$M_2^{2,\mathrm{sea}}$	0.7	0.69556	0.00166553
$M_2^{2,\mathrm{G}}$	0.7	0.718613	0.00153136
N_2^{sea}	0	0.026834	0.0000634117
N_2^{G}	0	0.0655444	0.000159079
α_2^{sea}	1.2	1.08425	0.000168532
α_2^{G}	1.2	1.19647	0.000237432
ν_X^{H}	1	0.987578	0.000421478
$\nu_{\rho^0}^{\mathrm{H}}$	1	1.01709	0.000464933
$\nu_{\rho^0}^{\mathrm{Z}}$	1	1.0698	0.000503358
ν_{ϕ}^{H}	1	0.719916	0.000443715
ν_{ϕ}^{Z}	1	0.926396	0.000529983

Table F.9.: Generic start, burn in start and standard deviation of the Gaussian proposal distribution for all parameters of the estimate F-nnl-Dt-C-NLO.

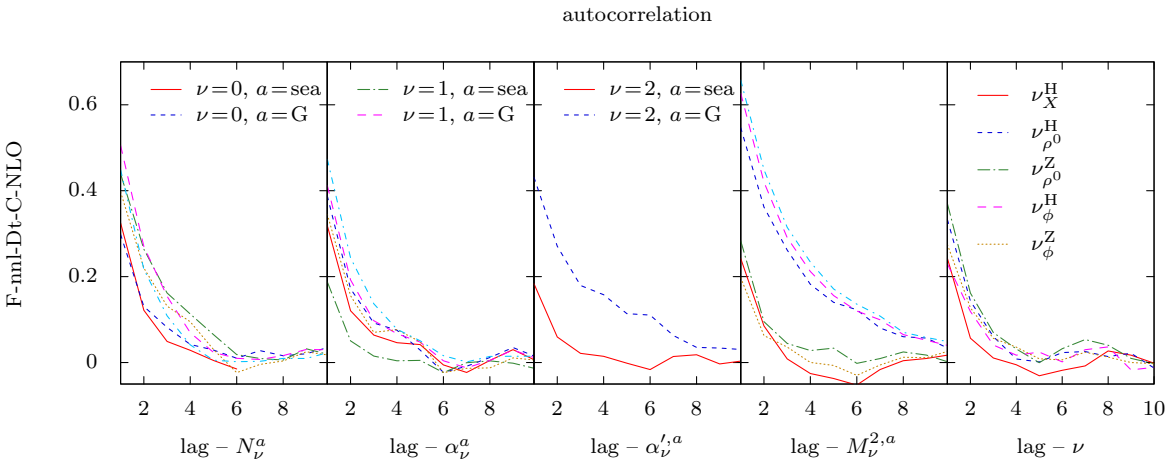

Figure F.3.: Autocorrelations of the parameters of the estimate for the data set C.

List of symbols

cdf cumulative distribution function

CFF Compton form factor

COPE conformal operator product expansion

COPE conformal operator product expansion

d.o.f. degrees of freedom

DA distribution amplitude

DIS deeply inelastic scattering

DVCS deeply virtual Compton scattering

DVMP deeply virtual meson production

F false

GPD generalized parton distribution

LIPS Lorentz invariant phase space

OPE operator product expansion

OS orthodox statistics

PDF parton distribution function

pdf probability distribution function

PTEL probability theory as extended logic

QCD quantum chromodynamics

T true

TFF transition form factor

Index

Acknowledgments

First of all, I want to thank Prof. Dr. Andreas Schäfer for giving me the opportunity to work on the highly interesting topic of this thesis and to follow my research interests under his guidance.
Furthermore, I am indebted to Dr. Dieter Müller for instructing this work. Without his deep knowledge about physics this thesis would not have been possible. I am grateful to Dr. Kornelija Passek-Kumerički and Dr. Krešimir Kumerički for all the interesting discussions. Moreover, I appreciate the feedback offered by Dr. Markus Diehl.
Thanks go to Monika Maschek for taking care of all administrative issues. In addition, a thank you to the Institute of Theoretical Physics II at the University Bochum and the Theoretical Physics Division at the Rudjer Bošković Institute in Zagreb for the hospitality during the conduction of this thesis. Moreover, I am grateful for the support by the German Ministry of Science and Education (BMBF grant OR 06RY9191 and 05P12WRFTE). I also want to thank Johannes Thalmayr and Florian Porkert for proofreading the manuscript.
I would like to acknowledge the support provided by my family during the preparation of my dissertation. Last but not least, I want to thank my wife Kathrin Graf.

References

[A+94] M. Arneodo et al., *Exclusive ρ^0 and ϕ muoproduction at large Q^2*, Nucl.Phys. **B429**, 503–529 (1994).

[A+96a] S. Aid et al., *A Measurement and QCD analysis of the proton structure function $F_2(x, Q^2)$ at HERA*, Nucl.Phys. **B470**, 3–40 (1996), hep-ex/9603004.

[A+96b] S. Aid et al., *Elastic electroproduction of ρ^0 and J/ψ mesons at large Q^2 at HERA*, Nucl.Phys. **B468**, 3–36 (1996), hep-ex/9602007.

[A+97a] M. Adams et al., *Diffractive production of $\rho^0(770)$ mesons in muon proton interactions at* 470 GeV, Z.Phys. **C74**, 237–261 (1997).

[A+97b] C. Adloff et al., *Proton dissociative ρ and elastic ϕ electroproduction at HERA*, Z.Phys. **C75**, 607–618 (1997), hep-ex/9705014.

[A+00a] C. Adloff et al., *Elastic electroproduction of ρ mesons at HERA*, Eur.Phys.J. **C13**, 371–396 (2000), hep-ex/9902019.

[A+00b] C. Adloff et al., *Elastic photoproduction of J/ψ and Υ mesons at HERA*, Phys.Lett. **B483**, 23–35 (2000), hep-ex/0003020.

[A+00c] A. Airapetian et al., *Exclusive leptoproduction of ρ^0 mesons from hydrogen at intermediate virtual photon energies*, Eur.Phys.J. **C17**, 389–398 (2000), hep-ex/0004023.

[A+01] C. Adloff et al., *Measurement of deeply virtual Compton scattering at HERA*, Phys.Lett. **B517**, 47–58 (2001), hep-ex/0107005.

[A+05] A. Aktas et al., *Measurement of deeply virtual compton scattering at HERA*, Eur.Phys.J. **C44**, 1–11 (2005), hep-ex/0505061.

[A+06] A. Aktas et al., *Elastic J/ψ Production at HERA*, Eur.Phys.J. **C46**, 585–603 (2006), hep-ex/0510016.

[A+08a] F. Aaron et al., *Measurement of deeply virtual Compton scattering and its t-dependence at HERA*, Phys.Lett. **B659**, 796–806 (2008), 0709.4114.

[A+08b] A. Airapetian et al., *Cross-sections for hard exclusive electroproduction of π^+ mesons on a hydrogen target*, Phys.Lett. **B659**, 486–492 (2008), 0707.0222.

[A+09a] F. Aaron et al., *Deeply Virtual Compton Scattering and its Beam Charge Asymmetry in $e^{\pm}p$ Collisions at HERA*, Phys.Lett. **B681**, 391–399 (2009), 0907.5289.

[A+09b] A. Airapetian et al., *Exclusive ρ^0 electroproduction on transversely polarized protons*, Phys.Lett. **B679**, 100–105 (2009), 0906.5160.

[A+10a] F. Aaron et al., *Combined Measurement and QCD Analysis of the Inclusive $e^{\pm}p$ Scattering Cross Sections at HERA*, JHEP **1001**, 109 (2010), 0911.0884.

[A+10b] F. Aaron et al., *Diffractive Electroproduction of ρ and ϕ Mesons at HERA*, JHEP **1005**, 032 (2010), 0910.5831.

[A+10c] A. Airapetian et al., *Single-spin azimuthal asymmetry in exclusive electroproduction of π^+ mesons on transversely polarized protons*, Phys.Lett. **B682**, 345–350 (2010), 0907.2596.

[A+12] G. Aad et al., *Observation of a new particle in the search for the Standard Model Higgs boson with the ATLAS detector at the LHC*, Phys.Lett. **B716**, 1–29 (2012), 1207.7214.

[AAA+12] C. Adolph, M. Alekseev, V. Y. Alexakhin, Y. Alexandrov, G. Alexeev et al., *Exclusive ρ^0 muoproduction on transversely polarised protons and deuterons*, Nucl.Phys. **B865**, 1–20 (2012), 1207.4301.

[Ale03] S. Alekhin, *Parton distributions from deep inelastic scattering data*, Phys.Rev. **D68**, 014002 (2003), hep-ph/0211096.

[APT00] I. Anikin, B. Pire and O. Teryaev, *On the gauge invariance of the DVCS amplitude*, Phys.Rev. **D62**, 071501 (2000), hep-ph/0003203.

[AS12] M. Abramowitz and I. Stegun, *Handbook of Mathematical Functions: with Formulas, Graphs, and Mathematical Tables*, Dover Books on Mathematics, Dover Publications, 2012.

[B+99] J. Breitweg et al., *Exclusive electroproduction of ρ^0 and J/ψ mesons at HERA*, Eur.Phys.J. **C6**, 603–627 (1999), hep-ex/9808020.

[B+00] J. Breitweg et al., *Measurement of exclusive ω electroproduction at HERA*, Phys.Lett. **B487**, 273–288 (2000), hep-ex/0006013.

[B+08] H. Blok et al., *Charged pion form factor between $Q^2 = 0.60$ and $2.45\,\mathrm{GeV}^2$. I. Measurements of the cross section for the ${}^1H(e, e'\pi^+)n$ reaction*, Phys.Rev. **C78**, 045202 (2008), 0809.3161.

[B+12a] I. Bedlinskiy et al., *Measurement of Exclusive π^0 Electroproduction Structure Functions and their Relationship to Transversity GPDs*, Phys.Rev.Lett. **109**, 112001 (2012), 1206.6355.

[B+12b] J. Beringer et al., *Review of Particle Physics (RPP)*, Phys.Rev. **D86**, 010001 (2012).

[BB96] P. Ball and V. M. Braun, *The ρ Meson Light-Cone Distribution Amplitudes of Leading Twist Revisited*, Phys. Rev. **D54**, 2182–2193 (1996), hep-ph/9602323.

[BBDM78] W. A. Bardeen, A. Buras, D. Duke and T. Muta, *Deep Inelastic Scattering Beyond the Leading Order in Asymptotically Free Gauge Theories*, Phys.Rev. **D18**, 3998 (1978).

[BBKT98] P. Ball, V. M. Braun, Y. Koike and K. Tanaka, *Higher twist distribution amplitudes of vector mesons in QCD: Formalism and twist - three distributions*, Nucl.Phys. **B529**, 323–382 (1998), hep-ph/9802299.

[BDKM99] V. M. Braun, S. E. Derkachov, G. Korchemsky and A. Manashov, *Baryon distribution amplitudes in QCD*, Nucl.Phys. **B553**, 355–426 (1999), hep-ph/9902375.

[BdT04] S. J. Brodsky and G. F. de Teramond, *Light front hadron dynamics and AdS/CFT correspondence*, Phys.Lett. **B582**, 211–221 (2004), hep-th/0310227.

[BGR99] J. Blumlein, B. Geyer and D. Robaschik, *The Virtual Compton amplitude in the generalized Bjorken region: twist-2 contributions*, Nucl.Phys. **B560**, 283–344 (1999), hep-ph/9903520.

[Bjo69] J. Bjorken, *Asymptotic Sum Rules at Infinite Momentum*, Phys.Rev. **179**, 1547–1553 (1969).

[BK99] J. Blumlein and S. Kurth, *Harmonic sums and Mellin transforms up to two-loop order*, Phys. Rev. **D60**, 014018 (1999), hep-ph/9810241.

[BKM03] V. M. Braun, G. P. Korchemsky and D. Müller, *The uses of conformal symmetry in QCD*, Prog. Part. Nucl. Phys. **51**, 311–398 (2003), hep-ph/0306057.

[Blu13] J. Blumlein, *The Theory of Deeply Inelastic Scattering*, Prog.Part.Nucl.Phys. **69**, 28–84 (2013), 1208.6087.

[BM98a] A. V. Belitsky and D. Müller, *Next-to-leading order evolution of twist-2 conformal operators: The Abelian case*, Nucl.Phys. **B527**, 207–234 (1998), hep-ph/9802411.

[BM98b] A. V. Belitsky and D. Müller, *Predictions from conformal algebra for the deeply virtual Compton scattering*, Phys.Lett. **B417**, 129–140 (1998), hep-ph/9709379.

[BM99] A. V. Belitsky and D. Müller, *Broken conformal invariance and spectrum of anomalous dimensions in QCD*, Nucl.Phys. **B537**, 397–442 (1999), hep-ph/9804379.

[BM00] A. V. Belitsky and D. Müller, *Twist- three effects in two photon processes*, Nucl.Phys. **B589**, 611–630 (2000), hep-ph/0007031.

[BM01] A. V. Belitsky and D. Müller, *Hard exclusive meson production at next-to-leading order*, Phys. Lett. **B513**, 349–360 (2001), hep-ph/0105046.

[BM09] C. Bechler and D. Müller, *Generic modelling of non-perturbative quantities and a description of hard exclusive π^+ electroproduction*, (2009), 0906.2571.

[BM11] V. Braun and A. Manashov, *Kinematic power corrections in off-forward hard reactions*, Phys.Rev.Lett. **107**, 202001 (2011), 1108.2394.

[BM12] V. Braun and A. Manashov, *Operator product expansion in QCD in off-forward kinematics: Separation of kinematic and dynamical contributions*, JHEP **1201**, 085 (2012), 1111.6765.

[BMK02] A. V. Belitsky, D. Müller and A. Kirchner, *Theory of deeply virtual Compton scattering on the nucleon*, Nucl.Phys. **B629**, 323–392 (2002), hep-ph/0112108.

[BMNS99] A. V. Belitsky, D. Müller, L. Niedermeier and A. Schäfer, *Evolution of nonforward parton distributions in next-to-leading order: Singlet sector*, Nucl.Phys. **B546**, 279–298 (1999), hep-ph/9810275.

[BMNS00] A. V. Belitsky, D. Müller, L. Niedermeier and A. Schäfer, *Deeply virtual Compton scattering in next-to-leading order*, Phys.Lett. **B474**, 163–169 (2000), hep-ph/9908337.

[BMP12a] V. Braun, A. Manashov and B. Pirnay, *Finite-t and target mass corrections to deeply virtual Compton scattering*, Phys.Rev.Lett. **109**, 242001 (2012), 1209.2559.

[BMP12b] V. Braun, A. Manashov and B. Pirnay, *Finite-t and target mass corrections to DVCS on a scalar target*, Phys.Rev. **D86**, 014003 (2012), 1205.3332.

[BR00] J. Blumlein and D. Robaschik, *On the structure of the virtual Compton amplitude in the generalized Bjorken region: Integral relations*, Nucl.Phys. **B581**, 449–473 (2000), hep-ph/0002071.

[BR05] A. V. Belitsky and A. V. Radyushkin, *Unraveling hadron structure with generalized parton distributions*, Phys. Rept. **418**, 1–387 (2005), hep-ph/0504030.

[BSMM00] I. Bronstein, K. Semendjajew, G. Musiol and H. Mühlig, *Taschenbuch der Mathematik*, Harri Deutsch, 5 edition, 2000.

[BST72] L. Bonora, G. Sartori and M. Tonin, *Conformal covariant operator-product expansions*, Nuovo Cim. **A10**, 667–681 (1972).

[Bur80] A. J. Buras, *Asymptotic Freedom in Deep Inelastic Processes in the Leading Order and Beyond*, Rev.Mod.Phys. **52**, 199 (1980).

[Bur03] M. Burkardt, *Impact parameter space interpretation for generalized parton distributions*, Int.J.Mod.Phys. **A18**, 173–208 (2003), hep-ph/0207047.

[C+02] S. Chekanov et al., *Exclusive photoproduction of J/ψ mesons at HERA*, Eur.Phys.J. **C24**, 345–360 (2002), hep-ex/0201043.

[C+03] S. Chekanov et al., *Measurement of deeply virtual Compton scattering at HERA*, Phys.Lett. **B573**, 46–62 (2003), hep-ex/0305028.

[C+04] S. Chekanov et al., *Exclusive electroproduction of J/ψ mesons at HERA*, Nucl.Phys. **B695**, 3–37 (2004), hep-ex/0404008.

[C+05] S. Chekanov et al., *Exclusive electroproduction of ϕ mesons at HERA*, Nucl.Phys. **B718**, 3–31 (2005), hep-ex/0504010.

[C+07] S. Chekanov et al., *Exclusive ρ^0 production in deep inelastic scattering at HERA*, PMC Phys. **A1**, 6 (2007), 0708.1478.

[C+09] S. Chekanov et al., *A Measurement of the Q^2, W and t dependences of deeply virtual Compton scattering at HERA*, JHEP **0905**, 108 (2009), 0812.2517.

[CAB+81] D. Cassel, L. Ahrens, K. Berkelman, C. Day, B. Gibbard et al., *Exclusive ρ^0, ω and ϕ Electroproduction*, Phys.Rev. **D24**, 2787 (1981).

[Car14] F. Carlson, *Sur une classe de séries de Taylor*, PhD thesis, Uppsala University, 1914.

[CDT85] N. Craigie, V. Dobrev and I. Todorov, *Conformally Covariant Composite Operators in Quantum Chromodynamics*, Annals Phys. **159**, 411–444 (1985).

[CF99] J. C. Collins and A. Freund, *Proof of factorization for deeply virtual Compton scattering in QCD*, Phys.Rev. **D59**, 074009 (1999), hep-ph/9801262.

[CFP80] G. Curci, W. Furmanski and R. Petronzio, *Evolution of Parton Densities Beyond Leading Order: The Nonsinglet Case*, Nucl.Phys. **B175**, 27 (1980).

[CFS97] J. C. Collins, L. Frankfurt and M. Strikman, *Factorization for hard exclusive electroproduction of mesons in QCD*, Phys. Rev. **D56**, 2982–3006 (1997), hep-ph/9611433.

[CG69] J. Callan, Curtis G. and D. J. Gross, *High-energy electroproduction and the constitution of the electric current*, Phys.Rev.Lett. **22**, 156–159 (1969).

[CJ01] S. Chib and I. Jeliazkov, *Marginal Likelihood From the Metropolis-Hastings Output*, Journal of the American Statistical Association **96**, 270–281 (March 2001).

[CKS00] K. Chetyrkin, J. H. Kuhn and M. Steinhauser, *RunDec: A Mathematica package for running and decoupling of the strong coupling and quark masses*, Comput.Phys.Commun. **133**, 43–65 (2000), hep-ph/0004189.

[Col84] J. Collins, *Renormalization: An Introduction to Renormalization, the Renormalization Group and the Operator-Product Expansion*, Cambridge University Press, 1984.

[Cox61] R. T. Cox, *The Algebra of Probable Inference*, The Johns Hopkins Press, 1961.

[CSI00] M.-H. Chen, Q.-M. Shao and J. G. Ibrahim, *Monte Carlo Methods in Bayesian Computation*, Springer, 2000.

[D'A03] G. D'Agostini, *Bayesian Reasoning in Data Analysis*, World Scientific Publishing Co. Pte. Ltd., 2003.

[D'A04] G. D'Agostini, *Asymmetric Uncertainties: Sources, Treatment and Potential Dangers*, ArXiv Physics e-prints (March 2004), arXiv:physics/0403086.

[Die03] M. Diehl, *Generalized parton distributions*, Phys.Rept. **388**, 41–277 (2003), hep-ph/0307382.

[DK07] M. Diehl and W. Kugler, *Next-to-leading order corrections in exclusive meson production*, Eur. Phys. J. **C52**, 933–966 (2007), 0708.1121.

[DM$^+$08] R. De Masi et al., *Beam spin asymmetry in deep and exclusive π^0 electroproduction*, Phys.Rev. **C77**, 042201 (2008), 0711.4736.

[ER80] A. Efremov and A. Radyushkin, *Factorization and Asymptotical Behavior of Pion Form-Factor in QCD*, Phys.Lett. **B94**, 245–250 (1980).

[Fey69] R. P. Feynman, *Very high-energy collisions of hadrons*, Phys.Rev.Lett. **23**, 1415–1417 (1969).

[FGG71a] S. Ferrara, R. Gatto and A. Grillo, *Conformal invariance on the light cone and canonical dimensions*, Nucl.Phys. **B34**, 349–366 (1971).

[FGG71b] S. Ferrara, A. Grillo and R. Gatto, *Improved light cone expansion*, Phys.Lett. **B36**, 124–126 (1971).

[FGG72] S. Ferrara, A. Grillo and R. Gatto, *Manifestly conformal-covariant expansion on the light cone*, Phys.Rev. **D5**, 3102–3108 (1972).

[Fie37] M. Fierz, *Zur Fermischen Theorie des β-Zerfalls*, Zeitschrift für Physik **104**(7-8), 553–565 (1937).

[FKL81] E. Floratos, C. Kounnas and R. Lacaze, *Higher Order QCD Effects in Inclusive Annihilation and Deep Inelastic Scattering*, Nucl.Phys. **B192**, 417 (1981).

[FKS96] L. Frankfurt, W. Koepf and M. Strikman, *Hard diffractive electroproduction of vector mesons in QCD*, Phys.Rev. **D54**, 3194–3215 (1996), hep-ph/9509311.

[FKS98] L. Frankfurt, W. Koepf and M. Strikman, *Diffractive heavy quarkonium photoproduction and electroproduction in QCD*, Phys.Rev. **D57**, 512–526 (1998), hep-ph/9702216.

[FM02] A. Freund and M. McDermott, *A Next-to-leading order analysis of deeply virtual Compton scattering*, Phys.Rev. **D65**, 091901 (2002), hep-ph/0106124.

[FPPS99] L. Frankfurt, P. Pobylitsa, M. V. Polyakov and M. Strikman, *Hard exclusive pseudoscalar meson electroproduction and spin structure of a nucleon*, Phys.Rev. **D60**, 014010 (1999), hep-ph/9901429.

[FPSV00] L. Frankfurt, M. V. Polyakov, M. Strikman and M. Vanderhaeghen, *Hard exclusive electroproduction of decuplet baryons in the large N_c limit*, Phys.Rev.Lett. **84**, 2589–2592 (2000), hep-ph/9911381.

[FS10] Y. Frishman and J. Sonnenschein, *Non-Perturbative Field Theory: From Two Dimensional Conformal Field Theory to QCD in Four Dimensions*, Cambridge University Press, 2010.

[FSW05] L. Frankfurt, M. Strikman and C. Weiss, *Small-x physics: From HERA to LHC and beyond*, Ann.Rev.Nucl.Part.Sci. **55**, 403–465 (2005), hep-ph/0507286.

[GIP66] V. Gribov, B. Ioffe and I. Y. Pomeranchuk, *What is the range of interactions at high-energies*, Sov.J.Nucl.Phys. **2**, 549 (1966).

[GK05] S. Goloskokov and P. Kroll, *Vector meson electroproduction at small Bjorken-x and generalized parton distributions*, Eur.Phys.J. **C42**, 281–301 (2005), hep-ph/0501242.

[GK08] S. Goloskokov and P. Kroll, *The Role of the quark and gluon GPDs in hard vector-meson electroproduction*, Eur.Phys.J. **C53**, 367–384 (2008), 0708.3569.

[GK10] S. Goloskokov and P. Kroll, *An Attempt to understand exclusive pi+ electroproduction*, Eur.Phys.J. **C65**, 137–151 (2010), 0906.0460.

[GL01] B. Geyer and M. Lazar, *Parton distribution functions from nonlocal light cone operators with definite twist*, Phys.Rev. **D63**, 094003 (2001), hep-ph/0009309.

[GP74] H. Georgi and H. D. Politzer, *Electroproduction scaling in an asymptotically free theory of strong interactions*, Phys.Rev. **D9**, 416–420 (1974).

[Gre05] P. C. Gregory, *Bayesian Logical Data Analysis for the Physical Science*, Cambridge University Press, 2005.

[GRSV96] M. Glück, E. Reya, M. Stratmann and W. Vogelsang, *Next-to-leading order radiative parton model analysis of polarized deep inelastic lepton - nucleon scattering*, Phys.Rev. **D53**, 4775–4786 (1996), hep-ph/9508347.

[GRV90] M. Glück, E. Reya and A. Vogt, *Radiatively generated parton distributions for high-energy collisions*, Z.Phys. **C48**, 471–482 (1990).

[GT71] D. J. Gross and S. Treiman, *Light cone structure of current commutators in the gluon quark model*, Phys.Rev. **D4**, 1059–1072 (1971).

[GT06] V. Guzey and T. Teckentrup, *The Dual parameterization of the proton generalized parton distribution functions H and E and description of the DVCS cross sections and asymmetries*, Phys.Rev. **D74**, 054027 (2006), hep-ph/0607099.

[GW74] D. Gross and F. Wilczek, *ASYMPTOTICALLY FREE GAUGE THEORIES. 2.*, Phys.Rev. **D9**, 980–993 (1974).

[H$^+$05] C. Hadjidakis et al., *Exclusive ρ^0 meson electroproduction from hydrogen at CLAS*, Phys.Lett. **B605**, 256–264 (2005), hep-ex/0408005.

[H$^+$08] P. Hagler et al., *Nucleon Generalized Parton Distributions from Full Lattice QCD*, Phys.Rev. **D77**, 094502 (2008), 0705.4295.

[Han63] L. Hand, *Experimental investigation of pion electroproduction*, Phys.Rev. **129**, 1834–1846 (1963).

[Has70] W. Hastings, *Monte Carlo sampling methods using Markov chains and their applications.*, Biometrika **57**, 97–109 (1970).

[HM08] D. Hwang and D. Müller, *Implication of the overlap representation for modelling generalized parton distributions*, Phys.Lett. **B660**, 350–359 (2008), 0710.1567.

[Hoo97] P. Hoodbhoy, *Wave function corrections and off forward gluon distributions in diffractive J / psi electroproduction*, Phys.Rev. **D56**, 388–393 (1997), hep-ph/9611207.

[Iof69] B. Ioffe, *Space-time picture of photon and neutrino scattering and electroproduction cross-section asymptotics*, Phys.Lett. **B30**, 123–125 (1969).

[ISK04] D. Y. Ivanov, L. Szymanowski and G. Krasnikov, *Vector meson electroproduction at next-to-leading order*, JETP Lett. **80**, 226–230 (2004), hep-ph/0407207.

[Jän01] K. Jänich, *Analysis für Physiker und Ingenieure: Funktionentheorie, Differentialgleichungen, Spezielle Funktionen*, Springer-Lehrbuch, Springer, 2001.

[Jay03] E. T. Jaynes, *Probability Theory: The Logic of Science*, Cambridge University Press, 2003.

[Jef39] H. Jeffreys, *Theory of Probability*, Clarendon Press, 1939.

[Ji97a] X.-D. Ji, *Deeply virtual Compton scattering*, Phys.Rev. **D55**, 7114–7125 (1997), hep-ph/9609381.

[Ji97b] X.-D. Ji, *Gauge-Invariant Decomposition of Nucleon Spin*, Phys.Rev.Lett. **78**, 610–613 (1997), hep-ph/9603249.

[JJ92] R. Jaffe and X.-D. Ji, *Chiral odd parton distributions and Drell-Yan processes*, Nucl.Phys. **B375**, 527–560 (1992).

[JO98a] X.-D. Ji and J. Osborne, *One loop corrections and all order factorization in deeply virtual Compton scattering*, Phys.Rev. **D58**, 094018 (1998), hep-ph/9801260.

[JO98b] X.-D. Ji and J. Osborne, *One loop QCD corrections to deeply virtual Compton scattering: The Parton helicity independent case*, Phys.Rev. **D57**, 1337–1340 (1998), hep-ph/9707254.

[KGB+96] K. Kerlikowske, D. Grady, J. Barclay, E. Sickles and V. Ernster, *Likelihood ratios for modern screening mammography. Risk of breast cancer based on age and mammographic interpretation.*, J. Am. Med. Ass. **276(1)**, 39–43 (1996).

[KM10] K. Kumerički and D. Müller, *Deeply virtual Compton scattering at small x_B and the access to the GPD H*, Nucl.Phys. **B841**, 1–58 (2010), 0904.0458.

[KMM13] K. Kumerički, D. Müller and M. Murray, *HERMES impact for the access of Compton form factors*, (2013), 1301.1230.

[KMPK08] K. Kumerički, D. Müller and K. Passek-Kumerički, *Towards a fitting procedure for deeply virtual Compton scattering at next-to-leading order and beyond*, Nucl. Phys. **B794**, 244–323 (2008), hep-ph/0703179.

[Lan75] S. Lang, $SL(2,\mathbb{R})$, Graduate Texts in Mathematics, Springer, 1975.

[LB79] G. P. Lepage and S. J. Brodsky, *Exclusive Processes in Quantum Chromodynamics: Evolution Equations for Hadronic Wave Functions and the Form-Factors of Mesons*, Phys.Lett. **B87**, 359–365 (1979).

[LMS13] T. Lautenschlager, D. Müller and A. Schäfer, *Global analysis of generalized parton distributions – collider kinematics –*, (2013), 1312.5493.

[M$^+$05] L. Morand et al., *Deeply virtual and exclusive electroproduction of ω mesons*, Eur.Phys.J. **A24**, 445–458 (2005), hep-ex/0504057.

[M$^+$09] S. Morrow et al., *Exclusive ρ^0 electroproduction on the proton at CLAS*, Eur.Phys.J. **A39**, 5–31 (2009), 0807.3834.

[Mak81] Y. Makeenko, *Conformal Operators in Quantum Chromodynamics*, Sov.J.Nucl.Phys. **33**, 440 (1981).

[MLPKS14] D. Müller, T. Lautenschlager, K. Passek-Kumericki and A. Schäfer, *Towards a fitting procedure to deeply virtual meson production - the next-to-leading order case*, Nucl.Phys. **B884**, 438–546 (2014), 1310.5394.

[MM14] M. Meskauskas and D. Müller, *A Fresh Look at Exclusive Electroproduction of Light Vector Mesons*, Eur.Phys.J. **C74**, 2719 (2014), 1112.2597.

[MMPK03] B. Melic, D. Müller and K. Passek-Kumericki, *Next-to-next-to-leading prediction for the photon-to-pion transition form factor*, Phys. Rev. **D68**, 014013 (2003), hep-ph/0212346.

[MMPR03] A. Mukherjee, I. Musatov, H. Pauli and A. Radyushkin, *Power law wave functions and generalized parton distributions for pion*, Phys.Rev. **D67**, 073014 (2003), hep-ph/0205315.

[MNP99] B. Melic, B. Nizic and K. Passek, *Complete next-to-leading order perturbative QCD prediction for the pion form-factor*, Phys.Rev. **D60**, 074004 (1999), hep-ph/9802204.

[MPR99] L. Mankiewicz, G. Piller and A. Radyushkin, *Hard exclusive electroproduction of pions*, Eur.Phys.J. **C10**, 307–312 (1999), hep-ph/9812467.

[MPS$^+$98] L. Mankiewicz, G. Piller, E. Stein, M. Vanttinen and T. Weigl, *NLO corrections to deeply virtual Compton scattering*, Phys.Lett. **B425**, 186–192 (1998), hep-ph/9712251.

[MPW98] L. Mankiewicz, G. Piller and T. Weigl, *Hard exclusive meson production and nonforward parton distributions*, Eur.Phys.J. **C5**, 119–128 (1998), hep-ph/9711227.

[MPW99] L. Mankiewicz, G. Piller and T. Weigl, *Hard leptoproduction of charged vector mesons*, Phys.Rev. **D59**, 017501 (1999), hep-ph/9712508.

[MRG$^+$94] D. Müller, D. Robaschik, B. Geyer, F. M. Dittes and J. Horejsi, *Wave functions, evolution equations and evolution kernels from light-ray operators of QCD*, Fortschr. Phys. **42**, 101 (1994), hep-ph/9812448.

[MRST98] A. D. Martin, R. Roberts, W. J. Stirling and R. Thorne, *Parton distributions: A New global analysis*, Eur.Phys.J. **C4**, 463–496 (1998), hep-ph/9803445.

[MS69] G. Mack and A. Salam, *Finite component field representations of the conformal group*, Annals Phys. **53**, 174–202 (1969).

[MS06] D. Müller and A. Schäfer, *Complex conformal spin partial wave expansion of generalized parton distributions and distribution amplitudes*, Nucl. Phys. **B739**, 1–59 (2006), hep-ph/0509204.

[MSTW09] A. D. Martin, W. J. Stirling, R. S. Thorne and G. Watt, *Parton distributions for the LHC*, Eur. Phys. J. **C63**, 189–285 (2009), 0901.0002.

[Mül94] D. Müller, *Conformal constraints and the evolution of the nonsinglet meson distribution amplitude*, Phys.Rev. **D49**, 2525–2535 (1994).

[Mül98] D. Müller, *Restricted conformal invariance in QCD and its predictive power for virtual two-photon processes*, Phys. Rev. **D58**, 054005 (1998), hep-ph/9704406.

[Mül99] D. Müller, *Scheme dependence of NLO corrections to exclusive processes*, Phys. Rev. **D59**, 116003 (1999), hep-ph/9812490.

[Mut98] T. Muta, *Foundations of Quantum Chromodynamics: An Introduction to Perturbative Methods in Gauge Theories*, World Scientific Lecture Notes in Physics, World Scientific, 1998.

[MvN96] R. Mertig and W. van Neerven, *The Calculation of the two loop spin splitting functions $P_{ij}^{(1)}(x)$*, Z.Phys. **C70**, 637–654 (1996), hep-ph/9506451.

[MVV04] S. Moch, J. Vermaseren and A. Vogt, *The Three loop splitting functions in QCD: The Nonsinglet case*, Nucl.Phys. **B688**, 101–134 (2004), hep-ph/0403192.

[Ohr82] T. Ohrndorf, *Constraints From Conformal Covariance on the Mixing of Operators of Lowest Twist*, Nucl.Phys. **B198**, 26 (1982).

[PBEoNR53] B. M. Project, H. Bateman, A. Erdélyi and U. S. O. of Naval Research, *Higher transcendental functions*, Number Bd. 1 in Higher Transcendental Functions, McGraw-Hill, 1953.

[Pól45] G. Pólya, *How to solve it*, Princton University Press, 1945.

[Pól54] G. Pólya, *Mathematics and Plausible Reasoning*, volume 2, Princton University Press, 1954.

[Pol99] M. V. Polyakov, *Hard exclusive electroproduction of two pions and their resonances*, Nucl.Phys. **B555**, 231 (1999), hep-ph/9809483.

[PPSS00] M. Penttinen, M. V. Polyakov, A. Shuvaev and M. Strikman, *DVCS amplitude in the parton model*, Phys.Lett. **B491**, 96–100 (2000), hep-ph/0006321.

[Rad96a] A. Radyushkin, *Asymmetric gluon distributions and hard diffractive electroproduction*, Phys.Lett. **B385**, 333–342 (1996), hep-ph/9605431.

[Rad96b] A. Radyushkin, *Scaling limit of deeply virtual Compton scattering*, Phys.Lett. **B380**, 417–425 (1996), hep-ph/9604317.

[Rad97] A. Radyushkin, *Nonforward parton distributions*, Phys.Rev. **D56**, 5524–5557 (1997), hep-ph/9704207.

[RW00] A. Radyushkin and C. Weiss, *DVCS amplitude with kinematical twist - three terms*, Phys.Lett. **B493**, 332–340 (2000), hep-ph/0008214.

[S$^+$08] J. Santoro et al., *Electroproduction of $\phi(1020)$ mesons at $1.4 \leq Q^2 \leq 3.8\,\mathrm{GeV}^2$ measured with the CLAS spectrometer*, Phys.Rev. **C78**, 025210 (2008), 0803.3537.

[TJG72] S. Treiman, R. Jackiw and D. Gross, *Lectures on Current Algebra and Its Applications*, Princeton Series in Physics, Princeton University Press, 1972.

[Ver99] J. A. M. Vermaseren, *Harmonic sums, Mellin transforms and integrals*, Int. J. Mod. Phys. **A14**, 2037–2076 (1999), hep-ph/9806280.

[VMV04] A. Vogt, S. Moch and J. Vermaseren, *The Three-loop splitting functions in QCD: The Singlet case*, Nucl.Phys. **B691**, 129–181 (2004), hep-ph/0404111.

[vNV00] W. van Neerven and A. Vogt, *NNLO evolution of deep inelastic structure functions: The Singlet case*, Nucl.Phys. **B588**, 345–373 (2000), hep-ph/0006154.

[Vog96] W. Vogelsang, *The Spin dependent two loop splitting functions*, Nucl.Phys. **B475**, 47–72 (1996), hep-ph/9603366.

[ZvN92] E. Zijlstra and W. van Neerven, *Order α_s^2 QCD corrections to the deep inelastic proton structure functions F_2 and F_L*, Nucl.Phys. **B383**, 525–574 (1992).

[ZvN94] E. Zijlstra and W. van Neerven, *Order α_s^2-corrections to the polarized structure function $g_1(x, Q^2)$*, Nucl.Phys. **B417**, 61–100 (1994).